2012

Synthesis of furo[2,3-d]pyrimidines, thieno[2,3-d]pyrimidines, pyrrolo[2,3-d]pyrimidines as classical and nonclassical antifolates, receptor tyrosine kinase (RTK) inhibitors and antimitotic agents

Xin Zhang

SYNTHESIS OF FURO[2,3-*d*]PYRIMIDINES, THIENO[2,3-*d*]PYRIMIDINES, PYRROLO[2,3-*d*]PYRIMIDINES AS CLASSICAL AND NONCLASSICAL ANTIFOLATES, RECEPTOR TYROSINE KINASE (RTK) INHIBITORS AND ANTIMITOTIC AGENTS

A Dissertation

Presented to the Graduate School of Pharmaceutical Sciences

of

Duquesne University

In Partial Fulfillment of the Requirements for

the Degree of Doctor of Philosophy

(Medicinal Chemistry)

by

Xin Zhang

March, 2012

Name: Xin Zhang

Dissertation: SYNTHESIS OF FURO[2,3-*d*]PYRIMIDINES, THIENO[2,3-*d*]PYRIMIDINES, PYRROLO[2,3-*d*]PYRIMIDINES AS CLASSICAL AND NONCLASSICAL ANTIFOLATES, RECEPTOR TYROSINE KINASE (RTK) INHIBITORS AND ANTIMITOTIC AGENTS

Degree: Doctor of Philosophy

Date Mar 16, 2012

APPROVED & ACCEPTED

Aleem Gangjee, Ph. D., Chair, Dissertation Committee
Professor of Medicinal Chemistry
Mylan School of Pharmacy Distinguished Professor
Graduate School of Pharmaceutical Sciences
Duquesne University Pittsburgh, Pennsylvania

APPROVED

Marc W. Harrold, Ph. D.
Professor of Medicinal Chemistry
Graduate School of Pharmaceutical Sciences,
Duquesne University Pittsburgh, Pennsylvania

APPROVED

Patrick T. Flaherty, Ph. D.
Assistant Professor of Medicinal Chemistry
Graduate School of Pharmaceutical Sciences,
Duquesne University Pittsburgh, Pennsylvania

APPROVED

David J. Lapinsky, Ph.D.
Assistant Professor of Medicinal Chemistry
Graduate School of Pharmaceutical Sciences,
Duquesne University Pittsburgh, Pennsylvania

APPROVED

Lawrence H. Block, Ph.D.
Professor of Pharmaceutics
Graduate School of Pharmaceutical Sciences,
Duquesne University Pittsburgh, Pennsylvania

APPROVED

Douglas J. Bricker, Ph.D.
Dean of the Mylan School of Pharmacy
Associate Professor of Pharmacology
Graduate School of Pharmaceutical Sciences,
Duquesne University Pittsburgh, Pennsylvania

Abstract

Dissertation Supervised by Professor Aleem Gangjee

An introduction, background and research progress in the areas of antifolates, receptor tyrosine kinase (RTK) inhbitors and antimitotic agents has been discussed .

Thymidylate synthase (TS), dihydrofolate reductase (DHFR) and glycinamide ribonucleotide formyltransferase (GARFTase) are important folate dependent enzymes that are targets for cancer chemotherapy and the treatment of infectious diseases. Classical antifolates, in most cases, are substrates for folypoly-γ-glutamate synthase (FPGS) and rely on folate transporter systems to enter cells. As a part of this study, twenty-eight compounds were designed on the basis of existing clinically active compounds and crystal structures, synthesized and evaluated as single and/or muliple targeted classical and nonclassical antifolates to decrease toxicity and improve the activity and selectivity of existing therapeutic agents. In addition, these structures provides an extension to the structure activity relationship in the antifolate area.

RTK inhibitors and antimitotic agents are important antitumor agents and are extensively used in the clinic for the treament of various types of cancers. Pgp overexpression is one of the common reasons for drug resistance to existing antitumor agents and consequently the reason for some chemotherapeutic failures. A furo[2,3-*d*]pyrimidine compound was discovered to have dual RTK inhibitory activity along with antimitotic activity that circumvent pgp over expression. Antimitotic activity via the binding at the colchicine site is one of the mechanisms of action. Molecular modelling and biological evaluation suggest the importance of conformational restriction for activity. Fifty-seven furo[2,3-*d*]pyrimidines and six thieno[2,3-*d*]pyrimidines were designed on

the basis of crustal structures and synthesized as potential RTK inhibitors with antimitotic antitumor activity. Four pyrrolo[2,3-*d*]pyrimidines were designed and synthesized as antimitotic anticancer agents that also reverse pgp action.

Table of Contents

List of Figures

List of Schemes

List of Tables

List of Abbreviations

5-FU	5-Fluorouracil
AB	acidic box
AICAR	Aminoimidazole-4-carboxamide ribosyl-5-phosphate
AICARFTase	Amino-imidazole-carboxamide-ribonuleotide formyl transferase
AIDS	Acquired immunodeficiency syndrome
AMT	Aminopterin
AR	amphiregulin
ATP	Adenosine-5'-triphosphate
Axl	a Tyro3 PTK
BTC	beta-cellulin
Bz_2O_2	Benzoyl perxoide
CA4	combretastatin A-4
CA4P	combretastatin A-4 phosphate
CadhD	cadherin-like domain
CM	Cross-metathesis
CML	chronic myelogenous leukemia
CRD	cysteine-rich domain
dATP	2'-Deoxyadenosine-5'-triphosphate
DDATHF	5,10-dideazatetrahydrofolic acid
DDR	discoidin domain receptor
dGTP	2'-deoxyguanosine-5'-triphosphate
dGTP	2'-Deoxyguanosine-5'-triphosphate
DHFR	dihydrofolate reductase
DiscD	discoidin-like domain
DNA	Deoxyribonucleic acid
dTDP	thymidine-5'-diphosphate
dTMP	2'-Deoxythymidylate-5'-monophosphate
dTTP	Deoxythymidine-triphosphate
dTTP	Deoxythymidine-triphosphate
dUMP	2'-Deoxyuridylate-5'-monophosphate
dUTP	2'-deoxyuridine-5'-triphosphate
E. coli	*Escherichia coli*
EGFD	epidermal growth factor-like domain
EGFR	epidermal growth factor receptor
EphR	ephrin receptor
EPR	epiregulin
FA	Folic acid
fAICAR	formyl-amino-imidazolecarboxamide ribosyl-5-phosphate
FdUMP	5-fluoro-2'-deoxyuridine-5'-monophosphate
FdUTP	5-fluoro-2'-deoxyuridine-5'-triphosphate
fGAR	Formyl-glycinamide ribosyl-5-phosphate
FGFR	fibroblast growth factor receptor
FH_2	7,8-Dihydrofolate
FH_4	5,6,7,8-Tetrahydrofolate

FNIII	fibronectin type III-like domain
FPGH	Folylpolyglutamate hydrolase
FPGS	folylpoly-γ-glutamate synthetase
FR	folate receptor
FR	Folate receptor
GAR	Glycinamide ribosyl-5-phosphate
GARFTase	Glycinamide-ribonucleotide transformylase
GISTs	gastrointestinal stromal tumors
GPI	glycosyl phosphatidylinositol
GTP	guanosine-5'-triphosphate
HB-EGF	hepairin-binding EGF-like growth factor
HGFR	hepatocyte growth factor receptor
IFN	Interferon
IgD	immunoglobulin-like domain
IGF-IR	Insulin-like growth factor-I receptor
IMP	inosine-5'- monophosphate
InsR	insulin receptor
IR	Insulin receptor
KLG/CCK	colon carcinoma kinase
KrinD	kringle-like domain
L. casei	*Lactobacillus casei*
L. major	*Leishmania major*
leucovorin	LV
LMR	Lemur. Other abbreviations
LMX	lometrexol
LRD	leucine-rich domain
LTK	leukocyte tyrosine kinase
M. avium	Mycobacterium avium
MDR	multiple drug resistance
MOE	Molecular Operating Environment
MRP	multidrug resistance protein
MRPs	multidrug-resistance-proteins
MTHFR	methylenetetrahydrofolate reductase
MTX	Methotrexate
MuSK	muscle-specific kinase
Mycobacterium avium	*M. avium*
N^{10}-CHO-FH_4	10-Formyltetrahydrofolate
N^5,N^{10}-CH_2-FH_4	5,10-Methylenetetrahydrofolate
N^5-CH=NH-FH_4	5-formiminotetrahydrofolate
N^5-CH_3-FH_4	5-Methyltetrahydrofolate
N^5-CHO-FH_4	5-Formyltetrahydrofolate
NADPH	Nicotinamide adenine dinucleotide phosphate
NBS	*N*-bromosuccinimide

NBS	N-bromosuccinamide
NGFR	nerve growth factor receptor
NRG	neuregulins
NRP-1	Neuropilin-1
NSCLC	non-small cell lung cancer
P. carinii	*Pneumocystis carinii*
PABA	*p*-Aminobenzoic acid
PCC	Pearson correlation coefficients
PCFT	proton coupled folate transporter
PCP	*P. carinii pneumonia*
PDDF	N^{10}-propargyl-5,8-dideazafolate
PDGFR	platelet-derived growth factor receptor
Pgp	P-glycoprotein
Piv	Pivaloyl (trimethyl acetyl)
PMX	pemetrexed
Pneumocystis jirovecii	*P. jirovecii*
PteGlu	Pteroylglutamic acid
PTX	piritrexim
Ret	rearranged during transfection
RFC	reduced folate carrier
rh GARFTase	recombinant human GARFTase
rl	rat liver
RNA	ribonucleic acid
ROR	receptor orphan
ROS	RPTK expressed in some epithelial cell types
Rr	resistance index
RTK	Receptor tyrosine kinase
RTKs	receptor tyrosine kinases
RTX	raltitrexed
RYK	receptor related to tyrosine kinases
SHMT	Serine hydroxymethyltransferase
T. gondii	*Toxoplasma gondii*
T. gondii	Toxoplasma gondii
TGF-α	transforming growth factor α
TIE	tyrosine kinase receptor in endothelial cells
TLC	Thin layer chromatography
TMP	trimethoprim
TMQ	trimetrexate
TS	Thymidylate synthase
VEGFR	vascular endothelial growth factor receptor
VGFR	Vascular endothelial growth factor receptor

I. BIOCHEMICAL REVIEW

1. Folate metabolism

Because of its critical importance in the biosynthesis of purine and pyrimidine nucleic acids, folate metabolism is an attractive target for chemotherapy. Folate coenzymes are required in more than twenty interrelated enzymatic reactions in cellular metabolism. These reactions are necessary to maintain *de novo* synthesis of the essential building blocks of deoxyribonucleic acid (DNA) as well as the synthesis of certain important amino acids.[1] Antimetabolites that interfere with this complex metabolism pathway are known as antifolates and are clinically useful as antimicrobial, antifungal, antiprotozoal, and antitumor agents.[2,3] Today, almost sixty years after the discovery of aminopterin (AMT),[4] the first important antifolate, the folate cycle remains an attractive target for drug development.

1.1 Folic acid and folates

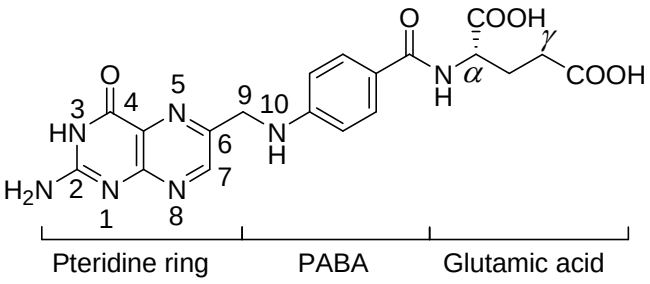

Figure 1. Structure of folic acid.

Folic acid (FA) is a water-soluble vitamin of the B-complex group for life sustaining process. In its various cofactor forms, FA is essential for different biological process and functions, including purine and pyrimidine biosynthesis and hence DNA synthesis and cell replication.[1,5,6]

FA was first reported more than 70 years ago as an anti-anemia agent in animals and as a growth factor in bacteria. It is also present in common foods such as peas, oranges, broccoli, and whole-wheat products. FA was named after folium, the Latin term for leaf, because in 1941, Mitchell *et al*[7] isolated the species from spinach leaves. Folates are obtained through two distinct pathways in eukaryotes and prokaryotes. Higher plants, fungi and bacteria synthesize folates *de novo*; however, mammalian cells (including human) are incapable of synthesizing FA and hence have to acquire preformed FA from the diet.[8]

From a structure point of view, FA consists of three elements: a hetero-bicyclic pteridine, a *p*-aminobenzoic acid (PABA) and a glutamic acid (Figure 1). Because of its structural features, FA is also called pteroylglutamic acid. FA can be regarded as the parent compound of a group of naturally occurring folates and exists in several oxidative states, including 7,8-dihydrofolate (FH_2), 5,6,7,8-tetrahydrofolate (FH_4), 5-methyltetrahydrofolate (N^5-CH_3-FH_4), 5,10-methylenetetrahydrofolate (N^5,N^{10}-CH_2-FH_4), 5-formyltetrahydrofolate (N^5-CHO-FH_4), 10-formyltetrahydrofolate (N^{10}-CHO-FH_4), 5-formiminotetrahydrofolate (N^5-CH=NH-FH_4) and others. All these folate cofactors are essential to the role of folate in metabolism.

Folates differ from FA in several respects: reduction states of the pteridine ring (oxidized, 7,8-H_2, and 5,6,7,8-H_4) may occur, one-carbon units may be attached to N5 (N^5-CH_3-FH_4, N^5-CHO-FH_4 and N^5-CH=NH-FH_4) or N10 (N^{10}-CHO-FH_4) or both (N^5,N^{10}-CH_2-FH_4), and additional glutamate residues (poly-γ-glutamates) may be attached to the glutamate moiety by unusual γ-peptide bonds, giving folate polyglutamates.

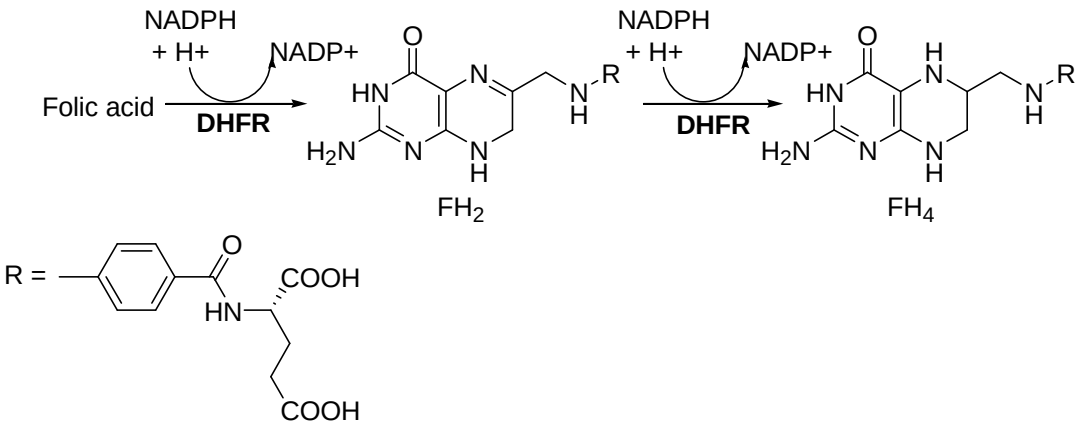

Figure 2. Biological conversion of folic acid to tetrahydrofolate.

Tetrahydrofolate is the central component of folate metabolism and is synthesized from FA through enzymatic process. Intracellular reduction of the pyrazine portion of the pteridine ring is catalyzed by a nicotinamide adenine dinucleotide phosphate (NADPH)-specific dihydrofolate reductase (DHFR) to form dihydrofolate, which is further reduced by DHFR to generate tetrahydrofolate (Figure 2).[9]

Tetrahydrofolate functions as the coenzyme in the utilization of one-carbon units and is capable of carrying single carbon units in various cofactor forms including N^5-CH_3-FH_4, N^5,N^{10}-CH_2-FH_4, N^5-CHO-FH_4, N^{10}-CHO-FH_4 and N^5-CH=NH-FH_4. In these folates cofactor forms, the one carbon unit may be attached to N5 or N10 or both positions. The conversion between folate cofactors are catalyzed by several different enzymes, as shown in Figure 3.

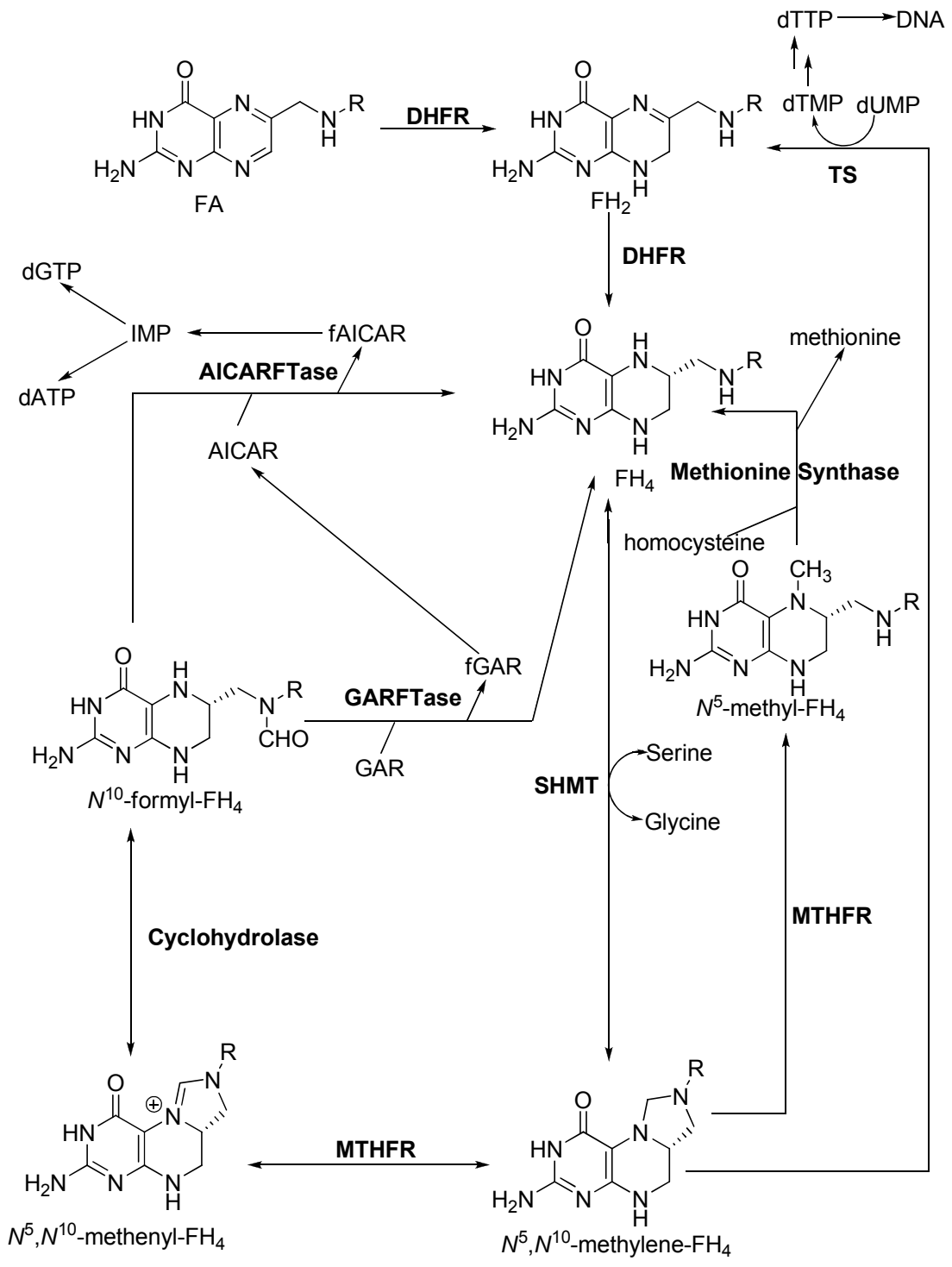

Figure 3. Folates metabolism. SHMT: Serine Hydroxymethyltransferase; MTHFR: Methylenetetrahydrofolate Reductase; GARFTase: Glycinamide-ribonucleotide Formyl Transferase; AICARFTase: Amino-imidazole-carboxamide-ribonuleotide Formyl

Transferase; AICAR: Aminoimidazole-4-carboxamide ribosyl-5-phosphate; dTMP: 2'-Deoxythymidylate 5'-monophosphate; dUMP: 2'-Deoxyuridylate-5'-monophosphate; dTMP: 2'-Deoxythymidylate 5'-triphosphate; GAR: Glycinamide Ribosyl-5-phosphate; DNA: Deoxyribonucleotide; IMP: Inositol monophosphate.

Folates are utilized as cofactors for one carbon unit transfer in a number of enzymatic processes, including the metabolism of amino acids (glycine, serine, methionine, and histidine), the biosynthesis of nucleic acid (purine nucleotide and the 5-methyl group of thymine) and the formation of formylmethionyl-tRNA.

During nucleic acid biosynthesis, folate cofactors play an important role in the conversion of 2'-deoxyuridylate-5'-monophosphate (dUMP) to 2'-deoxythymidylate-5'-monophosphate (dTMP) catalyzed by thymidylate synthase (TS) utilizing N^5,N^{10}- CH_2-FH_4 as the cofactor (Figure 4). This enzyme is unique among those which utilize FH_4 cofactor in that N^5,N^{10}-CH_2-FH_4 acts as the source of the methyl group as well as the reductant, by concerted transfer of its methylene moiety and the 6-hydrogen atom in the form of hydride to form the 5-methyl group of dTMP. TS catalyzes the only *de novo* synthesis of dTMP in dividing cells.

Severe deoxythymidine-triphosphate (dTTP) depletion due to TS inhibition, in the absence of salvage, leads to "thymineless death".[8] Unlike the deprivation of many other nutritional requirements, the deprivation of thymidine has a lethal effect rather than biostatic effects. Thymine starvation has both direct and indirect effects on dividing cells. The direct effects involve both single- and double-strand DNA breaks. The former may be repaired effectively, but the latter lead to cell death.

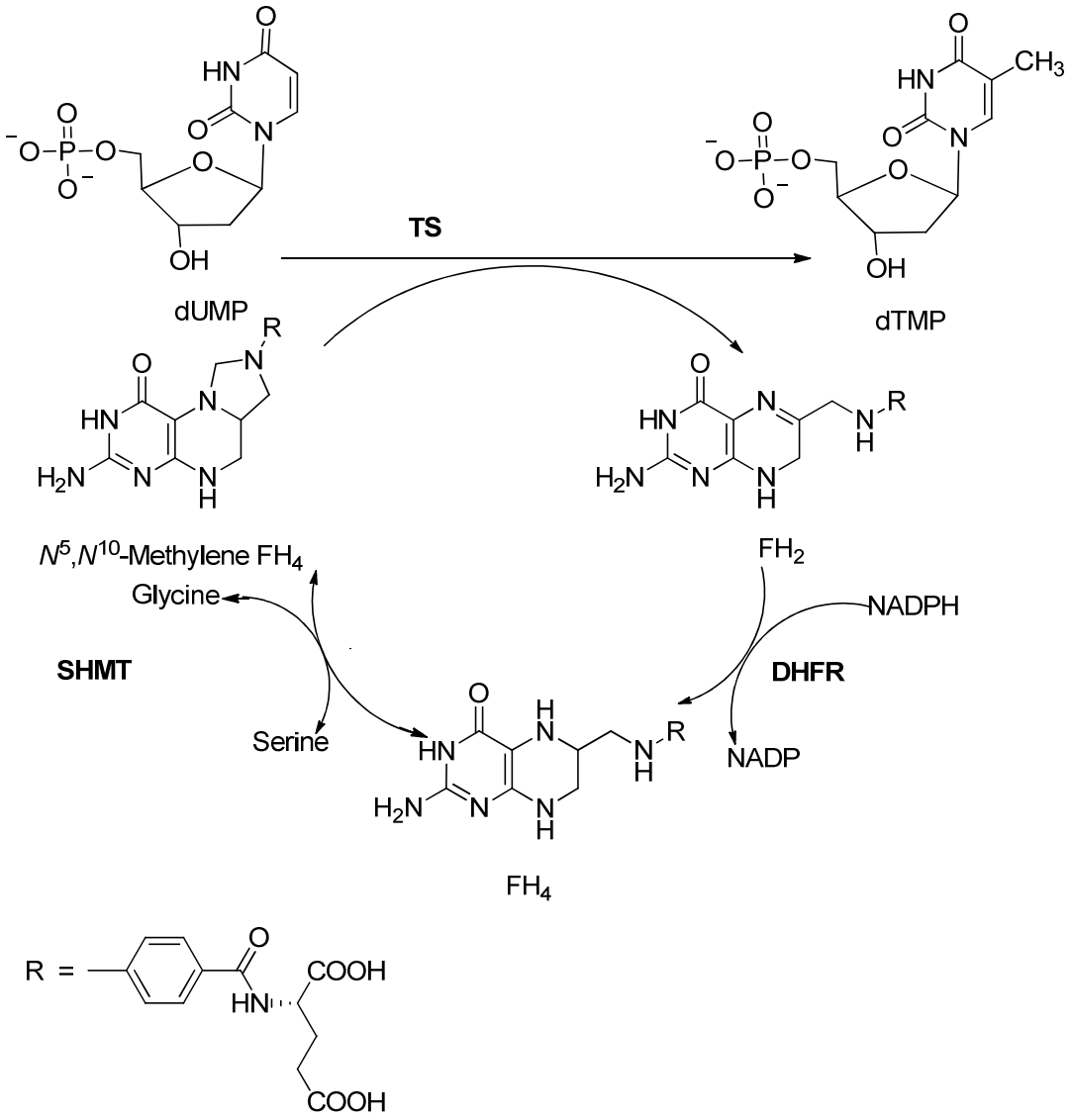

Figure 4. TS catalyzed biosynthesis of dTMP from dUMP.

Methotrexate (MTX) and 5-fluorouracil (5-FU) cause a decrease in dTTP levels and a concomitant increase in dUTP, which is incorporated into DNA. This leads to extensive DNA damage as a result of the active process of excision repair at the many uracil-containing sites in DNA, and thus trigger a DNA damage induced apoptosis.

During the TS catalyzed reaction, N^5,N^{10}-CH_2-FH_4 is oxidized to FH_2 and is

converted back to FH_4 by the action of DHFR, which functions to maintain the intracellular reduced folate pool. Thus the inhibition of DHFR leads to a partial depletion of the intracellular reduced folate pool which consequently limits cell growth.[10] Both human TS and human DHFR are crucial enzymes for cell growth and hence both represent attractive targets for developing chemotherapeutic agents.[11]

Another cofactor, N^{10}-CHO-FH_4 transfers one carbon units necessary in the *de novo* biosynthesis of purine nucleotides (Figure 5). These carbons comprise the C-8 carbon and C-2 carbon of purines. Glycinamide-ribonucleotide transformylase (GARFTase) catalyzes the conversion of glycinamide ribosyl-5-phosphate (GAR) to formyl-glycinamide ribosyl-5-phosphate (fGAR), utilizing N^{10}-formyl-FH_4. GARFTase occurs in mammals as a trifunctional protein which catalyzes three different steps in purine biosynthesis, including the second and the fifth steps of purine biosynthesis in addition to the third step. The fGAR formed is further converted to amino-imidazolecarboxamide ribosyl-5-phosphate (AICAR). Amino-imidazolecarboxamide ribosyl-5-phosphate formyl transferase (AICARFTase) is responsible for the catalysis of the last two steps in *de novo* purine biosynthesis. AICARFTase utilizes N^{10}-CHO-FH_4 and converts AICAR to formyl-amino-imidazolecarboxamide ribosyl-5-phosphate (fAICAR). The fAICAR formed continues along the purine biosynthetic pathway leading to the formation of inosine-5'-monophosphate (IMP), the precursor of adenosine-5'-triphosphate (ATP) and guanosine-5'-triphosphate (GTP) necessary for ribonucleic acid (RNA) synthesis and of 2'-deoxyadenosine-5'-triphosphate (dATP) and 2'-deoxyguanosine-5'-triphosphate (dGTP) necessary for DNA synthesis.[11,13]

,

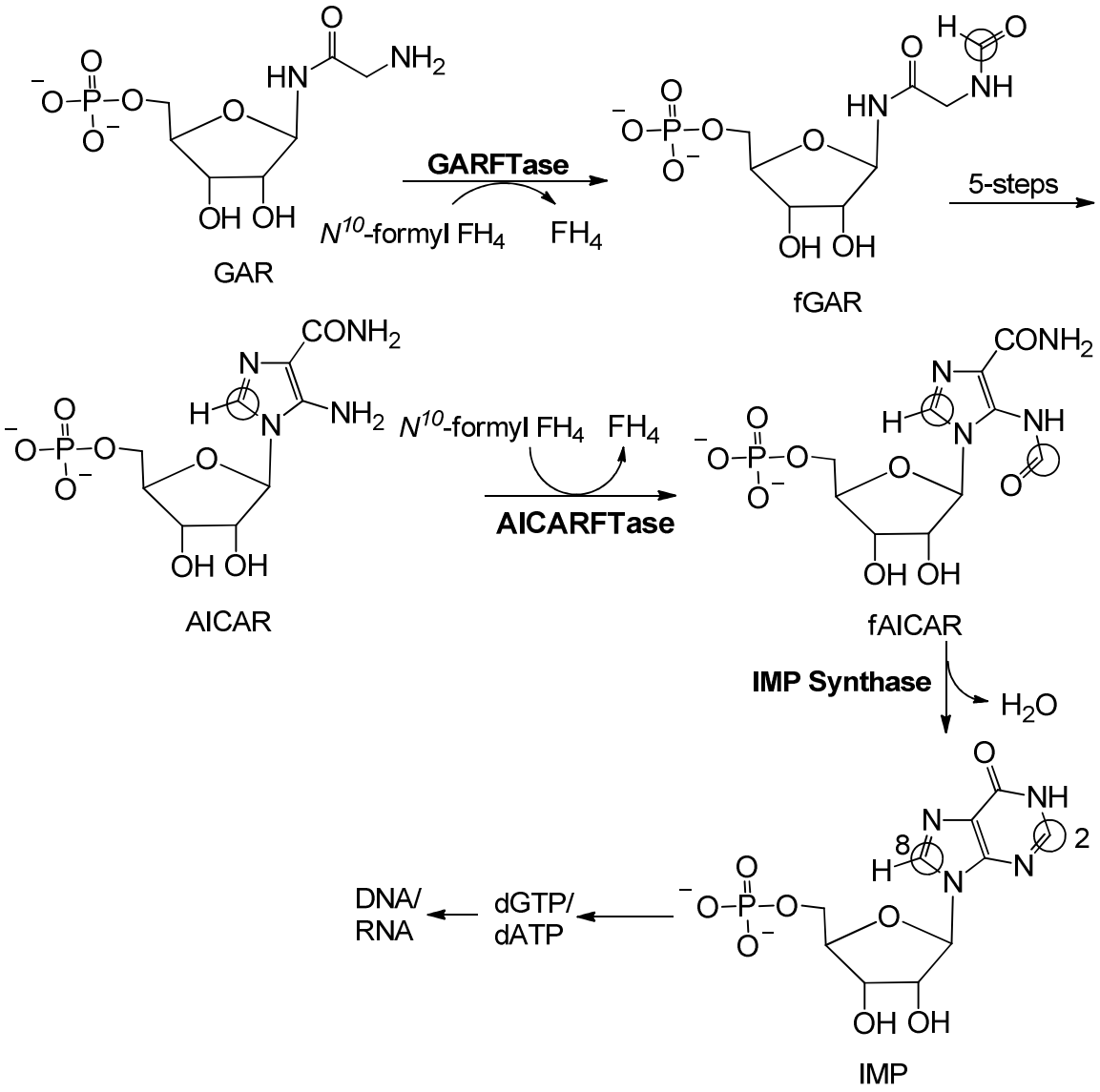

Figure 5. *De novo* synthesis of purines.

Mammalian cells have developed sophisticated folate uptake and retention system due to the importance of folate in the maintenance of single carbon metabolism.[6,11] Transport into the cell is usually accomplished by one of three carrier proteins present on the cell surface, reduced folate carrier (RFC), the membrane folate receptor (FR), and the proton coupled folate transporter (PCFT). The reduced form of FA including N^5-CH_3-FH_4 and N^{10}-CHO-FH_4 are actively taken up into the cell *via* the RFC system.[14] FA, however,

has a higher affinity for the FR, which has a higher affinity for the oxidized form of the folate cofactor than the reduced form.

Once inside the cell, FA or its cofactors are converted to the poly-γ-glutamyl species by the enzyme folylpoly-γ-glutamate synthetase (FPGS), which adds glutamic acid residues to the gamma carboxylic acid *via* amide bonds. The number of glutamate residues varies widely in naturally occurring folates. Usually 4-8 glutamate residues are added to the gamma carboxylic acid group of the FA. The polyglutamylated folate species have higher binding affinity to some folate dependent enzymes and have increased intracellular retention time.[6,15,16]

Folylpolyglutamate hydrolase (FPGH), which is an enzyme found in the lysosomes, catalyzes the hydrolysis of folates polyglutamates back to their monoglutamate form.[17] Through an ATP dependent process, folate monoglutamates can efflux from the cell *via* multidrug resistance protein (MRP) including P-glycoprotein (Pgp).[19]

1.2. Antifolates

Folate metabolism has long been recognized as an attractive target for cancer chemotherapy because of its crucial role in the biosynthesis of nucleic acid precursors. [20-23] Antimetabolites that interfere with this complex metabolism pathway are known as antifolates and are clinically useful as antimicrobial, antifungal, antiprotozoal, and antitumor agents.[24-27] Selective inhibition of folate-dependent enzymes in microbial cells,

cancer cells, and protozoan cells, provides opportunities for the design and synthesis of compounds which can be used to treat disorders like cancer and psoriasis, microbial and protozoan infections.

Based on their mechanism of transportation and the ability to undergo polyglutamylation, antifolates are classified into classical antifolates and nonclassical antifolate. Classical antifolates contain an intact L-glutamate side chain , while nonclassical antifolates contains a lipophilic side chain.[5,13] As shown in Figure 6, classical antifolates are typified by MTX, AMT, edatrexate, N^{10}-propargyl-5,8-dideazafolate (PDDF), raltitrexed (ZD1694, Tomudex) (RTX), pemetrexed (LY231514, Alimta) (PMX), GW1843, lometrexol (LMX) and plevitrexed (ZD9331). This group of analogs closely resembles the structure of endogenous folates and their metabolites. Classical antifolates are actively taken up into cells by folate transporter systems present on the cell surface.[14,15] The nonclassical antifolates are represented by structures such as AG337, nolatrexed (AG331, Thymitaq), pyrimethamine, trimethoprim (TMP), piritrexim (PTX) and trimetrexate (TMQ) (Figure 7). Nonclassical antifolates do not utilize the folate active transport systems (RFC and FR) and are presumably taken up by passive and/or facilitated diffusion.[14,15]

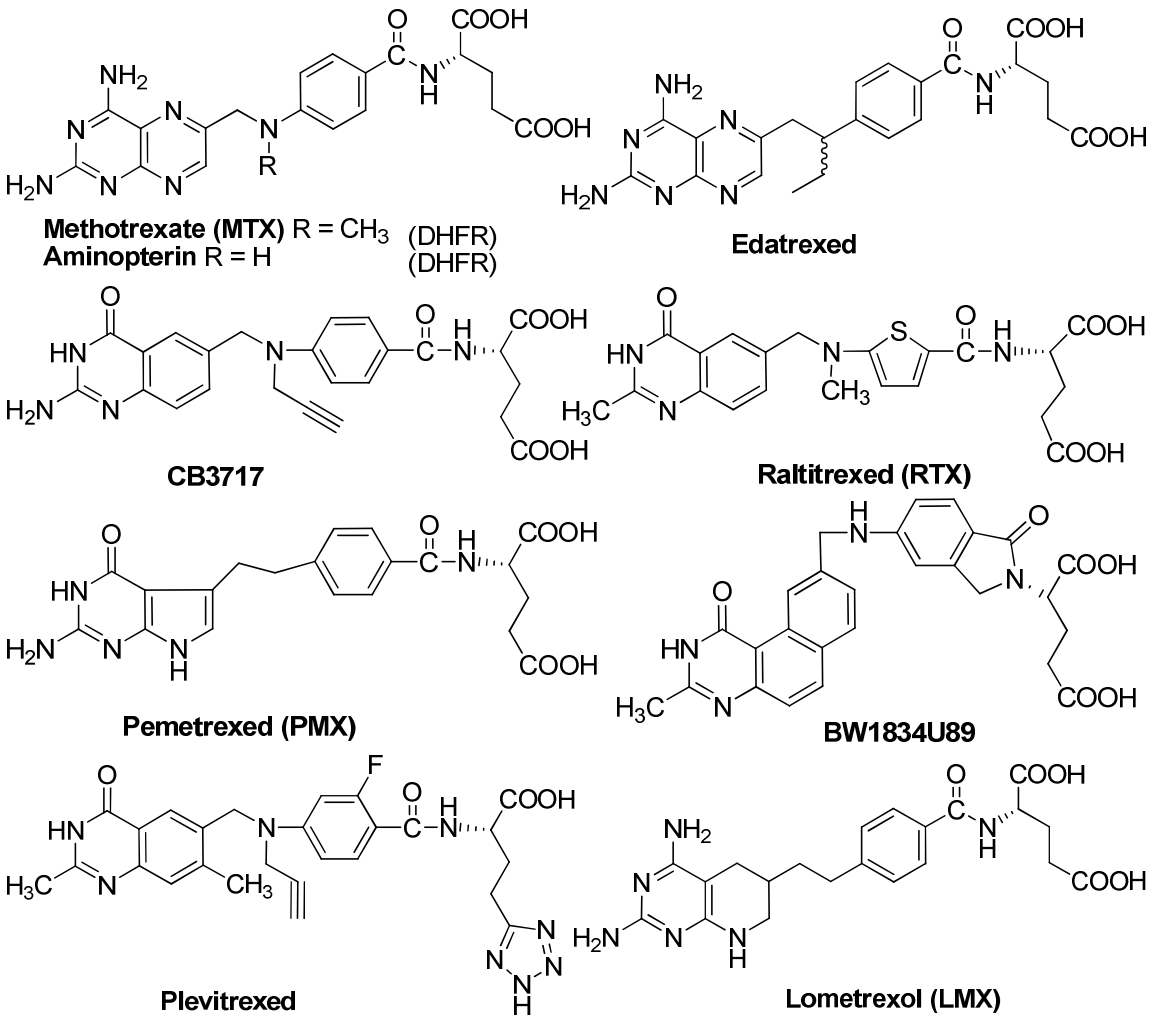

Figure 6. Representative examples of classical antifolates.

To overcome resistance associated with classical antifolates, non-classical antifolates have been developed as antitumor agents. In addition, nonclassical antifolates also provide selective treatment for pathogenic infections caused by organisms such as *Pneumocystis carinii* (*P. carinii*), *Toxoplasma gondii* (*T. gondii*), and *Mycobacterium avium* (*M. avium*).[17] Such infections are prevalent opportunistic infection in patients with compromised immune system, such as acquired immune deficiency syndrome (AIDS) patients, patients undergoing chemotherapy and organ transplant patients. The treatment

with antifolates of these infections takes advantage of the selective inhibition of pathogen DHFR over human DHFR.[5]

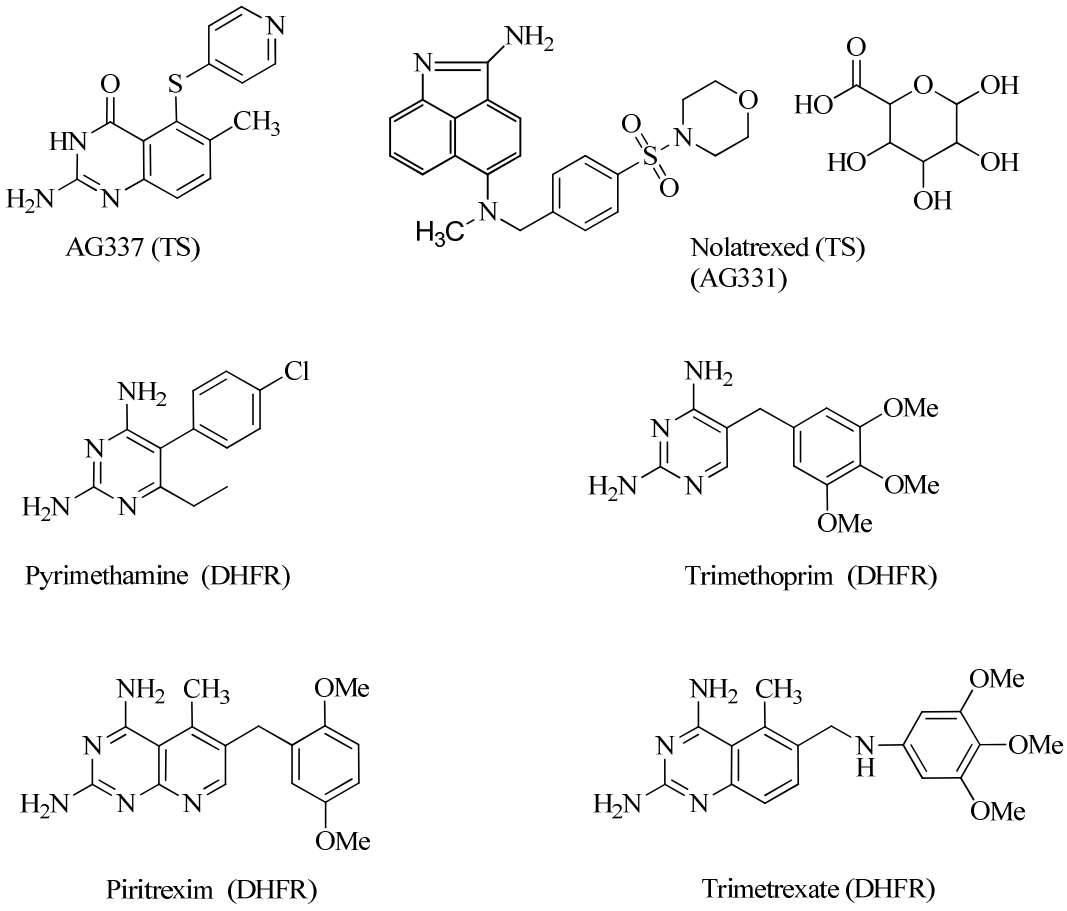

Figure 7. Representative examples of nonclassical antifolates (and their principal target(s)).

1.3. Dihydrofolate Reductase (DHFR)

DHFR functions as a catalyst for the reduction of dihydrofolate to tetrahydrofolate. The inhibition of DHFR leads to partial depletion of intracellular reduced folates with subsequent limitation of cell growth. Except for archaebacteria and a few parasitic protozoa, DHFR has been universally found in all organisms with the first

crystal structure reported more than three decades ago.[28] Since then, various x-ray crystal structures and solution NMR structures of DHFR from different species (bacteria, avian and mammalian) have been reported. The structures of DHFR bound to a variety of ligands, including cofactor(s) and their analogs, as well as inhibitors are recorded in the literature.[28-59] These X-ray crystal structures as well as NMR structures have provided insight into the various aspects of the structure and function of DHFR and have been extensively reviewed

1.3.1. Structure of DHFR

DHFR (EC 1.5.1.3) is a monomeric protein containing 159-250 amino acid residues with a molecular weight in the range of 18000-22000 Daltons. The overall tertiary structure from all known sources is very similar. The homology among vertebrate DHFR is 75-90% while in bacteria the homology decrease to 25-40%, with the highest homology observed at the N-terminal and least homology at the C-terminal.[60,61] The tertiary structure of DHFR has a α/β structure with the core made up of an eight-stranded β-sheet consisting of seven parallel strands, and one antiparallel strand at the C-terminal. It also contains at least four α-helices. Mammalian DHFR has longer sequences with the additional amino acid residues packed in the linkages between the βstrands. The active site can be described as a 15Å deep cleft stretching across one side of the enzyme. The binding site has a hydrophobic core with H-bond forming polar regions at both ends. The hydrophobic nature of the active site amino acid residues indicate that cofactors or inhibitors may bind with enzyme through hydrophobic and van der Walls interactions. This hydrophobic pocket serves as a binding site for the substrate folates or the

antifolates and nicotinamide portion of NADPH. The polarity of the substrate binding site is complementary to that of the folate or inhibitor.[62] The pteridine moiety and the glutamate side chain portions of the folate are surrounded by backbone carbonyls and polar side chains, while the benzoyl moiety of the folate forms hydrophobic interactions with the side-chains of surrounding non-polar hydrophobic residues. These 3D-structures of DHFR are used in structure-based drug design and to acquire information on inhibitor binding, enzyme-inhibitor-cofactor complexes and in particular to determine differences in amino acid location between parasite and host DHFR.

1.3.2. Species-difference among DHFR

To develop antiinfectious agents with selectivity for pathogen DHFR over human DHFR, the species-differences of the amino acid sequences among various DHFR in the active site has been exploited, which accounts for the differences in binding affinity for a variety of inhibitors against DHFR from different sources. Since the first report of diaminopyrimidine antifolates with selective, potent antibacterial and antiprotozoal activity but poor inhibitory activity against mammalian cells by Hitching and coworkers in 1979,[63] selective inhibition of pathogen DHFR has become a rational approach to drug development. As an example of such an approach, TMP (Figure 7) was developed as a potent antibacterial agent since its binding affinity for bacterial DHFR is five orders of magnitude greater than for mammalian DHFR. Patients with compromised immune system often suffer from *P. jirovecii*, *T. gondii*, and *M. avium* infections. Thus, the differences among these pathogen DHFR and human DHFR could be exploited to afford selectivity.

a. *Pneumocystis carinii* DHFR.

P. carinii DHFR is a small molecule of 24-26 KDa, consisting of 206 amino acids, and is similar to rat liver (rl) DHFR in size. *P. carinii* DHFR binds TMP and PTX in a fashion similar to that observed in bacterial enzyme,[64,65] although the *P. carinii* DHFR active site is intermediate in size between those of human (L1210) DHFR and bacterial (*E. coli*) DHFR. While most of the residues of the *P. carinii* DHFR involved in catalysis and binding are conserved in both human and *P. carinii* DHFR, x-ray crystal structures[41] indicate that the polar Asn64 residue in human DHFR, located just outside the binding site, is replaced by a nonpolar Phe69 in *P. carinii* DHFR.

TMP (Figure 7), in combination with sulfamethoxazole, is the agent of choice in the treatment of *P. carinii pneumonia* (PCP), although it is a relatively weak *P. carinii* DHFR inhibitor (IC_{50} = 12 μM) and has modest selectivity (14-fold) compared to rlDHFR.[66] TMQ, a much more poent but even less selective nonclassical antifolate, used along with leucovorin (LV) is an alternate therapy for moderate to severe PCP in patients who cannot tolerate TMP-sulfamethoxazole or pentamidine. TMQ (IC_{50} = 42 nM) is a potent inhibitor of *P. carinii* DHFR but is devoid of selectivity. It has been approved for the treatment of PCP when administered with the reduced folate LV to rescue host cells.[67] Since *P. carinii*, presumably lacks the carrier mediated uptake mechanisms[67] necessary for classical antifolates, it does not take up LV.

Recent study showed that *Pneumocystis jirovecii* (*P. jirovecii)* is the real opportunistic pathogen that infects human, while *P. carinii* is the pathogen that is derived from and infects rats.[68] According to Cody *et al*[69], the recombinant human-derived pneumocystis DHFR (*P. jirovecii* DHFR) differs from rat-derived *P. carinii* DHFR by

38% in amino acid sequences.

b. *Toxoplasma gondii* DHFR.

T. gondii belongs to genera of protozoan parasite and has a bifunctional DHFR-TS enzyme with the DHFR domain located at the N-terminus while the TS domain is at the C-terminus.[70] The DHFR domain and the TS domain are separated by a junction polypeptide.[71,72] The native protein is a dimmer of two such subunits. Roos and coworkers have reported the primary structure of the DHFR-TS gene from *T. gondii* .[73] Both enzyme domains of the DHFR-TS protein resemble the enzyme in eukaryotes with subtle differences, which could be exploited to design selective inhibitors. The major differences lie in the α-helices B and C, adjacent to the active site, which are known to participate in ligand interactions.[74,75] In the absence of the crystal structures of *T. gondii* DHFR, homology modeling and multiple sequence alignment studies were carried out to afford insight into the binding mode of inhibitors with *T. gondii* DHFR with inhibitors. It was found that a hydrophobic residue Phe91 aligns with Phe69 in *P. carinii* DHFR. Therefore, it should be possible to design inhibitors that interact productively with Phe69 in *P. carinii* DHFR and its putative counterpart hydrophobic residue in *T. gondii* DHFR thus providing selectivity not only for *P. carinii* DHFR, but perhaps also for *T. gondii* DHFR over human DHFR.

Several different DHFR inhibitors showed inhibitory activities against *T. gondii* DHFR. TMQ (IC_{50} = 10 nM), PTX (IC_{50} = 4.3 nM), TMP (IC_{50} = 2.8 μM), and pyrimethamine (IC_{50} = 0.39 μM, Figure 7), have activity against isolated *T. gondii* DHFR and against the growth of *T. gondii* cells in culture.[76]

1.3.3. The catalytic mechanism of DHFR.

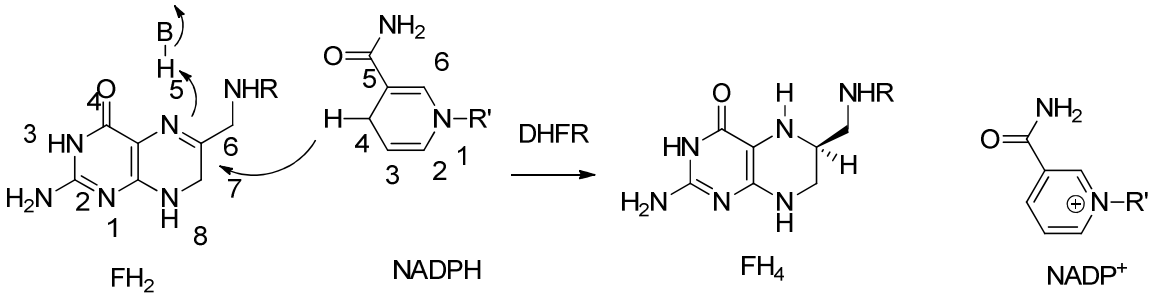

Figure 8. The reaction catalyzed by DHFR.

The catalytic mechanism of DHFR (Figure 8) has been chemically and structurally studied in detail. DHFR catalyzes a hydride transfer from NADPH to the C6 of FH_2, and at a much slower rate to the C7 of folate to form FH_4.[77,78] The generally accepted mechanism involves the initial protonation of N5 followed by a hydride transfer from the C4 of the cofactor NADPH to the adjacent C6. Studies on the effects of pH and deuterium isotope analysis on catalysis of 7,8-FH_2 reduction by E. coli DHFR suggest that the protonation at N5 either immediately precedes, or is concerted with, hydride transfer to C6. By analogy, a similar mechanism involving pre-protonation of N8 has been suggested as a means of promoting hydride transfer to C7 in folates. The hydride transfer from NADPH is much more facile to C6 of 7,8-FH_2 than to the C7 of folate.[77,78]

Three major differences between the mechanisms of folate reduction and FH_2 reduction are listed below: (A) pre-protonation of the ring nitrogen of the substrate adjacent to the hydride accepting carbon leads to a transition state stabilizing the hydrogen bond for folate, but to an unfavorable ionic-nonpolar interaction for FH_2, which favors delocalization of the positive charge to C6. (B) *Ab initio* calculations showed that

the protonation of N5 of FH_2 leads to a relatively localized positive charge build-up on the adjacent C6. The hydrogen bond of the N8 to the enzyme, which is suggested to stabilize the transition state for folate reduction, offers a path for further positive charge delocalization of the N8-protonated folate, thereby depleting the already partial positive charge on C7. (C) While the C-N bonds of the substrate that are reduced are not strictly syn or anti, the C6-N5 bond is closer to syn, while the C7-N8 bond is more anti. The angle defined by the donor-hydride acceptor atoms is 154° for hydride transfer to C6 of FH_2, which is considerably closer to the optimal value of 158° observed for syn hydride transfers than the 209° angle for hydride transfer to C7 of folate is to the optimal value of 173° required for anti hydride transfer transition states. In spite of the differences in the mechanism of the reduction of folate and FH_2, a common feature of both hypothetical transition states is the partial overlap of the pteridine and the nicotinamide binding sites, which allows for the dihydronicotinamide ring, with its potential "hydride", to be positioned close to the N5-C6 double bond of the pteridine ring.[78] Protonation of the N5 was first proposed to occur via the Asp27 (E. coli). However, Filman *et a1*. and Bystroff *et a1*. have noted that the distance between the Asp and the N5 of 7,8-FH2 is too large (6.3 Å) for direct protonation. Alternatively, they proposed an indirect mechanism for protonation via water molecules. NMR studies later detected two water molecules with long residence times (> 2 ns) bound to the active site of the enzyme, one of which has been implicated as the likely proton donor in the catalytic reduction.[79]

1.4. Thymidylate Synthase (TS)

TS (EC 2.1.1.45), a key enzyme in folate metabolism, present in almost all living organisms including bacteria, DNA viruses and protozoa.[80] It catalyzes the reductive

methylation of dUMP to dTMP, which is further phosphorylated to thymidine-5'-diphosphate (dTDP) and thymidine-5'-triphosphate (dTTP). The dTTP formed is utilized by DNA polymerase and is incorporated into DNA. The TS catalyzed reaction is a key step in DNA biosynthesis and the only *de novo* biosynthetic pathway to dTMP. TS inhibition results in a thymineless state, which prevents the growth of actively dividing cells.[81-83] This effect is probably due to increased DNA fragmentation resulting from dTTP depletion, which increases misincorporation of 2'-deoxyuridine-5'-triphosphate (dUTP). TS maintains the 2'-deoxyadenosine-5'-triphosphate/thymidine triphosphate ratio inside the cell, thus indirectly controls the incorporation of the component bases into DNA.[83] Due to its critical biological importance, TS has always been regarded as an valid target in anticancer chemotherapy. Several antimetabolites have been developed as TS inhibitors targeting both dUMP as well as folate cofactor (antifolates) binding site.

1.4.1. Structure of TS

The TS enzyme is a homodimmer with a molecular weight of 74,000 daltons and a primary sequence of approximately 316 amino acids long.[84-86] The dimmer interface consists of an extensive β-sheet. The primary structures of TS enzymes including those from humans, bacteriophages, and plants have been determined. TS enzymes from different species are highly conserved both in terms of structure and mechanism: 27 amino acids are completely conserved in TS from all species, and 165 (80%) are conserved in more than 60% of the organisms. Most notably, of 32 amino acid residues in the dUMP active site, 16 are conserved.[86]

The crystal structures of TS from various sources are available in the free enzyme form as well as in complex with cofactors and inhibitors.[87-92] The X-ray crystal structures of TS from several prokaryotic species, including *Escherichia coli* (*E. coli*),[93] and eukaryotes, such as *Lactobacillus casei* (*L. casei*),[94,95] *Leishmania major* (*L. major*),[96] *P. carinii*,[97] and T4 phage,[98] are known in the literature. The crystal structures of PMX and RTX with human TS are also known.[99,100] The existing crystal structures of TS in the native form or with ligands are important for the understanding of both TS mechanism and the inhibition of TS.[101-106] More importantly they allow a structure-based rational design of TS inhibitors.

Through site-directed mutagenesis, the function of each residue in the TS substrate binding site has been studied. Cys 198, Asn 229, Arg 178' and Arg 179', Glu 60 and Val 316 (lcTS numbering) were determined to be the most important residues in dUMP binding site. During the enzymatic reaction, the nucleophilic attacks of Cys 198 to the uracil ring resulted in the formation of a covalent bond between the enzyme and the substrate, thus no mutation is tolerated at Cys 198. Asn 229 (lcTS numbering) is another important residue in maintaining TS activity. Asn229 is an essential amino acid residue in the substrate binding site and is a part of a hydrogen bond network. Substitution of Asn229 by other amino acids causes a reduced or complete loss of catalytic activity,[107-109] but the resulting mutants can still catalyze the methylation reaction of 3-methyl dUMP. This amino acid also plays a very important role in enzyme specificity,[110,111] when replaced by Asp, the enzyme is no longer a deoxyuridylate methylase, but a cytidylate methylase, whose substrate is dCMP instead of dUMP. Two other amino acid residues, Arg 178' and Arg 179' (lcTS numbering), belong to the opposite subunit and interact

with the phosphate group of the deoxyribose ring. When these two amino acids are replaced, the catalytic activity decreased.[112] The importance of other amino acids in the active site has been studied also.[113,114]

Various spectroscopic methods including fluorescence,[115] UV-Vis,[116] circular dicroism,[117] and NMR[118] have detected the contribution of the C-terminal residue Val 316 (lcTS numbering) in the course of catalysis has been studied. Val 316 participates in the conformational change of the enzyme, which is necessary for the catalytic reaction, upon covalent binding of N^5, N^{10}-methylene-FH_4 to the binary complex TS-dUMP. When this conformational change takes place, the cofactor launches an electrophilic attack on the C5 of dUMP. X-ray crystallographic studies have revealed that in the TS-folate-FdUMP ternary complex the carboxy terminus residue shifts as far as about 4 Å from its original position in the unbound form towards the dUMP active site.[115-118]

1.4.2. Catalytic Mechanism of TS

The catalytic mechanism of human TS is summarized in Figure 9. Sequential binding of substrate (dUMP) and cofactor (N^5,N^{10}-CH_2-THF) with TS enzyme induces a conformational change to form a non-covalent ternary complex (TS-dUMP-cofactor).[9] In the initial step, the substrate dUMP is activated at the C5 position by a nucleophilic attack on the C6 of the uracil ring of dUMP by Cys195 of human TS. N^{10}-protonation changes the cofactor from an inactive tricyclic form to the active bicyclic form **2** in which the cofactor N^5,N^{10}-CH_2-FH_4 is in the iminium ion form at N^5. This results in the transformation of the non-covalent ternary complex into an unstable covalent ternary complex.

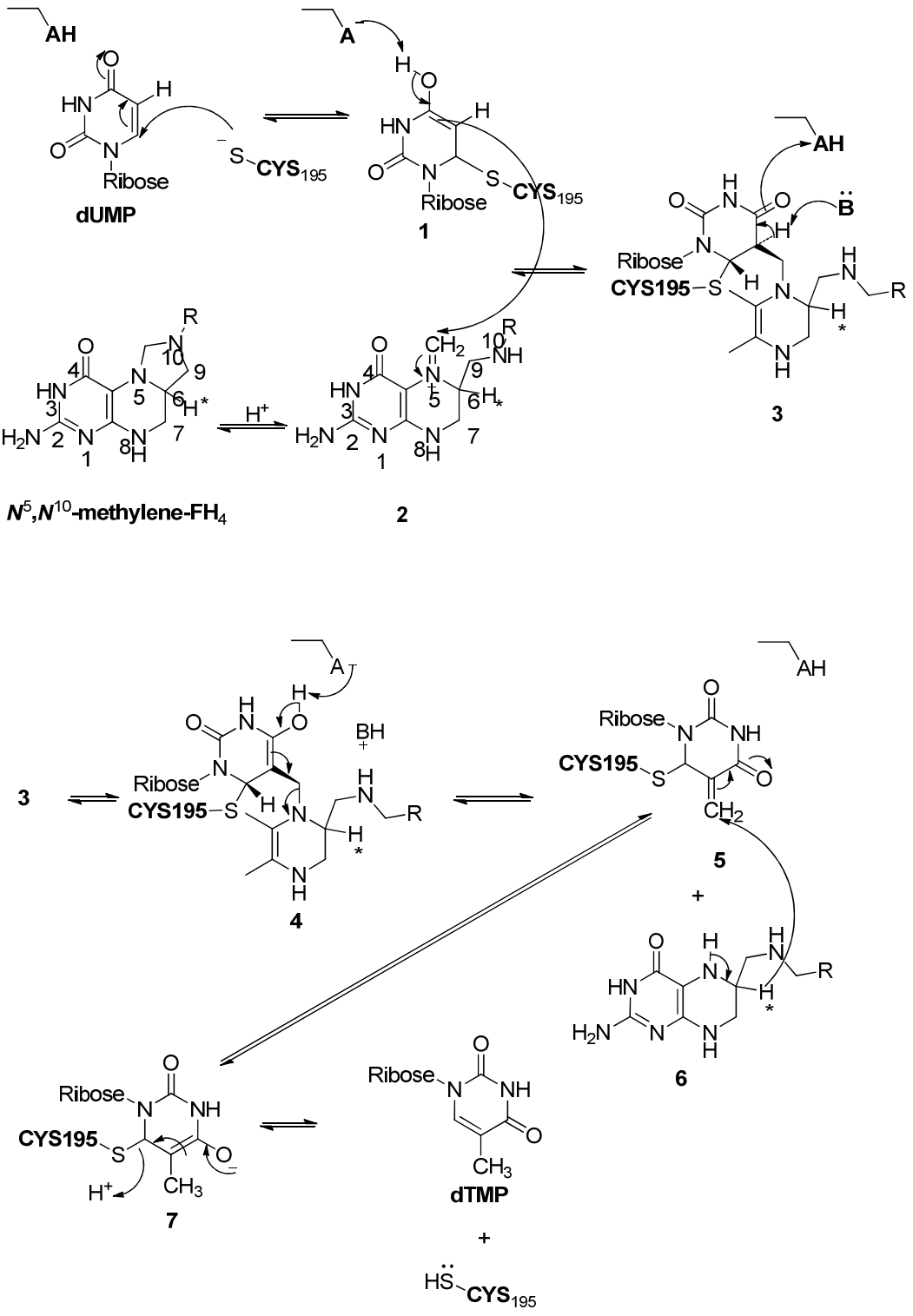

Figure 9. The catalytic mechanism of human TS.

The activated C5 of Michael-type adduct **1** is then trapped by the N^5-iminium ion of the reduced cofactor to form intermediate **3**. The proton at the C5-position of dUMP is abstracted by a base in the active site.The enzymatic reaction is completed by the reduction of the methylene of **5** *via* hydride transfer from C6 of the reduced cofactor **6**, which is simultaneously oxidized at the N^5–C6 bond to form FH_2. At the same time β-elimination of the sulfhydryl anion cys195 from C6 in **7** occurs to reform the double bond affording the product, dTMP, which is then released from the active site.

1.4.3. Typical TS inhibitors

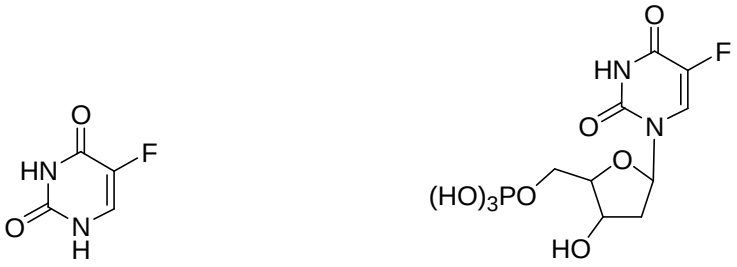

Figure 10. The structures of 5-FU and FdUMP.

In 1957 Heidelberger and coworkers synthesized 5-Fluorouracil (5-FU, Figure **10**), which belongs to the fluoropyrimidine class of antineoplastic agents.[119, 120] 5-FU is an antitumor agent with distinct antifolate and antipyrimidine properties. This agent represents the first class of clinically used TS inhibitors. It was proposed that a chemically modified uracil molecule might be effective in disrupting tumor DNA biosynthesis, thus 5-FU was rationally designed as a TS inhibitor. After it was introduced in the clinic, for 50 years, 5-FU still remains a useful agent with broad-spectrum activity

against many solid tumors, including colorectal, pancreas, breast, head and neck, gastric, and ovarian cancers.[121] The 5-FU prodrug Capecitabineis orally effective.

The mechanisms of action of 5-FU include inhibition of TS, incorporation into DNA, and/or incorporation into RNA.[122] The specific dose, administration route, and schedule all play important roles in determining the final mode(s) of action,[123-126] The native form of 5-FU is inactive, thus it must be converted to various nucleotide forms inside the cell. For example, 5-fluoro-2'-deoxyuridine-5'-monophosphate (FdUMP) is a critical nucleotide metabolite as it forms a covalent ternary complex with TS in the presence of N^5, N^{10}-methylene-FH_4, resulting in inhibition of the enzyme. Through a series of enzymatic steps, FdUMP is phosphorylated to 5-fluoro-2'-deoxyuridine-5'-triphosphate (FdUTP). The incorporation of FdUTP into DNA leads to the inhibition of DNA synthesis and function. The inhibition of TS results in an accumulation of dUMP , which can be subsequently converted to dUTP and misincorporated into DNA and result in the formation of single and double strand DNA breaks.

In both *in vitro* and *in vivo* studies, an inverse relationship between the level of TS enzyme activity in tumor cells and 5-FU sensitivity has been revealed.[126, 127] This relationship has also been confirmed in the clinic. In breast and colorectal cancer patients, a strong correlation has been observed between the expression level of TS and response to chemotherapy based on 5-FU. When treated with 5-FU-based chemotherapy, pretreatment levels of TS protein appear to be highly prognostic for patients with early-stage rectal cancer,[128] metastatic colorectal cancer,[129, 130] non-small-cell lung cancer,[131] breast cancer,[132] gastric cancer[133-135] and head and neck cancer.[136] Thus multiple pieces of evidence have confirmed that TS is the target of 5-FU.

The usage of LV in combination with 5-FU further supports the importance of TS inhibition in the mechanism of 5-FU. LV is intracellularly converted to the reduced folate 5, 10-methylenetetrahydrofolate, which then forms a ternary complex with FdUMP, the metabolite of 5-FU, and the target TS. Through this mechanism, the maximum enzyme inhibition state can be achieved. This effect of maintaining the enzyme in an inhibited state is critical as the TS-catalyzed reaction provides the essential nucleotide precursors for DNA biosynthesis. Subsequent work confirmed that when used in combination with LV, the cytotoxicity of 5-FU was significantly enhanced.[136]

Capecitabine a 5-FU prodrug is used clinically in the treatment of advanced breast or colorectal cancer. Novel combinations of 5-FU or its analogs with agents that have different mechanisms of actions (for example topoisomerase inhibitors, natural nucleosides, Platinum etc.) could also provide potential opportunities for improving the outlook of patients with various types of cancer.[142]

RTX is a more water-soluble analogue of PDDF and a less potent inhibitor of TS. Due to its improved water solubility, RTX does not cause renal toxicity. Similar to some classical antifolates, it is transported into cells via the RFC and undergoes rapid polyglutamylation by the enzyme FPGS. In its monoglutamate form, RTX is a mixed, noncompetitive inhibitor of human TS with a Ki of 90–100 nM. Polyglutamylation to higher glutamate forms improves its potency against TS by up to 100-fold. Compared to the monoglutamate form, the retention time of polyglutamylated RTX within cells is also significantly prolonged.[143]

RTX went through two phase I clinical trials, one in the UK[144] and the other by the National Cancer Institute in the United States.[145] In both studies, RTX was administered

as a 15-min infusion every 3 weeks. The dose-limiting toxicities in both trials included anorexia, fatigue, diarrhea, and myelosuppression. In the subsequent phase II trials, RTX displayed good activities in previously untreated patients with advanced colorectal and breast cancers with an overall response rates of 20–26%.[146, 147] Grade III/IV diarrhea, leukopenia, asthenia, and reversible elevation of serum transaminases were among the major toxicities. In 12% of the patients grade III/IV nausea and vomiting were observed and a maculopapular rash was noted in 14%. RTX was approved as first-line therapy for advanced colorectal cancer in several European countries, Australia, Canada, and Japan.

PMX is another TS inhibitor used in the clinic. While PMX inhibits TS, it also inhibits other folate-dependent enzymes including DHFR, ACARFTase, and GARFTase. Like RTX, it gain entry into cells through the function of RFC under normal pH and requires polyglutamylation for maximal inhibitory effects on the various target enzymes. It has shown activity *in vitro* against colon, renal, liver, and lung cancers.[155]

Based on the phase I clinical studies, the main toxicities associated with PMX include neutropenia, anorexia, thrombocytopenia, fatigue, gastrointestinal toxicity, and a reversible elevation of liver enzymes.[156]

In a phase II clinical studies, when PMX was used as single agent to treat previously untreated patients with non-small-cell lung cancer, it produced a 23% response rate. [157,158] A slightly higher partial response rate was observed in studies combining PMX with cisplatin (39%).[159] Another phase II study of PMX in advanced colorectal carcinoma showed a response rate of 15%.[160] PMX is approved in the USA for mesothelioma, breast cancer, colon cancer, pancreatic cancer and non-small cell lung cancer.

1.5. Glycinamide-ribonucleotide Transformylase (GARFTase)

Glycinamide-ribonucleotide transformylase (GARFTase) is a folate-dependent enzyme in the de novo purine biosynthetic pathway. It catalyzes the formyl transfer reaction that converts GAR to fGAR in the purine biosynthesis pathway, utilizing N10-formyl FH_4 as the cofactor. Cancer cells grow rapidly and require large amounts of purines, which are crucial components for the synthesis of DNA and RNA. Because cancer cells grow rapidly and require large amounts of purines to maintain such growth, the *de novo* purine biosynthetic pathway has attracted considerable attention as a target for cancer chemotherapy.[166] The inhibition of GARFTase in the *de novo* biosynthesis of purine thus has been considered an effective approach for cancer treatment.

1.5.1. The structure of GARFTase

Human GARFTase is located at C-terminus of a trifunctional enzyme human GART (*Hs*GART) encoded by purD-purM-purN with a molecular weight of 108 kD (1010 amino acids). [167] In addition to GARFTase activity, the trifunctional polypeptide also encodes GAR synthase (GARS, PurD, E.C. 6.3.4.13) and aminoimidazole ribonucleotide synthetase (AIRS, PurM, E.C. 6.3.3.1) activities.[167]

Because *E. coli* and human GARFTase share a 38% sequence identity, the *E. coli* GARFTase structure was considered an appropriate model for its eukaryotic counterpart. However, recent kinetic (17) and structural(18) studies revealed a number of important differences between the human and *E. coli* enzymes. [168,169] Monomeric *E. coli* GARFTase undergoes dimmerization below pH 6.8, while rh GARFTase remains be to a monomer at

a wide range of pH values. The active site loop-helix (residues 110-131) that undergoes pH-dependent order-disorder transition in *E. coli* GARFTase always adopts the same conformation under a wide range of pH conditions (pH 3.5-8) in the human enzyme. More importantly, the folate-binding loop, which intimately interacts with bound folate analogues, adopts different conformations in the unliganded human GARFTase from those described previously for *E. Coli* GARFTase.[168]

The human GARFTase domain of the trifunctional enzyme is readily available through cloning and overexpression.[168,170] The structures of human GARFTase in complex with various ligands including β-GAR[168], 10-trifluoroacetyl-5,10-dideaza-acyclic-5,6,7,8-tetrahydrofolic acid (10-CF3CO-DDACTHF)[171], and a series of folate inhibitors[172] at different pH have been reported.

Welin *et al.*[167]recently reported the structures of two functional domains of *Hs*GART: GARS and AIRS. Together with the previously reported the structures of the GARTfase domain of *Hs*GART [168,170], a completes structural characterization of the individual functional units of *Hs*GART was achieved, which allows for a structural understanding of substrate specificity and catalytic mechanism, as well as for a structure-based drug design. Although the construction of full-length *Hs*GART *via* crystalization of the enzyme in the intact form was not successful, Welin and coworkers [167]revealed the overall architecture of the trifunctional protein in the low-resolution *via* combining small angle X-ray scattering (SAXS) data with the high-resolution crystal structures.

1.5.2. Catalytic Mechanism of GARFTase

The catalytic mechanism of GARFTase has been reported by Shim and co-workers (Figure 11)[169]

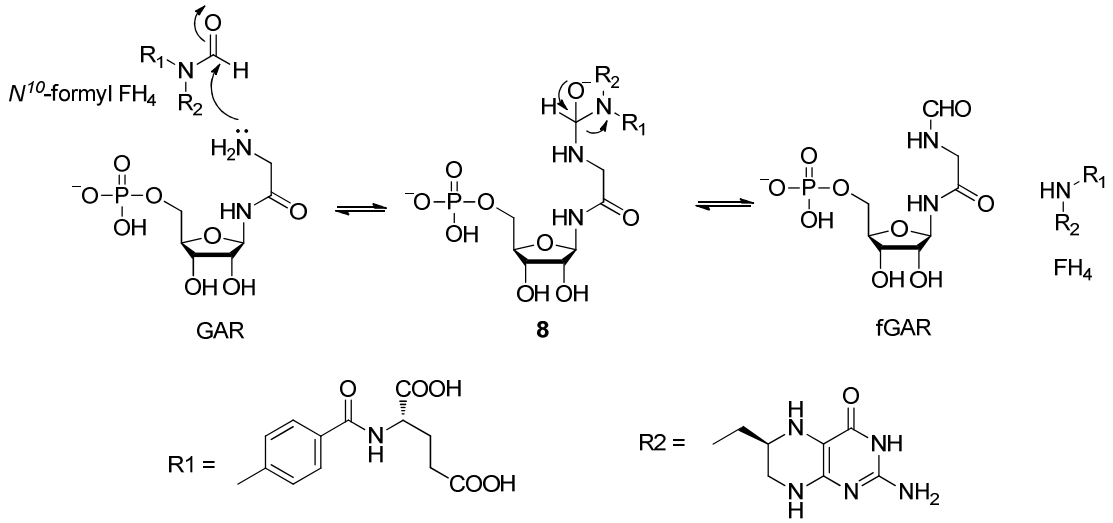

Figure 11. Proposed mechanism of GARFTase.

The formylation reactions catalyzed by the purN-encoded GARFTase are believed to proceed via a direct transfer mechanism. This would implicate the involvement of a negatively-charged tetrahedral intermediate. Nucleophilic attack by the amino group of GAR upon the formyl carbon of N^{10}-CHO-FH_4 leads to the formation of tetrahedral intermediate **8**,which is further converted to fGAR and FH_4 with the cleavage of the formyl carbon-N^{10} bond.

1.5.3. Typical GARFTase inhibitors

The discovery of the first potent and selective inhibitor, 5,10-dideazatetrahydrofolic acid (DDATHF) in 1980's validated GARFTase as an anti-cancer target.[173] This compound exhibits effective activity *in vivo* against solid murine and

human tumors, which rely on *de novo* purine synthesis. In contrast, the salvage pathway is the primary source of purines in most normal cells. LMX (Figure 6), the 6R diastereomer of DDATHF, has been in and out of clinical trials due to its toxicity.

1.6. Folates and antifolates transport systems

A high concentration of the folate pool is necessary for the normal activity of the cell. Since animal and humans lack the *de novo* biosynthesis of folates, cellular uptake of folates is essential for these species to maintain the concentration of the folate pool and to maintain normal tissue regeneration and cell growth. Because the α- and γ-carboxyl groups of the glutamate side chain are negatively charged at physiological pH, folates poorly penetrate biological membranes by diffusion alone. Transport of folates into the cell is usually accomplished by three carrier proteins present on the cell surface: RFC,[174,175] FR[176,177] and PCFT.[178] The biochemical and functional properties of these three transporters are compared in Table 1.

Goldman *et al*. [174] first reported the functional properties for murine leukemia cells in 1968. RFC, a member of the major facilitator superfamily of transporters, is characterized by its anion exchange property. As an integral transmembrane protein, RFC has a high affinity for reduced folates (Km ~1-5 μM) and a low affinity for FA (Ki ~ 200 μM) with a neutral pH optimum.

Ubiquitously expressed in normal tissues and tumor cells, RFC is the major transport system for folates in mammalian cells. More importantly, most antifolate drugs for cancer chemotherapy, including MTX, PMX, RTX and others, use RFC as the

primary transporter. A compromised RFC level or function is a common reason for antifolate resistance. For example, impaired RFC function is an important mechanism of tumor resistance to MTX and other antifolates *in vitro*.[174]

Table 1. Folate transporters in mammalian cells.

RFC	FR	PCFT
Integral protein	Anchored in plasma membranes by a glycosyl phosphatidylinositol (GPI) anchor.[174,176]	A member of the superfamily of facilitative carriers.[178,179]
Anion exchange mechanism	Endocytotic mechanism	H^+ symporter
The primary transporter of folates and antifolates.[174]		Transport wide range of folates and antifolates
High affinity for reduced folates (Km ~1-5 μM); Low affinity for FA (Ki ~ 200 μM)	High affinity for FA (1 nM) and reduced folates (5-10 nM)	
Ubiquitously expressed in normal tissues and tumor cells. [174]	Most normal cells do not express FRα; FRα are over expressed of on the surface of some tumor cells. [176]	Has wide but likely more restricted expression than hRFC. [178,179]
Optimum at physiological pH (~7.4)		Optimum at acidic pH (5.5~6.5). [179,180]

FRs are anchored in plasma membranes by a glycosyl phosphatidylinositol (GPI) anchor and mediate an endocytic mechanism. It shows high affinity for FA (1 nM) and reduced folates (5-10 nM). The FRs are high affinity folate binding proteins encoded by three distinct genes(α, β and γ).[180] FRα is overexpressed in some epithelial tumors, especially the kidney, placenta and choroid plexus, and has a restricted distribution in normal tissues, which provides an opportunity for the development of antifolates specifically targeted at FRα overexpressing tumours.[181-183] Antifolate toxicity mainly occurrrs in fast proliferating tissues such as bone marrow and gut. This could be because:(1) most antifolates are primarily transported into cells by the ubiquitously expressed RFC. (2) Proliferating tissues are highly dependent on the enzymes that the antifolates target. Thus antifolates that are specifically transported by FRα should show very low toxicity to normal tissues.

PCFT was recently identified as the third transporter for folates. As a proton-folate symporter that functions optimally at acidic pH (5.5~6.5), PCFT serves as the major transport system of folates at the acidic pH in the upper small intestine. [178,179] Although PCFT is widely expressed, the expression pattern is likely more restricted than hRFC. Since acidic microenvironment is characteristic of solid tumors, PCFT may play an important role in solid tumor cancer treatment. Recently it is reported that at pH 5.5, PCFT increased the inhibitory activity of PMX, which illustrats the unique property of PCFT as a transporter of antifolates.

1.7 Folyl poly-γ-glutamate synthetase (FPGS)

FPGS catalyzes the production of poly-γ-glutamates of folates and antifolates [11, 16, 184] and in some cases increases TS inhibitory activity for certain antifolates.[185-188] Classical antifolates, such as RTX and PMX, that have an *N*-benzoyl-L-glutamic acid side chain usually function as substrates for FPGS, the polyglutamates lead to high intracellular concentrations of these antitumor agents and increases TS inhibitory activity (RTX, 60-fold and PMX 130-fold) compared to their monoglutamate forms. Although polyglutamylation of certain antifolates (such as RTX and PMX) is necessary for their cytotoxic activity, it has also been implicated in toxicity to host cells, because of the longer cellular retention time of such polyanionic poly-glutamate metabolites. In addition, tumor cells develop resistance to antifolates (such as PMX) that depend on polyglutamylation for their antitumor effects by producing low concentration or defective FPGS, thus limiting the usefulness of such antifolates.[189-193]

Besides TS, polyglutamylation of antifolates can also increase the affinity of antifolates to other folate dependent enzymes including AICARFTase, GARFTase and methylenetetrahydrofolate reductase (MTHFR). Compared to its monoglutamate (K_i = 30 μM) form, the diglutamate of MTX (K_i = 6 μM) has a 5-fold increase in DHFR inhibition.[194] In addition to DHFR inhibition, the polyglutamate of MTX also inhibits TS, AICARFTase and MTHFR, which greatly increases the cytotoxicity of MTX. Similarly, the polyglutamates of PMX inhibits several folate requiring enzymes including TS, DHFR, GARFTase and AICARFTase to a greater extent than the monoglutamagtes.[195]

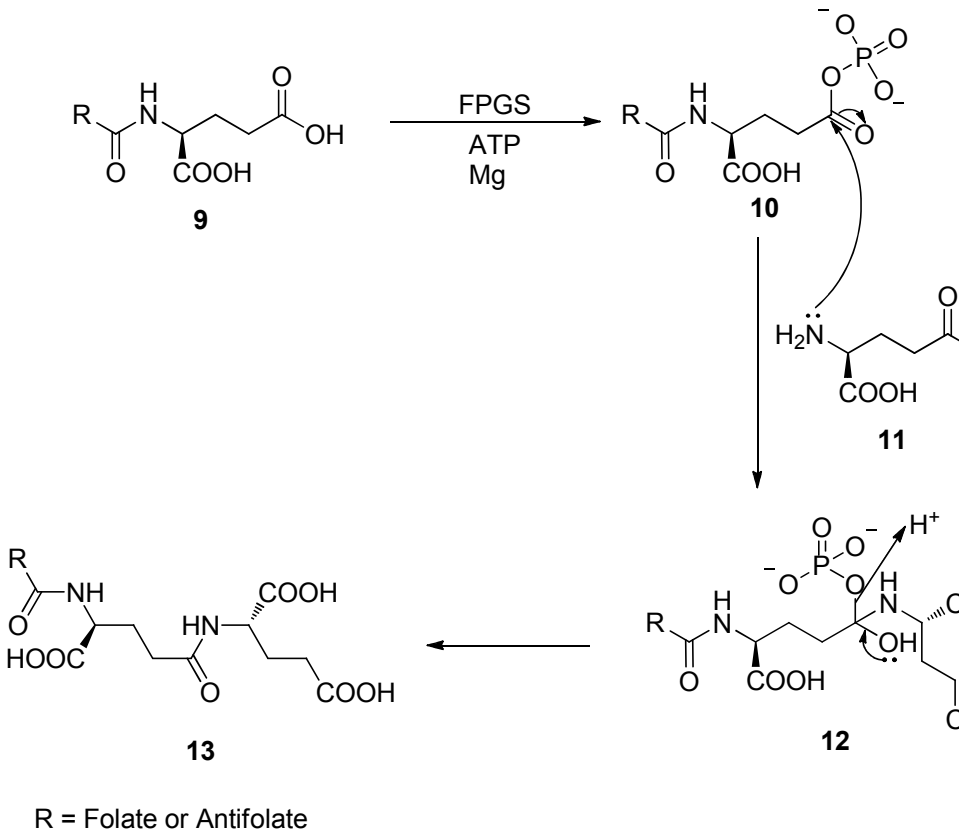

Figure 12. Mechanism of polyglutamylation by FPGS.

The mechanism of polyglutamylation by FPGS is shown in Figure 12. FPGS exists in both cytosolic and mitochondrial forms and is an ATP-dependent enzyme. The mechanism of polyglutamylation involves the binding of the folate or antifolate to the protein, subsequent activation by Mg-ATP, and then the attachment of L-glutamate to the γ-COOH. Folates attack the terminal phosphate of ATP catalyzed by FPGS to form an acyl-phosphate intermediate **10** and liberate ADP.[196-198] This activated mixed anhydride (**10**) is then attacked by the nucleophilic nitrogen of the co-substrate L-glutamate **11** to form a tetrahedral intermediate **12**, which then collapses to release polyglutamylated folates **13** and inorganic phosphate.

Due to the low-abundance and inherent instability, mammalian FPGS has not been isolated from natural source in sufficient quantities for crystallographic studies.[199] Although the dog liver enzyme has been cloned and purified[200] and recently a human cDNA encoding enzyme has been overexpressed in bacterial and insect cells.[201] In contrast highly purified enzyme from *L. casei* and *E. coli* are available, with the first x-ray crystal structure of the *L. casei* enzyme published in 1998.[202]The specificities of these bacterial enzymes for folate substrates are markedly different from the mammalian enzyme. Compared to *E. coli* FPGS, the catalytic efficiency of the human enzyme is higher for dihydrofolate, AMT, and MTX due to lower K_i values. [203]

2. Tubulin and microtubule.

Every nucleated cell in the human body has two types of spherical tubulin proteins, α and β tubulin. The spherical α and β tubulin assemble together to form heterodimmers, which undergoes energy dependent polymerization via complex polymerization dynamics. The tubulin heterodimmers line up in a head-to-tail arrangement to give the protofilaments, which group together to form a C-shaped protein sheet, and then curl around to give a pipe-like structure known as a microtubule with an external diameter of around 24 nm (Figure 13). At the time that tubulin adds to the microtubule ends, the hydrolysis of bounded GTP supplies energy for microtubule polymerization.[204]

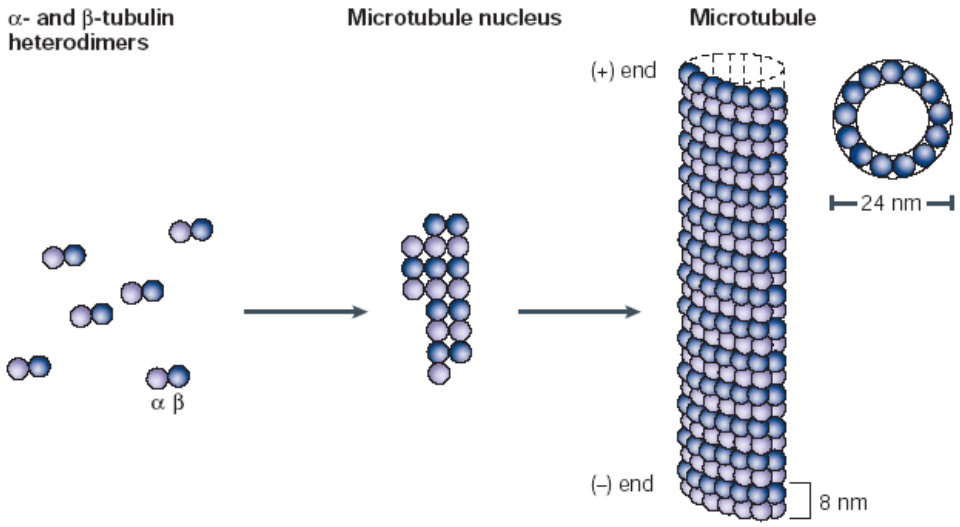

Figure 13. Polymerization of microtubles.[204]

The pipe-like microtubule has two ends, the “plus” (+) end and the “minus” (-) end. “Plus” (+) end is the end of microtubules with β tubulin exposed to solvent while the other end of microtubules is called “minus” (-) end.[205] After the microtubules are formed, the heterodimmers can be added or removed at either end of microtubules. Two kinds of non-equilibrium dynamics are known for microtubules: ‘dynamic instability’ and ‘treadmilling’.[206] Dynamic instability is the stochastic switching of microtubules between the growing and shrinking states. [207] Treadmilling is the process that tubulin subunits continuously flux from one end of the polymer to the other, due to net differences in the critical subunit concentrations at the opposite microtubule ends. This unidirectional flow of subunits is most readily detected at steady state under conditions where the polymers maintain a constant length.[208]

Dynamic instability and treadmilling are compatible behaviors, thus a specific population of microtubules can show primarily treadmilling behavior, dynamic-instability

behavior or both. By changing the parameters of these two dynamics, cells rearrange the microtubule network and quickly respond to environmental and developmental stimuli.[207]

2.1. Microtubule and mitosis.

The cell cycle process in which cells divide and distribute their chromosomes into two daughter cells is referred to mitosis. To ensure that the separation occurs in an ordered fashion, the chromosomes become aligned before partitioning can occur. Such alignment of replicated chromosomes and their separation into two daughter cells are called mitosis, which can be observed in virtually all eukaryotic cells.[209] Both the alignment and separation processes are the consequence of interactions between chromosomes and filamentous microtubules.

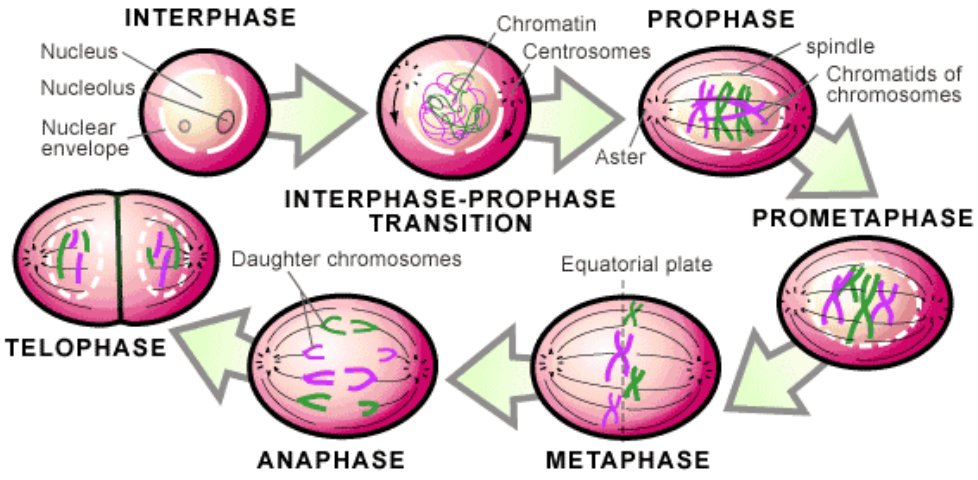

Figure 14. Stages of mitosis.[210]

The stages of mitosis are shown in Figure 14. The first phase of mitosis is called prophase, when the nucleolus fades and chromatin (replicated DNA and associated proteins) condenses into chromosomes. Each replicated chromosome comprises two chromatids, both with the same genetic information. Microtubules of the cytoskeleton, responsible for cell shape, motility and attachment to other cells during interphase, disassemble. And the building blocks of these microtubules are used to grow into a biconical array known as a spindle from the region of the centrioles.

Prometaphase is the second stage in mitosis, when the nuclear envelope breaks down. At this stage, some mitotic spindle fibers elongate from the centrioles and attach to kinetochores, with other spindle fibers elongate and overlap each other at the cell center. At the prometaphase, the nucleus is no longer recognizable.

During the next stage, metaphase, all chromosomes are aligned in one plane at the center of the cell by the tension of spindle fibers. Once all chromosomes are arranged at the exact position, the cell abruptly enters anaphase. At anaphase, microtubules shorten, the kinetochores separate, and the daughter chromosomes are pulled apart and begin moving to the cell poles.

Telophase is the final stage of mitosis, when the microtubules pulled the daughter chromosomes to arrive at the opposite poles of the cell and disappeared. The formation of new nuclear envelops around the daughter chromosomes is the mark of the end of mitosis.

In the process of mitosis the duplicated chromosomes of cells are divided into two identical sets and then divided into two daughter cells. Microtubules and their

polymerization dynamics play a pivotal role in this process of cell replication.[211] Thus the disruption in microtubules formation or their dynamics can interrupt the process of mitosis. This is even more important in tumor cells, because most tumor cells are fast growing and dividing cells. When mitosis in tumor cells are inhibited, the chromosomes can not separate, the cell can not reproduce and hence the tumor can not grow. The crucial involvement of microtubules in mitosis makes them a target for antitumor agents.

2.2. Mechanism of antimitotic drugs.

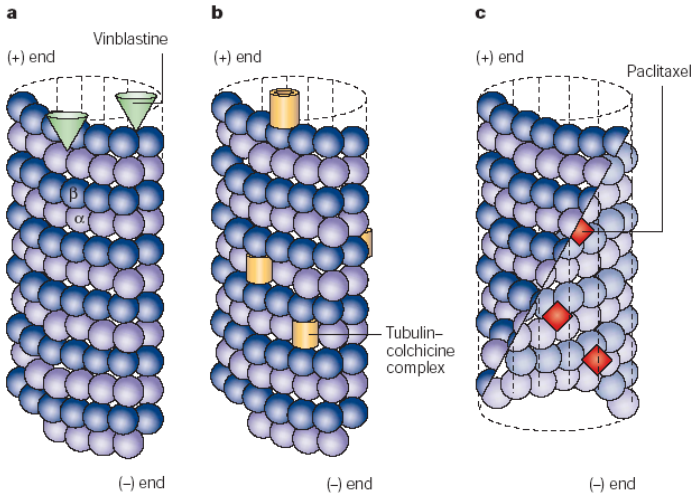

Figure 15. The binding sites of three major types of antimiotic drugs.[204]

Antimitotic drugs that target microtubules and mitosis cause either microtubule-stabilizing or microtubule-destabilizing effect. Most antimitotic drugs are classified into three major classes upon their binding sites on microtubules. The classification of a particular drug is dependent upon where it binds to microtubules. The common binding sites for antimitotic agents include the vinca alkaloid binding site, the colchicines binding site and the paclitaxel binding site (Figure 15).

2.2.1. The vinca alkaloid binding site.

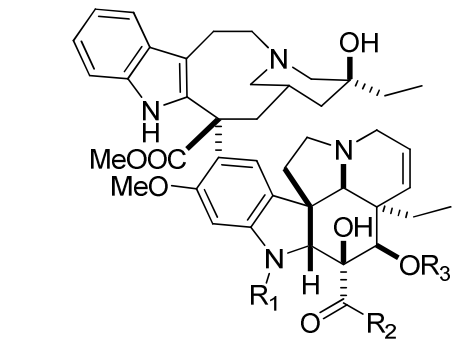

	R_1	R_2	R_3
vinblastine	Me	OMe	COMe
vincristine	CHO	OMe	COMe
vindesine	Me	NH2	H

Figure 16. Structures of representative vinca alkaloids.

Vinca alkaloids are a group of antimitotic agents with microtubules depolymerization effects. This group of drugs are used in the clinic or are under clinical investigation for cancer treatment. Vinblastine, vincristine, and vindesine are representative vinca alkaloids, the structures of which are shown in Figure 16. Other vinca alkaloids also include vinorelbine and vinflunine. Among them vinblastine (Velban), vincristine (Oncovin) and vinorelbine (Navelbine) are in clinical use while vinflunine is in phase III clinical trial. The binding of this class of compounds to soluble tubulin is rapid and reversible. Vinca alkaloids also bind with polymerous microtubules and rapidly and reversibly incorporate into the tubulin heterodimmers of microtubule. The β-subunit, where vinca alkaloids bind to microtubule is called Vinca-binding domain.[212] Vinca alkaloids also directly bind to the α-subunit of microtubules with high affinity in vitro, although such binding is not sufficient to suppress the growth of microtubules. The binding of vinca alkaloids with microtubules induce a conformational

change in tubulin, which lead to microtubule depolymerization and the subsequent destruction of mitotic spindles.

2.2.2 The colchicines binding site.

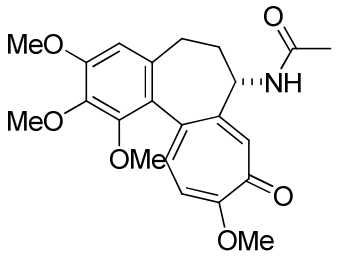

Colchicine

Figure 17. Structure of colchicine.

Colchicine (Figure 17) is a highly water-soluble tubulin-binding alkaloid,[213] which was found in the autumn crocus, a flower which resembles the true crocuses. Colchicine blocks or suppresses cell division by inhibiting the development of spindles as the nuclei are dividing. Thus it inhibits the division of the nucleus and mitosis. Colchicine binds to the soluble tubulin in solution, slowly changes the conformation of tubulin and then incorporates into the structure of microtubules (Figure 15, b). The involvment of tubulin-colchicine complexes in the formation of microtubules might induce a conformational change of microtubules, which slow the addition of new tubulin and suppresses the dynamics of microtubules. Due to its high toxicity and narrow therapeutic index colchicine has not been approved for the treatment of cancer. Instead, it is used in the treatment of gout.

2.2.3. The paclitaxel binding site.

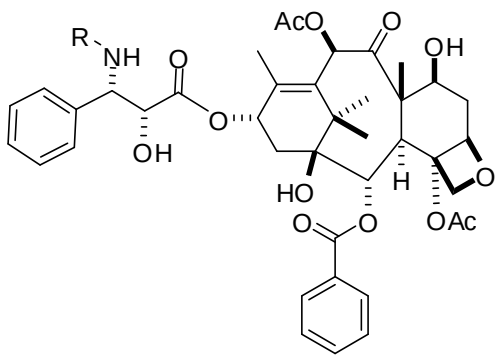

paclitaxel R=PhCO
docetaxel R=^{t}BuOCO

Figure 18. Structures of paclitaxel and docetaxel.

Paclitaxel, also known as taxol, was initially isolated from the bark of the pacific yew in 1967. Paclitaxel is widely used in the clinic for the treatment of different types of tumors including ovarian, breast and non-small cell lung cancer. Paclitaxel binds to the inside of the microtubule surface and stabilizes the structure of the microtubules by inhibiting the depolymerization to tubulin. The binding of paclitaxel leads to the stabilization of microtubules and an increase in net microtubule polymerization. Thus, the ability of the cells to break down the mitotic spindle during mitosis is inhibited by paclitaxel. With the spindle still in place, the cells can not divide into daughter cells. In contrast to drugs like colchicine and the Vinca alkaloids, which block mitosis by destabilizing the microtubules, paclitaxel is a microtubule stabilizing agent and has a different mechanism of action. Docetaxel, a semi-synthetic analogue of paclitaxel, is a clinically well established anti-neoplastic agent for the treatment of breast, ovarian and

non-small cell lung cancer. Similar to paclitaxel, docetaxel also serves as a microtubule stabilizing agent and prevents the mitotic spindle from being broken down.

2.2.4. Other binding sites.

Because most antimitotic agents bind to microtubules at the sites mentioned above, they are commonly categorized depending on whether they prevent the binding of vinca alkaloids, colchicine or paclitaxel to microtubules. However, some of the antimitotic agents do not have any effects on preventing the binding of these three classes of drug. Instead they have affinity for a separate, distinct region of tubulin. Although the binding site and mode of action of these drugs are not clear yet, they may bind covalently to certain reactive groups on the protein, particularly the tubulin sulfhydryl groups. [212]

2.3. Drug resistance to antimitotic agents.

Drug resistance is one of the major problems associated with antimitotic agents. The resistance to antimitotic agents can arise due to several different reasons. [213] Multidrug or multiple drug resistance (MDR) is a major drawback of cancer chemotherapy to a variety of drugs including the clinically used anti-microtubule agents. Ultimate failure of chemotherapy with antimitotic drugs often results due to MDR. MDR arises from intrinsic or acquired mechanisms of resistance. A major mechanism of MDR occurs via the overexpression of Pgp, which are an energy dependent (ATP), unidirectional transmembrane efflux pump. [214-216] Overexpression of Pgp has been reported in a number of tumor types, particularly after patients have received chemotherapy. [217-219] In addition, the expression of Pgp has been reported to be a

prognostic indicator in certain cancers and is associated with poor response to chemotherapy. [2220, 221] The over expression of a series of homologous proteins termed multidrug-resistance-proteins (MRPs) have also been reported to be a mechanism of MDR.[222, 223] The first MRP termed MRP1 was identified in a drug resistant lung cancer cell line that does not express Pgp.[224] All these transporters bind drugs within the cell and release them to the extracellular space in an ATP dependent fashion. Tumor cells preexposed to cytotoxic compounds often overexpress these efflux pumps to manifest resistance in the presence of cytotoxic agents.

The mutation in the genes that encode the α- and β-tubulin subunits is another common mechanism for antimitotic agent drug resistance. The mutation in the genes leads to structure changes in tubulin so that antimitotic agents can not recognize the binding site on the microtubule and hence the tumors develop drug resistance. [225, 226]

The altered expression pattern of tubulin isotypes is also responsible for the resistance to antimitotic agents. There are multiple isotypes of α- and β-tubulins expressed in varying ratios in different mammalian tissues.[227] Vertebrates have at least six of α- or β-tubulin isoforms, with a distinct pattern of expression. Although the functional significance of multiple β-tubulins has not been fully defined, there is evidence that the individual isotypes contribute to differences in microtubule dynamics and drug binding.[228] Under an altered tubulin isotype expression pattern, the binding efficiencies of anti-microtubule drugs might be ameliorated.

βIII tubulin expression is associated with resistance to taxane-based chemotherapy and is an independent prognostic factor for predicting poor progression-

free survival after docetaxel treatment alone.[229] According to a recent review, the correlation between βIII tubulin expression and response to anti-microtubule agents in advanced cases of non-small cell lung cancer (NSCLC) was noticed[230]. The corelation between a higher βIII tubulin expression level and a poorer outcome in patients with advanced NSCLC treated with paclitaxel-based or vinorelbine-based regimens were also reported . [229]

3. Antiangiogenesis

The biological process of new blood vessels formation from pre-existing vasculature is termed as angiogenesis.[231, 232] Angiogenesis occurs in normal adults only during wound healing, pregnancy and corpus luteum formation. Through the production of several proangiogenic and antiangiogenic factors, the complex cascade of physiological angiogenesis is tightly controlled and regulated. Unregulated angiogenesis is associated with several disease states and results in a number of pathological processes, including cancer, diabetic retinopathies, endometriosis, psoriasis, atherosclerosis, and rheumatoid arthritis.[233]

The cascade of angiogenesis is a complex process involving multiple steps. In the initial step, the stressed cells (injured cells or tumor cells) release proangiogenic factors, which then diffuse into nearby tissues. Upon the binding of proangiogenic factors with receptors on the endothelial cells of pre-existing blood vessel, the activation of these receptors as well as the secretion and activation of various proteolytic enzymes are initiated. These proteases then catalyze the degradation of basement membrane and the extracellular matrix in the parent vessels. The activated endothelial cells migrate through

the surrounding matrix and form a capillary sprout. These endothelial cells also proliferate when they migrate and eventually form new, lumen-containing vessels. Finally, the endothelial cells deposit a new basement membrane and secrete growth factors, that attract supporting cells to stabilize the new vessels. The vital importance of angiogenesis in tumor biology (such as the growth, invasion and metastasis) was first described in 1971 by Folkman.[231] To grow beyond 1-2 mm,[3] tumors require the formation of new blood vessels to supply nutrients.[233] In addition, metastasis requires angiogenesis to allow entrance into the circulation and to form tumors at sites distal to the primary tumor. Thus angiogenesis and metastasis contribute to the poor prognosis seen in patients with highly angiogenic tumors.[234] The inhibition of tumor angiogenesis has been considered an attractive target for the treatment of cancer. Since rarely does angiogenesis occur in normal adult, antiangiogenic cancer therapy is expected to provide selective treatment and have minimal side effects, compared with conventional chemotherapeutic agents. In addition, endothelial cells, the direct targets of antiangiogenic agents, are non-tumor cells and are expected to have less ability to mutate in order to produce resistance compared with tumor cells. Thus, antiangiogenic agents have afforded a new paradigm for the treatment of cancer.[235,236]

Intensive research efforts have been carried out to develop modulators to inhibit tumor angiogenesis and to regulate angiogenic disorders, in the last decade.[237, 238] Angiogenic signals are transmitted to the endothelial cells from the extracellular domain to the nucleus. This signal transduction is mediated by the membrane receptors including receptor tyrosine kinases (RTKs).[239,240] RTKs are primary mediators of angiogenic

signaling network, and thus inhibitors of RTKs are the predominant antiangiogenic agents.

3.1. Receptor Tyrosine Kinases (RTKs)

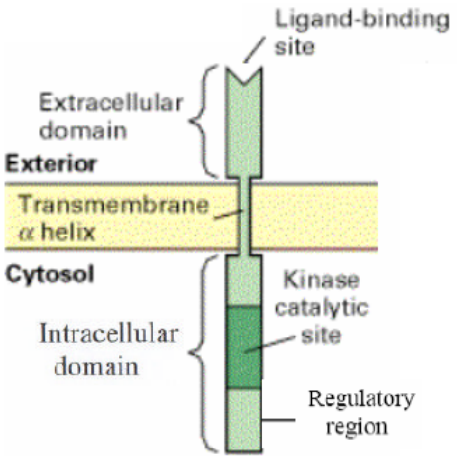

Figure 19. General structure of RTKs.

RTKs are membrane-spanning high-affinity cell surface receptors. RTKs not only function as key regulators of normal cellular processes but also play a critical role in the development and progression of many types of cancer. To date approximately twenty RTK families have been identified to include 58 different RTKs, which include platelet-derived growth factor receptor (PDGFR), fibroblast growth factor receptor (FGFR), vascular endothelial growth factor receptor (VEGFR), insulin receptor (InsR) and epidermal growth factor receptor (EGFR) among several others (Figure 20).[239, 241] The different RTK subfamily members have a similar molecular architecture including a ligandbinding domains in the extracellular region, a single transmembrane helix, and a cytoplasmic region (Figure 19).[240]

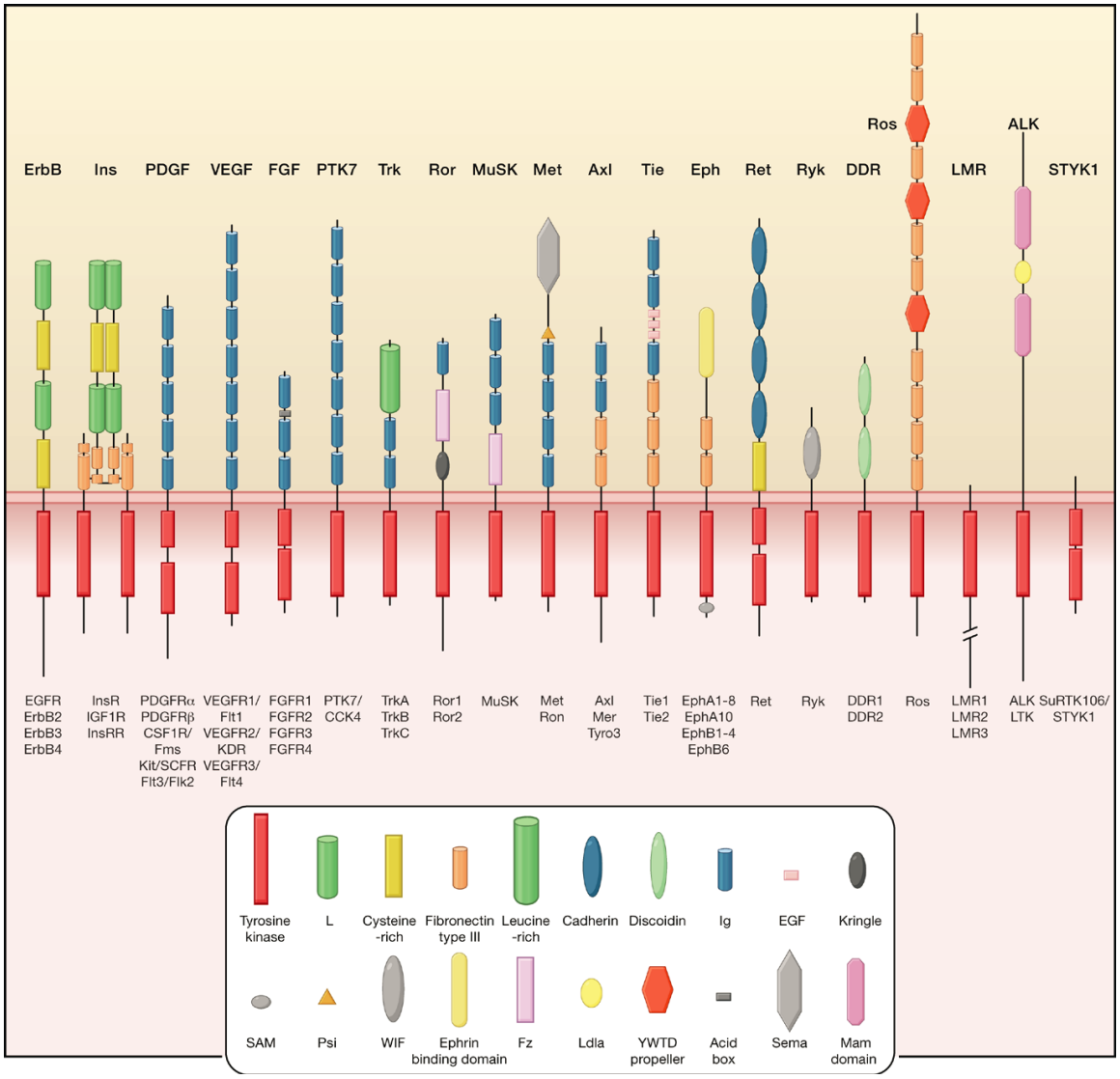

Figure 20. Receptor Tyrosine Kinase Families. [240]

Human receptor tyrosine kinases (RTKs) contain 20 subfamilies, shown in Figure 20 schematically with the family members listed beneath each receptor. Structural domains in the extracellular regions, identified by structure determination or sequence analysis, are marked according to the key.[240] The intracellular domains are shown as red rectangles. EGFR, epidermal growth factor receptor; InsR, insulin receptor; PDGFR, platelet-derived growth factor receptor; VEGFR; vascular endothelial growth factor

receptor; FGFR, fibroblast growth factor receptor; KLG/CCK, colon carcinoma kinase; NGFR, nerve growth factor receptor; HGFR, hepatocyte growth factor receptor, EphR, ephrin receptor; Axl, a Tyro3 PTK; TIE, tyrosine kinase receptor in endothelial cells; RYK, receptor related to tyrosine kinases; DDR, discoidin domain receptor; Ret, rearranged during transfection; ROS, RPTK expressed in some epithelial cell types; LTK, leukocyte tyrosine kinase; ROR, receptor orphan; MuSK, muscle-specific kinase; LMR, Lemur. Other abbreviations: AB, acidic box; CadhD, cadherin-like domain; CRD, cysteine-rich domain; DiscD, discoidin-like domain; EGFD, epidermal growth factor-like domain; FNIII, fibronectin type III-like domain; IgD, immunoglobulin-like domain; KrinD, kringle-like domain; LRD, leucine-rich domain.

Specific high-affinity binding site for the growth factor locates on the extracellular domain. As different sequence motifs have been identified within this domain, the extracellular ligand-binding site reveals the structural diversity of RTKs. The extracellular regions of RTKs may comprise cysteine-rich domains (CRD), EGF-like domains (EGFD), immunoglobulin-like domains (IgD), cadherin-like domains (CadhD), discoidin-like domains (DiscD), fibronectin-type III-like domain (FNIII), and kringle-like domains (KrinD) among others.

The transmembrane domain consists of about twenty-five hydrophobic amino acids residues embedded in the membrane lipid bilayer and plays an active role in signaling. They contribute to stabilize the full-length receptor dimers and to maintain a signaling-competent dimeric receptor conformation.[242]

The intracellular domain consists of a reasonably conserved tyrosine kinase domain and additional amino acid sequences that function as regulatory regions. The catalytic tyrosine kinase domain displays conservation between RTKs and is composed of about 250 amino acids. Sequence alignment has revealed that there are thirteen residues conserved in most RTKs. Crystal structure resolution of Insulin and FGF receptor fragments allowed homology models for the general structure of catalytic domains. The kinase domain is composed two lobes delimiting a central cleft. In the central cleft, the protein substrate and the complex ATP-Mg^{2+} ions are brought together and the phosphor-transfer reaction takes places. The N-terminal lobe contains glycine-rich motif and lysine residues which are critical for ATP binding. Protruding into the central cleft is the 'catalytic loop', in which an aspartic residue is the catalytic region and other residues allow recognition of tyrosine substrate. The C-terminal lobe contains a second loop, known as the 'kinase activation loop', frequently including one to three tyrosines endowed with regulatory functions.[243]

3. 2. Activation mechanism of RTKs

There is substantial evidence that activation of RTKs occurs through ligand-induced dimmerization (Figure 21). [244] Unbound receptor monomers are free to float in the lipid bilayer of the plasma membrane, where random reciprocal contacts occur in proportion to the number of receptor molecules present. Dimmerization can take place between two identical receptors, between different members of the same receptor family or even between a receptor and an accessory protein. In each family of RTKs, the binding of ligand, dimerization and activiation of RTK are specific.

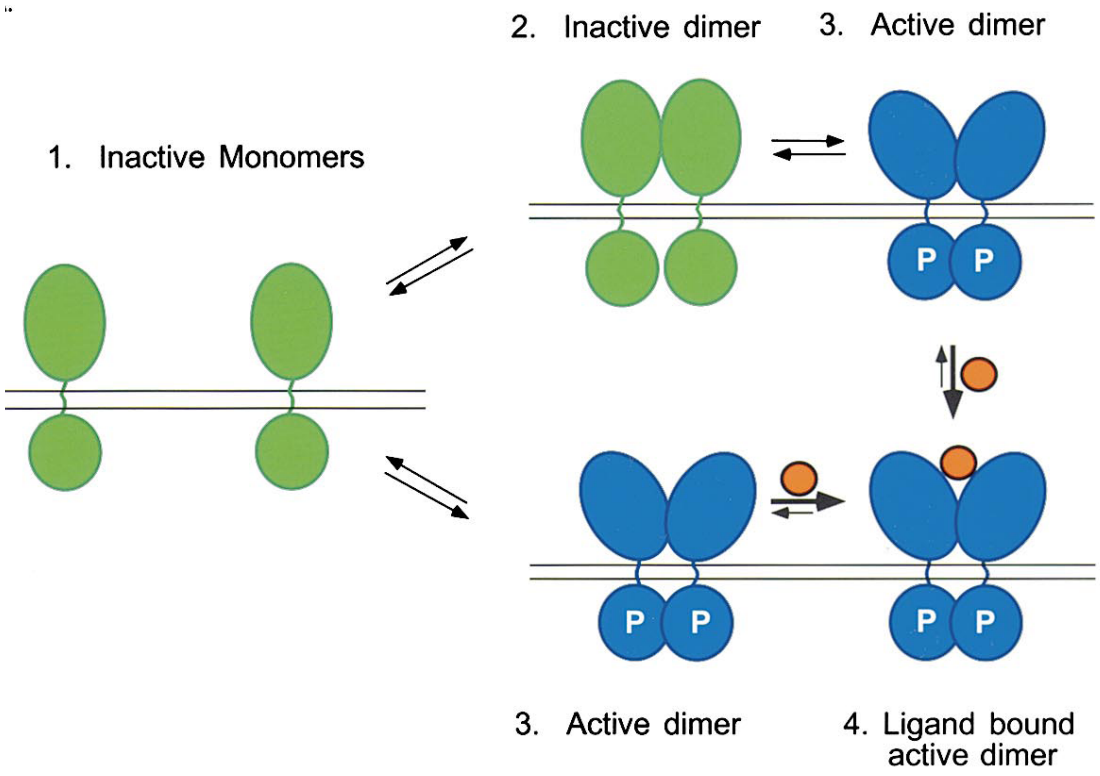

Figure 21. Mechanism activations of RTK.[244] Inactive receptor monomers (green) are in equilibrium with inactive (green) or active (blue) receptor dimers. The active receptor dimers exist in a conformation compatible with trans-autophosphorylation and stimulation of PTK activity (blue). Ligand binding stabilizes active dimer formation and hence PTK activation.[244]

For most receptors, ligand binding induces a conformational change that stabilizes the dimeric form. In the inactive state, this tyrosine prevents exogenous protein substrates from accessing the catalytic site, and the steric hindrance inhibits autophosphorylation of this residue. After ligand binding and the dimmerization of receptors, this tyrosine is trans-autophosphorylated and the equilibrium shifts towards a conformation that allows binding of exogenous substrates.

3.3. RTKs and human cancer

In normal cells, the activity of RTKs and their mediated cellular signaling is precisely coordinated and tightly controlled. Deregulation of this RTK signaling system, either by stimulation through autocrine–paracrine growth factor loops and/or genetic alteration, result in deregulated tyrosine kinase activity. Ullrich and coworkers made the first connection between a viral oncogene, a mutated RTK and human cancer in 1984.[245] Since then it is well known that aberrant signaling by RTKs is critically involved in human cancer and other hyper-proliferative diseases.[233] One of the common results of the RTKderegulation is that they result in RTKs with constitutive or strongly enhanced signaling capacity, which leads to malignant transformation. [247]Therefore, they are frequently linked to human cancer and also to other hyperproliferative diseases such as psoriasis. The tumor cells are known to use RTK transduction pathways to achieve tumor growth, angiogenesis and metastasis. The gene amplification and/or overexpression of RTKs occur in many human cancers, which might increase the response of cancer cells to normal growth factor levels. Additionally, overexpression of a specific RTK on the cell surface increases the incidence of receptor dimmerization even in the absence of an activating ligand. In many cases this results in constitutive activation of the RTK leading to aberrant and uncontrolled cell proliferation and tumor formation. The genetic alterations, including deletion or mutations, within the extracellular domain and the catalytic domain especially of the ATP-binding motif are another cause of uncontrolled cell proliferation and tumor formation. Autocrine-paracrine stimulation occurs when a RTK is aberrantly expressed or overexpressed in the presence of its ligand, or when overexpression of the ligand occurs in the presence of its associated receptor. For

example, it has been shown in many solid tumors that elevated levels of both growth factor receptor and its ligand are expressed concomitantly.[235,236,240]

3.4. Epidermal Growth Factor Receptor (EGFR)

EGFR is one of four closely related human epidermal growth factor receptor (HER or Erb) family RTKs and is a receptor tyrosine kinase that regulates fundamental processes of cell growth and differentiation.[248] The four EGFR family members share an overall structure of two cysteine-rich stretches in the extracellular region (Figure 22).Under normal physiological conditions, activation of the EGFR family is controlled by spatial and temporal expression of their ligands, members of the EGF-related peptide growth factor family.[240] These peptides are produced as transmembrane precursors, and are released as soluble growth factors after proteolytical cleavage. The mammalian EGFR ligands include epidermal growth factor (EGF), transforming growth factor α (TGF-α), hepairin-binding EGF-like growth factor (HB-EGF), amphiregulin (AR), beta-cellulin (BTC), epiregulin (EPR) and epigen. The neuregulins (NRG) binds to HER3 and HER4 (NRG1 and NRG2) or only HER4 (NRG3 and NRG4). The orphan HER2 (ErbB) has no ligands so far, and it is only activated following its heterodimmerization with another ligand-bound EGFR family receptor. Dimerization of ErbB receptors is mediated entirely by the receptor. [240]

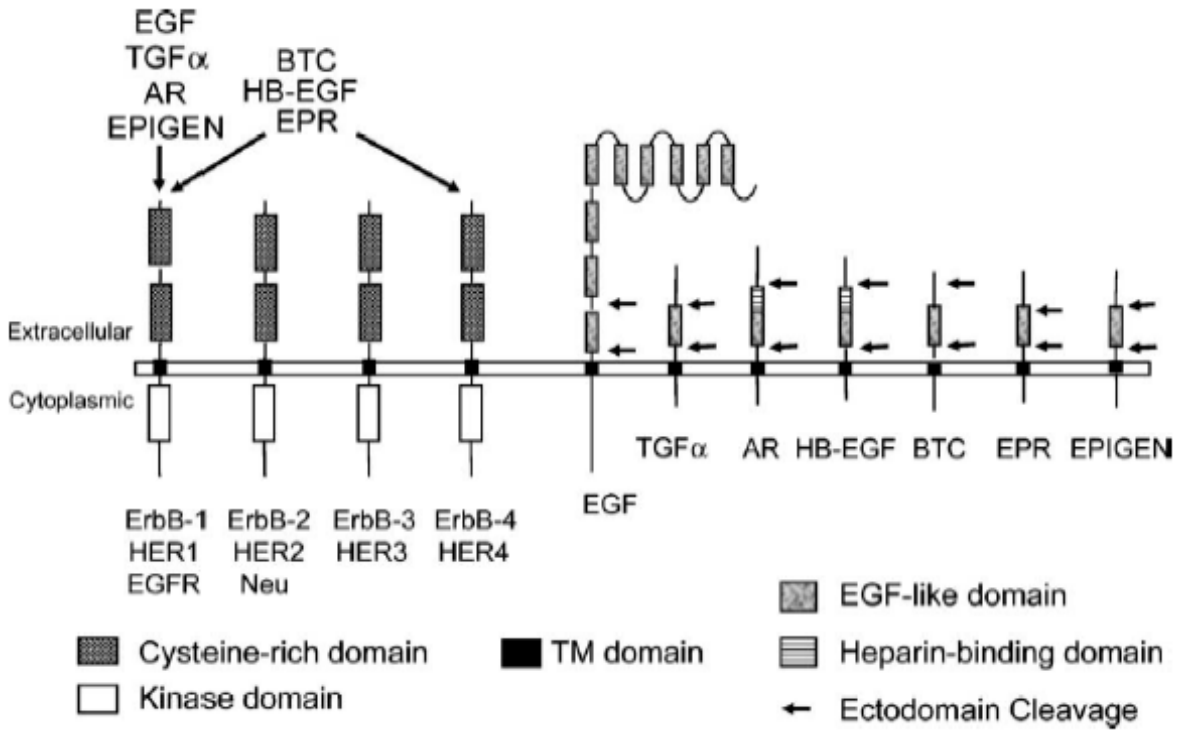

Figure 22. Mammalian family of epidermal growth factor receptors (EGFRs) and ligands.[249]

Over recent years, much evidence has been gathered to implicate the EGFR and its family members in the development and progression of numerous human tumors. [250, 251] Aberrant expression of EGFR in several types of cancer gene amplification has been implicated in the development, progression or aggressiveness of head and neck cancer, non-small cell lung cancer, breast cancer, colon cancer, glial tumors, prostate and epithelial cells cancer. Based on the clinical epidemiology and feasibility, the EGFR has been viewed as an ideal and viable target in drug discovery programs and represents one of the more advanced targets being explored clinically.[252,253] The role of EGFR in cell proliferation makes this an attractive target in other hyperproliferative disorders as well such as psoriasis.

3.5. Platelet-Derived Growth Factor Receptor (PDGFR)

Platelet-derived growth factor (PDGF) is a family of cationic dimeric protein which exists as various combinations, such as AA, BB and AB.[254]

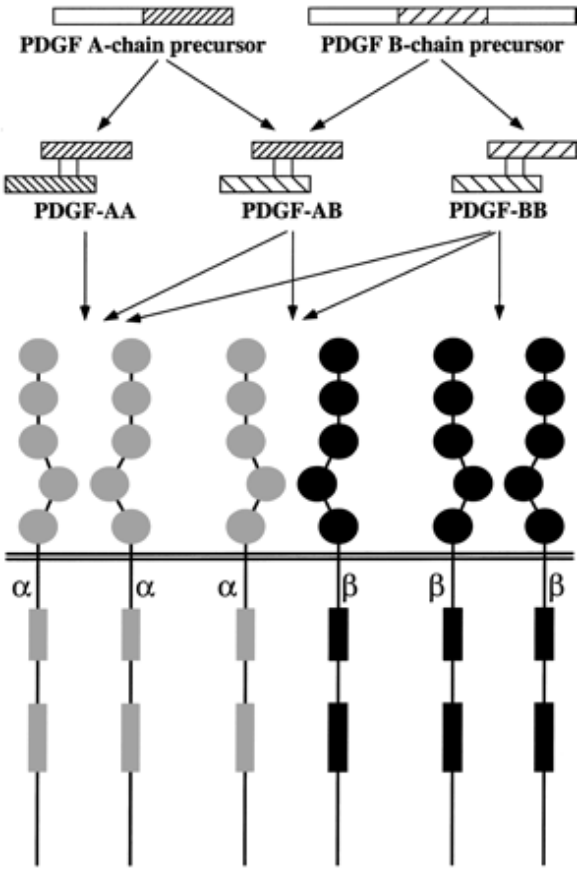

Figure 23. The structures of PDGFRs and their ligands A and B.[255]

PDGFRs have important functions during the embryogenesis, in particular for the development of kidneys, blood vessels, lungs, and CNS. The α-receptor plays important roles in the development of neural crest-derived cells and somites, and β receptor is crucial in the development of the mural cells of fibroblasts and blood vessels.

Overactivity of PDGFRs has been linked to several different disorders. In progression of glioblastoma and sarcomas, this action often causes autocrine stimulation of tumor cell growth. Overactivity of PDGFR signaling is a hallmark in a variety of diseases and has been implicated in atherosclerosis and several fibrotic conditions, including lung fibrosis, kidney fibrosis, liver cirrhosis, and myelofibrosis.[256, 257]

3.6. Vascular Endothelial Growth Factor Receptor (VEGFR)

The VEGF is a family of angiogenic proteins that now includes six secreted cysteine knot glycoproteins: VEGF-A, B, C, D, E and placental growth factor (PlGF).[258] It is well established that VEGF is a survival factor for endothelial cells in both developing tissues and tumor vessels. Because of its critical role in angiogenesis, VEGF is considered the master regulator of angiogenesis during growth and development, as well as in disease states such as cancer, diabetes, and macular degeneration.[258]

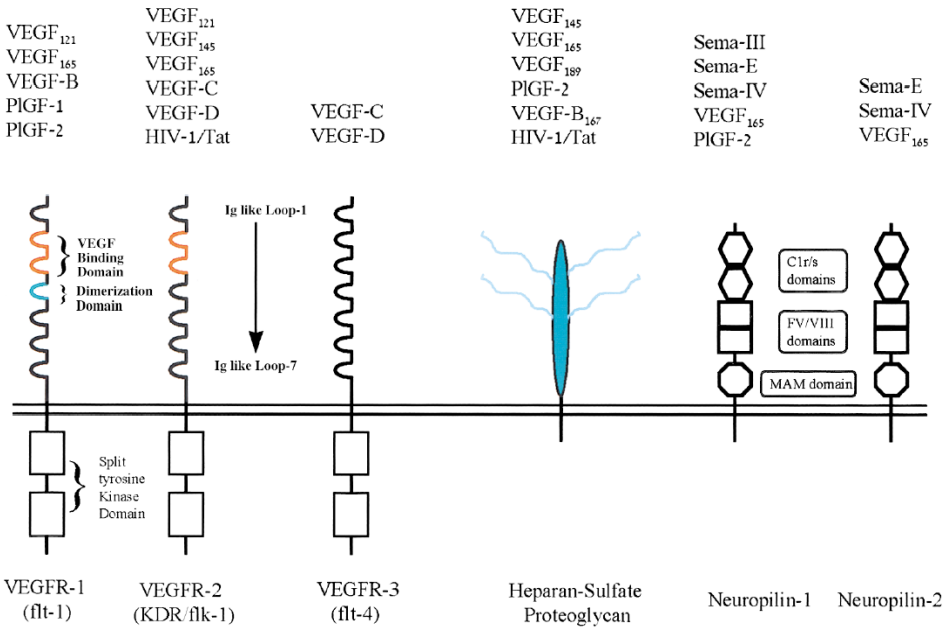

Figure 24. The Structure of VEGFRs and their factors.[259]

VEGF isoforms are the key factor involved in the regulation of many aspects of physiological and pathological angiogenesis by activating with their five endothelial growth factor receptors (VEGFRs) (Figure 24): VEGFR-1 (Flt-1, Fms-like tyrosine kinase), VEGFR-2 (KDR, kinase insert domain-containing receptor or Flk-1, fetal liver tyrosine kinase), VEGFR-3 (Flt-4), Neuropilin-1 and Neuropilin-2. The ligands that bind to VEGFR-1 are VEGF-A, VEGF-B, and also the related PIGF; whereas VEGFR-2 binds VEGF-A, VEGF-C, VEGF-D and VEGF-E. VEGFR-3 only binds VEGF-C and VEGF-D, and Neuropilin-1 and Neuropilin-2 bind VEGF-A, VEGF-E and PIGF.

Dimmerization of VEGFRs resulted in autophosphorylation on cytoplasmic tyrosine residues. Signal transduction through VEGFR affects several important functions and interactions between vascular, immune and neuronal cells. The function of VEGFRs in the angiogenesis process includes the production of proteases needed for the breakdown of blood vessel basement membranes, expression of certain integrins associated with angiogenesis, and stimulation of cell migration and proliferation. [260-262]

VEGFR-2 plays an abundant role in the most common forms of cancer. Overexpression of VEGFR-2 is frequently observed in the most common forms of cancer, whereas normal tissue displays only marginal expression of VEGFR-2. Moreover, the level of VEGFR-2 overexpression is often related to the stage of disease and the patient's prognosis.[263]

3.7. Fibroblast Growth Factor Receptor (FGFR)

The fibroblast growth factor receptors (FGFRs) are receptors that bind to members of the fibroblast growth factor (FGF) family of proteins. The family of FGFs comprises of at least 23 secreted glycoproteins including FGF-1 through FGF-23, and this number continues to increase.[264] The FGFRs include the four highly conserved transmembrane receptor tyrosine kinases FGFR1, FGFR2, FGFR3, and FGFR4 and one additional receptor, FGFR5 (FGFRL-1), which is able to bind FGFs but is devoid of kinase activity. [265] As for many other RTKs, dimmerization followed by conformational alterations of the FGFR appears to be an important requirement for activation of the tyrosine kinase activity.

FGF1 and in particular FGF2 are potent proangiogenic factors while FGF4 and −8 are less so.[236] FGFs are known to promote in vitro endothelial cell migration, proliferation, and differentiation. In a similar way to VEGF, FGFs appear to play a major role in vivo in the regulation of angiogenesis.[266]

Since RTKs have been implicated in a variety of cancer indications and other inappropriate mitogenic signaling disorders, RTKs and the activated signaling cascades represent promising targets for the development of therapeutic agents. Small molecule inhibition of a single RTK has been shown to be clinically effective as a novel approach to cancer chemotherapy.

Based on the mechanism of RTKs signal generation, several approaches of prevention of interception of cancer-relevant signaling have been pursued. These

approaches target either the extracellular ligand-binding domain, the intracellular tyrosine kinase or the substrate-binding region, such as monoclonal antibodies and antibody conjugates that are directed against the extracellular domain of RTKs. The development of adenosine triphosphate (ATP) competitive tyrosine kinase inhibitors (TKIs), which mimic ATP and compete for binding in the kinase active site, appears to be a promising approach for drug intervention. Thus several small-molecule TKIs have been developed to selectively interfere with the intrinsic tyrosine kinase activity and thereby block receptor autophosphorylation and activation of downstream signal transduction.

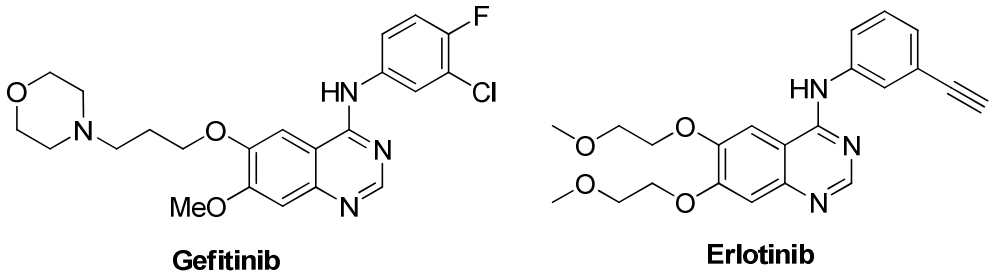

Figure 25. The structures of representative EGFR inhibitors.

Gefitnib and erlotinib are examples of small molecule of EGFR inhibitors. Both gefitnib and erlotinib are approved by the FDA for the treatment of non-small cell lung cancer. [267]

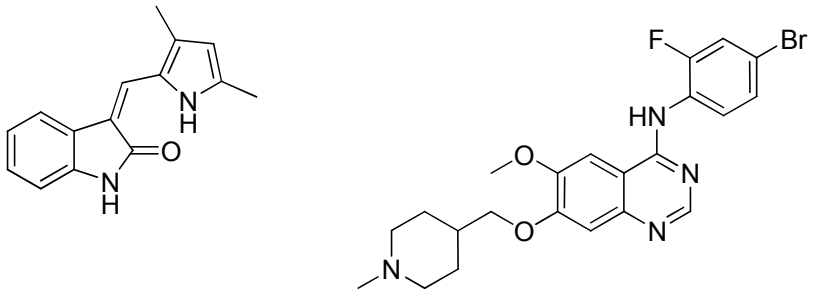

Figure 26. The structures of representative VEGFR-2 inhibitors.

Indolinones and quinazolines have been developed as potent VEGFR-2 inhibitors. Both semaxanib and vandetanib are important examples of VEGFR-2 inhibitors (Figure 25). Semaxanib (Figure 25) has undergone clinical trials as an antitumor agent, however, the study was discontinued due to ineffaciousness.[268, 269] Vandetanib was developed as a potential treatment for non-small cell lung cancer and showed promising result.

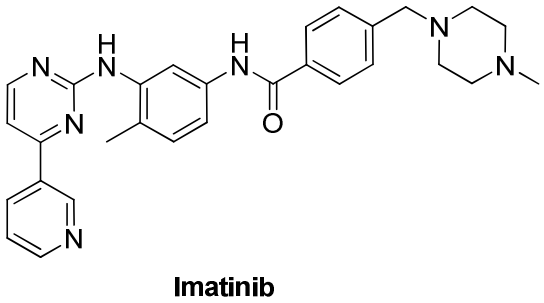

Figure 27. The Structure of PDGFRβ inhibitor: Imatinib.

Imatinib, a PDGFR inhibitor, has been approved by FDA for the treatment of chronic myelogenous leukemia (CML), gastrointestinal stromal tumors (GISTs) and a number of other malignancies .

In recent years, a number of RTK targeting small molecular inhibitors including Crizotinib[270], Sunitinib[271], Pazoparib[272], Sorafenib[273], Vemurafenib[274], Vandetanib[275],

Lapatinib[276] and Panzopinib[277] were approved by the FDA for the treatment of various typy of cancer.

1.2. ATP binding sites.

Despite two major obstacles, which include lack of access to the intracellular targets and the lack of selectivity of inhibition, the ATP-binding site of RTKs has been shown to be a viable target for rational drug design. Of the two obstacles, the selectivity issue has proven to be the more difficult one.[278] The commonality as well as diversity among the ATP-binding sites of kinases has allowed the development of pharmacophore models for rational drug design.[279] This along with reports of the x-ray crystal structures of protein kinases has validated that the ATP-binding site of RTKs is indeed an attractive target for small molecule drug design. A number of scaffolds including indoline, quinazolines and fused pyrimidines have been shown to be effective ATP competitive inhibitors of RTKs. [280,281]

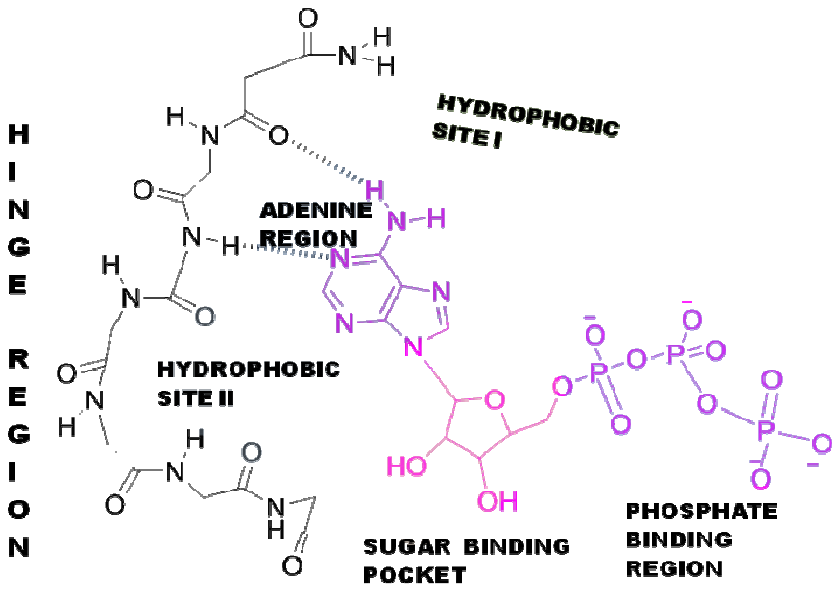

Figure 28: The general ATP-binding site of RTKs. The ATP-binding site of protein kinases. ATP is in pink. [282]

ATP binds to protein kinases within a deep cleft formed between the two lobes of the protein kinase. Apart from a bidentate donor-acceptor hydrogen bonding motif in the hinge region the interactions with the nucleotide are of a lipophilic/van der Waals nature (Figure 28).

Although the ATP-binding site is highly conserved among the kinases, several key diversities exist in the regions proximal to the ATP-binding site. For practical drug discovery purposes, the binding site of ATP can be divided into the following features:

1. Adenine region. This hydrophobic region contains the two key hydrogen bonds formed by the interaction of the N^1 and N^6 amino group of the adenine ring with the backbone NH and carbonyl group of the adenine anchoring hinge region of the RTKs. Although not used by ATP, some of the backbone carbonyl groups of residues in the hinge region can also serve as a hydrogen bond acceptor for inhibitor binding.

2. Hydrophobic region 1 pocket/selectivity pocket. This pocket is not used by ATP, but is exploited by several of the kinase inhibitors. It plays an important role in inhibitor design and selectivity. [281]

3. Hydrophobic region 2. This region is a slot that opens to solvent. As it is not used by ATP, it can also be exploited to gain binding affinity.

4. Sugar region. In most of the RTKs, this region is hydrophilic except in EGFR. This peculiarity has been exploited in the EGFR kinase project for the design of potent and selective inhibitors.

5. Phosphate binding region. This region appears to be the least important in terms of binding affinity, due to high solvent exposure. However, it is useful to improve

selectivity or to gain additional affinity in an inhibitor. The triphosphate group of ATP is constrained by a glycine-rich loop and is bound by the conserved array of basic amino acid residues, which, together with an invariant tyrosine (part of the tyrosine-phenylalanine-glycine triad) that deprotonates the phosphoacceptor OH group, are involved in the catalytic process.

II.CHEMICAL REVIEW

The chemistry related to the present work is reviewed and includes synthetic approaches to the following heterocyclic systems and relevent reactions.

A. Synthesis of furo[2,3-*d*]pyrimidines

B. Synthesis of pyrrolo[2,3-*d*]pyrimidines

C. Synthesis of thieno[2,3-*d*]pyrimidines

D. Sulfenilation reactions

E. Name reactions

A. Synthesis of Furo[2,3-*d*]pyrimidines

A few examples of the synthesis of furo[2,3-*d*]pyrimidines are known in the literature. A broad classification for the synthetic strategy for construction of this ring system is:

1. Route A: From furan precursors

2. Route B: From pyrimidine precursors

1. From furan precursors (Route A)

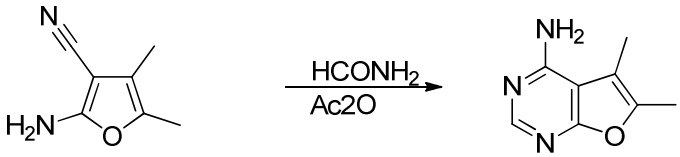

14 **15**

Scheme 1. Synthesis of 6-substituted furo[2,3-*d*]pyrimidines **15**.

In 1966, Gewald reported the synthesis of **15** (Scheme1) by the reaction of **14** with formamide in acetic anhydride.[283] This reaction represents the first synthesis of a furo[2,3-*d*]pyrimidine starting from a furan precursor.

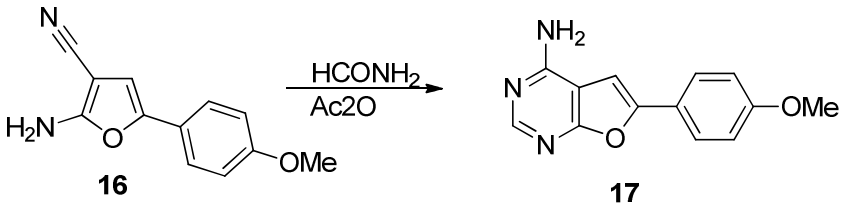

Scheme 2. Synthesis of 6-substituted furo[2,3-*d*]pyrimidines **17**.

The reaction between a 2-amino-3-nitrile-substituted furan and formamide has been utilized by several other groups to give furo[2,3-*d*]pyrimidines with a 2-hydrogen-4-amino-substitution. As shown in Scheme 2, Miyazaki and coworkers[284] reported the synthesis of **17** in 69% yield by using the above mentioned method.

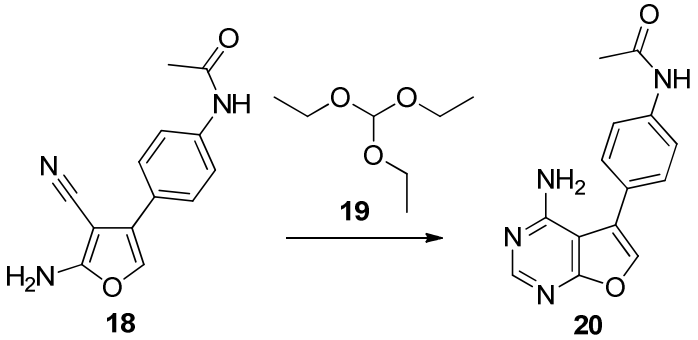

Scheme 3. Synthesis of 4-amino-5-substituted furo[2,3-*d*]pyrimidines **20**.

Furan precursors with 2-amino-3-nitrile-substitutions also react with triethylorthoformate to give 4-amino-substituted furo[2,3-*d*]pyrimidines. Miyazaki *et al*[285] also reported the synthesis of furo[2,3-*d*]pyrimidine **20** via condensation between **18** and **19** (Scheme 3).

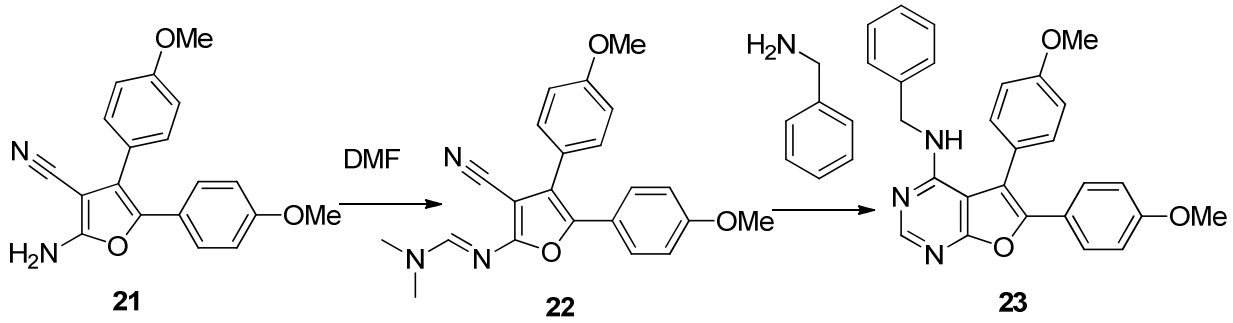

Scheme 4. Synthesis of furo[2,3-*d*]pyrimidine-4-amine derivative **23**.

Han and coworkers[286] reported a novel synthesis of furo[2,3-*d*]pyrimidin-4-amine derivative **23** (Scheme 4) by microwave irradiation. The reaction starts from readily available amines and substituted 2-aminofuran-3-carbonitrile which are converted into corresponding formamidines in DMF using benzenesulfonyl chloride and then cyclized with benzylamine to target compound.

The proposed reaction mechanism for the synthesis of furo[2,3-*d*]pyrimidine **23** is shown in Scheme 5. First, the nitrogen of amine attack the carbon of formamidine to give species **24**. Then an intramolecular reaction of **24** is folloewd by ring closure forms **25** followed elimination of dimethylamine, to yield product **26** (imino-product **26** is a kinetic product). Second, water as a nucleophile attacks the pyrimidine ring, and opens the ring to afford a ring-opened species **27**. Third, a subsequent electrocyclization to **28** and elimination of water yielded the thermodynamic stable product **23** (favored at high temperature).

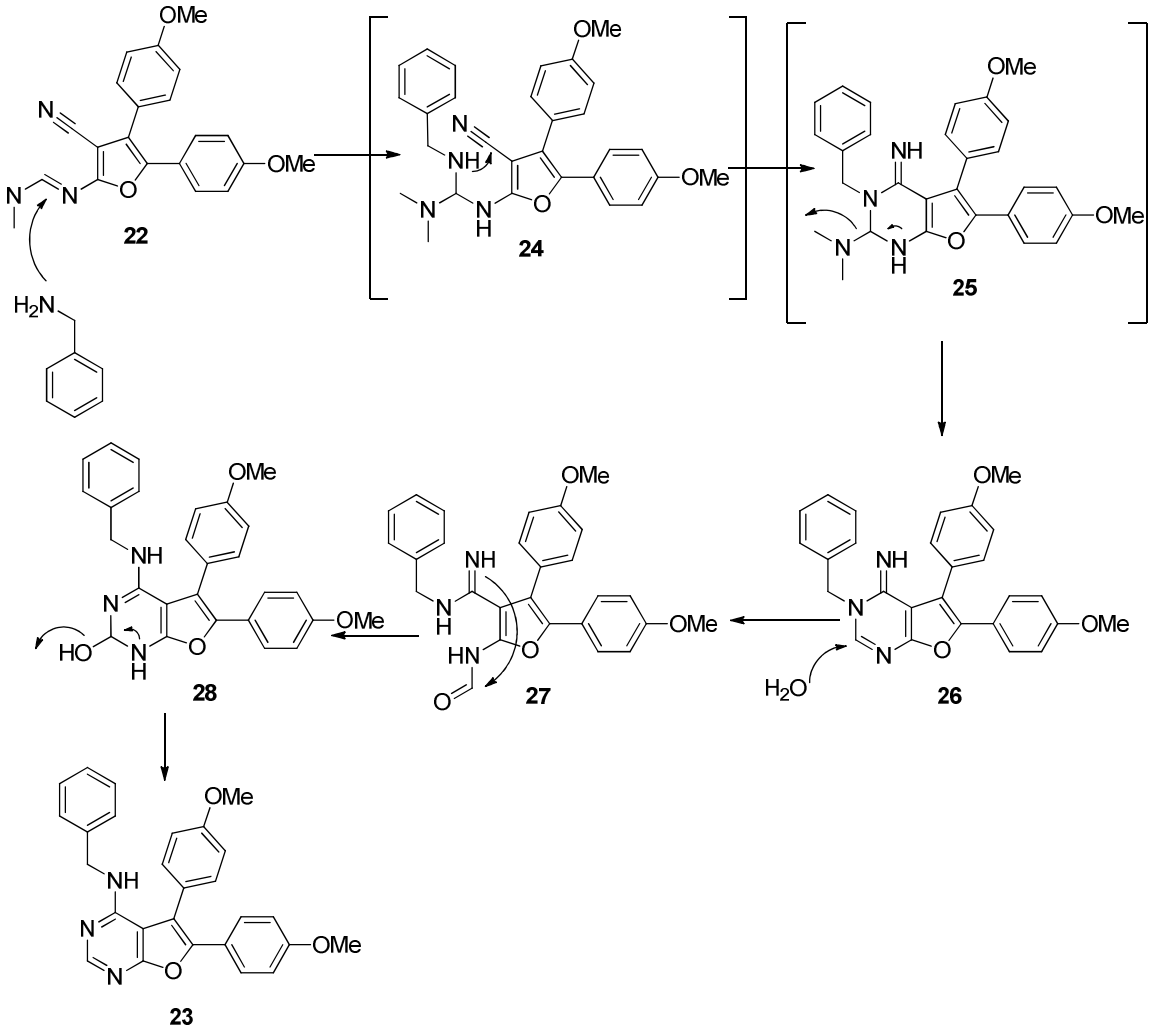

Scheme 5. Proposed mechanism for the synthesis of furo[2,3-*d*]pyrimidine-4-amine derivative **23**.

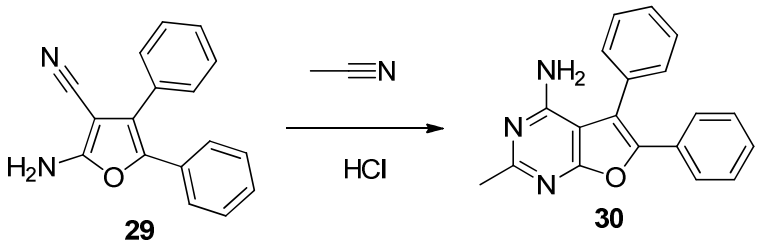

Scheme 6. Synthesis of furo[2,3-*d*]pyrimidines **30**.

In 1980, Dave *et al*[287] reported a facile synthesis of 2-methyl-4-amino-furo[2,3-

d]pyrimidine **30** (Scheme 6) via the condensation of **29** and acetonitrile under strong acidic HCl (g) conditions. [287]

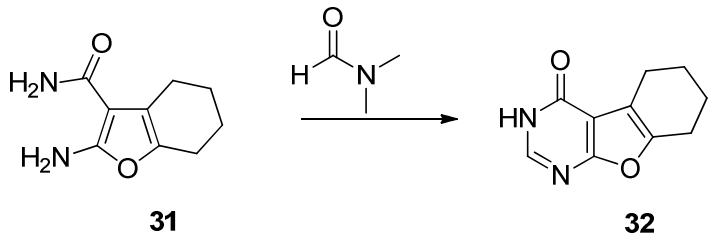

31 **32**

Scheme 7. Synthesis of furo[2,3-*d*]pyrimidines **32**.

The synthesis of furo[2,3-*d*]pyrimidine **32** (Scheme 7) was first reported by Manhas and Amin in 1977.[288] Compound **32** was obtained *via* the condensation of 2-amino-3-amide substituted furan **31** and DMF.

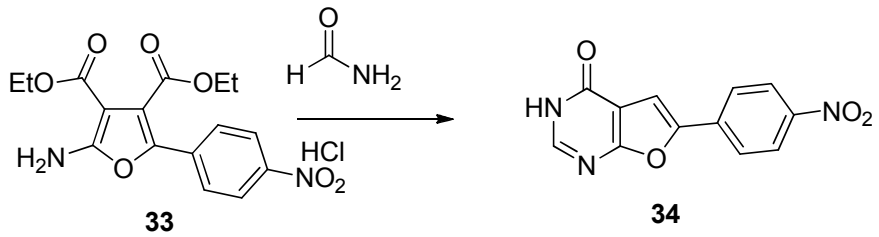

33 **34**

Scheme 8. Synthesis of furo[2,3-*d*]pyrimidines **34**.

Martin-Kohler and coworkers[289] reported a facile synthesis of furo[2,3-*d*]pyrimidines **34** (scheme 8) *via* condensation of furan **33** and formamide under acid conditions.

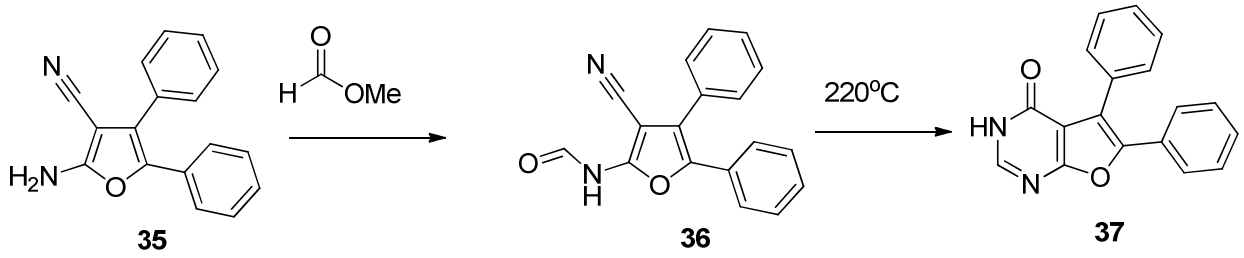

Scheme 9. Synthesis of furo[2,3-*d*]pyrimidines **37**.

In 2005, Foloppe and coworkers[290] reported the synthesis of furo[2,3-*d*]pyrimidines **37** (scheme 9) through the condensation between furan **35** and methyl formate followed by thermal cyclization *via* intermediate **36**.

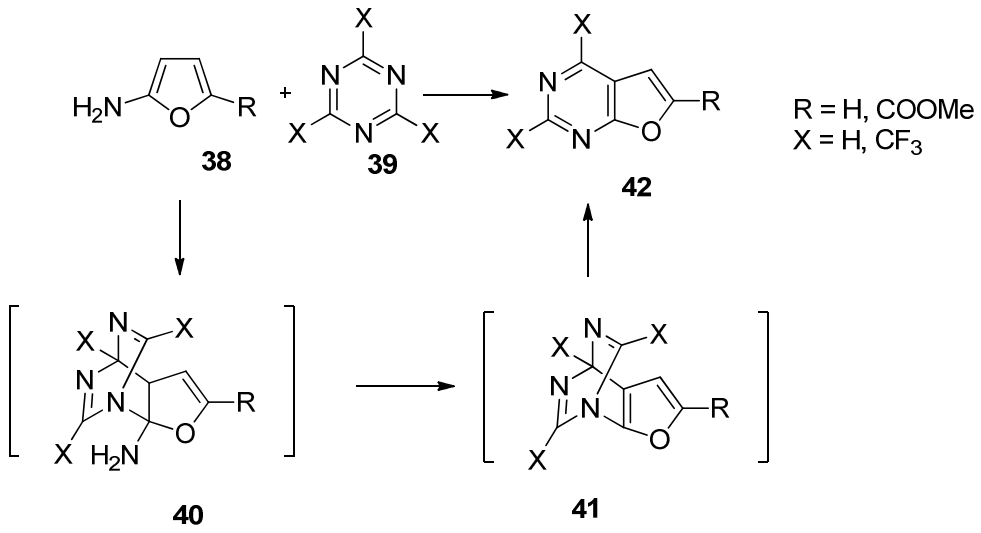

Scheme 10. Synthesis of furo[2,3-*d*]pyrimidines **42**.

In 2009, Dang and Liu[291] reported a novel approach for the synthesis of furo[2,3-*d*]pyrimidines **42** *via* Diels–Alder reactions of 2-aminofurans **38** with 1,3,5-triazines **39**. The reaction mechanism was envisioned to entail cascade reactions involving an inverse

electron demand Diels–Alder (IDA) reaction to give intermediate **40**, followed by the elimination of ammonia to afford intermediate **41**, and a final retro Diels–Alder reaction.[292.]

2. From pyrimidine precursors (Route B)

A majority of the literature methods for the synthesis of furo[2,3-*d*]pyrimidines start from pyrimidine precursors.

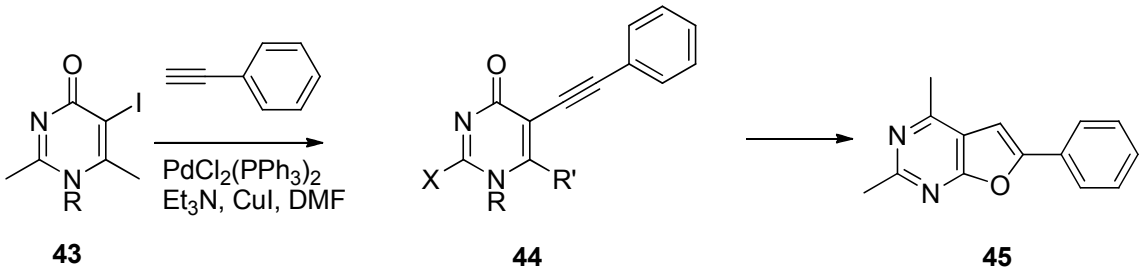

Scheme 11. Synthesis of 6-substituted furo[2,3-*d*]pyrimidines **45**.

In 1982, Sakamoto and coworkers[293] reported a facile approach for the synthesis of 6-substituted-furo[2,3-*d*]pyrimidines **45** (scheme 11) *via* a two step reaction starting from iodo-pyrimidine **43**. Sonogashira coupling of **43** and phenylacetylene afforded intermediate **44**, which was converted to **45** *via* thermal cyclization.

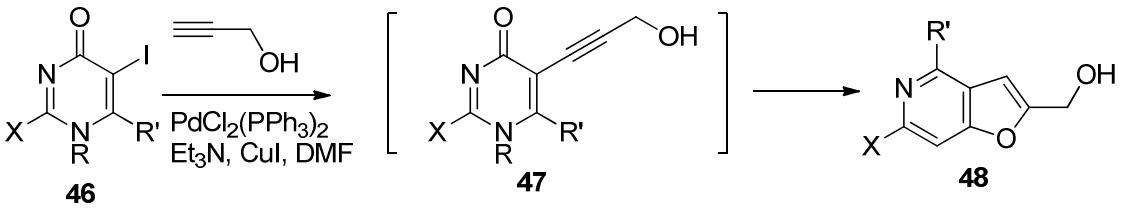

Scheme 12. Synthesis of 6-substituted furo[2,3-*d*]pyrimidines **48**.

In 2003, Petricci and coworkers[294] reported the synthesis of 6-substituted-furo[2,3-*d*]pyrimidines **48** (scheme 12) *via* cascade reactions involving microwave assisted Sonogashira coupling and intramolecular cyclization.

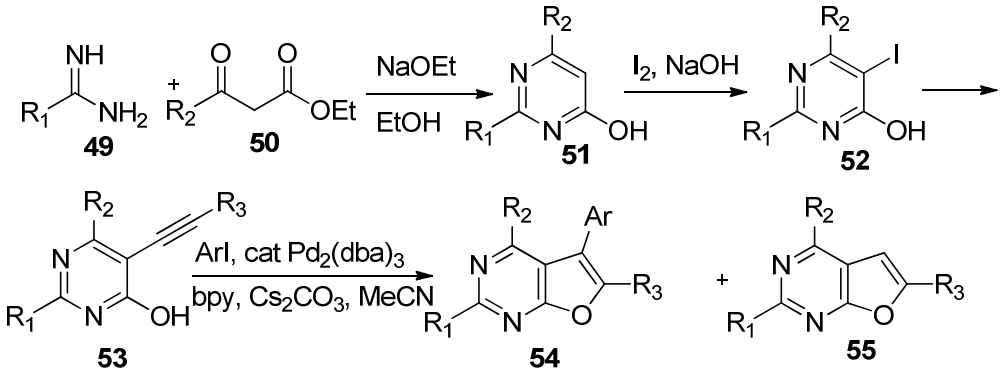

Scheme 13. Synthesis of furo[2,3-*d*]pyrimidines **54** and **55**.

Liu and coworkers[295] reported a modified approach for the synthesis of multi-substituted-furo[2,3-*d*]pyrimidines **54** and **55** (scheme 13) *via* Sonogashira coupling of iodopyrimidines and acetylenes, followed by metal catalyzed intramolecular cyclization. These iodopyrimidines precursors **52** were in turn obtained *via* condensation of amidines **49** with β ketoesters **50**, followed by iodination.

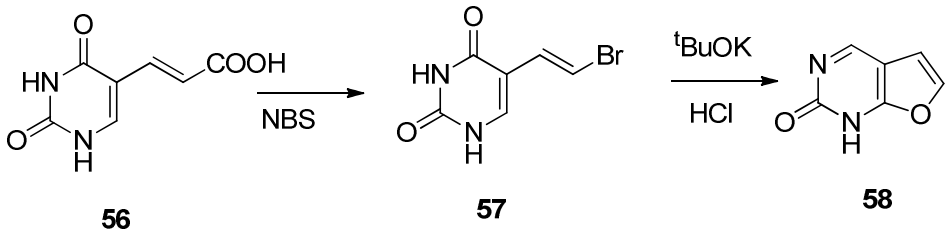

Scheme 14. Synthesis of 6-substituted furo[2,3-*d*]pyrimidines **58**.

Eger and coworkers[296] reported the novel synthesis of furo[2,3-*d*]pyrimidines **58**

(scheme 14) by intramolecular cyclocondensation of 5-(2-bromovinyl)-uracil **57**, which in turn was synthesized *via* the decarboxybromination of 5-(2-bromovinyl)-uracil **56**.

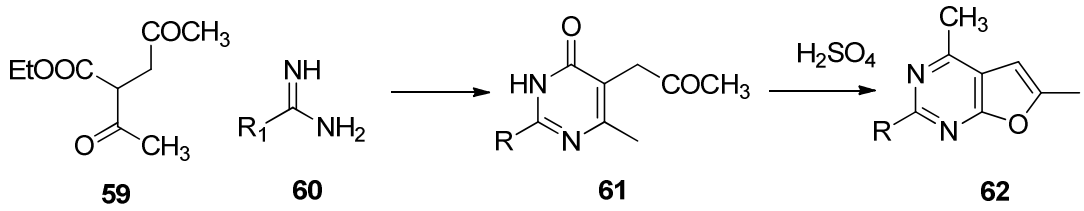

59 **60** **61** **62**

Scheme 15. Synthesis of 6-substituted furo[2,3-*d*]pyrimidines **62**.

Bisagni and coworkers[276] reported the synthesis of 4,6-dimethyl-2-substituted furo[2,3-*d*]pyrimidines **62** analogues (scheme 15) *via* a two-steps strategy. Condensation of β-ketoester **59** with amidines **60** afforded 5-acetone pyrimidines **61**. Cyclocondensation of the corresponding pyrimidine precursors in sulfuric acid afforded the desired 4,6-dimethyl-2-substituted furo[2,3-*d*]pyrimidines **62**.

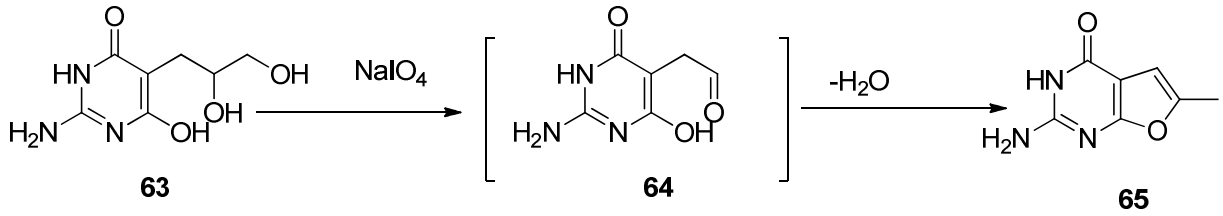

63 **64** **65**

Scheme **16**. Synthesis of 6-substituted furo[2,3-d]pyrimidines **65**.

Grindey and coworkers[298] reported a facile synthesis of 2-amino-4-oxo-furo[2,3-*d*]pyrimidine **65** (scheme 16) *via* the oxidative cyclization of 2-amino-4,6-dihydroxy-5-(2,3-dihydoxypropyl)-pyrimidine **63**. Periodate oxidation of **63** resulted in spontaneous

cyclization to afford furo[2,3-*d*]pyrimidin-4-one **65** *via* the intermediate aldehyde.

B. Synthesis of pyrrolo[2,3-*d*]pyrimidines

As deazapurine analogues, pyrrolo[2,3-*d*]pyrimidines have shown various biological activities and have found clinical use. Due to their important biological properties, a large body of literature exist for the synthesis of pyrrolo[2,3-*d*]pyrimidines. Generally, the synthesis of the pyrrolo[2,3-*d*]pyrimidine ring system can be achieved through following methods.

1. Route A: From pyrrole precursors

2. Route B: From pyrimidine precursors

3. Route C: From furan precursors

1. Route A: From pyrrole precursors

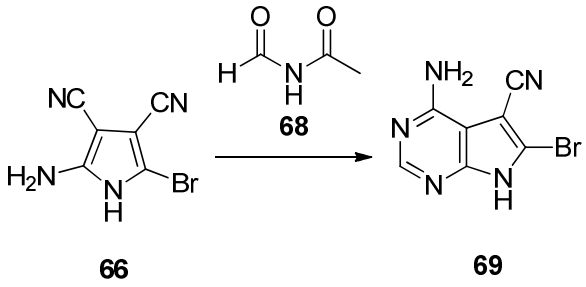

Scheme **17**. Synthesis of pyrrolo[2,3-d]pyrimidines **69**.

Tolman *et al*[299] in 1968 reported the ring closure of 2-amino-5-bromo-3,4-dicyanopyrrol with formamidine acetate in 2-ethoxyethanol at reflux temperature. The reaction furnished 4-amino-6-bromo-5-cyanopyrrolo[2,3-*d*]pyrimidine **69** (scheme 17) in 65% yield.

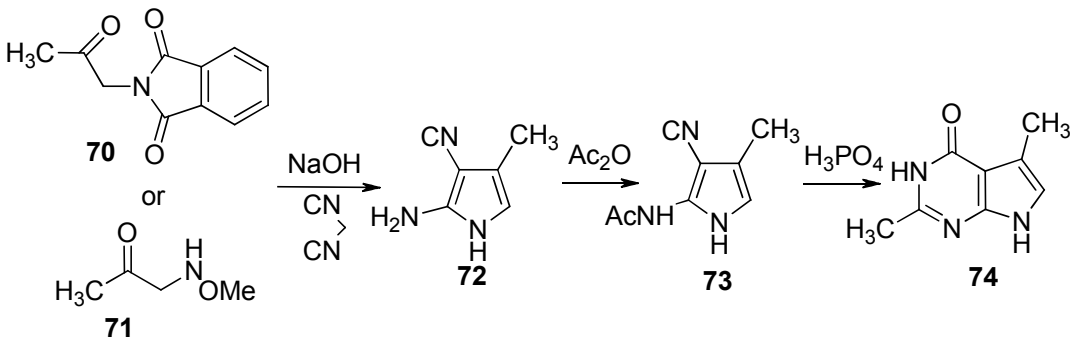

Scheme 18. Synthesis of 2,5-dimethyl-3*H*-pyrrolo[2,3-*d*]pyrimidin-4(7*H*)-one **74**.

Girgis *et al.* [300] in 1989 reported the synthesis of 2,5-dimethyl pyrrolo[2,3-*d*]pyrimidine **74** (Scheme 18) from 2-acetylamino-3-cyano-4-methylpyrrole **73** by with 85% phosphoric acid. The pyrrole **73** was in turn obtained by the reaction of either 2-(2-oxopropyl)isoindoline-1,3-dione **70** or 1-(methoxyamino)propan-2-one **71** with malononitrile to give 2-amino-4-methyl-1*H*-pyrrole-3-carbonitrile **72**, which was reacted with acetic anhydride to afford **73**.

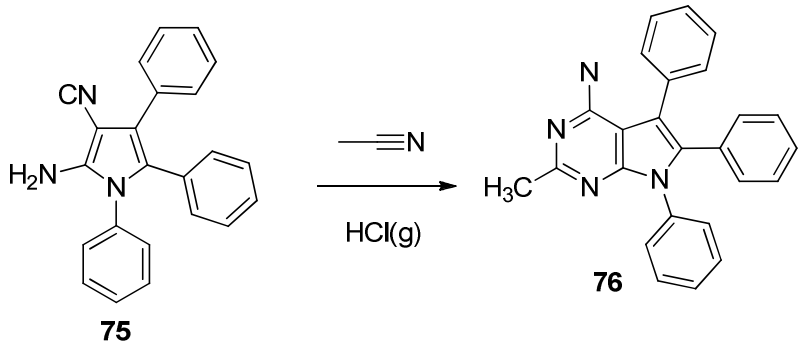

Scheme 19. Synthesis of 2-methyl-5-amino-pyrrolo[2,3-*d*]pyrimidine **76**.

Dave *et al* [287] in 1980 reported a general procedure for the synthesis of condensed pyrimidines. The condensation between acetonitrile and substituted pyrrole **75** (scheme 19) under HCl (g) condition afforded pyrrolo[2,3-*d*]pyrimidine **76** in 60% yield.

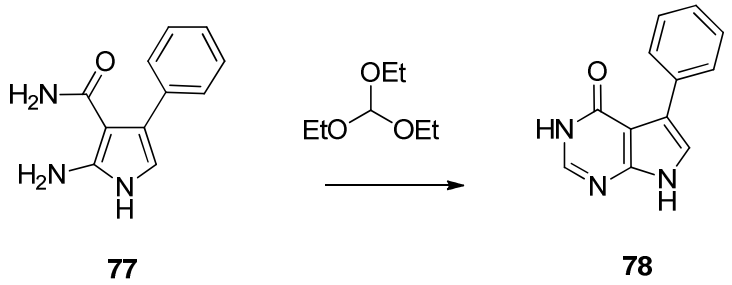

77 78

Scheme 20. Synthesis of 2-methyl-5-amino-pyrrolo[2,3-*d*]pyrimidine **78**.

Bookser *et al*[301] in 2005 reported the synthesis of pyrrolo[2,3-*d*]pyrimidine **78** (scheme 20) *via* the condensation between substituted pyrrole **77** and triethylorthoformate under acidic conditions.

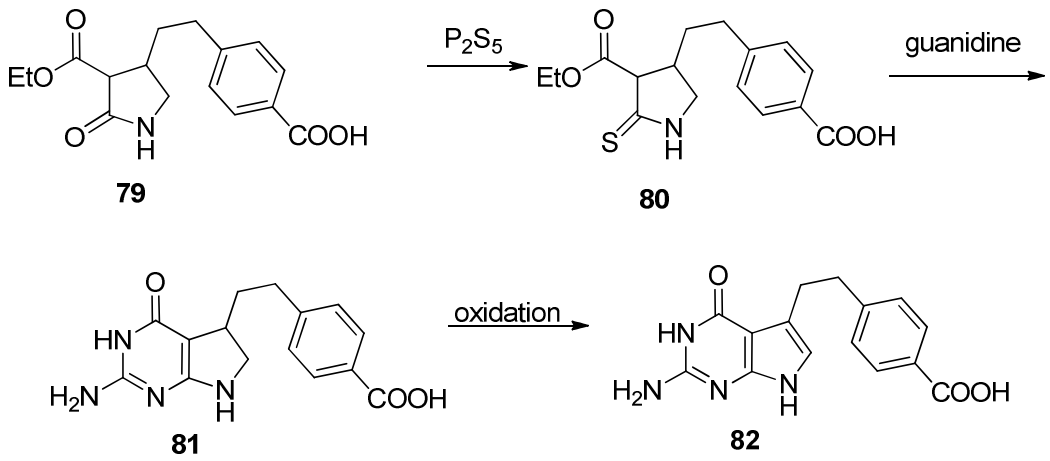

79 80 81 82

Scheme 21. Synthesis of 4-(2-(2-amino-4-oxo-4,7-dihydro-3*H*-pyrrolo[2,3-*d*]pyrimidin-5-yl)ethyl)benzoic acid **82**.

Barnett *et al*. [302] in 1993 reported the synthesis of 4-(2-(2-amino-4-oxo-4,7-dihydro-3*H*-pyrrolo[2,3-*d*]pyrimidin-5-yl)ethyl)benzoic acid **82** (scheme 21) *via* a guanidine cyclization of a preformed 3-carbethoxy-2-thiopyrrolidine intermediate **81** as

the key step.

2. Route B: From pyrimidine precursors

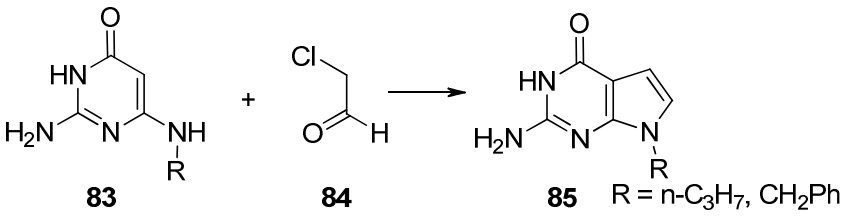

Scheme 22. Synthesis of pyrrolo[2,3-*d*]pyrimidines **85**.

In 1964, Noell *et al.* [303] first reported the synthesis of pyrrolo[2,3-*d*]pyrimidines **85** (Scheme 22) by the reaction of 2-amino-6-alkylamino-4-hydroxypyrimidines **83** with chloroacetaldehyde **84**.

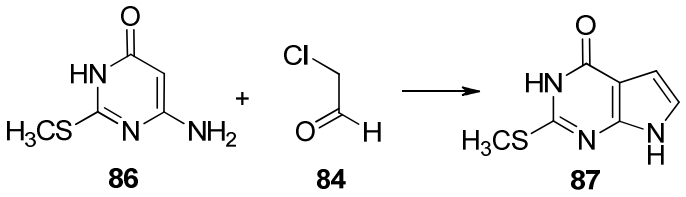

Scheme 23. Synthesis of 2-(methylthio)-3*H*-pyrrolo[2,3-*d*]pyrimidin-4(7*H*)-one **87**.

Noell and coworkers[303] also reported the synthesis of pyrrolo[2,3-*d*]pyrimidine **87** (Scheme 23) from 2-methylthio-6-amino-4-pyrimidone **86** and chloroacetaldehyde **84**.

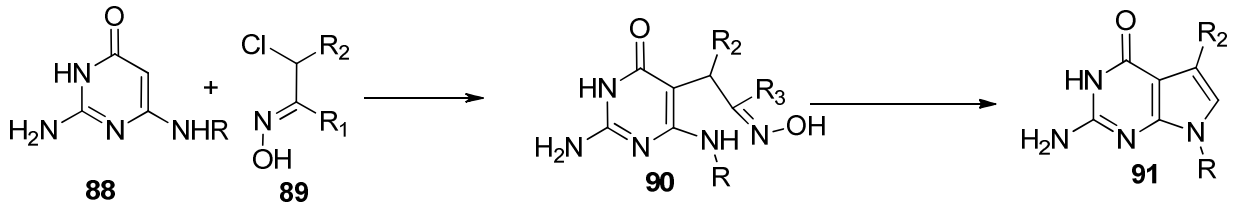

Scheme 24. Synthesis of pyrrolo[2,3-*d*]pyrimidines **91.**

Gibson and coworks[304] in 1998 reported the reaction of the diaminopyrimidine **88** (Scheme 24) with nitrosoalkenes **89** to provide a short synthesis of pyrrolo[2,3-*d*]pyrimidine **91** *via* pyrimidine intermediate **90.**

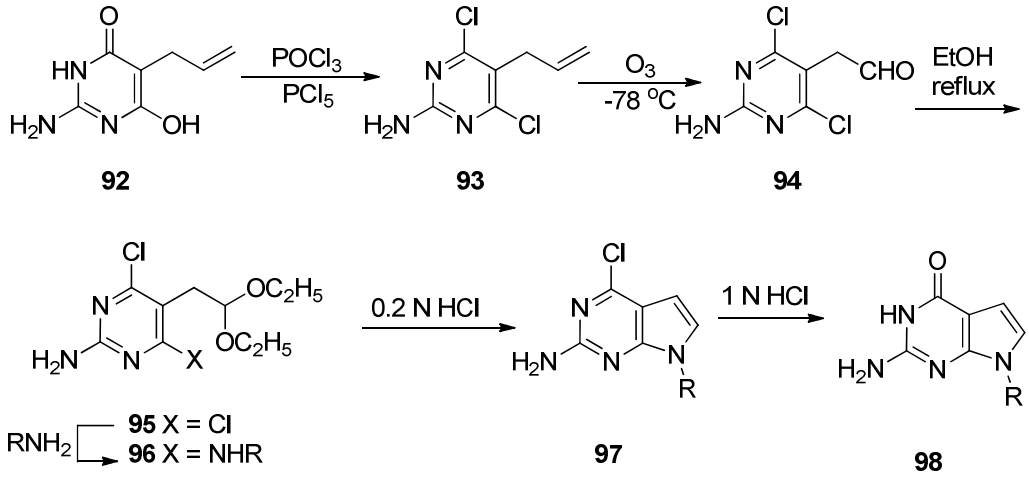

Scheme 25. Synthesis of 7-substituted-3*H*-pyrrolo[2,3-*d*]pyrimidin-4(7*H*)-one **98**.

Duffy and coworkers[305] in 1974 reported the synthesis of 2-amino-7-substituted-3*H*-pyrrolo[2,3-*d*]pyrimidin-4(7*H*)-one **98** from 2-amino-4,6-dichloro-5-(2,2-diethoxyethyl)pyrimidine **95** (Scheme 25). 5-Allyl-2-amino-4,6-dihydroxypyrimidine **92**,

prepared by the reaction of guanidine hydrochloride with diethyl allylmalonate, was converted to the 4,6-dichloro derivative **93** by treatment with $POCl_3$, and diethylaniline in the presence of PCl_5. The (2-amino-4,6-dichloropyrimidin-5-yl)acetaldehyde **94** was obtained from **93** by ozonolysis of the allyl group. Compound **94** was reacted with ethanol at reflux to give the corresponding acetal **95**, which was converted to **96** with the treatment of substituted amines followed by cyclization to give 2-amino-4-chloro-7-alkyl-7*H*-pyrrolo[2,3-*d*]pyrimidine **97** by treatment with dilute aqueous HCl at room temperature. The hydrolysis of **97** using 1 N HCl at 100 °C afforded **98**.

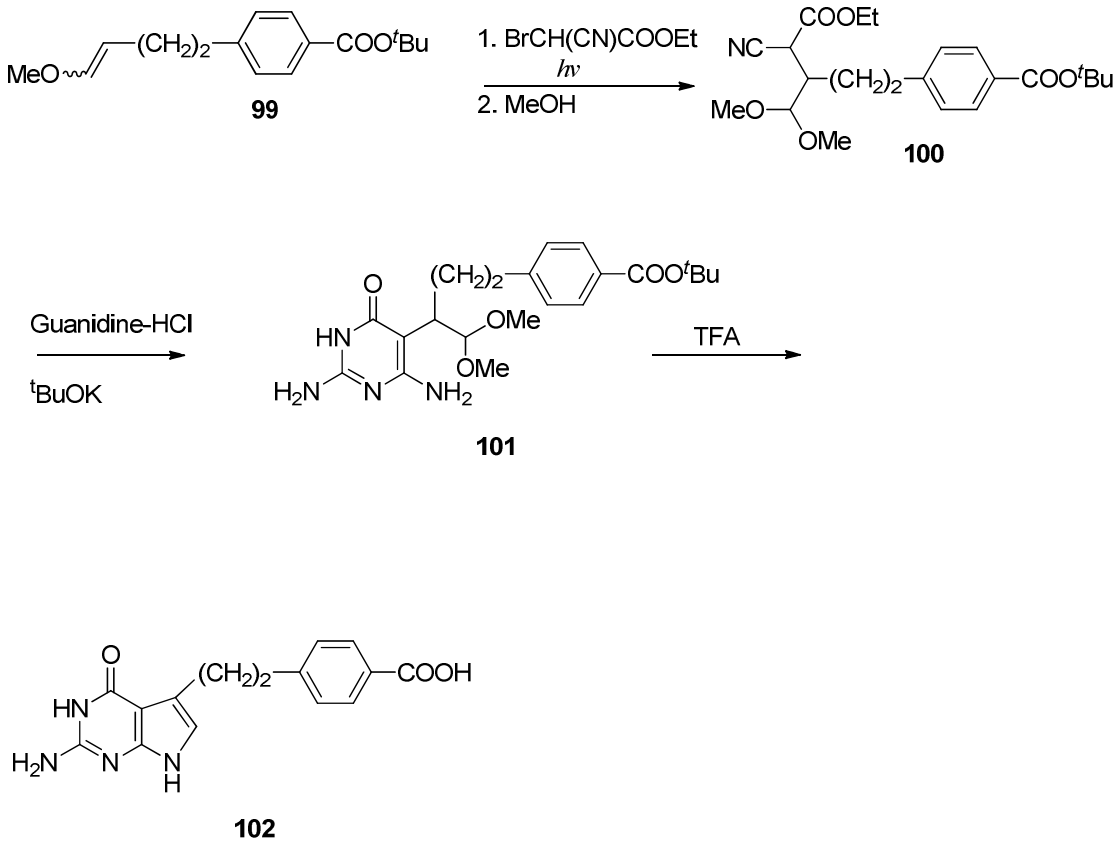

Scheme 26. Synthesis of pyrrolo[2,3-*d*]pyrimidines **102**.

Miwa *et al.*[306] in 1993 reported utilizing the spontaneous cyclization of 6-amino-5-pyrimidylacetaldehydes for the synthesis of pemetrexed (Scheme 26). The key step in the synthesis of the acetal protected aldehyde **100** was a photo-initiated free radical addition of ethyl bromocyanoacetate to the corresponding enol ether **99**. The reaction of the enol ether **99** with ethyl bromocyanoacetate in methanol under ultraviolet irradiation regioselectively afforded the acetal functionalized ethyl cyanoacetate **100**. Condensation of **100** and guanidine at reflux afforded the acetal protected 6-amino-5-pyrimidylacetaldehyde **101**. Acid catalyzed deprotection of the dimethyl acetal and *t*-butyl moieties of **101** afforded 4-[2-(2-amino-4-oxo-pyrrolo[2,3-*d*]pyrimidin-5-yl)-ethyl]-benzoic acid **102** *via* the free aldehyde.

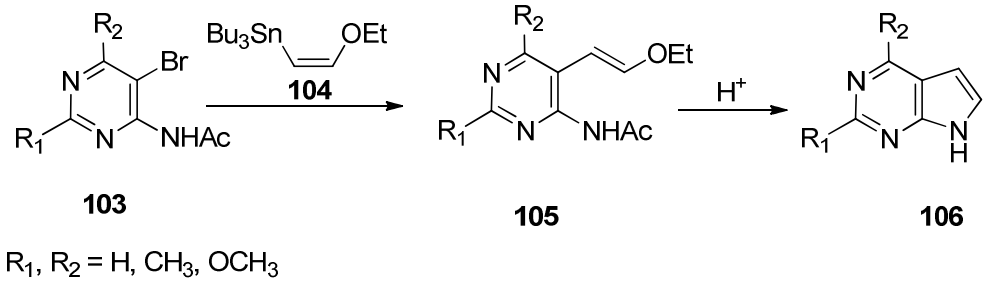

Scheme 27. Synthesis of pyrrolo[2,3-*d*]pyrimidines **105**.

Sakamoto *et al.* [307] in 1993 reported (Scheme **27**) the synthesis of pyrrolo[2,3-*d*]pyrimidines **106** by utilizing an intramolecular cyclization of protected 5-acetaldehyde pyrimidines **105**. Compound **105** was in turn synthesized by palladium(0) catalyzed coupling of the appropriate 2,4-disubstituted-5-bromo-6-acetamido pyrimidines **103** with (*Z*)-1-ethoxy-2-(tributylstannyl)ethane **104**.

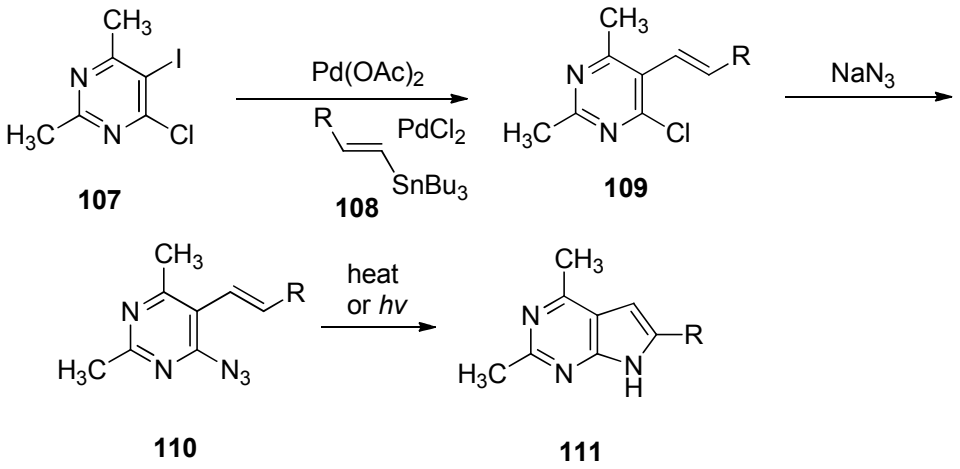

Scheme 28. Synthesis of 2,4 -dimethyl-6-substitued-7*H*-pyrrolo[2,3-*d*]pyrimidine **111**.

Kondo *et al.* [308] in 1989 reported the synthesis of 2,4-dimethyl-6-substitued-7*H*-pyrrolo[2,3-*d*]pyrimidine **111** (Scheme 28) *via* a photoinduced or thermal cyclization of 4-azidopyrimidines **110** containing an olefinic functionality at the 5-position. Intermediate **110** was in turn obtained by a palladium catalyzed cross-coupling between the 5-iodopyrimidine **107** and appropriate stannanes **108**, followed by nucleophilic displacement of the 4-chloro of pyrimidine **109** with sodium azide.

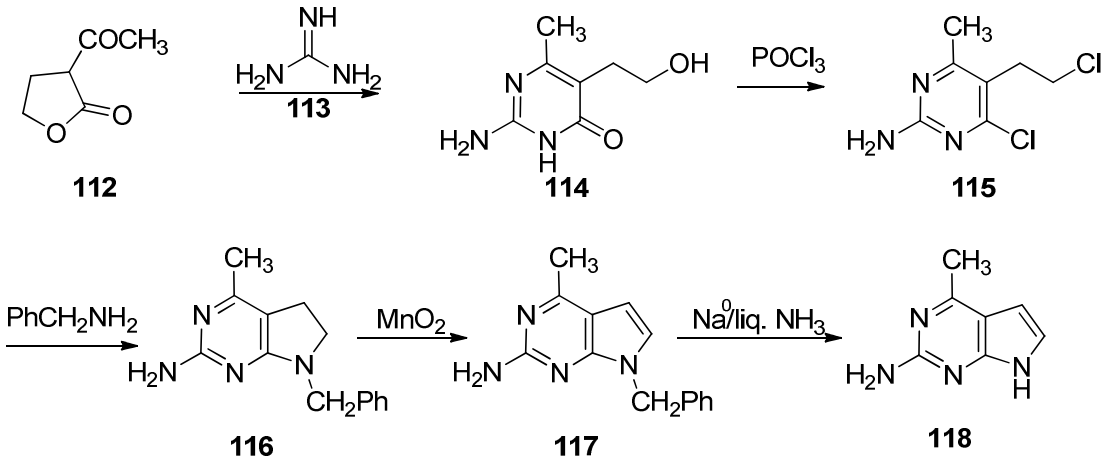

Scheme 29. Synthesis of 4-methyl-7*H*-pyrrolo[2,3-*d*]pyrimidin-2-amine **118**.

Gangjee *et al.* [309] in 2000 reported the synthesis of 2-amino-4-methyl-pyrrolo[2,3-*d*]pyrimidine **118** (Scheme 29) *via* a novel ring closure method. The synthesis commenced with the condensation of 2-acetylbutyrolactone **112** with guanidine carbonate **113** to afford 2-amino-5-(2-hydroxyethyl)-6-methylpyrimidin-4(3*H*)-one **114**. Chlorination with $POCl_3$ afforded the dichloro compound 4-chloro-5-(2-chloroethyl)-6-methylpyrimidin-2-amine **115**. Compound **115** was condensed with benzylamine to afford 2-amino-4-methyl-7-(*N*-benzyl)pyrrolidinyl[2,3-*d*]pyrimidine **116**. Oxidative aromatization of compound **116** with MnO_2 afforded the 7-benzyl-4-methyl-7*H*-pyrrolo[2,3-*d*]pyrimidin-2-amine **117**. Compound **118** was obtained following debenzylation of **117** with Na metal in ammonia.

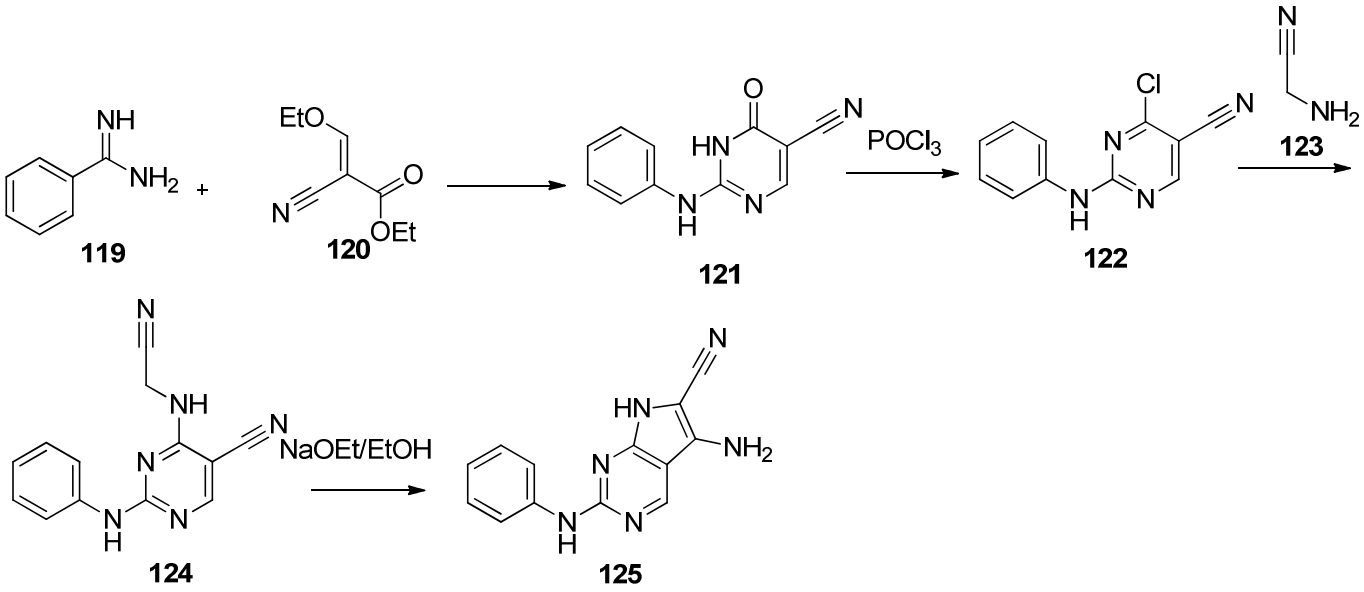

Scheme 30. Synthesis of pyrrolo[2,3-*d*]pyrimidine **125**.

Kim and Santilli [310] in 1971 reported the synthesis of multiple substituted

pyrrole[2,3-*d*]pyrimidine **125** (Scheme 30) via Dieckmann condensation of pyrimidine **124**.The condensation between amidine **119** and hemiacetalester **120** afforded hydroxylpyrimidine **121**, which was converted to 4-chloro analogue when treated with $POCl_3$. Upon treatment with amine **123**, 4-chloropyrimidine was converted to intermediate **124**, which cyclized under basic condition to afford pyrrolo[2,3-*d*]pyrimidine **125** in 97% yield**.**

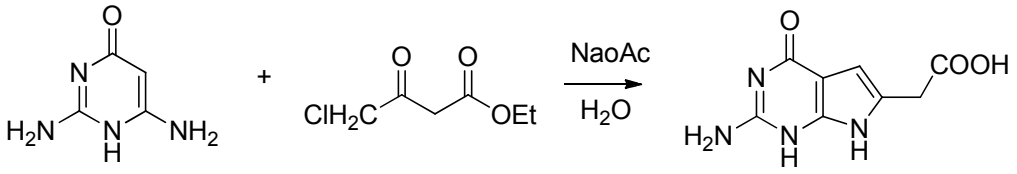

126 **127** **128**

Scheme 31. Synthesis of 2-(2-amino-4-oxo-4,7-dihydro-1*H*-pyrrolo[2,3-*d*]pyrimidin-6-yl)acetic acid **128**.

Gangjee *et al.* [311] in 2001 reported the synthesis of 2-(2-amino-4-oxo-4,7-dihydro-1*H*-pyrrolo[2,3-*d*]pyrimidin-6-yl)acetic acid **128** (Scheme 31)from the condensation of 2,6-diaminopyrimidin-4(1*H*)-one **126** with ethyl 4-chloro-3-oxobutanoate **127** in the presence of sodium acetate.

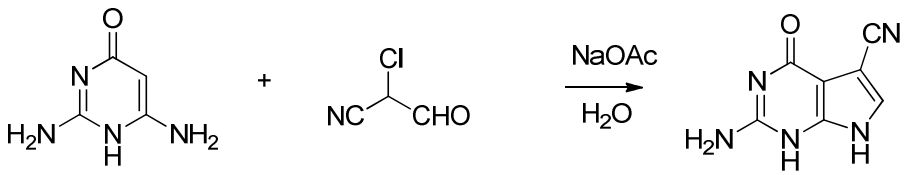

129 **130** **131**

Scheme 32. Synthesis of 2-amino-4-oxo-4,7-dihydro-1*H*-pyrrolo[2,3-*d*]pyrimidine-5-carbonitrile **131**.

In 2001, Gangjee *et al.* [312] also reported the synthesis of 2-amino-4-oxo-4,7-dihydro-1*H*-pyrrolo[2,3-*d*]pyrimidine-5-carbonitrile **131** (Scheme 32) from the condensation of compound **129** with 2-chloro-3-oxopropanenitrile **130** under basic condition.

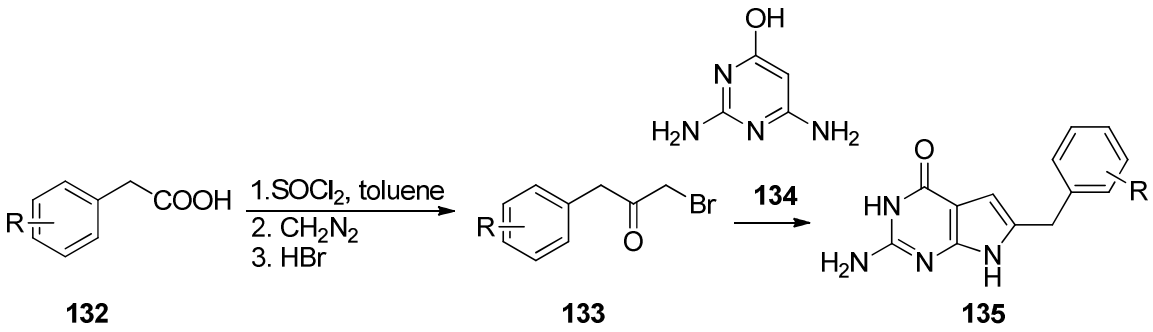

Scheme 33. Synthesis of 2-amino-6-substituted benzyl-3*H*-pyrrolo[2,3-*d*]pyrimidin-4(7*H*)-one **135**.

Gangjee *et al.*[313] in 2003 reported the synthesis of 2-amino-6-substituted benzyl-3*H*-pyrrolo[2,3-*d*]pyrimidin-4(7*H*)-one **135** (Scheme 33) from the condensation of 1-bromo-3-substituted phenylpropan-2-one **133** with **134**. Compound **133** was in turn obtained from the corresponding substituted benzyl acetic acid **132** reacting with thionyl chloride followed by the treatment of diazomethane and HBr (Conc.).

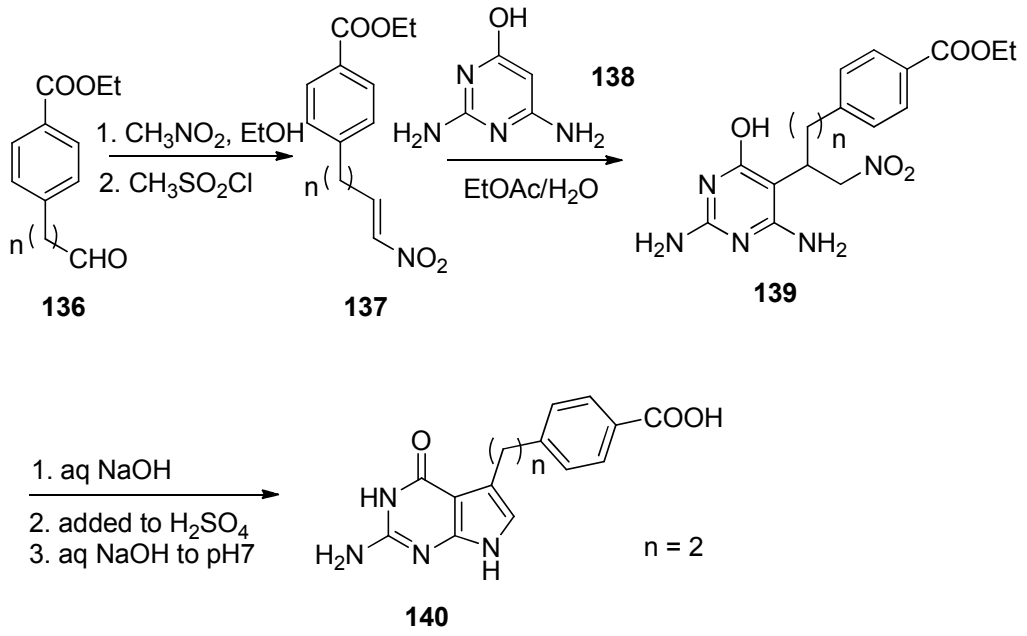

Scheme 34. Synthesis of pyrolo[2,3-*d*]pyrimidine **140**.

Taylor *et al.* [314] in 1999 reported a new and efficient synthesis of pyrrolo[2,3-*d*]pyrimidine **140** from aldehyde **136** (Scheme 34). A Henry reaction of **136** with nitromethane gave the nitro alcohol that was dehydrated by mesylation followed by treatment with triethylamine to yield **137**. Michael addition of pyrimidine **138** with **137** afforded **139**, which was then converted to pyrrolo[2,3-*d*]pyrimidine **140** *via* a one-pot three-step reaction.

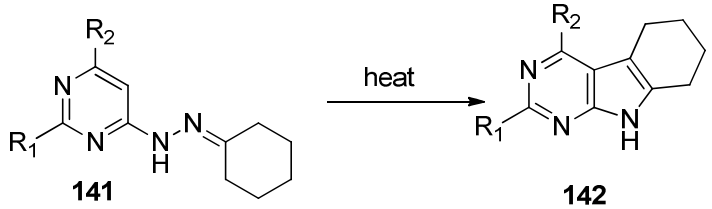

Scheme 35. Synthesis of pyrrolo[2,3-*d*]pyrimidine **142** *via* thermal Fisher indole cyclization.

Crooks *et al.* [315] reported the synthesis of tricyclic 5,6-fused pyrrolo[2,3-*d*]pyrimidine **142** (Scheme 35) *via* a thermal Fischer-indole reaction. Due to the limitation of thermal Fisher-indole cyclization, including steric rearrangement and high reaction temperatures, in the synthesis of pyrrolo[2,3-*d*]pyrimidines, acid-catalyzed Fischer-indole cyclizations have been developed as an alternate strategies for the of synthesis **142** in moderate to good yields. [316]

3. Route C: From furan precursors

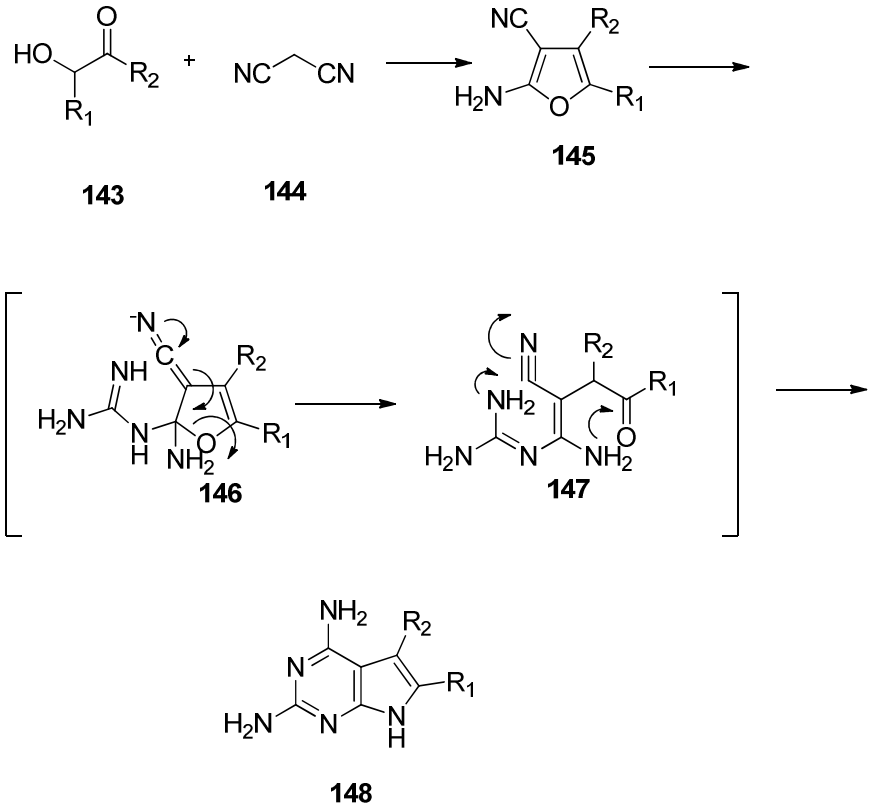

Scheme 36. Synthesis of 2,4-diaminopyrrolo[2,3-*d*]pyrimidine **148** from furan precursor.

In 1995, Taylor and coworkers [317] reported a general method to synthesize 5,6-disubstituted 2,4-diamino-pyrrolo[2,3-*d*]pyrimidines **148** (Scheme 36) from furan **145**.

The condensation between guanidine and 2-amino-3-cyanofuran **145** afforded pyrrolo[2,3-*d*]pyrimidine **148.** The key intermediate **145** was in turn obtained by the condensation of α-hydroxy-ketones **143** with malononitrile.

The reaction involved a ring-opening, ring-recyclization sequence whereby the starting furan 2-amino nitrogen (shown in Scheme 36) becomes the pyrrole nitrogen of the final product and one of the guanidine nitrogens becomes the N-1 of the fused pyrimidine ring **148**.[317]

C. Synthesis of thieno[2,3-*d*]pyrimidines

A broad classification for the synthetic strategy for construction of thieno[2,3-*d*]pyrimidines is:

1. Route A: From thiophene precursors

2. Route B: From pyrimidine precursors

1. From thiophene precursors (Route A)

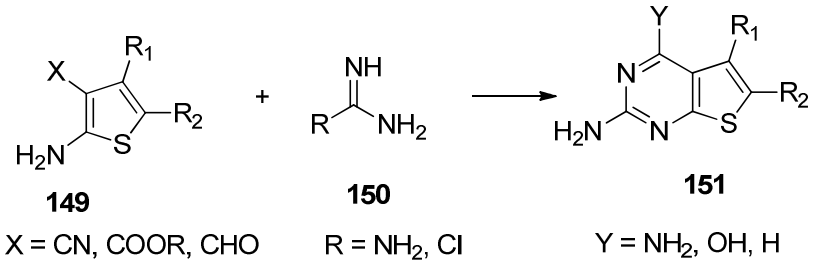

Scheme 37. Synthesis of thieno[2,3-*d*]pyrimidine **151**.

2-Amino-5,6-disubstituted thieno[2,3-*d*]pyrimidines **151** (Scheme 37) are synthesized *via* cyclocondensation of appropriate thiophenes **149** with an amidine

derivative **150**.[318] The thiophenes in turn can be synthesized from aldehydes or ketones through the Gewald reaction.[319] The amidines **150** can be guanidines (R = NH_2) or chloroformamidine hydrochloride (R = Cl). Depending on the nature of the X group in thiophene **149,** the 4-substitution (Y) in **151** can be H, NH_2 or OH.

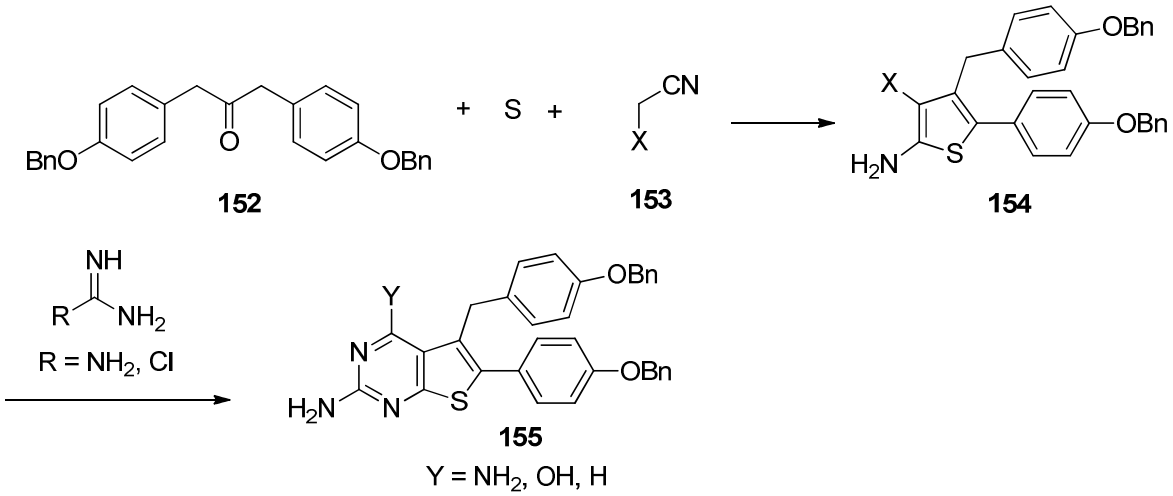

Scheme 38. Synthesis of thieno[2,3-*d*]pyrimidine **155**.

Zhang and coworkers[320] reported the synthesis of 2-amino-thieno[2,3-*d*]pyrimidines **155** through the condensation between amidines and substituted thiophenes (Scheme 38).Thiophene intermediate **154** in turn was synthesized from ketone **152**, sulfur and **153** *via* the Gewald reaction condition.[318] The target 2-amino-5,6-disubstituted thieno[2,3-*d*]pyrimidines **155** was obtained by the condensation of **154** with guanidine (R = NH_2) or chloroformamidine hydrochloride (R = Cl).

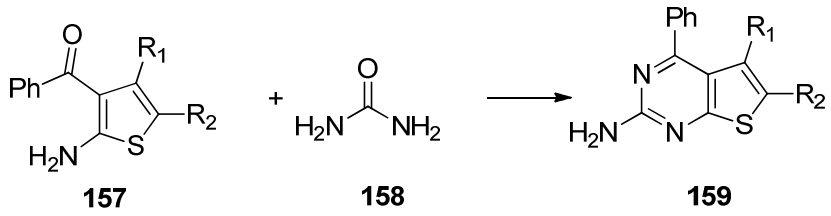

Scheme 39. Synthesis of thieno[2,3-*d*]pyrimidine **159**.

Ishikawa and coworkers[321] in 1980 reported a novel synthesis of 2-amino-4-phenyl substituted thieno[2,3-*d*]pyrimidines **159** (Scheme 39). The condensation between urea **158** and aminocarbonyl thiophenes **157** was utilized to synthesize thieno[2,3-*d*]pyrimidine **159**.

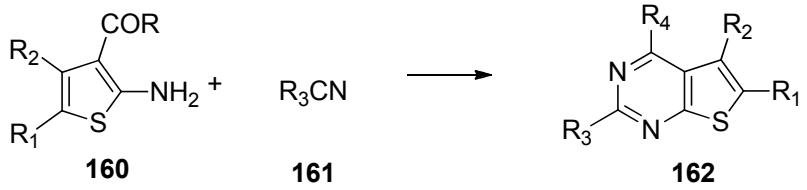

Scheme 40. Synthesis of thieno[2,3-*d*]pyrimidine **162**.

Dave and coworkers[322] reported a novel facile method for the synthesis of 2-alkyl thieno[2,3-*d*]pyrimidine in 1980. The cyclization between orthoaminocarboxylate thiophenes **160** (Scheme 40) and substituted nitriles **161** in the presence of HCl afforded thieno[2,3-d]pyrimidines **162**. Depending on the substitution groups on the carbonitrile **161**, different alkyl group can be introduced into the 2-postion in thieno[2,3-*d*]pyrimidine **162** . When acetonitrile was used as substrate 2-methyl-5,6-disubstituted thieno[2,3-*d*]pyrimidines were obtained. When the R groups in **160** were good leaving groups such as OR, NH_2, 4-oxo-substituted thieno[2,3-*d*]pyrimidines were obtained.

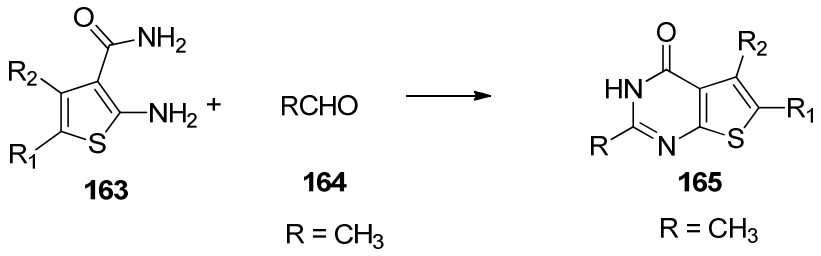

Scheme 41. Synthesis of thieno[2,3-*d*]pyrimidine **165**.

A novel approach for the synthesis of 2-substituted thieno[2,3-*d*]pyrimidines was reported by Cruceyra and coworkers. [323] The 2-substituted-4-oxo-thieno[2,3-*d*]pyrimidines was synthesized *via* condensation of thiophene **163** with aldehyde **164**. (Scheme 41). Various aliphatic and aromatic aldehydes can be utilized for the synthesis of thieno[2,3-*d*]pyrimidines. Acetaldehyde afforded 2-methyl-5,6-disubstituted thieno[2,3-*d*]pyrimidines **165**.

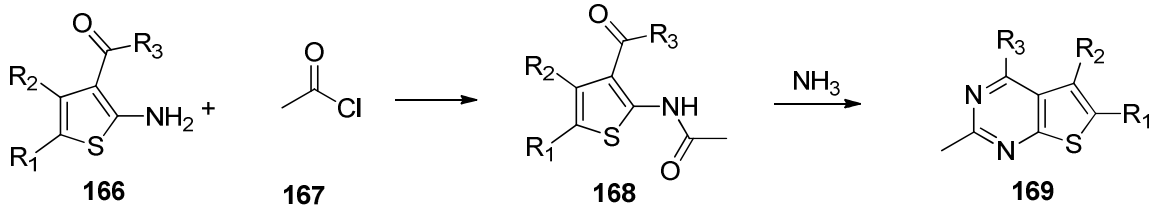

Scheme 42. Synthesis of thieno[2,3-*d*]pyrimidine **169**.

In 1978, Corral and coworkers[324] reported a modified approach for the synthesis of 2-alkyl thieno[2,3-*d*]pyrimidine **169** by using an acid chloride as the cyclization reagent instead of an aldehyde (Scheme 42). The amino group of the thiophene **166** reacted with acid chloride **167** to form the intermediate amide **168**, which cyclized with

NH_3 to afford thieno[2,3-*d*]pyrimidine **169**. When thiophenes **168** have good leaving groups as R_3 substitution, 4-oxo- thieno[2,3-*d*]pyrimidines were obtained. Compound **168** with methyl substitution as R_3 afforded 2-methyl-5,6-disubstituted thieno[2,3-*d*]pyrimidines.

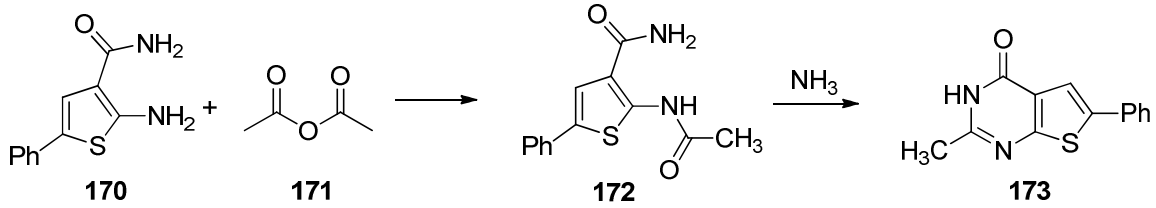

Scheme 43. Synthesis of thieno[2,3-*d*]pyrimidine **173**.

Konno and coworkers[325] reported the synthesis of 2-methyl-4-oxo-6-phenylthieno[2,3-*d*]pyrimidine **173** (Scheme 43) from intermediate **172**, which in turn was synthesized through the condensation of thiophene **170** with acetic anhydride **171**.

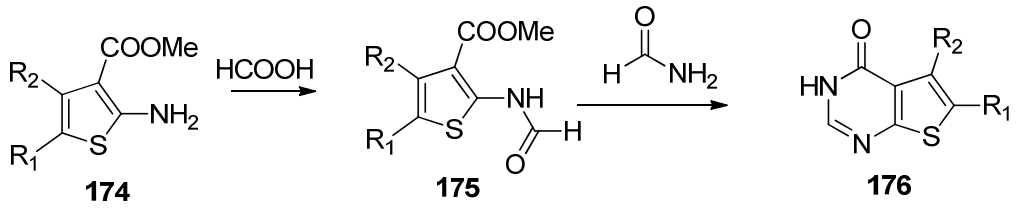

Scheme 44. Synthesis of thieno[2,3-*d*]pyrimidine **176**

In 1975, Robba and coworkers[326] reported the synthesis of thieno[2,3-*d*]pyrimidine **176** (Scheme 44). Thiophene **174** reacted with formic acid to give amide **175**, which then cyclized with formamide to afford **176**.

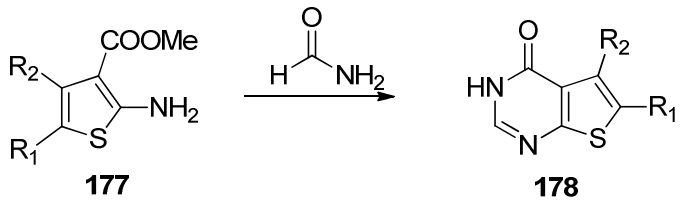

Scheme 45. Synthesis of thieno[2,3-*d*]pyrimidine **178**.

Horiuchi and coworkers[327] reported the one-pot synthesis of **178** via the condensation of thiophene **177** and formamide (Scheme 45) in 2009.

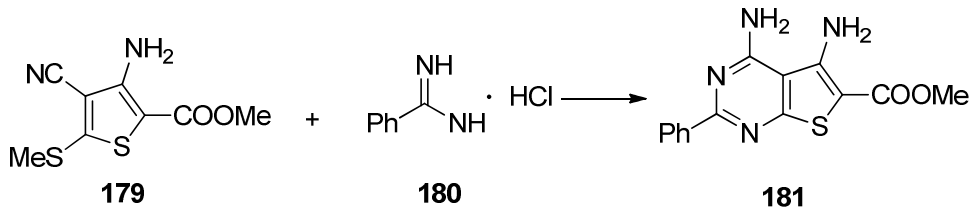

Scheme 46. Synthesis of thieno[2,3-*d*]pyrimidine **181**.

In 1998, Briel and coworkers[328] reported the synthesis of 2-phenyl substituted thieno[2,3-*d*]pyrimidine **181** *via* the condensation of thiophene **179** with benzamidine hydrochloride **180** (Scheme 46).

2. From pyrimidine precursors (Route B)

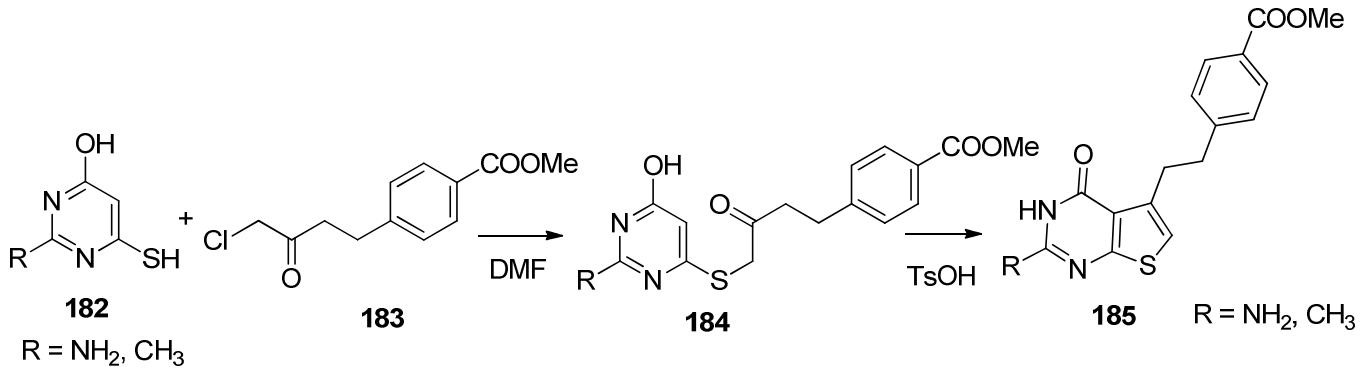

Scheme 47. Synthesis of thieno[2,3-*d*]pyrimidine **185**.

Taylor and coworkers[329] reported the synthesis of thieno[2,3-*d*]pyrimidine **185** (Scheme 47) as TS inhibitors and analogues of pemetrexed. Condensation of 2-substituted-4-hydroxy-6-mercaptopyrimidine **182** with α-chloroketone **183** gave pyrimidine sulfide **184**, which cyclized in the presence of p-toluenesulfonic acid to give **185**.

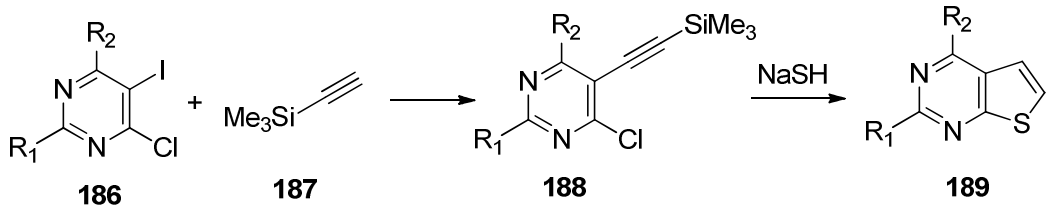

186 **187** **188** **189**

Scheme 48. Synthesis of thieno[2,3-*d*]pyrimidine **189**.

A novel approach for the synthesis of thieno[2,3-*d*]pyrimidine **189** was reported by Sakamoto and coworkers[330] in 1986 (Scheme 48). The intermediate **188** was synthesized by Sonogashira coupling of iodopyrimidines **186** and ethynyl-trimethyl-silane **187**, followed by the cyclization with NaSH.

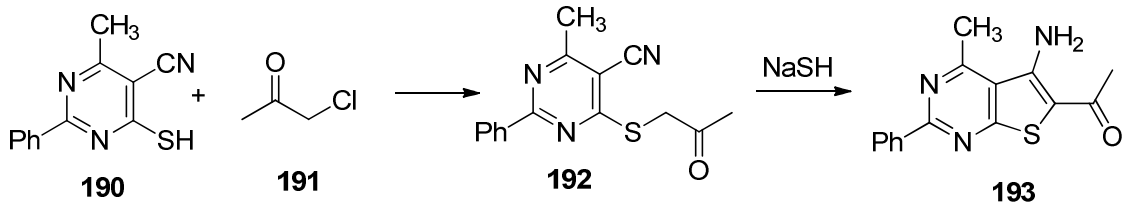

190 **191** **192** **193**

Scheme 49. Synthesis of thieno[2,3-*d*]pyrimidine **193**.

Ried and coworkers[331] In 1988 reported a novel approach for the synthesis of

thieno[2,3-*d*]pyrimidine **193** (Scheme 49) *via* the intramolecular cyclization of **192**, which in turn was synthesized through the condensation between 5-carbonitrile-6-mercaptopyrimidnes **190** and chloroacetone **191**.

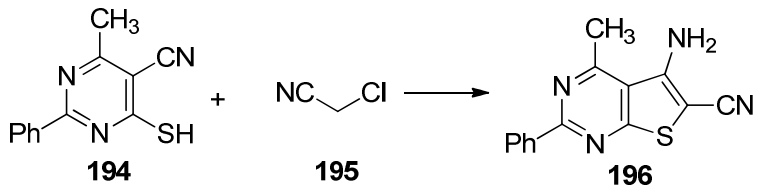

Scheme 50. Synthesis of thieno[2,3-*d*]pyrimidine **196**.

A similar approach was reported by El-Dean and coworkers[332] for the synthesis of thieno[2,3-*d*]pyrimidine **196** (Scheme 50). The condensation of substituted mercaptopyrimidine **194** and chloro-acetonitrile **195** afforded 5-amino-4-methyl-2-phenyl-thieno[2,3-*d*]pyrimidine-6-carbonitrile **196**.

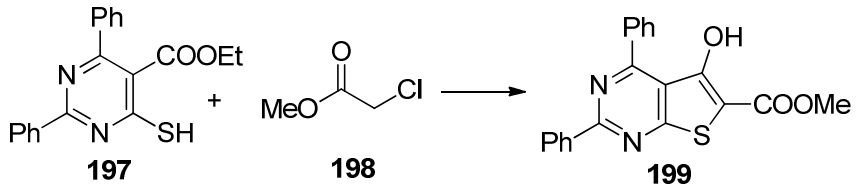

Scheme 51. Synthesis of thieno[2,3-*d*]pyrimidine **199**

Briel and coworkers[333] reported the synthesis of thieno[2,3-*d*]pyrimidine **199** (Scheme 51), which afford a further modification for the cyclization of the thieno[2,3-*d*]pyrimidine ring system. Chloroacetic acid methyl ester **198** reacted with 5-ethylester-6-mercaptopyrimidnes **197** afforded thieno[2,3-*d*]pyrimidine ring, a 5-hydoxy substitution

was achieved (Scheme 51).

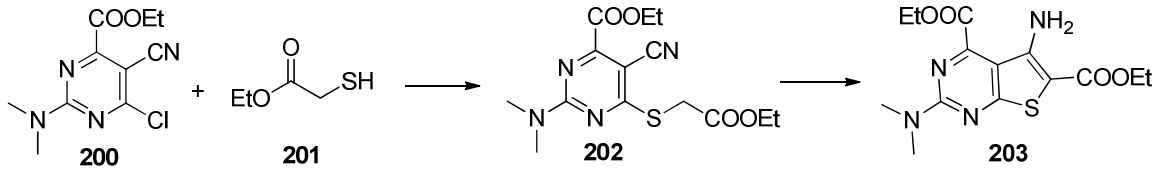

Scheme 52. Synthesis of thieno[2,3-*d*]pyrimidine **203**.

Ried and coworkers[331] reported a modified synthesis of thieno[2,3-*d*]pyrimidine. 5-Carbonitrile-6-chloropyrimidine **200** (Scheme 52) reacted with ethyl 2-mercaptoacetate **201** to form the intermediate **202**, which was further cyclized to afford **203**.

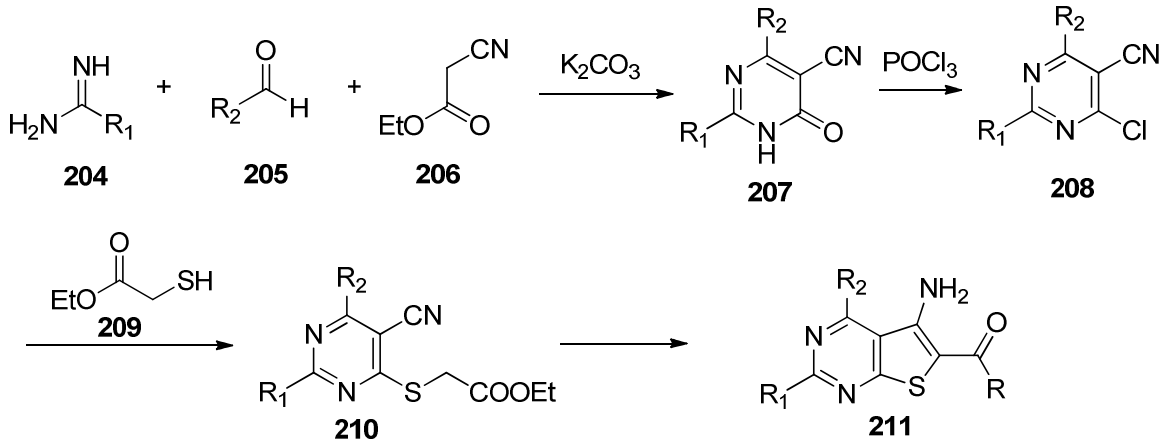

Scheme 53. Synthesis of thieno[2,3-*d*]pyrimidine **211.**

Van Straten and coworkers[334] reported the synthesis of **211** (Scheme 53) through a similar procedure. Condensation of amidine **204** with aldehyde **205** and ethyl cyanoacetate **206** in the presence of K_2CO_3 gave pyrimidone **207**, which was further

converted to 5-carbonitrile-6-chloropyrimidine **208** when treated with $POCl_3$. Upon base-mediated nucleophilic substitution and cyclization, intermediate **208** afforded thieno[2,3-*d*]pyrimidine **211**.

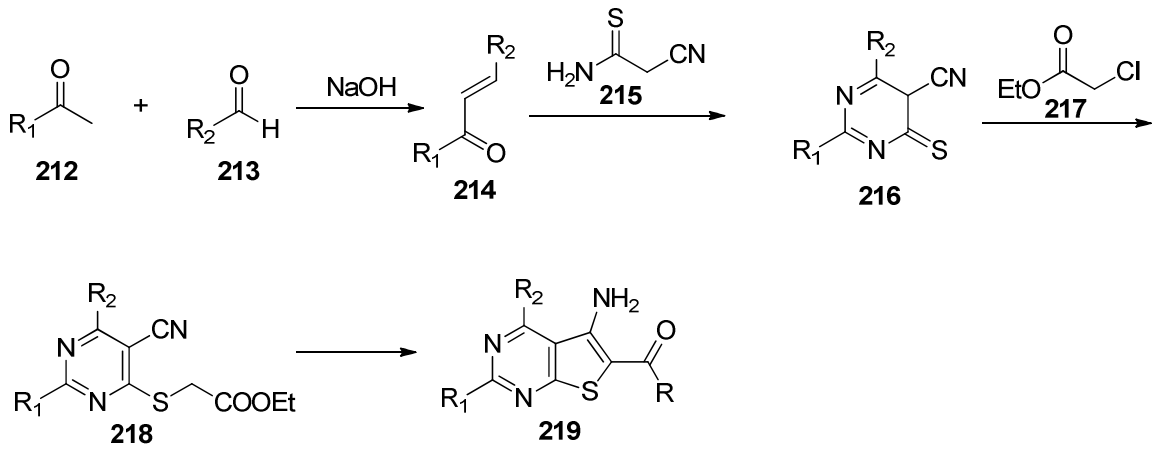

Scheme 54. Synthesis of thieno[2,3-*d*]pyrimidine **219**.

Van Straten and coworkers[334] reported the synthesis of **219** (Scheme 54) by the procedure depicted in Scheme 54. Aldol condensation of **212** and **213** afforded α,β-unsaturated ketone **214**, which condensed with 2-cyanothioacetamide **215** to afford thiopyridones **216**. Nucleophilic substitution of **216** and α-chloroester **217** followed by intramolecular cyclization afforded **219**.

D. Sulfenilation reaction to introduce side chain substitution

A few synthetic strategies are known in the literature to introduce thioester side chain substitution to pyrrolo[2,3-*d*]pyrimidines and other fused bicyclic pyrimidines. A broad classification for the synthesis of such system is:

1. Route A: Direct sulfenilation

2. Route B: Indirect sulfenilation via halogen substituted intermediate

1. Direct sulfenilation

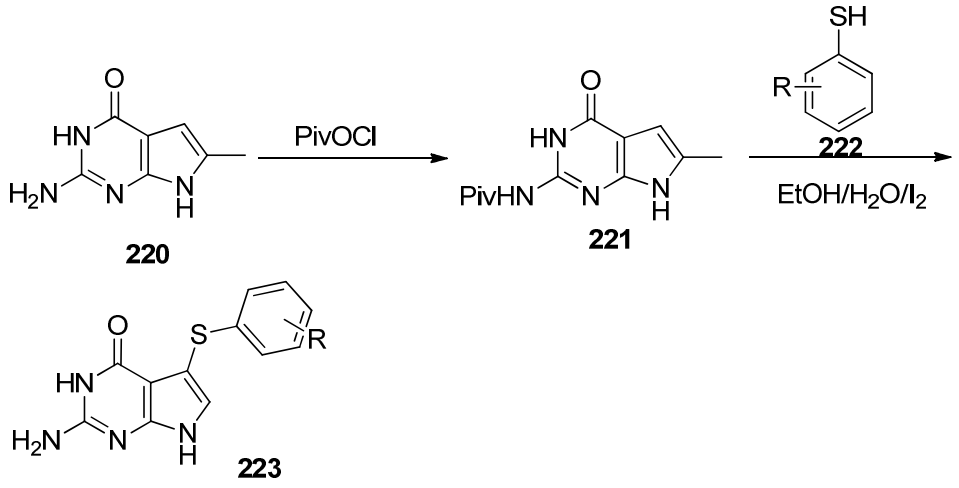

Scheme 55. Synthesis of nonclassical 5-arylthio substituted 2-amino-4-oxo-6-methylpyrrolo [2,3-*d*]pyrimidine antifolates **223**.

In 2004, Gangjee *et al.*[335] reported the synthesis of several nonclassical and a classical antifolate (Scheme 55) through a direct sulfenilation reaction. Compound **220** was converted to its pivaloyl protected derivative **221** to protect the amino group and to also improve the poor solubility of **220** for subsequent transformations. Sulfenilation was carried out with fused pyrimidine **221** and thiophenols **222** in a solution of ethanol/water with 2 equiv of iodine at 80 °C for a period of 16 h. Compound **221** was reacted with a variety of substituted thiophenols **222** to afford the 5-arylthiosubstituted compounds **223** in reasonably good yield with concomitant deprotection of the 2-pivaloyl group.

2. Indirect sulfenilation *via* halogen substituted intermediates

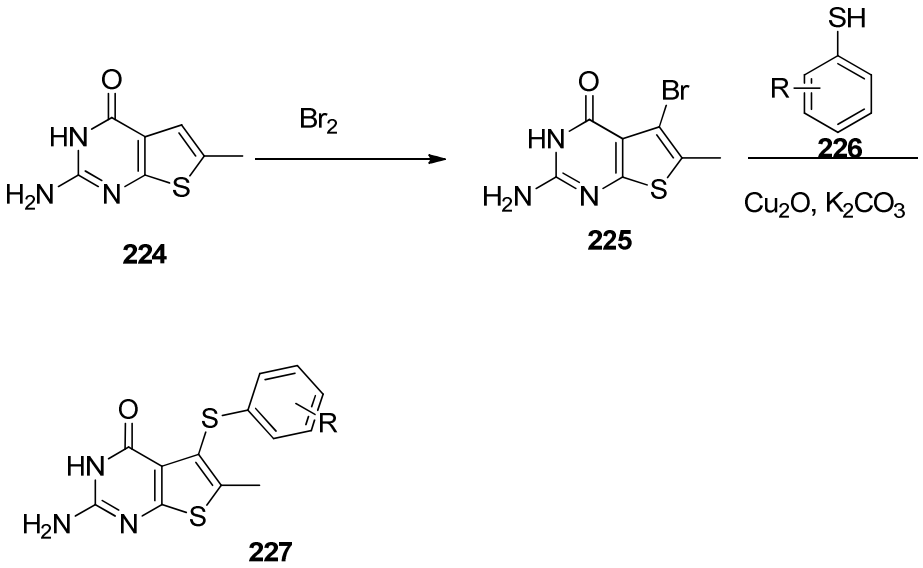

Scheme 56. Synthesis of classical and nonclassical 5-arylthio substituted 2-amino-4-oxo-6-methylthieno [2,3-*d*]pyrimidine antifolates **227**.

In 2008, Gangjee *et al*.[336] reported the synthesis of several nonclassical and a classical antifolate (Scheme 56) through indirect sulfenilation reaction *via* Ullmann coupling between arylbromide **225** and appropriate arylthiols in the presence of Cu_2O and K_2CO_3 in DMF under microwave irradiation at 180 °C for 30 min.

The required 2-amino-5-bromo-6-methylthieno[2,3-*d*]pyrimidin-4(3*H*)-one, **225** in turn was synthesized from **224** through bromination with Br_2 in acetic acid. The bromination of **224** under microwave irradiation with bromine in acetic acid at 150 °C for 30 min afforded **225** in a yield of 80%.

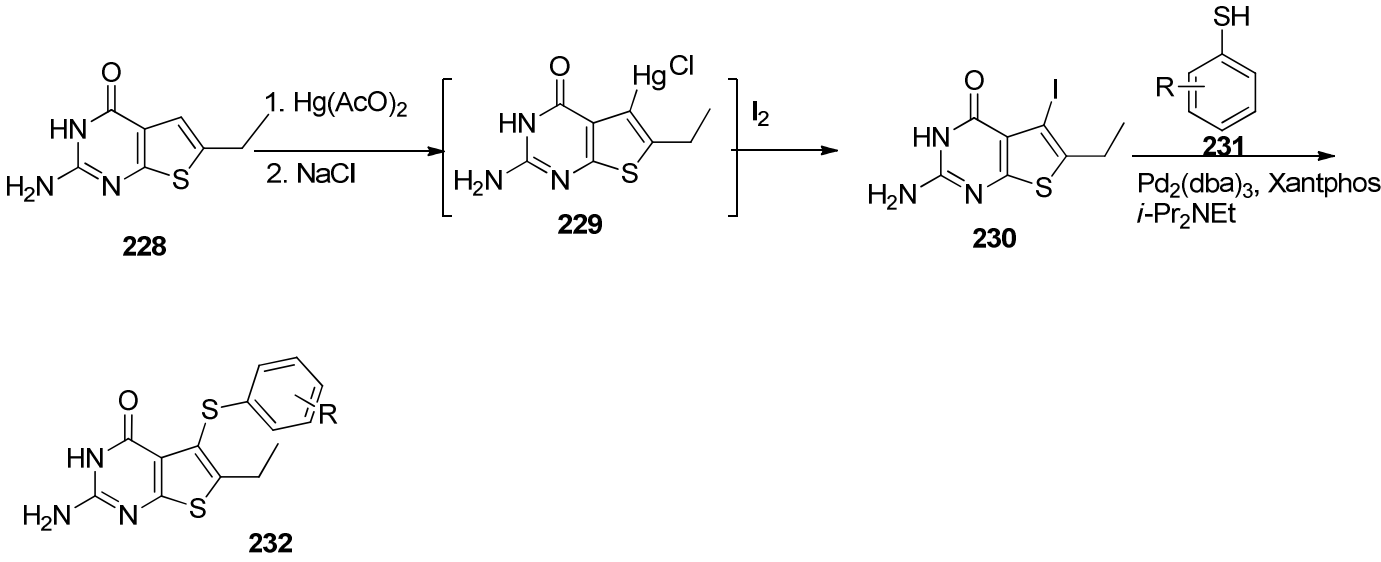

Scheme 57. Synthesis of classical and nonclassical 5-arylthio substituted 2-amino-4-oxo-6-ethylthieno [2,3-*d*]pyrimidine antifolates **232**.

In 2009, Gangjee *et al.* [337] reported an alternate strategy for the synthesis of nonclassical and classical antifolates **232** (Scheme 57) *via* indirect sulfenilation reaction between aryliodide **230** and appropriate arylthiols in the presence of palladium catalyst.

Mercuration of **228** with mercury(I) acetate in glacial acetic acid at 100 ^{o}C for 3 h, followed by treatment with NaCl solution, afforded 5-chloromercury-thieno[2,3-*d*]pyrimidine **229**. Without separation, **229** was treated with iodine in CH_2Cl_2 at room temperature for 5 h to afford **230** in 42% yield (over two steps). Palladium-catalyzed cross coupling reactions of **230**, the appropriate arylthiols **231**, and i-Pr_2NEt in DMF in the presence of $Pd_2(dba)_3$ and Xantphos under microwave irradiation at 190 ^{o}C for 1 h afforded 5-arylthio substituted 2-amino-4-oxo-6-ethylthieno[2,3-*d*]pyrimidine antifolates **232** in yields of 67-87%.

E. name reactions

The chemistry related to the present work will be reviewed and includes

1. Gewald reaction.

2. Sonogashira coupling.

3. Ullmann coupling.

4. Swern oxidation.

1. Gewald reaction.

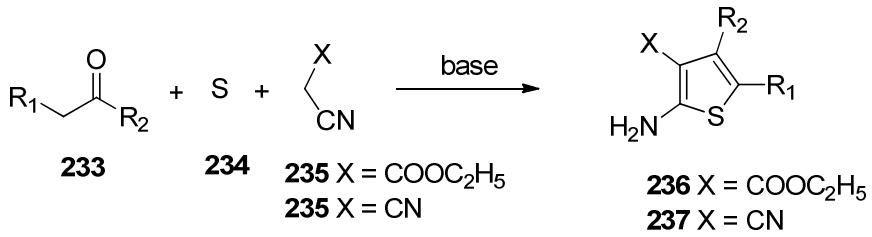

Scheme 58. A general model of the Gewald reaction.

Gewald reaction is a multi-component condensation reaction between sulfur, an α-methylene carbonyl compound and an α-cyanoester in the presence of morpholine as catalyst to give 2-aminothiophenes.[319] The Gewald reaction is the most convergent and well-established approach for the preparation of multiple substituted 2-aminothiophenes.

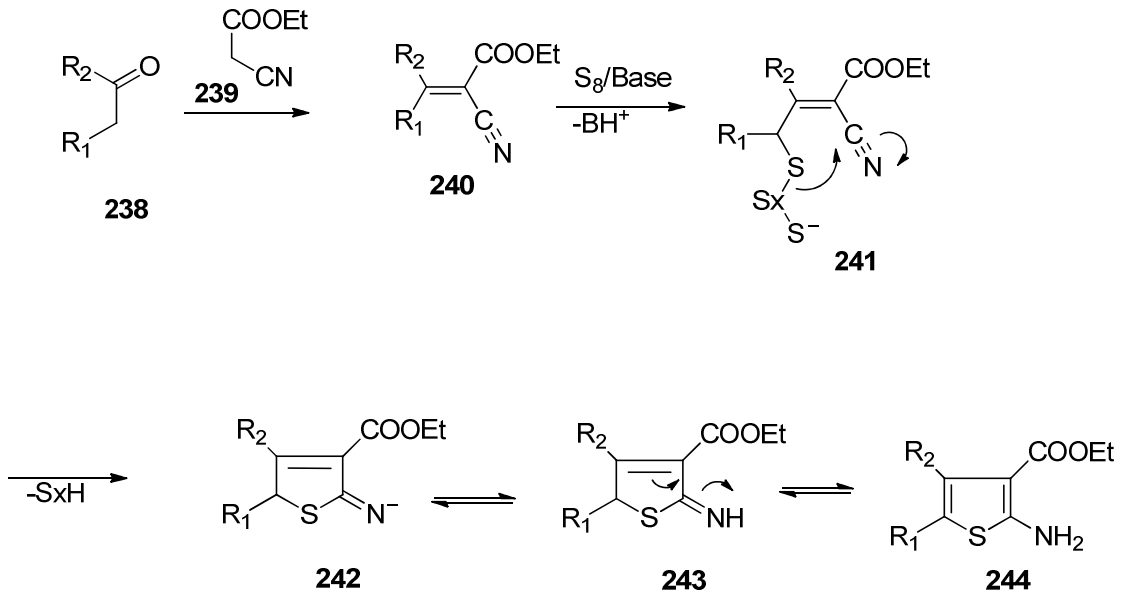

Scheme 59. The proposed mechanism of the Gewald reaction.

The reaction mechanism of the Gewald reaction has been recently elucidated As shown in Scheme 59, the first step is a Knoevenagel condensation between the α-methylene carbonyl compound **238** and an α-cyanoester **239** to produce intermediate **240**. Through an unknown mechanism, intermediate **240** reacts with elemental sulfur to afford intermediate **241**, which is further converted to 2-aminothiophenes via cyclization and tautomerization.

New procedures of the Gewald reactions have been developed under microwave or solvent free conditions. In 2007, Sridhar *et al*. reported[338] the first application of KF-alumina as a base for the preparation of 2-aminothiophenes by microwave accelerated multi-component condensation. Although the reactions proceeded well under conventional heating at reflux in ethanol, the microwave condition offered an efficient and convenient modification to the Gewald reaction as it can be carried out with very

short reaction times and excellent yields.

2. Sonogashira coupling.

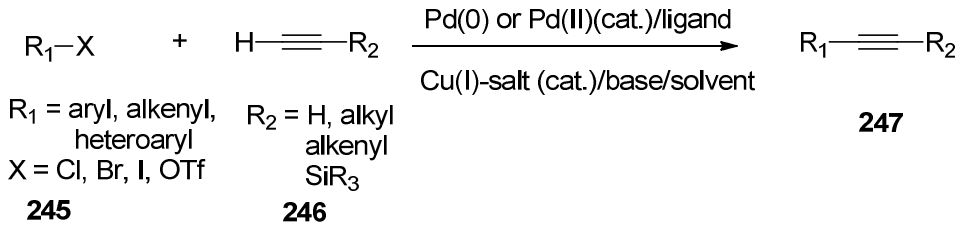

Scheme 60. A general model for Sonogashira cross-coupling.

In 1975, Sonogashira *et al.* [339] reported the synthesis of symmetrically substituted alkynes *via* a coupling reaction between acetylene gas and aryl iodides or vinyl bromides in the presence of catalytic amounts of $Pd(PPh_3)Cl_2$ and CuI under mild conditions. Thus, the copper-palladium catalyzed coupling of terminal alkynes with aryl and vinyl halides to give enynes is called the Sonogashira cross-coupling. Typically, two catalysts, a zerovalent palladium complex and a halide salt of copper(I), are necessary for the reaction. The reaction also requires basic medium to neutralize the hydrogen halide produced as the byproduct of this coupling reaction. The reactivity order of the aryl and vinyl halides is I ≈ OTf > Br >> Cl.[349]

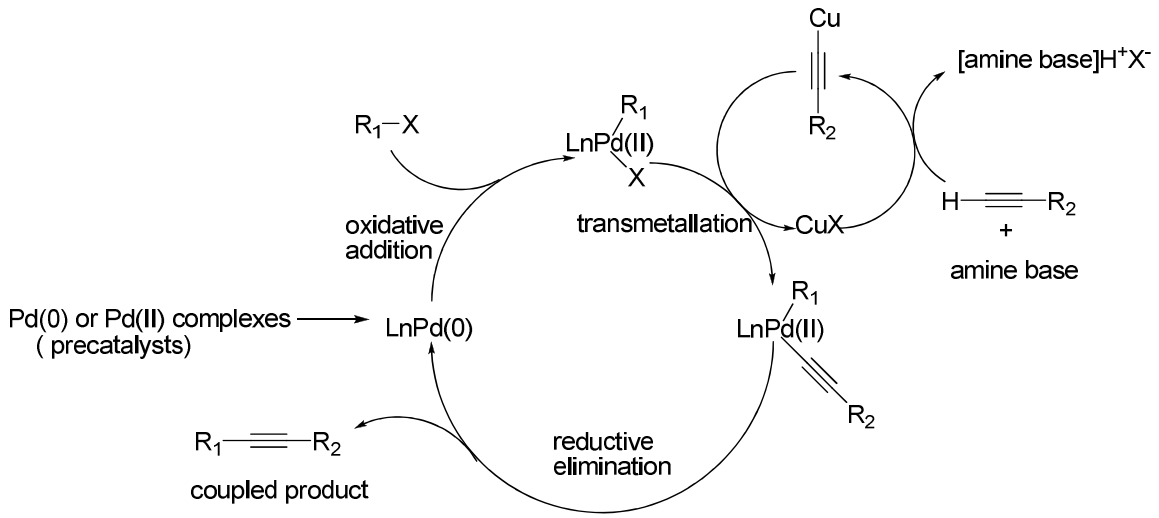

Scheme 61. Mechanism of Sonogashira cross-coupling.[340]

Sonogashira cross-coupling is believed to involve oxidative addition-reductive elimination pathway (Scheme 61), although the mechanism is not clearly understood.

.

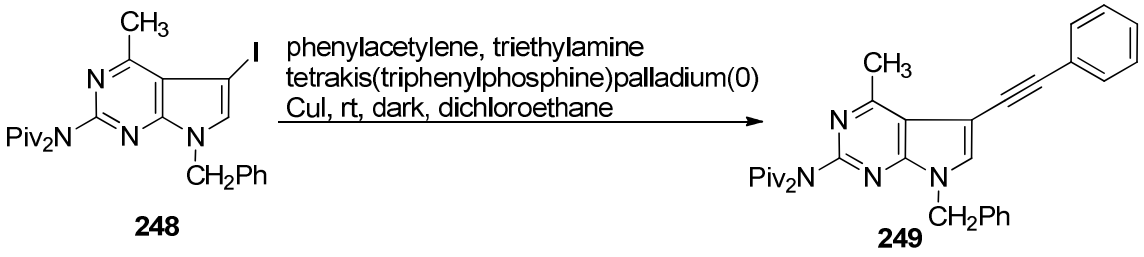

Scheme 62. Synthesis of *N*-(7-benzyl-4-methyl-5-(phenylethynyl)-7*H*-pyrrolo[2,3-*d*]pyrimidin-2-yl)-*N*-pivaloylpivalamide **249**.

In 2007, Gangjee *et al.* [341] reported the synthesis of *N*-(7-benzyl-4-methyl-5-(phenylethynyl)-7*H*-pyrrolo[2,3-*d*]pyrimidin-2-yl)-*N*-pivaloylpivalamide **249** (Scheme 62) from *N*-(7-benzyl-5-iodo-4-methyl-7*H*-pyrrolo[2,3-*d*]pyrimidin-2-yl)-*N*-

pivaloylpivalamide and phenylacetylene **248** *via* a Sonogashira cross-coupling in the presence of tetrakis(triphenylphosphine)palladium(0) and CuI as catalysts in dichloromethane (Scheme 62).

3. Ullmann coupling.

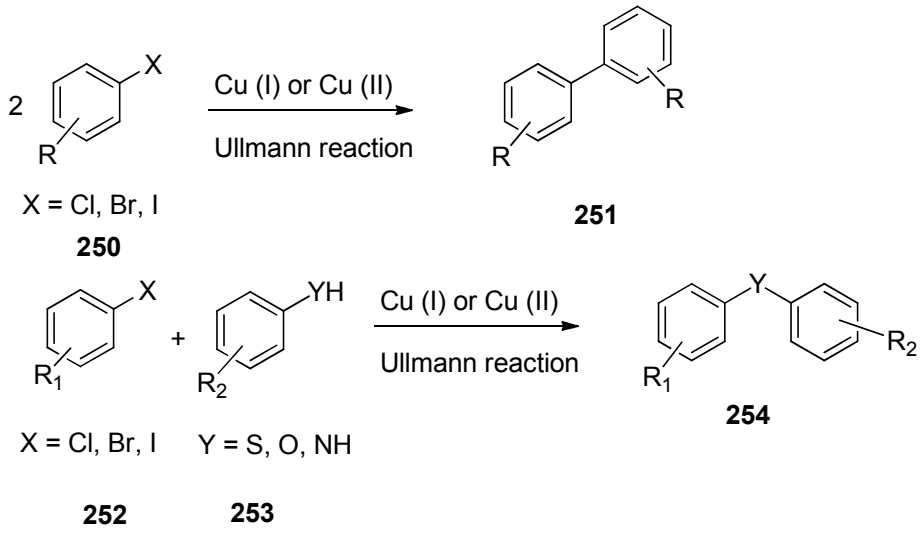

Scheme 63. A general model for Ullmann coupling.

Ullmann-coupling is the copper-catalyzed nucleophilic aromatic substitution between various nucleophiles with aryl halides (Scheme 63).[342, 343] The Ullmann coupling involves the formation of a C-O, C-N and C-S bond by the reaction between an aryl halide with phenol, aniline and thiophenol. Typically Ullmann coupling requires harsh reaction conditions including high temperatures (> 200 ^{o}C), strong bases, and long reaction times. In addition, the classical Ullmann reaction is limited to electron deficient aryl halides and can only affords moderate yields. The application of modern variants of the Ullmann reaction employing palladium and nickel have widened the substrate scope

of the reaction and rendered reaction conditions more mild. [344]

Although the reaction mechanism of the Ullmann reaction has been extensively studied, the exact mechanistic pathway is unknown.[345] According to radical scavenger experiments and electron spin resonance, radical mechanisms have been ruled out. Although the exact nature (oxidation state) of the Cu-intermediate is not known, the reaction is proposed to involve the formation of an organocopper compound (RCuX), which reacts with the other aryl reactant in a nucleophilic aromatic substitution.

In 2008, Gangjee *et al*. [336]reported the synthesis of several nonclassical and a classical antifolate *via* Ullmann coupling between arylbromide **225** (Scheme 53) and arylthiol nucleophiles in the presence of Cu_2O and K_2CO_3 in DMF under microwave irradiation at 180 °C for 30 min.

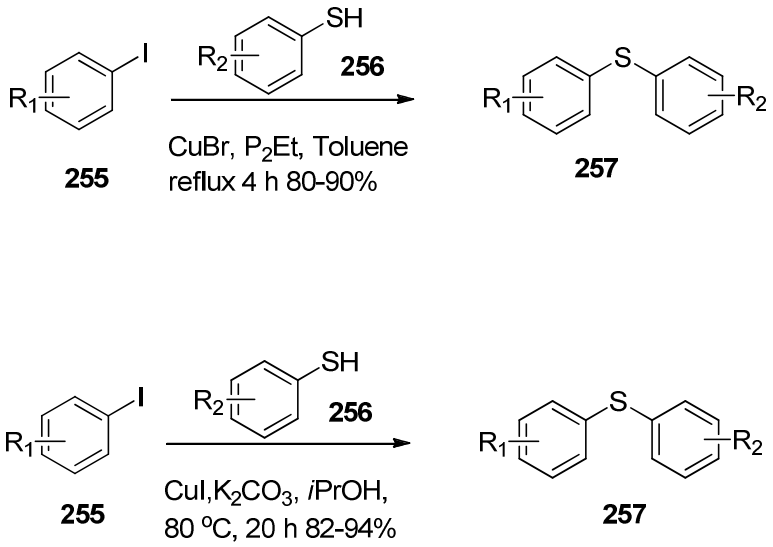

Scheme 64. Synthesis of thioether **257**.

Palomo *et al.*[346] have reported the formation of a C-S bond via Ullmann coupling

(Scheme 64) at lower temperature (80-110 ^{o}C) with high yield.

.

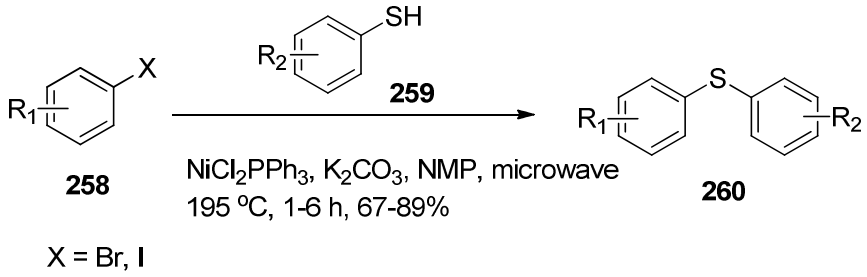

Scheme 65. Synthesis of thioether **260** under microwave assisted Ullmann coupling condition.

Microwave assisted organic synthesis has been widely used in organic synthesis, resulting in faster and cleaner reactions. In 2010, Chen and coworkers[347] reported Nickle catalyzed Ullmann coupling (Scheme 65).

4. Swern oxidation.

Swern oxidation is an oxidation procedure to convert primary or secondary alcohols to the corresponding aldehydes or ketones using dimethyl sulfoxide DMSO and oxalyl chloride.[348] The reaction has mild character and can tolerate a wide range of functional groups.

From a mechanistic point of view, the Swern oxidation proceeds through three steps (Scheme 66): the activation of DMSO, the activation of the alcohol and formation of the product.

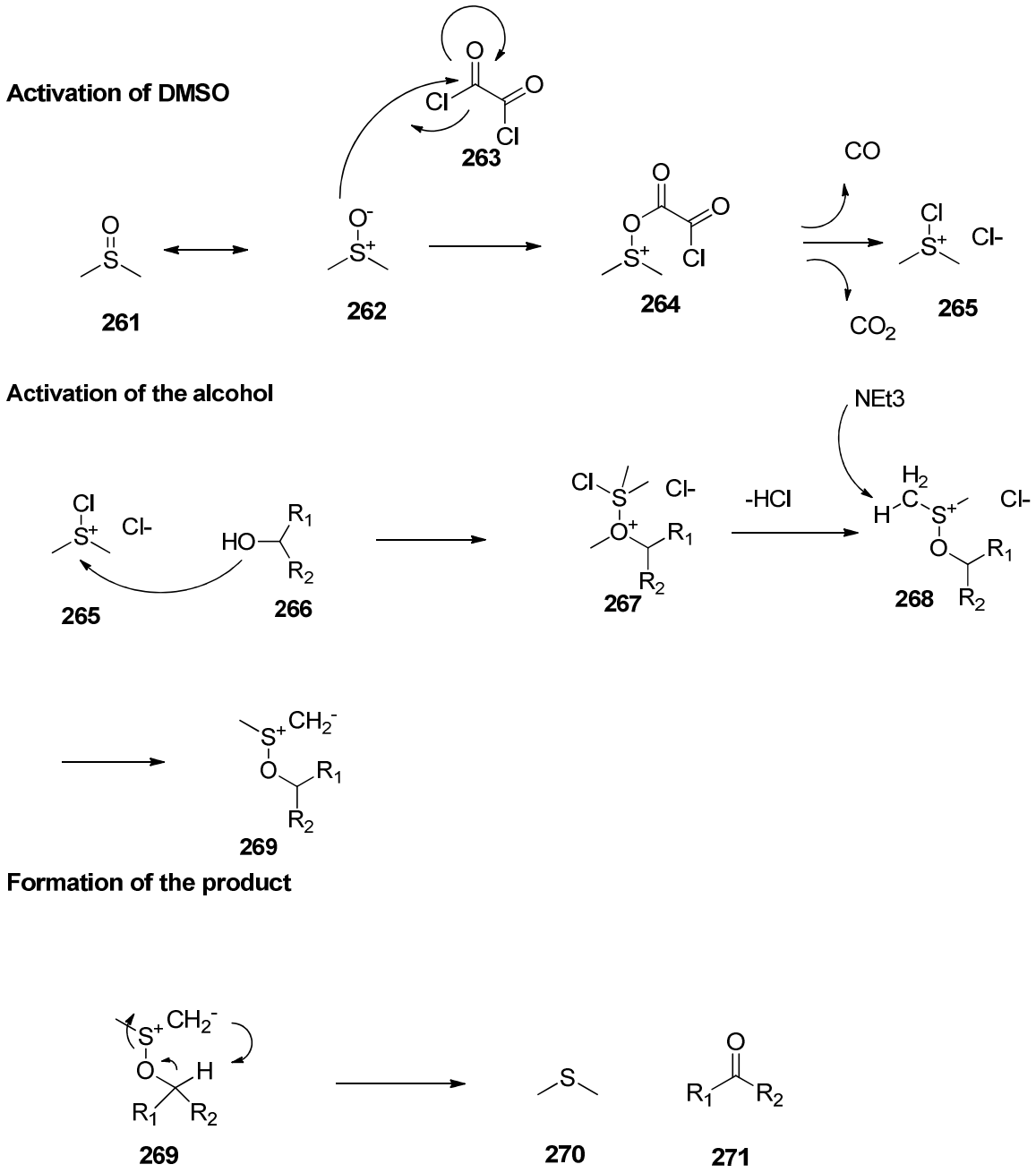

Scheme 66. The mechanism of Swern oxidation.

In the first stage, DMSO reacted with oxalyl chloride to form intermediate **264** , which quickly decomposed to release CO_2 and CO and to produce

dimethylchlorosulfonium chloride **265**.

After the addition of alcohol into the reaction medium, the dimethylchlorosulfonium chloride **265** reacted with the alcohol to give the key alkoxysulfonium ion intermediate **267**,which was deprotonated to give the sulfur ylide **269** upon treatment with base. The sulfur ylide **269** decomposed to give dimethyl sulfide and the desired aldehyde or ketone.

III. STATEMENT OF THE PROBLEM

1. 6,5,6-tricyclic Benzo[4,5]thieno[2,3-*d*]pyrimidines as Dual Thymidylate Synthase and Dihydrofolate Reductase Inhibitors

Folate metabolism is an attractive target for chemotherapy, because of its critical importance in the biosynthesis of purine and pyrimidine nucleic acids. Antifolates that target folate metabolism have found clinical utility as antitumor, antimicrobial, and antiprotozoal agents.[5,13,20,21,22] Among the folate dependent enzymes, thymidylate synthase (TS) and dihydrofolate reductase (DHFR) have been of particular interest. TS is a key enzyme in the *de novo* synthesis of 2'-deoxythymidine-5'-monophosphate (dTMP) from 2'-deoxyuridine-5'-monophosphate (dUMP).[26,349] The reaction requires 5,10-methylenetetrahydrofolate (5,10-CH_2THF) as a cofactor for one carbon unit transfer and represents the only *de novo* pathway for intracellular dTMP synthesis. DHFR catalyzes the reduction of dihydrofolate to tetrahydrofolate, and is indirectly responsible for dTMP synthesis by maintaining the reduced folate pool.[25]

Raltitrexed (RTX),[350] pemetrexed (PMX)[351] and methotrexate (MTX)[352] (Figure 29) are examples of TS and/or DHFR inhibitors used in the clinic. RTX, approved in several European countries, Australia, Canada, and Japan for the treatment of advanced colorectal cancer, is a TS inhibitor that undergoes rapid polyglutamylation by the enzyme folylpolyglutamate synthetase (FPGS).[186,353] PMX, in combination with cisplatin, was approved for the treatment of malignant pleural mesothelioma and also for non-small cell lung cancer. With TS inhibition as the primary mechanism of action, PMX was reported to inhibit several other folate-dependent enzymes including DHFR, glycinamide ribonucleotide formyltransferase (GARFTase), and aminoimidazole

carboxamideribonucleotide formyltransferase (AICARFTase).[351] Similar to RTX, polyglutamyltion by FPGS is essential for the cytotoxicity of PMX.

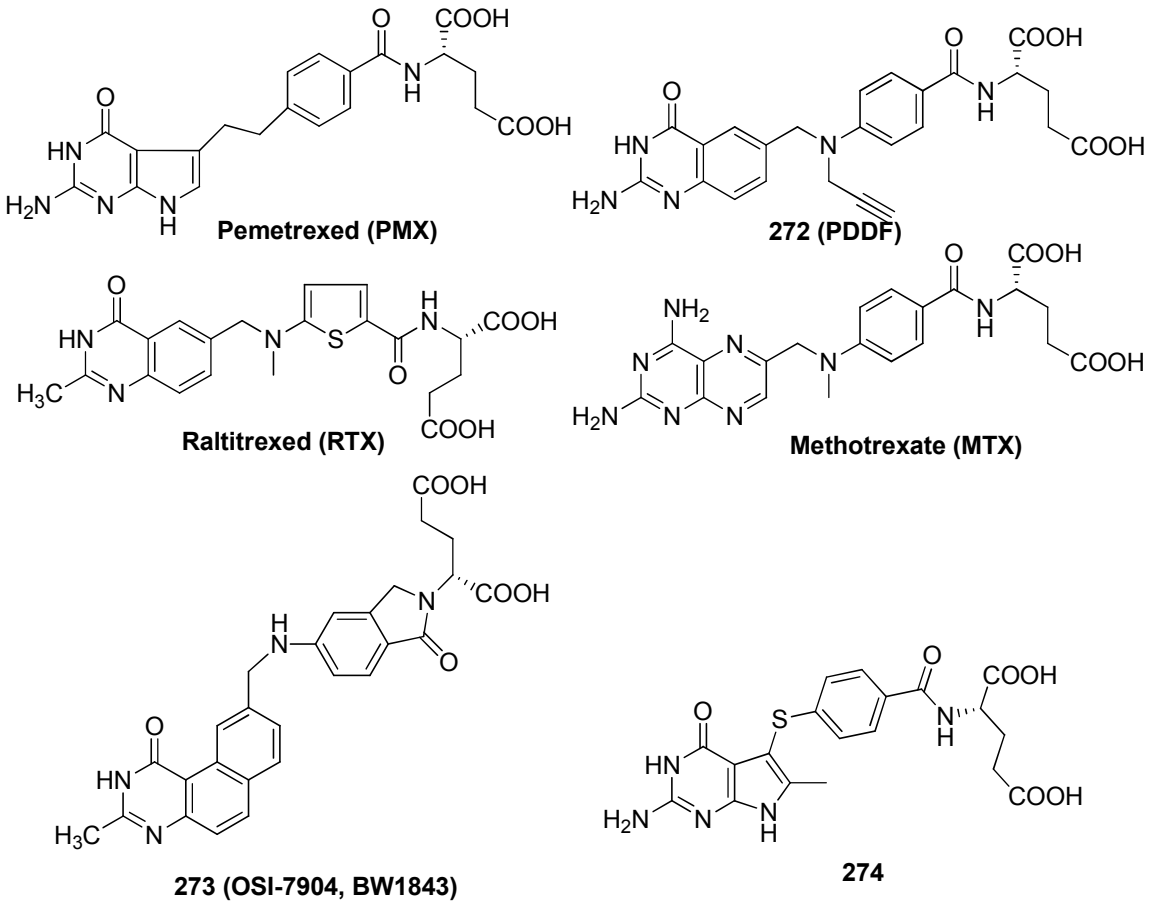

Figure 29. Antifolates

Classical antifolates, such as RTX and PMX, that have an *N*-benzoyl-L-glutamic acid side chain usually function as substrates for FPGS, which leads to high intracellular concentrations of these antitumor agents and increases TS inhibitory activity for some

antifolates (RTX, 60-fold and PMX 130-fold) compared to their monoglutamate forms.[187,188,350,351] Although polyglutamylation of certain antifolates (such as RTX and PMX) is necessary for their cytotoxic activity, it has also been implicated in toxicity to host cells, because of the longer cellular retention time of such polyanionic poly-glutamate metabolites.[190] In addition, reduced expression of FPGS in tumor cells can lead to resistance to FPGS dependent classical antifolates such as PMX.[192,193,194]

To circumvent the potential tumor resistance problems associated with FPGS, classical antifolates should have high enzyme inhibitory potency as their monoglutamate forms and not require polyglutamylation by FPGS to exert their antitumor activity.[354,355]

It has been of interest not only to design potent TS and DHFR inhibitors but also to design and synthesize single agents that have potent dual TS and DHFR inhibitory activity in a single molecule. Such dual inhibitors could act at two different sites (TS and DHFR) and might be capable of providing "combination chemotherapy" in single agents without the pharmacokinetic, overlapping toxicities and other disadvantages of two separate agents.[354] This strategy may also lead to an improved toxicity profile.

Typically, antifolates that contain a 2-methyl-4-oxo substitution in the pyrimidine ring (such as RTX) are TS inhibitors, while 2-amino-4-oxo substitution in the pyrimidine ring (such as PMX) may provide affinity for both TS and DHFR. 2,4-Diamino substitutions on the pyrimidine ring of antifolates is usually associated with DHFR inhibitory activity.

In an attempt to prevent or minimize the potential problems associated with FPGS, including tumor resistance, and to develop dual TS and DHFR inhibitors, Gangjee *et al*.[354] reported the synthesis of a classical antifolate *N*-{4-[(2-amino-6-methyl-4-oxo-4,7-

dihydro-3*H*-pyrrolo[2,3-*d*]pyrimidin-5-yl)thio]benzoyl}-L-glutamic acid, **274** (Figure 29), as a potent inhibitor of isolated hTS (IC_{50} = 42 nM) with a reasonable inhibition of human recombinant DHFR (IC_{50} = 2.2 μM) in its monoglutamate form thus providing dual inhibitory activity of TS and DHFR. Compound **274** was equipotent with **272** (Figure 29), a potent TS inhibitor, against hTS and was more potent than the clinically used RTX and PMX against isolated hTS in their monoglutamate forms. Molecular modeling (SYBYL 6.91)[356] suggested that the 6-methyl group in compound **274** makes important hydrophobic contacts with Trp109 in hTS and also serves to lock the 5-position side chain into favorable, low energy conformations. Both these factors probably contribute to the high inhibitory activity of **274** in its monoglutamate form against hTS.

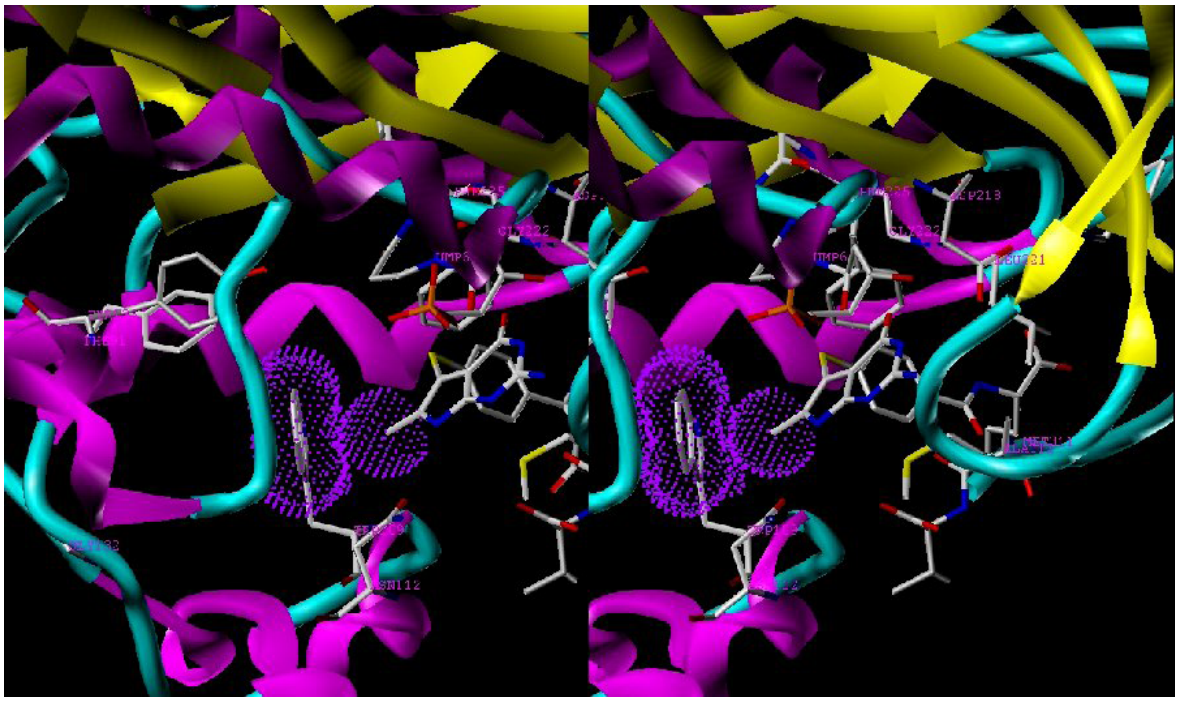

Figure 30. Stereoview compound **274** superimposed on pemetrexed (not shown) in human TS (PDB1JU6395), indicating the interaction of the 6-CH_3 with Trp109.

A potential advantage of compound **274** over RTX and PMX is that it is not a substrate for hFPGS, from CCRF-CEM cells, at concentrations up to 1045 μM.[354] The lack of hFPGS substrate activity of **274** was attributed, in part, to the presence of the 6-methyl group on the pyrrolo[2,3-*d*]pyrimidine of **274**. The 6-methyl group of **274** probably creates steric hindrance in its binding to the active site of hFPGS. Alternatively, the 6-methyl group of **274** may force the 5-position side chain into a conformation that is not conducive for binding to hFPGS. The fact that PMX, a pyrrolo[2,3-*d*]pyrimidine, much like **274**, lacks a 6-methyl group and is a substrate for FPGS lends credence to the involvement of the 6-methyl moiety in preventing FPGS substrate activity in **274**.

Tricyclic **273** (Figure 29) is a classical TS inhibitor with K_i = 0.09 nM.[354] Although this compound is an excellent substrate for FPGS, it is subject to the addition of only one additional glutamic acid. Moreover, the high potency of **273** does not rely on polyglutamation. The monoglutamate form is equi-potent with the diglutamate form.[116] Compound **273** is a noncompetitive TS inhibitor and its activity is not affected by the concentration of 5,10-CH_2THF.[357,358] In addition, it has been demonstrated that overexpression of the multidrug resistance proteins, MRP1 and MRP2, can confer tumor resistance to short term (4 h), but not long term (72 h), exposure of **273**.[19]

In the course of our structure-based drug design program it was of interest to synthesize classical antifolates **275-278** with a benzo[4,5]thieno[2,3-*d*]pyrimidine scaffold (Figure 31), as structural hybrids of **273** and **274**. Compounds **275** and **276,** similar to **273**, have a 2-methyl-4-oxo pyrimidine ring which is generally associated with TS inhibition. In contrast, 2**77** and 2**78** have a 2-amino-4-oxo substituent, which could

afford dual TS and DHFR inhibition, as observed for **274** and PMX.

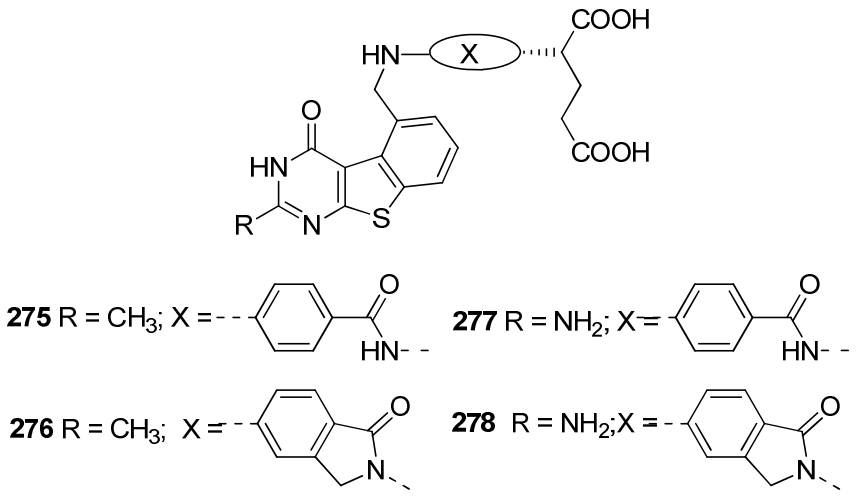

Figure 31. Target classical antifolates with the tricyclic benzo[4,5]thieno[2,3-*d*]pyrimidine scaffold.

The 2-substitutions on **275-278** would access the importance of hydrogen-bonding at this position (2**77, 278**) versus hydrophobic binding (**275, 276**) to biological activity. The size of a sulfur atom in **275-278** is larger than a nitrogen atom and smaller than two carbon atoms, thus the thiophene B-ring in benzo[4,5]thieno[2,3-*d*]pyrimidines **275-278** mimics both the smaller pyrrolo B-ring in **274** and the larger quinazoline B-ring in **273** (Figure 32).

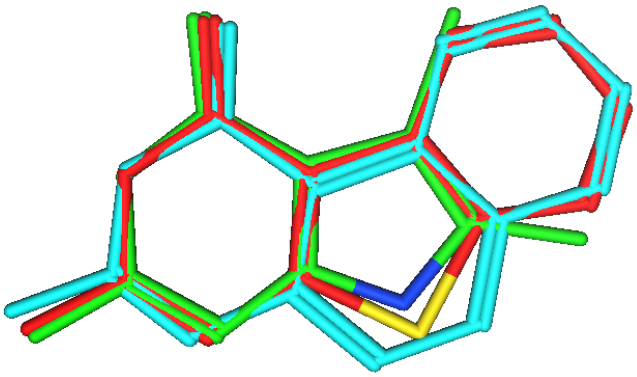

Figure 32. Superimposition of benzo[4,5]thieno[2,3-*d*]pyrimidine (red), pyrolo[2,3-*d*]pyrimidine (green) and benzo[*f*]quinazoline (cyan).

Similar to the C-ring in **273** and the 6-methyl group in **274**, the benzo C-ring in **275-278** makes hydrophobic contacts with Trp109 in hTS and restricts the side chain to a conformation conducive for potent TS activity but perhaps not for FPGS substrate activity.

To explore the effects of side chain flexibility on biological activity, **275** and **277** have the same benzoylglutamate side chain as **274**, while **276** and **278** have a more conformationally restricted 2-isoindolinyl-L-glutamate side chain like **273**. Unlike other classical TS inhibitors, the glutamate side chain in **273** is part of an isoindolinone system, which restricts the side chain conformation. The crystal structure of the ternary complex TS-dUMP-**273** (PDB: 1SYN) [359] revealed that the binding of **273** and the nucleotide induced a closed conformation of the TS protein, similar to other antifolates. Surprisingly, however, the binding surface of **273** includes a hydrophobic patch from Val 77 that is normally buried and not on the surface.[359]

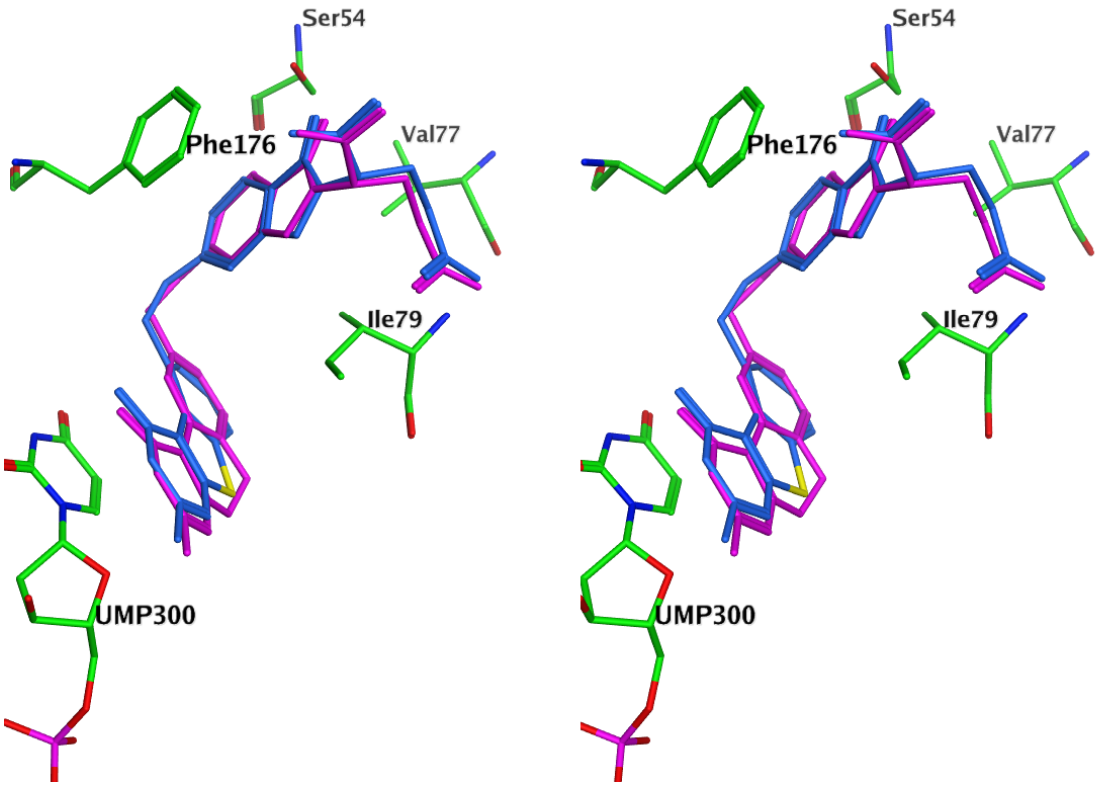

Figure 33. Stereoview of compound **276** (blue) superimposed on **273** (purple) in ecTS (green). Figure prepared with MOE 2008.10.[356]

As shown in Figure 33, molecular modeling using MOE 2008.10[356] revealed that when the central ring in **273** is truncated to a 5-member ring in the benzo[4,5]thieno[2,3-*d*]pyrimidine **276**, and the substitution is moved from the 6-position to the 5-position, the resulting compound binds to TS in a manner similar to **273**.

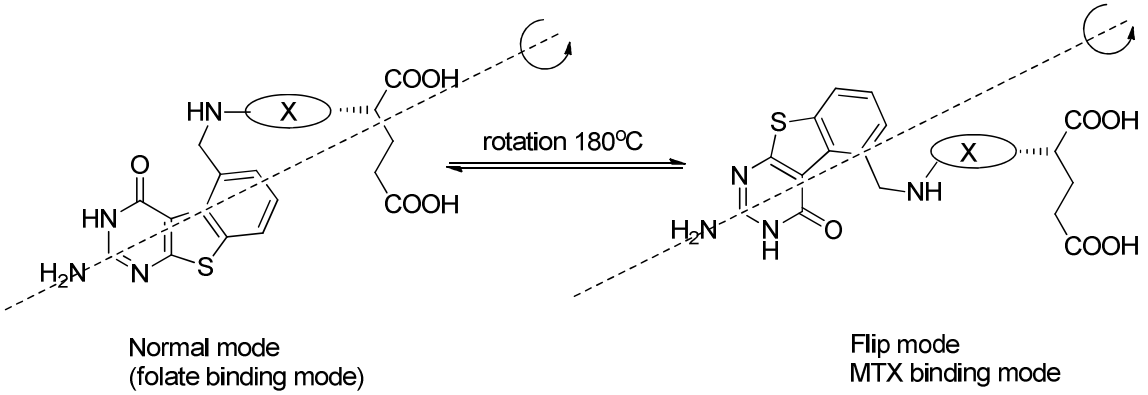

Figure 34. Proposed binding mode with DHFR. The "Normal mode" is defined as the binding mode of folic acid (a 2-amino-4-oxo pyrimidine system) to human DHFR. The "flipped" mode is defined as the binding mode when folic acid is rotated about the C_2-NH_2 bond by 180°.

Molecular modeling suggested that although 2-methyl substituted compounds **275** and **276** can not form a salt bridge with Glu30 of hDHFR at the N1 and $2NH_2$, like MTX, the 2-amino compounds **277** and **278** can bind just like folate (PDB: 1U72) in which the 2-amino-4-oxo group binds to the enzyme with hydrogen bonding and the heterocycle and the benzoyl moieties bind to Phe31, Phe34 and Ile 60. The α-carboxylic acid of the glutamate makes ionic contact with Arg70. According to molecular modeling, a second mode of binding would involve a 180° rotation about the C-2, NH_2 bond (Figure 34), whereby the sulfur of the thiophene ring is now superimposed on the 4-oxo group of folate, with all other interactions being the same. It is important to note that binding of **277** and **278** in the flip mode (Fig. 32) also allows the sulfur of the thiophene ring to mimic the 4-amino of MTX. To determine which of these two modes of binding the

molecule adopts to bind hDHFR, **277** and **278** were each cocrystalized with isolated hDHFR (Dr. Vivian Cody).

2. Classical and Nonclassical 2-Amino-4-oxo-5-arylthio-substituted-6-propyl thieno[2,3-*d*]pyrimidines as Dual Thymidylate Synthase and Dihydrofolate Reductase Inhibitors and Potential Agent for *Toxoplasma gondii* Infection

As mentioned before, classical antifolates that have an *N*-benzoyl-L-glutamic acid side chain such as RTX and PMX are, in most cases, able to function as substrates for folylpolyglutamate synthetase (FPGS),[350, 351] which leads to high intracellular concentrations of these antitumor agents and increases TS inhibitory activity for some antifolates (RTX 60-fold and PMX 130-fold) compared to their monoglutamate forms. Although polyglutamylation of certain antifolates is necessary for their cytotoxic activity, it has also been implicated in toxicity to host cells, because such polyanionic poly-glutamate metabolites have a longer cellular retention time and do not efflux from normal cells. Additionally, tumor cells can develop resistance to classical antifolates which depend on polyglutamylation for their antitumor effects by decreasing FPGS expression. The problem of resistance in tumors, due to low or defective FPGS, has placed limitations on the use of classical antifolates, which depend on polyglutamylation for their cytotoxicity. Classical antifolates also require carrier systems such as reduced folate carrier (RFC) to gain entry into the target cells. A decreased expression in folate transporter systems represents another mechanism for drug resistance.

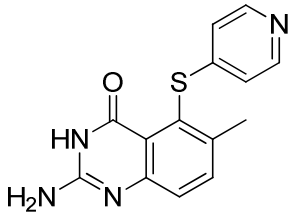

Nolatrexed

Figure 35. The structure of Nolatrexed.

Lipophilic nonclassical antifolates were designed to overcome the problem of drug resistance associated with classical antifolates. These lipophilic nonclassical antifolates lack the polar glutamate side chain found in classical antifolates and hence do not depend on FPGS for their inhibitory activity of the target enzymes. Additionally, they also do not require the RFC system for active uptake into the cell since they are lipophilic and are passively transported into cells. Nolatrexed (Figure 35) is the first nonclassical TS inhibitor in clinical trials as an antitumor agents.[364, 365]

Nonclassical dual TS and DHFR inhibitors also have the potential to treat opportunistic infections in immunocompromised patients such as those with acquired immunodeficiency syndrome (AIDS). The principal cause of death in patients with AIDS is opportunistic infections caused by *Pneumocystis carinii* (*P. carinii*) and *Toxoplasma gondii* (*T. gondii*).[366-368] Due to the limits of current therapies,[67,369-371] it is of considerable interest to incorporate selectivity and potency into a single nonclassical antifolate that can be used alone to treat these infections.

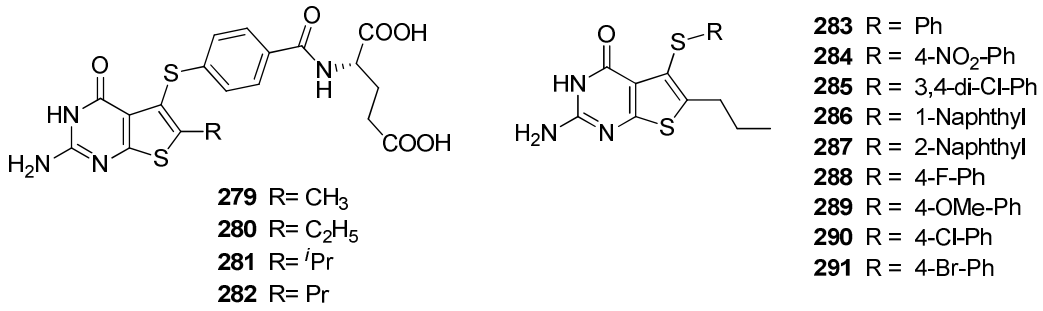

Figure 36. The structure of thieno[2,3-*d*]pyrimidine antifolates.

Gangjee *et al.* [337]recently discovered the potent TS inhibitory activity of a series of 2-amino-4-oxo-5-arylthio-substituted-6-ethylthieno[2,3-*d*]pyrimidine analogues. Compound **279** (Figure 36) is a potent dual inhibitor of human TS (IC_{50} = 54 nM) and human DHFR (IC_{50} = 19 nM). Molecular modeling using (SYBYL 8.0)[356] indicated that the 6-methyl group in **279** and the 6-ethyl group in **280** make important hydrophobic contacts with Trp109 in human TS and also sterically restrict the rotation of the 5-position side chain so that it adopts a favorable conformation for binding to human TS.

Gangjee *et al.*[337] previously reported the crystal structure of **279** and **280** bound to natural and mutant human DHFR (PDB: 3GHW & 3GHC). In both crystal structures, thieno[2,3-*d*]pyrimidine inhibitors were shown to bind with DHFR in the "normal" folate orientation. The crystal structures also indicated that the 6-substitutent interacted with a small hydrophobic pocket composed of Ile7, Thr56 and Val115 (Figure 37).

To determine the optimum size of the 6-alkyl group for TS and DHFR inhibitory activity, classical 6-isopropyl substituted thieno[2,3-*d*]pyrimidines **281** (Figure 36) and nonclassical analogues were also synthesized and evaluated.

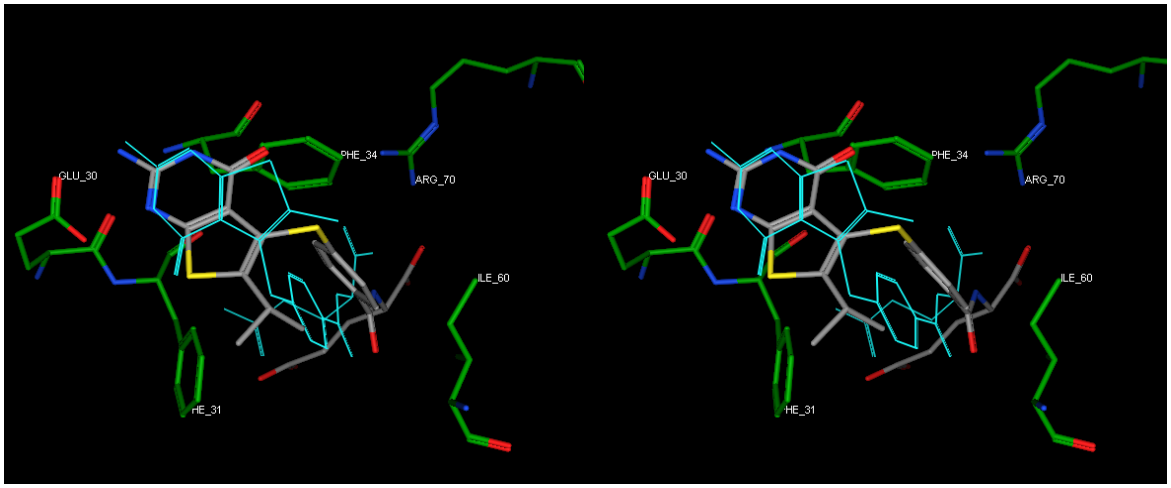

Figure 37. Stereoview: X-ray crystal structure of **280** with double mutant human DHFR (PDB : 3GHC), generated by MOE 2008.10**.**[363]

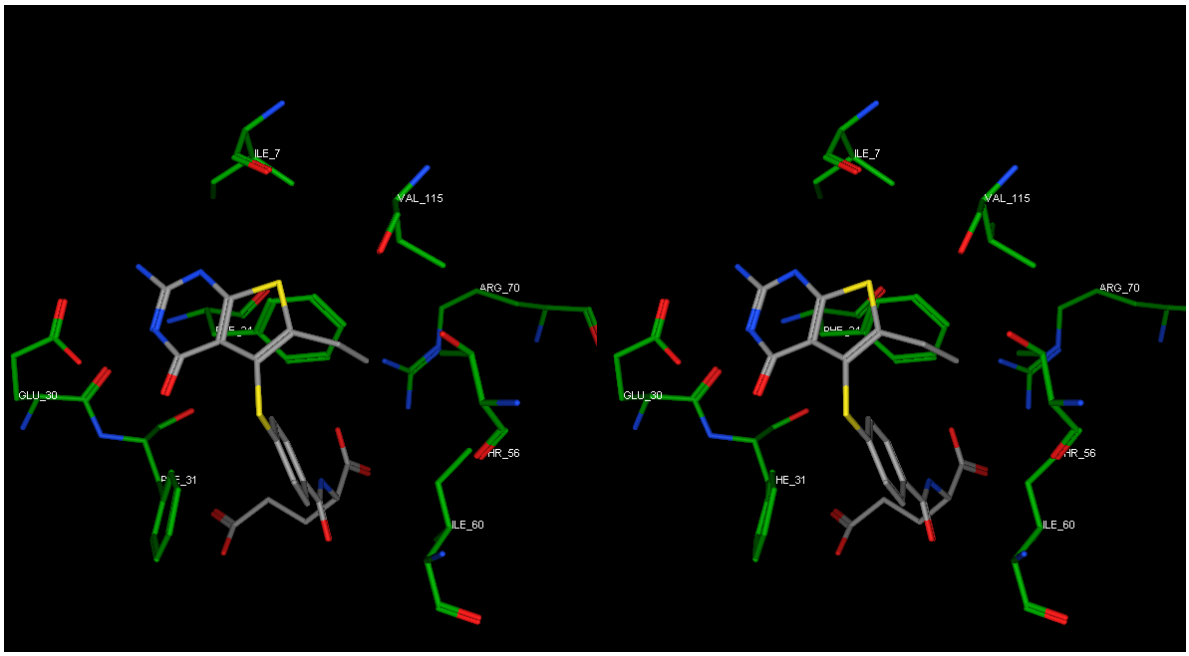

Figure 38. Stereoview: docking structure of **281** (gray) in human DHFR and **279** (blue) complex in the "flipped" mode (PDB : 3GHW), generated by MOE 2008.10.[363]

Molecular modeling revealed that compound **281** could not bind to human DHFR

in the “normal” mode, because of the steric clash between the bulky 6-isopropyl group and the narrow hydrophobic pocket (Ile 7, Thr 56 and Val 115). Instead, compound **281** adopts a “flipped” mode to bind with human DHFR compared to folic acid. Docking of **281** into the crystal structure of **279** (blue) in human DHFR (PDB : 3GHW) shows the sulfur atom of the thieno ring to be close to the 4-oxo group of **279** (Figure 38). In this binding mode, the Glu30 residue also interacts with the 2-NH_2 and N1 moieties of **281**. The *p*-aminobenzoyl ring along with thieno[2,3-*d*]pyrimidine ring makes hydrophobic interactions with Phe31, Phe34, and Ile60, and the α-COOH forms an ionic bond with Arg70 just as compound **279** does with human DHFR in the “normal” binding mode. The flipped mode of **281** resulted in a 10-fold decrease in its activity compared with compounds (**279**, **280)** having a straight chain substitution at 6-position.

To further explore the optimal size at the 6-position, classical and nonclassical 6-*n*-propyl straight chain substituted thieno[2,3-*d*]pyrimidines **282-291** (Figure 36) were designed.

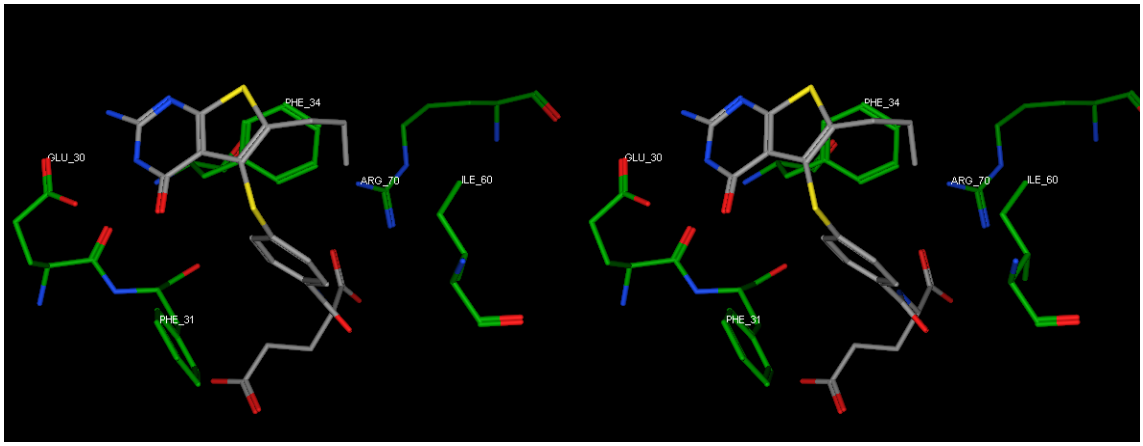

Figure 39. Stereoview: compound **282** bound to human DHFR in “normal” mode (PDB : 3GHW), generated by MOE 2008.10.[363]

Molecular modeling also revealed that when the 6-substitution was a straight chain propyl group, the compounds retain the ability to bind the human DHFR in the "normal" binding mode and restore human DHFR inhibitory activity. In the "normal" binding mode (Figure 39), compound **282** binds just like folic acid (PDB : 1DRF), **279** (PDB : 3GHW) and **280** (PDB : 3GHC). In this binding mode the 2-NH_2 and the N3 moieties form hydrogen bonds with Glu30. The α-carboxyl group of **282** interacts with Arg70 in an ionic bond and the thieno[2,3-*d*]pyrimidine and the phenyl ring make hydrophobic contacts with Phe31, Phe34, and Ile60 (Figure 39) in the binding pocket. The 6-propyl substitution contacts with Ile7 and Val115 in the hydrophobic pocket.

Gangjee *et al*. have previously shown that nonclassical analogues of **274** (Figure 29) with electron withdrawing groups in the phenyl ring of the side chain also enhance human TS inhibitory activity. SAR studies indicated that analogues with electron withdrawing groups at the 3- and/or 4-positions of the phenyl side chain provide optimum inhibitory potency against human TS. Certain analogues with electron withdrawing substitutions on the phenyl ring demonstrated greater potency against human TS than the clinically used RTX and PMX. In contrast to the requirements for human TS inhibition, electron donating substituents such as methoxy, methyl, and bulky substituents such as naphthyl are conducive for DHFR inhibition; hence nonclassical analogues containing these substituents were also synthesized in the 2-amino-4-oxo-5-arylthio-substituted-6-propyl thieno[2,3-*d*]pyrimidine series. As indicated above for the classical analogue **282,** it was anticipated that the nonclassical analogues **283-291** would also provide dual inhibitory activity against human TS and human DHFR.

3. Nonclassical 2-Amino-4-oxo-5-arylthio-substituted-6-methyl furo[2,3-*d*]pyrimidines as Dual Thymidylate Synthase and Dihydrofolate Reductase Inhibitors

Continuing the long standing goal of the Gangjee group to design and synthesize single agents with dual inhibitory activity against TS and DHFR as mentioned above, a series of 2-amino-4-oxo-5-arylthio-substituted-6-methyl furo[2,3-*d*]pyrimidines were designed. The furo[2,3-*d*]pyrimidine scaffold could be considered an isostere of the pyrrolo[2,3-*d*]pyrimidine system and thieno[2,3-*d*]pyrimidine ring systems.

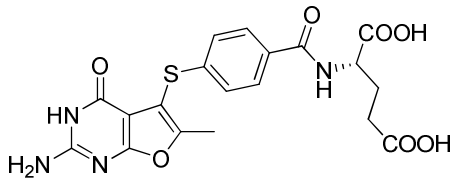

292

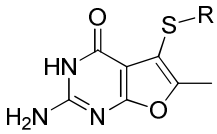

293 R = Ph
294 R = 1-Naphthyl
295 R = 4-OMe-Ph
296 R = 4-pyridinyl
297 R = 3,4-di-Cl-Ph
298 R = 4-Cl-Ph

Figure 40. The structure of furo[2,3-*d*]pyrimidine antifolates.

To develop potential dual TS and DHFR inhibitors, compound **292** (Figure 40) was designed as an isostere of **274** to determine the importance of the pyrrole 7-NH in **274** for binding to human TS and DHFR. The replacement of the NH of a pyrrolo[2,3-*d*]pyrimidine with an O to afford the furo[2,3-*d*]pyrimidine was also anticipated to evaluate the importance of a hydrogen bond donor (NH) versus a hydrogen bond acceptor (O). SAR studies in the pyrrolo[2,3-*d*]pyrimidine series showed that nonclassical analogues of **274** with electron withdrawing groups at the 3- and/or 4-positions of the phenyl ring of the side chain provide optimum inhibitory potency against human TS. Hence nonclassical analogues containing these substituents were also synthesized in the

furo[2,3-*d*]pyrimidine series. Since electron donating substituents such as methoxy and bulky substituents such as naphthyl are conducive for DHFR inhibition, nonclassical analogues containing these substituents were also designed in the a-Amino-4-oxo-5-arylthio-substituted-6-methyl furo[2,3-d]pyrimidine series.

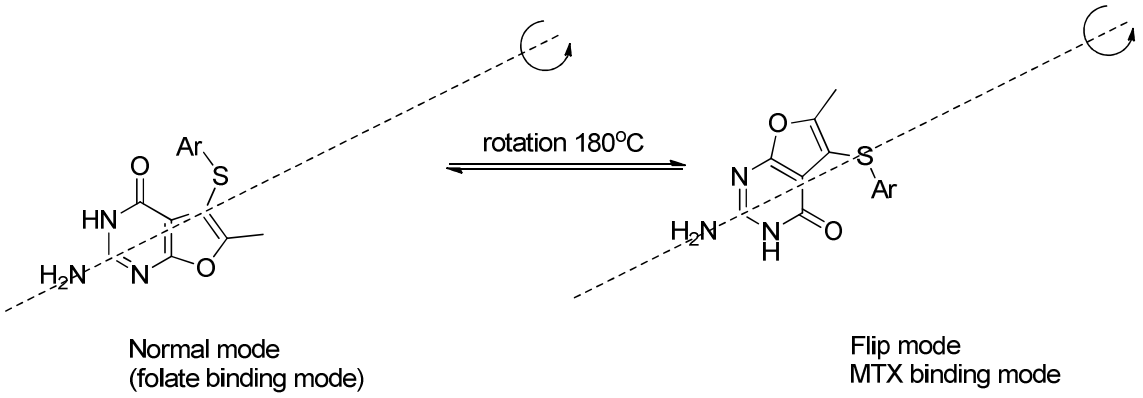

Figure 41. Proposed binding mode of 2-Amino-4-oxo-5-arylthio-substituted-6-methyl furo[2,3-*d*]pyrimidines. The "Normal mode" is defined as the binding mode of pemetrexed and raltitrexed to human TS and folic acid (a 2-amino-4-oxo pyrimidine system) to human DHFR. The "flipped" mode is defined as the binding mode when pemetrexed, raltitrexed or folic acid is rotated about the C_2-NH_2 bond by 180°.

For 2-amino-4-oxo-5-substituted-6-alkyl furo[2,3-*d*]pyrimidines two possible binding modes are shown in Figure 41. The 2-amino-4-oxo mode is defined as the normal mode and is proposed for TS and DHFR binding. A rotation about the C_2-NH_2 bond by 180° affords the flipped mode, which is also proposed for DHFR binding.

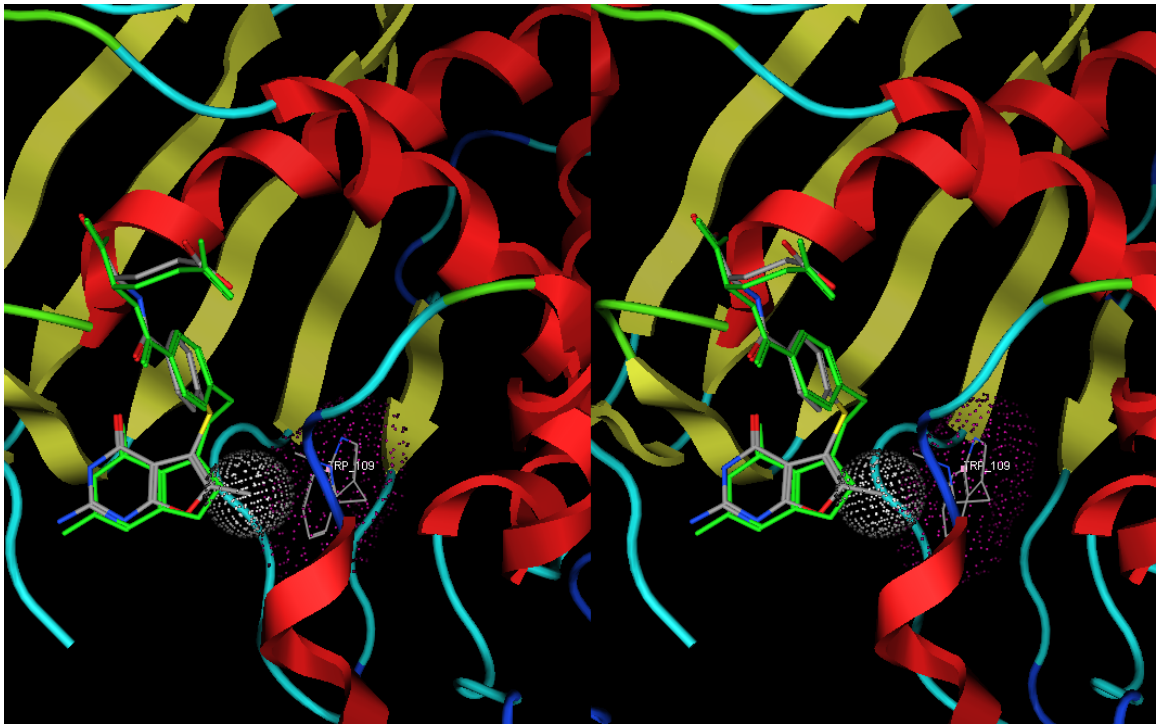

Figure 42. Stereoview of compound **292** (gray) superimposed on **274** (green) in ecTS. Figure prepared with MOE 2008.10.[363]

As shown in Figure 42, molecular modeling using MOE 2008.10[363] revealed that when the NH of a pyrrolo[2,3-*d*]pyrimidine was replaced with an O in the furo[2,3-*d*]pyrimidine, the resulting compound could bind to TS in a manner similar to **274**.

The 6-methyl substitution in the furo[2,3-*d*]pyrimidine antifolates makes hydrophobic contacts with Trp109 in hTS and restricts the side chain to a conformation conducive for potent TS activity but perhaps not for FPGS substrate activity.

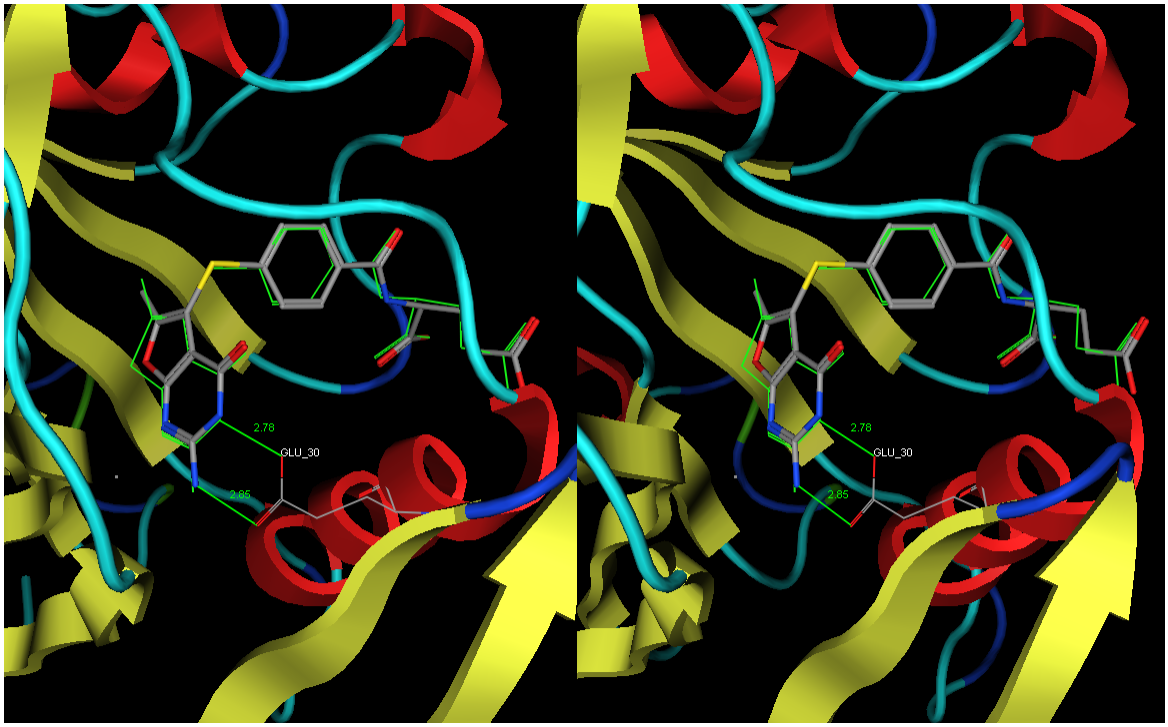

Figure 43. Stereoview: compound **292** bound to human DHFR in "normal" mode (PDB : 1U72), generated by MOE 2008.10.[363]

Molecular modeling suggested that compound **292** could also bind to human DHFR in either the "normal" folate binding mode (Figure 43) or the "flipped" folate binding mode (Figure 44). In the "Normal" binding mode compound **292** could bind just like folate (PDB: 1U72) in which the 2-NH_2 and N_3 moieties form hydrogen-bonds with Glu30 and the benzoyl moiety binds to Phe31, Phe34 and Ile 60. The α-carboxylic acid of the glutamate makes ionic contact with Arg70.

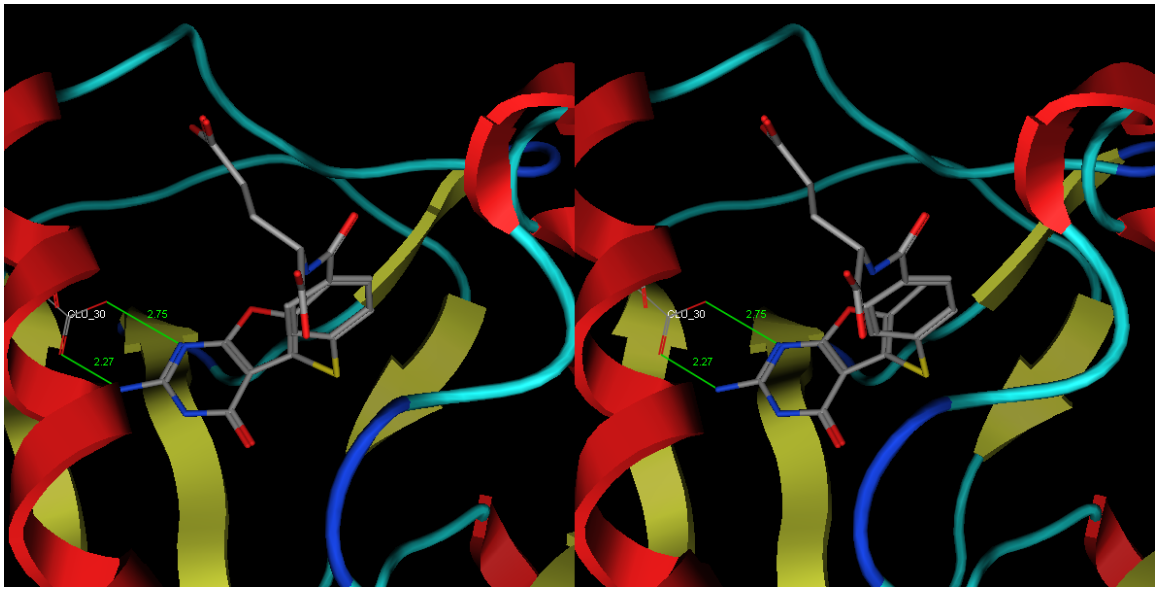

Figure 44. Stereoview: compound **292** bound to human DHFR in the "flipped" mode (PDB : 1U72), generated by MOE 2008.10

On the basis of molecular modeling, a second mode of binding would involve a 180° rotation about the C-2, NH_2 bond (Figure 44), whereby the oxygen of the furan ring is now superimposed on the 4-oxo group of folate, with all other interactions being the same. It is important to note that binding of **292** in the flip mode (Figure 44) also allows the oxygen of the furan ring to mimic the 4-amino of MTX. In this binding mode, the Glu30 residue interacts with 2-NH_2 and N1 moieties of **292**. The aminobenzoyl ring along with thieno[2,3-*d*]pyrimidine ring makes hydrophobic interactions with Phe31, Phe34 and Ile60 and the α-COOH forms an ionic bond with Arg70 just as MTX does with human DHFR.

4. 2,4-Diamino-6-substituted bicyclic pyrimidines as dihydrofolate reductase inhibitors.

The principal cause of death in patients with acquired immune deficiency syndrome (AIDS) are opportunistic infections caused by *Pneumocystis jirovecii* (*pj*) previously known as *Pneumocystis carinii* (*pc*), *Toxoplasma gondii* (*tg*) and *Mycobacterium avium* (*mav*) complex (MAC).[367,372] Selective inhibition of pathogen DHFR may provide a cure for such infections.

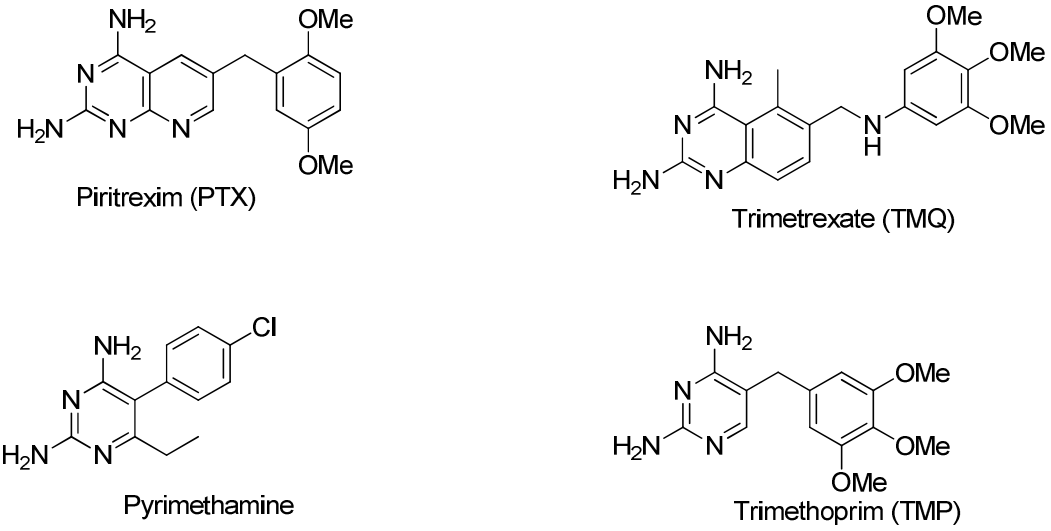

Figure 45. The structure of TMQ, TMP, PTX and pyrimethamine.

Several DHFR and TS inhibitors have found clinical utility as antitumor and antiopportunistic agents. Nonclassical lipophilic DHFR inhibitors are currently used to treat opportunistic infections caused in AIDS patients.[373] Current therapy for these opportunistic infections includes the selective but weakly potent monocyclic agents TMP and pyrimethamine. Both TMP and pyrimethamine are weak inhibitors of *pc*DHFR and *tg*DHFR and must be used with sulfonamides to provide a synergistic effect. However,

the combination therapy is successful in only 50-75% of the AIDS population and produces severe side effects in several cases. Up to 60% are unable to tolerate the combination therapy due to severe, adverse drug reactions.

Piritrexim (PTX) and trimetrexate (TMQ) are also nonclassical DHFR inhibitors. These are highly potent but lack selectivity toward the pathogen enzyme and show host toxicity. TMQ is coadministered with leucovorin, the classical folate cofactor (6R,6S)-5-formyl-5,6,7,8-THF, which selectively rescues host cells from TMQ toxicity.[371] Unfortunately, all these combinations cause serious toxicities that force the cessation of treatment in many cases.[37]

The existing regimen used to treat opportunistic infections in AIDS and other immunocompromised patients is suppressive rather than curative and the therapy must be continued indefinitely. Thus, it is of considerable interest to design single agents that have both the desired selectivity of TMP and the potency of TMQ. Patients with AIDS are often infected with multiple opportunistic infections, it is highly desirable to develop single agents that simultaneously target two or more opportunistic pathogen DHFR. However, the absence of any animal models for human *Pneumocystis jirovecii* pneumonia and the lack of crystal structures of *pj*DHFR and *tg*DHFR make the design of such analogs very difficult.

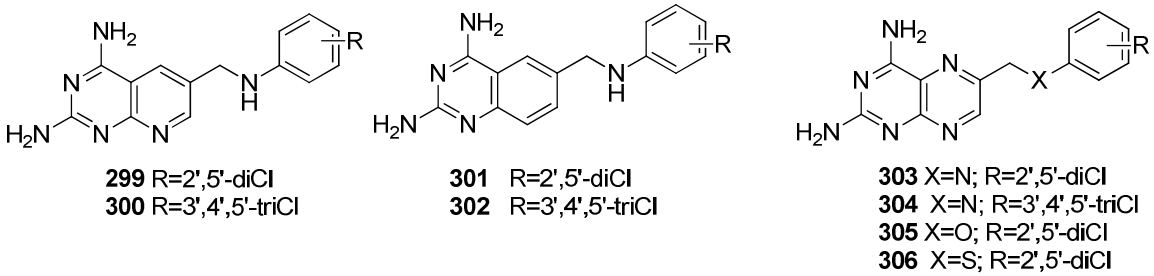

Figure 46. The structure of nonclassical 2,4-diamino-pyrido[2,3-*d*]pyrimidines **299**-**306**.

Gangjee *et al.*[145] as well as others,[18,135,377] have reported the investigation and structure-activity/selectivity relationships of several structural classes of DHFR inhibitors. Recently a series of pyrido[2,3-*d*]pyrimidines have been reported as potent and selective *pj*DHFR inhibitors.[69] Among them, compound **299** shows 2190-fold selectivity against *pj*DHFR, which is about 4-times higher than the selectivity index of clinically used TMP. Compared to **299** and TMP, the *pj*DHFR selectivity of **300** is not very high and its selectivity index is only 154. However, this compound has nanomolar *pj*DHFR inhibitory activity and is much more potent than TMP. These series of compounds also prove that *pj*DHFR and *pc*DHFR are different enzymes in different pathogen and drugs can behave quite differently against *pc*DHFR and *pj*DHFR.

Table 2: DHFR inhibitory activity of **299**, **300** and TMP[69]

	IC_{50}(μM)				
compound	rDHFR	rhDHFR	*pc*DHFR	*pj*DHFR	h/pj
299	4.7	4.6	0.184	0.004	2190
300	1.29	0.54	0.08	0.0035	154
TMP	129	188	22.4	0.33	564

To further explore the structure activity relationship (SAR) of this series of compounds and to improve the potency and selectivity against *pj*DHFR, structure modifications of **299** and **300** were carried out by using analogue design. The replacement of the nitrogen atom on the pyrido[2,3-*d*]pyrimidine ring with a carbon resulted in compounds **301** and **302**. This substitution causes the electron distribution on

the ring system to be altered and the loss of hydrogen bond formation at the 8-position. In addition, compounds **301** and **302** can be considered structural mimics of TMQ. Having the same 2,4-diamino quinazoline structure as TMQ, **301** and **302** were proposed to maintain high *pj*DHFR activity. By adding an additional nitrogen to the 5-position of the lead compound **299** and **300**, pteridine analogues **303** and **304** were designed. To explore the effects of different hetero atoms on the side chain, the nitrogen atom on the side chain of **303** was replaced by oxygen and sulfur to afford **305** and **306**. The replacement of the side chain NH of **303** a pyrrolo[2,3-*d*]pyrimidine with an O or S was also anticipated to evaluate the importance of a hydrogen bond donor (NH) versus hydrogen bond acceptor (O, S).

5. Importance of the Side Chain Aryl Group for Folate Receptor Targeting and GARFTase Inhibitory Activity in Classical Thieno[2,3-*d*]pyrimidine Antifolates

More than twenty interrelated enzymatic reactions in cellular metabolism require folate coenzymes. These reactions are essential to maintain *de novo* synthesis of deoxyribonucleic acid (DNA) and amino acids.[1]

Glycinamide-ribonucleotide transformylase (GARFTase) is the first folate-dependent enzyme in purine biosynthesis and catalyzes the conversion of glycinamide ribosyl-5-phosphate (GAR) to formyl-glycinamide ribosyl-5-phosphate (fGAR), utilizing N^{10}-formyl-FH_4 as a cofactor. The inhibition of GARFTase has potential importance in cancer treatment since it could lead to a depletion of purine nucleotide pools, which can limit nucleotides for DNA synthesis and repair.[374] High concentrations of the folate pool are necessary for normal activity of the cell. Since humans lack the *de novo* biosynthesis of folates, cellular uptake of these derivatives is essential for tissue regeneration and cell

growth. Transport into the cell is usually accomplished by three carrier proteins present on the cell surface: reduced folate carrier (RFC), the membrane folate receptor (FR) and the proton-coupled folate transporter (PCFT).[267]

Reduced folate carrier (RFC) is ubiquitously expressed in normal tissues and tumor cells. It has long been recognized as the major transport system for folates in mammalian cells[176] and the primary transporter of classical antifolate drugs used for cancer chemotherapy, such as methotrexate (MTX), pemetrexed (PMX), raltitrexed (RTX) (Figure 1). The decrease of RFC levels or functions is a common mechanism of antifolate resistance.[176,180]

Compared to the ubiquitously expressed RFC, α-folate receptor (FRα) has a restricted tissue distribution pattern. The FRα is overexpressed in some epithelial cells, especially the kidney, placenta and choroid plexus, and has a restricted distribution in normal tissues, which provides an opportunity to develop antifolates specifically targeted at FRα overexpressing tumors. Agents that are specific for the FRα are highly selective for tumors that overexpress FRα with the potential of little or no toxicity to normal cells.[376,377] PCFT was recently identified as a third transporter for folates. It was reported that PCFT increases the intracellular concentration of PMX at pH 5.5, which illustrated the unique property of PCFT as a transporter of antifolates.[375]

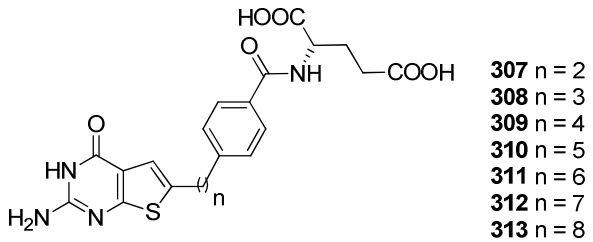

307 n = 2
308 n = 3
309 n = 4
310 n = 5
311 n = 6
312 n = 7
313 n = 8

Figure 47. The structure of antifolates **307-313**

Deng *et al*[377] reported a series of 6-substituted thieno[2,3-*d*]pyrimidine antifolates **307-313** (Figure 47) as potent and selective inhibitors of cells that express FRs α and β. The thieno[2,3-*d*]pyrimidines **307-313** are unique and distinct from all other clinically used classical antifolates, including the pyrrolo[2,3-*d*]pyrimidine (PMX), quinazoline (RTX), and pteridine (MTX) antifolates, in that they are neither substrates for RFC nor PCFT. In this series, compound **309** with a four carbon bridge is the most potent inhibitor of cells expressing FRs α and β, and this activity is directly related to intracellular GARFTase inhibition.[377]

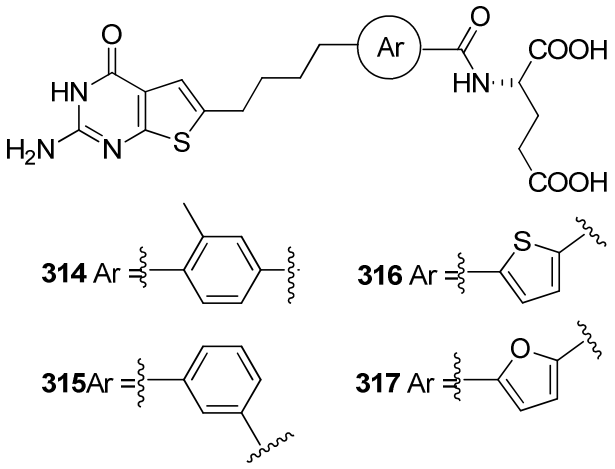

Figure 48. The structure of antifolates **314-317**.

To further investigate the structural requirements of the thieno[2,3-*d*]pyrimidine antifolates for FR transport and GARFTase inhibition, particularly the importance of the aromatic ring in the side-chain, a series of compounds **314-317** (Figure 48) with different aryl substitutions were designed, synthesized and evaluated. The aryl group in side-chain is believed not only to allow the appropriate relative orientation of the thieno[2,3-

d]pyrimidine scaffold (part A) and the glutamate portion (part B), but also allow important interactions with the transporter and the target enzyme.

Table 3. The angle of aryl disubstitutions.

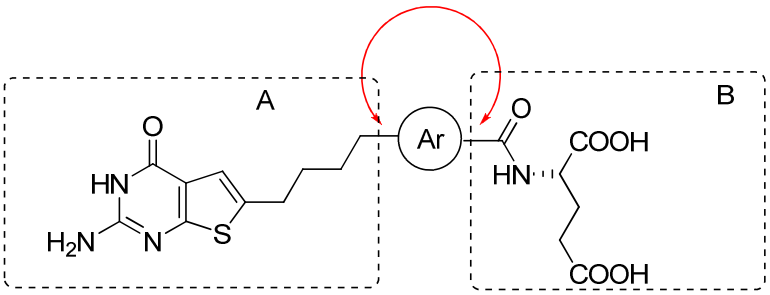

Compound	Ar	angle
309	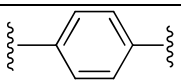	180°
314	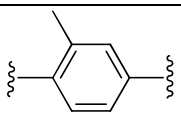	180°
315	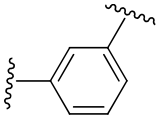	120°
316	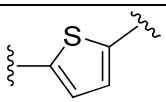	147.4°
317	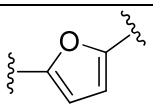	125.5°

As shown in Table 3, the angle between part A and part B is a measurement of the relative spatial orientation of A and B. For **314**, although A and B substitutions have the same angle (180°) as the parent **309**, the existence of an extra CH_3 in **314** *ortho* to the

alkyl chain in part A may restrict the free rotation of the otherwise flexible alkyl linker. Moreover, this methyl group could provide extra hydrophobic binding with the transporter FR and/or the enzyme GARFTase.

Depending on the angle, the overall distance between A and B in **315**, **316** and **317** are slightly different, which may also affect the binding affinity of the compounds with the transporter and/or target enzyme.

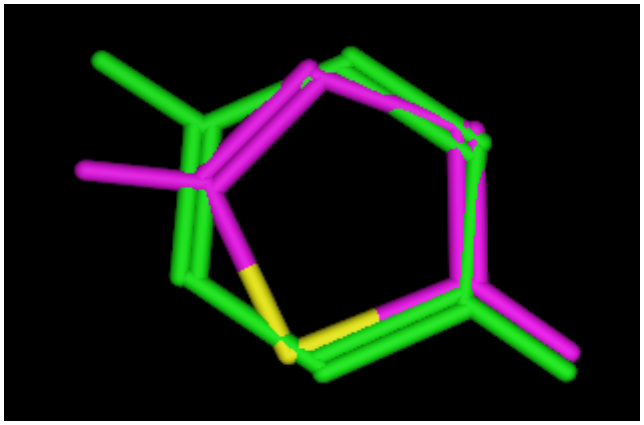

Figure 49. Structural alignment between 2,5-disubstituted thiophene (purple) and *para*-disubstituted benzene (green), generated by MOE 2008.10.

In **315**, a *meta* disubstitution pattern was adopted such that the angle between the two parts A and B is 120^{o}. 2,5-Disubstuted thiophene can mimic *para*-disubstituted benzene (Figure 49), while 2,5-disubstituted furan can mimic *meta*-disubstituted benzene (Figure 50). Thus, the benzoyl ring in **309** was bioisoterically replaced by a thienoyl ring or a furoyl ring, the resulting compounds **316** and **317** were able to explore 147.4^{o} and 125.5^{o} angles (Table 3) as well as the potential interactions between the hetero atoms in

the aryl ring and the transporter and/or enzyme.

Figure 50. Structural alignment between 2,5-disubstituted furan (purple) and 1,3-*meta*-disubstituted benzene (green), generated by MOE 2008.10.

6. Importance of the Glutamate Moiety for Folate Receptor Targeting and GARFTase Inhibitory Activity in Classical Thieno[2,3-*d*]pyrimidine Antifolates

As mentioned above, a series of thieno[2,3-*d*]pyrimidines **307-313** (Figure 47) were preparedas potent and selective inhibitors of cells that express FRs α and β.[369] This series of thieno[2,3-*d*]pyrimidine antifolates **307-313** are neither substrates for RFC nor PCFT, which is unique from all the other clinically used classical antifolates evaluated, including the pyrrolo[2,3-*d*]pyrimidine PMX, the quinazoline RTX, and the pteridine MTX antifolates. In this series, compounds **308** and **309** with a 3- or 4-methylene bridge were consistently the most potent inhibitors of cells expressing FRs α and β, and this was associated with potent inhibition of GARFTase.

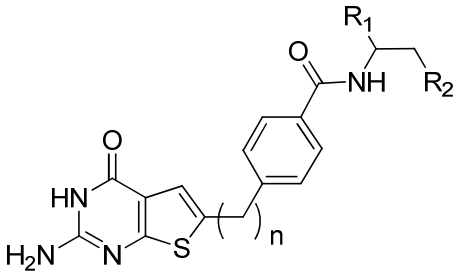

	n	R_1	R_2
318	4	CH_3	COOH
319	4	H	CH_2COOH
320	4	COOH	CH_2CH_3
321	4	COOH	CH_3
322	3	COOH	CH_2SH

Figure 51. The structure of antifolates **318-322**

To further investigate the structural requirements of the thieno[2,3-*d*]pyrimidine antifolates for GARFTase inhibition and selective FR binding, particularly the importance of the carboxylic acid moieties in the glutamate, a series of analogues **318-322** (Figure 51) with variation in the carboxylic acids of the L-glutamate moiety were designed, synthesized and evaluated. Compounds **318** and **319** have a CH_3 or H at the α-position instead of a carboxylic acid group to explore the importance of glutamate α-carboxylic acid. Compounds **320**-**322** maintain the α-carboxylic acid but have variations (CH_3 in **320**, H in **321** and SH in **322**) at the γ-carboxylic acid position.

7. Synthesis of *N*-aryl-2,6-dimethylfuro[2,3-*d*]pyrimidin-4-amines as RTK inhibitors.

Angiogenesis, the formation of new blood vessels from pre-existing vasculature, is essential for solid tumor proliferation and plays a key role in the growth of solid tumors, tumor invasion and metastasis.[378,379] Solid tumors depend on the newly formed vasculature network around the tumor mass to provide nutrients and to remove metabolic waste in order to grow beyond a few millimeters in diameter. [380]

The activation of RTKs regulates the transduction of signals from the extracellular domain of endothelial cells to the nucleus and represents the most pronounced factor that triggers angiogenesis.[238]

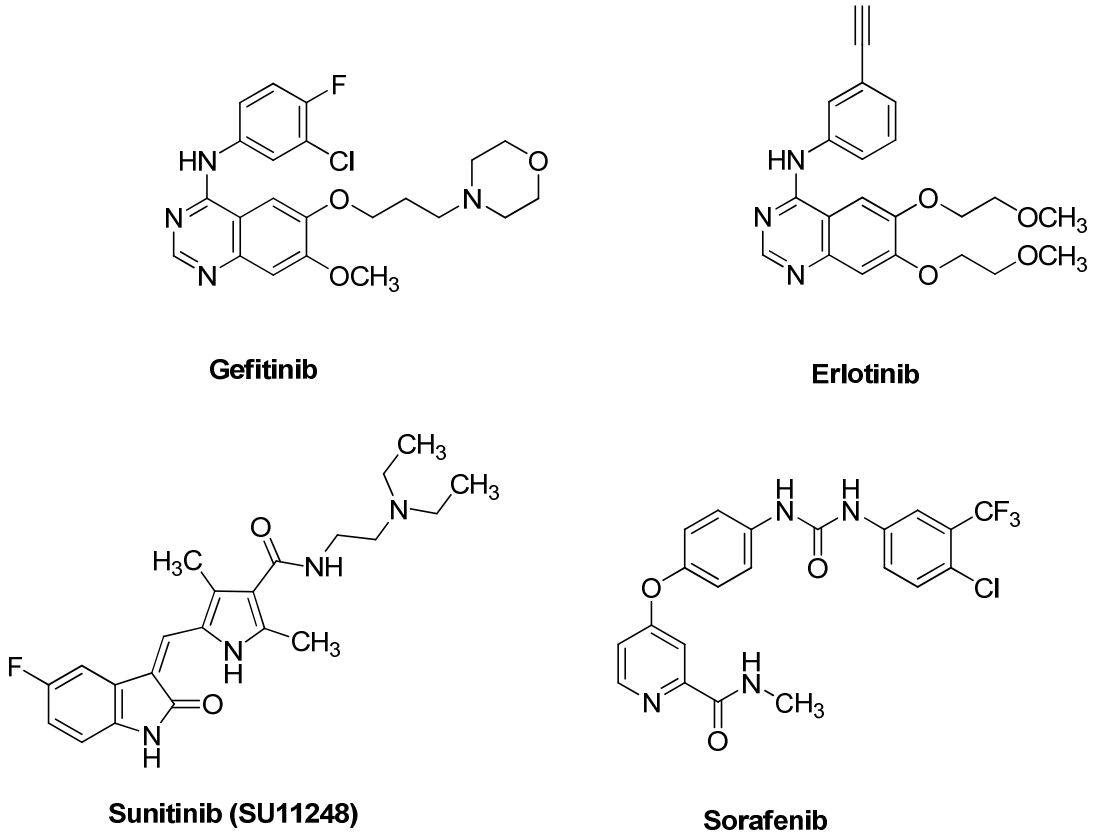

Figure 52. Representative RTK inhibitors.

The inhibition of RTK disrupts angiogenesis and provides an approach for the treatment of cancer. Previously, most of the development of RTK inhibitors was focused on targeting single RTKs. Inhibitors targeting single RTK do not allow for off target inhibition of other RTKs and hence have little toxicity issues. However, tumors often survive through an alternative signaling pathway to afford angiogenesis and thus develop resistance to these single targeting RTK inhibitors. Recently, preclinical studies have shown that the simultaneous inhibition of multiple

kinases by a single-agent has the potential to increase antitumor activity and delay resistance. Thus, multitargeting RTK inhibitors become the current paradigm in cancer chemotherapy. FDA has approved sunitinib and sorafenib as multitargeted agents which show clinical benefit with minor side effects as multi-kinase inhibitors (Figure 52). [381,382]

The ATP-binding site of RTKs is an attractive target for small molecule drug design. Structure determination of ATP-RTK complexes have revealed the regions within or close to the binding cleft not fully occupied by ATP. These unoccupied regions show structural diversity between members of the kinase family. The commonality as well as diversity among the ATP-binding sites of kinases has allowed the development of pharmacophore models for rational drug design.[259] The model proposed consists of an Adenine region which is a hydrophobic binding site for the adenine ring of ATP as well as for the heterocyclic scaffold of RTK inhibitors such as quinazolines and pyrimidines. The N1- and N6- amino nitrogen of the adenine ring of ATP are hydrogen bonded to two amino acid residues of the Hinge region (Figure 53). The Sugar binding pocket in the ATP binding site accommodates the sugar moiety of ATP and the Phosphate binding region binds the triphosphate moiety of ATP. In addition, a hydrophobic site I extends in the direction of the lone pair of the N7 of ATP and a Hydrophobic site II lies below the Adenine region. Both hydrophobic regions are unoccupied by ATP in the binding site.

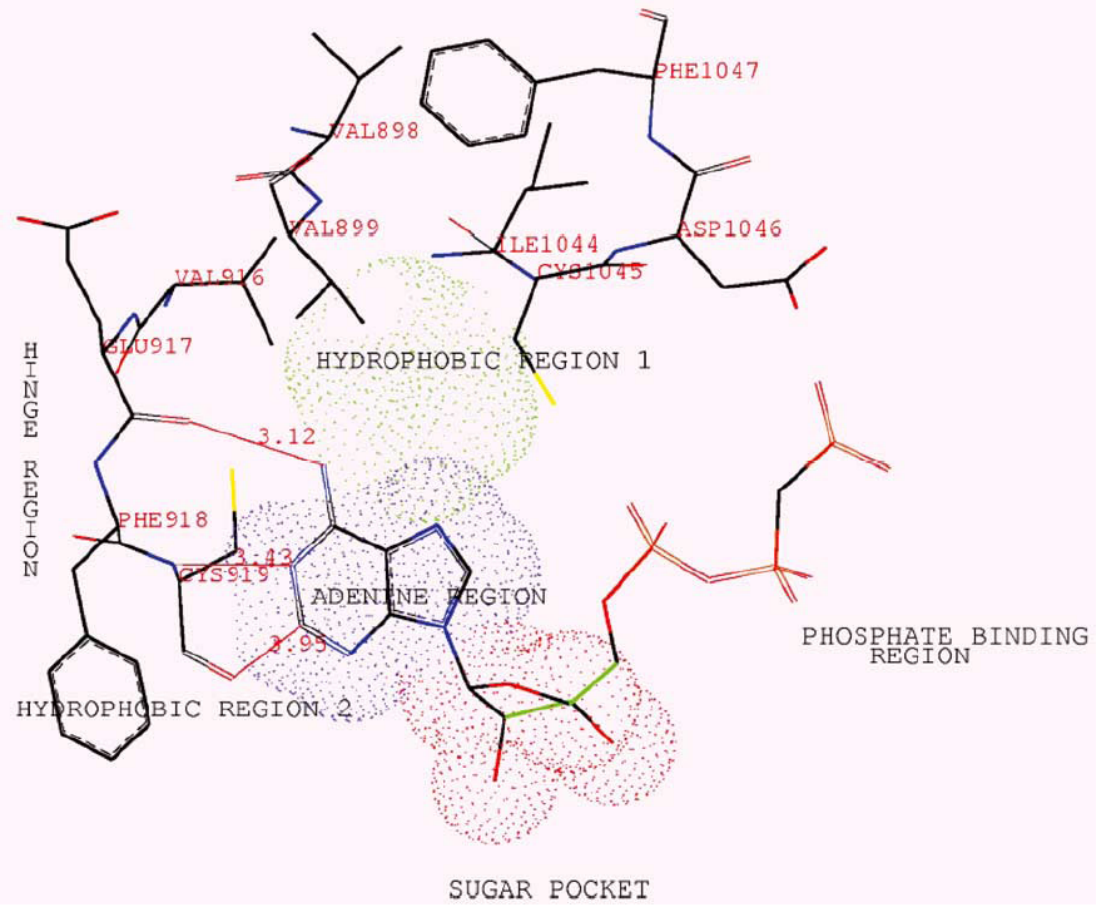

Figure 53. ATP from IRK modeled into VEGFR-2 using SYBYL 6.7.

Before the crystal structures of VEGFR2 or PDGFRβ with ATP or with quinazoline or pyrrolo[2,3-*d*]pyrimidine inhibitors became available, Gangjee *et al* modeled ATP from IRK into VEGFR-2 based on the proposed general pharmacophore for RTKs using SYBYL 6.7. For binding of ATP in VEGFR-2, the corresponding hinge region residues are Glu 917 and Cys 919 (Figure 53). These are important binding sites for ATP and ATP-competitive inhibitors and serve to anchor the heterocyclic portion of the molecule and appropriately orient the other parts of the molecule in the ATP binding site.

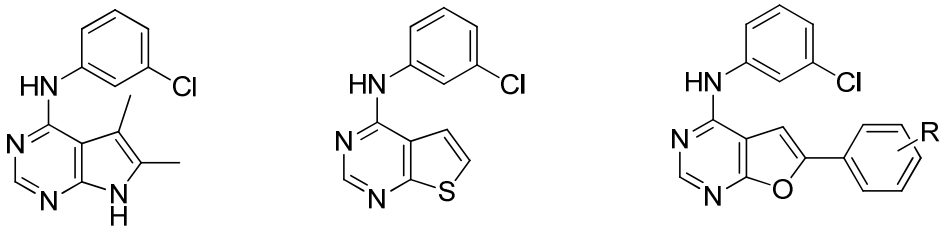

323 **324** **325**

Figure 54. The structure of 6-5 bicyclic RTK inhibitors **323-325**.

Compound **323-325** have been reported as 6-5 bicyclic RTK inhibitors. Compound **325** with a furo[2,3-*d*]pyrimidine scaffold was reported as an EGFR inhibitor with IC_{50} = 5-10 nM. On the basis of the general pharmacophore model and known 6-5 bicyclic RTK inhibitors, a series of furo[2,3-*d*]pyrimidine analogs of **326-334** were designed as RTK inhibitors.

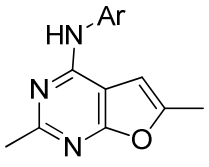

326 Ar = phenyl
327 Ar = naphthalen-1-yl
328 Ar = 3-ethynylphenyl
329 Ar = 4-(trifluoromethyl)phenyl
330 Ar = 3-chloro-4-fluorophenyl
331 Ar = 4-chlorophenyl
332 Ar = 1H-indol-4-yl
333 Ar = 4-methoxyphenyl
334 Ar = 3-fluorophenyl

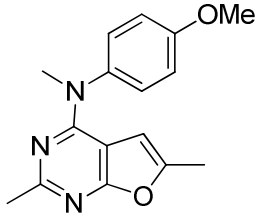

335

Figure 55. The structure of furo[2,3-*d*]pyrimidine RTK inhibitors **326-335**

These inhibitors contain a furo[2,3-*d*]pyrimidine scaffold rather than the purine scaffold of ATP with a 2,4,6-trisubstitution. The 2-substitution of **326-335** was designed as a methyl group, which is not present in most other 6-6 or 6-5 ring system RTK inhibitors reported. On the basis of molecular modeling, there is sufficient space in the ATP binding site of RTKs to

accommodate a 2-methyl group. In addition, further functionalization of the 2-methyl group can afford access to Hydrophobic region II thus perhaps increase the binding affinity with the enzymes and provide selectivity among different RTKs. Unlike **325**, compounds **326-334** have a 6-methyl substitution instead of a 6-phenyl substitution. Compared to a phenyl group, a methyl group has a smaller size, and can be accommodated in the phosphate or sugar binding site of multiple RTKs. Compounds **326-334** were designed to fit into the ATP binding site of multiple RTKs. In addition, the 6-methyl group provides a handle for further functionalization. When necessary, this methyl group can be converted to other groups to increase binding affinity with the enzyme or gain selectivity among different RTKs.

Similar to most of the known ATP competitive RTK inhibitors, **326-334** have a 4-anilino substitution. Different anilino substitutions at the 4-postion of the pyrimidine A-ring were expected to be involved in RTK binding at the Hydrophobic Region I and to influence inhibition, selectivity as well as the antitumor activity. Palmer *et al.*[383] reported in 1997 that small lipophilic electron-withdrawing groups at the 3-position of the anilino moiety in tricyclic ring system are beneficial for EGFR inhibition. Bold[384] reported that small lipophilic electron-withdrawing groups at the 4-position of the anilino moiety are also beneficial for VEGFR-2 and PDGFRβ inhibition. Thus, anilines with electron-withdrawing groups at either the 3- or 4-position were selected in compounds **329-331** and **334**. For comparison, compound **326** and **333** with a phenyl group and 4'-methoxy phenyl substitution were also included as 4-substitution on pyrimidine A ring. Compound **327** with a naphthalene substitution was design to determine the bulk tollerance in Hydrophobic region I among different RTKs. Similar to erlotinib, a 2-acetylenyl substitution was designed in compound **328**. The indole ring rather than a substituted phenyl ring has been reported to provide potent and selective RTK inhibition.[385] Thus in compound **332**, an indole ring

was designed as the 4-substitution on pyrimidine A-ring through a nitrogen linkage.

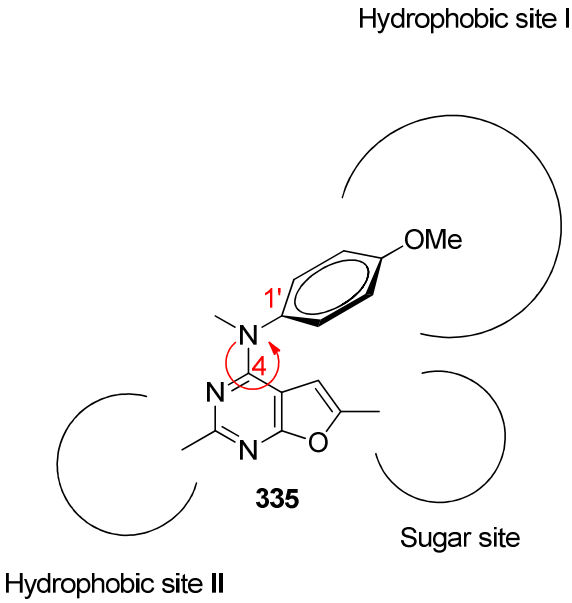

Figure 56. The proposed binding mode of **335**.

Compared to other compounds in the series, in compound **335**, an additional methyl group was designed on the aniline-nitrogen. This methyl group was introduced to restrict free rotation of the 4-position C-N bond as well as the 1'-position C_N bond (Figure 56) and influence the conformation of the compound. Thus an additional methyl group on the aniline-nitrogen could force the phenyl ring into the Hydrophobic site I and increase RTK inhibition, although the displacement of NH hydrogen with a methyl group could destroy hydrogen bond donor ability in the hinge region.

8. *N*-(4-methoxyphenyl)-*N*,2,6-trimethylfuro[2,3-*d*]pyrimidin-4-amine hydrochloride for improved water solubility.

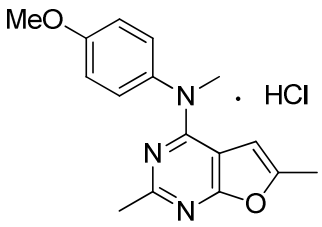

336

Figure 57. The Structure of *N*-(4-methoxyphenyl)-*N*,2,6-trimethylfuro[2,3-*d*]pyrimidin-4-amine hydrochloride **336**.

To define the mode(s) of binding and binding conformation with RTKs, an aniline N-methylated analog was designed in a series of furo[2,3-*d*]pyrimidine RTK inhibitors. Although compound **335** has an additional methyl group on the aniline-nitrogen, it showed moderate inhibition against certain RTKs. Compound **335** is a moderate inhibitor of RTKs and the inhibition potency of this compound is comparable to the NH analogs and the standard. Unlike typical RTK inhibitors and other compounds in the series, compound **335** showed potent antiproliferative activity, thus implying an additional mechanism of action. In the preclinical screening program of the National Cancer Institute in its 60 tumor cell line panel, **335** inhibited the proliferation of most of the 60 cancer cell lines with a GI_{50} of less than 500 nM.

The promising biological results for compound **335** against the NCI 60 cancer cell lines prompted further investigation this compound *in vivo*. However, this was hindered by its poor physiochemical properties. Compound **335** has poor water solubility (<1 mg/mL) and tends to absorb trace amount of hexane and HCl. Thus, it is desirable to covert **335** to its more water soluble hydrochloride salt **336** (Figure **57**).

9. Synthesis of *N*-(substitutedphenyl)-*N*,2,6-trimethylfuro[2,3-*d*]pyrimidin-4-amine as antimitotic anticancer agents.

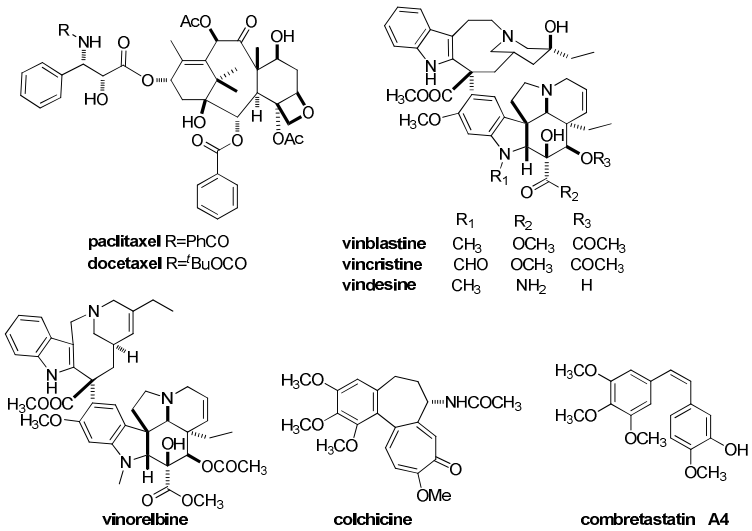

Figure 58. The structures of microtubule targeting agents.

Tubulin binding agents belong to a very important class of antitumore agents and are widely used in clinic for cancer chemotherapy. Half of all human tumors have mutations in the p53 gene, and the most effective drugs in p53 mutant cell lines are tubulin-binding agents.[386] Based on their binding sites, most antimicrotubule agents can be divided into three classes, taxoids, the vinca alkaloids and inhibitors that bind at colchicine site. [206, 387, 388] The first group includes paclitaxel (Taxol) and docetaxel (Taxotere), as well as the epothilones. Paclitaxel and other taxoids (and the epothilones) bind to the interior of the microtubule, [389,390] and the tubulin β-subunit. Unlike the other two classes of antimicrotubule agents, the taxoids stimulate tubulin polymerization and are designated microtubule-stabilizing agents. They are useful in the treatment of breast, lung, ovarian, head and neck and prostate carcinomas among others. The

second class are the vinca alkaloids including vincristine, vinblastine, vindesine and vinorelbine. The vinca alkaloids also bind at the β tubulin but is distinct from that of taxoids. The vinca alkaloids are important in the treatment of leukemias, lymphomas, non-small cell lung cancer and other cancers. A diverse collection of small molecules, including cochicine and combrestatatins, bind to the colchicine site on β-tubulin at its interface with α-tubulin, distinct from the vinca site. Similar to the vinca alkaloids, colchicine site agents inhibit tubulin polymerization. Colchicine itself is not used as an antitumor agent but is used in the treatment of gout and familial Mediteranean fever. Although there are no clinically approved antitumor agents that bind to the colchicine site, several of these agents are currrently in clinical trials.[391, 392] Combretastatins, as exemplified by combretastatin A-4 (CA4) and its phosphorylated prodrug combretastatin A-4 phosphate (CA4P) are currently in clinical trials,[206] which demonstrates the importance of developing colchicine site agents as antitumor agents.

Multidrug resistance (MDR) is a major limitation of cancer chemotherapy, and MDR tumors are usually resistant microtubule disrupting agents. Overexpression of P-glycoprotein (Pgp) represents one of the major mechanism of tumor resistance. An elevated Pgp level has been reported in the clinical setting in a number of tumor types, particularly after patients have received chemotherapy. [217,393] In addition, Pgp expression has also been reported to be a prognostic indicator in certain cancers and is associated with poor response to chemotherapy.[394,395] Due to the overwhelming lack of success of Pgp inhibitors in the clinic, new microtubule targeting agents unsusceptible to Pgp-mediated resistance are desired.[393,396] Such agents will fill an unmet need in the clinic for patients that develop resistance due to Pgp overexpression. The expression of βIII-tubulin is involved in resistance to taxoids and vinca alkaloids in multiple tumor types including non small cell lung,[397-399] breast,[400] and ovarian

cancers.[401,402] Stengel *et al*.[403] and Lee *et al*.[404] showed that colchicine site agents circumvent βIII-tubulin resistance, which indicated the critical importance of developing new agents that bind to the colchicine site as an alternative to the taxoids for the treatment of refractory cancers.

Poor water solubility is an additional problem associated with several of the currently used antitubulin agents, particularly the taxoids. It is necessary to formulate such drugs in Cremophor or polysorbate, which can cause hypersensitivity reactions and require long administration times. Thus the development of water soluble microtubule targeted agents are highly coveted, and attracted enormous research effort.

Table 4. Tumor cell inhibitory activity GI_{50} (nM) of **335** (NCI).

Panel/ Cell line	**GI_{50} (nM)**	**Panel/ Cell line**	**GI_{50} (nM)**	**Panel/ Cell line**	**GI_{50} (nM)**	**Panel/ Cell line**	**GI_{50} (nM)**
NSCLC		**Renal Cancer**		**Ovarian cancer**		**Prostate Cancer**	
A549/ATCC	37.6	786 - 0	43.6	IGROV1		PC-3	
EKVX	64.8	A498	19.5	OVCAR-3	29.1	DU-145	26.2
HOP-62	32.2	ACHN	55.9	OVCAR-4	60.4	**Breast Cancer**	
HOP-92		CAKI-1	16.3	OVCAR-5	55.8	MCF7	42.2
NCI-H226	84.1	RXF 393		OVCAR-8	36.6	MDA-MB-231/ATCC	44.3
NCI-H23	40.7	SN 12C	56.7	NCI/ADR-RES		HS 578T	15.3
NCI-H322M		TK-10		SK-OV-3	25.2	BT-549	48.0
NCI-H460	33.1	UO-31	75.2	**Melanoma**		MDA-MB-468	34.9
NCI-H522	<1	**Colon Cancer**		LOX IMVI	54.9	**Leukemia**	
CNS Cancer		COLO 205	20	MALME-3M	42.3	CCRF-CEM	25.3
SF-268	33.6	HCC-2998	28.5	M14	23.3	HL-60(TB)	17.3
SF-295	13.8	HCT-116	34	MDA-MB-435		K-562	13.2
SF-539	20.0	HCT-15	25.3	SK-MEL-2	33.9	MOLT-4	67.9
SNB-19	33.3	HT29	32.5	SK-MEL-28	37.7	RPMI-8226	42.8
SNB-75	53.2	KM12	21.1	SK-MEL-5	22.9	SR	32.0
U251	30.8	SW-620	29.8	UACC-62	14.6		

Compound **335** was originally designed as an inhibitor of multiple RTKs and to explore the effects of the N-methyl group on the binding conformation with RTKs. Compound **335** showed moderate activities against RTKs and the inhibition potency of this compound is comparable to the NH analogs and the standard. Unlike typical RTK inhibitors and other

compounds in the series, **335** showed potent antiproliferative activity. Compounds **335** showed potent GI_{50}s in most of the NCI 60 cancer cell lines (Table 4).

Table 5. NCI COMPARE analysis result for **335**.

Rank	**Vector**	**Correlation**	**Cell line**
1	vincristine sulfate S67574 -3M TGI 2 days AVGDATA	0.600	49
2	maytansine S 153858 -4M TGI 2 days AVGDATA	0.494	49
3	vinblastine sulfate S49842 -5.6M TGI 2 days AVGDATA	0.458	49

The potent activities of **335** prompted a COMPARE analysis,[405] which showed vincristine sulfate to have the closest Pearsons correlation coefficient with **335**. Other compounds, such as vinblastine sulfate and maytansine, also tubulin binding agents, were ranked as the next closest correlation (Table 5). This clearly warranted the evaluation of **335** as a tubulin binding agent.

Table 6. Microtubule depolymerization activities of **335**.

Compound	**EC_{50} for microtubule depolymerization**
Combretastatin A-4	7nM
335	103.2 nM

Compounds **335** caused dramatic reorganization of the interphase microtubule network, similar to the effects of colchicine and CA4P. The EC_{50} (concentration required to cause 50% loss of cellular microtubules) (Table 6) was calculated to be 7 nM for CA4P, [396] 103 nM for **335**. Compounds **335** is a potent microtubule depolymerizers in cells, confirming the COMPARE analysis results.

Table 7. The resistnace index of **335** in SK-OV-3 isogenic cell line pair.

	SKOV (nM)	**SKOV+pgp (nM)**	**Resistance Index**
335	36.7	171	4.7
Taxol	2.2	4400	2000

The ability of **335** to circumvent Pgp-mediated drug resistance was evaluated by using an SK-OV-3 isogenic cell line pair (Table 7). In this cell line pair the resistance index (Rr) of paclitaxel, a well known Pgp substrate is greater than 2000 while Rr values of 4.7 was obtained with **335**, consistent with the Rr values obtained with other colchicine site agents, CA4P and 2ME2 of 1.5-2.6. These data suggest that **335** is a poor substrates for transport by Pgp and thus has advantages over some clinically useful tubulin-targeting drugs like paclitaxel.

Table 8. The biological activities of **335** as a colchicine site binding agent

compound	**Inhibition tubulin assembly IC_{50}(μM)±SD**	**Inhibition of colchicine binding % inhibition ±SD**	
		1 μM	5 μM
Combretastatin A-4	1.0 ± 0.09	88 ± 2	99 ± 0.2
335	2.4 ± 0.01	63 ± 5	88 ± 3

Studies were conducted to determine if **335** inhibited the polymerization of purified bovine brain tubulin, as would be predicted from the effects in cells. These biochemical studies provide an indication of a direct interaction of the compounds with tubulin. An initial study indicated that **335** is a potent inhibitors of purified tubulin assembly. Compound **335** was also compared with CA4P as inhibitors of assembly in a quantitative study (Table 8). In this assay, **335** inhibited tubulin assembly about as well as CA4P (Table 8). The data in Table 4 also shows that **335** binds at the colchicine site on tubulin, since it inhibited [^{3}H]colchicine binding to the protein, although not as potently as CA4P.

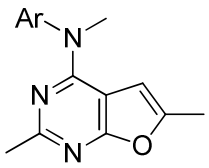

337 Ar = phenyl
338 Ar = 4-Me-phenyl
339 Ar = 3-Me-phenyl
340 Ar = 4-Cl-phenyl
341 Ar = 3,4-diCl-phenyl
342 Ar = 1-naphthyl

Figure 59. The structures of compound **337-342**.

To further improve the biological activity of **335** and to determine the pharmacophore, an additional series of compounds were designed through analog design. A topliss strategy was applied to determine the effects of substitution group on the phenyl ring and to determine the optimal substitutions. In this series, besides the parent 4-methoxy analogue **335**, six other analogues were designed to explore the electronic effects and steric effects. Compound **337** has an unsubstituted phenyl ring. Compound **338** and **339** have an electron donating methyl groups at the phenyl 3'- or 4'-position respectively. Compound **340** contains a single electron withdrawing chlorine substitution at the 4'-position. Compound **341** contains electron

withdrawing chlorine groups present at both the 3'- and 4'-positions. Compound **342** contains a bulky naphthyl substituent attached at the 1'-position in order to determine the bulk tollerance of the colchicine binding site.

10. Synthesis of conformational restricted *N*-(substituted)-2,6-dimethylfuro[2,3-*d*]pyrimidin-4-amine as antimitotic anticancer agents.

As mentioned above, the furo[2,3-*d*]pyrimidine **335** showed antiproliferative activity against the NCI-60 panel of tumor cells at low nanomolar levels and was active in taxol resistant tumor cell lines that over express Pgp. Compound **335** has additional advantages over clinical antimitotic agents, such as taxol, in that it is easily to be synthesized and is readily converted to the water soluble salt form. Microtubule depolymerization through the binding at the colchicine site was determined to be the primary mechanism of action for **335**.

Compared to the NH analogue, the N-methylated compound **335** showed spectacular antimitotic antitumor activity, which could be attributed, in part, to conformational restriction. A ^{1}HNMR study was carried out to explore the conformation of **333** and **335** (Figure 60). In compound **333**, the σ bonds ($C_{1'}$-N and N-C_4 bonds) connecting the phenyl ring and the pyrimidine ring are both free rotatable. While these bonds was restricted in **335**, where an additional methyl group was introduced on the N4-position. According to the ^{1}HNMR spectrum, the furo[2,3-*d*]pyrimidine 5-H in **335** is more shielded than in **333**, which suggested a nearby diamagnetic anisotropic cone. Due to the bulk of the N-methyl group, the conformation of **335** is restricted and the phenyl ring in **335** has to position itself on the top of 5-H proton, which leads to the shielding effect.

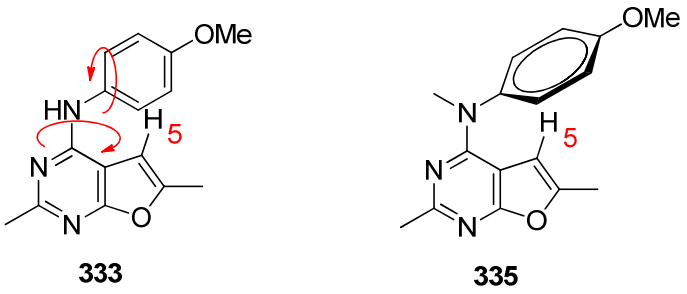

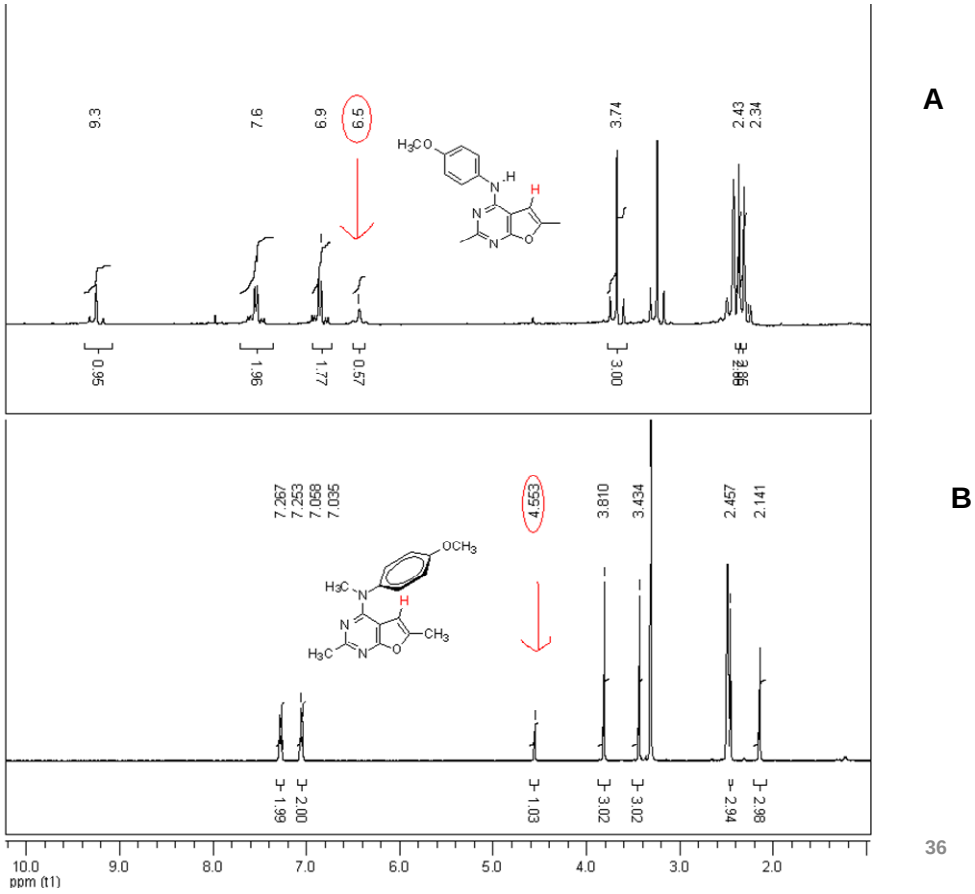

Figure 60. The conformations of compound **333 (A)** and **335 (B) and [1]HNMRS**.

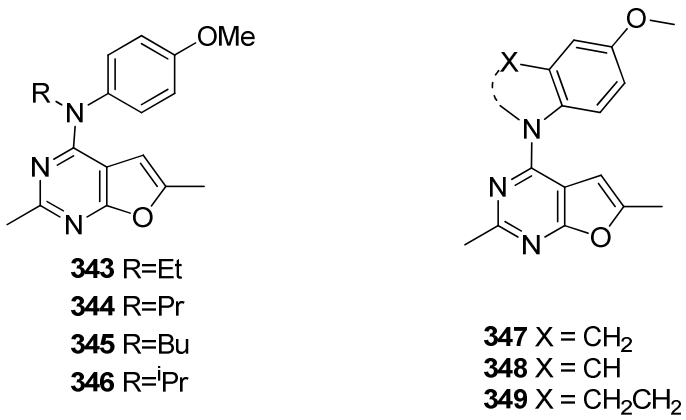

Figure 61. The structure of **343-349**

These larger groups require more space and further restrict the free rotation of C-N-C single bonds. In addition, these bulky group have larger hydrophobic surface and provide additional hydrophobic interactions with the protein. These compounds with larger N-substitutions may have greater affinity for the target protein and have more potent biological activities, compared to N-methylated compound.

An alternate strategy to explore the influence of conformational restriction was to restrict the free rotation of single bonds by incorporating them in ring systems. The single bonds in the ring system are no longer free rotatable. By changing the ring size and bond orders, the conformation of the compounds can be further attennuated. With optimal ring size and bond order, the low energy conformation of the compound is close to the biologically active conformation and affords potent activity. To further determine the optimal conformation, compound **347-349** (Figure 61) were designed. The N-methyl group and phenyl ring in compound **335** was linked through one additional carbon to afford compound **347**, which has a dihydroindole ring system. A two carbon atoms linker afforded tetrahydroquinoline **349**. Compound **348** has an indole ring to fix the position of the 4-methoxy phenyl.

11. Synthesis of *N*-(substituted)-2,6-dimethylfuro[2,3-*d*]pyrimidin-4-amine as antimitotic and anticancer agents.

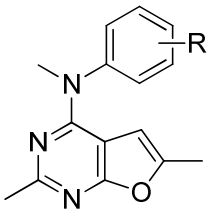

350 R = 2-OMe
351 R = 3-OMe
352 R = 4-CH_2Me
353 R = 4-SMe
354 R = 4-NHMe
355 R = 4-OEt
356 R = 4-OPr
357 R = 2,4-diOMe
358 R = 3,4-diOMe
359 R = 2,3,4-triOMe

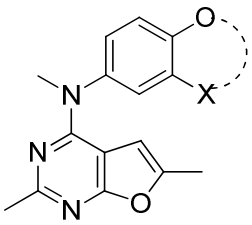

360 X = OCH_2
361 X = CH_2CH_2
362 X = CHCH

Figure 62. The structure of **350**-**362**

As mentioned above, **335** showed potent antimitotic antitumor activity. A topliss study was carried out to determine the optimal substitution on the phenyl ring and the importance of the 4-methoxy group. Replacement of 4'-methoxy group of **335** with hydrogen, electron donating methyl group or electron withdrawing 4'-chloro or 3',4'-dichloro substitutions resulted in compounds that lost both the antimitotic and antiproliferative activities. This result clearly indicated the critical importance of the 4'-methoxy group for biological activities. Thus it was of interest of determine the reason for the importance of the 4'-methoxy group and how it contributes to the activity. In an attempt to further clarify the interaction of the 4'-methoxy group with the colchicine binding site, compounds **350**-**362** was designed. The methoxy group was moved to the 2'- or 3'-positions in **350** and **351** respectively to determine the optimal

substitution position. The methoxy oxygen in **335** has two possible functions: providing interactions with the protein at the binding site through hydrogen bond or providing a linker between the methyl group and the phenyl ring and to position the methyl group in an appropriate region in the binding site. Due to the different hydrogen bonding possibilities, atom size and bond angles between oxygen, carbon, sulfur and nitrogen, compounds **352-354** were designed *via* a bioisosteric replacement of oxygen with carbon, sulfur and nitrogen. Compounds **355** and **356** were designed to explore the importance of the methyl group of the phenyl 4-methoxy substitution. It is hypothesized that the methyl group can interact with hydrophobic amino residues in the binding site. Thus, changing the methyl group to large alkyl groups could increase the hydrophobic interactions. To verify the hypothesis and to explore the size of the hypothetic hydrophobic pocket, compounds **355** and **356**, containing ethyl and propyl groups, were designed. Compound **335** was determined to be an inhibitor of the polymerization of purified bovine brain tubulin. In a quantitative study, compound **335** inhibited tubulin assembly about as well as CA4P. In addition, **335** was shown to bind at the colchicine site on tubulin, since it inhibited [^{3}H]colchicine binding to the protein. A structure activity relationship analysis indicated that colchicine, CA4P and several other colchicine site binding inhibitors have multimethoxy substitutions in their structures. Given the fact that **335** is a colchicine site binding inhibitor and contains one methoxy group, it is of interest to introduce additional methoxy groups in **335** to perhaps mimic colchicine and other related analogues. Thus **357-359** (Figure 62) with either dimethoxy or trimethoxy substitutions were designed.

The bond connecting the 4-methoxy group and the phenyl ring is free rotatable. To restrict the free rotation of the σ bond and to explore the optimal binding conformation, compound **360-362** (Figure 62) with fused bicyclic systems as 4-substitutions on the furo[2,3-

d]pyrimidine as the scaffolds were designed. The 4'-methoxy group in **335** was converted to the oxygen-methylene group and severed as part of the ring system in **360-362.** The benzodioxole in **360**, dihydrobenzofuran in **361** and benzofuran in **362** not only mimic the function of the 4'-methoxy group in **335** but perhaps also provide additional binding interactions with the target protein.

12. Synthesis of *N*-(4-methoxyphenyl)-*N*,2,6-trimethyl-5,6-dihydrofuro[2,3-*d*]pyrimidin-4-amine as antimitotic anticancer agents.

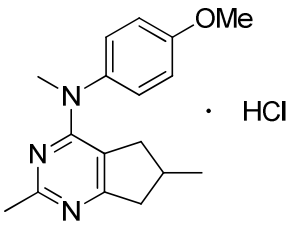

363

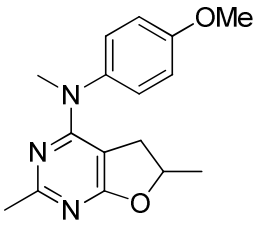

364

Figure 63. The structure of **363** and **364**

Gangjee *et al.*[406] recently reported the discovery of a potent antitubulin (R,S)-*N*-(4-methoxyphenyl)-*N*,2,6-trimethyl-6,7-dihydro-5H-cyclopenta[*d*]pyrimidin-4-aminium chloride **363** (Figure 63).

Similar to *N*-(4-methoxyphenyl)-2,6-dimethylfuro[2,3-*d*]pyrimidin-4-amine **335** mentioned above, **363** is a colchicine site binding, microtubule depolymerizing agent that inhibited the growth of cancer cells with GI_{50} in the nanomolar range. In addition, **363** overcomes the two most clinically relevant tumor resistance mechanisms that limit activity of microtubule targeting agents: overexpression of P-glycoprotein (Pgp) and βIII-tubulin.

Compound **335** and **363** share several common structure features including the 2,6-dimethyl substitution, 4-methoxyaniline substitution and the N-methyl substitution. The only difference between them is that the pyrimidine ring in **335** is fused to a unsaturated furan ring while the pyrimidine ring in **363** is fused to a saturated cyclopentane ring. A structural hybridid of **335** and **363** afforded 5,6-dihydrofuro[2,3-*d*]pyrimidine **364**, in which the pyrimidine ring is fused to a saturated ring system containing oxygen.

13. The synthesis of substituted furo[2,3-*d*]pyrimidin-4-amine as antimitotic anticancer agents.

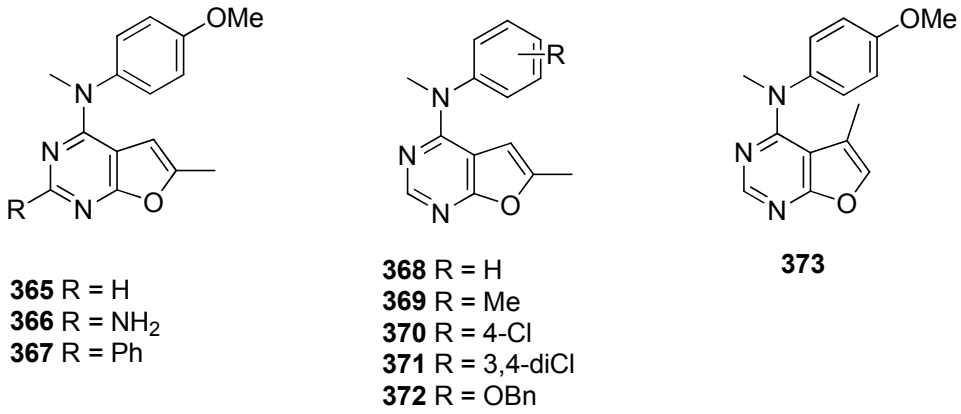

Figure 64. The structure of **365-373**

In an attempt to further explore the SAR of substituted furo[2,3-*d*]pyrimidin-4-amine as antimitotic anticancer agents and to improve the biological activity of **335**, a series of compounds **365-373** (Figure 64) were designed. Compound **365-367** were designed to determine the importance of the 2-methyl in **335**. The replacement of the 2-methyl group in **335** with a hydrogen, an amino group and a phenyl substitution resulted in the design of **365**, **366** and **367** respectively.

It was hypothesized that the introduction of a 2-NH_2 group on the pyrimidine ring could provide additional hydrogen bond interactions with the colchicine binding site. Compound **367**

has a phenyl substitution at the 2-position to explore the size limit and the effects of large hydrophobic group at this position. Compound **368-372** has the same 2-hydrogen as **365** and various electron donating and withdrawing groups on the 4-anilino ring. Compound **373** has a 2-hydrogen and 5-methyl substitution. This compound is the region isomer of **365** and can verify the importance of 6-methyl group in the lead compound. In addition, when the 6-methyl group was moved to the 5-position, the methyl group was anticipated to exert steric effects on the adjacent 4-substituted aniline thereby influencing the conformation of the compound and this could be reflected in perhaps higher activity.

14. The synthesis of substituted thieno[2,3-*d*]pyrimidin-4-amine as antimitotic anticancer agents.

As mentioned above, the furo[2,3-*d*]pyrimidine **335** showed antiproliferative activity against the NCI-60 panel tumor cells at low nanomolar levels and remained active in taxol resistant tumor cell lines that overexpress Pgp. Microtubule depolymerization through the binding at colchicine site was determined to be the primary site of action for this compound. A structure-activity relationship study revealed that the conformationally restricted analogue **349** (Figure 61), in which the *N*-methyl group and the phenyl ring were connected through two carbon atoms *via* a tetrahydroquinoline ring, showed potent antiproliferative activity against the NCI-60 tumor cells (Table 9) .

Table 9. Tumor cell inhibitory activity GI_{50} (nM) of **349** (NCI).

Panel/ Cell line	**GI_{50} (nM)**	**Panel/ Cell line**	**GI_{50} (nM)**	**Panel/ Cell line**	**GI_{50} (nM)**	**Panel/ Cell line**	**GI_{50} (nM)**
NSCLC		**Renal Cancer**		**Ovarian cancer**		**Prostate Cancer**	
A549/ATCC	<10	786 - 0	<10	IGROV1	<10	PC-3	<10
EKVX	<10	A498	<10	OVCAR-3	<10	DU-145	<10
HOP-62	<10	ACHN	<10	OVCAR-4	<10	**Breast Cancer**	
HOP-92	62.4	CAKI-1	<10	OVCAR-5	<10	MCF7	<10
NCI-H226	<10	RXF 393		OVCAR-8	<10	MDA-MB-231/ATCC	<10
NCI-H23	<10	SN 12C	<10	NCI/ADR-RES	<10	HS 578T	<10
NCI-H322M		TK-10	<10	SK-OV-3		BT-549	<10
NCI-H460	<10	UO-31		**Melanoma**		MDA-MB-468	<10
NCI-H522	<10	**Colon Cancer**		LOX IMVI	<10	**Leukemia**	
CNS Cancer		COLO 205	<10	MALME-3M		CCRF-CEM	<10
SF-268	11.1	HCC-2998	<10	M14	<10	HL-60(TB)	<10
SF-295	<10	HCT-116	<10	MDA-MB-435		K-562	<10
SF-539	<10	HCT-15	<10	SK-MEL-2	<10	MOLT-4	11.9
SNB-19	<10	HT29	<10	SK-MEL-28	<10	RPMI-8226	<10
SNB-75	<10	KM12	<10	SK-MEL-5	<10	SR	<10
U251	<10	SW-620	<10	UACC-62	<10		

Compound **349** was equipotent as CA4P and twice as potent as **335** as an inhibitor of tubulin assembly in a quantitative study (Table 10). Compound **349** also inhibited the binding of [^{3}H]colchicine to the protein as potently as CA4P. The quantitative study suggested that **349** is a more potent inhibitor than **335**.

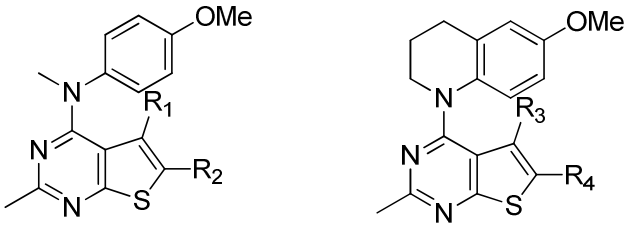

374 R_1 = H R_2 = Me
375 R_1 = Me R_2 = H

376 R_1 = H R_2 = Me
377 R_1 = Me R_2 = H

Figure 65. The structure of **374-377**.

Table 10. The biological activities of **349** as a colchicine site binding agent

Compound	**Inhibition tubulin assembly IC_{50}(μM)±SD**	**Inhibition of colchicine binding % inhibition ±SD**	
		1 μM	5 μM
Combretastatin A-4	1.0 ± 0.09	88 ± 2	99 ± 0.2
335	2.4 ± 0.01	63 ± 5	88 ± 3
349	1.1 ± 0.1	85 ± 3	96 ± 1

Thus the thieno[2,3-*d*]pyrimidine scaffold in this study was also of interest. This scaffold is an isostere of the furo[2,3-*d*]pyrimidine system of **335** and **349** and could afford more potential antimitotic anticancer inhibitors. Thus, compound **374** and **375** (Figure 65) were designed as isosteres of **335** and **369** to determine the importance of the furan oxygen in the furo[2,3-*d*]pyrimidine for binding to tubulin. The replacement of the O of a furo[2,3-*d*]pyrimidine with a S to afford the thieno[2,3-*d*]pyrimidine was also anticipated to evaluate the importance of electron distribution in the ring system. In addition the larger size of the sulfur atom compared to the oxygen allows the thieno[2,3-*d*]pyrimidines to more closely mimic the size of a 6-6-ring system, which may influence the conformation of the 4'-methoxy aniline substitution. As regional isomer of **374** and **375**, compound **376** and **377** can verify the importance of the 6-methyl group in the lead compounds. In addition, when the 6-methyl group was moved to the 5-

position, the methyl group was anticipated to exert steric effects on the adjacent 4-substitution thereby influence the conformation of the 4-anilino moiety and perhaps biological activities.

15. 7-substituted-5-arylethyl-4-methyl-7*H*-pyrrolo[2,3-*d*]pyrimidin-2-amines as antimitotic agents.

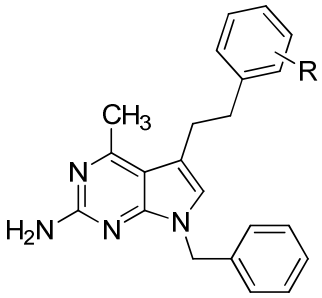

378 R = 3,4,5-triOMe
379 R = 4-OMe
380 R = 3-OMe
381 R = 2-OMe
382 R = H

Figure 66. The structure of **378-382**.[407]

Gangjee *et al.*[407] discovered compounds **378-382** (Figure 66) as novel antitumor antimitotic agents that also reverse tumor resistance. Compounds **378-382** caused dose dependent losses of microtubules in the cells and showed excellent to moderate inhibitory activity against tumor cells in the NCI preclinical 60 cell line panel. In addition, these compounds do not bind to the colchicine, taxol or vinca alkaloid or GTP or ATP binding sites on tubulin, and hence have a different binding site from that of all other known antimitotic agents. In addition, these compounds were also compared in human tumor cell lines with cell lines resistant to antimitotic agents due to overexpression of Pgp or MRP1 such as the NCI/ADR and MCF-7/VP cells. It was found that compounds **378** and **381** were the most potent compounds against all the tumor cell lines with nanomolar and submicromolar inhibitory activity, respectively. Compound **381** in addition to its antitumor activity, was the most effective for

reversing P-glycoprotein-mediated resistance to vinblastine.[408]

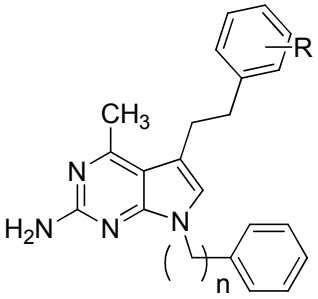

383 n = 0 R = 2-OMe
384 n = 0 R = 3,4,5-triOMe
385 n = 2 R = 2-OMe
386 n = 2 R = 3,4,5-triOMe
387 n = 3 R = 2-OMe
388 n = 3 R = 3,4,5-triOMe

Figure 67. 7-Substituted benzyl-5-(2-methoxyphenethyl)-4-methyl-7*H*-pyrrolo[2,3-*d*]pyrimidin-2-amines **383-388**.

*N*7-desbenzyl analogs of **379-383** were also synthesized and previously evaluated and were 100- to 10,000-fold less active than the corresponding benzylated compounds against the growth of tumor cells, which indicated the importance of the *N*7-benzyl substitution for tumor inhibitory activity. Thus, compounds **383-388** with variation of the chain length between *N*7-position and phenyl substitution were designed to explore initial structure-cytotoxicity and structure-resistance reversibility for other antimitotics with respect to the phenyl substitutions on the *N*7-benzyl of the lead analog **381**.

IV. CHEMICAL DISCUSSION

1. 6,5,6-tricyclic Benzo[4,5]thieno[2,3-*d*]pyrimidines as Dual Thymidylate Synthase and Dihydrofolate Reductase Inhibitors

It was envisioned that target compounds **275-278** would be synthesized *via* coupling between the benzo[4,5]thieno[2,3-*d*]pyrimidine scaffold and the glutamate side chain.

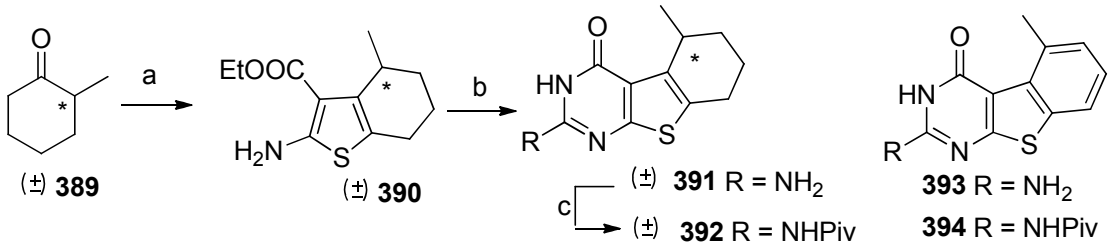

Reagents and conditions:
(a) ethylcyanoacetate, morpholine, sulfur, ethanol, 45 ^{o}C to rt, 12 h;
(b) chloroformamidine hydrochloride, $DMSO_2$, 150 ^{o} C; (c) $(Piv)_2O$, reflux, 3 h.

Scheme 67. Synthesis of tricyclic thieno[2,3-*d*]pyrimidines **391** and **392**.

The synthesis of benzo[4,5]thieno[2,3-*d*]pyrimidines started from commercially available α-methyl cyclohexanone (±)-**389** (Scheme 67) to the thiophene intermediate (±)-**390** via a Gewald reaction[319] in 81% yield. The reaction was attempted in several different solvents and bases, for example, methanol and triethyl amine, with the optimized results obtained with ethanol and morpholine. Cyclization of **390** *via* the partially aromatized tricyclic intermediate was expected to afford benzo[4,5]thieno[2,3-*d*]pyrimidines. To explore this strategy, (±)-**391** (Scheme 67) was synthesized *via* the condensation of **390** and chloroformamidine hydrochloride.[409] Aromatization of (±)-**391** was expected to afford **393** (Scheme 67).

Rosowsky *et al.*[410] reported aromatization of tetracyclic thieno-[2,3-*d*]pyrimidine *via* SeO_2

in acetic acid at reflux. Attempts at this reaction for the conversion of **391** to **393** were unsuccessful. Gangjee *et al.*[407] reported the oxidation of dihydropyrrolo[2,3-*d*]pyrimidines to their aromatic congeners *via* MnO_2 oxidation. However, MnO_2 oxidation for the aromatization of **391** was also unsuccessful. DDQ is reported[411] to serve as a dehydrogenation agent to effect aromatization. Reaction of **391** with DDQ at reflux in dioxane for up to 24 h afforded no new product (TLC). Other solvents with different boiling points including THF, DMSO and DMF among the others were also attempted at reflux and under microwave conditions. Trace amounts of a new product was observed under certain conditions, however, the yields were poor and precluded characterization.

The poor solubility of (±)-**391** in organic solvents could, in part, be responsible for the failure of aromatization. Thus, the 2-amino group in (±)-**391** was protected with a pivaloyl group at reflux with the anhydride $(Piv)_2O$ (Scheme 67) to give **392**, which was then subjected to DDQ oxidation under different reaction conditions. Unfortunately, no desired product was obtained.

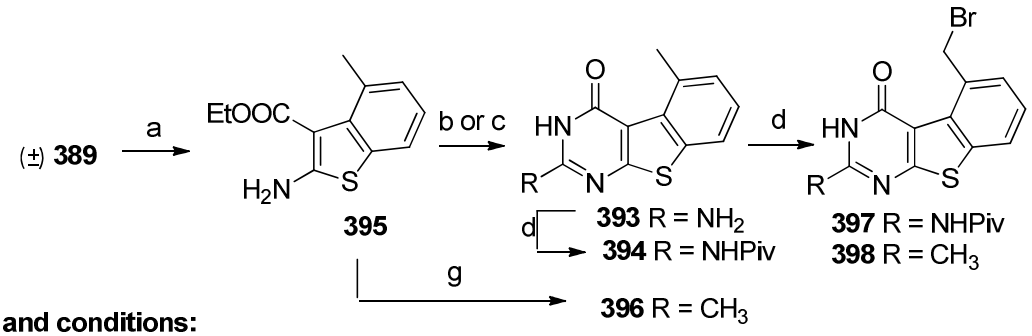

Reagents and conditions:
(a) Pd/C, toluene, reflux; (b) HCl (g), acetonitrile, ammonium hydroxide;
(c) chloroformamidine hydrochloride, $DMSO_2$, 150 °C; (d) $(Piv)_2O$, reflux, 3 h; (d) NBS, Bz_2O_2.

Scheme 68. Synthesis of tricyclic thieno[2,3-*d*]pyrimidines **397** and **398**.

The failure of the previous strategy prompted investigation of an alternate method, where the bicyclic scaffold was aromatized first (Scheme 68). Bicyclic intermediate **(±)-390** had good solubility in most organic solvents. With toluene as the solvent and MnO_2, SeO_2 or DDQ as the oxidant, under bench-top conditions or microwave irradiation no desired product was obtained. A literature search revealed Pd/C oxidation.[412,413] This allowed the conversion of **(±)-390** to the fully aromatized **395**. The solvent and time of the reaction were optimized for the aromatization with the optimal conditions being mesitylene as solvent at reflux for 48 h. Compared with **(±)-390**, the ^{1}H NMR of **395** showed the disappearance of protons at 1.54-3.17 ppm and the appearance of three aromatic protons at 6.98-7.43 ppm, which confirmed aromatization. In addition, the appearance of benzylic protons at 2.38 ppm as a singlet also confirmed aromatization. With **395** in hand, cyclization was carried out to afford the tricyclic scaffold. The substitution at the 2-position of the benzo[4,5]thieno[2,3-*d*]pyrimidine are predicated by the reactant. Cyclization of **395** (Scheme 68) with chloroformamidine hydrochloride afforded the 2-amino-4-oxo benzo[4,5]thieno[2,3-*d*]pyrimidine **393** in 60% yield. Pivaloylation of **393** with $(Piv)_2O$afforded **394**. The reaction of **395** in acetonitrile with hydrochloric acid gas afforded the 2-methyl-4-oxo product **396** in 57% yield. The 2-methyl and 5-methyl groups of **396** occur in the ^{1}H NMR at 2.35 ppm and 2.95 ppm respectively like similar dimethyl substituted quinazolines and benzoquinazolines.[414-417] Free radical bromination of **394** and **396** with *N*-bromosuccinimide (NBS) and a catalytic amount of benzoyl peroxide afforded intermediates **397** and **398** respectively.[414-417] By limiting the amount of NBS to just over one equivalent, the 5-methyl moiety of **396** was selectively brominated to afford **398**, similar to that reported for quinazolines and benzoquinazolines.[414-417] The 2-methyl moiety of **398** occurs in the ^{1}H NMR at 2.69 ppm and the 5-methylene protons occur at 5.84 ppm similar to the corresponding

quinazolines and benzoquinazolines.[414-417]

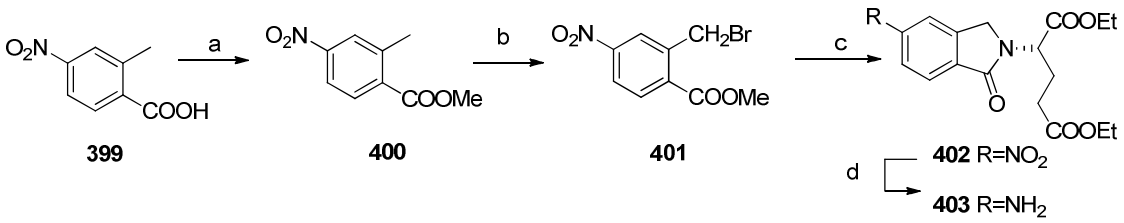

Reagents and conditions: (a) $SOCl_2$, MeOH; (b) NBS, Bz_2O_2; (c) diethyl glutamate, K_2CO_3; (d) H_2, Pd/C.

Scheme 69. Synthesis of side-chain **403**.

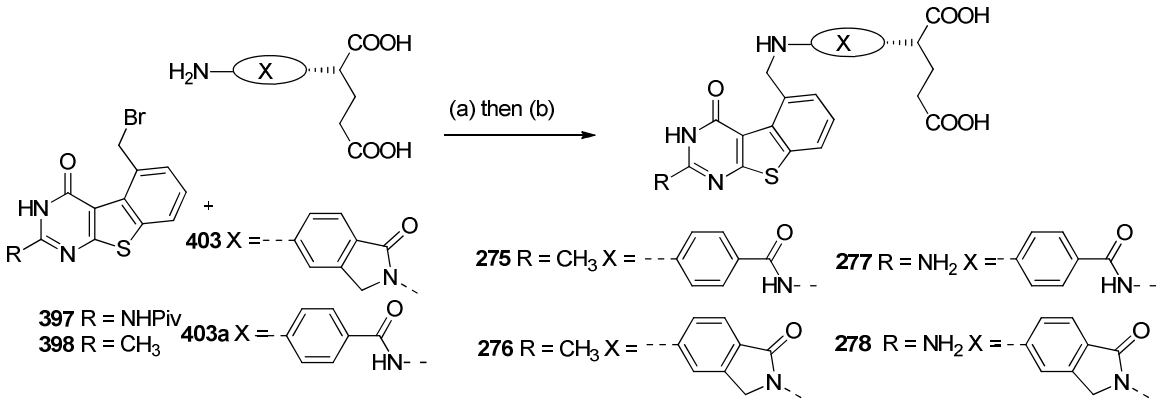

Reagents and conditions: (a) DMF, reflux; (b) 1 N NaOH, 60°C.

Scheme 70. Synthesis of classical analogues **275-278**.

The benzoylglutamate side chain for **275** and **277** is commercially available, however the 2-isoindolinylglutamate side chain for **276** and **278** was synthesized via a literature method (Scheme 69).[414] Esterification of **399** with $SOCl_2$ in methanol afforded **400** in 91% yield**.** Radical bromination of **400** with *N*-bromosuccinimide (NBS) and a catalytic amount of benzoyl

peroxide afforded **401** in 48% yield. The ^{1}H NMR of **401** showed the disappearance of protons at 2.69 ppm (CH_3) and appearance of methylene protons at 4.86 ppm (CH_2Br). Treatment of **401** with excess diethyl L-glutamate hydrochloride and K_2CO_3 in DMF at room temperature afforded isoindoline **402** as an orange oil in 56% yield. The ^{1}H NMR of **402** showed the appearance of protons at δ 4.51-4.83 ppm (isoindoline CH_2) and δ 5.09-5.14 ppm (Gluα-CH). Reduction of the nitro group in **402** afforded the amine **403** in 92.5% yield.

As shown in Scheme 67, *N*-alkylation[418] of **397** and **398** followed by hydrolysis of the ethyl ester (and the removal of pivaloyl protecting group in **277-278**) with 1 N NaOH and subsequent acid workup afforded target compounds **275-278**. The presence of glutamate in the side chain was confirmed from ^{1}H NMR. The expected NH at δ 6.74-7.40 ppm, exchanged with D_2O, and the benzylic protons occurred as a doublet at δ 5.13-5.24 ppm, which converts to a singlet upon D_2O exchange, indicated the success of the coupling reaction. High resolution MS (HRMS) and the presence of the requisite protons of the side chain via NMR confirmed the structure of **275-278**.

2. Classical and Nonclassical 2-Amino-4-oxo-5-arylthio-substituted-6-propyl thieno[2,3-*d*]pyrimidines as Dual Thymidylate Synthase and Dihydrofolate Reductase Inhibitors and Potential Agent for *Toxoplasma gondii* Infection

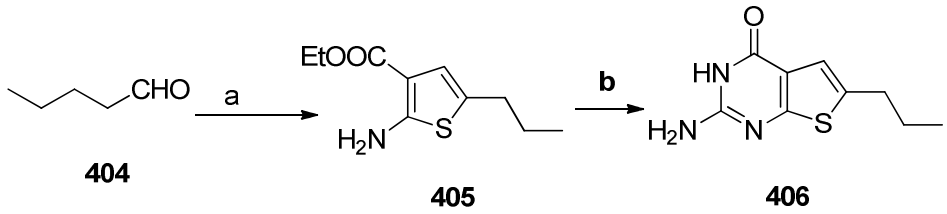

404 405 406

Reagents and conditions:
(a) Ethylcyanoacetate, morpholine, sulfur, ethanol, 45 ^{o}C to rt, 12 h;
(b) chloroformamidine hydrochloride, $DMSO_2$, 125 ^{o}C, 120 min

Scheme 71. Synthesis of thieno[2,3-*d*]pyrimidine **406**.

Commercially available pentaldehyde **404** (Scheme 71) reacted with sulfur, ethyl cyanoacetate and morpholine in EtOH for 24 h at room temperature under Gewald[319] reaction conditions to afford **405** in 78% yield. Cyclization of **405** with chloroformamidine hydrochloride afforded the thieno[2,3-*d*]pyrimidine **406** in yield of 80% (Scheme 71).

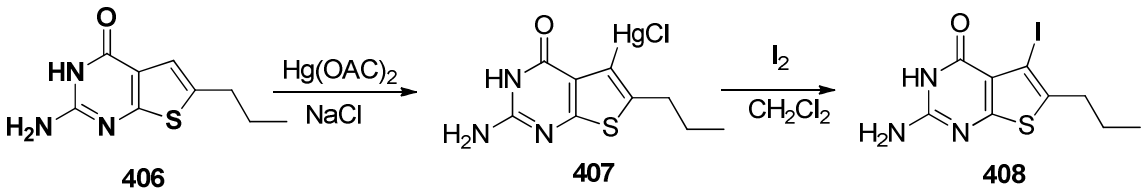

406 407 408

Scheme 72. Synthesis of key intermediate **408**.

Prior to thiolation at the 5-position, a two-step reaction was employed to introduce an iodo moiety on **408** (Scheme 72). Recently, Gangjee *et al.*[337] reported a mercuration methodology that could be adopted for the synthesis of the key intermediate 2-amino-6-propyl-5-iodothieno[2,3-*d*]pyrimidin-4(3*H*)-one **408**. Compound **406** was reacted with mercuric acetate at 150 ^{o}C and then treated with brine. The resulting solid **407** was collected by filtration and was

used for iodination without further purification. Iodine was added to the solution of **407** in CH_2Cl_2 and **408** was obtained in 68% yield (two-step reaction) (Scheme 72). The ^1H NMR of the compound **408** showed the disappearance of the C5 proton at 6.78 ppm, which confirmmed the substitution at the 5-position. Compound **408** was also characterized by elemental analysis.

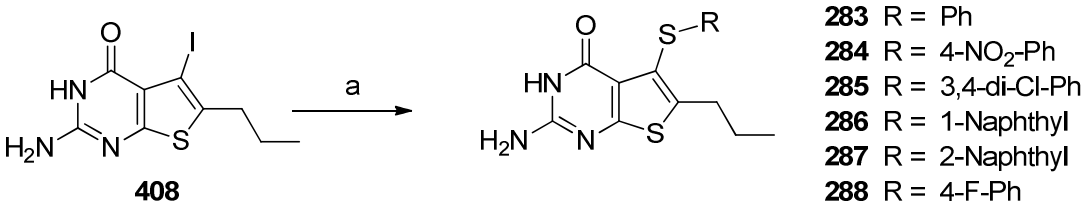

408

283 R = Ph
284 R = 4-NO_2-Ph
285 R = 3,4-di-Cl-Ph
286 R = 1-Naphthyl
287 R = 2-Naphthyl
288 R = 4-F-Ph
289 R = 4-OMe-Ph
290 R = 4-Cl-Ph
291 R = 4-Br-Ph

Reagents and conditions: (a) arylthiols, CuI, K_2CO_3, DMF, microwave 100 ^oC, 60-120 min.

Scheme 73. Synthesis of nonclassical analogues **283-291** *via* Ullmann coupling.

With the intermediate **408** in hand, two different coupling conditions, Buchwald coupling and Ullmann coupling could be employed for conversion of the 5-iodo substitution to the 5-thiol. A comparison of the two strategies suggested that Ullmann coupling had advantages of higher yields and ease of handling since the Buchwald reaction required evacuation and backfilling with nitrogen (3 cycles). Ullmann coupling[343] of **408** and the appropriate arylthiols in the presence of CuI and K_2CO_3 in DMF under microwave irradiation at 100 ^oC for 60-120 min afforded **283-291** in yields that ranged from 75-91% (Scheme 73).

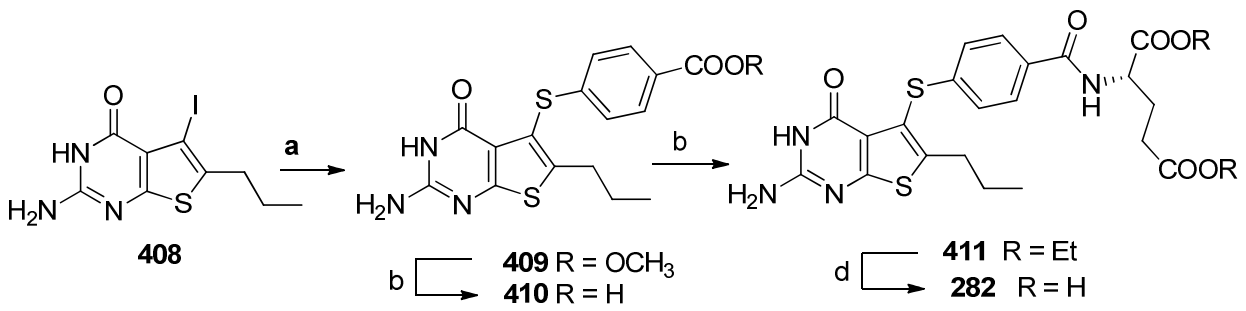

Reagents and conditions: (a) ethyl 4-mercaptobenzoate, CuI, K_2CO_3, DMF, microwave 100 °C, 60-120 min.; (b) 1 N NaOH, EtOH, rt, 18 h; (c) L-glutamic acid diethyl ester hydrochloride, 2-chloro-4,6-dimethoxy-1,3,5-triazine, N-methylmorpholine, DMF, rt, 5 h; (d) 1 N NaOH, EtOH, rt, 24 h.

Scheme 74. Synthesis of classical analogue **282** *via* Buchwald coupling.

For the synthesis of the classical compound **282**, the required intermediate **409** (Scheme 74) was prepared through the Ullmann coupling in 49 %yield. The ^{1}H NMR spectrum of **409** showed the presence of two aromatic doublets at 7.05 ppm and 7.77 ppm, which along with the other protons confirmed the structure of **409**. Hydrolysis of the ethyl ester of **409** with 1 N NaOH in ethanol followed by acid workup gave the corresponding acid **410** in 97% yield. With 2-Cl-4,6-dimethoxy-1,3,5-triazine and 4-methylmorpholine as the coupling reagents, acid **410** was coupled with diethyl-L-glutamate hydrochloride to afford compound **411** in 62% yield. The ^{1}H NMR spectrum of **411** revealed the expected peptide NH doublet at δ 8.60 ppm and δ 8.62 ppm, which exchanged on the addition of D_2O. The splitting pattern of Gluα-CH was simplified on addition of D_2O since the exchange of NH proton removes the coupling. Hydrolysis of **411** in 1 N NaOH followed by acid workup gave target compound **282** in 89% yield. Compound **282** was also characterized by elemental analysis.

3. Nonclassical 2-Amino-4-oxo-5-arylthio-substituted-6-methyl furo[2,3-*d*]pyrimidines as Dual Thymidylate Synthase and Dihydrofolate Reductase Inhibitors

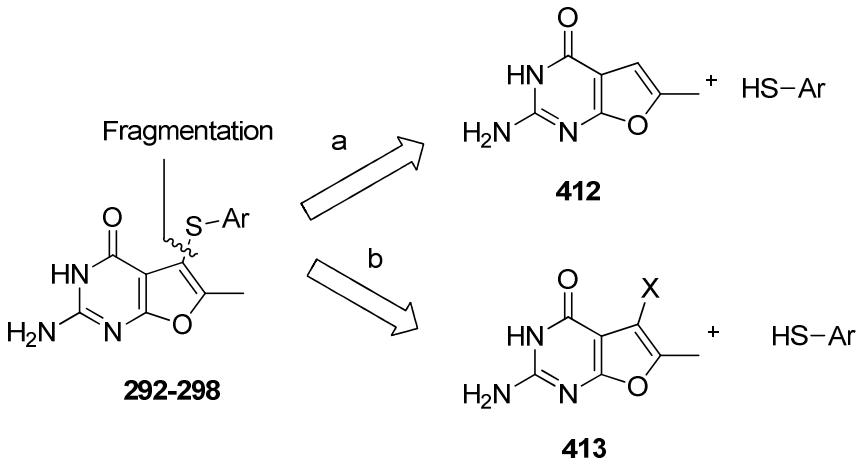

Scheme 75. Retro synthetic analysis to nonclassical 2-amino-5-arylthio-6-methylfuro[2,3-*d*]pyrimidin-4(3H)-one analogues.

From a retrosynthetic point of view (Scheme 75), two general strategies were envisioned for the synthesis of nonclassical 2-amino-5-arylthio-6-methylfuro[2,3-*d*]pyrimidin-4(3H)-one analogues **292-298**. The first strategy (Strategy A) involved the direct sulfenilation of 2-amino-4-oxo-furo[2,3-*d*]pyrimidine **412** with the corresponding thiols to afford **292-298**. The second strategy (Strategy B) involved a coupling of the 5-halogensubstituted-furo[2,3-*d*]pyrimidine **413** with the corresponding thiols. It was anticipated that the required 5-halogensubstituted-furo[2,3-*d*]pyrimidine for Strategy B could be synthesized *via* halogenation of furo[2,3-d]pyrimidine **412**. Thus, furo[2,3-*d*]pyrimidine **412** was the key intermediate for the synthesis of **292-298** in both strategies.

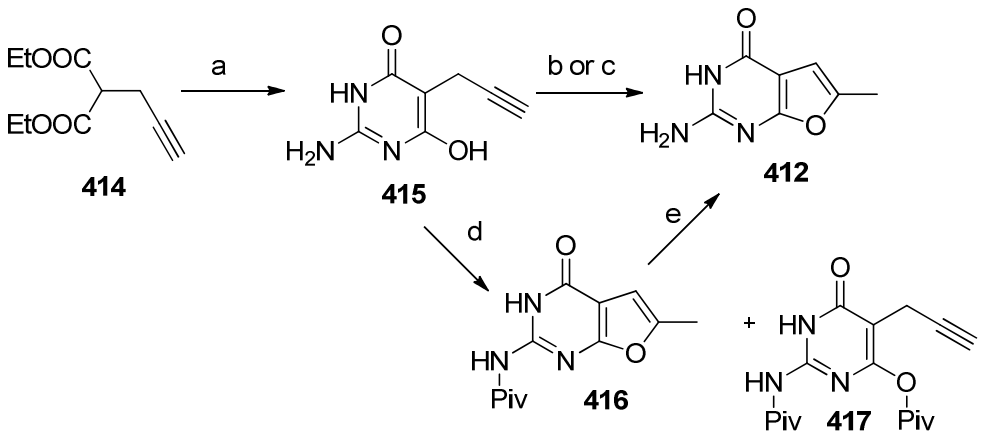

Reagents and conditions: (a) guanidine carbonate, MeOH, reflux, 24 h; (b) H_2SO_4 (conc.), r.t., overnight; (c) 2 N NaOH, microwave 180 ^oC, 30 min; (d) Piv_2O, reflux, 2 h; (e) 1,4-dioxane, 15% KOH, reflux, 10 h.

Scheme 76. The synthesis of intermediate **412**.

A literature search revealed that there was no synthesis or other report for this intermediate. The synthetic method utilized in this study (Scheme 76) was sparked by the report of the synthesis of 2-methyl-4-oxo-furo[2,3-*d*]pyrimidines from the Zimmerman group.[3] Propargyl malonate **414** was condensed with guanidine carbonate at reflux in methanol to afford the corresponding 5-propargyl-2-aminopyrimidine **415** in 40% yield. However, unlike the 2-methyl analogue described by Zimmerman et al., thermocyclization of **415** in DMSO did not afford the corresponding annulated furo analogue **412** but gave instead starting materials. Cyclization in conc. H_2SO_4, however, afforded intermediate **412** in 60% yield on gram scale. The reaction generates a considerable amount of heat that presents a possible physical hazard. It was thus decided to protect the 2-amino group of **415** prior further cyclization. It was interesting to note that during the pivaloylation, instead of the pivaloyl protected compound **417** as the major

product, a direct ring closure product **416** was isolated in good yield (67%) afterseparation from **417**.

With the intermediate **416** in hand, the 2-pivaloyl protecting group was easily removed in base to afford **412** in a yield of 76%. A possible explanation for the unexpected furan formation during pivaloylation could be that under the reaction conditions (high temperature, 120-130 ^{o}C oil bath) the acetylene moiety of **415** tautomerized to the ketene which could be partially stabilized by the conjugated aromatic system, the adjacent hydroxyl oxygen then undergoes an intramolecular cyclization with the reactive ketene to give the annulated compound **416**. Inspired by these initial results, an alternate direct thermocyclization of **415** was also attempted under microwave irradiation in 2 N NaOH at 180 ^{o}C, which affords **412** in a yield of 92%. The only limitation of this microwave condition is that it could not be used for the scale up to gram quantities of **412**.

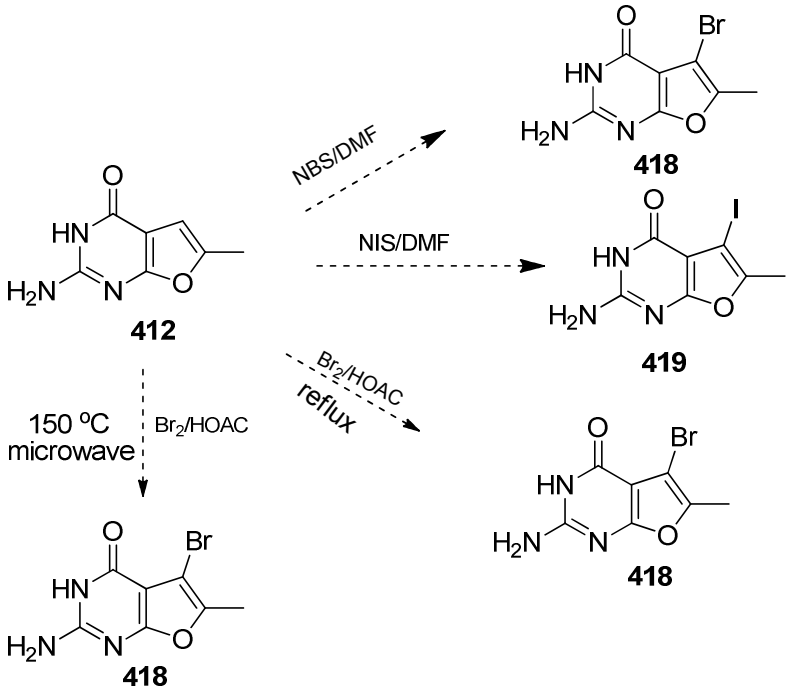

Scheme 77. Attempted halogenation reactions on **412**.

With the key intermediate **412** in hand, it was initially anticipated that different arylthiols could be easily appended to the 5-position of **412** via an oxidative addition reaction using iodine in ethanol/water at reflux as reported by Gangjee et al.[335-337] Unfortunately, all attempts at this oxidative addition using a variety of reaction conditions of time and temperature variations were unsuccessful. Failure of the above method led us to explore a new alternative strategy that involved the halogenation of the 5-position of intermediate **412** to give **418** or **419** (Scheme 77) followed by displacement with the appropriate arylthiols using Ullmann coupling or Buchwald reaction.

The initial approaches for the synthesis of **418** were bromination via NBS in DMF at room temperature or under reflux for 24 h (Scheme 77). Unfortunately, neither of these reactions afforded **418**. NIS did not afford **419** under similar reaction conditions either. Bromine in acetic acid under microwave irradiation at 150 ^{o}C for 30 min was also attempted but to no avail (Scheme 77).

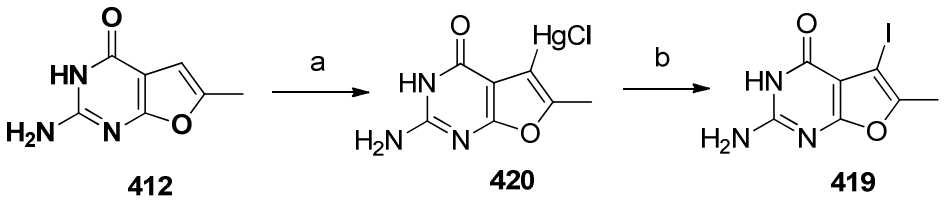

Reagents and conditions: (a) $Hg(OAc)_2$, AcOH, 100 ^{o}C, 3 h; (b) I_2, CH_2Cl_2, r.t., 12 h.

Scheme 78. The synthesis of **419**.

A two step iodonation reaction *via* mercury intermediate was successfully applied in the synthesis of the 5-iodo-thieno[2,3-*d*]pyrimidine **408** (Scheme 72). Thus the same strategy was applied for the synthesis of **419**. Compound **412** (Scheme 78) was reacted with mercuric acetate

at 100 ^{o}C and then treated with brine. The resulting solid **420** was collected by filtration and without further purification was iodinated with iodine in CH_2Cl_2 to afford **419** in 68% (over two-steps).

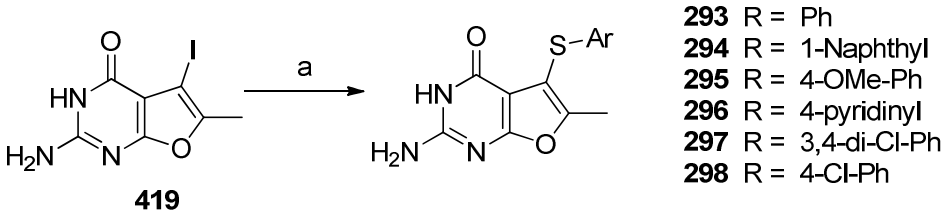

Reagents and conditions: (a) thiols, Cu_2O, K_2CO_3, DMF, microwave 150 ^{o}C, 1h.

Scheme 79. The synthesis of **293-298.**

With the intermediate **419** in hand, attention was turned to the synthesis of target nonclassical analogues **293-298** and intermediate **420** for the synthesis of the classical analogue. The Ullmann coupling of **419** with appropriate thiols in the presence of Cu_2O and K_2CO_3 in DMF under microwave irradiation at 150 ^{o}C for 1 h afforded target compounds in moderate to good yields (57%-70%).

4. 2,4-Diamino-6-substituted bicyclic-pyrimidines as dihydrofolate reductase inhibitors.

Gangjee *et al.*[280] reported the synthesis of 2,4-diamino-6-substituted-pyrido[2,3-*d*]pyrimidines through the reductive amination of the intermediate 2,4-diaminopyrido[2,3-*d*]pyrimidine-6-carbonitrile with appropriately substituted anilines. It was anticipated that 2,4-diamino-6-substituted-quinazoline could be synthesized through a similar reaction by the reductive amination of the 2,4-diaminoquinazoline-6-carbonitrile or 2,4-diaminoquinazoline-6-aldehyde with the appropriately substituted anilines.

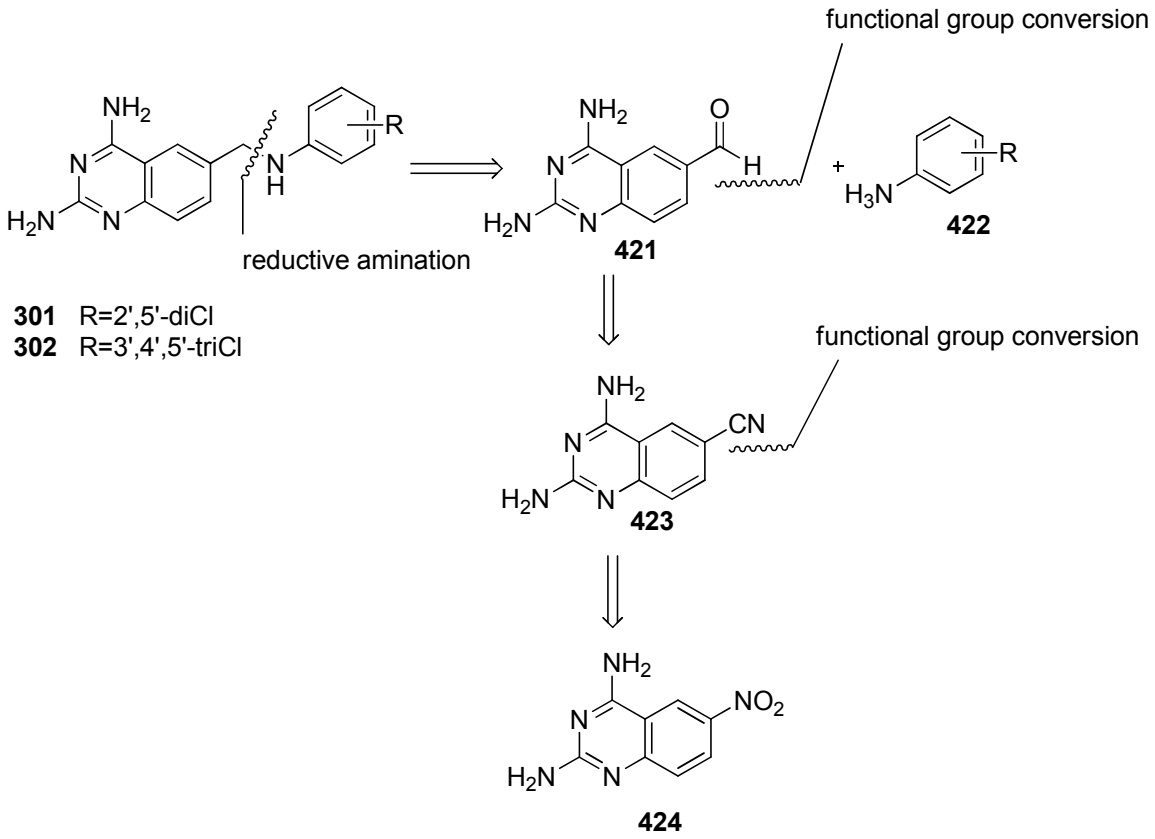

Scheme 80. Retro synthetic analysis to 2,4-diamino-6-substituted quinazoline **301** and **302** (Strategy A).

A search of the literature revealed that **421** and **423** (Scheme 80) are commercially available. However, the commercial sources of **421** and **423** are overseas and the prices are prohibitively high. A further literature search revealed that 2,4-diamino-6-nitroquinazoline **424**, the precursor for 2,4-diaminoquinazoline-6-carbonitrile also have a very limited commercial source and prohibitive price. It was therefore decided to develop another synthetic strategy for the synthesis of the target compounds **301-302**.

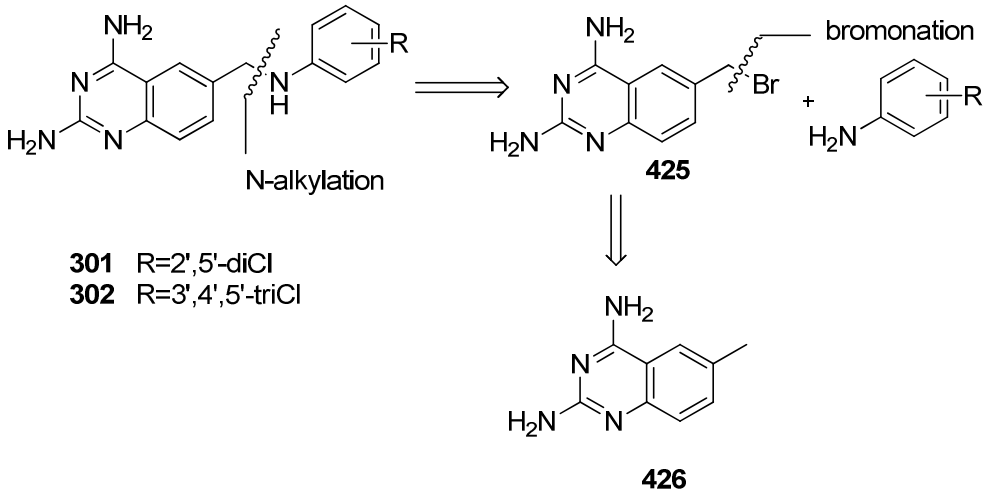

Scheme 81. Retro synthetic analysis to 2,4-diamino-6-substituted quinazoline **301** and **302** (Strategy B)**.**

From a retrosynthetic point of view (Scheme 81), it was anticipated that a benzyl bromination of **426** would afford the 6-bromomethyl substituted quinazoline **425**, which could undergo N-alkylation with appropriate anilines to afford the desired compounds.

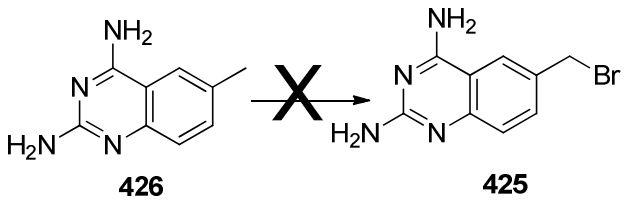

Scheme 82. Initial attemps for the synthesis of **425**.

Compound **426** (Scheme 82) was commercially available and was used directly in the bromination step, which however was unsuccessful. Radical reaction using NBS with catalytic amounts of AIBN in DMF at room temperature resulted in retention of the methyl group at the benzyl position, while no reaction occurred using several other conditions (e.g., NBS/Bz_2O_2,

DMF under microwave conditions 180 ^{o}C, 2 h; Br_2/AcOH under microwave condition 150 ^{o}C, 1 h or reflux); and the starting material **426** was recovered unchanged. Typically the free radical bromination reaction was carried out in nonpolar solvents such as benzene and carbon tetrachloride. Because compound **426** is almost insoluble in the above mentioned nonploar solvents, the bromonation raction has to be carried out in polar solvents, such as DMF and acetic acid, which may quench the free radio before the chain reaction was initiated.

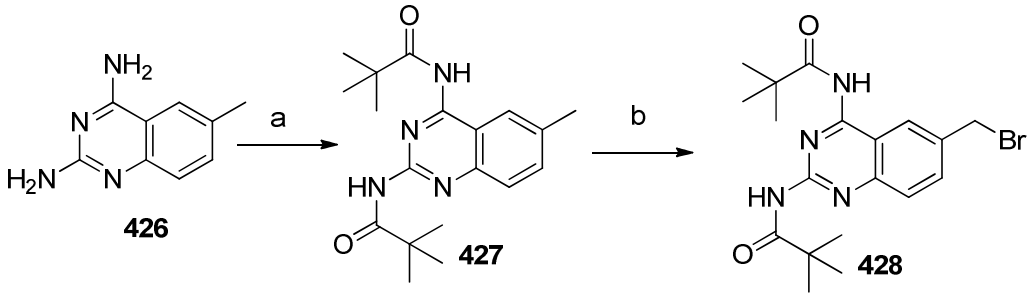

Reagents and conditions: (a) Piv_2O/reflux.; (b) NBS/Bz_{2O2}/ reflux

Scheme 83. The synthesis of **428**.

Failure of the above methods led to the exploration of a new alternate strategy where the free amino groups in quinoline **426** could be protected prior to any transformation. Compound **426** with the 2, 4-diamino groups has poor solubility in organic solvent and the existence of free amino moiety might interfere with the bromination reaction, both these two aspects probably contributed to the failure of the benzylic bromination. It was thus decided to protect the amino groups in **426** with pivaloyl group. Starting from commercially available 6-methylquinazoline-2,4-diamine, **427** was obtained by the protection of the 2,4-diamino groups. The reaction was carried out at reflux with pivaloyl anhydride. The protection of the diamino group not only boosts the solubility of the compound in nonpolar organic solvents but also avoids the possible

side reactions with the amino groups. The reaction between **427** and NBS was carried out in CH_2Cl_2 solution with benzoyl peroxide (Bz_2O_2) as the free radical initiator to afford intermediate **428**, the structure of which was confirmed by ^{1}HNMR. Under free radical bromination condition, the bromine atom was introduced to the benzylic position rather than aromatic positioins. On ^{1}HNMR spectrum, an integration of three protons in **427** changed to an integration of two protons, with all the other aromatic protons and aliphatic protons unchanged.

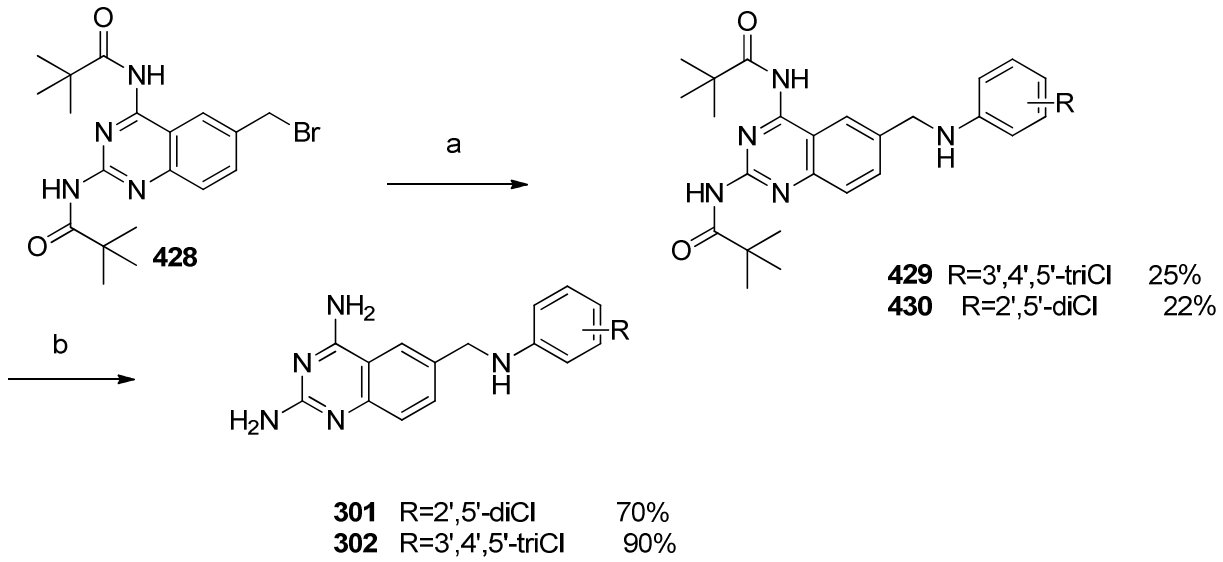

Reagents and conditions: (a) appropriate aniline/DMF/reflux.; (b) 1N NaOH/reflux

Scheme 84. The synthesis of **301** and **302**

The synthesis of the target compounds **301** and **302** were accomplished as indicated in Scheme 84. *N*-alkylation of the appropriate aniline benzyl bromide **428** was carried out at reflux in DMF to afford desired the intermediates **429** and **430**. Pivaloyl deprotection under basic condition converted **429** and **430** to the target compounds **301** and **302** respectively.

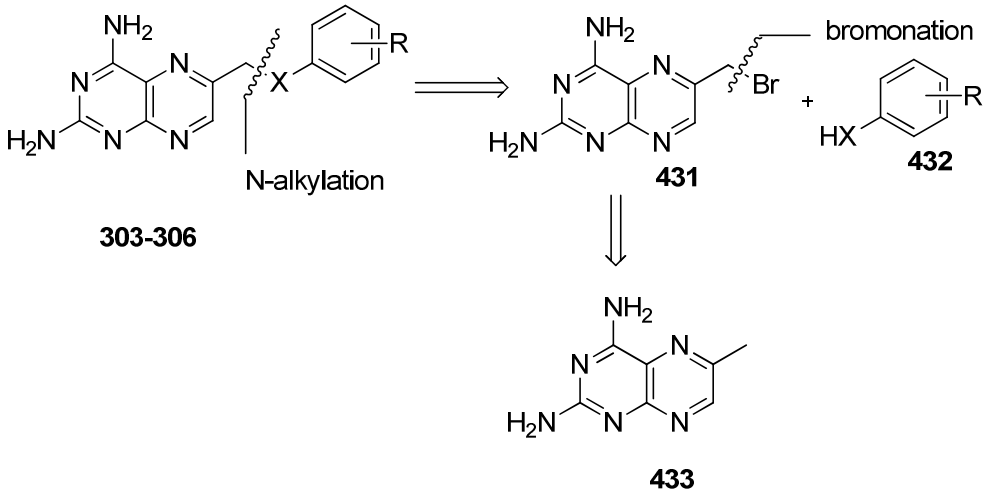

Scheme 85. Retro synthetic analysis to 2,4-diamino-6-pteridines **303** and **306**.

From a retrosynthetic point of view (Scheme 85), it was anticipated that target compounds **303-306** could be synthesized *via* the nucleophilic displacement of 6-bromomethyl substituted pteridine **431**, which in turn could be synthesized *via* bromination at the benzylic position catalyzed by a free radical initiator.

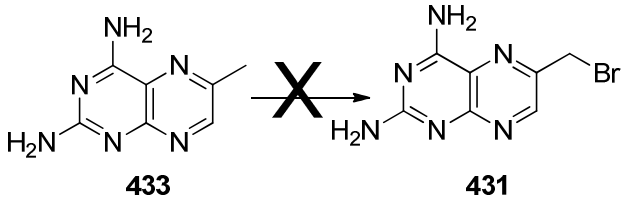

Scheme 86. Initial attemps for the synthesis of **431**

Compound **431** was commercially available and was used directly in the bromination step, which turned out to be unsuccessful. Radical reaction using NBS with catalytic amounts of AIBN in DMF at room temperature resulted in retention of the methyl group at the benzyl position, with no reaction. Several other conditions (e.g., NBS/Bz_2O_2, DMF under microwave

conditions 180 ^{o}C, 2 h; Br_2/AcOH under microwave condition 150 ^{o}C, 1 h or reflux); resulted in the starting material **433** being recovered unchanged.

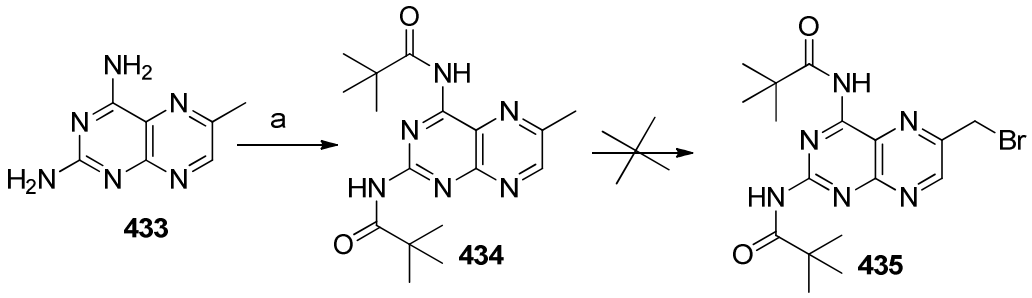

Reagents and conditions: (a) Piv_2O/reflux.

Scheme 87. Attemps for the synthesis of **435**.

Failure of the above methods led to the exploration of an alternate strategy where the free amino groups in pteridine **433** was protected prior to any further transformation. Compound **433** with the 2,4-diamino groups is poorly soluble in organic solvent and the existence of free amino groups could interfere with the bromination reaction. As discussed above, both these reasons contributed to the failure of the bromination step. It was thus decided to protect the amino groups in **433** with pivaloyl groups, as the strategy was showned to be effective in the synthesis of **428**. Starting from commercially available 6-methylquinazoline-2,4-diamine, **434** was obtained by the protection of the 2,4-diamino groups. The reaction was carried out at reflux in pivaloyl anhydride. Although the protection of the diamino group boosts the solubility of the compound in organic solvent, the attempted bromination of **434** were unsuccessful under various condtions. The existance of pteridine ring nitrogens may quenched free radicals in the reaction system and prohibited further chain reaction at the benzylic position.

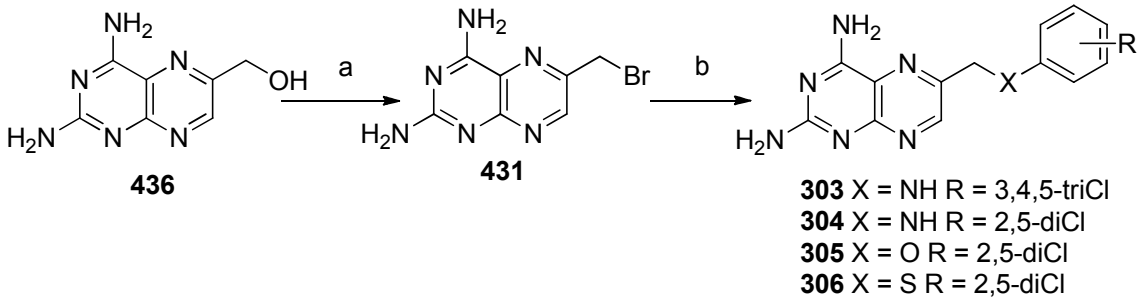

Reagents and conditions: (a) PPh_3Br_2; (b) appropriate neucleophile.

Scheme 88. The synthesis of **303-306**.

Failure of the above methods led to the exploration of yet another alternate strategy and is shown in Scheme 88. Reaction of commercially available (2,4-diaminopteridin-6-yl)methanol (**436**) with PPh_3Br_2 afforded 6-(bromomethyl)pteridine-2,4-diamine **431** as the key intermediate. The nucleophilic displacement of **431** with approriate anilines, phenols and thiophenols afforded target compounds **303-306**.

5. Importance of the Side Chain Aryl Group for Folate Receptor Targeting and GARFTase Inhibitory Activity in Classical Thieno[2,3-*d*]pyrimidine Antifolates

Esterification of commercially available **437** (Scheme 89) was achieved in methanol in the presence of $SOCl_2$ to afford methyl ester **438**. Subsequent Sonogashira coupling of **438** with **439** were in acetonitrile in the presence of $PdCl_2$, CuI and PPh_3 gave **440**. Pd/C catalyzed hydrogenation converted **440** to the corresponding alcohol **441**. A Swern oxidation of **441** with DMSO and oxalyl chloride afforded the corresponding aldehydes **442**.

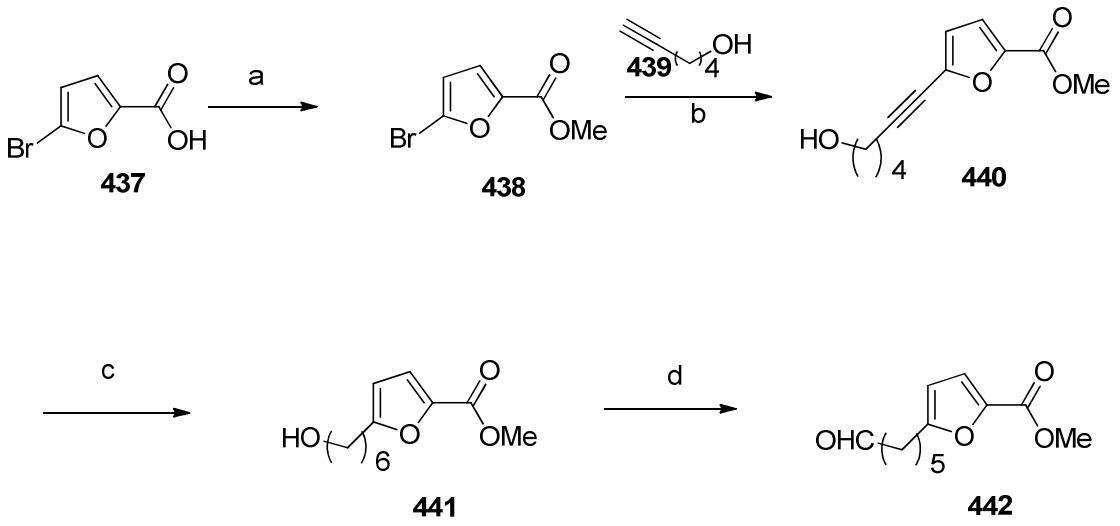

Reagents and conditions: (a) $SOCl_2$, MeOH, 12 h; (b) $PdCl_2$, CuI, PPh_3, NEt_3, microwave, 10 min; (c) 10% Pd/C, MeOH; (d) oxalyl chloride, DMSO, NEt_3.

Scheme 89. The synthesis of intermediate **442.**

With key aldehydes **442** in hand, a reaction of **442** (Scheme 90) with ethyl cyanoacetate and sulfur in the presence of morpholine was carried out according to the general procedure of Gewald and coworkers to afford the thiophene intermediate **443**. Cyclization of **443** with chloroformamidine hydrochloride afforded the thieno[2,3-*d*]pyrimidines **444**. Hydrolysis of the methyl ester of **444** with 1 N NaOH in ethanol followed by acid workup gave the corresponding acids **445**. Coupling of **445** with diethyl-L-glutamate followed by saponification afforded the desired product **317**.

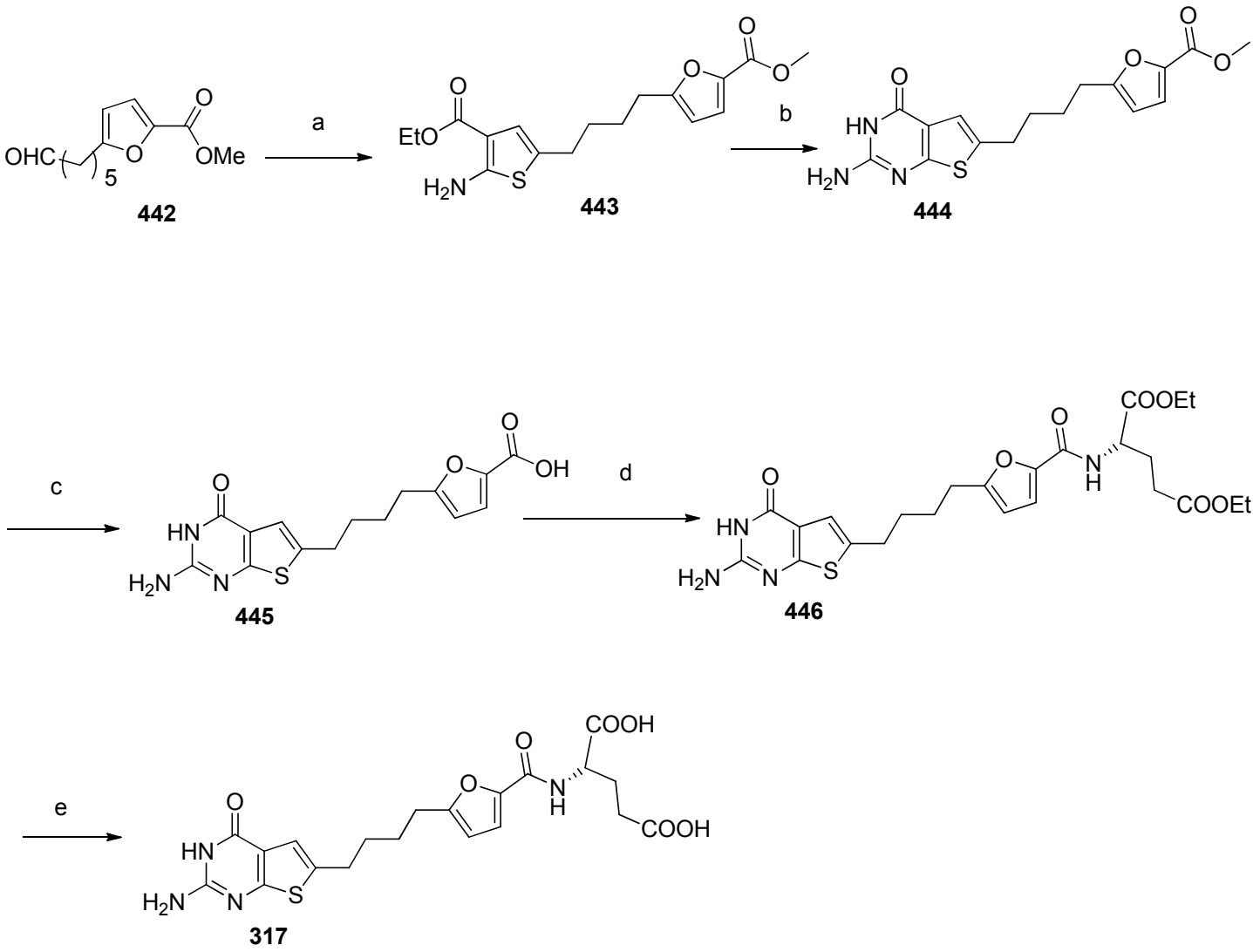

Reagents and conditions: (a) S, CN-CH_2-COOEt, Morpholine R.T. 24 h;
(b) Chloroformamidine hydrochloride, $DMSO_2$, 140 ^{0}C 4 h; (c) 1 N NaOH, EtOH, rt, 12h.
(d) Diethyl glutamate, 4-Methylmorpholine, 2-Cl-4,6-dimethoxy-1,3,5-triazine, DMF, 10 h; (e) 1 N NaOH, EtOH, rt, 24 h.

Scheme 90. The synthesis of intermediate **317.**

6. Importance of the Glutamate Moiety for Folate Receptor Targeting and GARFTase Inhibitory Activity in Classical Thieno[2,3-*d*]pyrimidine Antifolates

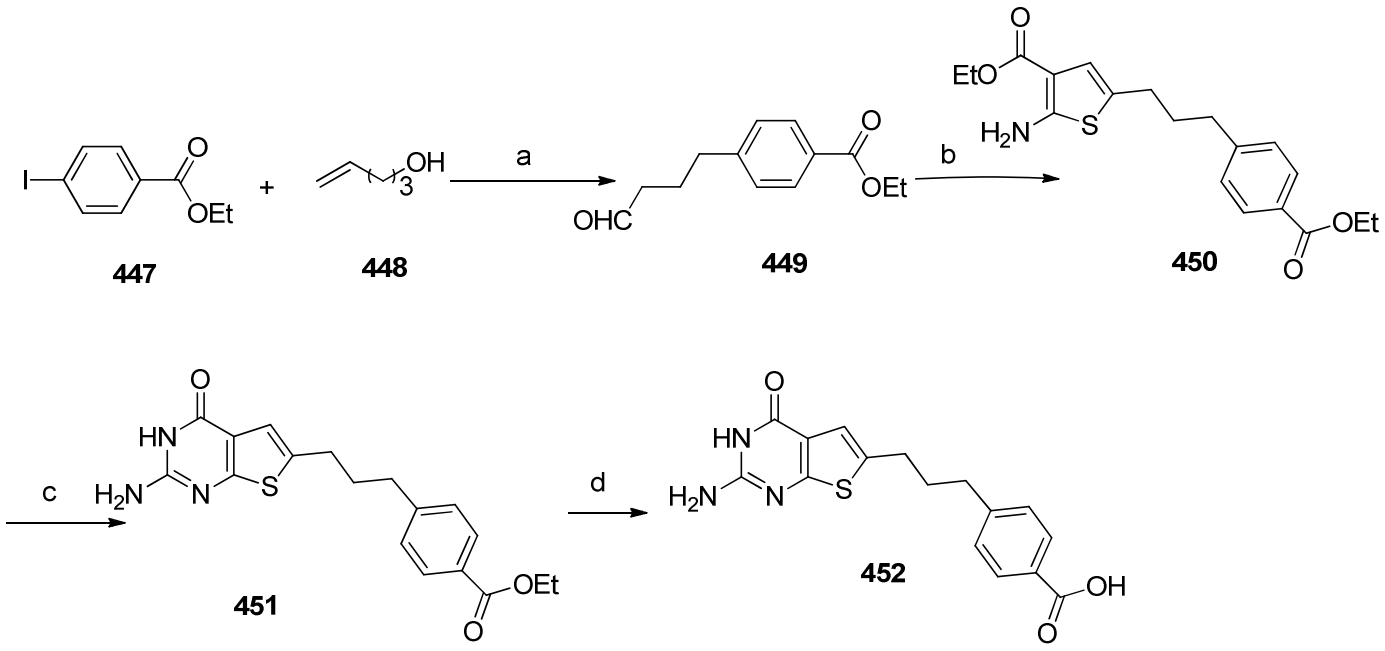

Reagents and conditions:
(a)10%$Pd(AcO)_2$, Bu_4NCl,LiCl, LiOAc, DMF 80 ^{0}C 12 h.; (b)S, CN-CH_2-COOEt, Morpholine R.T. 24 h;
(c) Chlorformamidine hydrochloride, $DMSO_2$, 140 ^{0}C 4 h; (d) 1 N NaOH, EtOH, rt, 12h;

Scheme 91. The synthesis of thieno[2,3-*d*]pyrimidine **452**

Allyl alcohol **448** was treated with palladium diacetate, ethyl 4-iodobenzoate **447**, LiCl, LiOAc and Bu_4NCl in DMF to afford the aldehyde **449**. A modified reaction temperature of 80 ^{o}C from that reported in the literature improved the yield. Aldehyde **449** was then reacted with sulfur, ethyl cyanoacetate and morpholine in EtOH for 24 h at room temperature under Gewald[319] reaction conditions to afford **450**. Cyclization of **450** with chloroformamidine hydrochloride afforded the thieno[2,3-*d*]pyrimidines **451** in 80% yield. Hydrolysis of the ethyl

ester of **451** with 1 N NaOH in ethanol followed by acid workup gave the corresponding acid **452.**

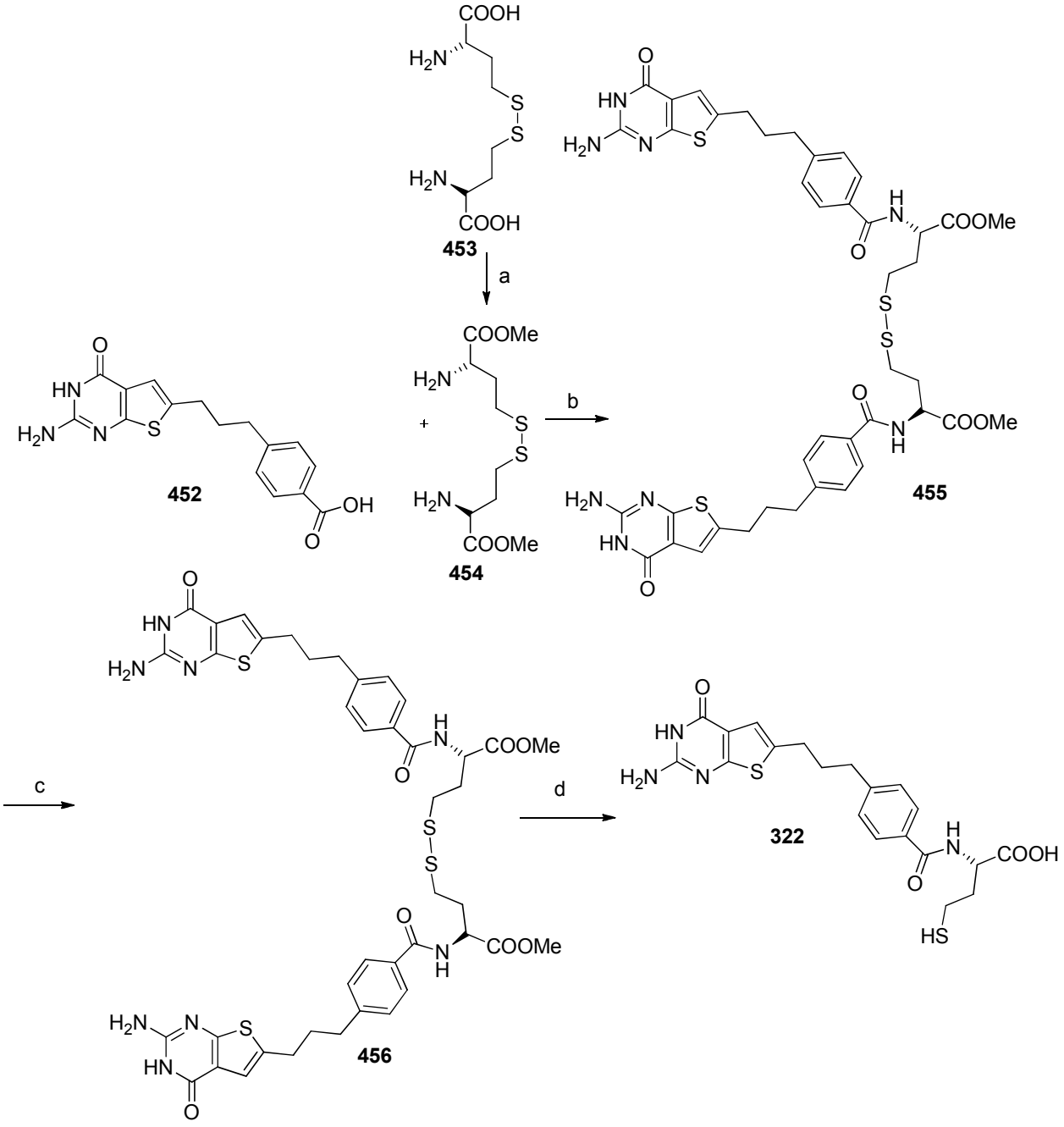

Reagents and conditions:
(a) $SOCl_2$, MeOH, 4 h; (b)4-methylmorpholine, 2-Cl-4,6-dimethoxy-1,3,5-triazine, DMF, 10 h;
(c) 1 N NaOH, EtOH, 12 h.; (d) DTT, 4 h

Scheme 92. The synthesis of **322**

The synthesis of compound **322** is shown in Scheme 92. Commercially available homocystine was converted to the corresponding dimethyl ester **454** by reacting with $SOCl_2$ in methanol solution. Peptide coupling of **452** and **454** in anhydrous DMF solution afforded disulfide **455**, which was further converted to **322** through deprotection and reduction. The reduction of the disulfide was carried out in aqueous solution using DTT as the reducing agent at pH = 9.

7. Synthesis of *N*-aryl-2,6-dimethylfuro[2,3-*d*]pyrimidin-4-amines as RTK inhibitors.

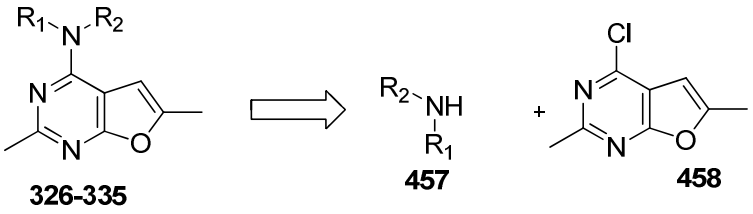

Scheme 93. Retro synthetic analysis to N-aryl-2,6-dimethylfuro[2,3-*d*]pyrimidin-4-amines **326-335**.

From a retrosynthetic analysis (Scheme 93), the desired *N*-aryl-2,6-dimethylfuro[2,3-*d*]pyrimidin-4-amines **326-335** could be synthesized from 2,6-dimethyl-4-chloro-furo[2,3-*d*]pyrimidine **458** *via* neucleophilic displacement. Compound **458** is a versatile intermediate and should react with a large variety of nucleophiles, thus **458** is the key intermediate for the synthesis of **326-335**.

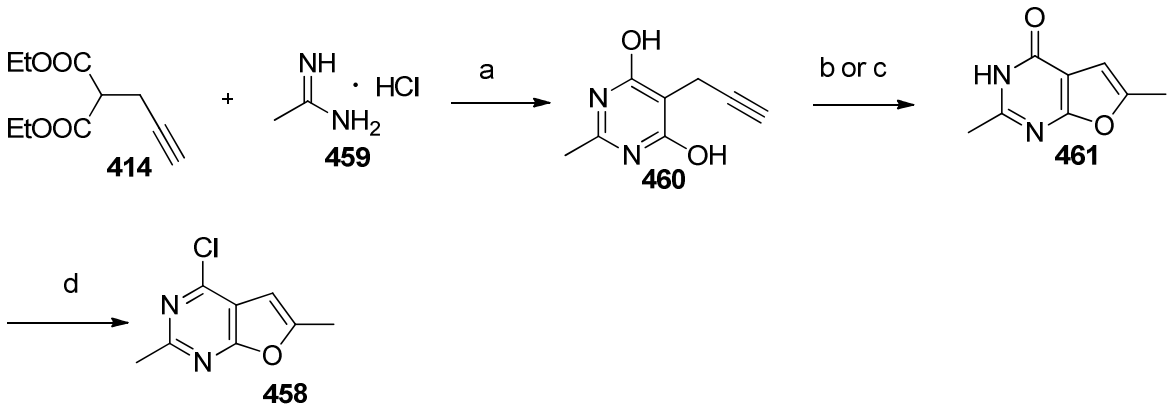

Reagents and conditions: (a) Na/MeOH/reflux; (b) H_2SO_4 (Conc.); (c) 2 N NaOH, 150^oC, microwave; (d) $POCl_3$, reflux

Scheme 94. The synthesis of 2,3-dimethyl-4-chloro-furo[2,3-*d*]pyrimidine **458**.

The synthesis of compound **458** is shown in Scheme 94. A two step reaction starting from dimethyl propargyl malonate **414** was successfully employed in the synthesis of 2-amino-4-oxo-6-methyl-furo[2,3-*d*]pyrimidine **412** (Scheme 76). It was anticipated that the same strategy could be extended to the synthesis of 2,6-dimethyl-4-oxo-furo[2,3-*d*]pyrimidine **461**. The condensation of dimethyl propargyl malonate **414** and acetamidine hydrochloride **459** was attempted as a route to pyrimidine **460**. The use of anhydrous MeOH and sodium metal are essential for the cyclization of the pyrimidine ring. With dihydroxyl pyrimidine **460** in hand, the next step was the intramolecular cyclization to give the furo[2,3-*d*]pyrimidine **461**. Two different strategies were developed for this cyclization. One was the cyclization under H_2SO_4 (Conc.) at r.t, and the other, the cyclization in 2N NaOH at 150 ^oC under microwave irradiation. The conversion under acidic conditions not only provide high yieldss (87%) of **461** but also leads itself to scale up and was used for the synthesis of gram quantities of **461** for in vivo evaluation. However, the use of large amount of H_2SO_4 (Conc.), especially for the scale up conditions, resulted in reaction temperature

control difficuties and posed a potential physical hazard. Due to the disadvantage of acid cyclization, using 2 N NaOH was developed for the conversion of **460** to **461**. The reaction was carried out under aqueous reaction conditions and the choice of base and reaction temperature was of critical importance for the cyclization. Several inorganic and organic bases including NaOH, Na_2CO_3, Ce_2CO_3, NaOMe and NEt_3 were attempted, with the best result obtained for NaOH. The optimal reaction temperature was above 150 ^oC. The desired product was not observed on TLC when the reaction was carried out at reflux or at 120 ^oC. Through the use of microwave irradiator, the reaction media could be heated to the required temperature (150 ^oC) in a fast and efficient manner. However, the attempt to further increase the reaction temperature was unsuccessful, due to the high pressure in the reaction vial of the microwave reactor.

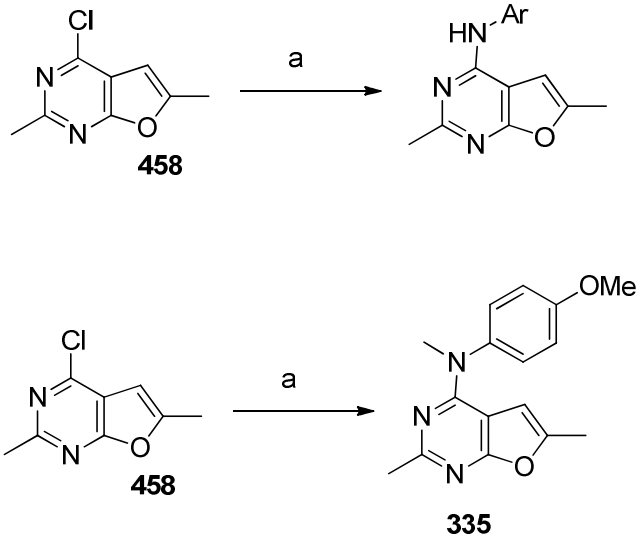

326 Ar = phenyl
327 Ar = naphthalen-1-yl
328 Ar = 3-ethynylphenyl
329 Ar = 4-(trifluoromethyl)phenyl
330 Ar = 3-chloro-4-fluorophenyl
331 Ar = 4-chlorophenyl
332 Ar = 1H-indol-4-yl
333 Ar = 4-methoxyphenyl
334 Ar = 3-fluorophenyl

Reagents and conditions: (a) the appropriate anilines, ^iPrOH or ^nBuOH, 1 drop of HCl (conc.), reflux

Scheme 95. The synthesis of *N*-aryl-2,6-dimethylfuro[2,3-*d*]pyrimidin-4-amines **326-335.**

Chlorination of **461** with $POCl_3$ afforded 2,6-dimethyl-4-chloro-furo[2,3-*d*]pyrimidine **458** (Scheme 95). This key intermediate was reacted with the appropriate nucleophiles to give the target compounds **326-335**. The reaction of **458** and the appropriate nucleophiles was carried out in ^{i}PrOH or ^{n}BuOH at reflux in the presence of a catalytic amount of HCl.

8. *N*-(4-methoxyphenyl)-*N*,2,6-trimethylfuro[2,3-*d*]pyrimidin-4-amine hydrochloride for improved water solubility.

Compound **335** is soluble in several different organic solvents, including methanol, acetone, ethyl acetate, ether and others. It was anticipated that the hydrochloric acid salt of **335** could have less solubility in organic solvent. Thus treatment of organic solutions of **335** with acid should afford the corresponding salt form, which could precipitate from the organic solvent.

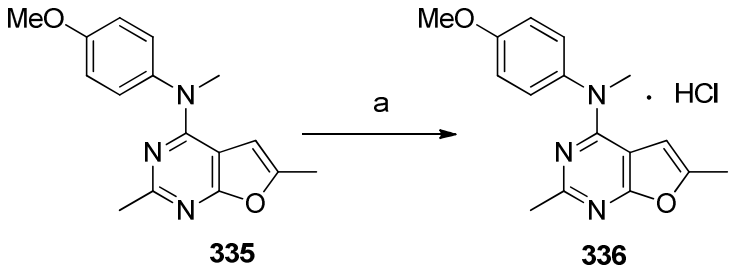

335 **336**

Reagents and conditions: (a) ether, HCl (g).

Scheme 96. The synthesis of hydrochloric acid salt **336**.

Treatment of **335** with HCl (g) in anhydrous ether (Scheme 97) afforded the hydrochloric acid salt **336**. Several different conditions were attempted to obtain **336** and are compared in table 11. In the initial attempt, 100 mg of **335** was dissolved in anhydrous ether to obtain a clear solution. After hydrochloric acid gas was bubbled through the solution, the formation of a white

precipitate was observed. However, the precipitate instantly redissolved. Similar phenomena were observed when the amount of **335** was increased up to 300 mg (entry 2 in table 1). Another method (entry 3 in table) was attempted to obtain **336** by using ^{i}PrOH as the solvent and concentrate HCl as the acid source. However, no precipitate was observed under these conditions.

Table 11. Attempted conditions for the synthesis of **336**.

Entry	amount	solvent	HCl source	Yield
1	100 mg	ether	G	precipitate redissolved
2	300 mg	ether	G	precipitate redissolved
3	100 mg	^{i}PrOH	Conc.	No precipitation
4	2 g	ether	G	96%

A literature search revealed that hydrochloric acid gas can react with ether to form an oxonium salt, which can dissolve a small amount but not large amounts of organic salts. Thus, the amount of **335** was increased to 2 g (entry 4 in table 1). Using ether as the solvent and HCl (g) as the acid source, **336** was obtained in 96% yield. Although the ^{1}HNMR spectrum did not show a distinguishable peak for the newly formed 1-N^{+}H proton, **335** and **336** have distinct melting point (108 ^{o}C for **335** and 273 ^{o}C for **336**). In addition, elemental analysis confirmed the stoichiometry of the salt as exact one molecule of hydrochloride per molecule of **336** with an additional 0.3 molecule of water.

Salt **336** has excellent water solubility (>2.5 mg/mL) and can be prepared as an aqueous solution for *in vivo* testing.

9. Synthesis of *N*-(substitutedphenyl)-*N*,2,6-trimethylfuro[2,3-*d*]pyrimidin-4-amine as antimitotic anticancer agents.

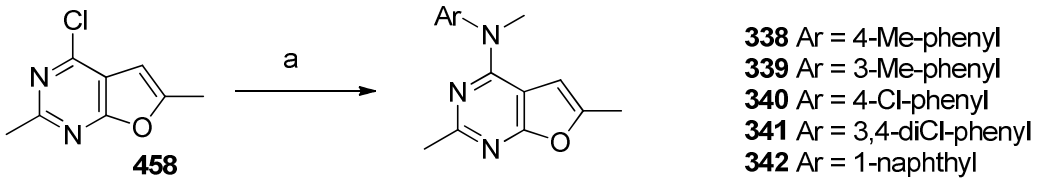

Reagents and conditions: (a) the appropriate anilines, ^{i}PrOH or ^{n}BuOH, 1 drop of HCl (conc.), reflux

Scheme 97. The synthesis of *N*-aryl-2,6-dimethylfuro[2,3-*d*]pyrimidin-4-amines **338-342.**

Target compounds **337-342** were synthesized using the method described for the synthesis of **335**, via the reaction of 2,3-dimethyl-4-chloro-furo[2,3-*d*]pyrimidine **458** and the appropriate N-methyl anilines (Scheme 97). The starting material **458** was treated with the appropriate N-methyl anilines and a catalytic amount of HCl in ^{i}PrOH or ^{n}BuOH at reflux. After the removal of the reaction solvent, the residue was purified through chromatography or recrystalized from ether to afford the target compounds in moderate to good yields (57%-74%). Anilines with electron donating group give high yilds, while the yields in anilines with electron withdrawing groups are lower. The structures of the **338-342** were confirmed by ^{1}HNMR and elemental analysis. After substituions, anilino aromatic protons can be clearly detected on the ^{1}HNMR spectrum around 6-7 ppm.

10. Synthesis of conformationally restricted *N*-(substituted)-2,6-dimethylfuro[2,3-*d*]pyrimidin-4-amine as antimitotic anticancer agents.

Compound **333**, the key intermediate for the synthesis of **343-346**, was synthesized from propargyl malonate *via* a four step strategy as described before (Scheme 92 and Scheme 93). The

reaction of **333** with NaH in anhydrous DMF resulted in the releasing of hydrogen gas and the deprotonation of **333** (Scheme 98).

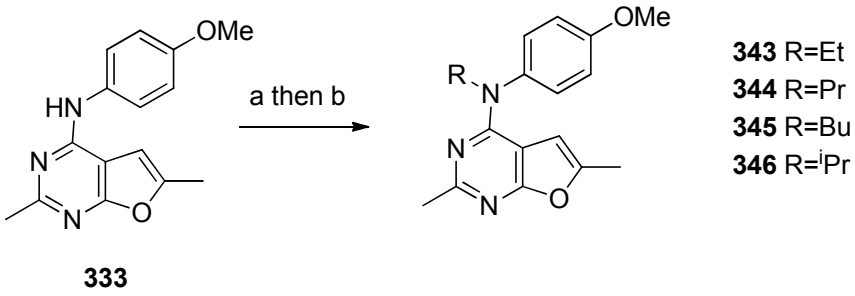

333

Reagents and conditions: (a) NaH, DMF; (b) alkyl iodide

Scheme 98. The synthesis of *N*-aryl-2,6-dimethylfuro[2,3-*d*]pyrimidin-4-amines **343-346**.

The resulting reaction mixture was then treated with the appropriate alkyl iodide to afford target compounds **343-346**.

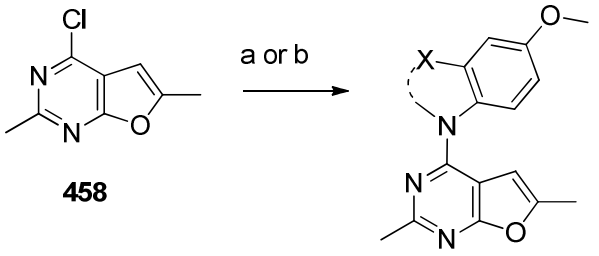

458

347 X = CH_2
349 X = CH_2CH_2

Reagents and conditions: (a) the apropriate aniline, ^{i}PrOH, 1 drop of HCl, reflux.;
(b) the appropriagte aniline, CuI, proline, Na_2CO_3

Scheme 99. The synthesis of *N*-aryl-2,6-dimethylfuro[2,3-*d*]pyrimidin-4-amines **347-349**.

With the intermediate **458** in hand, two different strategies, Ullmann coupling and neucleophilic displacement were developed for the synthesis of **347** and **349** (Scheme 99). The two strategies afforded identical products and in similar yields. Ullmann coupling of **458** and the

appropriate nucleophiles in the presence of CuI and K_2CO_3 in DMF under microwave irradiation at 100 ^oC for 60-120 min afforded **347** and **349** in moderate yields. The nucleophilic displacement at reflux in ^{i}PrOH and a catalytic amount of HCl provided slightly improved yields (63% and 48% respectively).

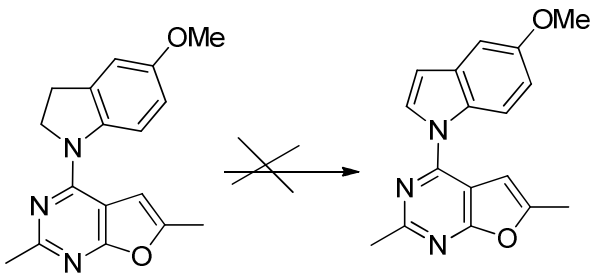

347 **348**

Scheme 100. The attempted synthesis of **348**.

Gangjee *et al.*[407] reported the oxidation of dihydropyrrolo[2,3-*d*]pyrimidines to their aromatic congeners *via* MnO_2 oxidation. In addition, stoimetric amount of Pd/C was reported as a dehydrogenation agent to effect aromatization. Thus, the direct oxidation of **347** to form **348** was attempted (Scheme 100). Reaction of **347** with MnO_2 at reflux in dioxane for up to 24 h afforded no new product (TLC). The oxidation of **347** in the presence of Pd/C did not provided the desired product **348** either.

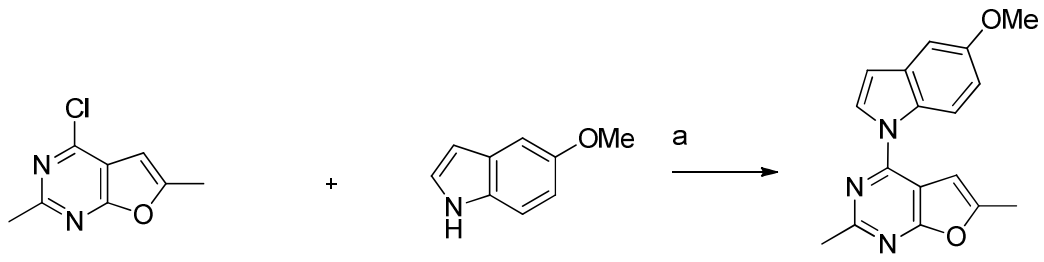

358 **462** **348**

Reagents and conditions: (a) NaH, DMF, 0^{o}C-r.t.

Scheme 101. The synthesis of compound **348**.

The failure of the above two strategies promoted us to develop a procedure for the synthesis of **348**. The deprotonation of 5-methoxyindoline with NaH in DMF resulted in the formation of indoline anion, which then reacted with **358** *via* a nucleophilic displacement to afford **348** in good yield. The structure of **348** was confirmed by ^{1}HNMR and elemental analysis.

11. Synthesis of *N*-(substituted)-2,6-dimethylfuro[2,3-*d*]pyrimidin-4-amines as antimitotic anticancer agents.

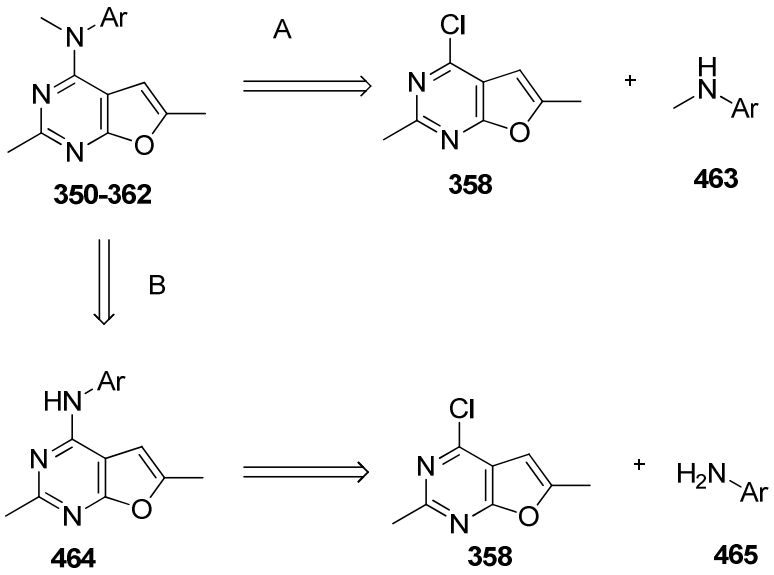

Scheme 102. Retro synthetic analysis to *N*-(substituted)-2,6-dimethylfuro[2,3-*d*]pyrimidin-4-amines **350-362**.

From a retrosynthetic point of view (Scheme 102), two general strategies were envisioned for the synthesis of *N*-(substituted)-2,6-dimethylfuro[2,3-*d*]pyrimidin-4-amines **350-362**. The first strategy (Strategy A) involved the direct nucleophilic displacement of 4-chloro-

2,6-dimethylfuro[2,3-*d*]pyrimidine **358** with the appropriate *N*-methyl anilines to afford **292-298**. The second strategy (Strategy B) involved the reaction of 4-chloro-2,6-dimethylfuro[2,3-*d*]pyrimidine **358** and the appropriate aniline followed by *N*-methylation. Thus, 4-chloro-2,6-dimethylfuro[2,3-*d*]pyrimidine **358** was the key intermediate for the synthesis of **350**-**362** in both strategies.

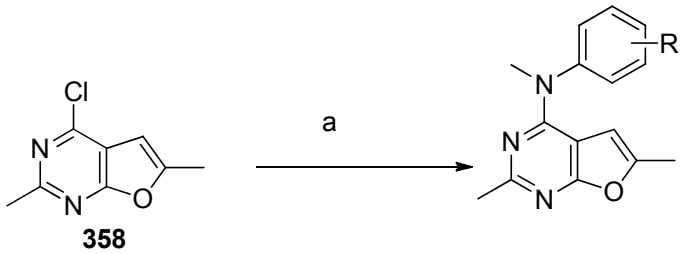

358

350 R = 2-OMe
351 R = 3-OMe

Reagents and conditions: (a) the apropriate N-methylaniline, ^{i}PrOH, 1 drop of HCl, reflux.;

Scheme 103. The synthesis of **350** and **351**.

Compound **358** was synthesized from propargyl dimethyl malonate via a 4 step sequence as described before (Scheme 94). With **358** in hand, compounds **350** and **351** were synthesized via strategy A. Compound **358** reacted with 3-methoxy-N-methyl aniline or 2-methoxy-N-methyl aniline in ^{i}PrOH at reflux to afford **350** and **351** respectively.

With **354** as the only exception, compounds **352-362** (Scheme 104) were synthesized *via* a two step strategy starting from **358**. The reaction of **358** and appropriate anilines in ^{i}PrOH at reflux afforded **466-473** (with **468** as the only exception). Intermediates **466-476** were subsequently treated with NaH and MeI to afford **352-362**.

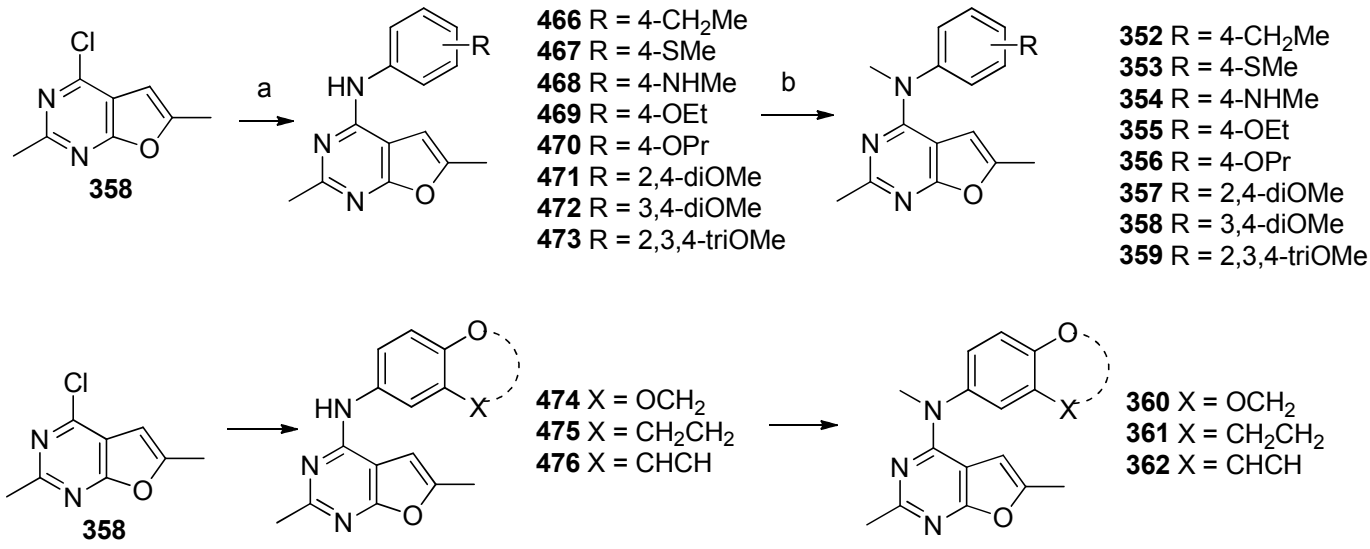

Scheme 104. The synthesis of **352** and **362**.

Several different strategies and reaction conditions were attempted for the synthesis of **468** and the corresponding **354** noted above and are summarized in Scheme 105. The reaction of **358** and anilines **477** or **478** were complex and no isolatable products were obtained, because both these anilines have two reactive anilino nitrogens. However when one of the reactive nitrogen was converted to the nitro group or when both aniline nitrogens were converted to the pivaloyl protected amides, the resulting compounds did not reacted with **358** under conventional conditions. In the case of 4-nitroaniline, the 4-nitro group is a strong electron withdrawing group, which decrease the electron density on the anilino nitrogen and hence nucleuphilicity. In the case of pivaloyl protected amides, the amide nitrogen was no longer a nucleuphile.

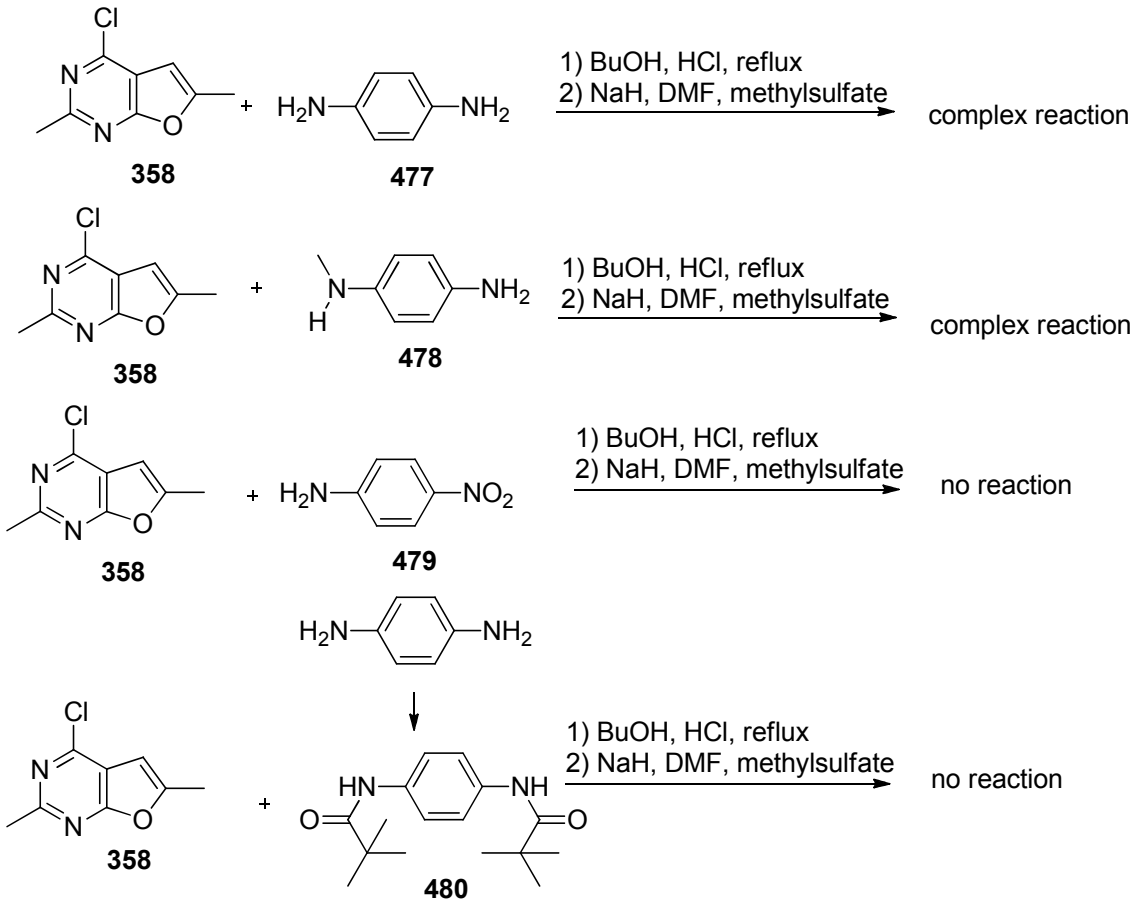

Scheme 105. The attempted synthesis of **468** and the corresponding **354**.

12. Synthesis of *N*-(4-methoxyphenyl)-*N*,2,6-trimethyl-5,6-dihydrofuro[2,3-*d*]pyrimidin-4-amine as antimitotic anticancer agents.

A retrosynthetic analysis (Scheme 106) suggested that the desired *N*-(4-methoxyphenyl)-*N*,2,6-trimethyl-5,6-dihydrofuro[2,3-*d*]pyrimidin-4-amine **364** could be synthesized from 2,6-dimethyl-4-oxo-5,6-dihydrofuro[2,3-*d*]pyrimidine **483** *via* chlorination and subsequent nucleophilic displacement. Thus, compound **483** was the key intermediate for the synthesis of **364**.

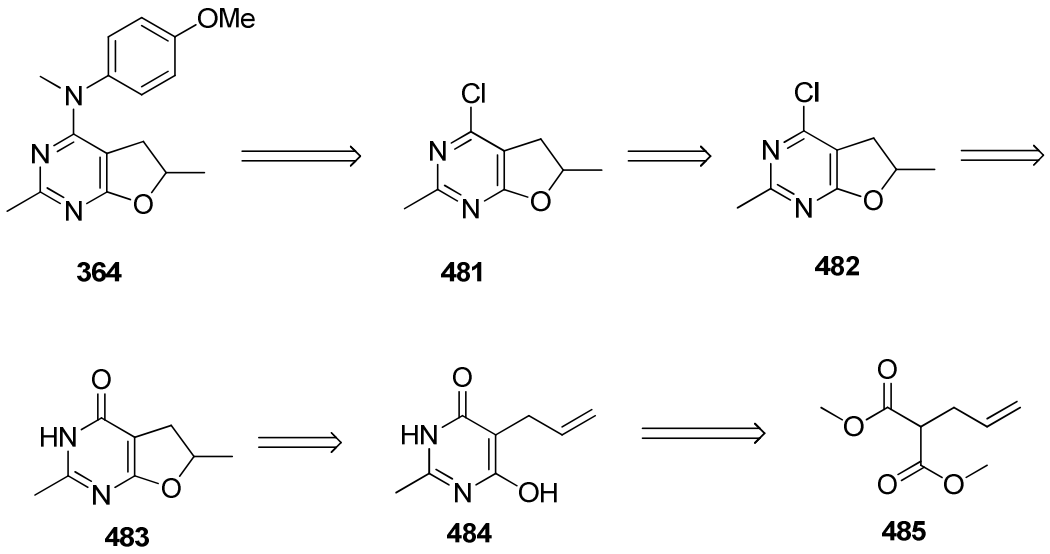

Scheme 106. Retro synthetic analysis to *N*-(4-methoxyphenyl)-*N*,2,6-trimethyl-5,6-dihydrofuro[2,3-*d*]pyrimidin-4-amine **364**.

A literature search revealed that there was no synthesis or other report for intermediate **483**. We had successfully developed a microwave promoted synthesis of 2-methyl-4-oxo-furo[2,3-*d*]pyrimidines in 2N NaOH starting from propargyl diethyl malonate (Scheme 94).

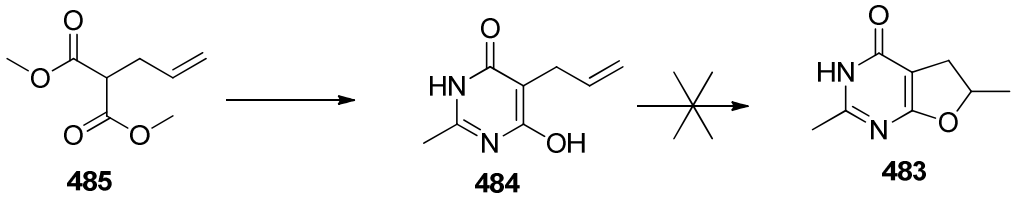

Scheme 107. The attempted synthesis of 2,6-dimethyl-4-oxo-5,6-dihydrofuro[2,3-*d*]pyrimidine **483**.

Thus, it appeared attractive to adopt this methodology for the synthesis of the corresponding 5,6-dihydrofuro[2,3-*d*]pyrimidine from allyl dimethyl malonate **485** (Scheme 107). Allyl dimethyl malonate **485** was condensed with guanidine carbonate at reflux in methanol to afford the corresponding 5-allyl-2-methylpyrimidine **484** in 40% yield. According to Baldwin

rule, both 5-exo-trig and 5-exo-dig are energy favorable for ring closure. However, unlike the 5-propargyl analogue described earlier, cyclization of **484** in 2N NaOH did not afford the corresponding annulated dihydrofuro analogue **483**.

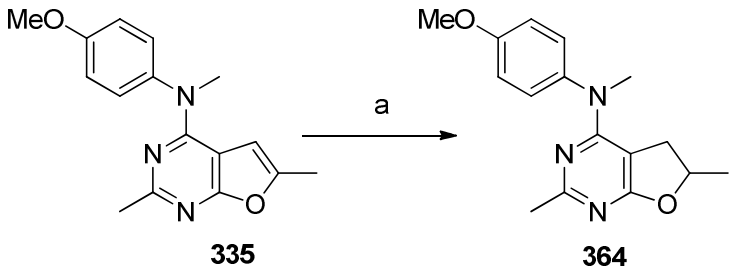

335 **364**

Reagents and conditions: (a) 20% Pd/C, H_2, MeOH/AcOH

Scheme 108. The synthesis of 2,6-dimethyl-4-oxo-5,6-dihydrofuro[2,3-*d*]pyrimidine **364**.

The failure of the above method prompted the development of a hydrogenation reaction to convert the furo[2,3-*d*]pyrimidine **335** to the reduced **364**. A literature search discovered no prior reports on the selective reduction of furo[2,3-*d*]pyrimidine, Thus a screening of the reduction condition is necessary. Both pyrimidine ring and furan ring in the furo[2,3-*d*]pyrimidine are unsaturated rings, hence are reducable. Various combination of catalyst loading, reaction solvents, reaction pressure and reaction time were attempted to achieve the conversion from **335** to **364**. The reaction required high reaction pressure (55 psi) and extended reaction time (overnight) .

13. The synthesis of substituted furo[2,3-*d*]pyrimidin-4-amine as antimitotic anticancer agents.

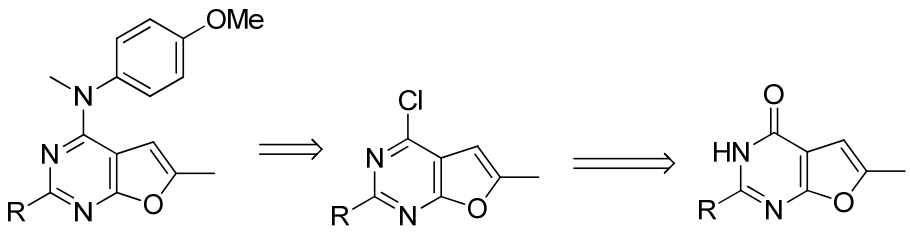

365 R = H
366 R = NH_2
367 R = Ph

486R = H
487 R = NH_2
488 R = Ph

489 R = H
412 R = NH_2
490 R = Ph

Scheme 109. Retro synthetic analysis to **365-367**.

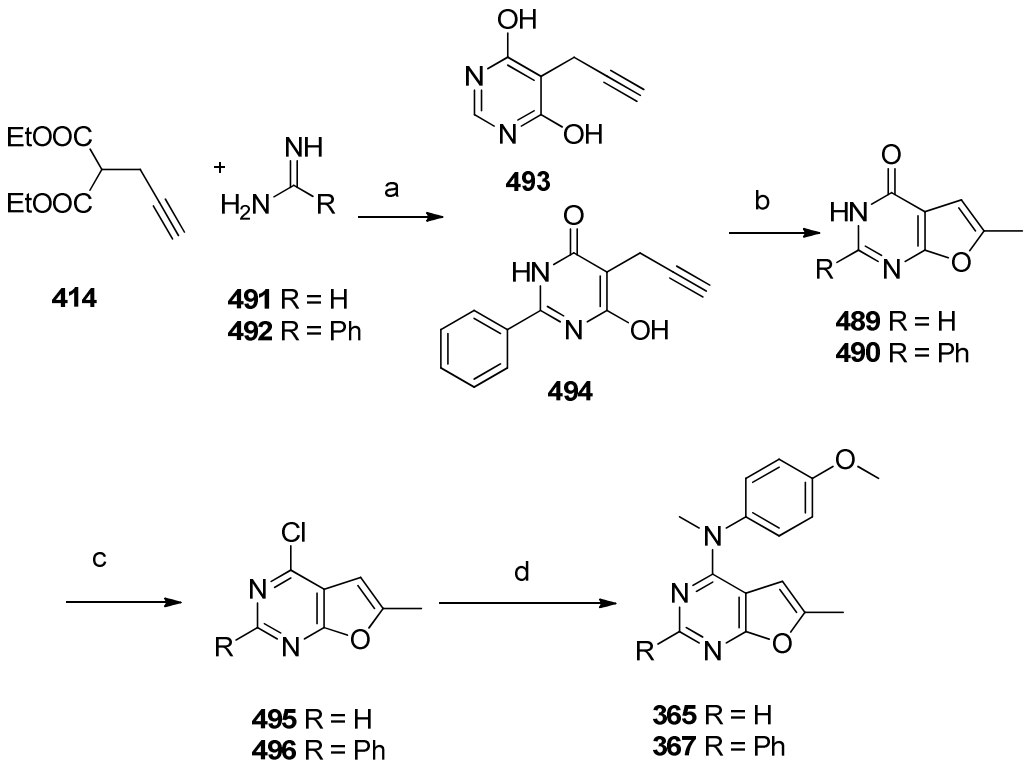

414

491 R = H
492 R = Ph

493

494

489 R = H
490 R = Ph

495 R = H
496 R = Ph

365 R = H
367 R = Ph

Reagents and conditions: (a) Na/MeOH/reflux; (b) 2 N NaOH, 150°C, microwave; (c) $POCl_3$, reflux; (d) 4-methoxy-N-methylaniline

Scheme 110. The synthesis of **365-367**.

It was envisioned that compounds **365-367** (Scheme 109) could be synthesized from 2-substituted-4-oxo-furo[2,3-*d*]pyrimidines **412**, **489** and **490** *via* chlorination and subsequent nucleophilic displacement. The required 2-substituted-4-oxo-furo[2,3-*d*]pyrimidines could be synthesized similar to 2-methyl-4-oxo-furo[2,3-*d*]pyrimidine described earlier (Scheme 94).

Compounds **489** and **490** (Scheme 110) were synthesized *via* a two step reactions starting from propargyl malonate **414**. Condensation of dimethyl propargyl malonate **414** and the appropriate amidines **491** or **492** in MeOH at reflux afforded the **493** and **494**, which were further cyclized in 2N NaOH, as described for the synthesis of **335,** to afford **489** and **490**.

^{1}HNMR showed that compound **493** and **494** exist in different tautomeric forms. In DMSO solution, **493** exists in the dihydroxyl pyrimidine form. In the dihydroxyl pyrimidine form, the two hydroxyl groups in **493** are identical, thus these two protons should only show one singlet on ^{1}HNMR spectrum, which was confirmed by the D_2O exchangable singlet at 11.94 ppm. While the ^{1}HNMR spectrum of **494** showed two seperate D_2O exchangable peaks at 11.61 ppm and 12.52 ppm, which are the characteristic of lactam form. When treated with $POCl_3$, **489** and **490** were chlorinated at the 4-position to give **495** and **496**. Reaction of **495** and **496** with N-methyl-4-methoxylaniline in ^{i}PrOH at reflux afforded **365** and **367**.

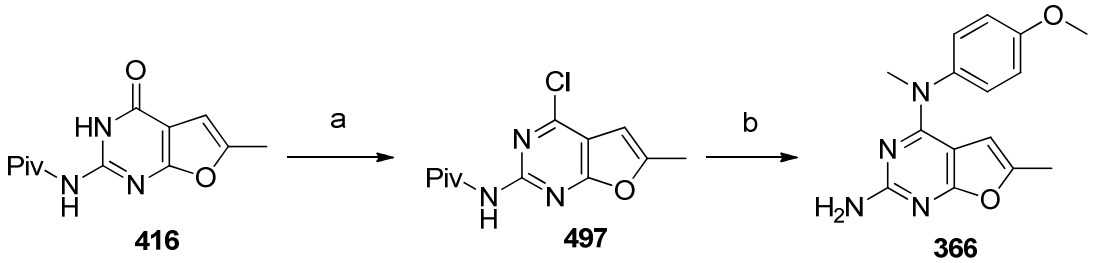

416 **497** **366**

Reagents and conditions: (a)$POCl_3$, (b) 4-methoxy-N-methylaniline, ^{i}PrOH, 1 drop of HCl, reflux.;

Scheme 111. The synthesis of **366**.

For the synthesis of **366**, compound **412** (Scheme 76) was the key intermediate, the synthesis of which was described in Scheme 76. Direct chlorination of **412** gave very low yields, hence the pivaloyl protected intermediate **416** (Scheme 112) was selected as the starting material for subsequent chlorination and nucleophilic displacement reactions. Similar to the synthesis of **365** and **367**, the treatment of **416** with $POCl_3$ afforded the 4-chlorinated **497**, which reacted with N-methyl-4-methoxylaniline in ^{i}PrOH at reflux to afford **366**.

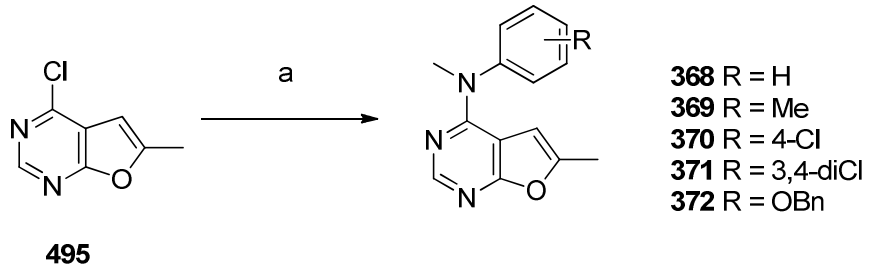

495

368 R = H
369 R = Me
370 R = 4-Cl
371 R = 3,4-diCl
372 R = OBn

Reagents and conditions: (a) the appropriate anilines, ^{i}PrOH or ^{n}BuOH, 1 drop of HCl (conc.), reflux

Scheme 112. The synthesis of **368-372**.

Compounds **368-372** (Scheme 112) were synthesized under the same reaction conditions as described for **365,** with the appropriate N-methylanilines.

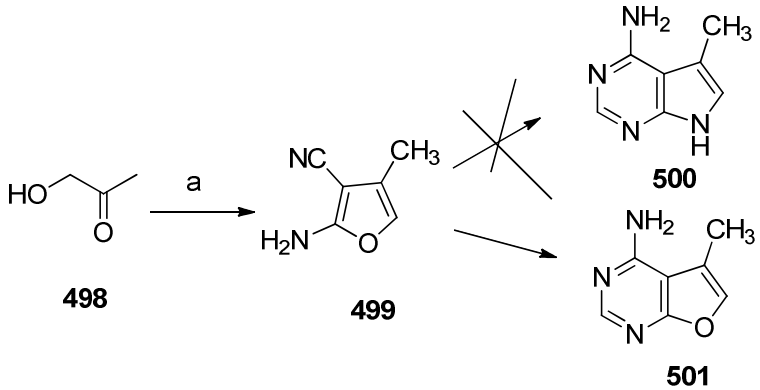

498

499

500

501

Reagents and conditions: (a) malononitrile, NEt_3, MeOH; (b) formamidine, NaOEt,EtOH, reflux

Scheme 113. The synthesis of intermediate **501**.

Intermediate **499** was synthesized by the published method from acetol **498** and malononitrile. The cyclization of **499** with formamidine free base afforded furo[2,3-*d*]pyrimidine **501** instead of expected pyrrolo[2,3-*d*]pyrimidine as per Taylor *et al*.[317] The structure of **501** was confirmed by ^{1}HNMR and elemental analysis. Compared to guanidine, which favors the formation of pyrrolo[2,3-*d*]pyrimidine, formamidine has less neucleophilicity and is also less basic. Both of these two properties may play a role in stabilizing the intermediate and favor the maintenance of furan ring, although the exact mechaism for this ring closure reaction is not clear yet.

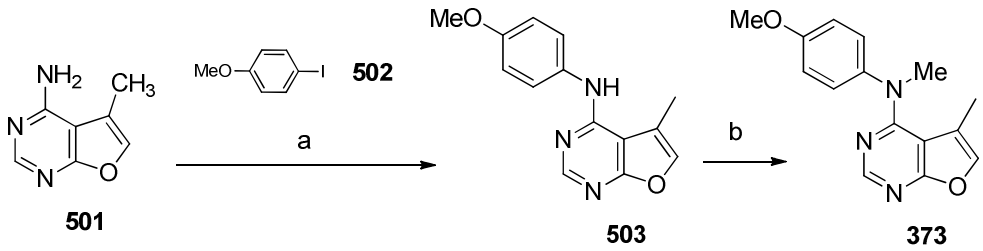

Reagents and conditions: (a) CuI, L-Proline, K_2CO_3,DMF, 110^{0}C, 24h;
(b) NaH, Dimethylsulfide, DMF, 0^{0}C-RT 8h

Scheme 114: The synthesis of **373**.

Compound **501** (Scheme 113) was as a suitable intermediate for elaboration to **503** and **373**. Under Ullman coupling reaction condition, the amino group of **501** was coupled with **502** using copper (I) iodide and L-proline as a chelating ligand in the presence of potassium carbonate in DMF to afford **503** (Scheme 114). Compound **503** was N-methylated with sodium hydride followed by dimethyl sulfate to obtain **373**.

14. The synthesis of substituted thieno[2,3-*d*]pyrimidin-4-amine as antimitotic anticancer agents.

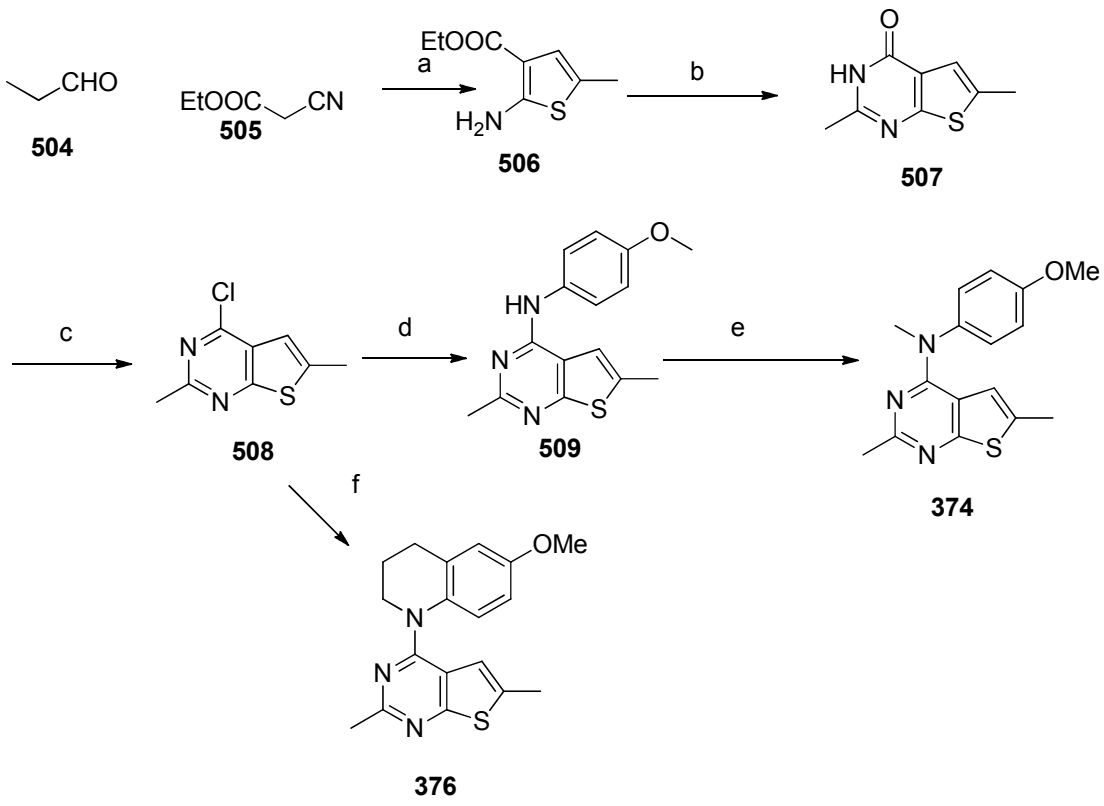

Reagents and conditions: (a) S, Morpholine; (b) HCl (g), CH_3CN; (c) $POCl_3$, reflux;
(d) 4-methoxyaniline, ^{i}PrOH, reflux; (e) NaH, DMF,Dimethylsulfate;
(f) 6-methoxy-1,2,3,4-tetrahydroquinoline, ^{i}PrOH, reflux

Scheme 115: The synthesis of target compounds **374** and **376**.

Compounds **374** and **376** were prepared as shown in Scheme **115**. Commercially available propaldehyde reacted with sulfur, ethyl cyanoacetate and morpholine in EtOH for 24 h at room temperature under Gewald reaction conditions to afford **506** in 73% yield. The reaction of **506** in acetonitrile with hydrochloric acid gas afforded the 2-methyl-4-oxo product **507** in 63% yield. Chlorination of **507** with $POCl_3$ for 3 h afforded **508** (84%). Reaction of **508** with 4-methoxylaniline in ^{i}PrOH in the presence of 2-3 drops of conc. HCl afforded **509** (74%). When sequentially treated with NaH and methyl sulfate, **509** was converted to **374** in 47% yield. The 2-

methyl and 6-methyl groups of **374** occur in the ^{1}H NMR at 2.34 ppm and 2.44 ppm. The reaction of **508** with 6-methoxy-1,2,3,4-tetrahydroquinoline produced **376**.

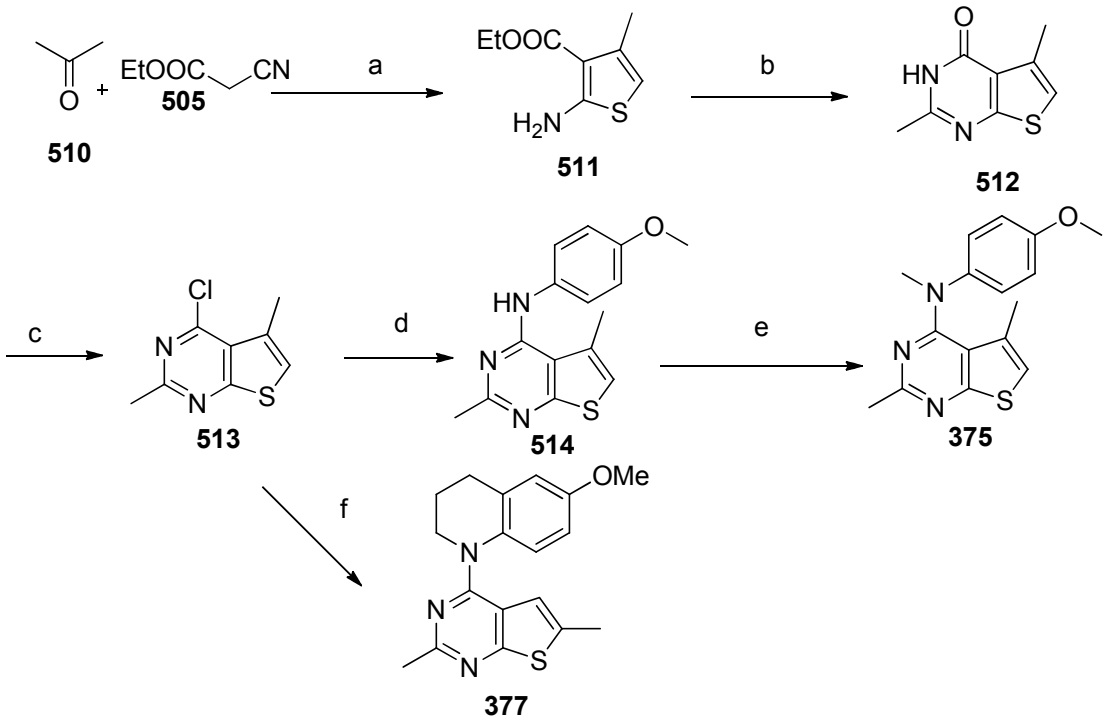

Reagents and conditions: (a) S, Morpholine; (b) HCl (g), CH_3CN; (c) $POCl_3$, reflux; (d) 4-methoxyaniline, ^{i}PrOH, reflux; (e) NaH, DMF,Dimethylsulfate; (f) 6-methoxy-1,2,3,4-tetrahydroquinoline, ^{i}PrOH, reflux

Scheme 116: The synthesis of target compounds **375** and **377.**

Compounds **375** and **377** were prepared as shown in Scheme **116**. Acetone reacted with sulfur, ethyl cyanoacetate and morpholine in ethanol for 24 h at room temperature under Gewald 319reaction conditions to afford **511** in 70% yield. The reaction of **511** in acetonitrile with hydrochloric acid gas afforded the 2-methyl-4-oxo product **512** in 59% yield. Chlorination of **512** with $POCl_3$ for 3 h afforded **513** (80%). Reaction of **513** with 4-methoxylaniline in ^{i}PrOH in the presence of 2-3 drops of conc. HCl afforded **514** (74%). When sequentially treated with NaH

and methyl sulfate, **514** was converted to **375** in 42% yield. The 2-methyl and 5-methyl groups of **375** occur in the ^{1}H NMR at 2.34 ppm and 2.48 ppm. The reaction of **513** with 6-methoxy-1,2,3,4-tetrahydroquinoline produced **377** in 62% yield.

15. 7-Substituted-5-arylethyl-4-methyl-7*H*-pyrrolo[2,3-*d*]pyrimidin-2-amines as antimitotic agents.

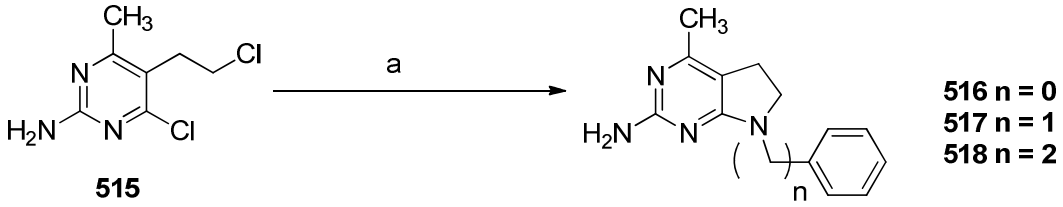

515

Reagents and conditions; (a) subsituted-benzylamine, NEt_3, ^{n}BuOH, reflux, 3 d

Scheme 117: The synthesis of compounds **516-518**.

The synthesis of the target compounds **516-518** (Scheme 117) were accomplished from a previously reported intermediate,[407] 4-chloro-5-(2-chloroethyl)-6-methylpyrimidin-2-amine **515**. Condensation of the appropriately substituted benzylamines with **515** in the presence of triethylamine at reflux in ^{n}BuOH afforded the bicyclic 7-substituted benzyl-4-methyl-6,7-dihydro-5*H*-pyrrolo[2,3-*d*]pyrimidin-2-amines **516-518** (34%~74%) (Scheme 118). Compounds **516-518** had very poor solubility in organic solvents including AcOEt and dichloromethane, and required a highly polar solvent system (methanol/dichloromethane) to isolate the compounds from column chromatography.

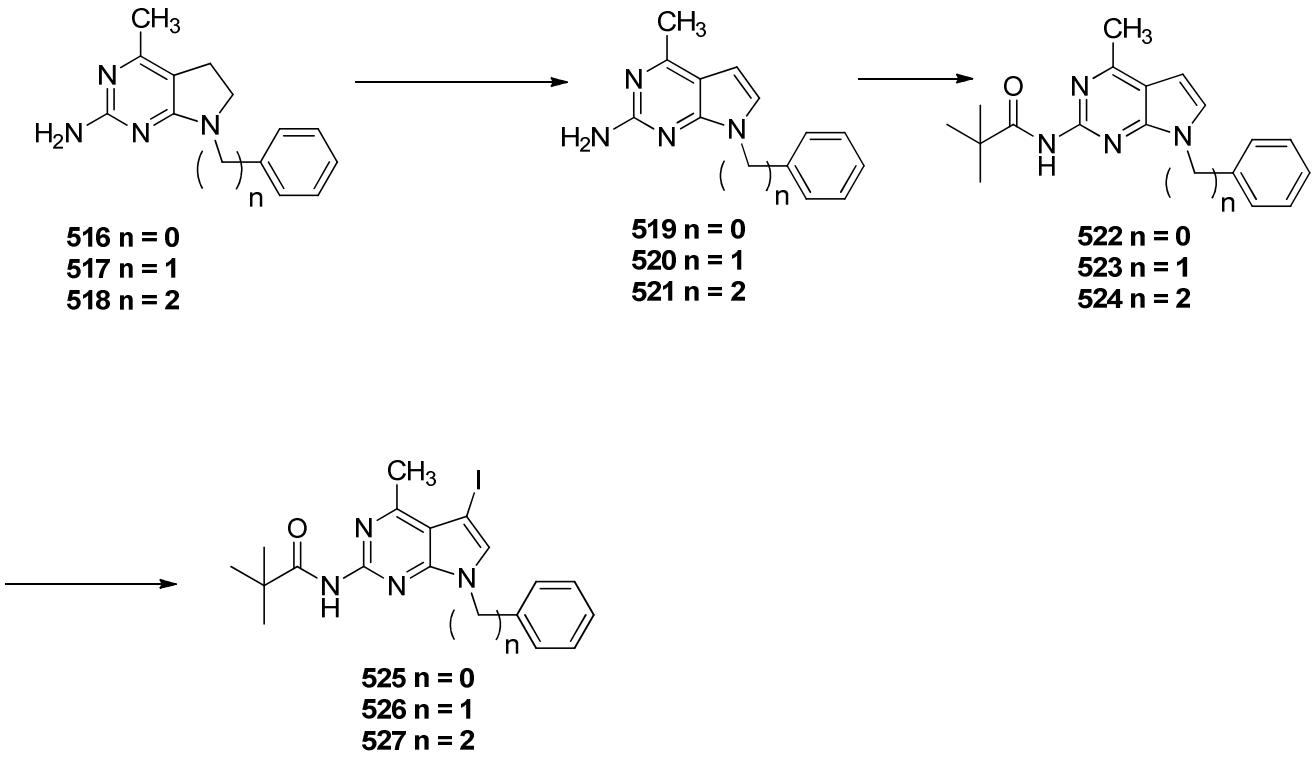

Reagents and conditions: (a) MnO_2,1,4-dioxane,120 ^oC, 24 h; (b) (Piv)2O, reflux; (c) NIS, THF, dark, rt.,18 h

Scheme 118. Synthesis of **525-527**.

Oxidation of **516-518** (Scheme 118) with MnO_2 at reflux in 1,4-dioxane for 24 h afforded aromatized compounds **519-521** (29%~60%). Treatment of **519-521** with pivaloyl chloride afforded a mixture of monoprotected and diprotected products, which are very difficult to seperate. Compounds **519-521** were reacted with pivaloyl anhydride at reflux to afford monoprotected compounds **522-524** (36%~72%). Using X-ray crystal structure, Gangjee *et al*.[418] demonstrated that selective iodonation at 5-position occured, when the 2-amino group was protected with mono or di pivaloyl group and NIS was used as iodonation agent. Thus regioselective iodination of **522-524** with NIS, with protection from air and light, gave compounds **525-527** (34%~83%).

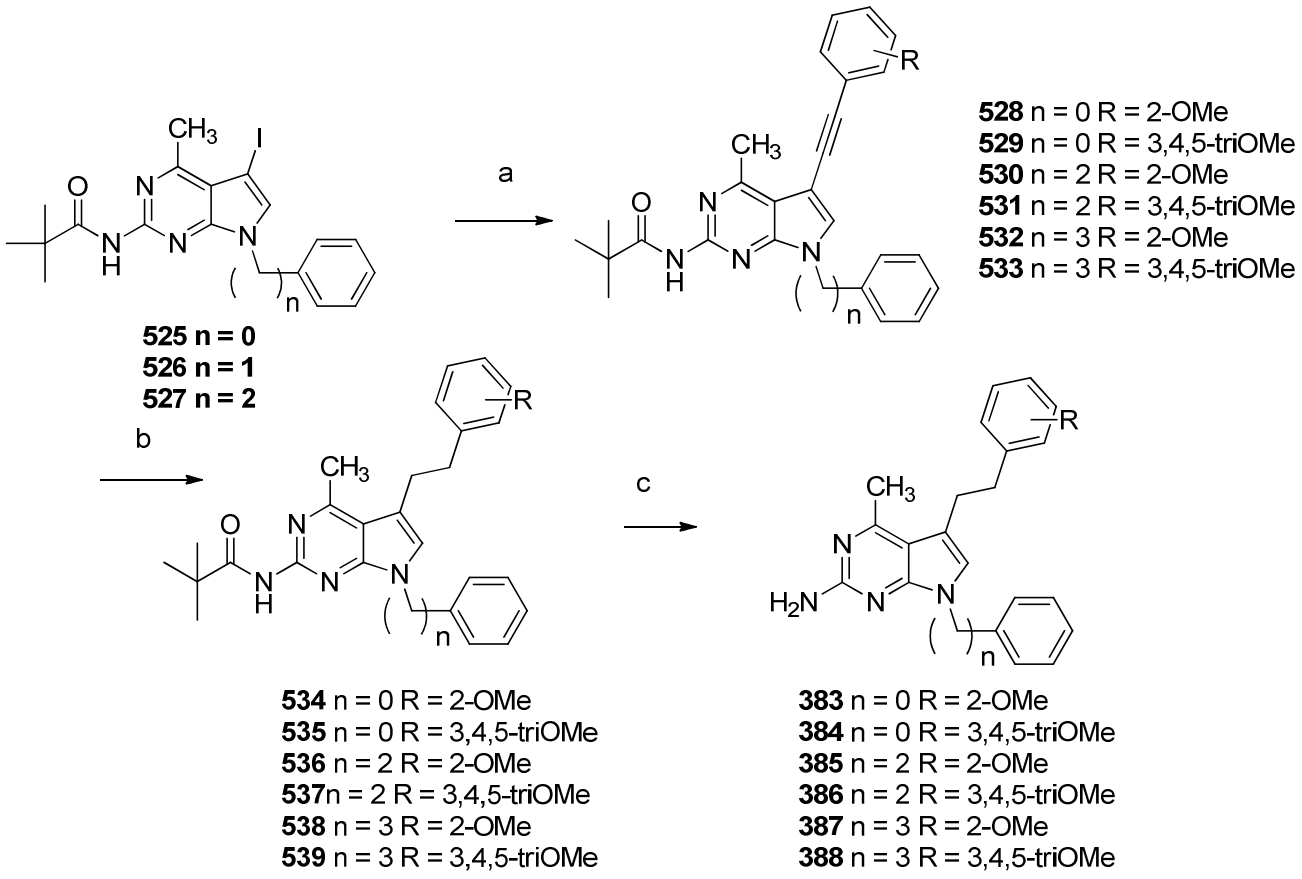

Reagents and conditions: (a) acetylene substituted benzenes, Pd/C, CuI, NEt_3, microwave; (b) Pd/C, H_2; (c) 1N NaOH

Scheme 119. The synthesis of **383-388**.

Sonogashira coupling of compounds **525-527** (Scheme 119) with 2-ethynylanisole or 3,4,5-trimethoxylethynylbenzene in the presence of Pd/C, copper(I) iodide, and triethylamine in acetonitrile gave compounds **528-533** (54%~92%) (Scheme 119). The use of other palladium catalysts including $Pd(OAc)_2$ and $PdCl_2$ also gave compounds **528-533** in good yield. The sequential hydrogenation and deprotection in 1N NaOH converted **528-533** to **383-388.**

V. SUMMARY

A total of Ninety-one new final target compounds were designed, synthesized and characterized from these projects. These compounds are as follows:

1. *N*-(4-{[(2-methyl-4-oxo-3,4-dihydro[1]benzothieno[2,3-*d*]pyrimidin-5-yl)methyl]amino}benzoyl)-L-glutamic acid (**275**)
2. (2S)-2-(5-{[(2-methyl-4-oxo-3,4-dihydro[1]benzothieno[2,3-*d*]pyrimidin-5-yl)methyl]amino}-1-oxo-1,3-dihydro-2H-isoindol-2-yl)pentanedioic acid (**276**)
3. *N*-(4-{[(2-amino-4-oxo-3,4-dihydro[1]benzothieno[2,3-*d*]pyrimidin-5-yl)methyl]amino}benzoyl)-L-glutamic acid (**277**)
4. (2S)-2-(5-{[(2-Amino-4-oxo-3,4-dihydro[1]benzothieno[2,3-*d*]pyrimidin-5-yl)methyl]amino}-1-oxo-1,3-dihydro-2H-isoindol-2-yl)pentanedioic acid (**278**)
5. 2-Amino-5-(phenylsulfanyl)-6-propylthieno[2,3-*d*]pyrimidin-4(3H)-one (**283**)
6. 2-Amino-5-[(4-nitrophenyl)sulfanyl]-6-propylthieno[2,3-*d*]pyrimidin-4(3H)-one (**284**)
7. 2-Amino-5-[(3,4-dichlorophenyl)sulfanyl]-6-propylthieno[2,3-*d*]pyrimidin-4(3H)-one (**285**)
8. 2-Amino-6-propyl-5-(1-naphthylsulfanyl)thieno[2,3-*d*]pyrimidin-4(3*H*)-one (**286**)
9. 2-Amino-6-propyl-5-(2-naphthylsulfanyl)thieno[2,3-*d*]pyrimidin-4(3*H*)-one (**287**)
10. 2-Amino-5-[(4-fluorophenyl)sulfanyl]-6-propylthieno[2,3-*d*]pyrimidin-4(3H)-one (**288**)
11. 2-Amino-5-[(4-methoxyphenyl)sulfanyl]-6-propylthieno[2,3-*d*]pyrimidin-4(3H)-one (**289**)
12. 2-Amino-5-[(4-chlorophenyl)sulfanyl]-6-propylthieno[2,3-*d*]pyrimidin-4(3H)-one (**290**)
13. 2-Amino-6-propyl-5-(4-bromophenyl sulfanyl)thieno[2,3-*d*]pyrimidin-4(3*H*)-one (**291**)
14. 2-Amino-6-methyl-5-(phenylsulfanyl)furo[2,3-*d*]pyrimidin-4(3*H*)-one (**293**)
15. 2-Amino-6-methyl-5-(naphthalen-1-ylsulfanyl)furo[2,3-*d*]pyrimidin-4(3*H*)-one (**294**)

16. 2-Amino-5-[(4-methoxyphenyl)sulfanyl]-6-methylfuro[2,3-*d*]pyrimidin-4(3*H*)-one (**295**)

17. 2-Amino-6-methyl-5-(pyridin-4-ylsulfanyl)furo[2,3-*d*]pyrimidin-4(3*H*)-one (**296**)

18. 2-Amino-5-[(3,4-dichlorophenyl)thio]-6-methylfuro[2,3-*d*]pyrimidin-4(3*H*)-one (**297**)

19. 2-Amino-5-[(4-chlorophenyl)sulfanyl]-6-methylfuro[2,3-*d*]pyrimidin-4(3*H*)-one (**298**)

20. 6-{[(2,5-Dichlorophenyl)amino]methyl}quinazoline-2,4-diamine (**301**)

21. 6-{[(3,4,5-Trichlorophenyl)amino]methyl}quinazoline-2,4-diamine (**302**)

22. 6-{[(3,4,5-Trichlorophenyl)amino]methyl}pteridine-2,4-diamine (**303**)

23. 6-{[(2,5-Dichlorophenyl)amino]methyl}pteridine-2,4-diamine (**304**)

24. 6-[(2,5-Dichlorophenoxy)methyl]pteridine-2,4-diamine (**305**)

25. 6-{[(2,5-Dichlorophenyl)sulfanyl]methyl}pteridine-2,4-diamine (**306**)

26. N-({5-[3-(2-amino-4-oxo-3,4-dihydrothieno[2,3-*d*]pyrimidin-6-yl)propyl]furan-2-yl}carbonyl)-L-glutamic acid (**317**)

27. N-{4-[3-(2-amino-4-oxo-3,4-dihydrothieno[2,3-*d*]pyrimidin-6-yl)propyl]benzoyl}-L-homocysteine (**322**)

28. 2,6-Dimethyl-*N*-phenylfuro[2,3-*d*]pyrimidin-4-amine (**326**)

29. 2,6-Dimethyl-*N*-(naphthalen-1-yl)furo[2,3-*d*]pyrimidin-4-amine (**327**)

30. N-(3-ethynylphenyl)-2,6-dimethylfuro[2,3-*d*]pyrimidin-4-amine (**328**)

31. 2,6-Dimethyl-*N*-[4-(trifluoromethyl)phenyl]furo[2,3-*d*]pyrimidin-4-amine (**329**)

32. N-(3-chloro-4-fluorophenyl)-2,6-dimethylfuro[2,3-*d*]pyrimidin-4-amine (**330**)

33. N-(4-chlorophenyl)-2,6-dimethylfuro[2,3-*d*]pyrimidin-4-amine (**331**)

34. N-(1*H*-indol-4-yl)-2,6-dimethylfuro[2,3-*d*]pyrimidin-4-amine (**332**)

35. N-(4-methoxyphenyl)-2,6-dimethylfuro[2,3-*d*]pyrimidin-4-amine (**333**)

36. N-(3-fluorophenyl)-2,6-dimethylfuro[2,3-*d*]pyrimidin-4-amine (**334**)

37. *N*-(4-methoxyphenyl)-*N*,2,6-trimethylfuro[2,3-*d*]pyrimidin-4-amine (**335**)

38. *N*-(4-methoxyphenyl)-*N*,2,6-trimethylfuro[2,3-*d*]pyrimidin-4-amine hydrochloride (**336**)

39. *N*,2,6-trimethyl-*N*-(4-methylphenyl)furo[2,3-*d*]pyrimidin-4-amine (**338**)

40. *N*,2,6-trimethyl-*N*-(3-methylphenyl)furo[2,3-*d*]pyrimidin-4-amine (**339**)

41. *N*-(4-chlorophenyl)-*N*,2,6-trimethylfuro[2,3-*d*]pyrimidin-4-amine (**340**)

42. *N*-(3,4-dichlorophenyl)-*N*,2,6-trimethylfuro[2,3-*d*]pyrimidin-4-amine (**341**)

43. *N*,2,6-trimethyl-*N*-(naphthalen-1-yl)furo[2,3-*d*]pyrimidin-4-amine (**342**)

44. *N*-ethyl-*N*-(4-methoxyphenyl)-2,6-dimethylfuro[2,3-*d*]pyrimidin-4-amine (**343**)

45. *N*-(4-methoxyphenyl)-2,6-dimethyl-*N*-propylfuro[2,3-*d*]pyrimidin-4-amine (**344**)

46. *N*-butyl-*N*-(4-methoxyphenyl)-2,6-dimethylfuro[2,3-*d*]pyrimidin-4-amine (**345**)

47. *N*-(4-methoxyphenyl)-2,6-dimethyl-*N*-(propan-2-yl)furo[2,3-*d*]pyrimidin-4-amine (**346**)

48. 4-(5-Methoxyindolin-1-yl)-2,6-dimethylfuro[2,3-*d*]pyrimidine (**347**)

49. 4-(5-Methoxy-1H-indol-1-yl)-2,6-dimethylfuro[2,3-*d*]pyrimidine (**348**)

50. 4-(6-Methoxy-3,4-dihydroquinolin-1(2H)-yl)-,2,6-trimethylfuro[2,3-*d*]pyrimidines (**349**)

51. *N*-(4-ethylphenyl)-2,6-dimethylfuro[2,3-*d*]pyrimidin-4-amine (**466**)

52. 2,6-Dimethyl-*N*-[4-(methylsulfanyl)phenyl]furo[2,3-*d*]pyrimidin-4-amine (**467**)

53. *N*-(4-ethoxyphenyl)-2,6-dimethylfuro[2,3-*d*]pyrimidin-4-amine (**469**)

54. 2,6-Dimethyl-*N*-(4-propoxyphenyl)furo[2,3-*d*]pyrimidin-4-amine (**470**)

55. *N*-(2,4-dimethoxyphenyl)-2,6-dimethylfuro[2,3-*d*]pyrimidin-4-amine (**471**)

56. *N*-(2,4-dimethoxyphenyl)-2,6-dimethylfuro[2,3-*d*]pyrimidin-4-amine (**472**)

57. 2,6-Dimethyl-*N*-(3,4,5-trimethoxyphenyl)furo[2,3-*d*]pyrimidin-4-amine(**473**)

58. *N*-(4-ethylphenyl)-*N*,2,6-trimethylfuro[2,3-*d*]pyrimidin-4-amine (**352**)

59. *N*,2,6-trimethyl-*N*-[4-(methylsulfanyl)phenyl]furo[2,3-*d*]pyrimidin-4-amine (**353**)

60. *N*-(4-ethoxyphenyl)-*N*,2,6-trimethylfuro[2,3-*d*]pyrimidin-4-amine (**355**)

61. *N*,2,6-trimethyl-*N*-(4-propoxyphenyl)furo[2,3-*d*]pyrimidin-4-amine (**356**)

62. *N*-(2,4-dimethoxyphenyl)-*N*,2,6-trimethylfuro[2,3-*d*]pyrimidin-4-amine (**357**)

63. *N*-(3,4-dimethoxyphenyl)-*N*,2,6-trimethylfuro[2,3-*d*]pyrimidin-4-amine (**358**)

64. *N*,2,6-trimethyl-*N*-(3,4,5-trimethoxyphenyl)furo[2,3-*d*]pyrimidin-4-amine (**359**)

65. *N*-1,3-benzodioxol-5-yl-2,6-dimethylfuro[2,3-*d*]pyrimidin-4-amine (**474**)

66. *N*-(2,3-dihydro-1-benzofuran-5-yl)-2,6-dimethylfuro[2,3-*d*]pyrimidin-4-amine (**475**)

67. *N*-1-benzofuran-5-yl-2,6-dimethylfuro[2,3-*d*]pyrimidin-4-amine (**476**)

68. *N*-1,3-benzodioxol-5-yl-*N*,2,6-trimethylfuro[2,3-*d*]pyrimidin-4-amine (**360**)

69. *N*-(2,3-dihydro-1-benzofuran-5-yl)-*N*,2,6-trimethylfuro[2,3-*d*]pyrimidin-4-amine (**361**)

70. *N*-1-benzofuran-5-yl-*N*,2,6-trimethylfuro[2,3-*d*]pyrimidin-4-amine (**362**)

71. *N*-(4-methoxyphenyl)-*N*,2,6-trimethyl-5,6-dihydrofuro[2,3-*d*]pyrimidin-4-amine (**364**)

72. *N*-(4-methoxyphenyl)-*N*,2,6-trimethylfuro[2,3-*d*]pyrimidin-4-amine (**365**)

73. *N*-(4-Methoxyphenyl)-*N*,6-dimethyl-2-phenylfuro[2,3-*d*]pyrimidin-4-amine (**367**)

74. *N*4-(4-methoxyphenyl)-*N*4,6-dimethylfuro[2,3-*d*]pyrimidine-2,4-diamine (**366**)

75. *N*-(3,4-dichlorophenyl)-N,2,6-trimethylfuro[2,3-*d*]pyrimidin-4-amine (**368**)

76. *N*,2,6-trimethyl-N-(4-methylphenyl)furo[2,3-*d*]pyrimidin-4-amine (**369**)

77. *N*-(4-chlorophenyl)-N,2,6-trimethylfuro[2,3-*d*]pyrimidin-4-amine (**370**)

78. *N*-(3,4-dichlorophenyl)-N,2,6-trimethylfuro[2,3-*d*]pyrimidin-4-amine (**371**)

79. *N*-(3,4-dichlorophenyl)-N,2,6-trimethylfuro[2,3-*d*]pyrimidin-4-amine (**372**)

80. *N*-(4-methoxyphenyl)-5-methylfuro[2,3-*d*]pyrimidin-4-amine (**503**)

81. *N*-(4-methoxyphenyl)-*N*,5-dimethylfuro[2,3-*d*]pyrimidin-4-amine (**373**)

82. *N*-(4-methoxyphenyl)-2,6-dimethylthieno[2,3-*d*]pyrimidin-4-amine (**509**)

83. *N*-(4-methoxyphenyl)-*N*,2,6-trimethylthieno[2,3-*d*]pyrimidin-4-amine (**374**)

84. *N*-(4-methoxyphenyl)-2,5-dimethylthieno[2,3-*d*]pyrimidin-4-amine (**514**)

85. *N*-(4-methoxyphenyl)-N,2,5-trimethylthieno[2,3-*d*]pyrimidin-4-amine (**375**)

86. 1-(2,5-Dimethylthieno[2,3-*d*]pyrimidin-4-yl)-6-methoxy-1,2,3,4-tetrahydroquinoline (**377**)

87. 4-Methyl-7-phenyl-5-[2-(3,4,5-trimethoxyphenyl)ethyl]-7*H*-pyrrolo[2,3-*d*]pyrimidin-2-amine (**384**)

88. 5-[2-(2-Methoxyphenyl)ethyl]-4-methyl-7-(2-phenylethyl)-7*H*-pyrrolo[2,3-*d*]pyrimidin-2-amine (**385**)

89. 4-Methyl-7-(2-phenylethyl)-5-[2-(3,4,5-trimethoxyphenyl)ethyl]-7*H*-pyrrolo[2,3-*d*]pyrimidin-2-amine (**386**)

90. 5-[2-(2-Methoxyphenyl)ethyl]-4-methyl-7-(3-phenylpropyl)-7*H*-pyrrolo[2,3-*d*]pyrimidin-2-amine (**387**)

91. 4-Methyl-7-(3-phenylpropyl)-5-[2-(3,4,5-trimethoxyphenyl)ethyl]-7*H*-pyrrolo[2,3-*d*]pyrimidin-2-amine (**388**)

Among them four benzo[4,5]thieno[2,3-*d*]pyrimidines were designed and synthesized as dual TS and DHFR inhibitors. Ten thieno[2,3-*d*]pyrimidines were designed and synthesized as dual TS and DHFR inhibitors. Six furo[2,3-*d*]pyrimidines were designed and synthesized as dual TS and DHFR inhibitors. Six 2,4-diamino-6-substituted bicyclic pyrimidines were designed and synthesized as selective *pj*DHFR inhibitors. Two thieno[2,3-*d*]pyrimidines were designed and synthesized as GARFTase inhibitors with folate receptor (FR) specificity and antitumor activity. Fifty-seven furo[2,3-*d*]pyrimidines and six thieno[2,3-*d*]pyrimidines were designed and synthesized as RTK inhibitors with antimitotic antitumor activity. Four pyrrolo[2,3-

d]pyrimidines were designed and synthesized as antimitotic anticancer agents that also reverse pgp action.

During this study, a novel synthetic procedure for the synthesis of benzo[4,5]thieno[2,3-*d*]pyrimidines were successfully exploited. The novel cyclization of furo[2,3-*d*]pyrimidine *via* H_2SO_4 (Conc.) or 2N NaOH have been developed. One of the furo[2,3-*d*]pyrimidine compounds showed dual RTK inhibitory activity and antimitotic activity. The compound showed a two digit nanomolar GI_{50} against most tumor cells in the preclinical NCI 60 tumor cell panel. Conformational resitriction in some of the moleculars led to increased inhibitory activities as RTK inhibitors as well as antimitotic activity. Several compounds were discovered that overcome the resistance mechanism s of tumor to standard antimicrotubule agents. In addition, highly coveted water soluble antimicrotubules were also synthesized.

VI. EXPERIMENTAL SECTION

All evaporations were carried out *in vacuo* with a rotary evaporator. Analytical samples were dried *in vacuo* (0.2 mmHg) in a CHEM-DRY drying apparatus over P_2O_5 at 80 ^oC. Melting points were determined on a MEL-TEMP II melting point apparatus with a FLUKE 51 K/J electronic thermometer and are uncorrected. Nuclear magnetic resonance spectra for proton (1H NMR) were recorded on either a Bruker WH-400 (400 MHz) spectrometer or a Bruker WH-300 (300 MHz) spectrometer. The chemical shift values are expressed in ppm (parts per million) relative to tetramethylsilane as an internal standard: s, singlet; d, doublet; t, triplet; q, quartet; m, multiplet; br, broad singlet. Mass spectra were recorded on a VG-7070 double-focusingmass spectrometer or in a LKB-9000 instrument in the electron ionization (EI) mode. Chemical names follow IUPAC nomenclature. Thin-layer chromatography (TLC) was performed on Whatman Sil G/UV254 silica gel plates with a fluorescent indicator, and the spots were visualized under 254 and 365 nm illumination. All analytical samples were homogeneous on TLC in three different solvent systems. Proportions of solvents used for TLC are by volume. Column chromatography was performed on a 230-400 mesh silica gel (Fisher, Somerville, NJ) column. Elemental analyses were performed by Atlantic Microlab, Inc., Norcross, GA. Element compositions are within 0.4% of the calculated values. Fractional moles of water frequently found in the analytical sample of antifolates could not be prevented in spite of 24-48 h of drying *in vacuo* and was confirmed where possible by the presence in the 1H NMR spectra. All solvents and chemicals were purchased from Aldrich Chemical Co. or Fisher Scientific and were used as received. For all the compounds submitted for biological evaluation, a single spot in three different solvent systems with three different R_f values confirmed >95% purity.

Ethyl 2-amino-4-methyl-4,5,6,7-tetrahydro-1-benzothiophene-3-carboxylate (390). A

mixture of sulfur (1.1 g, 36 mmol), 2-methylcyclohexanone (4.04 g, 36 mmol) , ethyl cyanoactetate (4.07 g, 36 mmol) and EtOH (150 mL) were placed in a round bottom flask and warmed to 45 ^{o}C and treated dropwise with morpholine (3.1 g, 36 mmol) over 15 min. The mixture was stirred for 5 h at 45 ^{o}C and 24 h at room temperature. Unreacted sulfur was removed by filtration, and the filtrate was concentrated under reduced pressure to afford an orange solid. The residue was loaded on a silica gel column packed with silica gel and eluted with 10% ethyl acetate in hexane. The fractions containing the desired product (TLC) were pooled and evaporated to afford **390** (6.97 g, 80.9 %) as an orange solid; mp 69.9-71 ^{o}C; R_f 0.44 (hexane/EtOAc 3:1); ^{1}H NMR (DMSO-d_6): δ 1.08-1.10 (d, 3 H, 4-CH_3), 1.25-1.28 (t, 3 H, $COOCH_2CH_3$), 1.57-1.78 (m, 4 H), 2.39-2.43 (m, 2 H), 3.15-3.17 (m, 1 H), 4.10-4.24 (q, 2 H, $COOCH_2CH_3$), 7.23 (s, 2 H, NH_2 exch).

2-Amino-5-methyl-5,6,7,8-tetrahydro[1]benzothieno[2,3-*d*]pyrimidin-4(3H)-one (391). A mixture of **390** (0.74 g, 3.28 mmol) and chloroformamidine hydrochloride (1.51 g, 13.12 mmol) in $DMSO_2$ (4 g) was heated at 140° C for 4 h. The mixture was cooled to room temperature and water (15 mL) was added and ammonium hydroxide was used to neutralize the suspension. The brown solid, obtained by filtration, was washed with water and dried over P_2O_5 in vacuum. The solid was dissolved in methanol and silica gel was added. A dry silica gel plug was obtained after evaporation of the solvent. The plug was loaded on to a silica gel column and eluted with 5% methanol in chloroform. The fractions containing the desired product (TLC) were pooled and evaporated to afford **391** (0.46 g, 59.7 %) as a light yellow solid; mp > 300 °C; R_f 0.5 (MeOH/$CHCl_3$, 1:6); ^{1}H NMR (DMSO-d_6) δ 1.18-1.20 (d, 3 H, CH_3), 1.59-1.61 (m, 1 H), 1.71-1.83 (m, 3 H), 2.54-2.64 (m, 2 H), 3.15-3.18 (m, 1 H), 6.39 (s, 2 H, 2-NH_2 exch), 10.73 (s, 1 H, 3-NH exch); Anal. calcd. for ($C_{11}H_{13}N_3SO \cdot 0.2\ H_2O$): C, 55.30; H, 5.65; N, 17.59; S, 13.42;

found: C, 55.19; H, 5.65; N, 17.33; S, 13.17.

2,2-Dimethyl-*N*-(5-methyl-4-oxo-3,4,5,6,7,8-hexahydro[1]benzothieno[2,3-*d*]pyrimidin-2-yl)propanamide (392). To a 100 mL round-bottomed flask was added **391** (0.706 g, 3 mmol) and excess Piv_2O (10 mL). The mixture was kept at reflux for 2 h. The excess Piv_2O was removed under vacuum and the residue was made into silica gel plug. The silica gel plug obtained was loaded onto a silica gel column and eluted with 1:8 ethyl acetate/hexane. The fraction containing the desired product were pooled afford **392** (0.956 g, 70.3 %) as a white solid; mp 236.6-237.8 °C; R_f 0.31 (hexane/EtOAc 3:1); ^{1}H NMR (DMSO-d_6) δ 1.22 (s, 12 H, 4 CH_3), 1.62-1.79 (m, 4 H), 2.58-2.73 (m, 2 H), 3.23 (br s, 1 H), 11.07 (s, 1 H, NH exch), 12.02 (s, 1 H, NH exch).

Ethyl 2-amino-4-methyl-1-benzothiophene-3-carboxylate (395). A mixture of **389** (0.239 g, 1 mmol), 10 % Pd/C (0.239 g) and mesitylene (50 mL) were placed in a round bottom flask and kept at reflux for 1-2 days. The mixture was cooled to room temperature and Pd/C was removed by filtration, and the filtrate was concentrated under reduced pressure to afford a brown oil. The residue was loaded on a silica gel column and eluted with 10% ethyl acetate in hexane. The fractions containing the desired product (TLC) were pooled and evaporated to afford **395** (0.123 g, 52.1%) as an orange semi solid; R_f 0.38 (hexane/EtOAc 3:1); ^{1}H NMR (DMSO-d_6): δ 1.29-1.32 (t, 3 H, $COOCH_2\mathit{CH_3}$), 2.38 (s, 3 H, CH_3), 4.25-4.30 (q, 2 H, $COO\mathit{CH_2}CH_3$), 6.98-7.04 (m, 2 H, C_6H_3), 7.44, 7.45 (d, 1 H, C_6H_3), 7.43 (s, 2 H, NH_2 exch).

2-Amino-5-methyl[1]benzothieno[2,3-*d*]pyrimidin-4(3H)-one (393). A mixture of **395** (0.49 g, 2.07 mmol) and chloroformamidine hydrochloride (1.19 g, 10.37 mmol) in $DMSO_2$ (2 g) was heated at 140° C for 2 h. The mixture was cooled to room temperature and water (15 mL) was added and ammonium hydroxide was used to neutralize the suspension. The brown solid,

obtained by filtration, was washed with water and dried over P_2O_5 vacuum. The solid was dissolved in methanol and silica gel (1.0 g) was added. A dry silica gel plug was obtained after evaporation of the solvent. The plug was loaded on to a silica gel column and eluted with 5% methanol in chloroform. The fractions containing the desired product (TLC) were pooled and evaporated to afford **393** (0.29 g, 60.7 %) as a yellow solid; mp > 300 °C; R_f 0.41 (MeOH/$CHCl_3$, 1:6); ^{1}H NMR (DMSO-d_6) δ 2.87 (s, 3 H, CH_3), 6.82 (s, 2 H, 2-NH_2 exch), 7.13- 7.17 (m, 2 H, C_6H_3), 7.57, 7.59 (d, 1 H, C_6H_3), 10.92 (s, 1 H, 3-NH exch).

2,2-Dimethyl-*N*-(5-methyl-4-oxo-3,4-dihydro[1]benzothieno[2,3-*d*]pyrimidin-2-yl)propanamide (394). To a 100 mL round-bottomed flask was added **393** (1.34 g, 5.8 mmol) and excess Piv_2O (4 eq). The mixture was kept at reflux for 2 h. The excess Piv_2O was removed under vacuum and the residue was made into silica gel plug. The silica gel plug obtained was loaded onto a silica gel column and eluted with 1:8 ethyl acetate/hexane to afford **394** (1.299 g, 70.9 %) as a white solid, mp 178.3-179.5 °C; R_f 0.35 (hexane/EtOAc 3:1); ^{1}H NMR ($CDCl_3$) δ 1.35 (s, 9 H, 3 CH_3 of Piv), 3.05 (s, 3 H, CH_3), 7.28 (m, 2 H, C_6H_3), 7.56, 7.59 (d, 1 H, C_6H_3), 8.14 (s, 1 H, NH exch), 11.86 (s, 1 H, NH exch).

2,5-Dimethyl[1]benzothieno[2,3-*d*]pyrimidin-4(3*H*)-one (396). To a 100 mL round flask were added **395** (2.35 g, 10 mmol) and CH_3CN (50 mL). Vigorous stirring afforded, a clear solution. Anhydrous HCl gas was bubbled into the solution for 1 h to give a thick precipitation, which then redissolved into the acid solution. Anhydrous HCl gas was added for an additional 3 h after which the reaction mixture became clear. Evaporation of the solvent under reduced pressure afforded a residue that was dissolved in water. Concentrated aqueous NH_4OH was added to afford a suspension at pH = 8. The precipitate was collected by filtration, washed with water and dried over P_2O_5 in a vacuum to afford **396** (1.0 g, 57%) as a yellow solid; mp > 300

^{o}C; R_f 0.58 (MeOH/$CHCl_3$, 1:6); ^{1}H NMR (DMSO-d_6) δ 2.348 (s, 3 H, 2-CH_3), 2.95 (s, 3 H, 5-CH_3). 7.29 (m, 2 H, C_6H_3), 7.78 (s, 1 H, C_6H_3), 12.54 (s, 1H, 3-NH exch). HRMS calcd for $C_{12}H_{10}N_2OS$ 231.0592, found 231.0584.

2,2-Dimethyl-*N*-(5-methyl-4-oxo-3,4-dihydro[1]benzothieno[2,3-*d*]pyrimidin-2-yl)propanamide (397) A solution of **394** (1.1 g, 3.49 mmol) in 1,2- dichloroethane (50 mL) was treated with *N*-bromosuccinimide (0.62 g, 3.49 mmol) and benzoyl peroxide (50 mg), and the mixture was maintained at reflux for 1 day. The mixture was cooled to room temperature and washed with water, and evaporated to an orange solid. The solid was dissolved in methanol and silica gel (1.5 g) was added. A dry silica gel plug was obtained after evaporation of the solvent. The plug was loaded on to a silica gel column and eluted with 6 % ethyl acetate in hexane to afford **397** (0.577 g, 41.9 %) as an orange solid; mp 217.8-219.1 °C; R_f 0.3 (hexane/EtOAc 3:1); ^{1}H NMR ($CDCl_3$) δ 1.27 (s, 9 H, 3 CH_3 of Piv), 5.71 (s, 2 H, CH_2Br), 7.30, 7.33 (d, 1 H, C_6H_3), 7.43, 7.46 (d, 1 H, C_6H_3), 7.64, 7.66 (d, 1 H, C_6H_3), 8.07 (s, 1 H, NH exch), 11.99 (s, 1 H, NH exch).

5-(Bromomethyl)-2-methyl[1]benzothieno[2,3-d]pyrimidin-4(3H)-one (398) To a 100 mL flask were added **396** (0.736 g, 3.2 mmol) and benzene (30 mL). The suspension was stirred at 60 ^{o}C for 30 min to afford a clear solution, followed by the addition of *N*-bromosuccinimide (0.620 g, 3.49 mmol) and benzoyl peroxide (50 mg). The mixture was maintained at reflux for 4h and then cooled to room temperature and washed with water, and evaporated to afford a yellow solid. The solid was dissolved in methanol and silica gel (1.5 g) was added. A dry silica gel plug was obtained after evaporation of the solvent. The plug was loaded on to a silica gel column and eluted with 6 % ethyl acetate in hexane to afford **398** (393 mg, 39%) as a white solid; mp 217.8-219.1 °C; R_f 0.3 (hexane/EtOAc 3:1); ^{1}H NMR ($CDCl_3$) δ 2.69 (s, 3 H, 2-CH_3), 5.84 (s, 2 H,

CH$_2$Br), 7.44-7.47 (t, 1 H, *J* = 7.2, C_6H_3), 7.57-7.58 (d, 1 H, *J* = 7.2, C_6H_3), 7.80-7.82 (d, 1 H, *J* = 7.2, C_6H_3). HRMS calcd for $C_{12}H_9N_2OSBr$ 307.9619, found 307.9613.

Methyl 2-methyl-4-nitrobenzoate (400). Thionyl chloride (4.3 g, 36.45 mmol) was added dropwise to a stirred solution of **399** (3 g, 16.57 mmol) in MeOH (25 mL) while maintaining the internal temperature below 12 ^oC. When the addition was complete the mixture was left to stand at room temperature for 12h to result a white precipitation. The mixture was filtered and the filtrate was concentrated under reduced pressure to afford white solid. The solid was washed with hexane and ethyl ether to afford **400** (2.95 g, 91.3 %); mp 153.7-154.4 °C (lit.[39] mp 153-154 °C); R_f 0.43 (hexane/EtOAc 3:1); ^{1}H NMR ($CDCl_3$) δ 2.69 (s, 3 H, CH_3), 3.95 (s, 3 H, $COOCH_3$), 8.02-8.11 (m, 3 H, C_6H_3).

Methyl 2-(bromomethyl)-4-nitrobenzoate (401). A solution of **400** (2.57 g, 13.19 mmol) in 1,2-dichloroethane (100 mL) was treated with *N*-bromosuccinimide (2.3 g, 13.19 mmol) and benzoyl peroxide (0.26 g), and the mixture was kept at reflux for 2 days, then cooled, washed with water, and evaporated to a yellow oil (3.52 g). The oil was dissolved in acetone and silica gel (4.0 g) was added. A dry silica gel plug was obtained after evaporation of the solvent. The plug was loaded on to a silica gel column and eluted with 10 % ethyl acetate in hexane to afford **401** (1.73 g, 48.2 %) as a yellow oil; R_f 0.53 (hexane/EtOAc 3:1); ^{1}H NMR ($CDCl_3$) δ 3.89 (s, 3 H, $COOCH_3$), 4.86 (s, 2 H, CH_2Br), 7.98-8.23 (m, 3 H, C_6H_3).

Diethyl (2S)-2-(5-nitro-1-oxo-1,3-dihydro-2H-isoindol-2-yl)pentanedioate (402). The oil **401** (0.85 g, 3.1 mmol) was stirred for 16 h with diethyl glutamate hydrochloride (1.54 g, 6.4 mmol) and powdered K_2CO_3 (1.7 g, 12 mmol) in DMA (3 mL) under argon. The reaction mixture was diluted with water (20 mL) and extracted with ethyl acetate (3 X 20 mL). The combined ethyl acetate solutions were washed twice with brine, dried, and evaporated to an

orange oil. The oil was dissolved in methanol and silica gel was added. A dry silica gel plug was obtained after evaporation of the solvent. The plug was loaded on to a silica gel column and eluted with 25 % ethyl acetate in hexane to afford **402** (0.63 g, 55.7 %) as an orange oil; R_f 0.44 (hexane/EtOAc 1:1); ^{1}H NMR ($CDCl_3$) δ 1.17-1.22 (t, 3 H, $COOCH_2\mathit{CH_3}$), 1.26-1.31 (t, 3 H, $COOCH_2\mathit{CH_3}$), 2.19-2.49 (m, 4 H, $CH\mathit{CH_2CH_2}COOEt$), 4.02-4.23 (2q, 4 H, $COO\mathit{CH_2}CH_3$), 4.51-4.83 (dd, 2 H, $-CH_2-$), 5.09-5.14 (m, 1 H, $\mathit{CH}CH_2CH_2COOEt$), 8.00-8.03 (d, 1 H, C_6H_3), 8.36 (br s, 2 H, C_6H_3).

Diethyl (2S)-2-(5-amino-1-oxo-1,3-dihydro-2H-isoindol-2-yl)pentanedioate (403). To a Parr hydrogenation bottle was added **402** (0.55 g, 1.51 mmol), 10% Pd/C (0.09 g) and acetyl acetate (30 mL). Hydrogenation was carried out at 55 psi for 12 h. After filtration, the organic phase was evaporated at vacuum to afford **403** (0.467 g, 92.5 %) as a orange oil; R_f 0.19 (hexane/EtOAc 1:1); ^{1}H NMR ($CDCl_3$) δ 1.17-1.19 (t, 3 H,$COOCH_2\mathit{CH_3}$), 1.20-1.25 (t, 3 H, $COOCH_2\mathit{CH_3}$), 2.20-2.51 (m, 4 H, $CH\mathit{CH_2CH_2}COOEt$), 4.02-4.28 (m, 6 H, 2 $COO\mathit{CH_2}CH_3$, NH_2 exch), 4.22-4.51 (dd, 2 H, $-CH_2-$), 5.03-5.07 (m, 1 H, $\mathit{CH}CH_2CH_2COOEt$), 6.69-6.73 (m, 2 H, C_6H_3), 7.60, 7.63 (d, 1 H, C_6H_3).

General Procedure for the Synthesis of Compounds 275-278. A stirred solution of the tricyclic bromide **397** or **398** (0.25 mmol) in dry DMF (5 mL) was treated with the appropriate amine **403** or **403a** (1 mmol) and K_2CO_3 (95 mg, 0.69 mmol). The solution was stirred for 1 h at 80 °C under argon. The cooled reaction mixture was filtered and the filtrate was evaporated to obtain an orange solid. The solid was dissolved in methanol and silica gel was added. A dry silica gel plug was obtained after evaporation of the solvent. The plug was loaded on to a silica gel column and eluted with ethyl acetate: hexane (1: 1). The fractions containing the desired product (TLC) were pooled and evaporated to afford a solid, to which a combined solution of

aqueous 1 N NaOH (3 mL) and methanol (12 mL) was added. The mixture was kept at reflux for 12 h. The methanol was evaporated under reduced pressure and the residue was dissolved in water (5 mL). The solution was cooled to 0 ^{o}C and carefully acidified to pH 3 with dropwise addition of 1 N HCl. The resulting suspension was left at 0 ^{o}C for 2 h and the precipitate was collected by filtration, washed with water (5 mL) and dried over P_2O_5/vacuum at 50 ^{o}C to afford target compounds **275-278**.

***N*-(4-{[(2-methyl-4-oxo-3,4-dihydro[1]benzothieno[2,3-*d*]pyrimidin-5-yl)methyl]amino}benzoyl)-L-glutamic acid (275).** Using the general procedure described above with **398** and **403a** afforded **275** (37 mg, 37 %) as a yellow solid; mp 219.6-221.3 °C; R_f 0.28 (MeOH/EtOAc, 1:6); R_f 0.32 (MeOH/ $CHCl_3$, 1:6 + 1 drop of NEt_3); R_f 0.34 (MeOH/$CHCl_3$, 1:6 + 1 drop of gl. HOAc); ^{1}H NMR (DMSO-d_6): δ 1.22 (s, 1 H, 2-CH_3), 1.88-2.01 (m, 2 H, Gluγ-CH_2CH_2), 2.29 (m, 2 H, Gluγ-CH_2CH_2), 4.31 (s, 1 H, Gluα-CH), 5.20 (s, 2 H, Benzylic CH_2), 6.56-6.58 (d, 2 H, J = 9.0), 7.38-7.40 (d, 1 H, J = 7.5), 7.49 (d, 2 H, 2-NH_2 exch), 7.58-7.59 (d, 2 H, J = 9.0), 7.88 (d, 1 H) 8.02 (s, 1 H, CO*NH*), 8.08 (d, 1H), 12.71 (s, 1 H, 3-NH exch); HRMS (ESI, pos mode) m/z [M + H^+] calcd for $C_{24}H_{23}N_4O_6S$ 495.1338, found 495.1345.

(2S)-2-(5-{[(2-methyl-4-oxo-3,4-dihydro[1]benzothieno[2,3-d]pyrimidin-5-yl)methyl]amino}-1-oxo-1,3-dihydro-2H-isoindol-2-yl)pentanedioic acid (276). Using the general procedure described above with **398** and **403** afforded **276** (35 mg, 34 %) as a yellow solid; mp 236.4-237.7 °C; R_f 0.29 (MeOH/EtOAc, 1:6); R_f 0.32 (MeOH/ $CHCl_3$, 1:6 + 1 drop of NEt_3); R_f 0.36 (MeOH/$CHCl_3$, 1:6 + 1 drop of gl. HOAc);^{1}H NMR (DMSO-d_6): δ 1.22 (s, 3 H, 2-CH_3), 1.95 (m, 2 H, Gluβ-CH_2), 2.18 (m, 2 H, Gluγ-CH_2), 4.22 (s, 2 H, isoindolinyl CH_2), 4.67-4.69 (m, 1 H, Gluα-CH), 5.21 (s, 2 H, Benzylic CH_2), 6.65 (s, 1 H, CH), 6.81 (s, 1 H, NH exch), 7.30-7.32 (d, 1 H, J = 6.0), 7.37-7.41 (d, 1 H, J = 12), 7.49-7.51 (d, 1 H, J = 6.0), 7.88-7.90 (d, 1

H, *J* = 6.0), 8.03 (s, 1 H),12.76 (s, 1 H, 3-NH exch), HRMS (ESI, pos mode) m/z [M + H^+] calcd for $C_{25}H_{23}N_4O_6S$ 507.1333, found 507.1362.

***N*-(4-{[(2-amino-4-oxo-3,4-dihydro[1]benzothieno[2,3-*d*]pyrimidin-5-yl)methyl]amino}benzoyl)-L-glutamic acid (277).** Using the general procedure described above with **397** and **403a** afforded **277** (39 g, 32 %) as an orange solid; mp > 300 °C; R_f 0.30 (MeOH/EtOAc, 1:6); R_f 0.34 (MeOH/ $CHCl_3$, 1:6 + 1 drop of NEt_3); R_f 0.34 (MeOH/$CHCl_3$, 1:6 + 1 drop of gl. HOAc);^{1}H NMR (DMSO-d_6): δ 1.85-1.98 (m, 2 H, Gluγ-CH_2*CH_2*), 2.27-2.32 (m, 2 H, Gluγ-*CH_2*CH_2),4.26-4.34 (m, 1 H, Gluα-CH), 5.10-5.14 (d, 2 H, Benzylic CH_2), 6.55 (s, H, CH_2*NH*), 6.55-6.58 (d, 2 H, *J* = 9.0, 2 CH), 6.94 (br s, 2 H, 2-NH_2 exch), 7.19-7.24 (t, 1 H, *J* = 7.5), 7.38-7.40 (d, 1 H, *J* = 7.5), 7.56-7.59 (d, 2 H, *J* = 9.0), 7.68-7.70 (d, 1 H, *J* = 7.5), 7.97-8.00 (d, 1 H, *J* = 6.9, NH exch), 11.19 (s, 1 H, 3-NH exch), 12.66 (s, 2 H, 2COOH exch); HRMS (ESI, pos mode) m/z [M + H^+] calcd for $C_{23}H_{22}N_5O_6S$ 496.1291, found 496.1316.

(2S)-2-(5-{[(2-Amino-4-oxo-3,4-dihydro[1]benzothieno[2,3-*d*]pyrimidin-5-yl)methyl]amino}-1-oxo-1,3-dihydro-2H-isoindol-2-yl)pentanedioic acid (278). Using the general procedure described above with **397** and **403a** afforded **278** (40 mg, 32 %) as a orange solid; mp > 300 °C; R_f 0.27 (MeOH/EtOAc, 1:6); R_f 0.30 (MeOH/ $CHCl_3$, 1:6 + 1 drop of NEt_3); R_f 0.33 (MeOH/$CHCl_3$, 1:6 + 1 drop of gl. HOAc);^{1}H NMR (DMSO-d_6): δ 1.97-2.20 (m, 4 H, Gluβ-CH_2, Gluγ-CH_2), 4.21-4.25 (m, 2 H, isoindolinyl CH_2), 4.68-4.71 (m, 1 H, Gluα-CH), 5.13, 5.14 (d, 2 H, benzylic CH_2), 6.64 (br s, 2 H, C_6H_3), 6.74 (s, 1 H, NH exch), 6.89 (s, 2 H, 2-NH_2 exch), 7.20-7.26 (t, 1 H, C_6H_3), 7.30-7.33 (d, 1 H, C_6H_3), 7.39-7.42 (dd, 1 H, C_6H_3), 7.69-7.72 (d, 1 H, C_6H_3), 11.11 (s, 1 H, 3-NH exch), 12.78 (s, 2 H, 2COOH exch). HRMS (ESI, pos mode) m/z [M + H^+] calcd for $C_{24}H_{21}N_5O_6S$, 508.1285; found, 508.1321.

Ethyl 2-amino-5-propylthiophene-3-carboxylate (405). A mixture of sulfur (1.92 g, 60 mmol),

pentanal (5.17 g, 60 mmol), ethyl cyanoactetate (6.78 g, 60 mmol) and EtOH (100 mL) were placed in a round bottom flask and warmed to 45 ^{o}C and treated dropwise with morpholine (5.23 g, 60 mmol) over 15 min. The mixture was stirred for 4 h at 45 ^{o}C and 24 h at room temperature. Unreacted sulfur was removed by filtration, and the filtrate was concentrated under reduced pressure to afford an orange oil. The residue was loaded on a silica gel column packed with silica gel and eluted with 10% ethyl acetate in hexane to afford **405** (9.97 g, 78%) as a orange liquid; R_f 0.66 (hexane/EtOAc 3:1); ^{1}H NMR ($CDCl_3$) δ 0.93-0.97 (t, 3 H, $CH_2CH_2\mathit{CH_3}$), 1.31-1.35 (t, 3 H, $COOCH_2\mathit{CH_3}$), 1.55-1.64 (m, 2 H, $CH_2\mathit{CH_2}CH_3$), 2.53-2.57 (t, 2 H, $\mathit{CH_2}CH_2CH_3$), 4.22-4.28 (q, 2 H, $COO\mathit{CH_2}CH_3$), 5.78 (s, 2 H, NH_2 exch), 6.63 (s, 1 H, 4-H). HRMS (EI) calcd for $C_{10}H_{15}NO_2S$ *m/z* = 213.0823, found *m/z* = 213.0828.

2-Amino-6-propylthieno[2,3-*d*]pyrimidin-4(3*H*)-one (406). A mixture of **405** (2.1 g, 9.8 mmol) and chloroformamidine hydrochloride (2.3 g, 29 mmol) in $DMSO_2$ (7.5 g, 7.5mmol) was heated at 150 ^{o}C for 2 h. The mixture was cooled to room temperature and water (30 mL) was added and ammonium hydroxide was used to neutralize the suspension. The brown solid, obtained by filtration, was washed with water and dried over P_2O_5 vacuum. The solid was dissolved in methanol and silica gel was added. The plug was loaded on to a silica gel column and eluted with 5% methanol in chloroform to afford **406** (1.63 g, 80%) as a yellow solid; mp > 300 ^{o}C; R_f 0.32 (MeOH/$CHCl_3$, 1:6); ^{1}H NMR (DMSO-d_6) δ 0.89-0.93 (t, 3 H, $CH_2CH_2\mathit{CH_3}$), 1.55-1.64 (m, 2 H, $CH_2\mathit{CH_2}CH_3$), 2.64-2.68 (t, 2 H, $\mathit{CH_2}CH_2CH_3$). 6.45 (s, 2 H, 2-NH_2 exch), 6.79 (s, 1 H, 5-H), 10.82 (s, 1 H, 3-NH exch); Anal. calcd. for ($C_9H_{11}N_3SO \cdot 0.2\ CH_3OH$): C, 51.23; H, 5.51; N, 19.48; S, 14.87; found: C, 51.26; H, 5.31; N, 19.34; S, 14.84.

2-Amino-5-iodo-6-propylthieno[2,3-*d*]pyrimidin-4(3*H*)-one (408). To a mixture of **406** (2.5 g, 11.9 mmol) in glacial acetic acid (60 mL) was added mercuric acetate (5.69 g, 17.93 mmol) at room temperature. The mixture was heated at 100 ^{o}C for 3 h. Then the mixture was poured into a brine solution (60 mL) and stirred for 30 min. The yellow solid **407** (4.2 g, 78.9%) obtained by filtration was washed with water and hexane and dried over P_2O_5 vacuum; mp 252.7 ^{o}C. Compound **407** (3.5 g, 7.8 mmol) was dissolved in CH_2Cl_2 (100 mL) and I_2 (3.85 g, 15.2 mmol) was added. The resulting mixture was stirred for 5 h at room temperature. The mixture was washed with 2 N NaS_2O_3 and dried over $MgSO_4$. The plug was loaded on to a silica gel column and eluted with 3% methanol in chloroform to afford **408** (2.25 g, 86%) as a yellow solid; mp 241 ^{o}C; R_f 0.26 (MeOH/$CHCl_3$, 1:10); ^{1}H NMR (DMSO-d_6) δ 0.91-0.95 (t, 3 H, $CH_2CH_2CH_3$), 1.53-1.63 (m, 2 H, $CH_2CH_2CH_3$), 2.65-2.68 (t, 2 H, $CH_2CH_2CH_3$), 6.56 (s, 2 H, 2-NH_2 exch), 10.91 (s, 1 H, 3-NH exch). HRMS (EI) calcd for $C_9H_{10}IN_3SO$ *m/z* = 335.9668, found *m/z* = 335.9641.

General procedure for the synthesis of compounds **283-291** and **409**.

A mixture of appropriate arylthiols (1.5 eq), K_2CO_3 (1.5 eq), CuI (1.3 eq) and **408** (1 eq) in dry DMF (5 mL) was irradiated in a microwave at 100 °C for 60-120 min. After the reaction mixture was cooled to room temperature, the mixture was filtered; the filtrate was concentrated under reduced pressure. The solid was dissolved in methanol and silica gel was added. A dry silica gel plug was obtained after evaporation of the solvent. The plug was loaded on to a silica gel column and eluted with 2 % methanol in chloroform.

2-Amino-5-(phenylsulfanyl)-6-propylthieno[2,3-d]pyrimidin-4(3H)-one (283). Using the general procedure above compound **283** (0.085 g, 54 %) was obtained as a light yellow solid by reacting **408** (0.167 g, 0.5 mmol), benzenethiol (0.083 g, 0.75 mmol), K_2CO_3 (0.103 g, 0.75

mmol) and CuI (0.124 g, 0.65 mmol) in DMF (5 mL) under microwave irradiation at 100 °C for 90 min. R_f 0.39 (MeOH/$CHCl_3$, 1:10); mp > 283.6-284.8 °C; ^{1}H NMR (DMSO-d_6) δ 0.82-0.86 (t, 3 H, $CH_2CH_2\mathit{CH_3}$), 1.48-1.57 (m, 2 H, $CH_2\mathit{CH_2}CH_3$), 2.8-2.84 (t, 2 H, $\mathit{CH_2}CH_2CH_3$), 6.56 (s, 2 H, 2-NH_2 exch), 6.96-6.99 (dd, 2 H, C_6H_5), 7.05-7.08 (t, 1 H, C_6H_5), 7.19-7.23 (t, 2 H, C_6H_5), 10.73 (s, 1 H, 3-NH exch); Anal. calcd. for ($C_{15}H_{15}N_3S_2O \cdot 0.5\ CH_3OH$): C, 55.83; H, 5.14; N, 12.60; S, 19.23; found: C, 55.82; H, 4.79; N, 12.39; S, 19.36.

2-Amino-5-[(4-nitrophenyl)sulfanyl]-6-propylthieno[2,3-d]pyrimidin-4(3H)-one (284). Using the general procedure above compound **284** (0.109 g, 60.2 %) was obtained as a light yellow solid by reacting **408** (0.167 g, 0.5 mmol), 4-nitrobenzenethiol (0.096 g, 0.75 mmol), K_2CO_3 (0.103 g, 0.75 mmol) and CuI (0.124 g, 0.65 mmol) in DMF (5 mL) under microwave irradiation at 100 °C for 90 min. R_f 0.39 (MeOH/$CHCl_3$, 1:10); mp 290.1-291.3 °C; ^{1}H NMR (DMSO-d_6) δ 0.83-0.86 (t, 3 H, $CH_2CH_2\mathit{CH_3}$), 1.52-1.57 (m, 2 H, $CH_2\mathit{CH_2}CH_3$), 2.81-2.84 (t, 2 H, $\mathit{CH_2}CH_2CH_3$), 6.63 (s, 2 H, 2-NH_2 exch), 7.16, 7.18 (d, 2 H, C_6H_4), 8.06, 8.08 (d, 2 H, C_6H_4), 10.81 (s, 1 H, 3-NH exch); Anal. calcd. for ($C_{15}H_{14}N_4S_2O_3 \cdot 0.2\ H_2O$): C, 49.22; H, 3.97; N, 15.31; S, 17.52; found: C, 49,46; H, 3.97; N, 14.98; S, 17.24.

2-Amino-5-[(3,4-dichlorophenyl)sulfanyl]-6-propylthieno[2,3-d]pyrimidin-4(3H)-one (285). Using the general procedure above compound **285** (0.141 g, 73.1 %) was obtained as a white solid by reacting **408** (0.167 g, 0.5 mmol), 3,4-dichlorobenzenethiol (0.134 g, 0.75 mmol), K_2CO_3 (0.103 g, 0.75 mmol) and CuI (0.124 g, 0.65 mmol) in DMF (5 mL) under microwave irradiation at 100 °C for 90 min. R_f 0.42 (MeOH/$CHCl_3$, 1:10); mp 284.4-284.9 °C; ^{1}H NMR (DMSO-d_6) δ 0.83-0.86 (t, 3 H, $CH_2CH_2\mathit{CH_3}$), 1.51-1.56 (m, 2 H, $CH_2\mathit{CH_2}CH_3$), 2.81-2.85 (t, 2 H, $\mathit{CH_2}CH_2CH_3$), 6.62 (s, 2 H, 2-NH_2 exch), 6.90, 6.92 (d, 1 H, C_6H_3), 7.22 (s, 1 H, C_6H_3), 7.45,

7.47 (d, 1 H, C_6H_3), 10.78 (s, 1 H, 3-NH exch); HRMS calcd for C15H14Cl_2N3OS_2 385.9950, found 385.9974.

2-Amino-6-propyl-5-(1-naphthylsulfanyl)thieno[2,3-*d*]pyrimidin-4(3*H*)-one (286). Using the general procedure above compound **286** (0.137 g, 74.9 %) was obtained as a yellow solid by reacting **408** (0.167 g, 0.5 mmol), naphthalene-1-thiol (0.12 g, 0.75 mmol), K_2CO_3 (0.103 g, 0.75 mmol) and CuI (0.124 g, 0.65 mmol) in DMF (5 mL) under microwave irradiation at 100 °C for 90 min. R_f 0.39 (MeOH/$CHCl_3$, 1:10); mp > 300 °C; ^{1}H NMR (DMSO-d_6) δ 0.80-0.83 (t, 3 H, $CH_2CH_2CH_3$), 1.49-1.56 (m, 2 H, $CH_2CH_2CH_3$), 2.8-2.83 (t, 2 H, $CH_2CH_2CH_3$), 6.59 (s, 2 H, 2-NH_2 exch), 6.77,6.79 (d, 1 H, $C_{10}H_7$), 7.28-7.32 (t, 1 H, $C_{10}H_7$), 7.55-7.66 (m, 3 H, $C_{10}H_7$), 7.91, 7.93 (d, 1 H, $C_{10}H_7$), 8.20, 8.22 (d, 1 H, $C_{10}H_7$), 10.73 (s, 1 H, 3-NH exch); HRMS (ESI, pos mode) m/z $[M + H]^+$ calcd for $C_{19}H_{17}N_3OS_2$, 368.0886; found, 368.0891.

2-Amino-6-propyl-5-(2-naphthylsulfanyl)thieno[2,3-*d*]pyrimidin-4(3*H*)-one (287). Using the general procedure above compound **287** (0.152 g, 83.1 %) was obtained as a light brown solid by reacting **408** (0.167 g, 0.5 mmol), naphthalene-2-thiol (0.12 g, 0.75 mmol), K_2CO_3 (0.103 g, 0.75 mmol) and CuI (0.124 g, 0.65 mmol) in DMF (5 mL) under microwave irradiation at 100 °C for 90 min. R_f 0.50 (MeOH/$CHCl_3$, 1:10); mp 257.3-257.6 °C; ^{1}H NMR (DMSO-d_6) δ 0.82-0.86 (t, 3 H, $CH_2CH_2CH_3$), 1.50-1.60 (m, 2 H, $CH_2CH_2CH_3$), 2.84-2.88 (t, 2 H, $CH_2CH_2CH_3$), 6.57 (s, 2 H, 2-NH_2 exch), 7.14, 7.17 (d, 1 H, $C_{10}H_7$), 7.43-7.45 (m, 3 H, $C_{10}H_7$), 7.70-7.81 (m, 3 H, $C_{10}H_7$), 10.71 (s, 1 H, 3-NH exch); HRMS (ESI, pos mode) m/z $[M + H]^+$ calcd for $C_{19}H_{17}N_3OS_2$, 368.0886; found, 368.0886.

2-Amino-5-[(4-fluorophenyl)sulfanyl]-6-propylthieno[2,3-d]pyrimidin-4(3H)-one (288). Using the general procedure above compound **288** (0.097 g, 58.1 %) was obtained as a light yellow solid by reacting **408** (0.167 g, 0.5 mmol), 4-fluorobenzenethiol (0.096 g, 0.75 mmol), K_2CO_3 (0.103 g, 0.75 mmol) and CuI (0.124 g, 0.65 mmol) in DMF (5 mL) under microwave irradiation at 100 °C for 90 min. R_f 0.41 (MeOH/$CHCl_3$, 1:10); mp > 300 °C; ^{1}H NMR (DMSO-d_6) δ 0.83-0.87 (t, 3 H, $CH_2CH_2\mathit{CH_3}$), 1.49-1.58 (m, 2 H, $CH_2\mathit{CH_2}CH_3$), 2.83-2.86 (t, 2 H, $\mathit{CH_2}CH_2CH_3$), 6.58 (s, 2 H, 2-NH_2 exch), 7.01-7.08 (m, 4 H, C_6H_4), 10.73 (s, 1 H, 3-NH exch); HRMS calcd for $C_{15}H_{15}FN_3OS_2$ 336.0635, found 336.0656.

2-Amino-5-[(4-methoxyphenyl)sulfanyl]-6-propylthieno[2,3-d]pyrimidin-4(3H)-one (289). Using the general procedure above compound **289** (0.085 g, 48.8 %) was obtained as a white solid by reacting **408** (0.167 g, 0.5 mmol), 4-methoxybenzenethiol (0.105 g, 0.75 mmol), K_2CO_3 (0.103 g, 0.75 mmol) and CuI (0.124 g, 0.65 mmol) in DMF (5 mL) under microwave irradiation at 100 °C for 90 min. R_f 0.44 (MeOH/$CHCl_3$, 1:10); mp 268.8-269.9 °C; ^{1}H NMR (DMSO-d_6) δ 0.84-0.88 (t, 3 H, $CH_2CH_2\mathit{CH_3}$), 1.48-1.57 (m, 2 H, $CH_2\mathit{CH_2}CH_3$), 2.84-2.87 (t, 2 H, $\mathit{CH_2}CH_2CH_3$), 3.68 (s, 3 H, OCH_3), 6.54 (s, 2 H, 2-NH_2 exch), 6.80, 6.82 (d, 2 H, C_6H_4), 7.04, 7.06 (d, 2 H, C_6H_4), 10.71 (s, 1 H, 3-NH exch); Anal. calcd. for ($C_{16}H_{17}N_3S_2O_2 \cdot 0.4\ CH_3OH$): C, 54.67; H, 5.20; N, 11.66; S, 17.80; found: C, 54.46; H, 4.85; N, 11.63; S, 17.71.

2-Amino-5-[(4-chlorophenyl)sulfanyl]-6-propylthieno[2,3-d]pyrimidin-4(3H)-one (290). Using the general procedure above compound **290** (0.118 g, 67.1 %) was obtained as a white solid by reacting **408** (0.167 g, 0.5 mmol), 4-chlorobenzenethiol (0.108 g, 0.75 mmol), K_2CO_3 (0.103 g, 0.75 mmol) and CuI (0.124 g, 0.65 mmol) in DMF (5 mL) under microwave irradiation at 100 °C for 90 min. R_f 0.39 (MeOH/$CHCl_3$, 1:10); mp 297.2-297.4 °C; ^{1}H NMR (DMSO-d_6) δ

0.83-0.86 (t, 3 H, $CH_2CH_2\mathit{CH_3}$), 1.51-1.59 (m, 2 H, $CH_2\mathit{CH_2}CH_3$), 2.81-2.84 (t, 2 H, $\mathit{CH_2}CH_2CH_3$), 6.58 (s, 2 H, 2-NH_2 exch), 6.98, 7.00 (d, 2 H, C_6H_4), 7.26, 7.28 (d, 2 H, C_6H_4), 10.71 (s, 1 H, 3-NH exch); Anal. calcd. for ($C_{15}H_{14}Cl\,N_3S_2O \cdot 0.05\ CHCl_3$): C, 50.51; H, 3.96; N, 11.74; S, 17.92; Cl, 11.39; found: C, 50.27; H, 3.93; N, 11.58; S, 17.58; Cl, 11.59.

2-Amino-6-propyl-5-(4-bromophenyl sulfanyl)thieno[2,3-*d*]pyrimidin-4(3*H*)-one (291). Using the general procedure above compound **291** (0.147 g, 88 %) was obtained as a light brown solid by reacting **408** (0.167 g, 0.5 mmol), 4-chlorobenzenethiol (0.096 g, 0.75 mmol), K_2CO_3 (0.103 g, 0.75 mmol) and CuI (0.124 g, 0.65 mmol) in DMF under microwave irradiation at 100 °C for 90 min. R_f 0.41(MeOH/$CHCl_3$, 1:10); mp 288.4-289.0 °C; ^{1}H NMR (DMSO-d_6) δ 0.83-0.86 (t, 3 H, $CH_2CH_2\mathit{CH_3}$), 1.48-1.58 (m, 2 H, $CH_2\mathit{CH_2}CH_3$), 2.80-2.84 (t, 2 H, $\mathit{CH_2}CH_2CH_3$), 6.58 (s, 2 H, 2-NH_2 exch), 6.91, 6.93 (d, 2 H, C_6H_4), 7.37, 7.40 (d, 2 H, C_6H_4), 10.74 (s, 1 H, 3-NH exch); HRMS (ESI, pos mode) m/z $[M + H]^+$ calcd for $C_{15}H_{14}BrN_3OS_2$, 396.9824; found, 396.9815.

Methyl 4-[(2-amino-4-oxo-6-propyl-3,4-dihydrothieno[2,3-d]pyrimidin-5-yl) sulfanyl]benzoate (409). Using the general procedure above compound **409** (0.176 g, 47.3 %) was obtained as a white solid by reacting **408** (0.334 g, 1 mmol), methyl 4-mercaptobenzoate (0.252 g, 1.5 mmol), K_2CO_3 (0.206 g, 1.5 mmol) and CuI (0.248 g, 1.3 mmol) in DMF (7 mL) under microwave irradiation at 100 °C for 90 min. R_f 0.38 (MeOH/$CHCl_3$, 1:10); mp 176.6-178.2 °C; ^{1}H NMR (DMSO-d_6) δ 0.81-0.85 (t, 3 H, $CH_2CH_2\mathit{CH_3}$), 1.49-1.59 (m, 2 H, $CH_2\mathit{CH_2}CH_3$), 2.79-2.83 (t, 2 H, $\mathit{CH_2}CH_2CH_3$), 3.79 (s, 3 H, $COOCH_3$), 6.60 (s, 2 H, 2-NH_2 exch), 7.05, 7.07 (d, 2 H, C_6H_4), 7.77, 7.79 (d, 2 H, C_6H_4), 10.77 (s, 1 H, 3-NH exch).

4-[(2-Amino-4-oxo-6-propyl-3,4-dihydrothieno[2,3-d]pyrimidin-5-yl)sulfanyl] benzoic acid (410). To a solution of **409** (0.14 g, 0.3 mmol) in ethanol (10 mL) was added

aqueous 1 N NaOH (5 mL) and the reaction mixture stirred at room temperature for 12 h. The ethanol was evaporated under reduced pressure and the residue was dissolved in water (5 mL). The solution was carefully acidified to pH 3 with the drop wise addition of 1 N HCl. The resulting suspension was left at 0 ^{o}C for an hour and then the residue was collected by filtration, washed with water (5 mL) and dried over P_2O_5/vacuum at 50 ^{o}C to afford **410** (0.105 g, 97.1 %) as a yellow solid. R_f 0.43 (MeOH/$CHCl_3$, 1:6+ 1drop of gl. HOAc); mp >300 °C; ^{1}H NMR (DMSO-d_6) δ 0.84 (m, 3 H, $CH_2CH_2\mathit{CH_3}$), 1.54 (m, 2 H, $CH_2\mathit{CH_2}CH_3$), 2.79-2.83 (m, 2 H, $\mathit{CH_2}CH_2CH_3$), 6.60 (s, 2 H, 2-NH_2 exch), 7.02, 7.04 (d, 2 H, C_6H_4), 7.74, 7.76 (d, 2 H, C_6H_4), 10.77 (s, 1 H, 3-NH exch), 12.77 (s, 1 H, COOH exch).

Diethyl *N*-{4-[(2-amino-4-oxo-6-propyl-3,4-dihydrothieno[2,3-d]pyrimidin-5-yl) sulfanyl]benzoyl}-L-glutamate (411). To a solution of **410** (0.1 g, 0.28 mmol) in anhydrous DMF (10 mL) was added N-methylmorpholine (0.034 g, 0.34 mmol) and 2-chloro-4,6-dimethoxy-1,3,5-triazine (0.06 g, 0.34 mmol). The resulting mixture was stirred at room temperature for 2 h. N-methylmorpholine (0.034 g, 0.34 mmol) and diethyl-L- glutamate hydrochloride (0.068 g, 0.28 mmol) were added to the mixture. The reaction mixture was stirred for an additional 3 h at room temperature and silica gel was added to this solution and the suspension evaporated under reduced pressure. The plug obtained was loaded on a silica gel column and eluted with 2% methanol in chloroform and **411** (0.095 g, 62.1 %) was obtained as a yellow solid. R_f 0.33 (MeOH/$CHCl_3$, 1:6); mp > 300 °C; ^{1}H NMR (DMSO-d_6) δ 0.83-0.87 (t, 3 H, $CH_2CH_2\mathit{CH_3}$), 1.13-1.18 (q, 6 H, 2 $COOCH_2\mathit{CH_3}$), 1.51-1.57 (m, 2 H, $CH_2\mathit{CH_2}CH_3$), 1.93-2.11 (m, 2 H Gluβ-CH_2), 2.39-2.43 (t, 2 H, Gluγ-CH_2), 2.80-2.84 (t, 2 H, $\mathit{CH_2}CH_2CH_3$), 4.00-4.11 (m, 4 H, 2 $COO\mathit{CH_2}CH_3$), 4.35-4.41 (1 H, m, Gluα-CH), 6.61 (s, 2 H, 2-NH_2 exch), 7.01, 7.03 (d, 2 H, C_6H_4), 7.68, 7.70 (d, 2 H, C_6H_4), 8.60-8.62 (d, 1H, CONH exch), 10.74 (s, 1 H, 3-

NH exch).

***N*-{4-[(2-Amino-4-oxo-6-propyl-3,4-dihydrothieno[2,3-d]pyrimidin-5-yl)sulfanyl]benzoyl}-L-glutamic acid (282).** To a solution of **411** (0.09 g, 0.165 mmol) in ethanol (7 mL) was added aqueous 1 N NaOH (4 mL) and the reaction mixture stirred at room temperature for 3 h. The ethanol was evaporated under reduced pressure and the residue was dissolved in water (5 mL). The solution was cooled to 0 ^{o}C and carefully acidified to pH 3 with drop wise addition of 1 N HCl. The resulting suspension was left at 0 ^{o}C for 2 h and the residue was collected by filtration. Washed with water (5 mL) and dried over P_2O_5/vacuum at 50 ^{o}C to afford **282** (0.072 g, 89.1%) as light yellow solid. R_f 0.41 (MeOH/$CHCl_3$, 1:6+ 1drop of gl. HOAc); mp 167.9-170 °C; ^{1}H NMR (DMSO-d_6) δ 0.83-0.87 (t, 3 H, $CH_2CH_2CH_3$), 1.51-1.57 (m, 2 H, $CH_2CH_2CH_3$), 1.86-2.13 (m, 2 H Gluβ-CH_2), 2.30-2.34 (t, 2 H, Gluγ-CH_2), 2.80-2.84 (t, 2 H, $CH_2CH_2CH_3$), 3.54-3.61 (m, 1 H), 4.32-4.39 (1 H, m, Gluα-CH), 6.58 (s, 2 H, 2-NH_2 exch), 7.01, 7.03 (d, 2 H, C_6H_4), 7.69, 7.71 (d, 2 H, C_6H_4), 8.47-8.49 (d, 1H, CONH exch), 10.75 (s, 1 H, 3-NH exch), 12.36 (s, 2H, COOH exch); Anal. calcd. for ($C_{21}H_{22}N_4S_6O_2$ ·1.5 H_2O): C, 48.73; H, 4.87; N, 10.82; S, 12.39; found: C, 48.49; H, 5.03; N, 10.63; S, 12.39.

2-Amino-5-(prop-2-yn-1-yl)pyrimidine-4,6-diol (415). A mixture of dimethyl prop-2-yn-1-ylmalonate **414** (10 g, 60 mmol) and guanidine carbonate (10.8 g, 60 mmol) was heated to reflux in MeOH (100 mL) for 24 h. The suspension was then cooled in an ice-bath to room temperature. The precipitate formed was collected by filtration and dissolved in 40 mL of water. The pH of this solution was adjusted to 3-4 with 1 N HCl whereupon a thick precipitate formed. The mixture was filtered and washed with a small amount of water followed by acetone and dried in vacuo to afford 3.4 g (40%) of **73c** as a light pink powder: mp 291.6-293.3 ^{o}C; 1H NMR (DMSO-*d*6) 2.45 (t, 1 H, *J* = 2.4 Hz), 2.95 (d, 2 H, *J* = 2.4 Hz), 6.53 (s, 2 H), 10.49 (br, 2H).

2,2-Dimethyl-*N*-(6-methyl-4-oxo-3,4-dihydrofuro[2,3-*d*]pyrimidin-2-yl)propanamide (416). To a 100 mL round-bottom flask was added **415** (3 g, 18 mmol) and pivaloyl anhydride (30 mL) and the resulting mixture was refluxed under N_2 atmosphere for 2.5 h. TLC showed the disappearance of the starting material **415** and the formation of a major spot at *Rf* = 0.42 ($CHCl_3$/MeOH 5:1). After evaporation of the solvent, the residue was loaded onto a silica gel column and eluted with hexane followed by hexane/EtOAc 2:1. The fractions containing the desired spot (TLC) were pooled and evaporated, the resulting residue was recrystallized from Et_2O/EtOAc to afford 3.0 g (67%) of **416** as light yellow crystals: mp 225-227 ^oC; *Rf* = 0.47 (MeOH/$CHCl_3$ 1 : 7); 1H NMR (DMSO-*d*6) 1.24 (s, 9 H), 2.34 (s, 3 H), 6.50 (s, 1 H), 11.26 (s, 1 H), 12.19 (s, 1 H). Anal. Calcd. for $C_{12}H_{15}N_3O_3$: C, 57.82; H, 6.07; N, 16.86 Found C, 58.10; H, 6.12; N,16.86.

2-Amino-6-methyl-furo[2,3-*d*]pyrimidin-4(3*H*)-one (412)

Method A.

To a suspension of **416** (2 g, 8 mmol) in 1,4-dioxane (20 mL) was added 50% KOH (15 mL) and the resulting mixture was refluxed over night. TLC indicated the diminishing of starting materials and the formation of a major spot at *Rf* = 0.12 [(CHCl3/MeOH 5:1)/(Hexane/EtOAc 2:1) 1:1]. After evaporation of the solvent, the residue was loaded onto a silica gel column and eluted with 2% MeOH in $CHCl_3$, followed by 5% MeOH in $CHCl_3$. The fractions containing the desired spot (TLC) were pooled and evaporated. The resulting residue was recrystallized from EtOAc/Et_2O to afford 1.1 g (76%) of **412** as yellow crystals: mp > 250 ^oC (dec); TLC *Rf* = 0.24 (MeOH/$CHCl_3$ 1: 3); 1H NMR (DMSO-*d*6) 2.23 (s, 3 H), 6.25 (s, 1 H), 6.56 (s, 2 H), 10.70 (s, 1 H). Anal. Calcd. for C7H7N3O2: C, 50.91; H, 4.27; N, 25.44 Found C, 50.71; H, 4.44; N, 25.05.

Method B.

The microwave reaction vial was charged with **415** (1.05 g, 3.3 mmol) and 15 mL 2 N NaOH. The reaction mixture was irradiated in a microwave apparatus at 180 °C, 30 min. After the reaction mixture was cooled to ambient temperature, the product was filtered, the filtrate was concentrated, and the crude mixture was purified by silica gel column chromatography using 2% MeOH in CHCl3 as the eluent. Fractions containing the product (TLC) were combined and evaporated to afford 0.98 g (93%) of **412** as a white crystals: mp > 250 ^{o}C (dec); TLC *Rf* = 0.24 (MeOH/CHCl3 1: 3); 1H NMR (DMSO-*d*6) 2.23 (s, 3 H), 6.25 (s, 1 H), 6.56 (s, 2 H), 10.70 (s, 1 H). HRMS (EI) calcd for C7H7N3O2 *m/z* = 165.0538, found *m/z* = 165.0537.

2-Amino-5-iodo-6-methylfuro[2,3-*d*]pyrimidin-4(3*H*)-one (419). To a suspension of **412** (0.9 g, 5.5 mmol) in 20 mL of glacial acetic acid at room temperature was added mercuric acetate (1.7 g, 5.5 mmol). The resulting solution was stirred at 100 oC for 3 h, then poured into a saturated NaCl (30 mL), and stirred for 20 min. The solid was collected by filtration, washed with water (10 mL), hexane (10 mL) and dried to give a dark solid (5-chloromercury derivative), which was directly used for iodination reaction without further purification. This dark material was dissolved in CH_2Cl_2 (30 mL) containing I_2 (1.4 g, 5.5 mmol), stirred for 2 h at room temperature. The solvent was evaporated, the residue was washed with 2 N NaS_2O_3 (15 mL) and dried in vacuo. The crude product was purified by column chromatography on silica gel with 3% MeOH/CHCl3 as the eluent to afford 0.51 g (32%) of **419** as a white solid: mp 214-215 °C; *Rf* 0.47 (MeOH/CHCl3, 1:5); 1H NMR (DMSO-*d*6) 2.25 (s, 3 H), 6.67 (s, 1 H), 10.84 (s, 1 H). HRMS (EI) calcd for C7H6IN3O2 *m/z* = 290.9504, found *m/z* = 290.9507.

2-amino-6-methyl-5-(phenylsulfanyl)furo[2,3-*d*]pyrimidin-4(3*H*)-one (293). The microwave reaction vial was charged with **419** (0.2 g, 0.7 mmol), K_2CO_3 (0.3 g, 2.1mmol) and 12 mL dry DMF. The mixture was evacuated and backfilled with nitrogen (3 cycles). Catalyst Cu2O (85 mg, 0.7 mmol) and benzenethiol (0.3 g, 2.8 mmol) were added and then the reaction mixture was degassed twice. The reaction mixture was irradiated in a microwave apparatus at 150 °C, for 1 h. After the reaction mixture was cooled to ambient temperature, the product was filtered, the filtrate was concentrated, and the crude mixture was purified by silica gel column chromatography using 2% MeOH in CHCl3 as the eluent. Fractions containing the product (TLC) were combined and evaporated to afford 0.12 g (62%) of **293** as a white solid: *Rf* = 0.42 (MeOH/CHCl3, 1:5); mp 121-122 °C; 1H NMR (DMSO-*d*6) 2.31 (s, 3 H), 6.70 (br s, 2 H, exch), 7.12-7.27 (m, 5 H, C_6H_5), 10.76 (s, 1 H).

2-amino-6-methyl-5-(naphthalen-1-ylsulfanyl)furo[2,3-*d*]pyrimidin-4(3*H*)-one (294). The microwave reaction vial was charged with **419** (0.2 g, 0.7 mmol), K_2CO_3 (0.3 g, 2.1mmol) and 12 mL dry DMF. The mixture was evacuated and backfilled with nitrogen (3 cycles). Catalyst Cu2O (85 mg, 0.7 mmol) and 4-methoxybenzenethiol (0.45 g, 2.8 mmol) were added and then the reaction mixture was degassed twice. The reaction mixture was irradiated in a microwave apparatus at 150 °C, for 1 h. After the reaction mixture was cooled to ambient temperature, the product was filtered, the filtrate was concentrated, and the crude mixture was purified by silica gel column chromatography using 2% MeOH in $CHCl_3$ as the eluent. Fractions containing the product (TLC) were combined and evaporated to afford 0.15 g (67%) of **294** as a white solid: *Rf* = 0.47 (MeOH/CHCl3, 1:5); mp 128-129 °C; 1H NMR (DMSO-*d*6) 2.33 (s, 3 H), 6.72 (s, 2 H, exch), 7.10-7.12 (d, 1 H, *J* = 7.2 Hz), 7.34-7.38 (t, 1 H, *J* = 7.6 Hz), 7.57-7.62 (m, 2 H), 7.71-7.73 (d, 1 H, 8.0 Hz), 7.94-7.96 (d, 1 H, 7.2 Hz), 8.24-8.26 (d, 1 H, 8.0 Hz), 10.69 (s, 1

H).

2-amino-5-[(4-methoxyphenyl)sulfanyl]-6-methylfuro[2,3-*d*]pyrimidin-4(3*H*)-one (295). The microwave reaction vial was charged with **419** (0.2 g, 0.7 mmol), K_2CO_3 (0.3 g, 2.1mmol) and 12 mL dry DMF. The mixture was evacuated and backfilled with nitrogen (3 cycles). Catalyst Cu2O (85 mg, 0.7 mmol) and 4-methoxybenzenethiol (0.4 g, 2.8 mmol) were added and then the reaction mixture was degassed twice. The reaction mixture was irradiated in a microwave apparatus at 150 °C, for 1 h. After the reaction mixture was cooled to ambient temperature, the product was filtered, the filtrate was concentrated, and the crude mixture was purified by silica gel column chromatography using 2% MeOH in $CHCl_3$ as the eluent. Fractions containing the product (TLC) were combined and evaporated to afford 0.14 g (64%) of **295** as a white solid: *Rf* = 0.43 (MeOH/CHCl3, 1:5); mp 122-124 °C; 1H NMR (DMSO-*d*6) 2.32 (s, 3 H), 3.69 (s, 3 H), 6.66 (s, 2 H, exch), 6.83-6.85 (d, 2 H, *J* = 8.0 Hz), 7.22-7.24 (d, 1 H, *J* = 8.0 Hz), 10.69 (s, 1 H).

2-amino-6-methyl-5-(pyridin-4-ylsulfanyl)furo[2,3-*d*]pyrimidin-4(3*H*)-one (296). The microwave reaction vial was charged with **419** (0.2 g, 0.7 mmol), K_2CO_3 (0.3 g, 2.1mmol) and 12 mL dry DMF. The mixture was evacuated and backfilled with nitrogen (3 cycles). Catalyst Cu_2O (85 mg, 0.7 mmol) and pyridine-4-thiol (0.3 g, 2.8 mmol) were added and then the reaction mixture was degassed twice. The reaction mixture was irradiated in a microwave apparatus at 150 °C, for 1 h. After the reaction mixture was cooled to ambient temperature, the product was filtered, the filtrate was concentrated, and the crude mixture was purified by silica gel column chromatography using 2% MeOH in $CHCl_3$ as the eluent. Fractions containing the product (TLC) were combined and evaporated to afford 0.1 g (57%) of **296** as a white solid: *Rf* = 0.38 (MeOH/CHCl3, 1:5); mp 140-142 °C; 1H NMR (DMSO-*d*6) 2.32 (s, 3 H), 6.76 (s, 2 H, exch), 7.30-7.32 (d, 2 H, *J* = 7.6 Hz), 7.08-7.10 (d, 1 H, *J* = 7.6 Hz), 10.82 (s, 1 H). HRMS (EI) calcd

for C12H10N4O2S *m/z* = 274.0524, found *m/z* = 274.0522.

2-Amino-5-[(3,4-dichlorophenyl)thio]-6-methylfuro[2,3-*d*]pyrimidin-4(3*H*)-one (297). The microwave reaction vial was charged with **419** (0.2 g, 0.7 mmol), K_2CO_3 (0.3 g, 2.1mmol) and 12 mL dry DMF. The mixture was evacuated and backfilled with nitrogen (3 cycles). Catalyst Cu_2O (85 mg, 0.7 mmol) and 3,4-dichlorobenzenethiol (0.5 g, 2.8 mmol) were added and then the reaction mixture was degassed twice. The reaction mixture was irradiated in a microwave apparatus at 150 °C, for 1 h. After the reaction mixture was cooled to ambient temperature, the product was filtered, the filtrate was concentrated, and the crude mixture was purified by silica gel column chromatography using 2% MeOH in $CHCl_3$ as the eluent. Fractions containing the product (TLC) were combined and evaporated to afford 0.33 g (70%) of **297** as a white solid: *Rf* = 0.42 (MeOH/CHCl3, 1:5); mp 126-128 °C; 1H NMR (DMSO-*d*6) 2.33 (s, 3 H), 6.77 (s, 2 H, exch), 7.09 (dd, 1 H, *J* = 2.4 Hz, *J* = 8.8 Hz), 7.38 (d, 1 H, *J* = 2.4 Hz), 7.49 (d, 1 H, *J* = 8.8 Hz), 10.82 (s, 1 H). HRMS (EI) calcd for $C_{13}H_9Cl_2N_3O_2S$ *m/z* = 340.9792, found *m/z* = 340.9797.

2-amino-5-[(4-chlorophenyl)sulfanyl]-6-methylfuro[2,3-*d*]pyrimidin-4(3*H*)-one (298). The microwave reaction vial was charged with **419** (0.2 g, 0.7 mmol), K_2CO_3 (0.3 g, 2.1mmol) and 12 mL dry DMF. The mixture was evacuated and backfilled with nitrogen (3 cycles). Catalyst Cu2O (85 mg, 0.7 mmol) and 4-chlorobenzenethiol (0.4 g, 2.8 mmol) were added and then the reaction mixture was degassed twice. The reaction mixture was irradiated in a microwave apparatus at 150 °C, for 1 h. After the reaction mixture was cooled to ambient temperature, the product was filtered, the filtrate was concentrated, and the crude mixture was purified by silica gel column chromatography using 2% MeOH in $CHCl_3$ as the eluent. Fractions containing the product (TLC) were combined and evaporated to afford 0.14 g (67%) of **298** as a white solid: *Rf* = 0.45 (MeOH/CHCl3, 1:5); mp 135-136 °C; 1H NMR (DMSO-*d*6) 2.32 (s, 3 H), 6.72 (s, 2 H,

exch), 7.13-7.15 (d, 2 H, *J* = 8.8 Hz), 7.29-7.32 (d, 1 H, *J* = 8.8 Hz), 10.77 (s, 1 H). HRMS (EI) calcd for $C_{13}H_{10}ClN_3O_2S$ *m/z* = 307.0182, found *m/z* = 307.0180.

Methyl 4-[(2-amino-6-methyl-4-oxo-3,4-dihydrofuro[2,3-*d*]pyrimidin-5-yl)sulfanyl]-benzoate (402). The microwave reaction vial was charged with **401** (0.4 g, 1.4 mmol), K2CO3 (0.6 g, 4.2 mmol) and 15 mL dry DMF. The mixture was evacuated and backfilled with nitrogen (3 cycles). Catalyst Cu2O (0.19 g, 1.4 mmol) and methyl 4-mercaptobenzoate (0.94 g, 5.6 mmol) were added and then the reaction mixture was degassed twice. The reaction mixture was irradiated in a microwave apparatus at 150 °C, for 1 h. After the reaction mixture was cooled to ambient temperature, the product was filtered, the filtrate was concentrated, and the crude mixture was purified by silica gel column chromatography using 2% MeOH in CHCl3 as the eluent. Fractions containing the product (TLC) were combined and evaporated to afford 0.36 g (75%) of **402** as a white solid: *Rf* = 0.47 (MeOH/CHCl3, 1:5); mp 156-158 °C; 1H NMR (DMSO-*d*6) □ 2.31 (s, 3 H), 3.80 (s, 3 H), 6.73 (s, 2 H), 7.18 (d, 2 H, *J* = 8.4 Hz), 7.80 (d, 2 H, *J* = 8.4 Hz), 10.82 (s, 1 H). HRMS (EI) calcd for C15H13N3O4S *m/z* = 331.0626, found *m/z* = 331.0628.

***N,N*'-(6-methylquinazoline-2,4-diyl)bis(2,2-dimethylpropanamide) (427)** To a 100 mL round-bottom flask was added **426** (0.342 g, 1 mmol) and pivaloyl anhydride (10 mL) and the resulting mixture was refluxed under N_2 atmosphere for 2.5 h. TLC showed the disappearance of the starting material **1** and the formation of a major spot at *Rf* = 0.42 (Hexane/AcOEt 5:1). After evaporation of the solvent, the residue was loaded onto a silica gel column and eluted with hexane followed by hexane/EtOAc 9:1. The fractions containing the desired spot (TLC) were pooled and evaporated, the resulting residue was recrystallized from Et_2O/EtOAc to afford 0.298 g (71%) of **427** as a white solid: mp 106.6-107.2 ^{o}C; *Rf* = 0.42 (Hexane/AcOEt 5 : 1); Anal.

Calcd. for $C_{19}H_{26}N_4O_2$: C, 66.64; H, 7.65; N, 16.36 Found C, 66.48; H, 7.80; N,16.33. Compound **427** was used directly for next step without further characterization.

***N,N'*-[6-(bromomethyl)quinazoline-2,4-diyl]bis(2,2-dimethylpropanamide) (428).** To a 100 mL flask were added **427** (1.09 g, 3.2 mmol) and benzene (30 mL). The suspension was stirred at 60 ^{o}C for 30 min to afford a clear solution, followed by the addition of *N*-bromosuccinimide (0.620 g, 3.49 mmol) and benzoyl peroxide (50 mg). The mixture was refluxed for 4h and then cooled to room temperature and washed with water, and evaporated to afford an yellow solid. The solid was dissolved in methanol and silica gel was added. A dry silica gel plug was obtained after evaporation of the solvent. The plug was loaded on to a silica gel column and eluted with 6 % ethyl acetate in hexane to afford **428** (457 mg, 34%) as a white solid; mp 148.1-148.9 °C; R_f 0.3 (hexane/EtOAc 3:1); ^{1}H NMR ($CDCl_3$) δ 1.37 (s, 9 H, Piv), 1.38 (s, 9 H, Piv), 4.73 (s, 2 H, CH_2Br), 7.44-7.47 (t, 1 H, J = 7.2, 8-C_6H_3), 7.78-7.82 (dd, 1 H, J_1 = 7.2, J_2 = 2.0, 7-C_6H_3),8.17 (s, 1 H, NH, exch), 8.50-8.51 (d, 1 H, J = 2.0, 6-C_6H_3), 15.78 (s, 1 H, NH, exch). HRMS calcd for $C_{12}H_9N_2OSBr$ 307.9619, found 307.9613.

***N,N'*-(6-{[(3,4,5-trichlorophenyl)amino]methyl}quinazoline-2,4-diyl)bis(2,2-dimethylpropanamide) (429)** A stirred solution of **428** (105 mg, 0.25 mmol) in dry DMF (5 mL) was treated with 3,4,5-trichloroaniline (194 mg, 1 mmol) and K_2CO_3 (95 mg, 0.69 mmol). The solution was stirred for 1 h at 80 °C under argon. The cooled reaction mixture was filtered and the filtrate was evaporated to obtain orange solid. The solid was dissolved in methanol and silica gel was added. A dry silica gel plug was obtained after evaporation of the solvent. The plug was loaded on to a silica gel column and eluted with ethyl acetate: hexane (7: 1) to afford 83 mg (62%) of **429** as a white solid, which was directly used for next step reaction.

***N,N'*-(6-{[(2,5-dichlorophenyl)amino]methyl}quinazoline-2,4-diyl)bis(2,2-**

dimethylpropanamide) (430) A stirred solution of **428** (105 mg, 0.25 mmol) in dry DMF (5 mL) was treated with 2,5-trichloroaniline (168 mg, 1 mmol) and K_2CO_3 (95 mg, 0.69 mmol). The solution was stirred for 1 h at 80 °C under argon. The cooled reaction mixture was filtered and the filtrate was evaporated to obtain orange solid. The solid was dissolved in methanol and silica gel was added. A dry silica gel plug was obtained after evaporation of the solvent. The plug was loaded on to a silica gel column and eluted with ethyl acetate: hexane (7: 1) to afford 80 mg (64%) **430** as a white solid; mp 129.7-130.2 °C; R_f 0.32 (hexane/EtOAc 3:1); ^{1}H NMR ($CDCl_3$) δ 1.32 (s, 9 H, Piv), 1.36 (s, 9 H, Piv), 4.50-4.51 (d, 2 H, *J* = 7.6, CH_2NH), 7.85-7.89 (t, 1 H, *J* = 7.6, CH_2*NH*), 6.61 (s, 1 H), 7.17-7.19 (d, 1 H), 7.26 (s, 1 H), 7.42-7.44 (d, 1 H), 7.68-7.70 (d, 1 H), 8.09 (s, 1 H, NH, exch), 8.46 (s, 1 H), 15.70 (s, 1 H, NH, exch). Compound **430** was used for the next step reaction without further characterization.

6-{[(2,5-dichlorophenyl)amino]methyl}quinazoline-2,4-diamine (301) To a combined solution of aqueous 1 N NaOH (1 mL) and methanol (4 mL) was added **429** (80 mg, 0.19 mmol). The mixture was refluxed for 12 h. The methanol was evaporated under reduced pressure and the residue was suspended in water (5 mL). The solution was cooled to 0 ^{o}C and carefully acidified to pH 8 with drop wise addition of 1 N HCl. The resulting suspension was left at 0 ^{o}C for 2 h and the residue was collected by filtration. Washed with water (3 X 1 mL) and dried over P_2O_5/vacuum at 50 ^{o}C to afford target **301** as a yellow solid; mp 167.2-167.9 °C; R_f 0.27 (MeOH/$CHCl_3$ 1:6); ^{1}H NMR ($CDCl_3$) δ 4.35-4.37 (d, 2 H, *J* = 7.6, CH_2NH), 5.74 (br s, 2 H, NH_2), 6.34 (t, 1 H, CH_2*NH*), 6.52 (s, 1 H), 6.54 (s, 1 H), 6.96-6.98 (d, 1 H, J = 8.4), 7.22-7.24 (d, 1 H, J = 8.4), 7.28-7.29 (d, 1 H, J = 2.0), 7.74 (s, 1 H); HRMS (ESI, pos mode) m/z [M + H^+] calcd for $C15H14N5Cl_2$ 334.0626, found 334.0617.

6-{[(3,4,5-trichlorophenyl)amino]methyl}quinazoline-2,4-diamine (302) To a combined

solution of aqueous 1 N NaOH (1 mL) and methanol (4 mL) was added **430** (50 mg, 0.11 mmol). The mixture was refluxed for 12 h. The methanol was evaporated under reduced pressure and the residue was suspended in water (5 mL). The solution was cooled to 0 ^{o}C and carefully acidified to pH 8 with drop wise addition of 1 N HCl. The resulting suspension was left at 0 ^{o}C for 2 h and the residue was collected by filtration. Washed with water (3 X 1 mL) and dried over P_2O_5/vacuum at 50 ^{o}C to afford target **302** as a yellow solid; mp 178.1-178.7 °C; R_f 0.29 (MeOH/$CHCl_3$ 1:6); HRMS (ESI, pos mode) m/z [M $^{+}$] calcd for C15H12N5Cl_3 367.0158, found 367.0612.

6-{[(3,4,5-trichlorophenyl)amino]methyl}pteridine-2,4-diamine (303) A stirred solution of **431** (63 mg, 0.25 mmol) in dry DMAC (5 mL) was treated with 3,4,5-trichloroaniline (194 mg, 1 mmol). The solution was stirred over night at room temperature under argon to obtain a yellow suspension. The solid was collected through filtration and then dissolved in methanol and silica gel was added. A dry silica gel plug was obtained after evaporation of the solvent. The plug was loaded on to a silica gel column and eluted with MeOH: $CHCl_3$ (7: 1) to afford 44 mg (48%) of **303** as a yellow solid; mp 179.2-179.7 °C; R_f 0.18 (MeOH/ $CHCl_3$ 4:1); ^{1}H NMR ($CDCl_3$) δ 4.50-4.51 (s, 2 H, CH_2NH), 6.66 (s, 2 H, C_6H_2), 6.93 (s, 2 H, exch), 7.00 (s, 1 H, exch), 7.82 (s, 2 H, exch), 8.7 (s, 1 H, C_4H_1); Anal. Calcd. for $C_{13}H_{10}Cl_3N_7$: C, 42.13; H, 2.72; N, 26.45; Cl, 28.70. Found C, 42.03; H, 2.65; N, 25.13; Cl, 29.87.

6-{[(2,5-dichlorophenyl)amino]methyl}pteridine-2,4-diamine (304) A stirred solution of **431** (63 mg, 0.25 mmol) in dry DMAC (5 mL) was treated with 2,5-dichloroaniline (168 mg, 1 mmol). The solution was stirred over night at room temperature under argon to obtain a yellow suspension. The solid was collected through filtration and then dissolved in methanol and silica gel was added. A dry silica gel plug was obtained after evaporation of the solvent. The plug was

loaded on to a silica gel column and eluted with MeOH: $CHCl_3$ (7: 1) to afford 57 mg (68%) of **304** as a yellow solid; mp 179.2-179.7 °C; R_f 0.18 (MeOH/ $CHCl_3$ 4:1); ^{1}H NMR ($CDCl_3$) δ 4.6 (s, 2 H, CH_2NH), 6.66 (m, 3 H, C_6H_2), 6.93 (s, 2 H, exch), 7.35 (s, 1 H, exch), 7.65 (s, 2 H, exch), 8.7 (s, 1 H, C_4H_1); Anal. Calcd. for $C_{13}H_{11}Cl_2N_7$: C, 46.45; H, 3.30; N, 29.17; Cl, 21.09. Found C, 45.71; H, 3.32; N, 28.56; Cl, 20.54.

6-[(2,5-dichlorophenoxy)methyl]pteridine-2,4-diamine (305)

A stirred solution of **431** (126 mg, 0.5 mmol) in dry DMAC (7.5 mL) was treated with 2,5-dichlorophenol (163 mg, 1 mmol). The solution was stirred over night at room temperature under argon to obtain a yellow suspension. The solid was collected through filtration and then dissolved in methanol and silica gel was added. A dry silica gel plug was obtained after evaporation of the solvent. The plug was loaded on to a silica gel column and eluted with MeOH: $CHCl_3$ (7: 1) to afford 49 mg (29%) of **305** as a yellow solid; mp 184.1-185.7 °C; R_f 0.19 (MeOH/ $CHCl_3$ 4:1); ^{1}H NMR ($CDCl_3$) δ 5.33 (s, 2 H, CH_2O), 6.76 (s, 2 H, NH_2 exch), 7.07 (1 H, d, C_6H_3), 7.49 (m, 2 H, C_6H_3), 7.65 (s, 2 H, NH_2 exch), 8.7 (s, 1 H, C_4H_1); HRMS (ESI, pos mode) m/z [M + H^+] calcd for C13H11N6OCl_2 337.0731, found 337.0355.

6-{[(2,5-dichlorophenyl)sulfanyl]methyl}pteridine-2,4-diamine (306)

A stirred solution of **431** (95 mg, 0.75 mmol) in dry DMAC (7.5 mL) was treated with 2,5-dichlorobenzenethiol (178 mg, 1 mmol). The solution was stirred over night at room temperature under argon to obtain a yellow suspension. The solid was collected through filtration and then dissolved in methanol and silica gel was added. A dry silica gel plug was obtained after evaporation of the solvent. The plug was loaded on to a silica gel column and eluted with MeOH: $CHCl_3$ (7: 1) to afford 98 mg (37%) of **306** as a yellow solid; mp 164.3-165.7 °C; R_f 0.19 (MeOH/ $CHCl_3$ 4:1); ^{1}H NMR ($CDCl_3$) δ 4.51 (s, 2 H, CH_2S), 6.69 (s, 2 H, NH_2 exch), 7.21 (1 H,

d, C_6H_3), 7.22 (s, 2 H, NH_2 exch), 7.46 (d, 1 H, C_6H_3), 7.70 (d, 1 H, C_6H_3), 8.78 (s, 1 H, C_4H_1); HRMS (ESI, pos mode) m/z [M + H^+] calcd for $C_{13}H_{11}N_6SCl_2$ 353.0143, found 353.0156.

methyl 5-bromofuran-2-carboxylate (438). Thionyl chloride (2.64g, 22 mmol) was added dropwise to a stirred solution of **437** (1.89 g, 10 mmol) in MeOH (20 mL) while maintaining the internal temperature below 12 ^oC. When addition was complete the mixture was left to stand at room temperature for 12h to obtain white solid. And the filtrate was concentrated under reduced pressure to afford white solid. The solid was washed with hexane and ethyl ether to afford **438** (1.93 g, 95%); R_f 0.55 (hexane/EtOAc 3:1); ^{1}H NMR (DMSO-d_6) δ 3.80 (s, 3 H), 6.84-6.85 (d, 1 H, J = 3.6), 7.35-7.36 (d, 1 H, J = 3.6).

methyl 5-(5-hydroxypent-1-yn-1-yl)furan-2-carboxylate (440). A mixture of **438** (0.2 g, 1 mmol), **439** (0.092 g, 1.1 mmol), $PdCl_2$ (11 mg), PPh_3 (44 mg), CuI (11 mg), NEt_3 (0.5 mL) and CH_3CN (2.5 mL) was irradiated to 100^oC for 10 min under microwave. The reaction mixture was then made in to plug and loaded on a silica gel column and eluted with hexane/EtOAc 5:1 to afford **440** (0.18 g, 85%) of as a yellow liquid; R_f 0.25 (hexane/EtOAc 1:1); ^{1}H NMR (DMSO-d_6) δ 1.51-1.58 (m, 4 H), 3.39-3.43 (m, 2 H), 3.79 (s, 3 H), 4.42-4.45 (t, 1 H, J = 5.2 Hz, OH exch), 6.83-6.84(d, 1 H, J = 3.6 Hz), 7.30-7.31(d, 1 H, J = 3.6 Hz).

methyl 5-(5-hydroxypentyl)furan-2-carboxylate (441). To a Parr hydrogenation bottle was added **440** (2.3 g, 11 mmol), 10% Pd/C (0.25 g) and MeOH(80 mL). Hydrogenation was carried out at 55 psi for 24 h. After filtration, the organic phase was evaporated at vacuum to afford **441** (2.09 g, 90%) as a yellow liquid; R_f 0.25 (hexane/EtOAc 1:1); ^{1}H NMR (DMSO-d_6) δ 1.27-1.30 (m, 4 H), 1.36-1.42 (m, 2 H), 1.55-1.62 (m, 2 H), 2.64-2.68 (t, 2 H), 3.33-3.38 (m, 2 H), 3.76 (s, 3 H), 4.31-4.34 (t, 1 H, J = 5.2 Hz, OH), 6.33-6.41 (d, 1 H, J = 3.6 Hz), 7.19-7.20 (d, 1 H, J = 3.6 Hz).

methyl 5-(5-oxopentyl)furan-2-carboxylate (442). A solution of CH_2Cl_2 (29 mL) and oxalyl chloride (1.2 mL, 12 mmol) was placed in a 100 mL 3-neck round bottom flask with an ballon and two dropping funnels containing DMSO (1.87 mL, 24 mmol) dissolved in CH_2Cl_2 (8 mL) and **441** (2.12 g, 10 mmol) in CH_2Cl_2 (15 mL). The DMSO was added to the stirred oxalyl chloride solution at -60^oC. The reaction mixture was stirred for 2 min and **7** was added within 20 min. Stirring was continued for an additional 15 min. NEt_3 (8.4 mL) was added and the reaction mixture was stirred for 5 min and the allowed to warm to room temperature. CH_2Cl_2 (40 mL) was added to the reaction mixture and then washed with H_2O (10 mL) for 3 times. The organic layer was then dried over anhydrous Na_2SO_4 to give **442** (1.99 g, 95%) as a yellow liquid; R_f 0.72 (hexane/EtOAc 1:1); ^{1}H NMR (DMSO-d_6) δ 1.24 (m, 2 H), 1.60 (m, 4 H), 2.43 (t, 2 H), 2.68 (t, 2 H), 3.68 (s, 3 H, CH_3), 6.34-6.35 (d, 1 H, J = 3.6 Hz), 7.20-7.21 (d, 1 H, J = 3.6 Hz), 9.63-9.65 (t, 1 H).

methyl 5-{3-[5-amino-4-(ethoxycarbonyl)thiophen-2-yl]propyl}furan-2-carboxylate (443). A mixture of **442** (2.6 g, 12.38 mmol), sulfur (0.397 g, 12.38 mmol), ethyl cyanoactetate (1.4 g, 12.38 mmol) and EtOH (100 mL) were placed in a round bottom flask and warmed to 45 ^oC and treated dropwise with morpholine (1.07 g, 12.4 mmol) over 15 min. The mixture was stirred for 4 h at 45 ^oC and 24 h at room temperature. Unreacted sulfur was removed by filtration, and the filtrate was concentrated under reduced pressure to afford an orange oil. The residue was loaded on a silica gel column packed with silica gel and eluted with 10% ethyl acetate in hexane to afford **443** (1.7 g, 41%) as a orange liquid; R_f 0.34 (hexane/EtOAc 3:1); ^{1}H NMR (DMSO-d_6) δ 1.20-1.24 (t, 3 H, J = 6.8 Hz, OCH_2CH_3), 1.49-1.63 (m, 4 H), 2.57-2.60 (t, 2 H, J = 7.2 Hz), 2.68-2.70 (t, 2 H, J = 7.2 Hz), 3.76 (s, 3 H, OCH_3), 4.09-4.15 (q, 2 H, J = 6.8 Hz, OCH_2CH_3), 6.33-6.34 (d, 1 H, J = 3.2 Hz), 6.49 (s, 1 H), 7.01 (s, 2 H, 2-NH_2 exch), 7.19-7.20 (d, 1 H, J = 3.2

Hz).

methyl 5-[3-(2-amino-4-oxo-3,4-dihydrothieno[2,3-*d*]pyrimidin-6-yl)propyl]furan-2-carboxylate (444) A mixture of **443** (1.82 g, 5.4 mmol) and chloroformamidine hydrochloride (2.46 g, 21.4 mmol) in $DMSO_2$ (5 g) was heated at 150 ^oC for 2 h. The mixture was cooled to room temperature. Water (40 mL) was added and ammonium hydroxide was used to neutralize the suspension. The brown solid, obtained by filtration, was washed with water and dried over P_2O_5 vacuum. The solid was dissolved in methanol and silica gel was added. The plug was loaded on to a silica gel column and eluted with 5% methanol in chloroformto to afford **444** (1.49g, 88%) as a yellow solid; mp 172.9-173.4 ^oC; R_f 0.3 (MeOH/$CHCl_3$, 1:6); ^1H NMR (DMSO-d_6) δ 1.61-1.63 (m, 4 H), 2.68-2.73 (m, 4 H), 3.76 (s, 3 H), 6.33-6.34 (d, 1 H, J = 3.6 Hz), 6.45 (s, 2 H, 2-NH_2 exch), 6.79 (s, 1 H), 7.19-7.20 (d, 1 H, J = 3.6 Hz), 10.82 (s, 1 H, 3-NH exch).

5-[3-(2-Amino-4-oxo-3,4-dihydrothieno[2,3-*d*]pyrimidin-6-yl)propyl]furan-2-carboxylic acid (445). To a solution of **444** (1.6 g, 4.81 mmol) in ethanol (130 mL) was added aqueous 1 N NaOH (68 mL) and the reaction mixture stirred at room temperature for 12 h. The ethanol was evaporated under reduced pressure and the residue was dissolved in water (40 mL). The solution was carefully acidified to pH 3 with the drop wise addition of 1 N HCl. The resulting suspension was left at 0 ^oC for an hour and then the residue was collected by filtration, washed with water (15 mL) and dried over P_2O_5/vacuum at 50 ^oC to afford **445** (1.3 g, 87 %) as a brown solid; mp >300 °C; R_f 0.40 (MeOH/$CHCl_3$, 1:6+ 1 drop of gl. HOAc); ^1H NMR (DMSO-d_6) δ 1.62-1.63 (m, 4 H), 2.67-2.74 (m, 4 H), 6.29-6.30 (d, 1 H, J = 3.2 Hz), 6.30 (s, 2 H, 2-NH_2 exch), 6.79 (s, 1 H), 7.09-7.10 (d, 1 H, J = 3.2 Hz), 10.83 (s, 1 H, COOH exch), 12.78 (s, 1 H, 3-NH exch).

Diethyl *N*-({5-[3-(2-amino-4-oxo-3,4-dihydrothieno[2,3-*d*]pyrimidin-6-yl)propyl]furan-2-yl}carbonyl)-L-glutamate (446). To a solution of **445** (1.05 g, 3.28 mmol) in anhydrous DMF (60 mL) was added N-methylmorpholine (0.39 g, 3.93 mmol) and 2-chloro-4,6-dimethoxy-1,3,5-triazine (0.69 g, 3.93 mmol). The resulting mixture was stirred at room temperature for 2 h. N-methylmorpholine (0.39 g, 3.93 mmol) and diethyl-L- glutamate hydrochloride (0.78 g, 3.28 mmol) were added to the mixture. The reaction mixture was stirred for an additional 3 h at room temperature and silica gel was added to this solution and the suspension evaporated under reduced pressure. The plug obtained was loaded on a silica gel column and eluted with 2% methanol in chloroform and **446** (1.02 g, 62 %) was obtained as a yellow solid; mp 185.4-186.7 °C; R_f 0.33 (MeOH/$CHCl_3$, 1:6); ^{1}H NMR (DMSO-d_6) δ 1.18-1.22 (m, 6 H), 1.65 (m, 4 H), 1.97-2.11 (m, 4 H), 2.36-2.40 (t, 2 H), 2.67-2.74 (m, 4 H), 2.83-2.87 (t, 2 H), 4.0--4.14 (m, 4 H), 4.34-4.40 (m, 1 H, Gluα-CH), 6.26-6.27 (d, 1 H, J = 3.6 Hz), 6.45 (s, 2 H, 2-NH_2 exch), 6.80 (s, 1 H), 7.06-7.07 (d, 1 H, J = 3.6 Hz), 8.43-8.45 (d, 1 H, J = 7.6, CONH exch), 10.81 (s, 1 H, 3-NH exch).

***N*-({5-[3-(2-Amino-4-oxo-3,4-dihydrothieno[2,3-*d*]pyrimidin-6-yl)propyl]furan-2-yl}carbonyl)-L-glutamic acid (317).** To a solution of **446** (0.28 g, 0.57 mmoL) in ethanol (22 mL) was added aqueous 1 N NaOH (11 mL) and the reaction mixture stirred at room temperature for 3 h. The ethanol was evaporated under reduced pressure and the residue was dissolved in water (8 mL). The solution was cooled to 0 ^{o}C and carefully acidified to pH 3 with drop wise addition of 1 N HCl. The resulting suspension was left at 0 ^{o}C for 2 h and the residue was collected by filtration. Washed with water (5 mL) and dried over P_2O_5/vacuum at 50 ^{o}C to afford **317** (0.23 g, 92%) as light brown powder; mp 224.7-225.6 °C; R_f 0.30 (MeOH/$CHCl_3$, 1:6+ 1 drop of gl. HOAc); ^{1}H NMR (DMSO-d_6) δ1.64 (m, 4 H), 1.88-2.07 (m, 2 H), 2.27-2.31 (m, 2 H),

2.67-2.74 (m, 4 H), 4.32-4.35 (m, 1 H, Gluα-CH), 6.26-6.27 (d, 1 H, *J* = 3.6 Hz), 6.45 (s, 2 H, 2-NH_2 exch), 6.80 (s, 1 H), 7.05-7.06 (d, 1 H, *J* = 3.6 Hz), 8.27-8.29 (d, 1 H, *J* = 7.6, CONH exch), 10.81 (s, 1 H, 3-NH exch), 12.55 (br, 2 H, 2 COOH); Anal. calcd. for ($C_{20}H_{22}N_4O_7S \cdot 0.5\ H_2O$): C, 50.95; H, 4.92; N, 11.88; S, 6.80; found: C, 50.94; H, 4.74; N, 11.73; S, 7.10.

Ethyl 4- (5-oxopentyl)benzoate (449) To a 250 mL round bottom flask, fitted with a magnetic stir bar, were placed palladium diacetate (0.269 g, 1.2 mmol), the appropriate allyl alcohol **448** (20 mmol), ethyl 4-iodobenzoate **447** (5.52 g, 20 mmol), LiCl (0.848 g, 20 mmol), LiOAc (3.3 g, 50 mmol) and Bu_4NCl (11.12 g, 40 mmol) and DMF (40 mL). The mixture was stirred vigorously at 70 ^oC for 24 h. The reaction mixture was cooled to room temperature and water (80 mL), ethyl acetate (100 mL) was added. The ethyl acetate layer was separated, washed with brine (30 mL x 3), dried over anhydrous sodium sulfate, and concentrated under reduced pressure to afford a brown oil. The residue was loaded on a silica gel column packed with silica gel and eluted with 5% ethyl acetate in hexane. The fractions containing the desired product (TLC) were pooled and evaporated to afford the product **449** as a colorless liquid (4.36 g, 87.9 %); R_f 0.71 (hexane/EtOAc 3:1); ^1H NMR ($CDCl_3$): δ 1.33-1.36 (t, 3 H, $COOCH_2\mathit{CH_3}$), 1.62-1.64 (m, 4 H, $CH_2\mathit{CH_2CH_2}CH_2CHO$), 2.38-2.42 (m, 2 H, $CH_2CH_2CH_2\mathit{CH_2}CHO$), 2.66-2.71 (m, 2 H, $\mathit{CH_2}CH_2CH_2CH_2CHO$), 4.32-4.37 (q, 2 H, $COO\mathit{CH_2}CH_3$), 7.22, 7.24 (d, 2 H, C_6H_4), 7.94, 7.96 (d, 2 H, C_6H_4), 9.79 (s, 1 H, CHO). HRMS (ESI, pos mode) m/z $[M + Na]^+$ calcd for $C_{14}H_{18}O_3$, 257.1154; found, 257.1144.

Ethyl 2-amino-5-{3-[4- (ethoxycarbonyl) phenyl]propyl}thiophene-3-carboxylate (450). A mixture of **449** (1.58 g, 6.31 mmol), sulfur (0.20 g, 6.31 mmol) and ethyl cyanoactetate (0.71 g, 6.31 mmol) and EtOH (5 mL) were placed in a round bottom flask and warmed to 45 ^oC and treated dropwise with morpholine (1 mmol) over 15 min. The mixture was stirred for 5 h at 45

^{o}C and 24 h at room temperature. Unreacted sulfur was removed by filtration, and the filtrate was concentrated under reduced pressure to afford an orange oil. The residue was loaded on a silica gel column packed with silica gel and eluted with 10% ethyl acetate in hexane. The fractions containing the desired product (TLC) were pooled and evaporated to afford the products. Compound **450** (1.49 g, 65.32 %) was obtained as an orange liquid; R_f 0.69 (hexane/EtOAc 3:1); ^{1}H NMR ($CDCl_3$): δ 1.32-1.36 (t, 3 H, $COOCH_2\mathit{CH_3}$), 1.37-1.42 (t, 3 H, $COOCH_2\mathit{CH_3}$) 1.88-1.98 (p, 2 H, C_6H_4-$CH_2\mathit{CH_2}CH_2$), 2.59-2.64 (t, 2 H, C_6H_4-$\mathit{CH_2}CH_2CH_2$), 2.69-2.74 (t, 2 H, C_6H_4-$CH_2CH_2\mathit{CH_2}$), 4.23-4.30 (q, 2 H, $COO\mathit{CH_2}CH_3$), 4.34-4.41 (q, 2 H, $COO\mathit{CH_2}CH_3$), 5.80 (s, 2 H, NH_2 exch), 6.65 (s, 1 H, 4-H), 7.23, 7.26 (d, 2 H, C_6H_4), 8.00, 8.03 (d, 2 H, C_6H_4). HRMS (ESI, pos mode) m/z $[M + Na]^+$ calcd for $C_{19}H_{23}NO_4S$, 384.1245; found, 384.1281.

Ethyl 4-[3- (2-amino-4-oxo-3,4-dihydrothieno[2,3-*d*]pyrimidin-6-yl)propyl]benzoate (451). A mixture of **450** (0.54 g, 1.49 mmol) and chloroformamidine hydrochloride (0.68 g, 5.9 mmol) (1:4) in $DMSO_2$ was heated at 140° C for 4 h. The mixture was cooled to room temperature and water (15 mL) was added.Ammonium hydroxide was used to neutralize the suspension. The brown solid, obtained by filtration, was washed with water and dried over P_2O_5 vacuum. The solid was dissolved in methanol and silica gel was added. A dry silica gel plug was obtained after evaporation of the solvent. The plug was loaded on to a silica gel column and eluted with 5% methanol in chloroform. The fractions containing the desired product (TLC) were pooled and evaporated to afford the **451** (0.43 g, 81.13 %) as a yellow solid; mp 224.4-225.3 °C; R_f 0.53 (MeOH/$CHCl_3$, 1:6); ^{1}H NMR (DMSO-d_6): δ 1.28-1.33 (t, 3 H, $COOCH_2\mathit{CH_3}$), 1.86-1.96 (p, 2 H, C_6H_4-$CH_2\mathit{CH_2}CH_2$), 2.68-2.74 (m, 4 H, C_6H_4-$\mathit{CH_2}CH_2\mathit{CH_2}$) 4.26-4.33 (q, 2 H, $COO\mathit{CH_2}CH_3$), 6.46 (s, 2 H, 2-NH_2 exch), 6.82 (s, 1 H, 5-H), 7.35, 7.37 (d, 2 H, C_6H_4), 7.87, 7.89 (d, 2 H, C_6H_4), 10.81 (s, 1 H, 3-NH exch). Anal. calcd. for ($C_{18}H_{19}N_3O_3S \cdot 0.4\ CH_3OH$): C, 59.69; H, 5.61; N,

11.35; S, 8.66; found: C, 59.73; H, 5.21; N, 11.55; S, 8.60.

4-[3-(2-Amino-4-oxo-3,4-dihydrothieno[2,3-*d*]pyrimidin-6-yl)propyl]benzoic acid (452). To a solution of **451** (0.22 g, 0.60 mmol) in ethanol (10-50 mL) was added aqueous 1 N NaOH and the reaction mixture stirred at room temperature for 12 h. The ethanol was evaporated under reduced pressure and the residue was dissolved in water (5-10 mL). The solution was carefully acidified to pH 3 with the drop wise addition of 1 N HCl. The resulting suspension was left at 0 ^{o}C for an hour and then the residue was collected by filtration, washed with water (5 mL) and dried over P_2O_5/vacuum at 50 ^{o}C to afford the free acids **452** as a white solid; mp 292.7-293.4 °C; R_f 0.52 (MeOH/$CHCl_3$, 1:6 + 1 drop of gl. HOAc); ^{1}H NMR (DMSO-d_6): δ 1.85-1.95 (m, 2 H, C_6H_4-CH_2*CH_2*CH_2), 2.66-2.73 (m, 4 H, C_6H_4-*CH_2*CH_2*CH_2*), 6.58 (s, 2 H, 2-NH_2 exch), 6.82 (s, 1 H, 5-H), 7.35, 7.39 (d, 2 H, C_6H_4), 7.85, 7.88 (d, 2 H, C_6H_4), 10.94 (s, 1 H, 3-NH exch), 12.79 (s, 1 H, COOH exch). Anal. calcd. for ($C_{16}H_{15}N_3O_3S \cdot 0.7\ CH_3OH$): C, 57.01; H, 5.10; N, 11.94; S, 9.11; found: C, 56.79; H, 4.75; N, 11.92; S, 9.20.

(S)-methyl 2-amino-4-(((R)-3-amino-4-methoxy-4-oxobutyl)disulfanyl)butanoate (452). To a suspension of **451** (2.68 g, 10 mmol) in 20 ml methanol was added $SOCl_2$ (1.28 g, 11 mmol) dropwise at 0 ^{o}C. The resulted mixture was stired at ambient temperature till a clear solution resulted. TLC indicated a full consumption of 451. The reaction solvent was removed under vacuum and the residue solid was slurried in water and then filtered to afford 2.75 g **452** (93%) as a white solid, which was dried and used directly in next step withough further characterization.

Dimethyl (2*S*,2'*S*)-4,4'-disulfanediylbis[2-({4-[3-(2-amino-4-oxo-3,4-dihydrothieno[2,3-*d*]pyrimidin-6-yl)propyl]benzoyl}amino)butanoate] 455. To a solution of **452** (0.10 g, 0.30 mmol) in anhydrous DMF (5-10 mL) was added N-methylmorpholine (0.12 mmol) and 2-chloro-4,6-dimethoxy-1,3,5-triazine (0.12 mmol). The resulting mixture was stirred at room temperature

for 2 h. N-methylmorpholine (0.12 mmol) and **452** (0.1 mmol) were added to the mixture. The reaction mixture was stirred for an additional 3 h at room temperature and silica gel was added to this solution and the suspension evaporated under reduced pressure. The plug obtained was loaded on a silica gel column and eluted with 2% methanol in chloroform. The fractions containing the desired product (TLC) were pooled and evaporated to afford 0.083g **455** as a yellow solid; mp 174.2-176.8 °C; R_f 0.63 (MeOH/$CHCl_3$, 1:6). The resulted compoudn was used directly for next step without further characterization.

(2*S*,2'*S*)-4,4'-disulfanediylbis[2-({4-[3-(2-amino-4-oxo-3,4-dihydrothieno[2,3-*d*]pyrimidin-6-yl)propyl]benzoyl}amino)butanoic acid] (456)

To a solution of **455** (0.083 g, 0.16 mmol) in ethanol (5-10 mL) was added aqueous 1 N NaOH and the reaction mixture stirred at room temperature for 3 h. The ethanol was evaporated under reduced pressure and the residue was dissolved in water (5-10 mL). The solution was cooled to 0 ^oC and carefully acidified to pH 3 with drop wise addition of 1 N HCl. The resulting suspension was left at 0 ^oC for 12 h and the residue was collected by filtration. Washed with water (5 mL) and dried over P_2O_5/vacuum at 50 ^oC to afford **456** (0.071 g, 96.5 %) as a yellow solid; mp 2442.-246.7 °C; R_f 0.62 (MeOH/$CHCl_3$, 1:6 + 1 drop of gl. HOAc); ^1H NMR (DMSO-d_6): δ 1.89 (m, 2 H, SCH_2), 2.08-2.23 (m, 2 H, SCH_2CH_2), 2.69-2.80 (m, 6 H, C_6H_4-$CH_2CH_2CH_2$), 4.43 (m, 1 H, Gluα-CH), 6.56 (s, 2 H, 2-NH_2 exch), 6.81 (s, 1 H, 5-H), 7.27 (d, 2 H, C_6H_4), 7.80 (d, 2 H, C_6H_4), 8.47 (d, 1 H, CONH exch), 10.98 (s, 1 H, 3-NH exch); HRMS (ESI, pos mode) m/z [M + H^+] calcd for $C40H43N8S_4O_8$ 891.2087, found 891.2059.

***N*-{4-[3-(2-amino-4-oxo-3,4-dihydrothieno[2,3-*d*]pyrimidin-6-yl)propyl]benzoyl}-L-homocysteine (322)**

To a solution of **456** (0.083 g, 0.16 mmol) in ethanol (5-10 mL) was added aqueous 1 N NaOH

and the reaction mixture stirred at room temperature for 3 h. The ethanol was evaporated under reduced pressure and the residue was dissolved in water (5-10 mL). To the solution was added DTT (300 mg). The solution was cooled to 0 ^{o}C and carefully acidified to pH 7 with drop wise addition of 1 N HCl. The resulting suspension was left at 0 ^{o}C for 12 h and the residue was collected by filtration. Washed with water (5 mL) and dried over P_2O_5/vacuum at 49 ^{o}C to afford **322** (0.071 g, 96.5 %) as a yellow solid; mp 190.0-192.1 °C; R_f 0.62 (MeOH/$CHCl_3$, 1:6 + 1 drop of gl. HOAc); ^{1}H NMR (DMSO-d_6): δ 1.24 (s, 1H, SH exch), 1.89 (m, 2 H, SCH_2), 2.08-2.23 (m, 2 H, SCH_2CH_2), 2.69-2.80 (m, 6 H, C_6H_4-$CH_2CH_2CH_2$), 4.55 (m, 1 H, Gluα-CH), 6.59 (s, 2 H, 2-NH_2 exch), 6.84 (s, 1 H, 5-H), 7.31 (d, 2 H, C_6H_4), 7.81 (d, 2 H, C_6H_4), 8.55 (d, 1 H, CONH exch), 10.95 (s, 1 H, 3-NH exch); HRMS (ESI, pos mode) m/z [M + H^+] calcd for $C_{20}H_{23}N_4S_2O_4$ 447.1161, found 447.1125.

2-Methyl-6-hydroxy-5-prop-2-yn-1-ylpyrimidin-4(3H)-one (**460**). A mixture of dimethyl prop-2-yn-1-ylmalonate **414** (11.9 g, 60 mmol), sodium metal (1.38 g, 60 mmol) and acetamidine hydrochloride (5.68 g, 60 mmol) was heated to reflux in MeOH (100 mL) for 24 h. The suspension was then cooled in an ice-bath to room temperature. The precipitate formed was collected by filtration and dissolved in 40 mL of water. The pH of this solution was adjusted to 3-4 with 1 N HCl whereupon a thick precipitate formed. The mixture was filtered and washed with a small amount of water followed by acetone and dried over P_2O_5 to afford 4.1 g (42%) of **460** as a white solid; mp >300°C; R_f 0.11 ($CHCl_3$/MeOH 6:1); ^{1}H NMR (DMSO-d_6) δ 2.23 (s, 3 H), 3.05 (s, 2 H), 3.32 (s, 1 H), 11.92 (s, 2 H).

2,6-Dimethylfuro[2,3-*d*]pyrimidin-4(3*H*)-one (**461**).

Method A

To a 25 mL round flask were added **460** (1.64 g,10 mmol) and concentrated sulfuric acid (15

mL). The resulting solution was stirred overnight and poured in to 100 mL distilled water and extracted by 3 X 30 mL chloroform. The organic layer was pooled and concentrated to afford **461** (1.36g, 83%) as a yellow powder; mp >300°C; R_f 0.35 ($CHCl_3$/MeOH 6:1); ^{1}H NMR (DMSO-d_6) δ 2.42 (s, 3 H, CH_3), 2.44 (s, 3 H, CH_3), 6.63 (s, 1 H, CH), 12.50 (s, 1 H, 3-NH exch).

Method B

The microwave reaction vial was charged with **460** (541 mg, 3.3 mmol) and 2 N NaOH (15 mL). The reaction mixture was irradiated in a microwave apparatus at 180 °C for 30 min. After the reaction mixture was cooled to ambient temperature, the product was filtered, the filtrate was concentrated, and the crude mixture was purified by silica gel column chromatography using 2% methanol in chloroform as the eluent. Fractions containing the product (TLC) were combined and evaporated to afford **461** (471 mg, 87%) as a yellow powder; mp >300°C; R_f 0.35 ($CHCl_3$/MeOH 6:1); ^{1}H NMR (DMSO-d_6) δ 2.42 (s, 3 H, CH_3), 2.44 (s, 3 H, CH_3), 6.63 (s, 1 H, CH), 12.50 (s, 1 H, 3-NH exch).

4-Chloro-2,6-dimethylfuro[2,3-*d*]pyrimidine (**458**). To a 50 mL flask were added **461** (1.64 g, 1 mmol) and 10 mL $POCl_3$. The resulting mixture was refluxed for 2 h, and the solvent was removed under reduced pressure to afford a dark residue. The crude mixture was purified by silica gel column chromatography using hexane: acetyl acetate = 20:1 as the eluent. Fractions containing the product (TLC) were combined and evaporated to afford 1.55 g (85%) **458** as a yellow solid; mp 47.6-48.1°C; R_f 0.26 (Hexane/EtOAC 15:1); ^{1}H NMR (DMSO-d_6) δ 2.48 (s, 3 H), 2.63 (s, 3 H), 6.77 (s, 1 H).

2,6-dimethyl-*N*-phenylfuro[2,3-*d*]pyrimidin-4-amine (326) To a 100-mL round-bottomed flask, flushed with nitrogen, were added **458** (127 mg, 0.7 mmol), aniline (97.6 mg, 1.05 mmol),

BuOH (20 mL), and 2-3 drops of concd HCl. The reaction mixture was heated at reflux with stirring for 2 h until the starting material **458** disappeared (TLC). The reaction solution was allowed to cool to room temperature; the solvent was removed under reduced pressure to dryness and the residue was purified by column chromatography on silica gel with 10% AcOEt/Haxene as the eluent. Fractions containing the product (TLC) were combined and evaporated to afford 137 mg (82%) of **326** as a yellow powder: mp 157.9-159.1 °C; *Rf* 0.16 (AcOEt/Haxene, 1:3); 1H NMR ($CDCl_3$) δ 2.32 (s, 3 H), 2.60 (s, 3 H), 5.64 (s, 1 H), 6.88 (s, 1 H, *exch*), 7.24-7.39 (m, 5 H), Anal. Calcd. for $C_{14}H_{13}N_3O{\cdot}0.1H_2O$: C, 69.75; H, 5.56; N, 17.43. Found C, 69.76; H, 5.56; N,17.40

2,6-dimethyl-*N*-(naphthalen-1-yl)furo[2,3-*d*]pyrimidin-4-amine (327) To a 100-mL round-bottomed flask, flushed with nitrogen, were added **458** (182 mg, 1 mmol), naphthalen-1-amine (150 mg, 1.05 mmol), BuOH (20 mL), and 2-3 drops of concd HCl. The reaction mixture was heated at reflux with stirring for 2 h until the starting material **458** disappeared (TLC). The reaction solution was allowed to cool to room temperature; the solvent was removed under reduced pressure to dryness and the residue was purified by column chromatography on silica gel with 10% AcOEt/Haxene as the eluent. Fractions containing the product (TLC) were combined and evaporated to afford 214 mg (74%) of **327** as a pale yellow powder: mp 253.6-254.7 °C; *Rf* 0.1 (AcOEt/Haxene, 1:3); 1H NMR ($CDCl_3$) δ 2.15 (s, 3 H), 2.60 (s, 3 H), 4.84 (s, 1 H), 7.52 (s, 1 H, *exch*), 7.51-8.07 (m, 7 H), Anal. Calcd. for $C_{18}H_{15}N_3O{\cdot}0.2H_2O$: C, 74.26; H, 5.26; N, 14.43. Found C, 74.25; H, 5.29; N,14.27

N-(3-ethynylphenyl)-2,6-dimethylfuro[2,3-*d*]pyrimidin-4-amine (328) To a 100-mL round-bottomed flask, flushed with nitrogen, were added **458** (182 mg, 1 mmol), 3-ethynylaniline (123 mg, 1.05 mmol), *i*-PrOH (20 mL), and 2-3 drops of concd HCl. The reaction mixture was heated

at reflux with stirring for 2 h until the starting material **458** disappeared (TLC). The reaction solution was allowed to cool to room temperature; the solvent was removed under reduced pressure to dryness and the residue was purified by column chromatography on silica gel with 10% AcOEt/Haxene as the eluent. Fractions containing the product (TLC) were combined and evaporated to afford 213 mg (81%) of **328** as a brown solid: mp 108.6-109.7 °C; *Rf* 0.15 (AcOEt/Haxene, 1:3); 1H NMR (DMSO-*d*6) δ 2.36 (s, 3 H), 2.50 (s, 3 H), 4.16 (s, 1 H), 6.74 (s, 1 H), 7.13 (d, 1 H, *J* = 7.7), 7.36 (t, 1 H, *J* = 7.7), 7.89 (d, 1 H, *J* = 7.7), 7.98 (s, 1 H), 9.56 (s, 1 H, *exch*), Anal. Calcd. for $C_{16}H_{13}N_3O \cdot 0.4H_2O$: C, 71.04; H, 5.14; N, 15.53. Found C, 70.81; H, 5.21; N,15.19

2,6-dimethyl-N-[4-(trifluoromethyl)phenyl]furo[2,3-*d*]pyrimidin-4-amine (329) To a 100-mL round-bottomed flask, flushed with nitrogen, were added **458** (182 mg, 1 mmol), 4-(trifluoromethyl)aniline (169 mg, 1.05 mmol),BuOH (20 mL), and 2-3 drops of concd HCl. The reaction mixture was heated at reflux with stirring for 2 h until the starting material **458** disappeared (TLC). The reaction solution was allowed to cool to room temperature; the solvent was removed under reduced pressure to dryness and the residue was purified by column chromatography on silica gel with 10% AcOEt/Haxene as the eluent. Fractions containing the product (TLC) were combined and evaporated to afford 174 mg (57%) of **329** as a yellow powder: mp 144.9-146.7 °C; *Rf* 0.16 (AcOEt/Haxene, 1:3); 1H NMR (DMSO-*d*6) δ 2.45 (s, 3 H), 2.50 (s, 3 H), 6.82 (s, 1 H), 7.68 (d, 2 H, *J* = 7.7), 8.08 (d, 1 H, *J* = 7.7), 9.85 (s, 1 H, *exch*), Anal. Calcd. for $C_{15}H_{12}FN_3O$: C, 58.63; H, 3.94; N, 13.68. Found C, 58.09; H, 4.07; N,13.40

N-(3-chloro-4-fluorophenyl)-2,6-dimethylfuro[2,3-*d*]pyrimidin-4-amine (330) To a 100-mL round-bottomed flask, flushed with nitrogen, were added **458** (182 mg, 1 mmol), 3-chloro-4-fluoroaniline (152 mg, 1.05 mmol),BuOH (20 mL), and 2-3 drops of concd HCl. The reaction

mixture was heated at reflux with stirring for 2 h until the starting material **458** disappeared (TLC). The reaction solution was allowed to cool to room temperature; the solvent was removed under reduced pressure to dryness and the residue was purified by column chromatography on silica gel with 10% AcOEt/Haxene as the eluent. Fractions containing the product (TLC) were combined and evaporated to afford 154 mg (53%) of **330** as a pale yellow powder: mp 191.6-193.1 °C; *Rf* 0.13 (AcOEt/Haxene, 1:3); 1H NMR (DMSO-*d*6) δ 2.40 (s, 3 H), 2.46 (s, 3 H), 6.70 (s, 1 H), 7.40 (t, 1 H, *J* = 7.6), 7.77 (d, 1 H, *J* = 7.6), 8.19 (d, 1 H, *J* = 7.6), 9.64 (s, 1 H, *exch*), Anal. Calcd. for $C_{14}H_{11}FClN_3O$: C, 57.63; H, 3.80; N, 14.40. Found C, 57.31; H, 3.82; N,14.27

N-(4-chlorophenyl)-2,6-dimethylfuro[2,3-*d*]pyrimidin-4-amine (331) To a 100-mL round-bottomed flask, flushed with nitrogen, were added **458** (182 mg, 1 mmol), 4-chloroaniline (133 mg, 1.05 mmol),BuOH (20 mL), and 2-3 drops of concd HCl. The reaction mixture was heated at reflux with stirring for 2 h until the starting material **458** disappeared (TLC). The reaction solution was allowed to cool to room temperature; the solvent was removed under reduced pressure to dryness and the residue was purified by column chromatography on silica gel with 10% AcOEt/Haxene as the eluent. Fractions containing the product (TLC) were combined and evaporated to afford 172 mg (63%) of **331** as a yellow powder: mp 156.6-157.2 °C; *Rf* 0.13 (AcOEt/Haxene, 1:3); 1H NMR (DMSO-*d*6) δ 2.43 (s, 3 H), 2.50 (s, 3 H), 6.77 (s, 1 H), 7.39 (d, 2 H, *J* = 8.4), 7.87 (d, 2 H, *J* = 8.4), 9.74 (s, 1 H, *exch*), Anal. Calcd. for $C_{14}H_{12}ClN_3O$: C, 61.43; H, 4.42; N, 15.35. Found C, 61.10; H, 4.44; N,14.93

***N*-(1*H*-indol-4-yl)-2,6-dimethylfuro[2,3-*d*]pyrimidin-4-amine (332)** To a 100-mL round-bottomed flask, flushed with nitrogen, were added **458** (127 mg, 0.7 mmol), 1*H*-indol-4-amine (138.6 mg, 1.05 mmol), *i*-PrOH (20 mL), and 2-3 drops of conc HCl. The reaction mixture was heated at reflux with stirring for 2 h until the starting material **458** disappeared (TLC). The

reaction solution was allowed to cool to room temperature; the solvent was removed under reduced pressure to dryness and the residue was purified by column chromatography on silica gel with 10% AcOEt/Haxene as the eluent. Fractions containing the product (TLC) were combined and evaporated to afford 122 mg (63%) of **75** as a brown powder: mp 241.0-242.2 °C; *Rf* 0.16 (AcOEt/Haxene, 1:1); 1H NMR ($CDCl_3$) δ 2.20 (s, 3 H), 2.61 (s, 3 H), 5.24 (s, 1 H), 6.49 (t, 1 H), 7.11 (m, 4 H, 1 H *exch*), 7.34 (d,1 H), 8.41 (s, 1 H, *exch*), Anal. Calcd. for $C_{16}H_{14}N_4O{\cdot}0.2H_2O$: C, 68.17; H, 5.15; N, 19.58. Found C, 67.86; H, 5.18; N,19.58

***N*-(4-methoxyphenyl)-2,6-dimethylfuro[2,3-*d*]pyrimidin-4-amine** (**333**). To a 50 mL flask was added **458** (91 mg, 0.5 mmol), 4-methoxyaniline (68 mg, 0.55 mmol) (0.55 mmol) and butanol (5 mL). To this solution was added 2 drops of concentrate HCl solution and the mixture was refluxed. After TLC indicated the disappearance of starting material amine, the solvent was removed under reduced pressure. To the residue obtained was added silica gel and methanol and the solvent was removed to make a plug. The plug was loaded on to a silica gel column and eluted with 10 % acetyl acetate in hexane to give **333** (110 mg, 82%) as a white powder; mp 135.2-136.7°C; R_f 0.28 (Hexane/AcOEt 3:1); ^{1}H NMR (DMSO-d_6) δ 2.34 (s, 3 H, CH_3), 2.39 (s, 3 H, CH_3), 3.74 (s, 3 H, OCH_3), 6.52 (s, 1 H, CH), 6.92 (d, 2 H, J = 8.8 Hz, C_6H_4), 7.61 (d, 2 H, J = 8.8 Hz, C_6H_4), 9.34 (s, 1 H, 4-NH exch); HRMS calcd for $C_{15}H_{16}N_3O_2$ 270.1243, found 270.1252.

N-(3-fluorophenyl)-2,6-dimethylfuro[2,3-*d*]pyrimidin-4-amine (334) To a 100-mL round-bottomed flask, flushed with nitrogen, were added **458** (182 mg, 1 mmol), 3-fluoroaniline (116 mg, 1.05 mmol),BuOH (20 mL), and 2-3 drops of concd HCl. The reaction mixture was heated at reflux with stirring for 2 h until the starting material **458** disappeared (TLC). The reaction solution was allowed to cool to room temperature; the solvent was removed under reduced

pressure to dryness and the residue was purified by column chromatography on silica gel with 10% AcOEt/Haxene as the eluent. Fractions containing the product (TLC) were combined and evaporated to afford 157 mg (61%) of **334** as a yellow powder: mp 169.2-170.8 °C; *Rf* 0.13 (AcOEt/Haxene, 1:3); 1H NMR (DMSO-*d*6) δ 2.43 (s, 3 H), 2.49 (s, 3 H), 6.82 (s, 1 H), 6.84 (t, 1 H, *J* = 8.4), 7.38 (dd, 1 H, J_1 = 12.0, J_2 = 7.8), 7.57 (d, 1 H, *J* = 7.8), 7.95 (d, 1 H, *J* = 12.0), 9.77 (s, 1 H, *exch*). Anal. Calcd. for $C_{14}H_{12}ClN_3O$: C, 61.43; H, 4.42; N, 15.35. Found C, 61.10; H, 4.44; N,14.93

***N*-(4-methoxyphenyl)-*N*,2,6-trimethylfuro[2,3-*d*]pyrimidin-4-amine** (**335**). To a 50 mL flask was added **458** (91 mg, 0.5 mmol), *N*-methyl-4-methoxylaniline (77 mg, 0.55 mmol) and butanol (5 mL). To this solution was added 2 drops of concentrate HCl solution and the mixture was refluxed. After TLC indicated the disappearance of starting material amine, the solvent was removed under reduced pressure. To the residue obtained was added silica gel and methanol and the solvent was removed to make a plug. The plug was loaded on to a silica gel column and eluted with 10 % acetyl acetate in hexane to give **335** (106 mg, 75%) as a white powder; mp 108-109°C; R_f 0.36 (Hexane/AcOEt 3:1); ^{1}H NMR (DMSO-d_6) δ 2.14 (s, 3 H, CH_3), 2.45 (s, 3 H, CH_3), 3.43 (s, 3 H, NCH_3), 3.81 (s, 3 H, OCH_3), 4.55 (s, 1 H, CH), 7.04 (d, 2 H, *J* = 9.2 Hz, C_6H_4), 7.25 (d, 2 H, *J* = 9.2 Hz, C_6H_4); HRMS calcd for $C_{16}H_{18}N_3O_2$ 284.1399, found 284.1387; Anal. Calcd. for $C_{16}H_{17}N_3O_2$: C, 67.83; H, 6.05; N, 14.83. Found C, 68.21; H, 6.23; N,14.33.

N-(4-methoxyphenyl)-N,2,6-trimethylfuro[2,3-d]pyrimidin-4-amine hydrochloride (**336**). To a 50 mL flask were added **335** (2.0 g, 7.07 mmol) and anhydrous ether (20 mL). The resulting mixture was stirred to afford a clear solution. Anhydrous hydrochloric acid gas was bubbled into the solution till no more solid precipitated out. The white solid was filtered out and then dried over P_2O_5 to afford 2.16 g (96%) of **336** as a colorless crystal; mp 287.3-287.7°C; R_f 0.01

(CH_3Cl/MeOH 6:1); ^{1}H NMR (DMSO-d_6) δ 2.14 (s, 3 H, CH_3), 2.46 (s, 3 H, CH_3), 3.44 (s, 3 H, NCH_3), 3.80 (s, 3 H, OCH_3), 4.55 (s, 1 H, *CH*), 7.04-7.06 (d, 2 H, *J* = 8.0 Hz, 2 *CH*), 7.26-7.28 (d, 2 H, *J* = 8.0 Hz, 2 *CH*); Anal. Calcd. for $C_{16}H_{18}ClN_3O_2 \cdot 0.3H_2O$: C, 59.09; H, 5.77; N, 12.92; Cl, 11.02. Found C, 59.02; H, 5.62; N,12.75; Cl, 11.02.

N,2,6-trimethyl-N-(4-methylphenyl)furo[2,3-d]pyrimidin-4-amine (**338**). To a 50 mL flask was added **458** (91 mg, 0.5 mmol), *N*,4-dimethylaniline (67 mg, 0.55 mmol) and BuOH (5 mL). To this solution was added 2 drops of concentrate HCl solution and the mixture was refluxed. TLC indicated the disappearance of starting material **458**, the solvent was removed under reduced pressure. To the residue obtained was added silica gel and MeOH and the solvent removed to make a plug. This plug was separated by column chromatography to give 99 mg (74%) of **338** as a white powder; mp 139.4-139.9°C; R_f 0.35 (Hexane/EtOAC 3:1); ^{1}H NMR (DMSO-d_6) δ 2.16 (s, 3 H, CH_3), 2.40 (s, 3 H, CH_3), 2.49 (s, 3 H, CH_3), 3.47 (s, 3 H, NCH_3), 4.58 (d, 1 H, *J* = 0.8 Hz, *CH*), 7.23-7.25 (d, 2 H, *J* = 8.0 Hz, 2 *CH*), 7.32-7.34 (d, 2 H, *J* = 8.0 Hz, 2 *CH*); Anal. Calcd. for $C_{16}H_{17}N_3O$: C, 71.89; H, 6.41; N, 15.72. Found C, 71.67; H, 6.50; N,15.75.

N,2,6-trimethyl-N-(3-methylphenyl)furo[2,3-d]pyrimidin-4-amine (**339**). To a 50 mL flask was added **458** (91 mg, 0.5 mmol), *N*,3-dimethylaniline (67 mg, 0.55 mmol) and BuOH (5 mL). To this solution was added 2 drops of concentrate HCl solution and the mixture was refluxed. TLC indicated the disappearance of starting material **458**, the solvent was removed under reduced pressure. To the residue obtained was added silica gel and MeOH and the solvent removed to make a plug. This plug was separated by column chromatography to give 92 mg (69%) of **339** as a white powder; mp 117.6-118.4 ^{o}C; R_f 0.37 (Hexane/EtOAC 3:1); ^{1}H NMR (DMSO-d_6) δ 2.14 (s, 3 H, CH_3), 2.34 (s, 3 H, CH_3), 2.47 (s, 3 H, CH_3), 3.47 (s, 3 H, NCH_3),

4.55 (s, 1 H, *CH*), 7.12-7.14 (d, 1 H, *J* = 7.6 Hz, 1 *CH*), 6.967.191 (s, 1 H, 1 *CH*), 7.25-7.27 (d, 1 H, *J* = 8.8 Hz, 1 *CH*), 7.37-7.40 (t, 1 H, J_1 = 8.8 Hz, J_2 = 7.6 Hz 1 *CH*); Anal. Calcd. for $C_{16}H_{17}N_3O$: C, 71.89; H, 6.41; N, 15.72. Found C, 71.93; H, 6.46; N,15.52.

N-(4-chlorophenyl)-N,2,6-trimethylfuro[2,3-d]pyrimidin-4-amine (**340**). To a 50 mL flask was added **458** (91 mg, 0.5 mmol), 4-chloro-*N*-methylaniline (78 mg, 0.55 mmol) and BuOH (5 mL). To this solution was added 2 drops of concentrate HCl solution and the mixture was refluxed. TLC indicated the disappearance of starting material **458**, the solvent was removed under reduced pressure. To the residue obtained was added silica gel and MeOH and the solvent removed to make a plug. This plug was separated by column chromatography to give 82 mg (57%) of **340** as a white powder; mp 162.3-163.5°C; R_f 0.34 (Hexane/EtOAC 3:1); ^{1}H NMR ($CDCl_3$) δ 2.22 (s, 3 H, CH_3), 2.64 (s, 3 H, CH_3), 3.57 (s, 3 H, NCH_3), 4.72 (d, 1 H, *J* = 0.8 Hz, *CH*), 7.20-7.23 (d, 2 H, *J* = 8.4 Hz, 2 *CH*), 7.45-7.43 (d, 2 H, *J* = 8.4 Hz, 2 *CH*); HRMS calcd for C15H14ClN3O 287.0825, found 287.0817.

N-(3,4-dichlorophenyl)-N,2,6-trimethylfuro[2,3-d]pyrimidin-4-amine (**341**). To a 50 mL flask was added **458** (91 mg, 0.5 mmol), 3,4-dichloro-*N*-methylaniline (96 mg, 0.55 mmol) and BuOH (5 mL). To this solution was added 2 drops of concentrate HCl solution and the mixture was refluxed. TLC indicated the disappearance of starting material **458**, the solvent was removed under reduced pressure. To the residue obtained was added silica gel and MeOH and the solvent removed to make a plug. This plug was separated by column chromatography to give 87 mg (59%) of **341** as a white crystal; mp 167.4-168.9°C; R_f 0.3 (Hexane/EtOAC 3:1); ^{1}H NMR ($CDCl_3$) δ 2.99 (s, 3 H, CH_3), 2.64 (s, 3 H, CH_3), 3.57 (s, 3 H, NCH_3), 4.90 (d, 1 H, *CH*), 7.11-7.14 (dd, 1 H, J_1 = 8.4 Hz, J_2 = 2.4 Hz, 1 *CH*), 7.40 (d, 1 H, *J* = 2.4 Hz, 1 *CH*), 7.51-7.54 (d, 1 H, *J* = 8.4 Hz, 1 *CH*); HRMS calcd for C15H13Cl_2N3O 321.0436, found 321.0426.

N,2,6-trimethyl-N-(naphthalen-1-yl)furo[2,3-d]pyrimidin-4-amine (**342**). To a 50 mL flask was added **458** (91 mg, 0.5 mmol), *N*-methylnaphthalen-1-amine hydrochloride (106 mg, 0.55 mmol) and BuOH (5 mL). The resulting mixture was refluxed. TLC indicated the disappearance of starting material **458**, the solvent was removed under reduced pressure. To the residue obtained was added silica gel and MeOH and the solvent removed to make a plug. This plug was separated by column chromatography to give 79 mg (52%) of **342** as a white crystal; mp 148.6-149.7°C; R_f 0.39 (Hexane/EtOAC 3:1); ^{1}H NMR ($CDCl_3$) δ 1.99 (s, 3 H, CH_3), 2.69 (s, 3 H, CH_3), 3.69 (s, 3 H, NCH_3), 4.99 (s, 1 H, *CH*), 7.44-7.58 (m, 4 H), 7.78-7.80 (d, 1 H, *J* = 8.0 Hz, 1 *CH*), 7.99-7.97 (d, 1 H, *J* = 8.0 Hz, 1 *CH*); HRMS calcd for C19H17N3O 303.1371, found 321.04303.1376.

General procedure for the synthesis of **343-346**. To a stirred suspension of **333** (1 mmol) in 2 ml DMF was added NaH (1.1 mmol) portionwise at 0 ^{o}C. The resulted mixture was stirred at ambient temperature till no more gas release. To the above mixture was added the appropriate alkyl iodide at ambient temperature. The resulted mixture was stirred at ambient temperature for 4 hours and then poured onto 10 ml H_20 to afford a white precipitate, which was collected through filtration and purified by colum chromatography to afford the desired compounds **343-346.**

***N*-ethyl-*N*-(4-methoxyphenyl)-2,6-dimethylfuro[2,3-*d*]pyrimidin-4-amine (343).** Above mentioned general procedure was applied to afford **343** as a colorless crystals: mp 87.6-88.7 ^{o}C; *Rf* = 0.30 (Hexane/EtOAC 3:1); 1H NMR (DMSO-*d*6) 1.13-1.16 (t, 3 H, J = 5.6 Hz, NCH_2CH_3), 2.15 (s, 3 H, CH_3), 2.47 (s, 3 H, CH_3), 3.84 (s, 3 H, OCH_3), 3.98-4.01 (q, 2 H, NCH_2CH_3), 4.47 (s, 1 H, 5-CH), 7.07-7.09 (d, 2 H, J = 6.8 Hz, C_6H_4), 7.24-7.26 (d, 2 H, J = 6.8 Hz, C_6H_4); Anal. Calcd. for $C_{17}H_{19}N_3O_2$: C, 68.67; H, 6.44; N, 14.13 Found C, 68.79; H, 6.51; N,14.02.

***N*-(4-methoxyphenyl)-2,6-dimethyl-*N*-propylfuro[2,3-*d*]pyrimidin-4-amine (344)**

Above mentioned general procedure was applied to afford **344** as a light yellow solid: mp 87.2-87.9 ^{o}C; *Rf* = 0.30 (Hexane/EtOAC 3:1); 1H NMR (DMSO-*d*6) 0.87-0.90 (t, 3 H, J = 6.0 Hz, $NCH_2CH_2CH_3$), 1.57-1.62 (m, 2 H, $NCH_2CH_2CH_3$), 2.15 (s, 3 H, CH_3), 2.46 (s, 3 H, CH_3), 3.84 (s, 3 H, OCH_3), 3.91-3.94 (t, 2 H, $NCH_2CH_2CH_3$), 4.46 (s, 1 H, 5-CH), 7.06-7.08 (d, 2 H, J = 7.2 Hz, C_6H_4), 7.24-7.26 (d, 2 H, J = 7.2 Hz, C_6H_4); Anal. Calcd. for $C_{18}H_{21}N_3O_2$: C, 69.43; H, 6.80; N, 13.49 Found C, 69.52; H, 6.91; N,13.39.

***N*-butyl-*N*-(4-methoxyphenyl)-2,6-dimethylfuro[2,3-*d*]pyrimidin-4-amine (345)** Above mentioned general procedure was applied to afford **345** as an orange crystal: mp 65.2-67.1 ^{o}C; *Rf* = 0.30 (Hexane/EtOAC 3:1); 1H NMR (DMSO-*d*6) 0.89-0.91 (t, 3 H, J = 5.6 Hz, $NCH_2CH_2CH_2CH_3$), 1.28-1.36 (m, 2 H, $NCH_2CH_2CH_2CH_3$), 1.52-1.58 (m, 2 H, $NCH_2CH_2CH_2CH_3$), 2.15 (s, 3 H, CH_3), 2.46 (s, 3 H, CH_3), 3.84 (s, 3 H, OCH_3), 3.97-3.98 (t, 2 H, $NCH_2CH_2CH_3$), 4.46 (s, 1 H, 5-CH), 7.06-7.08 (d, 2 H, J = 7.2 Hz, C_6H_4), 7.24-7.26 (d, 2 H, J = 7.2 Hz, C_6H_4); Anal. Calcd. for $C_{19}H_{23}N_3O_2$: C, 70.13; H, 7.12; N, 12.91 Found C, 70.12; H, 7.20; N,12.77.

***N*-(4-methoxyphenyl)-2,6-dimethyl-*N*-(propan-2-yl)furo[2,3-*d*]pyrimidin-4-amine (346)**

Above mentioned general procedure was applied to afford **343** as an orange crystal: mp 131.1-132.7 ^{o}C; *Rf* = 0.30 (Hexane/EtOAC 3:1); 1H NMR (DMSO-*d*6) 1.09-1.11 (d, 6 H, J = 6.4 Hz, 2 CH_3), 2.12 (s, 3 H, CH_3), 2.47 (s, 3 H, CH_3), 3.84 (s, 3 H, OCH_3), 4.20 (s, 1 H, 5-CH), 5.37-5.45 (m, 1 H, NCH), 7.08-7.10 (d, 2 H, J = 8.8 Hz, C_6H_4), 7.19-7.21 (d, 2 H, J = 8.8 Hz, C_6H_4); Anal. Calcd. for $C_{18}H_{21}N_3O_2$: C, 69.43; H, 6.80; N, 13.49 Found C, 69.23; H, 6.81; N,13.38.

4-(5-methoxyindolin-1-yl)-2,6-dimethylfuro[2,3-d]pyrimidine (347).

To a 100-mL round-bottomed flask, flushed with nitrogen, were added **458** (91 mg, 0.5 mmol), 5-methoxyindoline (82 mg, 0.55 mmol), BuOH (10 mL), and 2-3 drops of concd HCl. The

reaction mixture was heated at reflux with stirring for 12 h until the starting material **458** disappeared (TLC). The reaction solution was allowed to cool to room temperature; the solvent was removed under reduced pressure, and the residue was purified by column chromatography on silica gel with hexane: acetyl acetate = 20:1 as the eluent. Fractions containing the product (TLC) were combined and evaporated to afford 93 mg (63%) **347** as a white powder: mp 201.1-202.3 °C; R_f 0.5 (Hexane/EtOAC 3:1); ^{1}H NMR (DMSO-d_6) δ 2.42 (s, 3 H), 2.53 (s, 3 H), 3.25 (t, 2 H), 3.75 (s, 3 H), 4.39 (t, 2 H), 5.53 (s, 1 H), 6.79 (t, 2 H), 6.89 (d, 1 H), 8.48 (d, 1 H). Anal. $C_{17}H_{17}N_3O_2$ (C, 69.14; H, 5.80; N, 14.23; O, 10.83

4-(5-methoxy-1H-indol-1-yl)-2,6-dimethylfuro[2,3-*d*]pyrimidine (348). To a solution of 5-methoxy-1H-indole (74 mg, 0.5 mmol) in 5 mL DMF was added NaH (13 mg, 0.55 mmol). The resulted suspension was cooled to 0 ^{o}C and stirred for 30 min. To the solution was added **458** (273 mg, 1.5 mmol), the resulted mixture was stirred for another 2 h at ambient temperature. After adding 1 mL 1N HCl to terminate the reaction, the solvent was removed under reduced pressure. The crude mixture was purified by silica gel column chromatography using hexane: acetyl acetate=20:1 as the eluent. Fractions containing the product (TLC) were combined and evaporated to afford 66 mg (41%) **348** as a colorless crystal: mp 131.6-133.2 °C; R_f 0.28 (Hexane/EtOAC 3:1); ^{1}H NMR (DMSO-d_6) δ 2.51 (s, 3 H), 2.71 (s, 3 H), 3.81 (s, 3 H), 6.84 (d, 1 H, J = 2.8 Hz), 6.95 (dd, 1 H, J_1 = 7.2 Hz, J_2 = 2.0 Hz), 7.09 (s, 1 H), 7.20 (d, 1 H, J = 2.0 Hz), 8.04 (d, 1 H, J = 2.8 Hz), 8.57 (d, 1 H, J = 7.2 Hz). Anal. $C_{17}H_{15}N_3O_2$ (C, 69.61; H, 5.15; N, 14.33; O, 10.91)

4-(6-methoxy-3,4-dihydroquinolin-1(2H)-yl)-,2,6-trimethylfuro[2,3-*d*]pyrimidines (349).

To a 100-mL round-bottomed flask, flushed with nitrogen, were added **458** (91 mg, 0.5 mmol), 6-methoxy-1,2,3,4-tetrahydroquinoline (90 mg, 0.55 mmol), BuOH (10 mL), and 2-3 drops of

concd HCl. The reaction mixture was heated at reflux with stirring for 12 h until the starting material **458** disappeared (TLC). The reaction solution was allowed to cool to room temperature; the solvent was removed under reduced pressure, and the residue was purified by column chromatography on silica gel with hexane: acetyl acetate = 20:1 as the eluent. Fractions containing the product (TLC) were combined and evaporated to afford **349** as a pink powder 74 mg (48%): mp 108.9-109.6°C; R_f 0.5 (Hexane/EtOAC 3:1); ^{1}H NMR (DMSO-d_6) δ 1.90 (m, 2 H), 2.28 (s, 3 H), 2.48 (s, 3 H), 2.73 (t, 2 H), 3.75 (s, 3 H), 3.94 (t, 2 H), 5.53 (s, 1 H), 6.76 (dd, 1 H, J_1 = 7.2 Hz, J_2 = 2.0 Hz), 6.85 (d, 1 H, J = 2.0 Hz), 6.05 (d, 1 H, J = 7.2 Hz). Anal. $C_{18}H_{19}N_3O_2$ (C, 69.88; H, 6.19; N, 13.58; O, 10.34)

***N*-(4-ethylphenyl)-2,6-dimethylfuro[2,3-*d*]pyrimidin-4-amine** (**466**). To a 50 mL flask was added **358** (91 mg, 0.5 mmol), 4-ethylaniline (67 mg, 0.55 mmol) and BuOH (5 mL). To this solution was added 2 drops of concentrate HCl solution and the mixture was refluxed. TLC indicated the disappearance of starting material **5**, the solvent was removed under reduced pressure. To the residue obtained was added silica gel and MeOH and the solvent removed to make a plug. This plug was separated by column chromatography to give 99 mg (74%) of **466** as a off-white solid; mp 116.2-116.8 °C; R_f 0.52 (Hexane/EtOAC 3:1); ^{1}H NMR (DMSO-d_6) δ 1.18-1.21 (t, 3 H, J = 6.0 Hz, CH_2CH_3), 2.41 (s, 3 H), 2.48 (s, 3 H), 2.57-2.62 (q, 2 H, J = 6.0 Hz, CH_2CH_3), 6.65 (s, 1 H, 5-*CH*), 7.19-7.20 (d, 2 H, J = 6.8 Hz, C_6H_4), 7.67-7.69 (d, 2 H, J = 6.8 Hz, C_6H_4), 9.46 (s, 1 H, *NH* exch); Anal. Calcd. for $C_{16}H_{17}N_3O$: C, 71.89; H, 6.41; N, 15.72. Found C, 71.90; H, 6.46; N,15.64.

2,6-dimethyl-*N*-[4-(methylsulfanyl)phenyl]furo[2,3-*d*]pyrimidin-4-amine (**467**). To a 50 mL flask was added **358** (91 mg, 0.5 mmol), 4-(methylsulfanyl)aniline (76 mg, 0.55 mmol) and BuOH (5 mL). To this solution was added 2 drops of concentrate HCl solution and the mixture

was refluxed. TLC indicated the disappearance of starting material **5**, the solvent was removed under reduced pressure. To the residue obtained was added silica gel and MeOH and the solvent removed to make a plug. This plug was separated by column chromatography to give 97 mg (68%) of **467** as a yellow powder; mp 143.2-143.8 °C; R_f 0.4 (Hexane/EtOAC 3:1); ^{1}H NMR (DMSO-d_6) δ 2.43 (s, 3 H), 2.48 (s, 3 H), 2.49 (sq, 3 H), 6.70 (s, 1 H, 5-*CH*), 7.28-7.30 (d, 2 H, *J* = 8.0 Hz, C_6H_4), 7.78-7.80 (d, 2 H, *J* = 8.0 Hz, C_6H_4), 9.51 (s, 1 H, *NH* exch); Anal. Calcd. for $C_{15}H_{15}N_3OS$: C, 63.13; H, 5.30; N, 14.73, S, 11.24. Found C, 62.99; H, 5.27; N,14.56, S, 11.10.

***N*-(4-ethoxyphenyl)-2,6-dimethylfuro[2,3-*d*]pyrimidin-4-amine** (**469**). To a 50 mL flask was added **358** (91 mg, 0.5 mmol), 4-ethoxyaniline (75 mg, 0.55 mmol) and BuOH (5 mL). To this solution was added 2 drops of concentrate HCl solution and the mixture was refluxed. TLC indicated the disappearance of starting material **358**, the solvent was removed under reduced pressure. To the residue obtained was added silica gel and MeOH and the solvent removed to make a plug. This plug was separated by column chromatography to give 112 mg (80%) of **469** as a off-white powder; mp 160.6-162.1°C; R_f 0.51 (Hexane/EtOAC 3:1); ^{1}H NMR (DMSO-d_6) δ 1.32-1.35 (t, 3 H, *J* = 5.6 Hz, OCH_2CH_3), 2.40 (s, 3 H, 6-CH_3), 2.45 (s, 3 H, 2-CH_3), 4.00-4.04 (q, 2 H, *J* = 5.6 Hz, OCH_2CH_3), 6.50 (s, 1 H, 5-*CH*), 6.93-6.94 (d, 2 H, *J* = 6.8 Hz, C_6H_4), 7.61 (d, 2 H, *J* = 6.8 Hz, C_6H_4), 9.34 (s, 1 H, *NH* exch); Anal. Calcd. for $C_{16}H_{17}N_3O_2$: C, 67.83; H, 6.05; N, 14.83. Found C, 67.81; H, 6.08; N,14.71

2,6-Dimethyl-*N*-(4-propoxyphenyl)furo[2,3-*d*]pyrimidin-4-amine (**470**). To a 50 mL flask was added **358** (91 mg, 0.5 mmol), 4-propoxyaniline (83 mg, 0.55 mmol) and BuOH (5 mL). To this solution was added 2 drops of concentrate HCl solution and the mixture was refluxed. TLC indicated the disappearance of starting material **358**, the solvent was removed under reduced pressure. To the residue obtained was added silica gel and MeOH and the solvent removed to

make a plug. This plug was separated by column chromatography to give 99 mg (67%) of **470** as a colorless crystal; mp 136.3-137.1°C; R_f 0.51 (Hexane/EtOAC 3:1); ^{1}H NMR (DMSO-d_6) δ 0.98-1.00 (t, 3 H, $OCH_2CH_2CH_3$), 1.70-1.77 (m, 2 H, $OCH_2CH_2CH_3$), 2.40 (s, 3 H, 6-CH_3), 2.45 (s, 3 H, 2-CH_3), 3.91-3.94 (t, 2 H, $OCH_2CH_2CH_3$), 6.53 (s, 1 H, 5-*CH*), 6.93-6.94 (d, 2 H, *J* = 7.2 Hz, C_6H_4), 7.61-7.62 (d, 2 H, *J* = 7.2 Hz, C_6H_4), 9.33 (s, 1 H, *NH* exch); Anal. Calcd. for $C_{17}H_{19}N_3O_2$: C, 68.67; H, 6.44; N, 14.13. Found C, 68.52; H, 6.53; N,14.06.

***N*-(2,4-dimethoxyphenyl)-2,6-dimethylfuro[2,3-*d*]pyrimidin-4-amine** (**471**). To a 50 mL flask was added **358** (91 mg, 0.5 mmol), 2,4-dimethoxyaniline (84 mg, 0.55 mmol) and BuOH (5 mL). To this solution was added 2 drops of concentrate HCl solution and the mixture was refluxed. TLC indicated the disappearance of starting material **358**, the solvent was removed under reduced pressure. To the residue obtained was added silica gel and MeOH and the solvent removed to make a plug. This plug was separated by column chromatography to give 112 mg (77%) of **471** as a off-white powder; mp 97.7-97.9°C; R_f 0.62 (Hexane/EtOAC 1:1); ^{1}H NMR (DMSO-d_6) δ 2.31 (s, 3 H), 2.37 (s, 3 H), 3.73 (s, 3 H, OCH_3), 3.81 (s, 3 H, OCH_3), 5.93 (s, 1 H, 5-*CH*), 6.55-6.58 (dd, 1 H, *J* = 6.8 Hz, *J* = 2 Hz C_6H_3), 7.33-7.35 (d, 2 H, *J* = 6.8 Hz, C_6H_3), 8.78 (s, 1 H, *NH* exch); Anal. Calcd. for $C_{16}H_{17}N_3O_3$: C, 64.20; H, 5.72; N, 14.04. Found C, 64.57; H, 5.85; N,13.76.

***N*-(2,4-dimethoxyphenyl)-2,6-dimethylfuro[2,3-*d*]pyrimidin-4-amine** (**472**). To a 50 mL flask was added **358** (91 mg, 0.5 mmol), 3,4-dimethoxyaniline (84 mg, 0.55 mmol) and BuOH (5 mL). To this solution was added 2 drops of concentrate HCl solution and the mixture was refluxed. TLC indicated the disappearance of starting material **358**, the solvent was removed under reduced pressure. To the residue obtained was added silica gel and MeOH and the solvent removed to make a plug. This plug was separated by column chromatography to give 119 mg

(82%) of **472** as a gray solid; mp 150.8-151.4°C; R_f 0.50 (Hexane/EtOAC 1:1); ^{1}H NMR (DMSO-d_6) δ 2.41 (s, 3 H), 2.48 (s, 3 H), 3.75 (s, 3 H, O*CH*$_3$), 3.78 (s, 3 H, O*CH*$_3$), 6.57 (s, 1 H, 5-*CH*), 6.94-6.96 (d, 1 H, *J* = 7.2 Hz, C_6H_3), 7.24-7.26 (dd, 1 H, *J* = 7.2 Hz, C_6H_3), 7.54 (s, 1 H), 9.36 (s, 1 H, *NH* exch); Anal. Calcd. for $C_{16}H_{17}N_3O_3 \cdot H_2O$: C, 60.56; H, 6.03; N, 13.24. Found C, 60.67; H, 6.15; N,13.03.

2,6-dimethyl-*N*-(3,4,5-trimethoxyphenyl)furo[2,3-*d*]pyrimidin-4-amine(**473**). To a 50 mL flask was added **358** (91 mg, 0.5 mmol), 3,4,5-trimethoxyaniline (101 mg, 0.55 mmol) and BuOH (5 mL). To this solution was added 2 drops of concentrate HCl solution and the mixture was refluxed. TLC indicated the disappearance of starting material **358**, the solvent was removed under reduced pressure. To the residue obtained was added silica gel and MeOH and the solvent removed to make a plug. This plug was separated by column chromatography to give 137 mg (83%) of **473** as a yellow powder; mp 173.5-173.7°C; R_f 0.03 (Hexane/EtOAC 3:1); ^{1}H NMR (DMSO-d_6) δ 2.43 (s, 3 H), 2.50 (s, 3 H), 3.65 (s, 3 H, O*CH*$_3$), 3.80 (s, 6 H, 2 O*CH*$_3$), 6.71 (s, 1 H, 5-*CH*), 7.29 (s, 2 H, C_6H_2), 9.43 (s, 1 H, *NH* exch); Anal. Calcd. for $C_{17}H_{19}N_3O_4 \cdot 0.2H_2O$: C, 61.32; H, 5.87; N, 12.62. Found C, 61.41; H, 5.94; N,12.30.

***N*-(4-ethylphenyl)-*N*,2,6-trimethylfuro[2,3-*d*]pyrimidin-4-amine (352)** To a 25 mL round bottom flask was weighed **466** (134 mg, 0.5 mmol) and was added DMF (2 mL) to afford a solution. The flask was purged with argon for five min followed by cooling down to 0 °C using ice bath. Sodium hydride (36 mg, 1.5 mmol) was added to the solution at 0 °C. The solution was stirred for 30 min at 0 °C under argon atmosphere. Dimethyl sulfate (150 mg, 1.2 mmol) was introduced to the reaction mixture with the help of a syringe and the flask was warmed to room temperature. The mixture was stirred at room temperature for another 3h at the end of which 1 N Hydrochloric acid (5 mL) was added carefully to quench the reaction. The reaction solvent was

removed under reduced pressure and the residue was suspended in water (20 mL). The suspension was extracted using ethyl acetate (10 mL x 2). Combined organic extracts were washed with brine (10 mL) dried (anhydrous sodium sulfate) and concentrated under reduced pressure. Silica gel (200 mg) was added and solvent evaporated to afford a plug. Column chromatography by elution with hexanes: ethyl acetate (5:1) afforded 60 mg (43 %) of **352** as a colorless crystal: mp 105.0-105.7 °C; *Rf* 0.6 (AcOEt/Haxene, 1:3); 1H NMR (DMSO-*d*6) δ 1.23-1.26 (t, 3 H, J = 6.0 Hz, CH_2CH_3), 2.15 (s, 3 H, CH_3), 2.49 (s, 3 H, CH_3), 2.68-2.73 (q, 2 H, J = 6.0 Hz, CH_2CH_3), 3.48 (s, 3 H, NCH_3), , 4.53 (s, 1 H, 5-CH), 7.27-7.28 (d, 2 H, *J* = 6.8 Hz, C_6H_4), 7.36-7.37 (d, 2 H, *J* = 6.8 Hz, C_6H_4); Anal. Calcd. for $C_{17}H_{19}N_3O$: C, 72.57; H, 6.81; N, 14.94. Found C, 72.58; H, 6.83; N,14.77.

***N*,2,6-trimethyl-*N*-[4-(methylsulfanyl)phenyl]furo[2,3-*d*]pyrimidin-4-amine (353)** To a 25 mL round bottom flask was weighed **467** (143 mg, 0.5 mmol) and was added DMF (2 mL) to afford a solution. The flask was purged with argon for five min followed by cooling down to 0 °C using ice bath. Sodium hydride (36 mg, 1.5 mmol) was added to the solution at 0 °C. The solution was stirred for 30 min at 0 °C under argon atmosphere. Dimethyl sulfate (150 mg, 1.2 mmol) was introduced to the reaction mixture with the help of a syringe and the flask was warmed to room temperature. The mixture was stirred at room temperature for another 3h at the end of which 1 N Hydrochloric acid (5 mL) was added carefully to quench the reaction. The reaction solvent was removed under reduced pressure and the residue was suspended in water (20 mL). The suspension was extracted using ethyl acetate (10 mL x 2). Combined organic extracts were washed with brine (10 mL) dried (anhydrous sodium sulfate) and concentrated under reduced pressure. Silica gel (200 mg) was added and solvent evaporated to afford a plug. Column chromatography by elution with hexanes: ethyl acetate (5:1) afforded 78 mg (52 %) of

353 as a light yellow solid: mp 91.8-91.9 °C; *Rf* 0.5 (AcOEt/Haxene, 1:3); 1H NMR (DMSO-*d*6) δ 2.18 (s, 3 H, CH_3), 2.49 (s, 3 H, CH_3), 2.54 (s, 3 H, CH_3), 3.47 (s, 3 H, NCH_3), , 4.73 (s, 1 H, 5-CH), 7.30-7.32 (d, 2 H, *J* = 6.8 Hz, C_6H_4), 7.38-7.39 (d, 2 H, *J* = 6.8 Hz, C_6H_4); Anal. Calcd. for $C_{16}H_{17}N_3OS$: C, 64.19; H, 5.72; N, 14.04, S, 10.71. Found C, 64.26; H, 5.68; N,13.90, S, 10.80.

***N*-(4-ethoxyphenyl)-*N*,2,6-trimethylfuro[2,3-*d*]pyrimidin-4-amine (355)** To a 25 mL round bottom flask was weighed **469** (141 mg, 0.5 mmol) and was added DMF (2 mL) to afford a solution. The flask was purged with argon for five min followed by cooling down to 0 °C using ice bath. Sodium hydride (36 mg, 1.5 mmol) was added to the solution at 0 °C. The solution was stirred for 30 min at 0 °C under argon atmosphere. Dimethyl sulfate (150 mg, 1.2 mmol) was introduced to the reaction mixture with the help of a syringe and the flask was warmed to room temperature. The mixture was stirred at room temperature for another 3h at the end of which 1 N Hydrochloric acid (5 mL) was added carefully to quench the reaction. The reaction solvent was removed under reduced pressure and the residue was suspended in water (20 mL). The suspension was extracted using ethyl acetate (10 mL x 2). Combined organic extracts were washed with brine (10 mL) dried (anhydrous sodium sulfate) and concentrated under reduced pressure. Silica gel (200 mg) was added and solvent evaporated to afford a plug. Column chromatography by elution with hexanes: ethyl acetate (5:1) afforded 73 mg (49 %) of **355** as a colorless crystal: mp 107.6-108.2 °C; *Rf* 0.64 (AcOEt/Haxene, 1:3); 1H NMR (DMSO-*d*6) δ 1.36-1.38 (t, 3 H, *J* = 5.6 Hz, OCH_2CH_3), 2.16 (s, 3 H, CH_3),2.48 (s, 3 H, CH_3), 3.45 (s, 3 H, NCH_3), 4.85-4.10 (q, 2 H, O$CH_2$$CH_3$), 4.58 (s, 1 H, 5-CH), 7.04-7.06 (d, 2 H, *J* = 7.2 Hz, C_6H_4), 7.26-7.28 (d, 2 H, *J* = 7.2 Hz, C_6H_4); Anal. Calcd. for $C_{17}H_{19}N_3O_2$: C, 68.67; H, 6.44; N, 14.13. Found C, 68.89; H, 6.48; N,14.06.

***N*,2,6-trimethyl-*N*-(4-propoxyphenyl)furo[2,3-*d*]pyrimidin-4-amine (356)** To a 25 mL round bottom flask was weighed **470** (149 mg, 0.5 mmol) and was added DMF (2 mL) to afford a solution. The flask was purged with argon for five min followed by cooling down to 0 °C using ice bath. Sodium hydride (36 mg, 1.5 mmol) was added to the solution at 0 °C. The solution was stirred for 30 min at 0 °C under argon atmosphere. Dimethyl sulfate (150 mg, 1.2 mmol) was introduced to the reaction mixture with the help of a syringe and the flask was warmed to room temperature. The mixture was stirred at room temperature for another 3h at the end of which 1 N Hydrochloric acid (5 mL) was added carefully to quench the reaction. The reaction solvent was removed under reduced pressure and the residue was suspended in water (20 mL). The suspension was extracted using ethyl acetate (10 mL x 2). Combined organic extracts were washed with brine (10 mL) dried (anhydrous sodium sulfate) and concentrated under reduced pressure. Silica gel (200 mg) was added and solvent evaporated to afford a plug. Column chromatography by elution with hexanes: ethyl acetate (5:1) afforded 95 mg (61 %) of **356** as a light brown solid: mp 100.7-100.8 °C; *Rf* 0.7 (AcOEt/Haxene, 1:3); 1H NMR (DMSO-*d*6) δ 0.99-1.03 (t, 3 H, J = 5.6 Hz, $OCH_2CH_2CH_3$),1.75-1.79 (m, 2 H, *J* = 5.6 Hz, $OCH_2CH_2CH_3$), 2.17 (s, 3 H, CH_3), 2.48 (s, 3 H, CH_3), 3.45 (s, 3 H, NCH_3), 3.99-4.02 (t, 2 H, J = 5.6 Hz, $OCH_2CH_2CH_3$), 4.62 (s, 1 H, 5-CH), 7.05-7.07 (d, 2 H, *J* = 7.2 Hz, C_6H_4), 7.27-7.28 (d, 2 H, *J* = 7.2 Hz, C_6H_4); Anal. Calcd. for $C_{18}H_{21}N_3O_2$: C, 69.43; H, 6.80; N, 13.49. Found C, 69.42; H, 6.82; N,13.43.

***N*-(2,4-dimethoxyphenyl)-*N*,2,6-trimethylfuro[2,3-*d*]pyrimidin-4-amine (357)** To a 25 mL round bottom flask was weighed **471** (150 mg, 0.5 mmol) and was added DMF (2 mL) to afford a solution. The flask was purged with argon for five min followed by cooling down to 0 °C using ice bath. Sodium hydride (36 mg, 1.5 mmol) was added to the solution at 0 °C. The solution was

stirred for 30 min at 0 °C under argon atmosphere. Dimethyl sulfate (150 mg, 1.2 mmol) was introduced to the reaction mixture with the help of a syringe and the flask was warmed to room temperature. The mixture was stirred at room temperature for another 3h at the end of which 1 N Hydrochloric acid (5 mL) was added carefully to quench the reaction. The reaction solvent was removed under reduced pressure and the residue was suspended in water (20 mL). The suspension was extracted using ethyl acetate (10 mL x 2). Combined organic extracts were washed with brine (10 mL) dried (anhydrous sodium sulfate) and concentrated under reduced pressure. Silica gel (200 mg) was added and solvent evaporated to afford a plug. Column chromatography by elution with hexanes: ethyl acetate (5:1) afforded 74 mg (47 %) of **357** as a orange crystal: mp 166.1-166.4 °C; *Rf* 0.38 (AcOEt/Haxene, 1:1); 1H NMR (DMSO-*d*6) δ 2.16 (s, 3 H, *CH*$_3$), 2.47 (s, 3 H, *CH*$_3$), 3.41 (s, 3 H, N*CH*$_3$), 3.70 (s, 3 H, OCH_3), 3.85 (s, 3 H, OCH_3), 4.57 (s, 1 H, 5-CH), 6.62-6.64 (dd, 1 H, *J* = 6.8 Hz, *J* = 2.0 Hz, *C*$_6$*H*$_3$), 6.75-6.76 (d, 2 H, *J* = 6.8 Hz, *C*$_6$*H*$_3$), 7.24-7.22 (d, 2 H, *J* = 2.0 Hz, *C*$_6$*H*$_3$); Anal. Calcd. for $C_{17}H_{19}N_3O_3$: C, 65.16; H, 6.11; N, 13.41. Found C, 65.20; H, 6.16; N,13.21.

***N*-(3,4-dimethoxyphenyl)-*N*,2,6-trimethylfuro[2,3-*d*]pyrimidin-4-amine (358)** To a 25 mL round bottom flask was weighed **472** (150 mg, 0.5 mmol) and was added DMF (2 mL) to afford a solution. The flask was purged with argon for five min followed by cooling down to 0 °C using ice bath. Sodium hydride (36 mg, 1.5 mmol) was added to the solution at 0 °C. The solution was stirred for 30 min at 0 °C under argon atmosphere. Dimethyl sulfate (150 mg, 1.2 mmol) was introduced to the reaction mixture with the help of a syringe and the flask was warmed to room temperature. The mixture was stirred at room temperature for another 3h at the end of which 1 N Hydrochloric acid (5 mL) was added carefully to quench the reaction. The reaction solvent was removed under reduced pressure and the residue was suspended in water (20 mL). The

suspension was extracted using ethyl acetate (10 mL x 2). Combined organic extracts were washed with brine (10 mL) dried (anhydrous sodium sulfate) and concentrated under reduced pressure. Silica gel (200 mg) was added and solvent evaporated to afford a plug. Column chromatography by elution with hexanes: ethyl acetate (5:1) afforded 78 mg (50 %) of **358** as a orange crystal: mp 114.2-116.6 °C; *Rf* 0.28 (AcOEt/Haxene, 1:1); 1H NMR (DMSO-*d*6) δ 2.17 (s, 3 H, *CH*$_3$), 2.48 (s, 3 H, *CH*$_3$), 3.47 (s, 3 H, N*CH*$_3$), 3.73 (s, 3 H, OCH_3), 3.82 (s, 3 H, OCH_3), 4.64 (s, 1 H, 5-CH), 6.87-6.89 (dd, 1 H, *J* = 6.8 Hz, *J* = 2.0 Hz, *C*$_6$*H*$_3$), 7.02-7.07 (d, 2 H, *J* = 2.0 Hz, *C*$_6$*H*$_3$), 7.04-7.06 (d, 2 H, *J* = 6.8 Hz, *C*$_6$*H*$_3$); Anal. Calcd. for $C_{17}H_{19}N_3O_3$: C, 65.16; H, 6.11; N, 13.41. Found C, 65.11; H, 6.23; N,13.17.

***N*,2,6-trimethyl-*N*-(3,4,5-trimethoxyphenyl)furo[2,3-*d*]pyrimidin-4-amine (359)** To a 25 mL round bottom flask was weighed **473** (165 mg, 0.5 mmol) and was added DMF (2 mL) to afford a solution. The flask was purged with argon for five min followed by cooling down to 0 °C using ice bath. Sodium hydride (36 mg, 1.5 mmol) was added to the solution at 0 °C. The solution was stirred for 30 min at 0 °C under argon atmosphere. Dimethyl sulfate (150 mg, 1.2 mmol) was introduced to the reaction mixture with the help of a syringe and the flask was warmed to room temperature. The mixture was stirred at room temperature for another 3h at the end of which 1 N Hydrochloric acid (5 mL) was added carefully to quench the reaction. The reaction solvent was removed under reduced pressure and the residue was suspended in water (20 mL). The suspension was extracted using ethyl acetate (10 mL x 2). Combined organic extracts were washed with brine (10 mL) dried (anhydrous sodium sulfate) and concentrated under reduced pressure. Silica gel (200 mg) was added and solvent evaporated to afford a plug. Column chromatography by elution with hexanes: ethyl acetate (5:1) afforded 108 mg (63 %) of **359** as a light yellow crystal: mp 176.5-178.1 °C; *Rf* 0.19 (AcOEt/Haxene, 2:1); 1H NMR (DMSO-*d*6) δ

2.20 (s, 3 H, *CH*$_3$), 2.49 (s, 3 H, *CH*$_3$), 3.50 (s, 3 H, N*CH*$_3$), 3.74(s, 9 H, 3 OCH_3), 4.73 (s, 1 H, 5-CH), 6.73 (s, 2 H, *C*$_6$*H*$_2$); Anal. Calcd. for $C_{18}H_{21}N_3O_4$: C, 62.96; H, 6.16; N, 12.24. Found C, 63.18; H, 6.16; N,12.14.

***N*-1,3-benzodioxol-5-yl-2,6-dimethylfuro[2,3-*d*]pyrimidin-4-amine (474).** To a 50 mL flask was added **358** (91 mg, 0.5 mmol), benzo[d][1,3]dioxol-5-amine (75 mg, 0.55 mmol) and BuOH (5 mL). To this solution was added 2 drops of concentrate HCl solution and the mixture was refluxed. TLC indicated the disappearance of starting material **5**, the solvent was removed under reduced pressure. To the residue obtained was added silica gel and MeOH and the solvent removed to make a plug. This plug was separated by column chromatography to give 102 mg (72%) of **474**

as a brown solid; mp 185.5-187.1°C; R_f 0.10 (Hexane/EtOAC 3:1); ^{1}H NMR (DMSO-d_6) δ 2.40 (s, 3 H, CH_3), 2.46 (s, 3 H, CH_3), 6.01 (s, 2 H, OCH_2O), 6.59 (br, 1 H, NH exch), 6.89-6.91 (d, 1 H, J = 6.8 Hz), 7.09-7.11 (dd, 1 H, J = 8.4 Hz), 7.51 (s, 1 H), 9.37 (s, 1 H); Anal. Calcd. for $C_{15}H_{13}N_3O_2$: C, 63.60; H, 4.63; N, 14.83. Found C, 63.54; H, 4.56; N,14.90.

***N*-(2,3-dihydro-1-benzofuran-5-yl)-2,6-dimethylfuro[2,3-*d*]pyrimidin-4-amine (475).** To a 50 mL flask was added **358** (91 mg, 0.5 mmol), 2,3-dihydrobenzofuran-5-amine (74 mg, 0.55 mmol) and BuOH (5 mL). To this solution was added 2 drops of concentrate HCl solution and the mixture was refluxed. TLC indicated the disappearance of starting material **5**, the solvent was removed under reduced pressure. To the residue obtained was added silica gel and MeOH and the solvent removed to make a plug. This plug was separated by column chromatography to give 98 mg (70%) of **475** as a brown solid; mp 193.7-195.2°C; R_f 0.10 (Hexane/EtOAC 3:1); ^{1}H NMR (DMSO-d_6) δ 2.38 (s, 3 H, CH_3), 2.44 (s, 3 H, CH_3), 3.18-3.23 (t, 2 H, J = 8.4 Hz, CH_2*CH*$_2$), 4.52-4.56 (t, 2 H, J = 8.4 Hz, *CH*$_2$$CH_2$), 6.43 (br, 1 H, NH exch), 6.74-6.77 (d, 1 H, J

= 8.4 Hz), 7.33-7.35 (d, 1 H, J = 8.4 Hz), 7.57 (s, 1 H), 9.50 (s, 1 H); Anal. Calcd. for $C_{16}H_{15}N_3O_2$: C, 68.31; H, 5.37; N, 14.94. Found C, 68.39; H, 5.78; N,14.01.

***N*-1-benzofuran-5-yl-2,6-dimethylfuro[2,3-*d*]pyrimidin-4-amine (476).** To a 50 mL flask was added **358** (91 mg, 0.5 mmol), benzofuran-5-amine (73 mg, 0.55 mmol) and BuOH (5 mL). To this solution was added 2 drops of concentrate HCl solution and the mixture was refluxed. TLC indicated the disappearance of starting material **5**, the solvent was removed under reduced pressure. To the residue obtained was added silica gel and MeOH and the solvent removed to make a plug. This plug was separated by column chromatography to give 92 mg (66%) of **476** as a colorless crystal; mp 173.4-175.0°C; R_f 0.10 (Hexane/EtOAC 3:1); ^{1}H NMR (DMSO-d_6) δ 2.40 (s, 3 H, 6-*CH*$_3$), 2.49 (s, 3 H, 2-*CH*$_3$), 6.55 (br, 1 H, NH exch), 6.98 (d, 1 H, J = 1.6 Hz, 5-CH), 7.58-7.60 (d, 2 H, C_8H_5), 7.99 (d, 1 H, C_8H_5), 8.11-8.13 (t, 1 H, C_8H_5), 9.50 (s, 1 H, C_8H_5); Anal. Calcd. for $C_{16}H_{13}N_3O_2$: C, 68.81; H, 4.69; N, 15.05. Found C, 68.84; H, 4.77; N,14.96.

***N*-1,3-benzodioxol-5-yl-*N*,2,6-trimethylfuro[2,3-*d*]pyrimidin-4-amine (360).** To a 25 mL round bottom flask was weighed **474** (56.6 mg, 0.2 mmol) and was added DMF (2 mL) to afford a solution. The flask was purged with argon for five min followed by cooling down to 0 °C using ice bath. Sodium hydride (12 mg, 0.5 mmol) was added to the solution at 0 °C. The solution was stirred for 30 min at 0 °C under argon atmosphere. Dimethyl sulfate (50 mg, 0.4 mmol) was introduced to the reaction mixture with the help of a syringe and the flask was warmed to room temperature. The mixture was stirred at room temperature for another 3h at the end of which 1 N Hydrochloric acid (3 mL) was added carefully to quench the reaction. The reaction solvent was removed under reduced pressure and the residue was suspended in water (10 mL). The suspension was extracted using ethyl acetate (5 mL x 2). Combined organic extracts were washed with brine (5 mL) dried (anhydrous sodium sulfate) and concentrated under reduced

pressure. Silica gel (100 mg) was added and solvent evaporated to afford a plug. Column chromatography by elution with hexanes: ethyl acetate (5:1) afforded 40 mg (67%) of **360** as a colorless crystal; mp 200.0-200.7°C; R_f 0.48 (Hexane/EtOAC 1:1); ^{1}H NMR (DMSO-d_6) δ 2.21 (s, 3 H, CH_3), 2.48 (s, 3 H, CH_3), 3.44 (s, 3 H, OCH_3), 4.76 (s, 1 H, 5-CH), 6.14 (s, 2 H, OCH_2O), 6.82-6.84 (m, 1 H), 7.01-7.04 (m, 2 H); Anal. Calcd. for $C_{16}H_{15}N_3O_3$: C, 69.64; H, 5.09; N, 14.13. Found C, 64.63; H, 4.98; N,14.14.

***N*-(2,3-dihydro-1-benzofuran-5-yl)-*N*,2,6-trimethylfuro[2,3-*d*]pyrimidin-4-amine (361).** To a 25 mL round bottom flask was weighed **475** (43.6 mg, 0.2 mmol) and was added DMF (2 mL) to afford a solution. The flask was purged with argon for five min followed by cooling down to 0 °C using ice bath. Sodium hydride (12 mg, 0.5 mmol) was added to the solution at 0 °C. The solution was stirred for 30 min at 0 °C under argon atmosphere. Dimethyl sulfate (50 mg, 0.4 mmol) was introduced to the reaction mixture with the help of a syringe and the flask was warmed to room temperature. The mixture was stirred at room temperature for another 3h at the end of which 1 N Hydrochloric acid (3 mL) was added carefully to quench the reaction. The reaction solvent was removed under reduced pressure and the residue was suspended in water (10 mL). The suspension was extracted using ethyl acetate (5 mL x 2). Combined organic extracts were washed with brine (5 mL) dried (anhydrous sodium sulfate) and concentrated under reduced pressure. Silica gel (100 mg) was added and solvent evaporated to afford a plug. Column chromatography by elution with hexanes: ethyl acetate (5:1) afforded 35 mg (59%) of **361** as a colorless crystal; mp 167.2-168.4°C; R_f 0.16 (Hexane/EtOAC 3:1); ^{1}H NMR (DMSO-d_6) δ 2.18 (s, 3 H, CH_3), 2.48 (s, 3 H, CH_3), 3.21-3.25 (t, 3H, J = 6.8 Hz, CH_2CH_2), 3.45 (s, 3 H, OCH_3), 4.61-4.64 (t, 3H, J = 6.8 Hz, CH_2CH_2), 4.65 (s, 1 H, 5-CH), 6.86-6.88 (d, 1 H, J = 6.8 Hz), 7.05-7.07 (dd, 1 H, J = 8.4 Hz), 7.24 (s, 1 H); Anal. Calcd. for $C_{17}H_{17}N_3O_2$: C, 69.14; H,

5.80; N, 14.23. Found C, 68.97; H, 5.88; N,14.12.

***N*-1-benzofuran-5-yl-*N*,2,6-trimethylfuro[2,3-*d*]pyrimidin-4-amine (362).** To a 25 mL round bottom flask was weighed **476** (58.6 mg, 0.2 mmol) and was added DMF (2 mL) to afford a solution. The flask was purged with argon for five min followed by cooling down to 0 °C using ice bath. Sodium hydride (12 mg, 0.5 mmol) was added to the solution at 0 °C. The solution was stirred for 30 min at 0 °C under argon atmosphere. Dimethyl sulfate (50 mg, 0.4 mmol) was introduced to the reaction mixture with the help of a syringe and the flask was warmed to room temperature. The mixture was stirred at room temperature for another 3h at the end of which 1 N Hydrochloric acid (3 mL) was added carefully to quench the reaction. The reaction solvent was removed under reduced pressure and the residue was suspended in water (10 mL). The suspension was extracted using ethyl acetate (5 mL x 2). Combined organic extracts were washed with brine (5 mL) dried (anhydrous sodium sulfate) and concentrated under reduced pressure. Silica gel (100 mg) was added and solvent evaporated to afford a plug. Column chromatography by elution with hexanes: ethyl acetate (5:1) afforded 37 mg (63%) of **362** as a colorless crystal; mp 193.0-194.2°C; R_f 0.22 (Hexane/EtOAC 3:1); ^{1}H NMR (DMSO-d_6) δ 2.10 (s, 3 H, CH_3), 3.38 (s, 3 H, OCH_3), 4.37 (s, 1 H, 5-CH), 7.03 (s, 1 H), 7.30-7.32 (d, 1 H, J = 6.8 Hz), 7.69 (s, 1 H), 7.74-7.76 (d, 1 H, J = 6.8 Hz), 8.13 (s, 1 H); Anal. Calcd. for $C_{17}H_{15}N_3O_2$: C, 69.61; H, 5.15; N, 14.33. Found C, 69.54; H, 5.17; N, 14.21.

***N*-{4-[(2,2-dimethylpropanoyl)amino]phenyl}-*N*,2,2-trimethylpropanamide (480).** To a 100 mL round-bottom flask was added 1,4-phenyl-diamine (2.19 g, 18 mmol) and pivaloyl anhydride (30 mL) and the resulting mixture was refluxed under N_2 atmosphere for 2.5 h. TLC showed the disappearance of the starting material **73c** and the formation of a major spot at *Rf* = 0.32 (AcOEt/Haxene, 1:3). After evaporation of the solvent, the residue was loaded onto a silica gel

column and eluted with hexane followed by hexane/EtOAc 5:1. The fractions containing the desired spot (TLC) were pooled and evaporated, the resulting residue was recrystallized from Et2O/EtOAc to afford 4.38 g (84%) of **480** as colorless crystals: mp 181.3-182.7 ^{o}C; *Rf* = 0.32 (AcOEt/Haxene, 1:3); 1H NMR (DMSO-*d*6) 0.96 (s, 9 H, Piv), 1.24 (s, 9 H, Piv), 3.07 (s, 3 H, CH_3), 7.22-7.23 (d, 2 H, *J* = 6.8 Hz, C_6H_4), 7.69-7.71 (d, 2 H, *J* = 6.8 Hz, C_6H_4), 9.31 (s, 1 H).

2-Methyl-5-(allyl)pyrimidine-4,6-diol (484). A mixture of **485** (8.6 g, 50 mmol) and acetamidine hydrochloride (5.42 g, 60 mmol) was heated to reflux in methanol (100 mL), followed by the addition of sodium metal (1.52 g, 66 mmol). The mixture was refluxed for 24 h to afford a thick yellow precipitation. The suspension was then cooled in an ice-bath to room temperature. The precipitate formed was collected by filtration and dissolved in 40 mL of water. The pH of this solution was adjusted to 3-4 with 1 N HCl whereupon a thick precipitate formed. The mixture was filtered and washed with a small amount of water followed by acetone and dried in vacuo to afford **73c** (4.7g, 57%) as a light yellow powder; mp >300°C; R_f 0.11 ($CHCl_3$/MeOH 6:1). The comound was used directly in next step without further purification.

***N*-(4-methoxyphenyl)-*N*,2,6-trimethyl-5,6-dihydrofuro[2,3-*d*]pyrimidin-4-amine** (**364**). To a solution of **335** (283 mg, 1 mmol) in a mixture of MeOH (15 mL) and AcOH (3 mL) was added 10% palladium on activated carbon (100 mg), and the suspension was hydrogenated in a Parr apparatus at room temperature and 55 psi for 20 h. The reaction was stopped, when TLC indicated the disappearance of the starting material and the formation of single new spot. The reaction mixture was filtered through Celite, washed with 50 mL MeOH. To this solution was added 1 g silica gel and the mixture was evaporated under reduced pressure to dryness. The residue was purified by column chromatography on silica gel with hexane: acetyl acetate = 20:1 as the eluent. Fractions containing the product (TLC) were combined and evaporated to afford

364 as a white crystal 252 mg (88%). mp 200.2-200.7 °C; R_f 0.27 (Hexane/EtOAC 1:1); ^{1}H NMR (DMSO-d_6) δ 1.34 (d, 3 H, J = 6 Hz), 1.68 (dd, 1 H, J_1= 15.2 Hz, J_2 = 6.8 Hz), 2.20 (dd, 1 H, J_1= 15.2 Hz, J_2 = 6.8 Hz), 2.33 (s, 3 H), 3.36 (s, 3 H), 3.82 (s, 3 H), 4.60 (q, 1 H, J = 6 Hz), 6.96 (d, 2 H, J = 8 Hz), 7.22 (d, 2 H, J = 8 Hz).

2-Methyl-5-(prop-2-yn-1-yl)pyrimidine-4,6-diol (493). A mixture of dimethyl prop-2-yn-1-ylmalonate (10 g, 60 mmol) and formamidine hydrochloride (4.8 g, 60 mmol) was heated to reflux in MeOH (100 mL), followed by the addition of sodium metal (1.52 g, 66 mmol). The mixture was refluxed for 24 h to afford a thick yellow precipitation. The suspension was then cooled in an ice-bath to room temperature. The precipitate formed was collected by filtration and dissolved in 40 mL of water. The pH of this solution was adjusted to 3-4 with 1 N HCl whereupon a thick precipitate formed. The mixture was filtered and washed with a small amount of water followed by acetone and dried in vacuo to afford 6.2 g (69%) of **493** as a white powder: mp 256.4-257.1°C; R_f 0.11 ($CHCl_3$/MeOH 6:1); ^{1}H NMR (DMSO-d_6) δ 2.56-2.58 (t, 1 H, J = 2.8, *CH*), 3.07-3.08 (d, 2 H, J = 2.8, CH_2), 7.98 (s, 1 H, *CH*), 11.94 (s, 2 H, 2 *OH* exch).

6-Methylfuro[2,3-*d*]pyrimidin-4(3H)-one (489). The microwave reaction vial was charged with **493** (150 mg, 1 mmol) and 5 mL 2 N NaOH. The reaction mixture was irradiated in a microwave apparatus at 180 °C for 30 min. After the reaction mixture was cooled to ambient temperature, the product was filtered, the filtrate was concentrated, and the crude mixture was purified by silica gel column chromatography using 2% MeOH in $CHCl_3$ as the eluent. Fractions containing the product (TLC) were combined and evaporated to afford 124 mg (83%) of **489** as a white powder: mp 220-221.3°C; R_f 0.69 ($CHCl_3$/MeOH 6:1); ^{1}H NMR (DMSO-d_6) δ 2.36 (s, 3 H, CH_3), 6.52 (s, 1 H, *CH*), 7.99 (s, 1 H, *CH*), 12.49 (s, 1 H, 3-*NH* exch); Anal. Calcd. for $C_7H_6N_2O_2$: C, 56.00; H, 4.03; N, 21.31. Found C, 55.35; H, 4.08; N,18.21.

4-Chloro-2,6-dimethylfuro[2,3-*d*]pyrimidine (495). To a 50-mL round-bottomed flask was added **489** (1.5 g, 10 mmol) in 25 mL phosphorus oxychloride. The reaction mixture was heated at reflux with stirring in an anhydrous atmosphere for 4 h. All the suspensions were dissolved after heating to afford a dark solution. The dark orange solution was allowed to cool to room temperature and concentrated in vacuo. Water (40 mL) was then added to the residue at 0 ^{o}C with vigorous stirring to give an exothermic reaction. Concentrated aqueous ammonium hydroxide was added to afford a pH = 5 solution. The aqueous solution was extracted with AcOEt (3 x 20 mL) and the organic layer was pooled and dried in vacuo. The crude product was purified by silica gel column chromatography with 10% AcOEt/Haxene to afford 1.2 g (72%) of **495** as a white crystal: TLC *Rf* 0.24 (Hexane/EtOAC 15:1); mp 45.6-46.3°C; 1H NMR (DMSO-*d*6) δ 2.55 (s, 3 H, *CH*$_3$), 6.53 (s, 1 H, *CH*), 8.69 (s, 1 H, *CH*); Anal. Calcd. for $C_7H_5ClN_2O$: C, 49.87; H, 2.99; N, 16.62; Cl, 21.03. Found C, 50.04; H, 3.03; N,16.50; Cl, 20.98.

***N*-(4-methoxyphenyl)-*N*,2,6-trimethylfuro[2,3-*d*]pyrimidin-4-amine** (**365**). To a 50 mL flask was added **495** (84 mg, 0.5 mmol), N-methyl-4-methoxylaniline (77 mg, 0.55 mmol) and BuOH (5 mL). To this solution was added 2 drops of concentrate HCl solution and the mixture was refluxed. TLC indicated the disappearance of starting material **495**, the solvent was removed under reduced pressure. To the residue obtained was added silica gel and MeOH and the solvent removed to make a plug. This plug was separated by column chromatography to give 104 mg (77%) of **365** as a light yellow crystal; mp 79.1-79.8°C; R_f 0.19 (Hexane/EtOAC 3:1); ^{1}H NMR (DMSO-d_6) δ 2.19 (s, 3 H, *CH*$_3$), 3.46 (s, 3 H, N*CH*$_3$), 3.82 (s, 3 H, O*CH*$_3$), 4.64 (s, 1 H, *CH*), 7.05-7.07 (d, 2 H, *J* = 8.8 Hz, 2 *CH*), 7.29-7.31 (d, 2 H, *J* = 8.8 Hz, 2 *CH*), 8.31 (s, 1 H, *CH*); Anal. Calcd. for $C_{15}H_{15}N_3O_2$: C, 66.90; H, 5.61; N, 15.60. Found C, 67.18; H, 5.58; N,15.40.

6-Hydroxy-2-phenyl-5-(prop-2-yn-1-yl)pyrimidin-4(3*H*)-one (494). A mixture of dimethyl

prop-2-yn-1-ylmalonate (10 g, 60 mmol) and benzenecarboximidamide hydrochloride (9.4 g, 60 mmol) was heated to reflux in MeOH (100 mL), followed by the addition of sodium metal (1.52 g, 66 mmol). The mixture was refluxed for 24 h to afford a thick yellow precipitation. The suspension was then cooled in an ice-bath to room temperature. The precipitate formed was collected by filtration and dissolved in 40 mL of water. The pH of this solution was adjusted to 3-4 with 1 N HCl whereupon a thick precipitate formed. The mixture was filtered and washed with a small amount of water followed by acetone and dried in vacuo to afford 8.6 g (63%) of **494** as a white powder: mp >300°C; R_f 0.12 ($CHCl_3$/MeOH 6:1); ^{1}H NMR (DMSO-d_6) δ 2.62 (s, 1 H, CH), 7.50-7.58 (m, 3 H, C_6H_5), 8.04-8.06 (d, 2 H, J = 7.6 Hz, C_6H_5) 11.61 (s, 1 H, OH exch), 12.52 (s, 1 H, NH exch)

6-Methyl-2-phenylfuro[2,3-*d*]pyrimidin-4(3*H*)-one (490). The microwave reaction vial was charged with **494** (226 mg, 1 mmol) and 5 mL 2 N NaOH. The reaction mixture was irradiated in a microwave apparatus at 180 °C for 30 min. After the reaction mixture was cooled to ambient temperature, the product was filtered, the filtrate was concentrated, and the crude mixture was purified by silica gel column chromatography using 2% MeOH in $CHCl_3$ as the eluent. Fractions containing the product (TLC) were combined and evaporated to afford 196 mg (87%) of **490** as a yellow powder: mp 234.1-234.9°C; R_f 0.7 ($CHCl_3$/MeOH 6:1); ^{1}H NMR (DMSO-d_6) δ 2.39 (d, 3 H, J = 1.2 Hz, 6-CH_3), 6.59 (d, 1 H, J = 1.2 Hz, 5-CH), 7.50-7.57 (m, 3 H, C_6H_5), 8.09-8.11 (dd, 2 H, J_1 = 7.6 Hz, J_2 = 1.2 Hz, C_6H_5), 12.68 (s, 1 H, NH exch).

4-Chloro-6-methyl-2-phenylfuro[2,3-*d*]pyrimidine (496). To a 50-mL round-bottomed flask was added **490** (2.26 g, 10 mmol) in 25 mL phosphorus oxychloride. The reaction mixture was heated at reflux with stirring in an anhydrous atmosphere for 4 h. All the suspensions were

dissolved after heating to afford a dark solution. The dark orange solution was allowed to cool to room temperature and concentrated in vacuo. Water (40 mL) was then added to the residue at 0 ^{o}C with vigorous stirring to give an exothermic reaction. Concentrated aqueous ammonium hydroxide was added to afford a pH = 5 solution. The aqueous solution was extracted with AcOEt (3 x 20 mL) and the organic layer was pooled and dried in vacuo. The crude product was purified by silica gel column chromatography with 10% AcOEt/Haxene to afford 1.65 g (68%) of **496** as a white crystal: mp 139.4-139.7°C; *Rf* 0.24 (Hexane/EtOAC 15:1); 1H NMR (DMSO-*d*6) δ 2.53-2.54 (d, 3 H, *J* =1.2 Hz, 6-CH_3), 6.86 (s, 1 H, *J* =1.2 Hz 5-CH), 7.53-7.55 (m, 3 H, C_6H_5), 8.33-8.36 (dd, 2 H, J_1 = 6.8 Hz, J_2 = 2.4 Hz, C_6H_5).

***N*-(4-Methoxyphenyl)-*N*,6-dimethyl-2-phenylfuro[2,3-*d*]pyrimidin-4-amine** (**367**).

To a 25 mL round bottom flask was weighed **496** (66 mg, 0.2 mmol) and was added DMF (2 mL) to afford a solution. The flask was purged with argon for five min followed by cooling down to 0 °C using ice bath. Sodium hydride (14.4 mg, 0.6 mmol) was added to the solution at 0 °C. The solution was stirred for 30 min at 0 °C under argon atmosphere. Dimethyl sulfate (75.7 mg; ≈ 57μl; 0.6 mmol) was introduced to the reaction mixture with the help of a syringe and the flask was warmed to room temperature. The mixture was stirred at room temperature for another 3h at the end of which 1 N Hydrochloric acid (5 mL) was added carefully to quench the reaction followed by water (20 mL) to afford a precipitate. Product was extracted using ethyl acetate (10 mL x 2). Combined organic extracts were washed with brine (10 mL) dried (anhydrous sodium sulfate) and concentrated under reduced pressure. Silica gel (200 mg) was added and solvent evaporated to afford a plug. Column chromatography by elution with hexanes: ethyl acetate (5:1) afforded 45 mg of **367** (65 %) as a colorless crystal: mp 151.4-152.7 °C; R_f 0.22 (hexane: AcOEt, 3:1); ^{1}HNMR (400 MHz) (DMSO-d_6): δ 2.21 (s, 1H, 6-CH_3), 3.59 (s, 3H, NCH_3), 3.83 (s, 3H,

OCH_3), 4.67 (s, 1H, 5-CH), 7.07-7.09 (d, 2H, *J* = 8.8 Hz, C_6H_4,), 7.35-7.37 (d, 2H, *J* = 8.4 Hz , C_6H_4), 7.48-7.55 (m, 3H, C_6H_5), 8.39-8.41 (m, 2H, C_6H_5). Anal. Calcd for $C_{21}H_{19}N_3O_2$: C, 73.03; H, 5.54; N, 12.17; Found: C, 73.13; H, 5.61; N, 12.03.

2,2-Dimethyl-*N*-(6-methyl-4-oxo-3,4-dihydrofuro[2,3-*d*]pyrimidin-2-yl)propanamide (416). To a 100 mL round-bottom flask was added **415** (3 g, 18 mmol) and pivaloyl anhydride (30 mL) and the resulting mixture was refluxed under N_2 atmosphere for 2.5 h. TLC showed the disappearance of the starting material **415** and the formation of a major spot at *Rf* = 0.42 ($CHCl_3$/MeOH 5:1). After evaporation of the solvent, the residue was loaded onto a silica gel column and eluted with hexane followed by hexane/EtOAc 2:1. The fractions containing the desired spot (TLC) were pooled and evaporated, the resulting residue was recrystallized from Et2O/EtOAc to afford 3.0 g (67%) of **416** as light yellow crystals: mp 225-227 ^oC; *Rf* = 0.47 (MeOH/CHCl3 1 : 7); 1H NMR (DMSO-*d*6) 1.24 (s, 9 H), 2.34 (s, 3 H), 6.50 (s, 1 H), 11.26 (s, 1 H), 12.19 (s, 1 H). Anal. Calcd. for C12H15N3O3: C, 57.82; H, 6.07; N, 16.86 Found C, 58.10; H, 6.12; N,16.86.

***N*-(4-chloro-6-methylfuro[2,3-*d*]pyrimidin-2-yl)-2,2-dimethylpropanamide (497).** To a 50-mL round-bottomed flask was added **416** (249 mg, 1 mmol) in 5 mL phosphorus oxychloride. The reaction mixture was heated at reflux with stirring in an anhydrous atmosphere for 3 h. All the suspensions were dissolved after heating to afford a dark solution. The dark orange solution was allowed to cool to room temperature and concentrated in vacuo. Water (10 mL) was then added to the residue at 0 ^oC with vigorous stirring to give an exothermic reaction. Concentrated aqueous ammonium hydroxide was added to afford a pH = 5 solution. The aqueous solution was extracted with AcOEt (3 x 5 mL) and the organic layer was pooled and dried in vacuo. The crude product was purified by silica gel column chromatography with 10% AcOEt/Haxene to afforded

192 mg (72%) of **497** as a brown solid: TLC *Rf* 0.38 (Hexane/EtOAC 15:1); mp 141.7-143.2°C; 1H NMR (DMSO-*d*6) δ 1.23 (s, 9 H, *Piv*), 2.36 (s, 3 H, CH_3), 6.76 (s, 1 H, *CH*), 10.38 (s, 1 H, *NH exch*).

***N*4-(4-methoxyphenyl)-*N*4,6-dimethylfuro[2,3-*d*]pyrimidine-2,4-diamine** (**366**). To a 50 mL flask was added **497** (134 mg, 0.5 mmol), N-methyl-4-methoxylaniline (77 mg, 0.55 mmol) and BuOH (10 mL). To this solution was added 2 drops of concentrate HCl solution and the mixture was refluxed. TLC indicated the disappearance of starting material **366**, the solvent was removed under reduced pressure. To the residue obtained was added silica gel and MeOH and the solvent removed to make a plug. This plug was separated by column chromatography to give 57 mg (57%) of **497** as a white powder; mp 169.5-171.3°C; R_f 0.13 (Hexane/EtOAC 2:1); ^{1}H NMR (DMSO-d_6) δ 2.06 (s, 3 H, CH_3), 3.38 (s, 3 H, NCH_3), 3.82 (s, 3 H, OCH_3), 4.41 (s, 1 H, *CH*), 4.14 (s, 2 H, CH_2), 7.03-7.05 (d, 2 H, *J* = 8.8 Hz, 2 *CH*), 7.24-7.26 (d, 2 H, *J* = 8.8 Hz, 2 *CH*); HRMS calcd for C16H18N3O$_2$ 284.1399, found 284.1387; Anal. Calcd. for $C_{15}H_{16}N_4O_2 \cdot 0.2H_2O$: C, 62.57; H, 5.74; N, 19.46. Found C, 62.69; H, 5.73; N,19.16.

***N*-(3,4-dichlorophenyl)-N,2,6-trimethylfuro[2,3-d]pyrimidin-4-amine** (**368**). To a 50 mL flask was added **495** (84 mg, 0.5 mmol), aniline (51g, 0.55 mmol) and BuOH (5 mL). To this solution was added 2 drops of concentrate HCl solution and the mixture was refluxed. TLC indicated the disappearance of starting material **495**, the solvent was removed under reduced pressure. To the residue obtained was added silica gel and MeOH and the solvent removed to make a plug. This plug was separated by column chromatography to give 94 mg (79%) of **368** as a light yellow crystal; mp 97.7-98.2°C; R_f 0.11 (Hexane/EtOAC 3:1); ^{1}H NMR ($CDCl_3$) δ 2.19 (s, 3 H, CH_3), 3.51 (s, 3 H, NCH_3), 4.59 (s, 1 H, *CH*), 7.8-7.5 (m, 5 H, 5*CH*), 8.33 (s, 1 H, *CH*); Anal. Calcd. for $C_{14}H_{13}N_3O$: C, 70.28; H, 5.48; N, 17.56. Found C, 70.43; H, 5.53; N,17.62.

***N*,2,6-trimethyl-N-(4-methylphenyl)furo[2,3-d]pyrimidin-4-amine** (**369**). To a 50 mL flask was added **495** (84 mg, 0.5 mmol), *N*,4-dimethylaniline (67 mg, 0.55 mmol) and BuOH (5 mL). To this solution was added 2 drops of concentrate HCl solution and the mixture was refluxed. TLC indicated the disappearance of starting material **495**, the solvent was removed under reduced pressure. To the residue obtained was added silica gel and MeOH and the solvent removed to make a plug. This plug was separated by column chromatography to give 97 mg (77%) of **369** as a yellow solid; mp 77.5-77.9 °C; R_f 0.46 (Hexane/EtOAC 1:1); ^{1}H NMR (DMSO-d_6) δ 2.18 (s, 3 H, *CH*$_3$), 2.39 (s, 3 H, *CH*$_3$), 3.47 (d, 3 H, *J* = 0.4 Hz,*CH*$_3$), 4.64-4.65 (t, 1 H, *J* = 0.8 Hz, *CH*), 7.24-7.26 (d, 2 H, *J* = 8.4 Hz, 2 *CH*), 7.32-7.34 (d, 2 H, *J* = 8.4 Hz, 2 *CH*), 8.32 (s, 1H, CH); Anal. Calcd. for $C_{15}H_{15}N_3O$: C, 71.13; H, 5.97; N, 16.59. Found C, 70.94; H, 5.98; N,16.60.

***N*-(4-chlorophenyl)-N,2,6-trimethylfuro[2,3-d]pyrimidin-4-amine** (**370**). To a 50 mL flask was added **495** (84 mg, 0.5 mmol), 4-chloro-*N*-methylaniline (78 mg, 0.55 mmol) and BuOH (5 mL). To this solution was added 2 drops of concentrate HCl solution and the mixture was refluxed. TLC indicated the disappearance of starting material **495**, the solvent was removed under reduced pressure. To the residue obtained was added silica gel and MeOH and the solvent removed to make a plug. This plug was separated by column chromatography to give 83 mg (61%) of **370** as a light yellow powder; mp 117.6-117.9 °C; R_f 0.19 (Hexane/EtOAC 3:1); ^{1}H NMR ($CDCl_3$) δ 2.23 (s, 3 H, *CH*$_3$), 3.57 (s, 3 H, N*CH*$_3$), 4.89 (s, 1 H, CH), 7.42-7.44 (d, 2 H, *J* = 8.8 Hz, 2 *CH*), 7.45-7.43 (d, 2 H, *J* = 8.8 Hz, 2 *CH*), 8.35 (s, 1 H, CH); Anal. Calcd. for $C_{14}H_{12}ClN_3O$: C, 61.43; H, 4.42; N, 15.35; Cl, 12.95. Found C, 61.51; H, 4.44; N,15.31; Cl, 12.86.

***N*-(3,4-dichlorophenyl)-N,2,6-trimethylfuro[2,3-d]pyrimidin-4-amine** (**371**). To a 50 mL flask

was added **495** (84 mg, 0.5 mmol), 3,4-dichloro-*N*-methylaniline (96 mg, 0.55 mmol) and BuOH (5 mL). To this solution was added 2 drops of concentrate HCl solution and the mixture was refluxed. TLC indicated the disappearance of starting material **495**, the solvent was removed under reduced pressure. To the residue obtained was added silica gel and MeOH and the solvent removed to make a plug. This plug was separated by column chromatography to give 78 mg (51%) of **371** as a colorless crystal; mp 147.6-147.9°C; R_f 0.19 (Hexane/EtOAC 3:1); ^{1}H NMR ($CDCl_3$) δ 2.28 (s, 3 H, *CH*$_3$), 3.52 (s, 3 H, N*CH*$_3$), 5.20 (s, 1 H, *CH*), 7.38-7.40 (dd, 1 H, J_1 = 8.4 Hz, J_2 = 2.4 Hz, 1 *CH*), 7.73-7.75 (d, 1 H, *J* = 8.4 Hz, 1 *CH*), 7.78-7.79 (d, 1 H, *J* = 2.4 Hz, 1 *CH*), 8.37 (s, 1 H, *CH*); Anal. Calcd. for $C_{14}H_{11}Cl_2N_3O$: C, 54.47; H, 3.60; N, 13.64; Cl, 23.01. Found C, 54.84; H, 3.57; N,13.36; Cl, 22.72.

***N*-(3,4-dichlorophenyl)-N,2,6-trimethylfuro[2,3-d]pyrimidin-4-amine** (**372**). To a 50 mL flask was added **495** (84 mg, 0.5 mmol), 4-(benzyloxy)-*N*-methylaniline (117g, 0.55 mmol) and BuOH (5 mL). To this solution was added 2 drops of concentrate HCl solution and the mixture was refluxed. TLC indicated the disappearance of starting material **495**, the solvent was removed under reduced pressure. To the residue obtained was added silica gel and MeOH and the solvent removed to make a plug. This plug was separated by column chromatography to give 112 mg (65%) of **372** as a brown solid; mp 148.5-149.1°C; R_f 0.64 (Hexane/EtOAC 3:1); ^{1}H NMR ($CDCl_3$) δ 2.18 (s, 3 H, *CH*$_3$), 3.46 (s, 3 H, N*CH*$_3$), 4.60 (s, 1 H, *CH*), 5.20 (s, 2 H, *CH*$_2$) 7.13-7.49 (m, 9 H, 9 *CH*), 8.30 (s, 1 H, *CH*); Anal. Calcd. for $C_{21}H_{19}N_3O$: C, 73.03; H, 5.54; N, 12.17. Found C, 73.10; H, 5.56; N,12.01.

5-Methylfuro[2,3-*d*]pyrimidin-4-amine (501). Sodium metal (2.3 g; 0.1 M) was added cautiously to stirred anhydrous Ethanol (5.8 mL, 0.1 M) over 10 min at room temperature. After stirring the resulting slurry for additional 5 min, formamidine hydrochloride (8.05 gm, 0.1 M)

was added. The slurry was stirred at room temperature for 30 min after which solution of **499** (crude; 13 g, ≈ 0.1 M) in anhydrous ethanol (200 mL) was added. The mixture was heated at reflux for 8 h. After cooling the reaction mixture to room temperature, silica gel (25 g) was added and solvents evaporated under reduced pressure to obtain a plug. Purification was done by flash chromatography using 1% methanol in chloroform. The fractions corresponding to the product spot were pooled and evaporated under reduced pressure to obtain **501** (5.3 g, 35 %) as lustrous pink crystals. TLC R_f 0.29 ($CHCl_3$: MeOH, 10:1); mp 240.2-242.5 °C; ^{1}HNMR (300 MHz) (DMSO-d_6): δ 2.28 (s, 3H, CH_3); 7.01 (br, 2H, NH_2, exch), 7.52 (s, 1H, C6-C*H*), 8.12 (s, 1H, C2-C*H*). Anal. Calcd for $C_7H_7N_3O$: C, 56.37; H, 4.73; N, 28.17; Found: C, 56.48; H, 4.74; N, 28.17.

***N*-(4-methoxyphenyl)-5-methylfuro[2,3-*d*]pyrimidin-4-amine (503):** A 50 mL round bottom flask with a stir bar was charged with copper iodide (66.5 mg, 0.35 mmol), anhydrous potassium carbonate (480 mg, 3.5 mmol), L-proline (80 mg, 0.7 mmol), **501** (150 mg, 1 mmol) and **502** (135 mg, 1.1 mmol). The flask was connected to vacuum for 3 min followed by the addition of anhydrous DMF (5 mL) using syringe. The flask was purged with argon for 5 min and then heated in an oil bath maintained at 110 °C. On heating the suspension became bluish grey which lasted for about 2 h. The reaction was stirred for additional 22 h at 110 °C at the end of which the mixture was allowed to cool to room temperature. Ethyl acetate (25 mL) was added and the mixture was poured into water (100 mL). The product was extracted with ethyl acetate (100 mL x 2). The combined organic extracts were washed with brine (100 mL) and dried (anhydrous sodium sulfate) and concentrated under reduced pressure. Silica gel (500 mg) was added and solvent evaporated to obtain a plug. Purification by column chromatography using hexanes and ethyl acetate (10:1 to 2:1) afforded **503** (140 mg, 56 %) as light brown solid. TLC R_f 0.77

($CHCl_3$: MeOH, 10:1); mp 99-101.6 °C; ^{1}HNMR (400 MHz) (DMSO-d_6): δ 2.38-2.38 (d, 3H, CH_3, J = 1.2 Hz); 3.74 (s, 3H, OCH_3), 6.91-6.94 (d, 2H, C_6H_4, J = 8.8 Hz), 7.46-7.48 (d, 2H, C_6H_4, J = 8.8 Hz), 7.65-7.65 (d, 1H, C6-C*H*, J = 1.2 Hz), 8.23 (s, 1H, C2-C*H*), 8.38 (s, 1H, 4-N*H*, exch). Anal. Calcd for $C_{14}H_{13}N_3O_2$: C, 65.87; H, 5.13; N, 16.46; Found: C, 65.94; H, 5.13; N, 16.42.

***N*-(4-methoxyphenyl)-*N*,5-dimethylfuro[2,3-*d*]pyrimidin-4-amine (373):**

To a 25 mL round bottom flask was weighed **503** (51 mg, 0.2 mmol) and was added DMF (2 mL) to afford a solution. The flask was purged with argon for five min followed by cooling down to 0 °C using ice bath. Sodium hydride (14.4 mg, 0.6 mmol) was added to the solution at 0 °C. The solution was stirred for 30 min at 0 °C under argon atmosphere. Dimethyl sulfate (75.7 mg; ≈ 57μl; 0.6 mmol) was introduced to the reaction mixture with the help of a syringe and the flask was warmed to room temperature. The mixture was stirred at room temperature for another 3h at the end of which 1 N Hydrochloric acid (5 mL) was added carefully to quench the reaction followed by water (20 mL) to afford a precipitate. Product was extracted using ethyl acetate (10 mL x 2). Combined organic extracts were washed with brine (10 mL) dried (anhydrous sodium sulfate) and concentrated under reduced pressure. Silica gel (200 mg) was added and solvent evaporated to afford a plug. Column chromatography by elution with hexanes: ethyl acetate (5:1) afforded **3** (20 mg; 37 %) as light brown semisolid; which was triturated with hexanes to afford light brown solid. TLC R_f 0.79 ($CHCl_3$: MeOH, 10:1); mp 84-85.6 °C; ^{1}HNMR (400 MHz) (DMSO-d_6): δ 1.03 (d, 3H, CH_3, J = 1.2 Hz); 3.42 (s, 3H, NCH_3), 3.75 (s, 3H, OCH_3), 6.94-6.96 (d, 2H, C_6H_4, J = 9.2 Hz), 7.17-7.19 (d, 2H, C_6H_4, J = 9.2 Hz), 7.50 (d, 1H, C6-C*H*, J = 1.2 Hz), 8.23 (s, 1H, C2-C*H*). Anal. Calcd for $C_{15}H_{15}N_3O_2 \cdot 0.28\ C_6H_{14} \cdot 0.05$ HCl: C, 67.84; H, 6.48; N, 14.22; Found: C, 67.89; H, 6.18; N, 14.06.

Ethyl 2-amino-5-methylthiophene-3-carboxylate (506). A mixture of sulfur (1.1 g, 36 mmol), propanal (2.09 g, 36 mmol) , ethyl cyanoactetate (4.07 g, 36 mmol) and EtOH (150 mL) were placed in a round bottom flask and warmed to 45 ^{o}C and treated dropwise with morpholine (3.1 g, 36 mmol) over 15 min. The mixture was stirred for 5 h at 45 ^{o}C and 24 h at room temperature. Unreacted sulfur was removed by filtration, and the filtrate was concentrated under reduced pressure to afford an orange oil. The residue was loaded on a silica gel column packed with silica gel and eluted with 10% ethyl acetate in hexane. The fractions containing the desired product (TLC) were pooled and evaporated to afford 4.45 g of **7** (73 %) as an orange solid; R_f 0.45 (hexane/EtOAc 3:1); ^{1}H NMR (DMSO-d_6): δ 1.22-1.25 (t, 3 H, J = 6.8 Hz, $COOCH_2CH_3$), 2.17-2.18 (d, 3 H, J = 1.2 Hz, 2-CH_3), 4.12-4.17 (q, 2 H, J = 6.8 Hz, $COOCH_2CH_3$), 6.49 (d, 1 H, J = 1.6 Hz, 3-CH), 7.09 (s, 2 H, NH_2 exch).

2,6-dimethylthieno[2,3-*d*]pyrimidin-4(3*H*)-one (507). To a 100 mL round flask were added **506** (1.85 g, 10 mmol) and CH_3CN (50 mL). After vigorous stirring, a clear solution was afforded. Anhydrous hydrochloric acid gas was bubbled into the solution for 1 h to give a thick precipitation, which then redissolved into the acid solution. Anhydrous hydrochloric acid gas was continued for an additional 3 h after the reaction solution became clear. After evaporation of the solvent under reduced pressure, the residue was dissolved in water. Concentrated aqueous ammonium hydroxide was added to afford a pH = 8 suspension. The precipitate was collected by filtration, washed with water and dried over P_2O_5 vacuum to afford **507** (1.1 g, 63%) as a white solid; mp > 300 ^{o}C; R_f 0.58 (MeOH/$CHCl_3$, 1:6); ^{1}H NMR (DMSO-d_6) δ 2.34 (s, 3 H), 2.44 (s, 3 H). 7.0 (s, 1 H,5-CH), 7.78 (s, 1 H, C_6H_3), 12.31 (s, 1H, 3-NH exch).

4-chloro-2,6-dimethylthieno[2,3-*d*]pyrimidine (508). To a 50-mL round-bottomed flask was added **507** (900 mg, 5 mmol) in 15 mL phosphorus oxychloride. The reaction mixture was heated

at reflux with stirring in an anhydrous atmosphere for 3 h. All the suspensions were dissolved after heating to afford a dark solution. The dark orange solution was allowed to cool to room temperature and concentrated in vacuo. Water (20 mL) was then added to the residue at 0 ^{o}C with vigorous stirring to give an exothermic reaction. Concentrated aqueous ammonium hydroxide was added to afford a pH = 5 solution. The aqueous solution was extracted with AcOEt (3 x 15 mL) and the organic layer was pooled and dried in vacuo. The crude product was purified by silica gel column chromatography with 10% AcOEt/Haxene. Recrystallization from AcOEt afforded 831 mg (84%) of **508** as a white crystal: mp 102.1-103.7; *Rf* 0.54 (Hexane/EtOAC 3:1); 1H NMR (DMSO-*d*6) δ 2.59-2.60 (d, 2 H, *J* = 1.2 Hz, 6-CH_3), 2.69 (s, 3 H, 2-CH_3), 6.63 (s, 1 H, *J* = 1.2 Hz, 5-CH).

***N*-(4-methoxyphenyl)-2,6-dimethylthieno[2,3-*d*]pyrimidin-4-amine** (**509**). To a 50 mL flask was added **508** (99 mg, 0.5 mmol), 4-methoxyaniline (68 mg, 0.55 mmol) and BuOH (5 mL). To this solution was added 2 drops of concentrate HCl solution and the mixture was refluxed. TLC indicated the disappearance of starting material **5**, the solvent was removed under reduced pressure. To the residue obtained was added silica gel and MeOH and the solvent removed to make a plug. This plug was separated by column chromatography to give 105 mg (74%) of **509** as a white crystal; mp 164.2-166.8°C; R_f 0.08 (Hexane/EtOAC 3:1); ^{1}H NMR (DMSO-d_6) δ 2.50 (s, 3 H, CH_3), 2.57 (s, 3 H, CH_3), 3.78 (s, 3 H, OCH_3), 6.97-6.99 (d, 2 H, *J* = 8.8 Hz, C_6H_4), 7.49 (s, 1 H, *CH*), 7.67-7.69 (d, 2 H, *J* = 8.8 Hz, C_6H_4), 9.76 (s, 1 H, NH exch)

***N*-(4-methoxyphenyl)-*N*,2,6-trimethylthieno[2,3-*d*]pyrimidin-4-amine (374):**

To a 25 mL round bottom flask was weighed **509** (57 mg, 0.2 mmol) and was added DMF (2 mL) to afford a solution. The flask was purged with argon for five min followed by cooling down to 0 °C using ice bath. Sodium hydride (14.4 mg, 0.6 mmol) was added to the solution at 0 °C. The

solution was stirred for 30 min at 0 °C under argon atmosphere. Dimethyl sulfate (75.7 mg; ≈ 57µl; 0.6 mmol) was introduced to the reaction mixture with the help of a syringe and the flask was warmed to room temperature. The mixture was stirred at room temperature for another 3h at the end of which 1 N Hydrochloric acid (5 mL) was added carefully to quench the reaction followed by water (20 mL) to afford a precipitate. Product was extracted using ethyl acetate (10 mL x 2). Combined organic extracts were washed with brine (10 mL) dried (anhydrous sodium sulfate) and concentrated under reduced pressure. Silica gel (200 mg) was added and solvent evaporated to afford a plug. Column chromatography by elution with hexanes: ethyl acetate (5:1) afforded 28 mg of **374** (47 %) as a yellow solid: mp 108.6-109.2 °C; R_f 0.13 (hexane: AcOEt, 3:1); ^{1}HNMR (400 MHz) (DMSO-d_6): δ 2.20-2.21 (d, 3H, J = 1.2 Hz, 6-CH_3); 2.51 (s, 3H, 2-CH_3), 3.46 (s, 3H, NCH_3), 3.83 (s, 3H, OCH_3), 5.16 (d, 1H, J = 1.2 Hz, 5-CH), 7.05-7.07 (d, 2H, J = 9.2 Hz, C_6H_4,), 7.17-7.19 (d, 2H, J = 9.2 Hz , C_6H_4). Anal. Calcd for $C_{16}H_{17}N_3OS$: C, 64.19; H, 5.72; N, 14.04; Found: C, 64.33; H, 5.68; N, 13.90.

1-(2,6-dimethylthieno[2,3-d]pyrimidin-4-yl)-6-methoxy-1,2,3,4-tetrahydroquinoline (376)

To a 100-mL round-bottomed flask, flushed with nitrogen, were added **508** (198 mg, 1 mmol), 6-methoxy-1,2,3,4-tetrahydroquinoline (171 mg, 1.05 mmol), BuOH (20 mL), and 2-3 drops of concd HCl. The reaction mixture was heated at reflux with stirring for 2 h until the starting material **508** disappeared (TLC). The reaction solution was allowed to cool to room temperature; the solvent was removed under reduced pressure to dryness and the residue was purified by column chromatography on silica gel with 10% AcOEt/Haxene as the eluent. Fractions containing the product (TLC) were combined and evaporated to afford 120 mg (37%) of **376** as a light yellow powder: mp 140.5-142.0 °C; *Rf* 0.21 (AcOEt/Haxene, 1:3); 1H NMR (DMSO-*d*6) δ 1.91-1.97 (oct, 2 H, J = 6.4, $CH_2CH_2CH_2$), 2.35 (s, 3 H, CH_3), 2.52 (s, 3 H, CH_3), 2.74-2.77 (t, 2

H, *J* = 6.4, $CH_2CH_2\mathit{CH_2}$), 3.76 (s, 3 H, $O\mathit{CH_3}$), 3.92-3.95 (t, 2 H, *J* = 6.4, $\mathit{CH_2}CH_2CH_2$), 6.03 (s, 1 H, *CH*), 6.68-6.71 (dd, 1 H, J_1 = 8.8, J_2 = 2.8 , *CH*), 6.84-6.86 (d, 1 H, *J* = 8.8, *CH*), 6.87-6.88 (d, 1 H, *J* = 2.8, *CH*); Anal. Calcd. for $C_{18}H_{19}N_3OS$: C, 66.43; H, 5.88; N, 12.91. Found C, 66.62; H, 5.87; N,12.81.

ethyl 2-amino-4-methylthiophene-3-carboxylate (511). A mixture of sulfur (1.92 g, 60 mmol), acetone (3.48 g, 60 mmol), ethyl cyanoactetate (6.78 g, 60 mmol) and EtOH (100 mL) were placed in a round bottom flask and warmed to 45 ^oC and treated dropwise with morpholine (5.23 g, 60 mmol) over 15 min. The mixture was stirred for 4 h at 45 ^oC and 24 h at room temperature. Unreacted sulfur was removed by filtration, and the filtrate was concentrated under reduced pressure to afford an orange oil. The residue was loaded on a silica gel column packed with silica gel and eluted with 10% ethyl acetate in hexane to afford **511** (8.1 g, 72%) as a yellow solid; mp 76.2-76.7 ^oC; R_f 0.66 (hexane/EtOAc 3:1); ^1H NMR ($CDCl_3$) δ 1.24-1.28 (t, 3 H, *J* = 6.4, $OCH_2\mathit{CH_3}$), 2.18 (s, 3 H, $\mathit{CH_3}$), 4.15-4.21 (q, 2 H, *J* = 6.4, $O\mathit{CH_2}CH_3$), 5.93 (s, 1 H, *CH*), 7.29 (s, 2 H, $\mathit{NH_2}$ exch).

2,5-dimethylthieno[2,3-d]pyrimidin-4(3H)-one (512). To a 100 mL round flask were added **511** (1.81 g, 9.8 mmol) and 30 mL CH_3CN. After vigorous stirring, a clear solution was afforded. Anhydrous hydrochloric acid gas was bubbled into the solution for 1 h to give a thick precipitation, which then redissolved into the acid solution. Anhydrous hydrochloric acid gas was continued for an additional 3 h after the reaction solution became clear. After evaporation of the solvent under reduced pressure, the residue was dissolved in water. Concentrated aqueous ammonium hydroxide was added to afford a pH = 8 suspension. The precipitate was collected by filtration, washed with water and dried over P_2O_5 vacuum to afford **512** (1.0 g, 57%) as a yellow solid; mp 285.4-286.7 ^oC; R_f 0.58 (MeOH/$CHCl_3$, 1:6); ^1H NMR (DMSO-d_6) δ 2.34 (s, 3 H,

CH$_3$), 2.48 (s, 3 H, *CH*$_3$). 7.02 (s, 1 H, *CH*), 12.33 (s, 1 H, *3-NH* exch).

4-Chloro-2,5-dimethylthieno[2,3-d]pyrimidine (513). To a 50-mL round-bottomed flask was added **512** (900 mg, 5 mmol) in 15 mL phosphorus oxychloride. The reaction mixture was heated at reflux with stirring in an anhydrous atmosphere for 3 h. All the suspensions were dissolved after heating to afford a dark solution. The dark orange solution was allowed to cool to room temperature and concentrated in vacuo. Water (20 mL) was then added to the residue at 0 ^{o}C with vigorous stirring to give an exothermic reaction. Concentrated aqueous ammonium hydroxide was added to afford a pH = 5 solution. The aqueous solution was extracted with AcOEt (3 x 15 mL) and the organic layer was pooled and dried in vacuo. The crude product was purified by silica gel column chromatography with 10% AcOEt/Haxene. Recrystallization from AcOEt afforded 831 mg (84%) of **513** as a yellow crystal: mp 67.4-67.7 °C; *Rf* 0.5 (Hexane/AcOEt, 3:1); 1H NMR (DMSO-*d*6) δ 2.62-2.63 (d, 3 H, *J* = 1.2, *CH*$_3$), 2.68 (s, 3 H, *CH*$_3$), 7.22-7.23 (d, *J* = 1.2,1 H, *CH*).

***N*-(4-methoxyphenyl)-2,5-dimethylthieno[2,3-d]pyrimidin-4-amine (514)** To a 100-mL round-bottomed flask, flushed with nitrogen, were added **513** (198 mg, 1 mmol), 4-methoxylaniline (129 mg, 1.05 mmol), *i*-PrOH (20 mL), and 2-3 drops of concd HCl. The reaction mixture was heated at reflux with stirring for 2 h until the starting material **513** disappeared (TLC). The reaction solution was allowed to cool to room temperature; the solvent was removed under reduced pressure to dryness and the residue was purified by column chromatography on silica gel with 10% AcOEt/Haxene as the eluent. Fractions containing the product (TLC) were combined and evaporated to afford 210 mg (74%) of **514** as a brown crystal: mp 111.2-111.9 °C; *Rf* 0.08 (AcOEt/Haxene, 1:3); 1H NMR (DMSO-*d*6) δ 2.43 (s, 3 H, *CH*$_3$), 2.69 (d, 3 H, *J* = 0.8, *CH*$_3$), 3.77 (s, 3 H, O*CH*$_3$), 6.94-6.96 (d, 2 H, *J* = 9.2, 2 *CH*), 7.15 (d, 2 H, *J*

= 0.8, 2 *CH*), 7.58-7.61 (d, 2 H, *J* = 9.2, 2 *CH*), 8.04 (s, 1 H, *NH exch*), Anal. Calcd. for $C_{15}H_{15}N_3OS$: C, 63.13; H, 5.30; N, 14.73. Found C, 63.30; H, 5.27; N,14.58.

***N*-(4-methoxyphenyl)-N,2,5-trimethylthieno[2,3-d]pyrimidin-4-amine (375)** To a 25 mL round bottom flask was weighed **514** (144 mg, 0.5 mmol) and was added DMF (2 mL) to afford a solution. The flask was purged with argon for five min followed by cooling down to 0 °C using ice bath. Sodium hydride (36 mg, 1.5 mmol) was added to the solution at 0 °C. The solution was stirred for 30 min at 0 °C under argon atmosphere. Dimethyl sulfate (150 mg, 1.2 mmol) was introduced to the reaction mixture with the help of a syringe and the flask was warmed to room temperature. The mixture was stirred at room temperature for another 3h at the end of which 1 N Hydrochloric acid (5 mL) was added carefully to quench the reaction. The reaction solvent was removed under reduced pressure and the residue was suspended in water (20 mL). The suspension was extracted using ethyl acetate (10 mL x 2). Combined organic extracts were washed with brine (10 mL) dried (anhydrous sodium sulfate) and concentrated under reduced pressure. Silica gel (200 mg) was added and solvent evaporated to afford a plug. Column chromatography by elution with hexanes: ethyl acetate (5:1) afforded 70 mg (47 %) of **375** as a yellow powder: mp 113.5-113.9 °C; *Rf* 0.13 (AcOEt/Haxene, 1:3); 1H NMR (DMSO-*d*6) δ 1.55 (d, 3 H, *J* = 0.8, CH_3), 2.59 (s, 3 H, CH_3), 3.45 (s, 3 H, NCH_3), 3.72 (s, 3 H, OCH_3), 6.85-6.87 (d, 2 H, *J* = 8.8, 2 *CH*), 6.94-6.96 (d, 2 H, *J* = 8.8, 2 *CH*), 7.03 (d, 1 H, *J* = 0.8, *CH*); Anal. Calcd. for $C_{16}H_{17}N_3OS$: C, 64.19; H, 5.72; N, 14.04. Found C, 64.38; H, 5.73; N,13.81.

1-(2,5-Dimethylthieno[2,3-d]pyrimidin-4-yl)-6-methoxy-1,2,3,4-tetrahydroquinoline (377) To a 100-mL round-bottomed flask, flushed with nitrogen, were added **513** (198 mg, 1 mmol), 6-methoxy-1,2,3,4-tetrahydroquinoline (171 mg, 1.05 mmol), BuOH (20 mL), and 2-3 drops of concd HCl. The reaction mixture was heated at reflux with stirring for 2 h until the starting

material **513** disappeared (TLC). The reaction solution was allowed to cool to room temperature; the solvent was removed under reduced pressure to dryness and the residue was purified by column chromatography on silica gel with 10% AcOEt/Haxene as the eluent. Fractions containing the product (TLC) were combined and evaporated to afford 120 mg (37%) of **377** as a light yellow crystal: mp 102.6-102.8 °C; *Rf* 0.29 (AcOEt/Haxene, 1:3); 1H NMR (DMSO-*d*6) δ 1.73 (s, 3 H, *J* = 1.2, *CH*$_3$), 2.00-2.03 (m, 2 H, *J* = 5.2, $CH_2CH_2CH_2$), 2.79 (s, 3 H, *CH*$_3$), 2.79-2.82 (t, 2 H, *J* = 5.2, $CH_2CH_2CH_2$), 3.69 (s, 3 H, O*CH*$_3$), 3.78-3.81 (t, 2 H, *J* = 5.2, $CH_2CH_2CH_2$), 6.35-6.37 (d, 1 H, *J* = 7.2, *CH*), 6.52-6.55 (dd, 1 H, J_1 = 7.2, J_2 = 2.4 , *CH*), 6.80 (d, 1H, *J* = 2.4, *CH*), 7.15 (d, 1 H, *J* = 1.2, *CH*); Anal. Calcd. for $C_{18}H_{19}N_3OS$: C, 66.43; H, 5.88; N, 12.91; S, 9.85. Found C, 66.66; H, 5.88; N,12.77; S, 9.63.

General procedure for the synthesis of 516-518: Compound **515** (2.05 g, 10 mmol) was dissolved into *n*-butanol (20 mL). To this solution were added the appropriate amine (10 mmol) and triethylamine (6 mL). The mixture was refluxed for 3 days before the solvent was removed by evaporation. To the residue was added methanol (50 ml) and silica gel (6 g) and the solvent was evaporated to make a plug. The silica gel plug obtained was loaded onto a silica gel column and eluted with 1:1:7 ethyl acetate/triethylamine/hexanes. Fractions containing the product (TLC) were pooled and the solvent evaporated to afford analytically pure compounds **6**, respectively.

4-Methyl-7-phenyl-6,7-dihydro-5*H*-pyrrolo[2,3-*d*]pyrimidin-2-amine (516). Compound **516** was synthesized from **515** and aniline. The general procedure described above was applied to afford 768 mg of **516** (34%) as a colorless crystal: R_f 0.17 (EtOAc/TEA/hexane, 3:1:5); mp 215.4-216.2 °C; ^{1}H NMR (DMSO-d_6) δ 2.05 (s, 3 H, CH_3), 2.87-2.93 (t, 2 H, *J* = 11.6 Hz, CH_2), 3.93-3.99 (t, 2 H, *J* = 11.6 Hz, CH_2), 6.07 (s, 2 H, NH_2, exch.), 6.94-6.99 (t, 1 H, *J* = 9.6 Hz, 3'-CH), 7.29-7.34 (t, 2 H, *J* = 10.0 Hz, 2'-CH), 7.84-7.87 (d, 2 H, *J* = 12 Hz, 1'-CH); Anal. Calcd.

for $C_{13}H_{14}N_4$: C, 69.00; H, 6.24; N, 24.76. Found C, 69.07; H, 6.29; N, 24.74.

4-Methyl-7-(2-phenylethyl)-6,7-dihydro-5*H*-pyrrolo[2,3-*d*]pyrimidin-2-amine (517). Compound **517** was synthesized from **515** and aniline. The general procedure described above was applied to afford 1.75 g of **517** (69%) as a colorless crystal. The compound was used directly in the next step without further characterization.

4-Methyl-7-(3-phenylpropyl)-6,7-dihydro-5*H*-pyrrolo[2,3-*d*]pyrimidin-2-amine (518). Compound **518** was synthesized from **515** and aniline. The general procedure described above was applied to afford 1.98 g of **518** (74%) as a colorless crystal. The compound was used directly in the next step without further characterization.

General procedure for the synthesis of 326a-m: Compound **516-518** was dissolved in anhydrous 1,4-dioxane in a 250 mL round bottom flask and manganese dioxide was added to the solution. The reaction mixture was heated in oil bath at 120 °C for 24 h. The resulting slurry was filtered through celite pad. To the filtration was added silica gel (6 g) and the solvent was evaporated to make a plug. The silica gel plug obtained was loaded onto a silica gel column and eluted with 1:1 hexane/EtOAc. Fractions containing the product (TLC) were pooled and the solvent evaporated to afford analytically pure compound.

4-Methyl-7-phenyl-7*H*-pyrrolo[2,3-*d*]pyrimidin-2-amine (519)

Using the general procedure described above, compound **516** reacted with MnO_2 to afford **519** (176 mg, 29%) as a colorless crystal: R_f 0.48 (EtOAc/TEA/hexane, 3:1:5); mp 202.6-202.9 °C; ^{1}H NMR (DMSO-d_6) δ 2.47 (s, 3 H, CH_3), 6.24 (s, 2 H, NH_2, exch.), 6.60-6.62 (d, 1 H, J = 4.8 Hz, 5-CH), 7.29-7.34 (t, 1 H, J = 10.0 Hz, C_6H_5), 7.29-7.31 (d, 2 H, J = 4.8 Hz, 6-CH), 7.48-7.53 (t, 2 H, J = 10.0 Hz, C_6H_5), 7.81-7.84 (d, 2 H, J = 10.0 Hz, C_6H_5); Anal. Calcd. for $C_{13}H_{14}N_4$: C, 69.62; H, 5.39; N, 24.98. Found C, 69.65; H, 5.48; N, 24.21.

4-Methyl-7-(2-phenylethyl)-7*H*-pyrrolo[2,3-*d*]pyrimidin-2-amine (520). Using the general procedure described above, compound **517** reacted with MnO_2 to afford **520** (1.14 g, 60%) as a colorless crystal. The resulted compound was used directly in next step without further characterization.

4-Methyl-7-(3-phenylpropyl)-7*H*-pyrrolo[2,3-*d*]pyrimidin-2-amine (521). Compound 521 was synthesized from 518 (2.5 g, 14 mmol), manganese dioxide (5.5 g, 63 mmol) using the general procedure described above to afford after purification 1.06 g (45%) as a yellow solid: R_f 0.53 (EtOAc/TEA/Hexane, 3:1:5); mp 129.3-130.5 °C; ^{1}H NMR (DMSO-d_6) δ 2.43 (s, 3 H, CH_3), 3.85 (s, 3 H, OCH_3), 5.17 (s, 2 H, CH_2Ph), 6.13 (s, 2 H, NH_2, exch.), 6.42 (d, 1 H, 5-H), 6.93 (d, 1 H, 6-H), 6.95-7.32 (m, 4 H, C_6H_4). Anal. calcd. for ($C_{15}H_{16}N_4O$): C, 67.15; H, 6.01; N, 20.88; found: C, 66.84; H, 6.02; N, 20.74.

General procedure for the synthesis of 522-524: To a 100 mL round-bottom flask was added **519-521** and pivaloyl anhydride (5 eq) and the resulting mixture was refluxed under N_2 atmosphere for 2.5 h. TLC showed the disappearance of the starting material **522-524** and the formation of a new spot. After evaporation of the solvent, the residue was loaded onto a silica gel column and eluted with hexane followed by 25% ethyl acetate in hexane. Fractions containing the product (TLC) were pooled and the solvent evaporated to afford analytically pure compound.

2,2-Dimethyl-*N*-(4-methyl-7-phenyl-7*H*-pyrrolo[2,3-*d*]pyrimidin-2-yl)propanamide (522)

Using the general procedure described above, compound **519** reacted with pivalyl anhydride to afford **522** (460 mg, 54%) as a light yellow solid: R_f 0.54 (EtOAc/hexane, 3:5); mp 168.4-168.7 °C; ^{1}H NMR (DMSO-d_6) δ 1.07 (s, 9 H, Piv), 2.34 (s, 3 H, CH_3), 6.70 (d, 1 H, 5-CH), 7.20 (t, 1 H, C_6H_5), 7.39 (t, 2 H, C_6H_5), 7.71 (d, 1 H, 6-CH), 7.82 (d, 2 H, C_6H_5).

2,2-Dimethyl-*N*-[4-methyl-7-(2-phenylethyl)-7*H*-pyrrolo[2,3-*d*]pyrimidin-2-yl]propanamide

(523)

Using the general procedure described above, compound **520** reacted with pivalyl anhydride to afford **523** (849 mg, 36%) as a light yellow solid: R_f 0.62 (EtOAc/ hexane, 3:1:5); mp 148.5-148.7 °C; ^{1}H NMR (DMSO-d_6) δ 1.27 (s, 9 H, Piv), 2.64 (s, 3 H, CH_3), 3.14-3.17 (t, 2 H, J = 5.6 Hz, CH_2), 4.42-4.45 (t, 2 H, J = 5.6 Hz, CH_2), 7.19-7.35 (m, 5 H, C_6H_5), 10.05 (br, NH exch).

2,2-Dimethyl-*N*-[4-methyl-7-(3-phenylpropyl)-7*H*-pyrrolo[2,3-*d*]pyrimidin-2-yl]propanamide (524).

Using the general procedure described above, compound **521** reacted with pivalyl anhydride to afford **524** (1.3 g, 72%) as a light yellow solid: R_f 0.66 (EtOAc/ hexane, 3: 5); mp 150.1-150.3 °C; ^{1}H NMR (DMSO-d_6) δ 1.24 (s, 9 H, Piv), 2.04 (m, 2 H, CH_2), 2.60 (s, 3 H, CH_3), 2.54 (m, 2 H, CH_2), 4.17 (t, 2 H, CH_2), 6.63 (d, 1 H, 5-CH), 7.27-7.35 (m, 5 H, C_6H_5), 7.47 (d, 2 H, 6-CH), 9.73 (br, NH exch).

General procedure for the synthesis of 525-527: Compound **522-524** was dissolved into anhydrous DMF in a 100 mL round bottom flask protected from light with aluminum foil. To this solution was added *N*-iodosuccinimide. The dark brown solution was stirred at room temperature under nitrogen for 18 h. The solvent was stripped off in vacuum and the residue was dissolved in dichloromethane (100 mL), washed with brine (100 mL x 2). The organic layer was dried over sodium sulfate. To the filtration was added silica gel (3.0 g) and the solvent was evaporated to make a plug. The silica gel plug obtained was loaded onto a silica gel column and eluted with 15:1 hexane/EtOAc. Fractions containing the product (TLC) were pooled and the solvent evaporated to afford products.

***N*-(5-iodo-4-methyl-7-phenyl-7*H*-pyrrolo[2,3-*d*]pyrimidin-2-yl)-2,2-dimethylpropanamide**

(525).

Compound **525** was synthesized from **522** (0.93 g, 2.21 mmol), *N*-iodosuccinimide (0.58g, 2.43 mmol) using the general procedure described above to afford after purification 0.90 g (74%) as a light yellow solid. The compound was used directly in next step without further characterization.

***N*-[5-iodo-4-methyl-7-(2-phenylethyl)-7*H*-pyrrolo[2,3-*d*]pyrimidin-2-yl]-2,2-dimethylpropanamide (526).** Using the general procedure described above, compound 6 reacted with NIS to afford **526** (327 mg, 34%) as a yellow crystal: R_f 0.17 (EtOAc /hexane, 1:5); mp 142.2-142.5 °C; ^{1}H NMR (DMSO-d_6) δ 1.21 (s, 9 H, Piv), 2.80 (s, 3 H, 4-CH_3), 3.10-3.17 (t, 2 H, J = 9.9 Hz, CH_2), 4.36-4.41 (t, 2 H, J = 9.9 Hz, CH_2), 7.24 (m, 5 H, C_6H_5), 7.58 (s, 1 H, 6-CH), 9.86 (br, 1 H, NH exch).

***N*-[5-iodo-4-methyl-7-(3-phenylpropyl)-7*H*-pyrrolo[2,3-*d*]pyrimidin-2-yl]-2,2-dimethylpropanamide (527).** Compound **527** was synthesized from **523**, *N*-iodosuccinimide using the general procedure described above to afford after purification 1.22 g (83%) light yellow solid. The compound was used directly in next step without further characterization.

General procedure for the synthesis of 528-533: To a 50-mL round-bottom flask covered with aluminum foil were added **525-527**, ethynyl benzene, copper (I) iodide and tetrakis(triphenylphosphine)palladium(0) dissolved in anhydrous dichloroethane (5 mL) and triethylamine. The resulting, dark brown, solution was stirred at room temperature under nitrogen for 3.5 h. Then CH_2Cl_2 (50 mL) was added to the solution and the reaction mixture was washed with brine (20 mL x 2), the organic layer separated and dried over Na_2SO_4 and filtered. The filtrate was evaporated *in vacuo*. To this residue was added silica gel (10 g) and methanol (20 mL) and the solvent evaporated to afford a plug. The silica gel plug obtained was loaded onto a silica gel column and eluted with 1:1:10 ethyl acetate/triethylamine/hexanes. Fractions containing the

product (TLC) were pooled and the solvent evaporated to afford products.

***N*-{5-[(2-methoxyphenyl)ethynyl]-4-methyl-7-phenyl-7*H*-pyrrolo[2,3-*d*]pyrimidin-2-yl}-2,2-dimethylpropanamide (528).** Using the general procedure described above, **525** reacted with 1-ethynyl-2-methoxybenzene to afford **528** (65 mg, 54%) as a yellow solid, the compound was used directly for next step hydrogenation without further characterization.

2,2-Dimethyl-*N*-{4-methyl-7-phenyl-5-[(3,4,5-trimethoxyphenyl)ethynyl]-7*H*-pyrrolo[2,3-*d*]pyrimidin-2-yl}propanamide (529). Using the general procedure described above, **525** reacted with 5-ethynyl-1,2,3-trimethoxybenzene to afford **529** (74 mg, 67%) as a yellow solid: the compound was used directly for next step hydrogenation without further characterization.

***N*-{5-[(2-methoxyphenyl)ethynyl]-4-methyl-7-(2-phenylethyl)-7*H*-pyrrolo[2,3-*d*]pyrimidin-2-yl}-2,2-dimethylpropanamide (530).** Using the general procedure described above, **526** reacted with 1-ethynyl-2-methoxybenzene to afford **532** (103 mg, 92%) as a yellow solid, the compound was used directly for next step hydrogenation without further characterization.

2,2-Dimethyl-*N*-{4-methyl-7-(2-phenylethyl)-5-[(3,4,5-trimethoxyphenyl)ethynyl]-7*H*-pyrrolo[2,3-*d*]pyrimidin-2-yl}propanamide (531). Using the general procedure described above, **526** reacted with 5-ethynyl-1,2,3-trimethoxybenzene to afford **531** (87 mg, 84%) as a yellow solid: R_f 0.69 (EtOAc/ hexane, 3: 5); mp 136.2-136.7 °C; ^{1}H NMR ($CDCl_3$) δ 1. 23 (s, 9 H, Piv), 2.87 (s, 3 H, 4-CH_3), 3.24 (m, 2 H, 2 CH_2), 3.86 (s, 9 H, 3 OCH_3), 4.47 (t, 2 H, CH_2), 6.62 (s, 2 H, C_6H_2), 7.02 (s, 1 H, 6-CH), 7.06-7.28 (m, 5 H, C_6H_5), 8.13 (s, 1 H, NH exch).

***N*-{5-[(2-methoxyphenyl)ethynyl]-4-methyl-7-(3-phenylpropyl)-7*H*-pyrrolo[2,3-*d*]pyrimidin-2-yl}-2,2-dimethylpropanamide (532).** Using the general procedure described above, **527** reacted with 1-ethynyl-2-methoxybenzene to afford **532** (94 mg, 86%) as a yellow solid: R_f 0.68 (EtOAc/TEA/hexane, 3: 5); mp 128.3.-128.7 °C; ^{1}H NMR ($CDCl_3$) δ 1. 24 (s, 9 H,

Piv), 2.45 (m, 2 H, CH_2), 2.88 (s, 3 H, 4-CH_3), 3.40 (m, 2 H, 2 CH_2), 3.87 (s, 3 H, OCH_3), 4.22 (t, 2 H, CH_2), 7.90-7.28 (m, 11 H), 7.93 (s, 1 H, NH exch).

2,2-Dimethyl-*N*-{4-methyl-7-(3-phenylpropyl)-5-[(3,4,5-trimethoxyphenyl)ethynyl]-7*H*-pyrrolo[2,3-*d*]pyrimidin-2-yl}propanamide (533). Using the general procedure described above, **527** reacted with 5-ethynyl-1,2,3-trimethoxybenzene to afford **533** (77mg, 83%) as a yellow solid, the compound was used directly for next step hydrogenation without further characterization.

General procedure for the synthesis of 534-539. To a Parr hydrogenation bottle was added **528-533** dissolved in dichloromethane (20 mL) and methanol (20 mL), followed by the addition of 5% Pd/C. The mixture was hydrogenated at 50 psi at room temperature for 3h, respectively. After filtration through celite, the catalyst was thoroughly washed with hot methanol (20 mL x 3). The filtrate was concentrated *in vacuo* and silica gel (10 g) and methanol (20 mL) were added to the residue. The solvent was evaporated to afford a plug. The silica gel plug obtained was loaded onto a silica gel column and eluted with 1:1:7 ethyl acetate/triethylamine/hexanes. Fractions containing the product (TLC) were pooled and the solvent evaporated to afford product.

***N*-{5-[2-(2-methoxyphenyl)ethyl]-4-methyl-7-phenyl-7*H*-pyrrolo[2,3-*d*]pyrimidin-2-yl}-2,2-dimethylpropanamide (534).** Compound **534** was synthesized from **528** (44 mg, 0.1 mmol), 30 mg of 5% palladium on carbon using the general procedure described above to afford after purification 36 mg (82%) as a yellow solid. Compound **528** was used directly in the deprotection step without further characterization.

2,2-Dimethyl-*N*-{4-methyl-7-phenyl-5-[2-(3,4,5-trimethoxyphenyl)ethyl]-7*H*-pyrrolo[2,3-*d*]pyrimidin-2-yl}propanamide (535).

Compound **535** was synthesized from **529** (50 mg, 0.1 mmol), 30 mg of 5% palladium on carbon

using the general procedure described above to afford after purification 42 g (85%) as a yellow solid. Compound **535** was used directly in the deprotection step without further characterization.

***N*-{5-[2-(2-methoxyphenyl)ethyl]-4-methyl-7-(2-phenylethyl)-7*H*-pyrrolo[2,3-*d*]pyrimidin-2-yl}-2,2-dimethylpropanamide (536).** Compound **536** was synthesized from **530** (47 mg, 0.1mmol), 30 mg of 5% palladium on carbon using the general procedure described above to afford after purification 37 mg (80%) as a yellow solid. Compound **536** was used directly in the deprotection step without further characterization.

2,2-Dimethyl-*N*-{4-methyl-7-(2-phenylethyl)-5-[2-(3,4,5-trimethoxyphenyl)ethyl]-7*H*-pyrrolo[2,3-*d*]pyrimidin-2-yl}propanamide (537). Using the general procedure described above, **531** was hydrogenated to afford **537** (48 mg, 91%) as a yellow solid: R_f 0.55 (EtOAc/TEA/hexane, 3:1:5); mp 117.6-117.9 °C; ^{1}H NMR ($CDCl_3$) δ 1. 39 (s, 9 H, Piv), 2.73 (s, 3 H, 4-CH_3), 2.81 (t, 2 H, 2 CH_2), 3.03 (t, 2 H, CH_2), 3.09 (t, 2 H, CH_2), 3.81 (s, 9 H, 3 OCH_3), 4.39 (t, 2 H, CH_2), 6.36 (s, 2 H, C_6H_2), 6.51 (s, 1 H, 6-CH), 7.15-7.22 (m, 5 H, C_6H_5), 8.07 (s, 1 H, NH exch).

***N*-{5-[2-(2-methoxyphenyl)ethyl]-4-methyl-7-(3-phenylpropyl)-7*H*-pyrrolo[2,3-*d*]pyrimidin-2-yl}-2,2-dimethylpropanamide (538).** Compound **538** was synthesized from **532** (48 mg, 0.1mmol), 30 mg of 5% palladium on carbon using the general procedure described above to afford after purification 43 g (90%) as a yellow solid. Compound **538** was used directly in the deprotection step without further characterization.

2,2-Dimethyl-*N*-{4-methyl-7-(3-phenylpropyl)-5-[2-(3,4,5-trimethoxyphenyl)ethyl]-7*H*-pyrrolo[2,3-*d*]pyrimidin-2-yl}propanamide (539). Compound **539** was synthesized from **533** (54g, 0.1mmol), 30 mg of 5% palladium on carbon using the general procedure described above to afford after purification 47 mg (88%) as a yellow solid. Compound **539** was used directly in

the deprotection step without further characterization.

General Procedure for the Synthesis of 383-388: To a round-bottom flask was added **534-539** in methanol (10 mL), followed by the addition of 1 N NaOH (2 mL). The reaction mixture was heated at reflux at 80 °C for 24 h. The reaction was then cooled and the MeOH evaporated under vacuum. The slurry was diluted with 50ml water, and then extracted with ethyl acetate. The organic layer was dried with anhydrous sodium sulfate and evaporated to afford a plug. The silica gel plug obtained was loaded onto a silica gel column and eluted with 1:1:7 ethyl acetate/triethylamine/hexanes. Fractions containing the product (TLC) were pooled and the solvent evaporated to afford analytically pure product.

5-[2-(2-Methoxyphenyl)ethyl]-4-methyl-7-phenyl-7*H*-pyrrolo[2,3-*d*]pyrimidin-2-amine (383). Using the general procedure described above, **534** was deprotected to afford **384**. Not enough material was obtained for subsequent chariacterization and biological evaluation.

4-Methyl-7-phenyl-5-[2-(3,4,5-trimethoxyphenyl)ethyl]-7*H*-pyrrolo[2,3-*d*]pyrimidin-2-amine (384)

Using the general procedure described above, **535** was deprotected to afford **384** (26 mg, 72%) as a yellow solid: R_f 0.28 (EtOAc/TEA/hexane, 3:1:5); mp 137.4-137.9 °C; ^{1}H NMR (DMSO-d_6) δ 2.71 (s, 3 H, 4-CH_3), 2.96 (t, 2 H, CH_2), 3.12 (t, 2 H, CH_2), 3.85 (s, 9 H, 3 OCH_3), 4.83 (br, 2 H, NH_2 exch), 6.43 (s, 2 H, C_6H_2), 6.86 (s, 1 H, 6-CH), 7.31 (m, 1 H, C_6H_5), 7.48 (m, 2 H, C_6H_5), 7.67 (m, 2 H, C_6H_5), Anal. Calcd. for $C_{24}H_{26}N_4O_3$: C, 66.88; H, 6.26; N, 13.39 Found C, 68.61; H, 6.36; N,12.18.

5-[2-(2-Methoxyphenyl)ethyl]-4-methyl-7-(2-phenylethyl)-7*H*-pyrrolo[2,3-*d*]pyrimidin-2-amine (385)

Using the general procedure described above, **536** was deprotected to afford **385** (44 mg, 69%)

as a yellow solid: R_f 0.27 (EtOAc/TEA/hexane, 3:1:5); mp 141.6-141.9 °C; ^{1}H NMR ($CDCl_3$) δ 2.68 (s, 3 H, 4-CH_3), 2.89 (m, 4 H, 2 CH_2), 3.04 (t, 2 H, CH_2), 3.82 (s, 3 H, OCH_3), 4.22 (t, 2 H, CH_2), 4.95 (br, 2 H, NH_2 exch), 6.41 (s, 1 H, 6-CH), 6.89 (m, 1 H), 7.10-7.32 (m, 7 H, C_6H_5); HRMS calcd for C24H26N4O 386.2107, found 386.2107.

4-Methyl-7-(2-phenylethyl)-5-[2-(3,4,5-trimethoxyphenyl)ethyl]-7*H*-pyrrolo[2,3-*d*]pyrimidin-2-amine (386) Using the general procedure described above, **537** was deprotected to afford **386** (35 mg, 72%) as a yellow solid: R_f 0.28 (EtOAc/TEA/hexane, 3:1:5); mp 140.1-140.5 °C; ^{1}H NMR (DMSO-d_6) δ 1.14 (s, 3 H, 4-CH_3), 2.67 (t, 2 H, CH_2), 2.84 (m, 4 H, 2 CH_2), 3.72 (s, 9 H, 3 OCH_3), 4.12 (t, 2 H, CH_2), 5.02 (s, 1 H, 6-CH), 6.24 (s, 2 H, C_6H_2), 7.03-7.15 (m, 5 H, C_6H_5), 7.15 (br, 2 H, NH_2 exch); Anal. Calcd. for $C_{24}H_{26}N_4O_3$: C, 66.88; H, 6.26; N, 13.39 Found C, 68.61; H, 6.36; N,12.18.

5-[2-(2-Methoxyphenyl)ethyl]-4-methyl-7-(3-phenylpropyl)-7*H*-pyrrolo[2,3-*d*]pyrimidin-2-amine (387). Using the general procedure described above, **538** was deprotected to afford **387** (66 mg, 83%) as a yellow solid: R_f 0.30 (EtOAc/TEA/hexane, 3:1:5); mp 137.8-137.0°C; ^{1}H NMR ($CDCl_3$) δ 2.10 (m, 2 H, CH_2), 2.61 (t, 2 H, CH_2), 2.68 (s, 3 H, 4-CH_3), 2.95-2.97 (m, 4 H, 2 CH_2), 3.82 (s, 3 H, OCH_3), 4.02 (t, 2 H, CH_2), 4.79 (br, 2 H, NH_2 exch), 6.54 (s, 1 H, 6-CH), 6.88-7.25 (m, 9 H); Anal. Calcd. for $C_{25}H_{28}N_4O$: C, 74.97; H, 7.05; N, 13.99 Found C, 74.80; H, 7.07; N, 13.78.

4-Methyl-7-(3-phenylpropyl)-5-[2-(3,4,5-trimethoxyphenyl)ethyl]-7*H*-pyrrolo[2,3-*d*]pyrimidin-2-amine (388). Using the general procedure described above, **539** was deprotected to afford **388** (27 mg, 52%) as a yellow solid: R_f 0.31 (EtOAc/TEA/hexane, 3:1:5); mp 144.3-144.6°C; ^{1}H NMR ($CDCl_3$) δ 1.98 (s, 3 H, 4-CH_3), 2.51 (m, 4 H), 2.72 (m, 2 H, CH_2), 2.91 (m, 2 H, CH_2), 3.71 (s, 9 H, 3 OCH_3), 3.91 (t, 2 H, CH_2), 5.47 (br, 2 H, NH_2 exch), 6.25 (s, 2 H, C_6H_2),

6.41 (s, 1 H, 6-CH), 7.03-7.15 (m, 5 H, C_6H_5); HRMS (ESI, pos mode) m/z [M + H^+] calcd for $C_{27}H_{33}N_4O_3$ 461.2553, found 461.2538.

VII. BIBLIOGRAPHY

1. Kisliuk, R. L. Folate Biochemistry in Relation to Antifolate Selectivity. In *Antifolate Drugs in Cancer Therapy*. Jackman, A., Ed.; Humann Press: Totowa, **1999**, pp 13-36.
2. Kisliuk, R. L.; Gaumont, Y.; Powers, J. F.; Thorndike, J.; Nair, M. G.; Piper, J. R. Synergistic Growth Inhibition by Combination of Antifolates. In *Evaluation of Folate Metabolism in Health and Disease*. Picciano, M. F.; Stokstad, E. L. R.; Gregory, J. F.; Alan R.; Ed.; Liss: New York, **1990**, pp 79-89.
3. Hitchings, G. A. Folate Antogonists as Antibacterial and Antiprotozoal Agents. *Ann. N. Y. Acad. Sci.* **1971**, *186*, 444-451.
4. Seeger, Doris R.; Cosulich, Donna B.; Smith, James M., Jr.; Hultquist, Martin E. Analogs of pteroylglutamic acid. III. 4-Amino derivatives. *J. Am. Chem. Soc.* **1949**, *71*, 1753-1758.
5. Gangjee, A.; Elzein, E.; Kothare, M.; Vasudevan, A. Classical and Nonclassical Antifolates as Potential Antitumor, Antipneumocystis and Antitoxoplasma Agents. *Curr. Pharm. Des.* **1996**, *2*, 263-280.
6. Calvert, H. An Overview of Folate Metabolism: Features Relevant to the Action and Toxicities of Antifolate Anticancer Agents. *Semin. Oncol.* **1999**, *26*, 3-10
7. Mitchell, H. K.; Snell, E. E.; Williams, R. J. (1941). The concentration of "folic acid"". *J Am Chem Soc*. 1941, *63*, 2284.
8. Blakley, R. L. *The Biochemistry of Folic Acid and Related Pteridines*; Neuberger, A., Tatum, E. L., Eds.; North Holland Publishing Co.: Amsterdam, 1969; pp 92-94.
9. Schnell, J. R.; Dyson, H. J.; Wright, P. E. Structure, Dynamics, and Catalytic Function of Dihydrofolate Reductase. *Annu. Rev. Biophys. Biomol. Struct*. **2004**, *33*, 119-140.
10. Roth, B. Design of Dihydrofolate Reductase Inhibitors from X-Ray Crystal Structures. *Fed.*

Proc. **1986**, *45*, 2765-2772.

11. Costi, M. P.; Ferrari, S. Update on Antifolate Drugs Targets. *Curr. Drug Targets*. **2001**, *2*, 135-166.
12. Carreras, C. W.; Santi, D. V. The Catalytic Mechanism and Structure of Thymidylate Synthase. *Ann. Rev. Biochem*. **1995**, *64*, 721-762.
13. Jackman, A. L. Antifolate Drugs: Past and Future Perspectives. In *Antifolate Drugs in Cancer Therapy*; Jackman. A. L., Ed.; Humana Press: Totowa, NJ, 1999; pp 1-12.
14. Jansen, G. Receptor- and Carrier-Mediated Transport Systems for Folates and Antifolates: Exploitation for Folate-Based Chemotherapy and Immunotherapy. In *Antifolate Drugs in Cancer Therapy*; Jackman. A. L., Ed.; Humana Press: Totowa, NJ, 1999; pp 293-321.
15. Brzezińska, A.; Wińska, P.; Balińska, M. Cellular Aspects of Folate and Antifolate Membrane Transport. *Acta Biochim. Pol.*, **2000**, *47*, 735-749.
16. Moran, R. G. Roles of Folylpoly-γ-glutamate Synthetase in Therapeutics with Tetrahydrofolate Antimetabolites: An Overview. *Semin. Oncol.* **1999**, *26*, 24-32.
17. Yao, R.; Schneider, E.; Ryan, T. J.; Galivan, J. Human Gamma-Glutamyl Hydrolase: Cloning and Characterization of the Enzyme Expressed *in vitro*. *Proc. Natl. Acad. Sci. USA* **1996**, *93*, 10134-10138.
18. Barrueco, J. R.; O'Leary, D. F.; Sirotnak, F. M. Facilitated Transport of Methotrexate Polyglutamates into Lysosomes Derived from S180 Cells. Further Characterization and Evidence for a Simple Mobile Carrier System with Broad Specificity for Homo- or Heteropeptides Bearing a C-Terminal Glutamyl Moiety. *J. Biol. Chem.* **1992**, *267*, 19986-19991.

19. Hooijberg, J. H.; Broxterman, H. J.; Kool, M.; Assaraf, Y. G.; Peters, G. J.; Noordhuis, P.; Scheper, R. J.; Borst, P.; Pinedo, H. M.; Jansen, G. Antifolate Resistance Mediated by the Multidrug Resistance Proteins MRP1 and MRP2. *Cancer Res.* **1999**, *59*, 2532-2535.

20. DeGraw, J. I.; Colwell, W. T.; Piper, J. R.; Sirotnak, F. M.; Smith, R. L. New Analogs of Methotrexate in Cancer and Arthritis. *Curr. Med. Chem.* **1995**, *2*, 630-653.

21. Huennekens, F. M.; Duffy, T. H.; Vitols, K. S. Folic Acid Metabolism and its Disruption by Pharmacologic Agents. *NCI monographs.* **1987**, *5*, 1-8.

22. Berman, E. M.; Werbel, L. M. The Renewed Potential for Folate Antagonists in Contemporary Cancer Chemotherapy. *J. Med. Chem.* **1991**, *34*, 479-485.

23. Weinstein, G. D. Biochemical and Pathophysiological Rationale for Amethopterin in Psoriasis. *Ann. N. Y. Acad. Sci.* **1971**, *186*, 452-465.

24. Rader, J. I., Huennekens, F. M. Folate Coenzyme-mediated Transfer of One-Carbon Groups. In *The Enzymes*; Beyer, P.D., Ed.; Academic Press: New York, **1973**; Vol. IX, pp 197-223.

25. Hitchings, G. H. Functions of Tetrahydrofolate and the Role of Dihydrofolate Reductase. In *Cellular Metabolism in Inhibition of Folate Metabolism in Chemotherapy*; Hitchings, G. H., Ed.; Springer Verlag: New York. **1983**, 11-23.

26. Danenberg, P. V. Thymidylate Synthetase: A Target Enzyme in Cancer Chemotherapy. *Biochim. Biophys. Acta*. **1977**, *47*, 73-92.

27. Harrap, K. R.; Jackman, A. L.; Newell, D. R.; Taylor, G. A.; Hughes, J. R.; Calvert, A. H. Thymidylate Synthase: A Target for Anticancer Drug Design. In *Advanced in Enzyme Regulation*. Weber, G., Ed.; Pergamon Press: **1989**, Vol. *29*, pp161-179.

28. Matthews, D. A.; Alden, R. A.; Bolin, J. T.; Freer, S. T.; Hamlin, R.; Xuong, N.; Kraut, J.; Poe, M.; Williams, M.; Hoogsteen, K. Dihydrofolate Reductase: X-Ray Structure of the Binary Complex with Methotrexate. *Science* **1977**, *197*, 452-455.
29. Bolin, J. T.; Filman, D. J.; Matthews, D. A.; Hamlin, R. C.; Kraut, J. Crystal Structures of *Escherichia coli* and *Lactobacillus casei* Dihydrofolate Reductase Refined at 1.7 Å Resolution. I. General Features and Binding of Methotrexate. *J. Biol. Chem.* **1982**, *257*, 13650-13662.
30. Baker, D. J.; Beddell, C. R.; Champness, J. N.; Goodford, P. J.; Norrington, F. E. A.; Smith, D. R.; Stammers, D. K. The Binding of Trimethoprim to Bacterial Dihydrofolate Reductase. *FEBS Lett*. **1981**, *126*, 49-52.
31. Matthews, D. A.; Biolin, J. T.; Burridge, J. M.; Filman, D. J.; Volz, K. W.; Kaufman, B. T.; Beddell, C. R.; Champness, J. N.; Stammers, D. K.; Kraut, J. Refined Crystal Structures of *Escherichia coli* and Chicken Liver Dihydrofolate Reductase Containing Bound Trimethoprim. *J. Biol. Chem.* **1985**, *260*, 381-391.
32. Bystroff, C.; Oatley, S. J.; Kraut, J. Crystal Structures of *Escherichia coli* Dihydrofolate Reductase: The $NADP^+$ Holoenzyme and Folate•$NADP^+$ Ternary Complex. Substrate Binding and a Model for the Transition State. *Biochemistry* **1990**, *29*, 3263-3277.
33. Champness, J. N.; Stammers, D. K.; Beddell, C. R. Crystallographic Investigation of the Cooperative Interaction Between Trimethoprim, Reduced Cofactor and Dihydrofolate Reductase. *FEBS Lett.* **1986**, *199*, 61-67.
34. Bystroff, C.; Kraut, J. Crystal Structure of Unliganded *Escherichia coli* Dihydrofolate Reductase. Ligand-Induced Conformational Changes and Cooperativity in Binding. *Biochemistry* **1991**, *30*, 2227-2239.

35. Reyes, V. M.; Sawaya, M. R.; Brown, K. A.; Kraut, J. Isomorphous Crystal Structures of *Escherichia coli* Dihydrofolate Reductase Complexed with Folate, 5-Deazafolate and 5,10-Dideazatetrahydrofolate: Mechanistic Implications. *Biochemistry* **1995**, *34*, 2710-2723.
36. Lee, H.; Reyes, V. M.; Kraut, J. Crystal Structures of *Escherichia coli* Dihydrofolate Reductase Complexed with 5-Formyltetrahydrofolate in Two Space Groups: Evidence for Enolization of Pteridine O4. *Biochemistry* **1996**, *35*, 7012-7022.
37. Sawaya, M. R.; Kraut, J. Loop and Subdomain Movements in the Mechanism of *Escherichia coli* Dihydrofolate Reductase: Crystallographic Evidence. *Biochemistry* **1997**, *36*, 586-603.
38. Matthews, D. A.; Alden, R. A.; Bolin, J. T.; Filman, D. J.; Freer, S. T.; Hamlin, R.; Hol, W. G.; Kisliuk, R. L.; Pastore, E. J.; Plante, L. T.; Xuong, N.; Kraut, J. Dihydrofolate Reductase from *Lactobacillus casei*. X-ray Structure of the Enzyme Methotrexate•NADPH Complex. *J. Biol. Chem.* **1978**, *253*, 6946-6954.
39. Matthews, D. A.; Alden, R. A.; Freer, S. T.; Xuong, N.; Kraut, J. Dihydrofolate Reductase from *Lactobacillus casei*. Stereochemistry of NADPH Binding. *J. Biol. Chem.* **1979**, *254*, 4144-4151.
40. Filman, D.; Bolin, J. T.; Burder, J. M.; Filman, D.; Volz, K. W.; Kraut, J. Dihydrolate Reductase. The Stereochemistry of Inhibitor Selectivity. *J. Biol. Chem.* **1985**, *260*, 392-399.
41. Matthews, D. A.; Bolin, J. T.; Burridge, J. M.; Filman, D. J.; Volz, K. W.; Kraut, J. Dihydrofolate Reductase. The Stereochemistry of Inhibitor Selectivity. *J. Biol. Chem.* **1985**, *260*, 392-399.
42. Volz, K. W.; Matthews, D. A.; Alden, R. A.; Freer, S. T.; Hansch, C.; Kaufman, B. T.; Kraut, J. Crystal Structure of Avian Dihydrofolate Reductase Containing Phenyltriazine and NADPH. *J. Biol. Chem.* **1982**, *257*, 2528-2536.

43. McTigue, M. A.; Davies, J. F., II; Kaufman, B. T.; Kraut, J. Crystal Structures of Chicken Liver Dihydrofolate Reductase: Binary ThioNADP$^+$ and Ternary ThioNADP$^+$•Biopterin Complexes. *Biochemistry* **1993**, *32*, 6855-6862.

44. McTigue, M. A.; Davies, J. F., II; Kaufman, B. T.; Kraut, J. Crystal Structure of Chicken Liver Dihydrofolate Reductase Complexed with NADP$^+$ and Biopterin. *Biochemistry* **1992**, *31*, 7264-7273.

45. Stammers, D. K.; Champness, J. N.; Beddell, C. R.; Dann, J. G.; Eliopoulos, E.; Geddes, A. J.; Ogg, D.; North, A. C. The Structure of Mouse L1210 Dihydrofolate Reductase-Drug Complexes and the Construction of a Model of Human Enzyme. *FEBS Lett*. **1987**, *218*, 178-184.

46. Tsitsa, P.; Antoniadou-Vyza, E.; Hamodrakas, S. J.; Eliopoulos, E. E.; Tsantili-Kakoulidou, A.; Lada-Hytiroglou, E.; Roussakis, C.; Chinou, I.; Hempel, A.; Camerman, L.; Ottensmeyer, F. P.; Vanden Berghe, D. A. Synthesis, Crystal Structure and Biological Properties of a New Series of Lipophilic *s*-Triazines, Dihydrofolate Reductase Inhibitors. *Eur. J. Med. Chem.* **1993**, *28*, 149-158.

47. Ofner, C.; D'Arcy, A.; Winkler, F. K. Crystal Structures of Human Dihydrofolate Reductase Complexes with Folate. *Eur. J. Biochem.* **1998**, *174*, 377-385.

48. Davies, J. F.; Delcamp, T. J.; Prendergast, N. J.; Ashford, V. A.; Freisheim, J. H.; Kraut, J. Crystal Structures of Recombinant Human Dihydrofolate Reductase Complexed with Folate and 5-Deazafolate. *Biochemistry* **1990**, *29*, 9467-9479.

49. Morrison, J. F.; Stone, S. R. Mechanism of the Reaction Catalyzed by DHFR from *E. coli*: pH and Deuterium Isotope Effects with NADPH as the Variable Substrate. *Biochemistry* **1998**, *37*, 5499-5506.

50. Cody, V.; Galitsky, N.; Luft, J. R.; Pangborn, W.; Rosowsky, A.; Blakley, R. L. Comparison of Two Independent Crystal Structures of Human Dihydrofolate Reductase Ternary Complexes Reduced with Nicotinamide Adenine Dinucleotide Phosphate and the Very Tight-Binding Inhibitor PT523. *Biochemistry* **1997**, *36*, 13897-13903.
51. Champness, J. N.; Achari, A.; Ballantine, S. P.; Bryant, P. K.; Delves, C. J.; Stammers, D. K. The Structure of *Pneumocystis carinii* Dihydrofolate Reductase to 1.9 Å Resolution. *Structure* **1994**, *2*, 915-924.
52. Cody, V.; Galitsky, N.; Luft, J. R.; Pangborn, W.; Gangjee, A.; Devraj, R.; Queener, S. F.; Blakely, R. L. Comparison of Ternary Complexes of *Pneumoucystis carinii* and Wild-Type Human Dihydrofolate Reductase with Coenzyme NADPH and a Novel Classical Antitumor Furo[2,3-*d*]pyrimidine Antifolate. *Acta Crystallogr. D.* **1997**, *D53*, 638-649.
53. Cody, V.; Galitsky, N.; Luft, J. R.; Pangborn, W.; Gangjee, A.; Queener, S. F. Crystal Structures of *Pneumocystis carinii* Dihydrofolate Reductase Cofactor Ternary Complexes with the Selective Furopyrimidinesulfo-2-naphthalene Antifolate and with Methotrexate. In *Chemistry and Biology of Pteridines and Folates*; Pfleiderer, W., Rokos, H., Eds.; Blackwell Science: Berlin, 1997; pp 399-402.
54. Gangjee, A.; Guo, X.; Queener, S. F.; Cody, V.; Galitsky, N.; Luft, J. R.; Pangborn, W. Selective *Pneumocystis carinii* Dihydrofolate Reductase Inhibitors: Design, Synthesis, and Biological Evaluation of New 2,4-Diamino-5-substituted furo[2,3-*d*]pyrimidines. *J. Med. Chem.* **1998**, *41*, 1263-1271.
55. Cody, V.; Galitsky, N.; Rak, D.; Luft, J. R.; Pangborn, W.; Queener, S. F. Ligand-Induced Conformational Changes in the Crystal Structures of *Pneumocystis carinii* Dihydrofolate Reductase Complexes with Folate and $NADP^+$. *Biochemistry* **1999**, *38*, 4303-4312.

56. Chunduru, S. K.; Cody, V.; Luft, J. R.; Pangborn, W.; Appleman, J. R.; Blakely, R. L. Methotrexate-Resistant Variants of Human Dihydrofolate Reductase. Effects of Phe31 Substitutions. *J. Biol. Chem.* **1994**, *269*, 9547-9555.

57. Lewis, W. S.; Cody, V.; Galitsky, N.; Luft, J. R.; Pangborn, W.; Chunduru, S. K.; Spencer, H. T.; Appleman, J. R.; Blakley, R. L. Methotrexate-Resistant Variants of Human Dihydrofolate Reductase with Substitutions of Leucine 22. Kinetics, Crystallography and Potential as Selectable Markers. *J. Biol. Chem.* **1995**, *270*, 5057-5064.

58. Li, R.; Sirawaraporn, R.; Chitnumsub, P.; Sirawaraporn, W.; Wooden, J.; Athappilly, F.; Turley, S.; Hol, W. G. J. Three-Dimensional Structure of *M. tuberculosis* Dihydrofolate Reductase Reveals Opportunities for the Design of Novel Tuberculosis Drugs. *J. Mol. Biol.* **2000**, *295*, 307-323.

59. Dams, T.; Auerbach, G.; Bader, G.; Jacob, U.; Ploom, T.; Huber, R.; Jaenicke, R. The Crystal Structure of Dihydrofolate Reductase from *Thermotoga maritima*: Molecular Features of Thermostability. *J. Mol. Biol.* **2000**, *297*, 659-672.

60. Freisham, J. H.; Matthews, D. A. The Comparative Biochemistry of DHFR. In *Folate as Therapeutic Agents*. Sirotnak, Burchall, Ensminger, Montgomery, Eds., Academic Press, Inc., Orlando, **1984**, *I*, 69-131.

61. Blakeley, R. L.; Appleman, J. R. Recent Advances in the Study of Dihydrofolate Reductase. In *Chemistry and Biology of Pteridines*. Cooper and Whitehead, Eds.; Walter de Gruyter Berlin N.Y. **1986**, 769-772.

62. Davies, J. F.; Delcamp, T. J.; Prendergast, N. J.; Ashford, V. A.; Freisheim, J. H.; Kraut, J. Crystal Structures of Recombinant Human Dihydrofolate Reductase Complexed with Folate and 5-Deazafolate. *Biochemistry* **1990**, *29*, 9467-9479.

63. Hitchings. G. H.; Smiths, S. L. Dihydrofolate Reductases as Targets. In *Adv. Enzyme Regulation*. Weber; Ed., Pergamon Press: **1979**, Vol *18*, pp 349-371.

64. Kovacs, J. A.; Allegra, C. J.; Masur, H. Characterization of DHFR *of Pneumocystis carinii* and *Toxoplasma gondii*. *Experimental Parasitology* **1990**, *71*, 60-68.

65. Edman. U.; Edman, J. C.; Lundgren, B.; Santi. D. V. Isolation and Expression of the *Pneumocystis carinii* Thymidylate Synthase Gene. *Proc. Natl. Acad. Sci. USA* **1989**, *86*, 6503-6507.

66. Kovacs. J. A.: Masur, H. *Pneumocystis carinii* Pneumonia: A Comparison Between Patients with Acquired Immunodeficiency Syndrome and Patients with Other Immunodeficiencies. *Ann. Int. Med.* **1984**, *100*, 663-671.

67. Allegra, C. J.; Kovacs, J. A.; Drake, J. C.; Swan, J. C.; Chabner, B. A.; Masur, H. Activity of Antifolates Against *Pneumocystis carinii* Dihydrofolate Reductase and Identification of a Potent New Agent. *J. Exp. Med.* **1987**, *165*, 926-931.

68. Hughes, W. T.; Bartley, D. L.; Smith, B. M. A Natural Source of Infection due to *Pneumocystis carinii*. *J. Infect. Dis.* **1983**, *147*, 595.

69. Cody, V.; Chisum, K.; Pope, C.; Queener, S. F. Purification and Characterization of Human-Derived *Pneumocystis jirovecii* Dihydrofolate Reductase Expressed in Sf21 Insect Cells and in *Escherichia coli*. *Protein Expr. Purif.* **2005**, *40*, 417-423.

70. Ivanetich, K. M.; Santi, D. V. Thymidylate Synthase-Dihydrofolate Reductase in Protozoa. *Exp. Parasitol.* **1990**, *70*, 367-371.

71. Garrett, C. E.; Coderra, J. A.; Meek, T. D.; Garvey, E. P.; Claman, D.M.; Beverly, S. M.; Santi, D. V. Bifunctional Thymidylate Synthase-DHFR in Protozoa. *Mol. Biochem. Parasitol.* **1984**, *11*, 257-265.

72. Grumont, R.; Washtein, W. L.; Caput, D.; Santi, D. V. Bifunctional Thymidylate Synthase-Dihydrofolate from *Leishmania tropica*: Sequence Homology with the Corresponding Monofuctional Proteins. *Proc. Natl. Acad. Sci. USA*. **1986**, *83*, 5387-5391.

73. Roos, D. S. Primary Structure of the Dihydrofolate Reductase-Thymidylate Synthase Gene from *Toxoplasma gondii*. *J. Biol.Chem.* **1993**, *268*, 6269-6280.

74. Deroin, F.; Chastang, C. In vitro Effect of Folate Inhibitors on *Toxoplasma gondii*. *Antimicrobial Agents and Chemotherapy*. **1989**, *33*, 1753-1759.

75. Matthews, D. A.; Appelt, K.; Oatley, S. J.; Xuong, N. H. Crystal Structure of *E. coli* TS with FdUMP and 5,8-Dideazafolate. *J. Mol. Biol.* **1990**, *214*, 923-936.

76. Derouin, F.; Chastang, C. *In vitro* Effects of Folate Inhibitors on *Toxoplasma gondii*. *Antimicrob. Agents Chemother.* **1989,** *33*, 1753-1759.

77. Cummins, P. L. and Gready, J. E. Energetically Most Likely Substrate and Activityt-site Protonation sites and Pathways in the Catalytic Mechanism of Dihydrofolate Reductase. *J. Am. Chem. Soc*., **2001**, *123*, 3418-3428.

78. Gready, J. E. Theoretical Studies on the Activation of the Pterin Cofactor in the Catalytic Mechanism of Dihydrofolate Reductase. *Biochemistry*, **1985**, *24*, 4761-4766.

79. Wu, Y-D; Houk, K. N. Theoretical Transition Structures for Hydride Transfer to Methyleniminium Ion from Methylamine and Dihydropyridine. On the Nonlinearit, of Hydride Transfer. *J. Am. Chem. Soc*. **1987**, *109*, 2226-2227.

80. Harrison, P. T.; Scott, J. E.; Hutchinson, M. J.; Thompson, R. Site-directed Mutagenesis of Varicella-zoster Virus Thymidylate Synthase. Analysis of Two Highly Conserved Regions of the Enzyme. *Eur. J. Biochem.* **1995**, *230*, 511-516.

81. Douglas, K. T. The Thymidylate Synthesis cycle and anticancer drugs. *Med. Res. Rev.*, **1987**, *7*, 441-475.

82. Cisneros, R. J.; Silks, L. A.; Dunlap, R. B. *Drugs Fut.* **1988**, *13*, 859.

83. Pogolotti, A. L., Jr.; Santi, D. V. The Catalytic Activity of Thymidylate Synthase. In *Bioorganic Chemistry*; van Tamelen, E. E., Ed.; Academic Press: Orlando, FL, 1977; Vol. 1, pp 277-311.

84. Perry, K. M.; Fauman, E.; Finer-Moore, J. S.; Montfort, W. R.; Maley, C. F.; Maley, F.; Stroud, R. M. Plastic Adaptation toward Mutations in Proteins: Structural Comparison of Thymidylate Synthases. *Proteins* **1990**, *8*, 315-313.

85. Ercikan, E.; Banerjee, D.; Waltham, M.; Schnieders, B.; Scotto, K. W., Bertino, J. R. Translational Regulation of the Synthesis of Dihydrofolate Reductase. *Adv. Exp. Med. Biol.* **1993**, *338*, 537-540.

86. Ercikan-Abali, E. A.; Banerjee, D.; Waltham, M. C.; Skacel, N.; Scotto, K. W.; Bertino, J. R. Dihydrofolate Reductase Protein Inhibits Its Own Translation by Binding to Dihydrofolate Reductase mRNA Sequences within the Coding Region. *Biochemistry* **1997**, *36*, 12317-12322.

87. Ercikan, E.; Banerjee, D.; Waltham, M.; Schnieders, B.; Scotto, K. W., Bertino, J. R. Translational Regulation of the Synthesis of Dihydrofolate Reductase. *Adv. Exp. Med. Biol.* **1993**, *338*, 537-540.

88. Kamb, A.; Finer-Moore, J. S.; Stroud, R. M. Structural Basis for Recognition of Polyglutamyl Folates by Thymidylate Synthase. *Biochemistry* **1992**, *31*, 9883-9890.

89. Kamb, A.; Finer-Moore, J. S.; Stroud, R. M. Cofactor triggers the conformational change in thymidylate synthase: implications for an ordered binding mechanism. *Biochemistry* **1992**, *31*, 12876-12884.

90. Matthews, D. A.; Appelt, K.; Oatley, J. S.; Xuong, N. H. Crystal Structure of *Escherichia coli* Thymidylate Synthase Containing Bound 5-Fluoro-2'-deoxyuridylate and 10-Propargyl-5,8-dideazafolate. *J. Mol. Biol.*, **1990**, *214*, 923-936.

91. Matthews, D. A.; Villafranca, J. E.; Janson, C. A.; Smith, W. W.; Welsh, K.; Freer, S. Stereochemical Mechanism of Action for Thymidylate Synthase Based on the X-ray Structure of the Covalent Inhibitory Ternary Complex with 5-Fluoro-2'-deoxyuridylate and 5,10-Methylenetetrahydrofolate. *J. Mol. Biol.* **1990**, *214*, 937-948.

92. Montfort, W. R.; Perry, K. M.; Fauman, E. B.; Finer-Moore, J. S.; Maley, G. F.; Maley, F.; Stroud, R. M. Pairwise Specificity and Sequential Binding in Enzyme Catalysis: Thymidylate Synthase. *Biochemistry*, **1990**, *29*, 6977-6986.

93. Perry, K. M.; Fauman, E.; Finer-Moore, J. S.; Montfort, W. R.; Maley, C. F.; Maley, F.; Stroud, R. M. Plastic Adaptation toward Mutations in Proteins: Structural Comparison of Thymidylate Synthases. *Proteins* **1990**, *8*, 315-313.

94. Hardy, L. W. Finer-Moore, J. S. Montfort, W. R. Jones, M. O. Santi, D. V. Stroud, R. M. Atomic Structure of Thymidylate Synthase: Target for Rational Drug Design. *Science* **1987**, *35*, 448-455.

95. Finer-Moore, J.; Fauman, E. B.; Foster, P. G.; Perry, K. M.; Santi, D. V.; Stroud, R. M. Refined Structures of Substrate-bound and Phosphate-bound Thymidylate Synthase from *Lactobacillus casei*. *J. Mol. Biol.* **1993**, *232*, 1101-1116.

96. Knighton, D. R.; Kan, C. C.; Howland, E.; Janson, C. A.; Hostomska, Z.; Welsh, K. M.; Matthews, D. A. Structure of and Kinetic Channeling in Bifunctional Dihydrofolate Reductase-thymidylate Synthase. *Nat. Struct. Biol.* **1994**, *1*, 186-194.

97. Anderson, A. C.; Perry, K. M.; Freymann, D. M.; Stroud, R. M. The Crystal Structure of Thymidylate Synthase from *Pneumocystis carinii* Reveals a Fungal Insert Important for Drug Design. *J. Mol. Biol.* **2000**, *297*, 645-657.

98. Finer-Moore, J. S.; Maley, G. F.; Maley, F.; Montfort, W. R.; Stroud, R. M. Crystal Structure of Thymidylate Synthase from T4 Phage: Component of a Deoxynucleoside Triphosphate-synthesizing Complex. *Biochemistry*, **1994**, *33*, 15459-15468.

99. Phan, J.; Koli, S.; Minor, W.; Dunlap, R. B.; Berger, S. H.; Lebioda, L. Human Thymidylate Synthase is in the Closed Conformation when Complexed with dUMP and Raltitrexed, An Antifolate Drug. *Biochemistry* **2001**, *40*, 1897-1902.

100. Sayre, P. H.; Finer-Moore, J. S.; Fritz, T. A.; Biermann, D.; Gates, S. B.; MacKellar, W. C.; Patel, V. F.; Stroud, R. M. Multi-Targeted Antifolates Aimed at Avoiding Drug Resistance Form Covalent Closed Inhibitory Complexes with Human and *Escherichia coli* Thymidylate Synthases. *J. Mol. Biol.* **2001**, *313*, 813-829.

101. Finer-Moore, J. S.; Montfort, W. R.; Stroud, R. M. Structure, Multiple Site Binding, and Segmental Accommodation in Thymidylate Synthase on Binding dUMP and an Anti-folate. *Biochemistry* **1990**, *29*, 6964-6977.

102. Finer-Moore, J. S.; Liu, L.; Schafmeister, C. E.; Bridsall, D. L.; Mau, T.; Santi, D. V.; Stroud, R. M. Partitioning Roles of Side Chains in Affinity, Orientation, and Catalysis with Structures for Mutant Complexes: Asparagine-229 in Thymidylate Synthase. *Biochemistry* **1996**, *35*, 5125-5136.

103. Appelt, K.; Bacquet, R. J.; Bartlett, C. A.; Booth, C. L. J.; Freer, S. T. Design of Enzyme Inhibitors Using Iterative Protein Crystallographic Analysis. *J. Med. Chem.* **1991**, *34*, 1925-1934.

104. Reich, S. H.; Fuhry, A. M. Nguyen, D. Pino, M. J. Design and Synthesis of Novel 6,7-Imidazotetrahydroquinoline Inhibitors of Thymidylate Synthase Using Iterative Protein Crystal Structure Analysis. *J. Med. Chem.* **1992**, *35*, 847-858.

105. Shoichet, B. K.; Stroud, R. M.; Santi, D. V.; Kuntz, I. K.; and Perry, K. M. Structure-based Discovery of Inhibitors of Thymidylate Synthase. *Science* **1993**, *259*, 1445-1450.

106. Varney, M. D.; Marzoni, G. P.; Palmer, C. L.; Deal, J. G.; Webber, S.; Welsh, K. M.; Bacquet, R. J.; Bartlett, C. A.; Morse, C. A.; Booth, C. L. J.; Herrmann, S. M.; Howlland, E. F.; Ward, R. W.; White, J. Crystal-structure-based Design and Synthesis of Benz[*cd*]indole-containing Inhibitors of Thymidylate Synthase. *J. Med. Chem.* **1992**, *35*, 663-676.

107. Liu, L.; Santi, D. V. Exclusion of 2'-Deoxycytidine 5'-Monophosphate by Asparagine 229 of Thymidylate Synthase. *Biochemistry* **1993**, *32*, 9263-9267.

108. Liu L.; Santi, D. V. 5-Fluoro-2'-deoxycytidine 5'-Monophosphate is a Mechanism-based Inhibitor of Thymidylate Synthase. *Biochem. Biophys. Acta* **1994**, *1209*, 89-94.

109. Liu L.; Santi, D. V. Asparagine 229 in Thymidylate Synthase Contributes to, but is not Essential for, Catalysis. *Proc. Natl. Sci. U. S. A.* **1993**, *90*, 8604-8068.

110. Costi, M. P.; Liu, L.; Finer-Moore, J.; Stroud, R. M.; Santi, D. V. Asparagine 229 Mutants of Thymidylate Synthase Catalyze the Methylation of 3-Methyl-2'-deoxyuridine 5'-Monophosphate. *Biochemistry* **1996**, *35*, 3944-3949.

111. Rastelli, G.; Thomas, B.; Kollman, P. A.; Santi, D. V. Insight into the Specificity of Thymidylate Synthase from Molecular Dynamics and Free Energy Perturbation Calculations. *J. Am. Chem. Soc.* **1995**, *117*, 7213-7227.

112. Climie, S.; Ruiz-Perez, L.; Gonzales-Pacanowska, D. Prapunwattana, P.; Cho, S. W. Saturation Site-directed Mutagenesis of Thymidylate Synthase. *J. Biol. Chem.* **1990**, *265*, 18776-18779.

113. Zapf, J. W.; Weir, M. S.; Emerick, V.; Villafranca, J. E.; Dunlap, R. B. Substitution of Glutamine for Glutamic Acid-58 in *Escherichia coli* Thymidylate Synthase Results in Pronounced Decreases in Catalytic Activity and Ligand Binding. *Biochemistry* **1993**, *32*, 9274-9281.

114. Kealey, J. T.; Eckstein, J.; Santi, D. V. *Chem. & Biol.* Role of the Conserved Tryptophan 82 of *Lactobacillus casei* Thymidylate Synthase. **1995**, *2*, 609-614.

115. Leary, R. P.; Kisliuk, R. L. Crystalline Thymidylate Synthetase from Dichloromethotrexate Resistant *Lactobacillus casei*. *Prep. Biochem.* **1971**, *1*, 47-54.

116. Dev, I. K.; Dallas, W. S.; Ferone, R.; Hanlon, M.; McKee, D. D.; Yates, B. B. Mode of Binding of Folate Analogs to Thymidylate Synthase. Evidence for Two Asymmetric but Interactive Substrate Binding Sites. *J. Biol. Chem.* **1994**, *269*, 1873-1882.

117. Galivan, J. H.; Maley, G. F.; Maley, F. The Effect of Substrate Analogs on the Circular Dichroic Spectra of Thymidylate Synthetase from *Lactobacillus casei*. *Biochemistry* **1975**, *14*, 3338-3844.

118. Connick, T. J.; Reilly, R. T.; Dunlap, R. B.; Ellis, P. D. Phosphorus-31 Nuclear Magnetic Resonance Studies of Complexes of thymidylate synthase. *Biochimica et Biophysica Acta* **1994**, *1208*, 118-126.

119. Heidelberger, C. On the Rational Development of a New Drug: the Example of the Fluorinated Pyrimidines. *Cancer Treat Rep.* 1981, **65**, 3-9.

120. Heidelberger, C.; Chaudhuri, N. K.; Danenberg, P.; Duchinsky, R., Schnitzer, R. J.; Pleven, E.; Schener, J. Fluorinated Pyrimidines: a New Class of Tumor-inhibitory Compounds. *Nature* **1957**, *179*, 663-666.

121. Pinedo, H. M.; Peters, G. F. Fluorouracil: biochemistry and pharmacology. *J. Clin. Oncol.* **1988**, *6*, 1653-1664.

122. Aschele, C.; Sobrero, A.; Faderan, M. A.; Bertino, J. R. Novel Mechanism(s) of Resistance to 5-Fluorouracil in Human Colon Cancer (HCT-8) Sublines Following Exposure to Two Different Clinically Relevant Dose Schedules. *Cancer Res*. **1992**, *52*, 1855-1864.

123. Lokich, J. Infusional 5-FU: Historical Evolution, Rationale, and Clinical Experience. *Oncology* **1998**, *12*, 19-22.

124. Meta-analysis Group in Cancer Efficacy of Intravenous Continuous Infusion of Fluorouracil Compared with Bolus Administration in Advanced Colorectal Cancer. *J. Clin. Oncol.* **1998**, *16*, 301-308.

125. Sobrero, A. F.; Aschele, C.; Bertino, J. R. Fluorouracil in Colorectal Cancer—a Tale of Two Drugs: Implications for Biochemical Modulation. *J. Clin. Oncol.* **1997**, *15*, 368-381.

126. Chu, E.; Allegra, C. J. Antifolates. In: *Cancer chemotherapy*. Chabner, B. A.; Collins, J. M. Eds. Lippincott-Raven, New York, **1996**, pp 109.

127. Johnston, P. G.; Lenz, H. J.; Leichman, C. G.; Danenberg, K. D.; Allegra, C. J.; Danenberg, P. V.; Leichman, L. Thymidylate Synthase Gene and Protein Expression Correlate and are Associated with Response to 5-Fluorouracil in Human Colorectal and Gastric Tumors. *Cancer Res.* **1995**, *55*, 1407-1412.

128. Johnston, P. G.; Fisher, E. R.; Rockette, H. E.; Fisher, B. Wolmark, N.; Drake, J. C.; Chabner, B. A.; Allegra, C. J. The Role of Thymidylate Synthase Expression in Prognosis and Outcome of Adjuvant Chemotherapy in Patients with Rectal Cancer. *J. Clin. Oncol.* **1994**, *12*, 2640-2647.

129. Edler, D.; Hallstrom, M.; Johnston, P. G.; Magnusson, I.; Ragnhammar, P.; Blomgren, H. Thymidylate Synthase Expression: an Independent Prognostic Factor for Local Recurrence, Distant Metastasis, Disease-free and Overall Survival in Rectal Cancer. *Clin. Cancer Res.* **2000**, *6*, 1378-1384.

130. Salonga, D.; Danenberg, K. D.; Johnson, M.; Metzger, R.; Groshen, S.; Tsao-Wei, D. D.; Lenz, H. J.; Leichman, C. G.; Leichman, L.; Diasio, R. B.; Danenberg, P. V. Colorectal Tumors Responding to 5-Fluorouracil Have Low Gene Expression Levels of Dihydropyrimidine Dehydrogenase, Thymidylate Synthase, and Thymidine Phosphorylase. *Clin. Cancer Res.* **2000**, *6*, 1322-1327.

131. Huang, C. L.; Yokomise, H.; Kobayashi, S.; Fukushima, M.; Hitomi, S.; Wada, H. Intratumoral Expression of Thymidylate Synthase and Dihydropyrimidine Dehydrogenase in Non-small Cell Lung Cancer Patients Treated with 5-FU-based Chemotherapy. *Int. J. Oncol.* **2000**, *17*, 47-54.

132. Nishimura, R.; Nagao, K.; Miyayama, H.; Matsuda, M.; Baba, K.; Matsuoka, Y.; Yamashita, H.; Fukuda, M.; Higuchi, A.; Satoh, A.; Mizumoto, T.; Hamamoto, R. Thymidylate Synthase Levels as a Therapeutic and Prognostic Predictor in Breast Cancer. *Anticancer Res.* **1999**, *19*, 5621-5626.

133. Ishikawa, Y.; Kubota, T.; Otani, Y.; Watanabe, M.; Teramoto, T.; Kumai, K.; Takechi, T.; Okabe, H.; Fukushima, M.; Kitajima, M. Thymidylate Synthetase and Dihydropyrimidine Dehydrogenase Levels in Gastric Cancer. *Anticancer Res.* **1999**, *19*, 5635-5640.

134. Lenz, H. J.; Leichman, C. G.; Danenberg, K. D.; Danenberg, P. V.; Groshen, S.; Cohen, H.; Laine, L.; Crookes, P.; Silberman, H.; Baranda, J.; Garcia, Y.; Li, J.; Leichman, L. Thymidylate Synthase mRNA Level in Adenocarcinoma of the Stomach: a Predictor for Primary Tumor Response and Overall Survival. *J. Clin. Oncol.* **1996**, *14*, 176-182.

135. Johnston, P. G.; Mick, R.; Recant, W.; Behan, K. A.; Dolan, M. E.; Ratain, M. J.; Beckmann, E.; Weichselbaum, R. R.; Allegra, C. J.; Vokes, E. E. Thymidylate Synthase Expression and Response to Neoadjuvant Chemotherapy in Patients with Advanced Head and Neck Cancer. *J. Natl. Cancer. Inst.* **1997**, *89*, 308-313.

136. Sotos, G. A.; Grogan, L.; Allegra, C. J. Preclinical and Clinical Aspects of Biomodulation of 5-Fluorouracil. *Cancer Treat. Rev.* **1994**, *20*, 11-49.

137. Bobbio-Pallavicini, E.; Porta, C.; Moroni, M.; Spaghi, A.; Casagranda, I.; Nastasi, G. Folinic Acid Does Improve 5-Fluorouracil Activity in vivo. Results of a Phase III Study Comparing 5-Fluorouracil to 5-Fluorouracil and Folinic Acid in Advanced Colon Cancer Patients. *J. Chemother.* **1993**, *5*, 52-55.

138. Buyse, M.; Thirion, P.; Carlson, R. W.; Burzykowski, T.; Molenberghs, G.; Piedbois, P. Relation between Tumour Response to First-line Chemotherapy and Survival in Advanced Colorectal Cancer: a Meta-analysis. *Lancet* **2000**, *356*, 373-378.

139. Doroshow, J. H.; Multhauf, P.; Leong, L.; Margolin, K.; Litchfield, T.; Akman, S.; Carr, B.; Bertrand, M.; Goldberg, D.; Blayney, D. Prospective Randomized Comparison of Fluorouracil Versus Fluorouracil and High-dose Continuous Infusion Leucovorin Calcium

for the Treatment of Advanced Measurable Colorectal Cancer in Patients Previously Unexposed to Chemotherapy. *J. Clin. Oncol.* **1990**, *8*, 491-501.

140. O'Connell, M. J.; Martenson, J. A.; Wieand, H. S.; Krook, J. E.; Macdonald, J. S.; Haller, D. G.; Mayer, R. J.; Gunderson, L. L.; Rich, T. A. Improving Adjuvant Therapy for Rectal Cancer by Combining Protracted-Infusion Fluorouracil with Radiation Therapy after Curative Surgery. *N. Engl. J. Med.* **1994**, 331, 502-507.

141. Papamichael, D. The Use of Thymidylate Synthase Inhibitors in the Treatment of Advanced Colorectal Cancer: Current Status. *Oncologist*, **1999**, *4*, 478-487.

142. Peters, G. J.; Kohne, C. H. Fluoropyrimidines as antifolate drugs. In *Antifolate Drugs in Cancer Therapy*; Jackman, A. L., Ed.; Humana Press: Totowa, NJ, 1999; pp 101-145.

143. Jackman, A. L.; Calvert, A. H. Folate-based Thymidylate Synthase Inhibitors as Anticancer Drugs. *Ann. Oncol.* **1995**, *6*, 871-881.

144. Clarke, S. J.; Hanwell, J.; de Boer, M.; Planting, A.; Verweij, J.; Walker, M.; Smith, R.; Jackman, A. L.; Hughes, L. R.; Harrap, K. R.; Kennealey, G. T.; Judson, I. R. Phase I trial of ZD1694, a New Folate-based Thymidylate Synthase Inhibitor, in Patients with Solid Tumors. *J. Clin. Oncol.* **1996**, *14*, 1495-1503.

145. Sorensen, J. M.; Jordan, E.; Grem, J. L.; Arbuck, S. G.; Chen, A. P.; Hamilton, J. M.; Johnston, P.; Kohler, D. R.; Goldspiel, B. R.; Allegra, C. J. Phase I Trial of ZD1694 (Tomudex), a Direct Inhibitor of Thymidylate Synthase. *Ann. Oncol.* **1994**, *4*, 132-142.

146. Smith, I.; Jones, A.; Spielmann, M.; Namer, M.; Green, M. D.; Bonneterre, J.; Wander, H. E.; Hatschek, T.; Wilking, N.; Zalcberg, J.; Spiers, J.; Seymour, L. A Phase II Study in Advanced Breast Cancer: ZD1694 (’Tomudex’) a Novel Direct and Specific Thymidylate Synthase Inhibitor. *Br. J. Cancer* **1996**, *74*, 479-481.

147. Zalcberg, J. R.; Cunningham, D.; Van Cutsem, E.; Francois, E.; Schornagel, J.; Adenis, A.; Green, M.; Iveson, A.; Azab, M.; Seymour, I. ZD1694: a Novel Thymidylate Synthase Inhibitor with Substantial Activity in the Treatment of Patients with Advanced Colorectal Cancer. *J. Clin. Oncol.* **1996**, *14*, 716-721.

148. Cocconi, G.; Cunningham, D.; Van Cutsem, E.; Francois, E.; Gustavsson, B.; Van Hazel, G.; Kerr, D.; Possinger, K.; Hietschold, S. M. Open, Randomized Multicenter Trial of Raltitrexed versus Fluorouracil plus High-dose Leucovorin in Patients with Advanced Colorectal Cancer. *J. Clin. Oncol.* **1998**, *16*, 2943-2952.

149. Cunningham, D.; Zalcberg, J. R.; Rath, U.; Oliver, I.; Van Cutsem, E.; Svensson, C.; Seitz, J. F.; Harper, P.; Kerr, D.; Perez-Manga, G Final Results of a Randomised Trial Comparing 'Tomudex' (raltitrexed) with 5-Fluorouracil plus Leucovorin in Advanced Colorectal Cancer. *Ann. Oncol.* **1996**, *7*, 961-965.

150. Pazdur, R.; Vincent, M. Raltitrexed (Tomudex) versus 5-fluorouracil and leucovorin (5-FU + LV) in patients with advanced colorectal cancer (ACC): results of a randomized, multicenter, North American trial (abstract 801). *Proc. Am. Soc. Clin. Oncol.* **1997**.

151. Comella, P.; De Vita, F.; Mancarella, S.; De Lucia, L.; Biglietto, M.; Casaretti, R.; Farris, A.; Ianniello, G. P.; Lorusso, V.; Avallone, A.; Carteni, G.; Leo, S. S.; Catalano, G.; De Lena, M.; Comella, G. Biweekly Irinotecan or Raltitrexed plus 6S-leucovorin and Bolus 5-Fluorouracil in Advanced Colorectal Carcinoma: a Southern Italy Cooperative Oncology Group Phase II-III Randomized Trial. *Ann. Oncol.* **2000**, *11*, 1323-1333.

152. Lewis, N.; Scher, R.; Weiner, L. M.; Engstrom, P.; Szarka, C.; Gallo, J.; Adams, A.; Litwin, S.; Kilpatrick, D.; Brady, D.; Meropol, N. Phase I and Pharmacokinetic Study of Irinotecan in Combination with Raltitrexed (abstract 757). *Proc. Am. Soc. Clin. Oncol.* **2000**.

153. Scheithauer, W.; Kornek, G. V.; Ulrich-Pur, H.; Penz, M.; Raderer, M.; Salek, T.; Haider, K.; Kwasny, W.; Depisch, D. Oxaliplatin plus Raltitrexed in Patients with Advanced Colorectal Carcinoma: Results of a Phase I-II Trial. *Cancer* **2001**, *91*, 1264-1271.

154. Botwood, N.; James, R.; Vernon, C.; Price, P. Raltitrexed ('Tomudex') and Radiotherapy Can Be Combined as Postoperative Treatment for Rectal Cancer. Ann Oncol **2000**, *11*, 1023-1028.

155. Schultz, R. M.; Chen, V. J.; Bewley, J. R.; Roberts, E. F.; Shih, C.; Dempsey, J. A. Biological Activity of the Multitargeted Antifolate, MTA (LY231514), in Human Cell Lines with Different Resistance Mechanisms to Antifolate Drugs. *Semin. Oncol.* **1999**, *26*, 68-73.

156. Rinaldi, D. A. Overview of Phase I Trials of Multitargeted Antifolate (MTA, LY231514). *Semin. Oncol.* **1999**, *26*, 82-88.

157. O'Dwyer, P. J.; Nelson, K.; Thornton, D. E. Overview of Phase II Trials of MTA in Solid Tumors. *Semin. Oncol.* **1999**, *26*, 99-104.

158. Rusthoven, J. J.; Eisenhauer, E.; Butts, C.; Gregg, R.; Dancey, J.; Fisher, B.; Iglesias, J. Multitargeted Antifolate LY231514 as First-line Chemotherapy for Patients with Advanced Non-small-cell Lung Cancer: a Phase II Study. *J. Clin. Oncol.* **1999**, *17*, 1194-1199.

159. Manegold, C.; Gatzemeier, U.; von Pawel, J.; Pirker, R.; Malayeri, R.; Blatter, J.; Krejcy, K. Front-line Treatment of Advanced Non-small-cell Lung Cancer with MTA (LY231514, Pemetrexed Disodium, Alimta) and Cisplatin: a Multicenter Phase II Trial. *Ann. Oncol.* **2000**, *11*, 435-440.

160. John, W.; Picus, J.; Blanke, C. D.; Clark, J. W.; Schulman, L. N.; Rowinsky, E. K.; Thornton, D. E.; Loehrer, P. J. Activity of Multitargeted Antifolate (Pemetrexed Disodium,

LY231514) in Patients with Advanced Colorectal Carcinoma: Results from a Phase II Study. *Cancer* **2000**, *88*, 1807-1813.

161. Calvert, A. H.; Hughes, A. N.; Calvert, P. M.; Plummer, R.; Highley, M. Alimta in Combination with Carboplatin Demonstrates Clinical Activity against Malignant Mesothelioma in Phase I Trial (abstract 1936). *Proc. Am. Soc. Clin. Oncol.* **2000**.

162. Celio, L.; Bajetta, E.; Buzzoni, R.; Ferrari, L.; Martinetti, A.; Longaridini, R.; Marchano, A.; Ilardi, C.; Gentile, A. Efficacy and Toxicity of Pemetrexed Disodium (Alimta) with Folic Acid (FA) in Gastric Cancer (abstract 660). *Proc. Am. Soc. Clin. Oncol.* **2001**.

163. Scagliotti, G.; Shin, D.; Kindler, H.; Johnson, D.; Keppler, U. Phase II Study of Alimta Single Agent in Patients with Malignant Pleural Mesothelioma. *Eur. J. Cancer* **2001**, *37*, S20-S21.

164. Theodoulou, M.; Llombart, A.; Cruciani, G.; Bloch, R.; Campos, L.; Tung, N.; Borges, V.; Perry, M.; Rowland, K.; Schuster, M.; Kneuper-Hall, R.; Hudis, C. Pemetrexed Disodium (Alimta, LY231514, MTA) in Locally Advanced or Metastatic Breast Cancer (MBC) Patients (Pts) with Prior Anthracycline or Anthracenedione and Taxane Treatment: Phase II Study (abstract 506). *Proc. Am. Soc. Clin. Oncol.* **2000**.

165. Vogelzang, N.; Rusthoven, J.; Paoletti, P.; Denham, C.; Kaukel, E,; Ruffie, P.; Gatzemeier, U.; Boyer, M. J.; Emri, S.; Niyikiza, C. Phase III Single-blinded Study of Pemetrexed + Cisplatin vs. Cisplatin alone in Chemonaive Patients with Malignant Pleural Mesothelioma (abstract 5). *Proc. Am. Soc. Clin. Oncol.* **2002**.

166. Adam T. Purine *de novo* Synthesis - Mechanisms and Clinical Implications. *Klin. Biochem. Metab.* 2005;**13**:177–181

167. Welin, M.; Grossmann, J. G.; Flodin, S.; Nyman, T.; Stenmark, P.; Trésaugues, L.; Kotenyova, T.; Johansson, I.; Nordlund, P.; Lehtiö, L. Structural Studies of Tri-functional Human GART. *Nucleic Acids Res***. 2010**, *38*,7308–7319.

168. Zhang, Y., Desharnais, J., Greasley, S. E., Beardsley, G. P., Boger, D. L., and Wilson, I. A. Crystal Structures of Human GAR Tfase at Low and High pH and with Substrate β-GAR. *Biochemistry*, **2002**, *41*, 14206-14215.

169. Shim, J. H.; Benkovic, S. J., Catalytic Mechanism of Escherichia coli Glycinamide Ribonucleotide Transformylase Probed by site-directed Mutagenesis and pH-dependent Studies. *Biochemistry*, **1999**, 38, 10024-10031.

170. Dahms, T. E. S.; Sainz, G.; Giroux, E. L.; Caperelli, C. A.; Smith, J. L. The Apo and Ternary Complex Structures of a Chemotherapeutic Target: Human Glycinamide Ribonucleotide Transformylase. *Biochemistry*, **2005**, 44, 9841-9850.

171. Zhang, Y.; Desharnais, J.; Marsilje, T. H.; Li, C.; Hedrick, M. P.; Gooljarsingh, L. T.; Tavassoli, A.; Benkovic, S. J.; Olson, A. J.; Boger, D. L.; Wilson, I. A. Rational design, synthesis, evaluation, and crystal structure of a potent inhibitor of human GAR Tfase: 10-(trifluoroacetyl)-5,10-didedideaza-acyclic-5,6,7,8-tetrahydrofolic acid, *Biochemistry*, **2003**, *42*, 6043-6056

172. Varney, M. D.; Palmer, C. L.; Romines, W. H. III.; Boritzki, T.; Margosiak, S. A.; Almassy, R.; Janson, C. A., Bartlett, C.; Howland, E. J.; Ferre, R. Protein structure-based design, synthesis, and biological evaluation of 5-thia-2,6-diamino-4(3H)-oxopyrimidines: potent inhibitors of glycinamide ribonucleotide transformylase with potent cell growth inhibition, *J. Med. Chem.* **1997**, *40*, 2502-2524.

173. Taylor, E. C.; Harrington, P. J.; Fletcher, S. R., Beardsley, G. P.; Moran, R. G. Synthesis of the antileukemic agents 5,10-dideazaaminopterin and 5,10-dideaza-5,6,7,8 tetrahydroaminopterin. *J. Med. Chem.* **1985**, *28*, 914-921

174. Matherly, L. H.; Goldman, I. D. Membrane Transport of Folates. Vitam. Horm. **2003**, 66, 403–456.

175. Matherly, L. H.; Hou, Z.; Deng, Y. Human Reduced Folate Carrier: Translation of Basic Biology to Cancer Etiology and Therapy. *Cancer Metastasis Re*v. **2007**, *26*, 111–128.

176. Salazar, M. D.; Ratnam, M. The Folate Receptor: What Does It Promise in Tissue-Targeted Therapeutics. *Cancer Metastasis Rev*. **2007**, *26*, 141–152.

177. Hilgenbrink, A. R.; Low, P. S. Folate Receptor-Mediated Drug Targeting: From Therapeutics to Diagnostics. *J. Pharm. Sci*. **2005**, *94*, 2135–2146.

178. Qiu, A.; Jansen, M.; Sakaris, A.; Min, S. H.; Chattopadhyay, S.; Tsai, E.; Sandoval, C.; Zhao, R.; Akabas, M. H.; Goldman, I. D. Identification of an Intestinal Folate Transporter and the Molecular Basis for Hereditary Folate Malabsorption. *Cell*, **2006**, *127*, 917–928

179. Zhao, R.; Goldman, I. D. Resistance to Antifolates. *Oncogene.* **2003**, *22,* 7431-7457.

180. Ragoussis, J.; Senger, G.; Trowsdale, J.; Campbell, I. G. Genomic Organization of the Human Folate Receptor Genes on Chromosome 11q13. *Genomics* **1992**, 14, 423–430.

181. Elnakat, H.; Ratnam, M. Distribution, Functionality and Gene Regulation of Folate Receptor Isoforms: Implications in Targeted Therapy. *Adv. Drug Delivery*, **2004**, *56*, 1067–1084.

182. Toffoli, G.; Cernigoi, C.; Russo, A.; Gallo, A.; Bagnoli, M.; Boiocchi, M. Overexpression of Folate Binding Protein in Ovarian Cancers. *Int. J. Cancer*, **1997**, *74*, 193–198.

183. Wu, M.; Gunning, W.; Ratnam, M. Expression of Folate Receptor Type Alpha in Relation to Cell Type, Malignancy, and Differentiation in Ovary, Uterus, and Cervix. *Cancer Epidemiol., Biomarkers rev.* **1999**, *8*, 775–782.

184. Gangjee, A.; Dubash, N.P.; Zeng, Y.; McGuire, J.J. Recent Advances in the Chemistry and Biology of Folypoly-γ-glutamate Synthetase Substrates and Inhibitors. *Curr. Med. Chem. Anticancer Agents*, **2002**, *2*, 331-355.

185. Sikora, E.; Jackman, A. L.; Newell, D. R.; Calvert, A. H. Formation and Retention and Biological Activity of N^{10}-Propargyl-5,8-dideazafolic Acid (CB 3717) Polyglutamates in L1210 Cells *In Vitro. Biochem. Pharmacol.* **1988**, *37*, 4047-4054.

186. Jackman, A. L.; Newell, D. R.; Gibson, W.; Jodrell, D. I.; Taylor, G. A.; Bishop, J. A.; Hughes, L. R.; Calvert, A. H. The Biochemical Pharmacology of the Thymidylate Synthase Inhibitor 2-Desamino-2-methyl-N^{10}-propargyl-5,8-dideazafolic Acid (ICI 198583). *Biochem. Pharmacol.* **1991**, *42*, 1885-1895.

187. Nair, M. G.; Abraham, A.; McGuire, J. J.; Kisliuk, R. L.; Galivan, J. H.; Ferone, R. Polyglutamylation as a Determinant of Cytotoxicity of Classical Folate Analog Inhibitors of Thymidylate Synthase and Glycinamide Ribonucleotide Formyltransferase. *Cell. Pharmacol.* **1994**, *1*, 245-249.

188. Bisset, G. M. F.; Pawelczak, K.; Jackman, A. L.; Calvert, A. H.; Hughes, L. R. Syntheses and Thymidylate Synthase Inhibitory Activity of the Poly-γ-glutamyl Conjugates of *N*-[5-[*N*-(3,4- Dihydro-2-methyl-4-oxoquinazolin-6-ylmethyl)-*N*-methylamino]- 2-thienoyl]-L-glutamic Acid (ICI D1694) and Other Quinazoline Antifolates. *J. Med. Chem.* **1992**, *35*, 859-866.

189. Jackman, A. L.; Kelland, L. R.; Kimbell, R.; Brown, M.; Gibson, W.; Aherne, G. W.; Hardcastle, A.; Boyle, F. T. Mechanisms of Acquired Resistance to the Quinazoline Thymidylate Synthase Inhibitor ZD1694 (Tomudex) in One Mouse and Three Human Cell Lines. *Br. J. Cancer.* **1995**, *71*, 914-924.

190. Barakat, R. R.; Li, W. W.; Lovelace, C.; Bertino, J. R. Intrinsic Resistance of Cervical Squamous Cell Carcinoma Cell Lines to Methotrexate (MTX) as a Result of Decreased Accumulation of Intracellular Methotrexate Polyglutamates. *Gynecol. Oncol.* **1993**, *51,* 54-60.

191. McCloskey, D. E.; McGuire, J. J.; Russell, C. A.; Rowan, B. G.; Bertino, J. R.; Pizzorno, G.; Mini, E. Decreased Folylpolyglutamate Synthetase Activity as a Mechanism of Methotrexate Resistance in CCRF-CEM Human Leukemia Sublines. *J. Biol. Chem.* **1991**, *266*, 6181-6187.

192. Braakhuis, B. J. M.; Jansen, G.; Noordhius, P.; Kegel, A.; Peters, G. J. Importance of Pharmacodynamics in the *In Vitro* Antiproliferative Activity of the Antifolates Methotrexate and 10-Deazaaminopterin Against Human Head and Neck Squamous Cell Carcinoma. *Biochem. Pharmacol.* **1993**, *46*, 2155-2161.

193. Liani, E.; Rothem, L.; Bunni, M. A.; Smith, C. A.; Jansen, G.; Assaraf, Y. G. Loss of Folylpoly-γ-glutamate Synthetase Activity is a Dominant Mechanism of Resistance to Polyglutamylation-Dependent Novel Antifolates in Multiple Human Leukemia Sublines. *Int. J. Cancer* **2**Sheng, Y.; Sun, X.; Shen, Y.; Bognar, A. L.; Baker, E. N.; Smith, C. A. Structural and Functional Similarities in the ADP-forming Amide Bond Ligase Superfamily: Implications for a Substrate-Induced Conformational Change in Folylpolyglutamate Synthetase. *J. Mol. Biol.* **2000**, *302*, 427-440.

194. Kalman, T. I. Mechanism Based Approaches to Inhibition of the Synthesis and Degradation of Folate and Antifolate Polyglutamates. *Adv. Exp. Med. Biol.* **1993**, *338*, 639-643.

195. Blakeley, R. L.; Appleman, J. R. Recent Advances in the Study of Dihydrofolate Reductase. In *Chemistry and Biology of Pteridines*. Cooper and Whitehead, Eds.; Walter de Gruyter Berlin N.Y. **1986**, 769-772.

196. Cichowicz, D. J.; Shane, B. Mammalian Folylpoly-y glutamate Synthetase 2. Substrate Specificity and Kinetic Properties. *Biochemistry*, **1987**, *26*, 513-521.

197. Sheng, Y.; Sun, X.; Shen, Y.; Bognar, A. L.; Baker, E. N.; Smith, C. A. Structural and Functional Similarities in the ADP-forming Amide Bond Ligase Superfamily: Implications for a Substrate-Induced Conformational Change in Folylpolyglutamate Synthetase. *J. Mol. Biol.* **2000**, *302*, 427-440.

198. Kalman, T. I. Mechanism Based Approaches to Inhibition of the Synthesis and Degradation of Folate and Antifolate Polyglutamates. *Adv. Exp. Med. Biol.* **1993**, *338*, 639-643.

199. Shane, B.; Garrow, T.; Brenner, A.; Chen, L.; Choi, Y. J.; Hsu, J. C.; Stover, P. Folylpoly-γ-glutamate Synthetase. *Adv. Exp. Med. Biol.* **1993**, *338*, 629-634.

200. Cichowicz, D. J.; Shane, B. Mammalian Folylpoly-γ-glutamate Synthetase. 1. Purification and General Properties of the Hog Liver Enzyme. *Biochemistry*, **1987**, *26*, 504-512.

201. Garrow, T. A.; Admon, A.; Shane, B. Expression Cloning of a Human cDNA Encoding Folylpoly(γ-glutamate)Synthetase and Determination of its Primary Structure. *Proc. Natl. Acad. Sci. USA* **1992**, *89*, 9151-9155.

202. Sun, X.; Cross, J.A.; Bognar, A.L.; Baker, E.N. and Smith, C.A. Folate-binding Triggers the Activation of Folypolyglutamate Synthetase, *J. Mol. Biol*., **2001**, 310, 1067-1078.

203. McGuire, J. J.; Coward, J. K. Folylpolyglutamate Synthetase as a Target for Therapeutic Intervention. *Drugs Fut.*, **2003**, *28*, 967-974.

204. Jordan, M. A. and Wilson L. Microtubules as a Target for Anticancer Drugs. *Nat. Rev., Cancer*, **2004**, *4*, 253-265.

205. Valiron, O.; Caudron, N.; Job, D. Microtubule dynamics. *Cell Mol. Life Sci*. **2001**, *58*, 2069-2084.

206. Vos, J. W.; Dogterom, M.; Emons, A. M.. Microtubules Become More Dynamic but not Shorter During Preprophase Band Formation: A Possible 'Search-and capture' Mechanism for Microtubule translocation. *Cell Motil Cytoskeleton*, **2004**, *57*, 246-258.

207. Desai, A.; Mitchison, T. J. Microtubule Polymerization Dynamics. *Annu. Rev. Cell. Dev. Biol.* **1997**, *13*, 83-117.

208. Margolis R.L. and Wilson, L. Microtubule Treadmilling: What Goes Around Comes Around. *BioEssays* , **1998,** *20*, 830–836.

209. Jordan, A.; Hadfield, J. A.; Lawrence, N. J.; and McGown, A. T.. Tubulin as a Target for Anticancer Drugs: Agents which Interact with the Mitotic Spindle. *Med Res Rev*. **1998**, *4*, 259-96.

210. Heald, R. and Nogales, E. Microtubule Dynamics. *J. Cell Sci.*, **2002**, *115*, 3-4.

211. Bai, R. B., Pettit, G. R. & Hamel, E.. Binding of Dolastatin 10 to Tubulin at a Distinct Site for Peptide Antimitotic Agents near the Exchangeable Nucleotide and Vinca Alkaloid Sites. *J. Biol. Chem.* **1990**, *265*, 17141–17149.

212. Correia, J. J. Effects of Antimitotic Agents on Tubulin-nucleotide Interactions. *Pharmacol. Ther.*, **1991**, *51*, 127.

213. Checchi, P. M.; Nettles, J. H.; Zhou, J.; Snyder, J. P. and Joshi, H. C.. Microtubule-Interacting Drugs for Cancer Treatment. *Trends. Pharmcol. sci.*, **2003**, *24*, 361-365.

214. Sikic, B.; Fisher, G.; Lum, B.; Halsey, J.; Beketic-Oreskovic, L.. Modulation and Prevention of Multidrug Resistance by Inhibitors of P-glycoprotein. *Cancer Chemother. Pharmacol.*, **1997**, *40*, S13-S19.

215. Ling, V. Multidrug Resistance: Molecular Mechanisms and Clinical Relevance. *Cancer Chemother.*, **1997**, *40*, S3-8.

216. Tan, B. Multidrug Resistance Transporters and Modulation. *Appl. Biochem. Biotechnol.*, **2000**, *87*, 233-245.

217. Goldstein, L. J.; Galski, H.; Fojo, A.; Willingham, M.; Lai, S. L. ; et al. Expression of a Multidrug Resistance Gene in Human Cancers. *J. Natl. Cancer Inst.*, **1989**, *81*, 116-124.

218. Fojo, A. T.; Ueda, K.; Slamon, D. J.; Poplack, D. G.; Gottesman, M. M. *and Pastan, I.* Expression of a Multidrug-Resistance Gene in Human Tumors and Tissues. *Proc. Natl. Acad. Sci.,* **1987***, 84*, 265-269.

219. Ma, D. D.; Scurr, R. D.; Davey, R. A.; Mackertich, S. M.; Harman, D. H.; et al. Detection of a Multidrug Resistant Phenotype in Acute Non-Lymphoblastic Leukaemia. *Lancet*, **1987**, *1*, 135-137.

220. Van de Vrie, W.; Marquet, R. L.; Stoter, G.; De Bruijn, E. A. and Eggermont, A. M. *In vivo* Model Systems in P-glycoprotein-Mediated Multidrug Resistance. *Crit. Rev. Clin. Lab Sci.*, **1998**, *35*, 1-57.

221. Trock, B. J.; Leonessa, F.; and Clarke, R. Multidrug Resistance in Breast Cancer: A Meta-Analysis of MDR1/gp170 Expression and Its Possible Functional Significance. *J. Natl. Cancer Inst.*, **1997**, *89*, 917-931.

222. Grant, C. E.; Valdimarsson, G.; Hipfner, D. R.; Almquist, K. C.; Cole, S. P.; et al. Overexpression of Multidrug Resistance-Associated Protein (MRP) Increases Resistance to Natural Product Drugs. *Cancer Res.*, **1994**, *54*, 357-361.

223. Kruh, G. D.; Chan, A.; Myers, K.; Gaughan, K.; Miki, T. *and Aaronson, S. A.* Expression Complementary DNA library Transfer Establishes MRP as a Multidrug Resistance Gene. *Cancer Res.*, **1994**, *54*, 1649-1652.

224. Cole, S. P.; Bhardwaj, G.; Gerlach, J. H.; Mackie, J. E.; Grant, C. E.; et al. Overexpression of a Transporter Gene in a Multidrug-Resistant Human Lung Cancer Cell Line. *Science*, **1992**, *258*, 1650-1654.

225. Giannakakou P.;Sackeet. D. L.; Kang, Y.; Zhan, Z.; Buters. J. T. M.; Fojo, T. and Poruchynsky, M. S.. Paclitaxel-resistant Human Ovarian Cancer Cells Have Mutant β-Tubulins that Exhibit Impaired Paclitaxel-driven Polymerization. *J. Biol. Chem.* **1997,** *272,* 17118–17125.

226. Gonzalez-Garay M.L.; Gussio, R.; Nogales, E.; Downing, K. H.; Zaharevitz, D.; Bollbuck, B.; Poy, G.; Sackett, D.; Nicolaou, K. C. and Fojo, T. A β-tubulin Leucine Cluster Involved in Microtubule Assembly and Paclitaxel Resistance. *J. Biol. Chem.* **1999,** *274,* 23875–23882.

227. Sullivan, K.F. Structure and Utilization of Tubulin Isotypes**.** *Annu.Rev.Cell Biol*. **1988**, *4*, 687-716.

228. Lewis, S. A.; Cowan, N. J. Microtubule Proteins (Avila J., ed) 1990, pp. 37–65, CRC Press, Boca Raton, FL.

229. Kaira, K.; Takahashi, T.; Murakami, H.; Shukuya, T.; Kenmotsu, H.; Ono, A.; Naito, T.; Tsuya, A.; Endo, Y. N. M.; Kondo, H.; Nakajima, T.; Yamamoto, N. The role of βIII-tubulin in Non-small Cell Lung Cancer Patients Treated by Taxane-based Chemotherapy. *Int. J. Clin. Oncol.* Online First™, 23 February 2012.

230. Seve, P.; Reiman, T.; Dumontet, C. The Role of βIII-tubulin in Predicting Chemoresistance in Non-small Cell Lung Cancer. *Lung Cancer*, **2010**, *67*,136–143.

231. Folkman, J. Tumor Angiogenesis: Therapeutic Implications. *N. Eng. J. Med.* **1971**, *285*, 1182-1186.

232. Carmeliet, P. Mechanisms of Angiogenesis and Arteriogenesis. *Nature Med.*, **2000**, *6*, 389-395.

233. Choura, M.; Reba, A. Receptor tyrosine kinases: from biology to pathology. *J Recept Signal Transduct Res.* **2011**, *31*, 387-394.

234. Haroon, Z.; Peters, K.G.; Greenberg, C.S. and Dewhirst, M.W. Angiogenesis and Blood Flow in the Solid Tumors. In: Antiangiogenic Agents in Cancer Therapy, Edited by Beverly A. Teicher, Totowa, New Jersey, Humana Press. pp3-22, **1999**.

235. Bar, J.; Goss, G. D. L. K. Tumor Vasculature as a Therapeutic Target in Non-small Cell Lung Cancer. *J Thorac Oncol*. **2012**, *7*, 609-620.

236. Daniele, G.; Corral, J.; Molife, L. R.; de Bono, J. S. G. FGF Receptor Inhibitors: Role in Cancer Therapy. *Curr Oncol Rep*. **2012** Feb 5. [Epub ahead of print]

237. Fabbro, D., McCormick, F., Eds. *Protein Tyrosine Kinases: From Inhibitors to Useful Drugs*; Humana Press, Totowa, NJ, 2006; 290 pp.

238. Reckamp, K.L. Antiangiogenic Agents as Second-line Therapy for Advanced Non-small Cell Lung Cancer. *Cancer Lett.* **2012** Feb 3. [Epub ahead of print]

239. Ellis, L. M. Epidermal Growth Factor Receptor in Tumor Angiogenesis. *Hematol. Oncol. Clin. North America*, **2004**, *18*, 1007-1021.

240. Lemmon1, M. A.; Schlessinger, J. Cell Signaling by Receptor Tyrosine Kinases. Cell, **2010**, *141*, 1117-1134.

241. Dan, R. Robinson.; Yi-Mi, Wu.; Su-Fang Lin. The protein tyrosine kinase family of the human genome. *Oncogene* , **2000**, *19*, 5548–5557.

242. Li, E.; Hristova, K. Receptor Tyrosine Kinase Transmembrane Domains Function, Dimer Structure and Dimerization Energetics. *J Recept Signal Transduct Res*. **2011**, *31*, 387-394.

243. Peter, Geer.; Tony, Hunter.; Richard, A., Lindberg. Receptor Protein-tyrosine Kinases and Their Signal Transduction Pathway. *Ann. Rev. Cell Biol*., **1994**, *10*, 251–337.

244. Joseph, S. Cell Signaling by Receptor Tyrosine Kinases. *Cell*, **2000**, *103*, 211-225.

245. A., Ullrich.; L., Coussens., J. S., Hayflick.; T., J., Dull.; A., Gray.; A. W., Tam.; J., Lee.; Y., Yarden.; T. A., Libermann.; J., Schlessinger.; J., Downward.; E. L. V., Mages.; N., Whittle.; M. D., Warfield.; P. H., Seeburg. Human epidermal growth factor receptor cDNA sequence and aberrant expression of the amplified gene in A431 epidermoid carcinoma cells. *Nature*, **1984**, *309*, 418–425.

246. Kolibaba, K. S.; Druker, B. J. Protein Tyrosine Kinases and Cancer. *Biochimica et Biophysica Acta*, **1997**, *1333*, F217–F248.

247. Thogersen, V. B.; Jorgensen, P. E.; Sorensen, B. S.; Bross, P.; Orntoft, T.; Wolf, H.; Nexo, E. Expression of Transforming Growth Factor Alpha and Epidermal Growth Factor Receptor in Human Bladder Cancer. *Scand. J. Clin. Lab Invest.* **1999**, *59*, 267-277.

248. Batchu, S.N.; Korshunov, V. A. Novel Tyrosine Kinase Signaling Pathways: Implications in Vascular Remodeling. *Curr Opin Nephrol Hypertens*. **2012**, *21*, 122-127.

249. Hynes, N. E; Lane, H.A. ERBB Receptors and Cancer: The Complexity of Targeted Inhibitors. *Nat Rev Cancer.* **2005**, *5*, 341–354.

250. Shelton, J. G.; Steelman, L. S; Abrams, S. L.; Bertrand, F. E.; Franklin, R. A.; McMahon, M.; McCubrey, J. A. The Epidermal Growth Factor Receptor Gene Family as a Target For Therapeutic Intervention in Numerous Cancers: What's Genetics Got to Do With It? *Expert. Opin. Ther. Targets.* **2005**, *9*, 1009-1030.

251. Seshacharyulu, P. ; Ponnusamy, M. P.; Haridas, D.; Jain, M.; Ganti, A. K.; Batra, S. K. Targeting the EGFR Signaling Pathway in Cancer Therapy. *Expert. Opin. Ther. Targets.* **2005** [Epub ahead of print].

252. Salomon, D. S.; Brandt, R.; Ciardiello, F.; Normanno, N. Epidermal Growth Factor-Related Peptides and Their Receptors in Human Malignancies. *Crit. Rev. Oncol. Hematol*. **1995**, *19*, 183−232.

253. Ritter, C. A.; Artega, C. L. The Epidermal Growth Factor Receptor-tyrosine Kinase: A Promising Therapeutic Target in Solid Tumors. *Semin. Oncol*.**2003**, *30*, 993−1011.

254. Andrae J, Gallini R, Betsholtz C. Role of platelet-derived growth factors in physiology and medicine. *Genes Dev*, **2008**, *22*, 1276–1312.

255. Board, R.; Jayson, G. C.Platelet-Derived Growth Factor Receptor (PDGFR): A Target for Anticancer Therapeutics. *Drug Resist. Updates*, **2005**, *8*, 75-83.

256. Ostman, A. PDGF Receptors-Mediators of Autocrine Tumor Growth and Regulators of Tumor Vasculature and Stroma. *Cytokine Growth F R*, **2004**, *15*, 275-286.

257. Shima, A. H.; Liua, H.; Fociaa, P. J.; Chena, X.; Linb, P. C.; Hea, X. Structures of a Platelet-derived Growth Factor/propeptide Complex and a Platelet-Derived Growth Factor/receptor Complex. *PNAS*, **2010**, *107*, 11307-11312.

258. Otrock, Z. K.; Makarem, J. A.; and Shamseddine, A. I. Vascular Endothelial Growth Factor Family of Ligands and Receptors: Review. *Blood Cells Mol. Dis*. **2007**, *38*, 258–268.

259.

260. Anan, K.; Morisaki, T.; Katano, M.; Ikubo, A.; Kitsuki, H.; Uchiyama, A.; Kuroki, S.; Tanaka, M.; Torisu, M. Vascular Endothelial Growth Factor and Platelet-Derived Growth Factor are Potential Angiogenic and Metastatic Factors in Human Breast Cancer. *Surgery* **1996**, *119*, 333-339.

261. Brown, L. F.; Jackman, R. W.; Tognazzi, K.; Manseau, E. J.; Senger, D. R.; Dvorak, H. F. Expression of Vascular Permeability Factor (Vascular Endothelial Growth Factor) and Its Receptors in Adenocarcinomas of the Gastrointestinal Tract. *Cancer Res.* **1993**, *53*, 4727-4735.

262. Takahashi, A.; Sasski, H.; Kim, S. J.; Tobisu, K.-I.; Kakizoe, T.; Tsukamoto, T.; Kumamoto, Y.; Sugimura, T.; Terada, M. Markedly Increased Amounts of Messenger RNAs for Vascular Endothelial Growth Factor and Placenta Growth Factor in Renal Cell Carcinoma Associated with Angiogenesis. *Cancer Res.* **1994**, *54*, 4233-4237.

263. Kampen, K. R. The Mechanisms That Regulate the Localization and Overexpression of VEGF Receptor-2 are Promising Therapeutic Targets in Cancer Biology. *Anticancer Drugs*. **2012**, *23*, 347-354.

264. Beenken, A.; Mohammadi, M. The FGF Family: Biology, Pathophysiology and Therapy. *Nat Rev Drug Discov*. **2009**, *8*, 235–253.

265. Johnson, D.E.; Williams, L.T. Structural and Functional Diversity in the FGF Receptor Multigene Family. *Adv Cancer Res*. **1993**, *60*, 1-41.

266. Presta, M.; Dell'Era, P.; Mitola, S. Fibroblast Growth Factor/Fibroblast Growth Factor Receptor System in Angiogenesis. *Cytokine Growth Factor Rev*. **2005**,*16*, 159–178.

267. Takimoto CH, Calvo E. Principles of Oncologic Pharmacotherapy. in Pazdur R, Wagman LD, Camphausen KA, Hoskins WJ (Eds) Cancer Management: A Multidisciplinary Approach. 11 ed. **2008**

268. Mendel, D. B.; Laird, A. D.; Smolich, B. D.; Blake, R. A.; Liang, C.; Hannah, A. L.; Shaheen, R. M.; Ellis, L. M.; Weitman, S.; Shawver, L. K.; Cherrington, J. M. Development of SU5416, a Selective Small Molecule Inhibitor of VEGF Receptor Tyrosine Kinase Activity, as an Anti-angiogenesis Agent. *Anti-Cancer Drug Des.* **2000**, *15*, 29-41.

269. Hoff, PM, Wolff, R. A.; Bogaard, K.; Waldrum, S. and Abbruzzese J. L.. A Phase I Study of Escalating Doses of the Tyrosine Kinase Inhibitor Semaxanib (SU5416) in Combination with Irinotecan in Patients with Advanced Colorectal Carcinoma. *Jpn. J. Clin. Oncol.* **2006**, *36*, 100–103.

270. Crizotinib

271. Faivre, S.; Delbaldo, C.; Vera, K.; Robert, C.; Lozahic, S.; Lassau, N.; Bello, C.; Deprimo, S.; Brega, N.; Massimini, G.; Armand, J.-P.; Scigalla, P.; Raymond, E. Safety, pharmacokinetic, and antitumor activity of SU11248, a novel oral multitarget tyrosine kinase inhibitor, in patients with cancer. *J. Clin. Oncol.* **2006**, *24*, 25-35.

272. Harris, P. A.; Boloor, A.; Cheung, M.; Kumar, R.; Crosby, R. M.; Davis-Ward, R. G.; Epperly, A. H.; Hinkle, K. W.; Hunter III, R. N.; Johnson, J. H.; Knick, V. B.; Laudeman, C. P.; Luttrell, D. K.; Mook, R. A.; Nolte, R. T.; Rudolph, S. K.; Szewczyk, J. R.; Truesdale, A.

T.; Veal, J. M.; Wang, L.; Stafford, J. A. Discovery of 5-[[4-[(2,3-dimethyl-2*H*-indazol-6-yl)methylamino]-2-pyrimidinyl]amino]-2-methylbenzenesulfonamide (Pazopanib), a novel and potent vascular endothelial growth factor receptor inhibitor. *J. Med. Chem.* **2008**, *51*, 4632-4640.

273. Wilhelm, S. M.; Carter, C.; Tang, L.; Wilkie, D.; McNabola, A.; Rong, H.; Chen, C.; Zhang, X.; Vincent, P.; McHugh, M.; Cao, Y.; Shujath, J.; Gawlak, S.; Eveleigh, D.; Rowley, B.; Liu, L.; Adnane, L.; Lynch, M.; Auclair, D.; Taylor, I.; Gedrich, R.; Voznesensky, A.; Riedl, B.; Post, L. E.; Bollag, G.; Trail, P. A. BAY 43-9006 exhibits broad spectrum oral antitumor activity and targets the RAF/MEK/ERK pathway and receptor tyrosine kinases involved in tumor progression and angiogenesis. *Cancer Res.* **2004**, *64*, 7099-7109.

274. Bollag, G.; Hirth, P.; Tsai, J. *et al*. Clinical efficacy of a RAF inhibitor needs broad target blockade in BRAF-mutant melanoma. *Nature*, **2010**, 467, 596-599.

275. Morabito, A.; Piccirillo, M. .; Costanzo, R.; Sandomenico, C.; Carillio, G.; Daniele, G.; Giordano, P.; Bryce, J.; Carotenuto, P.; La Rocca, A.; Di Maio, M.; Normanno, N.; Rocco, G.; Perrone, F. Vandetanib: An Overview of its Clinical Development in NSCLC and other Tumors. *Drugs Today*, **2010**, *46*, 683-698.

276. Kenny, L. M.; Lam, E. W. Review: lapatinib in metastatic colorectal cancer-another strategy for disease control? *Clin Adv Hematol Oncol*, 2011, 9, 500-501.

277. Melichar, B.; Studentová, H.; Zezulová, M. Pazopanib: a new multiple tyrosine kinase inhibitor in the therapy of metastatic renal cell carcinoma and other solid tumors. *J BUON*, **2011**, *16*, 203-209.

278. Traxler, P.; Bold, G.; Buchdunger, E.; Caravatti, G.; Furet, P.; Manley, P.; O'Reilly, T.; Wood, J.; Zimmermann, J. Tyrosine Kinase Inhibitors: From Rational Design to Clinical Trials. *Med. Res. Rev.* **2001**, *21*, 499-512

279. Fabbro, D.; Ruetz, S.; Buchdunger, E.; Cowan-Jacob, S. W.; Fendrich, G.; Liebetanz, J.; Mestan, J.; O'Reilly, T.; Traxler, P.; Chaudhuri, B.; Fretz, H.; Zimmermann, J.; Meyer, T.; Caravatti, G.; Furet, P.; Manley, P. W. Protein Kinases as Targets for Anticancer Agents: From Inhibitors to Useful Drugs. *Pharmacol. Ther.* **2002**, *93*, 79-98.

280. Gangjee, A.; Yang, J.; Ihnat M. A. and Kamat, S. Antiangiogenic and Antitumor Agents: Design, Synthesis, and Evaluation of Novel 2-Amino-4-(3-bromoanilino)-6-benzylsubstituted Pyrrolo[2,3-*d*]pyrimidines as Inhibitors of Receptor Tyrosine Kinases *Bioorg. Med. Chem*. **2003,** *11*, 5155-5170.

281. Laufer, S. A.; Domeyer, D. M.; Scior, T. R. F.; Albrecht, W.; Hauser, D. R. J. Synthesis and Biological Testing of Purine Derivatives as Potential ATP-Competitive Kinase Inhibitors. *J. Med Chem.* **2005**, *48*, 710-722.

282. ATP-binding site

283. Gewald, K. Heterocycles from CH-acidic nitriles. IX. Reaction of α-hydroxy Ketones with Malononitrile. *Chem. Ber.* **1996**, *99*, 1002-1007.

284. Miyazaki, Y.; Matsunaga, S.; Tang, J.; Maeda, Y.; Nakano, M.; Philippe, R. J.; Shibahara, M.; Liu, W.; Sato, H.; Wang, L.; Nolte, R. T. Novel 4-aminofuro[2,3-d]pyrimidines as Tie-2 and VEGFR2 Dual Inhibitors. *Bio. Med. Chem. Lett.***2005**, *15*, 2203-2207.

285. Miyazaki, Y.; Maeda, Y.; Sato, H.; Nakano, M.; Mellor, G. W. Rational Design of 4-amino-5,6-diaryl-furo[2,3-d]pyrimidines as Potent Glycogen Synthase Kinase-3 Inhibitors. *Bio. Med. Chem. Lett.***2008**, *18*, 1967-1971.

286. Han, Y.; Ebinger, K.; Vandevier, L., E.; Maloney, J. W.; Nirschl, D. S.; Weller, H. N. Efficient and library-friendly Synthesis of furo- and thieno[2,3-d] pyrimidin-4-amine Derivatives by Microwave Irradiation.*Tetrahedron Lett*, **2010**, *51*, 629-632.

287. Dave, K. G.; Shishoo, C. J.; Devani, M. B.; Kalyanaraman, R.; Ananthan, S.; Ullas, G. V.; Bhadti, V. S. Reaction of Nitriles under Acidic cConditions. Part I. A General Method of Synthesis of Condensed Pyrimidines. *Heterocycl Chem*, **1980**, *17*, 1497-1500.

288. Manhas, M. S. ; Amin, S. G. Heterocyclic compounds. VIII. Synthesis of 3- and 2,3-substituted thienopyrimidones. *Heterocycl Chem*, **1977**, *14*, 161-164.

289. Martin-Kohler, Andreas; Widmer, Jorg; Bold, Guido; Meyer, Thomas; Sequin, Urs; Traxler, Peter. Furo[2,3-*d*]pyrimidines and Oxazolo[5,4-*d*]pyrimidines as Inhibitors of Receptor Tyrosine Kinases (RTK). *Helvetica Chimica Acta*, **2004**, *87*, 956-975.

290. Foloppe, Nicolas; Fisher, Lisa M.; Howes, Rob; Kierstan, Peter; Potter, Andrew; Robertson, Alan G. S.; Surgenor, Allan E. Structure-Based Design of Novel Chk1 Inhibitors: Insights into Hydrogen Bonding and Protein-Ligand Affinity.

291. Dang, Qun; Liu, Yan. An efficient entry to furo[2,3-*d*]pyrimidines via inverse electron demand Diels-Alder reactions of 2-aminofurans with 1,3,5-triazines. *Tetrahedron Lett*, **2009**, *50*, 6758-6760.

292. Iaroshenko, Viktor O. Synthesis of some Fluorinated Heteroannulated Pyrimidines - Purine Isosteres - via Inverse-electron-demand Diels-Alder Protocol. *Synthesis*, **2009**, *23*, 3967-3974.

293. Sakamoto, Takao; Kondo, Yoshinori; Yamanaka, Hiroshi. Studies on Pyrimidine Derivatives. XXIX. Synthesis of Pyrimidines Fused with Five-membered Heterocycles by

Cross-Coupling of 5-iodopyrimidines with Phenylacetylene and Styrene. *Chem Pharm Bull*, **1982**, *30*, 2417-2420.

294. Petricci, E.; Radi, M.; Corelli, F.; Botta, M. Microwave-enhanced Sonogashira Coupling Reaction of Substituted Pyrimidinones and Pyrimidine Nucleosides. *Tetrahedron Lett*., **2003**,*44*, 9181–9184.

295. Liu, Z.; Li, D.; Li, S.; Bai, D.; He, X.; Hu, Y. Synthesis of Novel 5,6-substituted Furo[2,3-*d*]pyrimidines *via* Pd-catalyzed Cyclization of Alkynylpyrimidinols with Aryl Iodides. *Tetrahedron*, **2007**, *63*, 1931-1936.

296. Eger, Kurt; Jalalian, Mohammad; Schmidt, Mathias. Steric Fixation of Bromovinyluracil: Synthesis of furo[2,3-*d*]pyrimidine Nucleosides. *Heterocycl Chem*, **1995**, *32*, 211-218.

297. Bisagni, E.; Marquet, J. P.; Andre-Louisfert, J. 2,3-Disubstituted Furans and Pyrroles. VI. Synthesis of Some New Pyrimidines and their Transformation into Furo- and Pyrrolo[2,3-*d*]pyrimidines. Bull. Soc. Chim. Fr. 1969, 3, 803-811.

298. Grindey, G. B.; Wang, M. C.; Kinahan, J. J. Thymidine Induced Perturbations in Ribonucleoside Triphosphate Pools in Human Leukemic CCRF-CEM Cells. *Mol. Pharmacol*.**1979**, *16*, 601-606.

299. Tolman, Richard L.; Robins, Roland K.; Townsend, Leroy B. Pyrrolo[2,3-d]pyrimidine Nucleoside Antibiotics. Total Synthesis and Structure of Toyocamycin, Unamycin B, Vengicide, Antibiotic E-212, and Sangivamycin (BA-90912). *J. Am. Chem. Soc*, **1968**, *90*, 524-526.

300. Girgis, N. S.; Joergensen, A.; Pedersen, E. B. Phosphorus Pentoxide in Organic Synthesis; XI. A New Synthetic Approach to 7-Deazahypoxanthines. *Synthesis*, **1985**, *1*, 101-104.

301. Bookser, Brett C.; Ugarkar, Bheemarao G.; Matelich, Michael C.; Lemus, Robert H.; Allan, Matthew; Tsuchiya, Megumi; Nakane, Masami; Nagahisa, Atsushi; Wiesner, James B.; Erion, Mark D. Adenosine Kinase Inhibitors. 6. Synthesis, Water Solubility, and Antinociceptive Activity of 5-Phenyl-7-(5-deoxy-β-D-ribofuranosyl)pyrrolo[2,3-d]pyrimidines Substituted at C4 with Glycinamides and Related Compounds. *J. Med. Chem.* **2005**, *48*, 7808-7820.

302. Barnett, C. J.; Wilson, T. M.; Grindley, G. B. Synthesis and Antitumor Activity of LY288601, the 5,6-Dihydro analog of LY231514. *Adv. Exp. Med Biol*. **1993**, *338*, 409-412.

303. Noell, C. W.; Robins, R. K. Aromaticity in Heterocyclic Systems. II. The Application of NMR in a Study of the Synthesis and Structure of Certain Imidazo[1,2-*c*]pyrimidines and Related Pyrrolo[2,3-*d*]pyrimidines. *J. Heterocycl. Chem.* **1964**, *1*, 34-41.

304. Gibson, Colin L.; Ohta, Kyuji; Paulini, Klaus; Suckling, Colin J. Specific Inhibitors in Vitamin Biosynthesis. Part 10. Synthesis of 7- and 8-substituted 7-deazaguanines. *J. Chem. Soc., Perkin Trans. 1*, **1998**, *18*, 3025-3032.

305. Duffy, T. D.; Wibberley, D. G. Pyrrolo[2,3-*d*]pyrimidines. Synthesis from 4-Pyrimidylhydrazones, a 2-Bis(ethylthio)methyleneaminopyrrolo-3-carbonitrile and a Pyrrolo[2,3-*d*][1,3]thiazine-2(1*H*)-thione. *J. Chem. Soc., Perkin Trans. 1* **1974**, *16*, 1921-1929.

306. Miwa, T.; Hitaka, T.; Akirnoto, H. A Novel Synthetic Approach to Pyrrolo[2,3-*d*]pyrimidine Antifolates. *J. Org. Chem.* **1993**, *58*, 1696-1701.

307. Sakamoto, T.; Satoh, C.; Kondo, Y.; Yamanaka, H. Condensed Heteroaromatic Ring Systems. XXI. Synthesis of Pyrrolo[2,3-*d*]pyrimidines and Pyrrolo[3,2-*d*]pyrimidines. *Chem. Pharm. Bull.* **1993**, *41*, 81-86.

308. Kondo, Y.; Watanabe, R.; Sakamoto, T.; Yamanaka, H. Condensed Heteroaromatic Ring Systems. XVI. Synthesis of Pyrrolo[2,3-*d*]pyrimidine Derivatives. *Chem. Pharm. Bull*., **1989**, *37*, 2933-2936.

309. Gangjee, A.; Yu, J.; McGuire, J. J.; Cody, V.; Galitsky, N.; Kisliuk, R. L.; Queener, S. F. Design, Synthesis, and X-Ray Crystal Structure of a Potent Dual Inhibitor of Thymidylate Synthase and Dihydrofolate Reductase as an Antitumor Agent. *J. Med. Chem*., **2000**, *43*, 3837-3851.

310. Kim, D. H.; Santilli, A. A. 7-Deazapurines. II. Syntheses and Reactions of 5-aminopyrrolo[2,3-d]pyrimidine-6-carbonitrile and Related Compounds. *Heterocycl Chem*, **1971**, *8*, 715-719.

311. Gangjee, A.; Dubash, N. P.; Kisliuk, R. L. Synthesis of Novel, Nonclassical 2-Amino-4-oxo-6-(arylthio)ethylpyrrolo[2,3-*d*]pyrimidines as Potential Inhibitors of Tymidylate Synthase, *J. Heterocycl. Chem.* **2001**, *38*, 349-354.

312. Gangjee, A.; Vidwans, A.; Elzein, E.; McGuire, J. J.; Queener, S. F.; Kisliuk, R. L.Synthesis, Antifolate, and Antitumor Activities of Classical and Nonclassical 2-Amino-4-oxo-5-substituted-pyrrolo[2,3-*d*]pyrimidines. *J. Med. Chem.* **2001**, *44*, 1993-2003.

313. ?????

314. Taylor, Edward C.; Liu, Bin. A Simple and Concise Synthesis of LY231514 (MTA). *Tetrahedron Lett.* **1999**, *40*, 4023-4026.

315. Crooks, P. A.; Robinson, B. Thermal Indolization of 4-Pyrimidinylhydrazones and 4-Pyridylhydrazones. *Chem. Ind.* **1967**, 547-548.

316. Wright, G. E. 9*H*-Pyrimido[4,5-*b*]indole-2,4-diones. The Acid-catalyzed Cyclization of 6-(phenylhydrazino)uracils. *J. Heterocycl. Chem.* **1976**, 13, 539-545.

317. Taylor, E. C.; Young, W. B.; Chaudhari, R.; Patel, M. Synthesis of a Regioisomer of N-{4-[2-(2-amino-4(3*H*)-oxo-7*H*-pyrrolo[2,3-*d*]pyrimidin-5-yl)ethyl]benzoyl}-L-glutamic Acid (LY231514), an Active Thymidylate Synthase Inhibitor and Antitumor Agent. *Heterocycles* **1993**, *36*, 1897-1908.

318. Rosowsky, A.; Chaykovsky, M.; chen, K. K. N.; Lin, M.; Modest, E. J. 2,4-Diaminothieno[2,3-*d*]Pyrimidines as Antifolates and Antimalarials. 1. Synthesis of 2,4-Diamino-5,6,7,8-Tetrahydrothianaphtheno[2,3-*d*]pyrimidines and Related Compounds. J. *Med. Chem.* **1973,** *16*, 185-188

319. Gewald, K. Heterocyclen aus CH-aciden nitrilen. VII. 2-Aminothiophene aus α-oxo-Mercaptanen und Methylen aktiven Nitrilen. *Chem. Ber*. **1966**, *98*, 3571-3577.

320. Zhang, M.; Harper, R. W. A Concise Synthetic Entry to Substituted 2-Aminothieno[2,3-*d*]pyrimidines Via a Gewald Precursor. B*ioorganic & med. Chem. Letters* **1997,** *7*, 1629-1634.

321. Ishikawa, F.; Yamaguchi, H. Cyclic Guanidines. Xiii. Synthesis of 2-Amino-4-Phenyl-3,4-Dihydrothieno[2,3-*d*]Pyrimidine Derivatives. *Chem. Pharm. Bull.* **1980,** *28*, 3172-3177.

322. Dave, K. G.; Shishoo, C. J.; Devani, M. B.; Kalyanaraman, R.; Ananthan, S. *et al*. Reaction of Nitriles under Acidic Conditions. Part I. Ageneral Method of Synthesis of Condensed Pyrimidines. J. *Heterocyclic Chem.* **1980,** *17*, 1497-1500.

323. Cruceyra, A.; Gomez Parra, V.; Madronero, R. Thiophene Bioisosteres. Iii. 4-Oxo-1,2,3,4-Tetrahydrothieno[2,3-*d*]Pyrimidines. A*nales de Quimica* **1975,** *71*,103-106.

324. Corral, C.; Madronero, R.; Ulecia, N. Bischler and Friedlaender Reactions with 2-Amino-3-Aroylthiophenes. A*finidad* **1978,** *35*, 129-133.

325. Konno, S.; Tsunoda, M.; Watanabe, R.; Yamanaka, H.; Fujita, F. et al. Synthesis of Thieno[2,3-*d*]pyrimidine Derivatives and Their Antifungal Activities. Y*akugaku Zasshi* **1989,** *109,* 464-473.

326. Robba, M.; de Sevricourt, M. C.; Lecomte, J. M. Thienopyrimidines. VII. Reactions of the 4-hydrazinothieno[2,3-*d*]pyrimidines. *J. Heterocycl. Chem.* **1975**, *12*, 525-527.

327. Horiuchi,T.; Chiba, J.; Uoto, K.; Soga, T. *Bioorg. Med. Chem. Lett.* **2009**, *19,* 305-308.

328. Briel, D. Synthesis of Thieno-Heterocycles from Substituted 5-(Methylthio)Thiophene-4-Carbonitriles. *Pharmazie* **1998,** *53,* 227-231.

329. Taylor, E. C.; Patel, H. H.; Sabitha, G.; Chaudhari, R. Synthesis of Thieno[2,3 -*d*]pyrimidine Analogues of the Potent Antitumor Agent, N-{4-[2-(2- Amino-4(3H)-oxo-7H-pyrrolo [2,3-*d*]pyrimidin-5-yl)ethyl]B enzoyl }-Lglutamic Acid. (LY 231514) *Heterocycles.* **1996**, *43,* 349-365.

330. Sakamoto, T.; Kondo, Y.; Watanabe, R.; Yamanaka, H. Condensed Heteroaromatic Ring Systems. Vii. Synthesis of Thienopyridines, Thienopyrimidines, and Furopyridines from O-Substituted Heteroarylacetylenes. *Chem. Pharm. Bull.* **1986,** *34,* 2719-2724.

331. Ried, W.; Beller, G. Synthesis of Thieno[2,3-*d*]Pyrimidines and Pyrrolo[2,3-*d*]Pyrimidines. L*iebigs Annalen der Chemie* **1988,** *7,* 633-642.

332. El-Dean, A. K. Synthesis of Some Pyrimidothienopyrimidine Derivatives. M*onatshefte fuer chemie* **1998,** *129,* 523-533.

333. Briel, D.; Wagner, G.; Lohmann, D.; Laban, G. Preparation of 2,4-Diaryl-5-Hydroxythieno[2,3-*d*]Pyrimidines as Drugs and Drug Intermediates.: Ger. (East), 1**988.**

334. Van Straten

335. Gangjee, A.; Lin, X.; Queener, S. F. Design, Synthesis, and Biological Evaluation of 2,4-Diamino-5-methyl-6-substituted-pyrrolo[2,3-*d*]pyrimidines as Dihydrofolate Reductase Inhibitors. *J. Med. Chem*. **2004**, *47*, 3689-3692.

336. Gangjee, A.; Qiu, Y.; Li, W.; Kisliuk, R. L. Potent Dual Thymidylate Synthase and Dihydrofolate Reductase Inhibitors: Classical and Nonclassical 2-Amino-4-oxo-5-arylthio-substituted-6-methylthieno[2,3-d]pyrimidine Antifolates. *J. Med. Chem*. **2008**, *51*, 5789-5797.

337. Gangjee, A.; Li, W.; Kisliuk, R. L.; Cody, V.; Pace, J.; Piraino, J.; Makin. J. Design, Synthesis, and X-ray Crystal Structure of Classical and Nonclassical 2-Amino-4-oxo-5-substituted-6-ethylthieno[2,3-*d*]pyrimidines as Dual Thymidylate Synthase and Dihydrofolate Reductase Inhibitors and as Potential Antitumor Agents. *J. Med. Chem*. **2009**, *52*, 4892-4902.

338. Sridhar, M.; Rao, R. M.; Baba, N. H. K.; Kumbhare, R. M. Microwave Accelerated Gewald Reaction: Synthesis of 2-aminothiophenes. *Tetrahedron Lett.* **2007**, *48*, 3171-3172.

339. Sonogashira, K. Tohda, Y.; Hagihara, N. Convenient Synthesis of Acetylenes. Catalytic Substitutions of Acetylenic Hydrogen with Bromo Alkenes, Iodo Arenes, and Bromopyridines. *Tetrahedron Lett*. **1975**, *16*, 4467-4470.

340. Negishi, E.-I., Anastasia, L. Palladium-Catalyzed Alkynylation. *Chem. Rev*. **2003**, *103*, 1979-2017.

341. Gangjee, A.; Yu, J. M.; Copper, J. E.; Smith, C. D., Discovery of Novel Antitumor Antimitotic Agents that also Reverse Tumor Resistance. *J. Med. Chem.* **2007**, *50*, 3290-3301.

342. Ullmann, F.; Bielecki, J. "Ueber Synthesen in der Biphenylreihe". *Chem Ber*, **1901**, *34*, 2174–2185.

343. Hassan, J., Sevignon, M., Gozzi, C., Schulz, E., Lemaire, M. Aryl-Aryl Bond Formation One Century after the Discovery of the Ullmann Reaction. *Chem. Rev*. **2002**, *102*, 1359-1469.

344. Nelson, T. D.; Crouch, R. D. Cu, Ni, and Pd Mediated Homocoupling Reactions in Biaryl Syntheses: The Ullmann Reaction .*Org. React*. **2004**, *63*, 265.

345. Kornblum, N.; Kendall, D. L. The use of dimethylformamide in the Ullmann reaction. *J. Am. Chem. Soc.* **1952**, *74*, 5782

346. Palomo, C.; Oiarbide, M.; Lopez, R.; Gomez-Bengoa, E. *J. Chem. Soc., Chem. Commun*. **1998**, 2091

347. Chen, W.; Zhao, Q.; Xu, M.; Lin, G. Nickel-Catalyzed Asymmetric Ullmann Coupling for the Synthesis of Axially Chiral Tetra-ortho-Substituted Biaryl Dials. *Org. Lett*. **2010**,*12*,1072-1075.

348. Omura, K.; Swern, D. Oxidation of Alcohols by "activated" Dimethyl Sulfoxide. A Preparative, Steric and Mechanistic study. *Tetrahedron*. **1978** ,*34*, 1651-1660.

349. Chu, E.; Callender, M. A.; Farrell, M. P.; Schmitz, J. C. Thymidylate Synthase Inhibitors as Anticancer agents: from Bench to Bedside. *Cancer Chemother Pharmacol.* **2003**, 80-89.

350. Jackman, A. L.; Taylor, G. A.; Gibson, W.; Kimbell, R.; Brown, M.; Calvert, A. H.; Judson, I. R.; Hughes, L. R. ICI D1694, a Quinazoline Antifolate Thymidylate Synthase Inhibitor That Is a Potent Inhibitor of L1210 Tumour Cell Growth in Vitro and in Vivo: A New Agent for Clinical Study. *Cancer Res*. **1991**, *51*, 5579-5586.

351. Taylor, E. C.; Kuhnt, D.; Shih, C.; Rinzel, S. M.; Grindey, G. B.; Barredo, J.; Jannatipour,M.; Moran, R. A Dideazatetrahydrofolate Analogue Lacking a Chiral Center at C-6, N-[4-[2-(2-Amino-3,4-dihydro-4-oxo-7H-pyrrolo[2,3-d]pyrimidin-5-y1)ethylbenzoyl]-

L-glutamic Acid, Is an Inhibitor of Thymidylate Synthase. *J. Med. Chem*.**1992**, *35*, 4450–4454.

352. Bertino, J. R.; Kamen, B.; Romanini, A. Folate Antagonists. In Cancer Medicine; Holland, J. F., Frei, E., Bast, R. C., Kufe, D. W., Morton, D. L., Weichselbaum, R. R., Eds.; Williams and Wilkins:Baltimore, MD, 1997; Vol. 1, pp 907-921.

353. Gibson, W.; Bisset, G. M. F.; Marsham, P. R.; Kelland, L. R.; Judson, I. R.; Jackman, A. L. The Measurement of Polyglutamate Metabolites of the Thymidylate Synthase Inhibitor, ICI D1694, in Mouse and Human Cultured Cells. *Biochem. Pharmacol*. **1993**, *45*, 863-869.

354. Gangjee, A.; Devraj, R.; McGuire, J. J.; Kisliuk, R. L. 5-Arylthio Substituted 2-Amino-4-oxo-6-methylpyrrolo[2,3-*d*]pyrimidine Antifolates as Thymidylate Synthase Inhibitors and Antitumor Agents. *J. Med. Chem.* **1995**, *38*, 4495-4502.

355. Marsham, P. R.; Jackman, A. L.; Barker, A. J.; Boyle, F. T.; Pegg, S. J.; Wardleworth, J. M.; Kimbell, R.; O'Connor, B. M.; Calvert, A. H.; Hughes, L. R. Quinazoline Antifolate Thymidylate Synthase Inhibitors: Replacement of Glutamic Acid in the C2-Methyl Series. *J. Med. Chem.* **1995**, *38*, 994-1004.

356. Tripos Inc., 1699 South Hanley Road, St. Louis, MO 63144.

357. Pendergast, W.; Dickerson, S. H.; Dev, I. K.,; Ferone, R.,; Duch, D. S.; Smith, G. K. Benzo[*f*]quinazoline Inhibitors of Thymidylate Synthase: Methyleneamino-linked Arylglutamate Derivatives. *J Med Chem.* **1994**, *37*, 838-844.

358. Beutel, G.; Glen, H.; Schoffski, P.; Chick, J.; Gill, S.; Cassidy, J.; Twelves, C. Phase I Study of OSI-7904L, a Novel Liposomal Thymidylate Synthase Inhibitor in Patients with Refractory Solid Tumors. *Clin Cancer Res.* **2005**, *11*, 5487-5495.

359. Montfort, W. R.; Weichsel, A. Thymidylate Synthase: Structure, Inhibition, and Strained Conformations During Catalysis. *Pharmacol. Ther.* **1997**, *76*, 29-43.

360. Stout, T. J.; Stroud, R. M. the Complex of the Anticancer Therapeutic, BW1843U89, with Thymidylate Synthase at 2.0 Å Resolution: Implications for a New Mode of Inhibition. *Structure*, **1996**, *4*, 67-77.

361. Weichsel, A.; Montfort, W. R. Ligand-induced Distortion of an Active Site in Thymidylate Synthase upon Binding Anticancer Drug 1843U89. *Nature Struct. Biol.* **1995**, 2, 1095-l 101.

362. Weichsel, A.; Montfort, W. R.; Ciesla, J.; Maley, F. Promotion of Purine Nucleotide Binding to Thymidylate Synthase by a Potent Folate Analogue Inhibitor, 1843U89. *Proc. Natl. Acad. Sci.* **1995**, *92*, 3493-3497

363. Vainio, M. J.; Johnson, M. S. Generating conformer ensembles using a Multiobjective Genetic Algorithm. *J. Chem. Inf. Model.* **2007**, *47*, 2462-2474.

364. Zakrzewski, S. F.; Dave, C.; Rosen, F. Comparison of the Antitumor Activities and Toxicity of the 2,4-5(1-adamantyl)-6-methylpyrimidine and 2,4-Diamino-5-(I-adarnantyl)6-ethyl-pyrimidine. *J. Natl. Caner. Invest.* **1978,** 60, 1029-1033.

365. Bliss, E. A.; Griffin, R. J.; Stevens, M. F. G. Structural Studies on Bioactive Compounds. Part 5. Synthesis and Properties of 2,4-Diaminopyrimidine DHFR Inhibitors Bearing Lipophilic Azido Groups. *J. Chem. Soc. Perk.Trans.I* **1987,** *1*, 2217- 2228.

366. Seage, G. R.; Losina, E.; Goldie, S. J.; Paltiel, A. D.; Kimmel, A. D.; Freedberg, K. A. The Relationship of Preventable Opportunistic Infections, HIV-1 RNA, and CD4 Cell Counts to Chronic Mortality. *JAIDS, J. Acquired Immune Defic. Syndr.* **2002**, *30*, 421-428.

367. Klepser, M. E.; Klepser, T. B. Drug Treatment of HIV-Related Opportunistic Infections. *Drugs* **1997**, *53*, 40–73.

368. DeClercq, E. Toward Improved Anti-HIV Chemotherapy: Therapeutic Strategies for Intervention with HIV Infections. *J. Med. Chem.* **1995**, *38*, 2491–2517.

369. Masur, H.; Polis, M. A.; Tuazon, C. V.; Ogota-Arakaki, D.; Kovacs, J. A.; Katz, D.; Hilt, D.; Simmons, T.; Feuerstein, I.; Lundgren, B.; Lane, H. C.; Chabner, B. A.; Allegra, C. J. Salvage Trial of Trimetrexate-Leucovorin for the Treatment of Cerebral Toxoplasmosis. *J. Infect. Dis.* **1993**, *167*, 1422-1426.

370. Gangjee, A.; Vasudevan, A; Queener, S. F.; Kisliuk, R. L. 2,4-Diamino-5-Deaza-6-Substituted Pyrido[2,3-*d*]pyrimidine Antifolates as Potent and Selective Nonclassical Inhibitors of Dihydrofolate Reductases. *J. Med. Chem.* **1996**, *39*, 1438-1446.

371. News. FDA Approves Trimetrexate as Second line Therapy of *Pneumocystis carinii* Pneumonia *Am. J. Hosp. Pharm.* **1994**, *51*, 591-592.

372. Willemot, P.; Klein, M. B. Prevention of HIV-associated Opportunistic Infections and Diseases in the Age of Highly Active Antiretroviral Therapy. *Expert Rev. Anti-Infect. Ther*. **2004**, *2*, 521–532.

373. Walzer, P. D.; Foy, J.; Steele, P.; White, M. Synergistic combinations of Ro 11-8958 and other dihydrofolate reductase inhibitors with sulfamethoxazole and dapsone for therapy of experimental pneumocystosis. *Antimicrobial agents and chemotherapy* **1993**, *37*, 1436-43.

374. Hertz, R.; Tullner, W. W. Inhibition of Estrogen-induced Growth in the Genital Tract of the Female Chick by a Purine Antagonist; Reversal by Adenine. *Science.* **1949**, *109*, 539.

375. Zhao, R. B.; Qiu, A. D.; Tsai, E.; Jansen, M.; Akabas, M. H.; Goldman, I. D. The Proton-coupled Folate Transporter: Impact on Pemetrexed Transport and on Antifolates Activities Compared with the Reduced Folate Carrier. *Mol. Pharmacol.* **2008**, *74*, 854-862.

376. Deng, Y. J.; Wang, Y. Q.; Cherian, C.; Hou, Z. J.; Buck, S. A.; Matherly, L. H.; Gangjee, A., Synthesis and Discovery of High Affinity Folate Receptor-specific Glycinamide Ribonucleotide Formyltransferase Inhibitors with Antitumor Activity. *J. Med.Chem.* **2008**, *51*, 5052-5063.

377. Deng, Y.; Zhou, X.; Desmoulin, S. K.; Wu, J. Cherian, C. Hou, Z.; Metherly, L. H.; Gangjee, A. Synthesis and Biological Activity of a Novel Series of 6-Substituted Thieno[2,3-*d*]pyrimidines Antifolate Inhibitors of Purine Biosynthesis with Selectivity for High Affinity Folate Receptors over the Reduced Folate Carrier and Proton-Coupled Folate Transporter for Cellular Entry. *J. Med.Chem.* **2009**, *52*, 2940-2951.

378. Folkman, J. The influence of angiogenesis research on management of patients with breast cancer. *Breast Cancer Res. Treat.* **1995**, *36*, 109–118.

379. Hanahan, D. and Folkman, J. Patterns and Emerging Mechanisms of the Angiogenic Switch during Tumorigenesis. *Cell* **1996**, *1996*, 353–364.

380. Folkman, J. Angiogenesis: An Organizing Principle for Drug Discovery? *Nature Rev. Drug Discov.* **2007**, *6*, 273-286.

381. Mandel, D. B.; Laird, A. D.; Xin, X.; Louie, S. G.; Christensen, J. G.; Li, G.; Schreck, R. E.; Abrams, T. J.; Ngai, T. J.; Lee, L. B.; Murray, L. J.; Carver, J.; Chan, E.; Moss, K. G.; Haznedar, J. O.; Sukbuntherng, J.; Blake, R. A.; Sun, L.; Tang, C.; Miller, T.; Shirazian, S.; McMahon, G.; Cherrington, J. M. *In Vivo* Antitumor Activity of SU11248, A Novel Tyrosine Kinase Inhibitor Targeting Vascular Endothelial Growth Factor and Platelet-derived Growth

Factor Receptors: Determination of a Phamarcokinetic/Pharmacodynamic Relationship. *Clin. Cancer Res.* **2003**, *9*, 327–337.

382. Wilhelm, S. M.; Carter, C.; Tang, L.; Wilkie, D.; McNabola, A.; Rong, H.; Chen, C.; Zhang, X.; Vincent, P.; McHugh, M.; Cao, Y.; Shujath, J.; Gawlak, S.; Eveleigh, D.; Rowley, B.; Liu, L.; Adnane, L.; Lynch, M.; Auclair, D.; Taylor, I.; Gedrich, R.; Voznesensky, A.; Riedl, B.; Post, L. E.; Bollag, G.; Trail, P. A. BAY 43–9006 Exhibits Broad Spectrum Oral Antitumor Activity and Targets the RAF/MEK/ERK Pathway and Receptor Tyrosine Kinases Involved in Tumor Progression and Angiogenesis. *Cancer Res.* **2004**, *64*, 7099–7109.

383. Palmer B. D., Trumppkallmeyer S., Fry D. W., Nelson J. M.,Showalter H. D. H., Denny W. A. Tyrosine Kinase Inhibitors. 11. Soluble Analogues of Pyrrolo- and Pyrazoloquinazolines as Epidermal Growth Factor Receptor Inhibitors: Synthesis, Biological Evaluation, and Modeling of the Mode of Binding. *J. Med. Chem.* **1997**, *40*, 1519–1529.

384. Bold, G. G., Frei, J., Traxler, P., Altmann, K., Mett, H., Strover, D., Wood, J. WO9835958.

385. Ple, P. A.; Green, T. P.; Hennequin, L. F.; Curwen, J.; Fennell, M.; Allen, J.; Lambert-van der B., Christine; Costello, G.. Discovery of a New Class of Anilinoquinazoline Inhibitors with High Affinity and Specificity for the Tyrosine Kinase Domain of c-Src. *J. Med. Chem.* **2004**, *47*, 871-887.

386. O'Connor, P. M.; Jackman, J.; Bae, I.; Myers, T. G.; Fan, S.; Mutoh, M.; Scudiero, D. A.; Monks, A.; Sausville, E. A.; Weinstein, J. N.; Friend, S.; Fornace, A. J. Jr. and Kohn, K. W. Characterization of the p53 Tumor Suppressor Pathway in Cell Lines of the National Cancer Institute Anticancer Drug Screen and Correlations with the Growth-inhibitory Potency of 123 Anticancer Agents. *Cancer Res.*, **1997**, *57*, 4285-4300.

387. Jordan, M. A. and Kamath, K. How do Microtubule-Targeted Drugs Work? An Overview. *Curr. Cancer Drug Targets*, **2007**, *7*, 730-742.

388. Lee, J. F. and Harris, L. N. Antimicrotubule Agents. In *Cancer: Principles & Practice of Oncology* 8th ED., V. T. DeVita, Jr., T. S. Lawrence and S. A. Rosenberg Eds., Lippincott Williams & Wilkins, **2008**, 447-456.

389. Löwe, J.; Li, H.; Downing, K. H. and Nogales, E. Refined Structure of αβ-Tubulin at 3.5Å Resolution. *J. Mol. Biol.*, **2001**, *313*, 1045-1057.

390. Huey, R. M.; Calvo, E.; Barasoain, I.; Pineda, O.; Edler, M. C.; Matesanz, R.; Cerezo, G.; Vanderwal, C. D.; Day, B. W.; Sorensen, E. J.; Lopez, J. A.; Andreu, J. M.; Hamel, E. and Diaz, J. F. Cyclostreptin Binds Covalently to Microtubule Pores and Lumenal Taxoid Binding Sites. *Nat. Chem. Biol.*, **2007**, *3*, 117-125.

391. Kanthou, C. and Tozer, M. T. Microtubule Depolymerizing Vascular Disrupting Agents: Novel Therapeutic Agents for Oncology and Other Pathologies. *Int. J. Exp. Path.*, 2009, *90*, 284-294.

392. Carlson, R. O. New Tubulin Targeting Agents Currently in Clinical Development. *Expert Opin. Investig. Drugs*, **2008**, *17*, 707-722.

393. Leonard, G. D.; Fojo, T. and Bates, S. E. The Role of ABC Transporters in Clinical Practice. *Oncologist*, **2003**, *8*, 411-424.

394. Yeh, J. J.; Hsu, W. H.; Wang, J. J.; Ho, S. T. and Kao, A. Predicting Chemotherapy Response to Taxol-based Therapy in Advanced Non-Small-Cell Lung Cancer with P-glycoprotein Expression. *Respiration*, **2003**, *70*, 32 – 35.

395. Chiou, J. F.; Liang, J. A.; Hsu, W. H.; Wang, J. J.; Ho, S. T. and Kao, A. Comparing the Relationship of Taxol-based Chemotherpay Response with P-glycoprotein and Lung

Resistance-related Protein Expression in Non-Small Cell Lung Cancer. *Lung*, **2003**, *181*, 267 – 273.

396. Fojo, T. and Menefee, M. Mechanisms of Multidrug Resistance: The Potential Role of Microtubule-stabilizing Agents. *Ann. Oncol.*, **2007**, *18*, 3 – 8.

397. Rosell, R.; Scagliotti, G.; Danenberg, K. D.; Lord, R. V. N.; Bepler, G.; Novello, S.; Cooc, J.; Crino, L.; Sanchez, J. J.; Taron, M.; Boni, C.; De Marinis, F.; Tonato, M.; Marangolo, M.; Gozzelino, F.; Di Costanzo, F.; Rinaldi, M.; Salonga, D.; Stephens, C. Transcripts in Pretreatment Biopsies From A Three-Arm Randomized Trial In Metastatic Non-Small-Cell Lung Cancer. *Oncogene*, **2003**, *22*, 3548 – 3553.

398. Dumontet, C.; Isaac, S.; Souquet, P.-J.; Bejui-Thivolet, F.; Pacheco, Y.; Peloux, N.; Frankfurter, A.; Luduena, R.; Perol, M. Expression of Class III Beta Tubulin In Non-Small Cell Lung Cancer Is Correlated With Resistance To Taxane Chemotherapy. *Bull. Cancer*, **2005**, *92*, 25 – 30.

399. Seve, P.; Isaac, S.; Tredan, O.; Souquet, P.-J.; Pacheco, Y.; Perol, M.; Lafanechere, L.; Penet, A.; Peiller, E.-L.; Dumontet, C. Expression of Class III β -Tubulin Is Predictive of Patient Outcome in Patients with Non-Small Cell Lung Cancer Receiving Vinorelbine-Based Chemotherapy *Clin. Cancer Res.*, **2005**, *11*, 5481 – 5486.

400. Tommasi S.; Mangia A.; Lacalamita R.; Bellizzi A.; Fedele V.; Chiriatti A.; Thomssen C.; Kendzierski N.; Latorre A.; Lorusso V.; Schittulli F.; Zito F.; Kavallaris M.; Paradiso A. Cytoskeleton and Paclitaxel Sensitivity In Breast Cancer: The Role Of Beta-Tubulins. *Int. J. Cancer*, **2007**, *120*, 2078 – 2085.

401. Mozzetti, S.; Ferlini, C.; Concolino, P.; Filippetti, F.; Raspaglio, G.; Prislei, S.; Gallo, D.; Martinelli, E.; Ranelletti, F. O.; Ferrandina, G.; Scambia, G. Class III β-tubulin

Overexpression Is A Prominent Mechanism Of Paclitaxel Resistance In Ovarian Cancer Patients. *Clin. Cancer Res.* **2005**, *11*, 298 – 305.

402. Ferrandina, G.; Zannoni, G. F.; Martinelli, E.; Paglia, A.; Gallotta, V.; Mozzetti, S.; Scambia, G.; Ferlini, C. Class III β -Tubulin Overexpression Is A Marker Of Poor Clinical Outcome In Advanced Ovarian Cancer Patients. *Clin. Cancer Res.*, **2006**, *12*, 2774 – 2779.

403. Strengel, C,.; Newman, S. P.; Lesse, M. P.; Potter, B. V. L.; Reed, M. J. and Purohit, A. Class III Beta- Tubulin Expression and in vitro Resistance To Microtubule Targeting Agents. *Brit. J. Cancer, **2010**, 102,* 316 – 324.

404. Lee L., Robb L.M., Lee M., Davis R., Mackay, H., Chavda, S., O'Brien, E.L., Risinger, AL, Mooberry, SL, Lee, M. Design, Synthesis and Biological Evaluations of 2,5-Diaryl-2,3-dihydro-1,3,4-oxadiazoline Analogs of Combretastatin-A4. *J. Med. Chem.* **2010**, *53*, 325 – 334.

405. Paull, K. D.; Lin, C. M.; Malspeis, L. and Hamel, E. Identification of Novel Antimitotic Agents Acting at the Tubulin Level by Computer-assisted Evaluation of Differential Cytotoxicity Data. *Cancer Res.*, **1992**, *52*, 3892 – 3900.

406. Gangjee, A.; Zhao, Y.; Hamel, E.; Westbrook, C.; Mooberry, S. L. Synthesis and Biological Activities of (R)- and (S)-N-(4-Methoxyphenyl)-N,2,6-trimethyl-6,7-dihydro-5H-cyclopenta[d]pyrimidin-4-aminium Chloride as Potent Cytotoxic Antitubulin Agents. *J. Med. Chem.* **2011**, *54*, 6151 – 6154.

407. Gangjee, A.; Yu, J.; Keller, S. N.; Smith, C. D.; Discovery of Novel Antitumor Antimitotic Agents that Also Reverse Tumor Resistance. Abstract of Papers, 232nd ACS National Meeting, San Francisco, CA, United States, Sept, 10-14, **2006**, MEDI-142

408. Zhang, M.; Harper, R. W. A Concise Synthetic Entry to Substituted 2-Amino-thieno[2,3-*d*]pyrimidines *via* a Gewald Precursor. *Bioorg. Med. Chem. Lett*. **1997**, *7*, 1629-1634.

409. Rosowsky, A.; Chen, K. K.; Lin, M., 2,4-Diaminothieno[2,3-*d*]pyrimidines as Antifolates and Antimalarials. 3. Synthesis of 5,6-Disubstituted Derivatives and Related Tetracyclic Analogs. *J. Med. Chem.* **1973**, *16*, 191-194.

410. Yadav, P. P.; Gupta, P.; Chaturvedi, A. K.; Shukla, P. K.; Maurya, R., Synthesis of 4-Hydroxy-1-methylindole and Benzo[b]thiophen-4-ol Based Unnatural Flavonoids as New Class of Antimicrobial Agents. *Bioorg. Med. Chem.* **2005**, *13*, 1497-1505.

411. Sengupta, S. K.; Chatterjee, S.; Protopapa, H. K.; Modeat, E. J., 2,3-Diaminopyrimidines from Dicyandiamide. IV. Condensation with Bicyclic Aromatic Ketones. *J. Org. Chem* **1972**, *37*, 1323-1328.

412. Wartenberg, F. H.; Koppe, T.; Wetzel, W.; Wydra, M.; Benz, A., Method for Producing Benzo Annelated Heterocycles. PCT Int. Appl.(2001), CODEN: PIXXD2 WO 01/77099 A1 19980305.

413. Rosowsky, A.; Forsch, R. A.; Null, A.; Moran, R. G., 5-Deazafolate Analogues with a Rotationally Restricted Glutamate or Ornithine Side Chain: Synthesis and Binding Interaction with Folylpolyglutamate Synthetase. *J. Med. Chem*. **1999**, *42*, 3510-3519.

414. Pendergast, W.; Dickerson, S. H.; Dev, I. K.; Ferone, R.; Duch, D. S.; Smith, G. K. Benzo[*f*]quinazoline Inhibitors of Thymidylate Synthase: Methyleneamino-Linked Aroylglutamate Derivatives *J. Med. Chem*. **1994**, *37*, 838-844.

415. Patil, S. D.; Jones, C.; Nair, M. G.; Galivan, J.; Maley, F.; Kisliuk, R. L.; Gaumont, Y; Duch, D.; Ferone, R. Folate analogs. 32. Synthesis and Biological Evaluation of 2-desamino-

2-methyl-N10-propargyl-5,8-dideazafolic Acid and Related Compounds J. *Med. Chem*. **1989**, *32*, 1284-1289.

416. Hughes, L. R.; Jackman, A. L.; Oldfield, J.; Smith, R. C.; Burrows, K. D.; Marsham, P. R.; Bishop, J. A. M.; Jones, T. R.; O'Connor, B. M. and Calvert, A. H. Quinazoline Antifolate Thymidylate Synthase Iinhibitors: Alkyl, Substituted Alkyl, and Aryl Substituents in the C-2 position *J. Med. Chem*., **1990**, *33*, 3060-3067.

417. Marsham, P. R.; Jackman, A. L.; Hayter, A. J.; Daw, M. R.; Snowden, J. L.; O'Connor, B. M.; Bishop, J. A.; Calvert, A. H.; Hughes, L. R., Quinazoline Antifolate Thymidylate Synthase Inhibitors: Bridge Modifications and Conformationally Restricted Analogues in the C2-methyl Series. *J. Med. Chem.* **1991**, *34*, 2209-2218.

418. Namjoshi, O. Dessertation. Duquesne University.

Appendix

The biological evaluations of the analogs listed in the following tables were performed by Dr. Michael Ihnat (Department of Cell Biology, University of Oklahoma Health Science Center) against various kinase (VEGFR-1, VEGFR-2, EGFR and PDGFRβ), A431 cytotoxicity and the chorioallantonic membrane (CAM) assay (as described below), Dr. Roy L. Kisliuk (Department of Biochemistry, Tufts University School of Medicine) against rhTS, rhDHFR, *E. coli* TS and *E. coli* DHFR; Dr. Sherry F. Queener (Department of Pharmacology and Toxicology, Indiana University School of Medicine) against rat liver (rl)DHFR, *P. carinii* DHFR, *T. gondii* DHFR, and *M. avium* DHFR; Dr. Susan Mooberry (Co-leader of Experimental and Developmental Therapeutics, CTRC at UTHSCSA) against MDA MB 435 breast tumor cells and effects on microtubule depolymerization, Dr.Vivian Cody (Hauptman-Woodward Medical Research Institute), Dr. Ernest Hamel and National Cancer Institute (NCI).

X-ray Structure Determination and Refinement of 277 and 278. Expression and purification of hDHFR were carried out as previously described.[41] Recombinant hDHFR was washed in a Centricon-10 with 10 mM HEPES buffer, pH 7.4, and concentrated to 11.9 – 12.1 mg/mL for the two samples. The hDHFR protein was incubated with NADPH and an excess of compounds **277** and **278** for 1hr over ice prior to crystallization using the hanging drop vapor diffusion method. The reservoir solution for inhibitor **277** contained 100 mM KPO_4, pH 6.9, 66% saturated NH_4SO_4, 3% v/v ethanol and 70% saturated NH_4SO_4 for compound **278**. Crystals of hDHFR complex grew over serval days at 14^oC and were trigonal, space group H3. Data were collected to 1.35A resolution for both complexes using the remote access robot[42-44] at liquid N2 temperatures on beamline 9-2 at the Stanford Synchrotron Research Laboratory (SSRL) imaging plate system. The data were processed using Mosflm.[45] The diffraction statistics are shown in Table 2 for the two complexes.

Table 12. Data collection and refinement statistics for hDHFR-NADPH-**277** and **278** ternary complexes.

Data collection	hDHFR NADPH-**277**	hDHFR NADPH-**278**
PDB accession #	3ntz	3nu0
Space group	H3	H3
Cell dimensions (Å)	84.29 77.79	84.39 78.19
Beamline	SSRL 9-2	SSRL 9-2
Resolution (Å)	1.35	1.35
Wavelength (Å)	0.975	0.975
R_{sym} (%) [a,b]	0.061 (0.72)	0.066 (0.45)
R_{merge}	0.053 (0.62)	0.063 (0.39)
Completeness (%) [a]	100.0 (100.0)	100.0 (100.0)
Observed reflections	169,016	569,239
Unique reflections	45,260	45,587
I/□(I)	15.3 (1.6)	27.0 (8.6)
Multiplicity [a]	3.7 (3.7)	12.5 (12.1)

Refinement and model quality

Resolution range (Å)	26.6 – 1.35	33.1 – 1.35
No. of reflections	45,259	45,587
R-factor [c]	18.6	18.0
R_{free}-factor [d]	20.5	20.9
Total protein atoms	1817	1868
Total water atoms	164	187
Average B-factor (Å^2)	18.9	15.7
Rms deviation from ideal		
Bond lengths (Å)	0.031	0.035
Bond angles (^{o})	2.84	2.99
Luzzati	0.159	0.145
Ramachandran plot		
Most favored regions (%)	97.8	97.8
Additional allowed regions (%)	2.2	2.2
Generously allowed regions (%)	0.0	0.0
Disallowed regions (%)	0.0	0.0

[a] The values in parentheses refer to data in the highest resolution shell.
[b] $R_{sym} = \Sigma_h\Sigma_i|I_{h,i} - \langle I_h\rangle| / \Sigma_h\Sigma_i|I_{h,i}|$, where $\langle I_h\rangle$ is the mean intensity of a set of equivalent reflections.
[c] R-factor = $\Sigma|F_{obs} - F_{calc}| / \Sigma F_{obs}$, where F_{obs} and F_{calc} are observed and calculated structure factor amplitudes.
[d] R_{free}-factor was calculated for R-factor for a random 5% subset of all reflections.

The structures were solved by molecular replacement methods using the coordinates for hDHFR (u072) in the program Molref.[45] Inspection of the resulting difference electron density maps made using the program COOT[46] running on a MacG5 workstation revealed density for the ternary complex in both crystals. The final cycles of refinement were carried out using the program Refmac5 in the CCP4 suite of programs. The Ramachandran conformational parameters from the last cycle of refinement generated by PROCHECK[47] showed that more than 98% of the residues have the most favored conformation and none are in the disallowed regions. Coordinated for these structures have been deposited with the Protein Data Bank (3ntz, 3nu0).

Table 13. Inhibitory Concentrations of **275-278** (IC_{50} in μM) against TS and DHFR.[a]

	TS(μM)			**DHFR**(μM)		
compound	**human**[b]	***E. coli***[b]	***T. gondii***[c]	**human**[d]	***E. coli***[e]	***T. gondii***[c]
272[f]	0.072	0.027	0.09	nd	Nd	nd
273[g]	0.085	0.085	nd	nd	Nd	nd
274[h]	0.042	nd	nd	2.2	Nd	nd
275	0.26	0.82	1.7	>20(35)	15	1.4
276	0.8	0.85	3.7	>20(24)	>20(38)	1.8
277	0.068	0.017	0.14	0.09	0.4	0.02
278	0.034	0.05	0.17	0.1	0.4	0.01
PMX[i]	9.5	76	2.8	6.6	2300	0.43
MTX	Nd	nd	nd	0.022	0.0066	0.022

[a] The percent inhibition was determined at a minimum of four inhibitor concentrations within 20% of the 50% point. The standard deviations for determination of 50% points were within ± 10% of the value given. [b] Kindly provided by Dr. Frank Maley, New York State Department of Health. [c] Kindly provided by Dr. Karen Anderson, Yale Univerisy, New Haven CT. [d] Kindly provided by Dr. J. H. Freisheim, Medical College of Ohio, Toledo, OH. [e] Kindly provided by Dr. R. L. Blakley, St. Jude Children's hospital, Memphis TN. [f] Kindly provided by Dr. M. G. Nair, University of South Alabama. [g] Kindly provided by Dr. J. J. McGuire, Roswell Park Cancer Institute, Buffalo, NY. [h] Data derived from ref 20. [i] Kindly provided by Dr. Chuan Shih, Eli Lilly and Co. nd = not determined

Table 14. Inhibitory Concentrations of **283-291** (IC_{50} in μM) against TS and DHFR.[a]

compound	TS(μM)			DHFR (μM)			
	human[b]	***E. coli***[b]	***T. gondii***[c]	**human**[d]	***E. coli***[e]	***T. gondii***[c]	***DHFR Selectivity (h/t.g.)***
279[f]	0.04	0.04	0.036	0.02	0.2	0.008	2.5
280[g]	0.054	0.018	0.09	0.019	1.0	0.0021	9
281[h]	0.08	0.06	0.096	0.95	>19 (43)	0.19	5
282	0.084	0.08	0.16	0.029	5.7	0.0057	5
283	>2.5 (41)	>2.5 (0)	>2.5 (21)	9.0	12.0	0.03	300
284	0.23	1.8	0.35	0.57	> 2.7 (0)	0.016	35.6
285	0.31	>2.2 (33)	1.1	2.6	>26 (23)	0.023	113
286	>1.4 (16)	>1.4 (24)	>1.4 (15)	17.0	> 17 (0)	0.017	1000
287	0.21	2.3	1.8	> 2.6 (0)	> 2.6 (0)	0.023	>113
288	2.0	>2.5 (16)	>2.5 (34)	6.0	> 30 (27)	0.024	250
289	0.46	2.3	1.8	2.8	> 28 (0)	0.014	200
210	0.92	>2.3 (25)	1.8	> 28 (24)	> 28 (0)	0.031	>903
211	0.23	>2.1 (25)	1.1	2.2	> 25 (17)	0.02	110
PMX[i]	9.5	76	2.8	6.6	230	0.43	15
PDDF[j]	0.085	0.019	0.43	1.9	23	0.22	8.6
MTX	nd	Nd	nd	0.02	0.0088	0.033	0.6
Trimethoprim	nd	Nd	nd	>340 (22)	0.01	6.8	>50

[a] The percent inhibition was determined at a minimum of four inhibitor concentrations within 20% of the 50% point. The standard deviations for determination of 50% points were within ± 10% of the value given. [b] Kindly provided by Dr. Frank Maley, New York State Department of Health. [c] Kindly provided by Dr. Karen Anderson, Yale Univerisy, New Haven CT. [d] Kindly provided by Dr. J. H. Freisheim, Medical College of Ohio, Toledo, OH. [e] Kindly provided by Dr. R. L. Blakley, St. Jude Children's hospital, Memphis TN. [f] Data derived from ref 7. [g] Data derived from ref 2. [h]Data derived from ref 6. nd = not determined. [i] Kindly provided by Dr. Chuan Shih, Eli Lilly and Co. [j] Kindly provided by Dr. M. G. Nair, University of South Alabama.

Table 15. Inhibitory Concentrations of **292-298** (IC_{50} in μM) against TS and DHFR.[a]

	TS(μM)			**DHFR** (μM)		
compound	**human**[b]	***E. coli***[b]	***T. gondii***[c]	**human**[d]	***E. coli***[e]	***T. gondii***[c]
272[f]	0.04	0.04	0.036	0.02	0.2	0.008
292	0.11	0.18	0.72	0.16	22	0.026
293	0.24	0.96	0.6	0.29	>2.9	0.015
295	2.2	28	25	>33 (0)	>33 (0)	1.7
296	3.3	13	26	>40 (15)	>40 (33)	4.4
297	0.11	2.3	1.2	2.8	>2.8 (0)	0.028
298	1.4	22	22	16	>32 (0)	0.32
pemetrexed[g]	9.5	76	2.8	6.6	230	0.43
PDDF[h]	0.085	0.019	0.43	1.9	23	0.22
MTX	nd	nd	nd	0.02	0.0088	0.033
trimethoprim	nd	nd	nd	>340 (22)	0.01	6.8

[a] The percent inhibition was determined at a minimum of four inhibitor concentrations within 20% of the 50% point. The standard deviations for determination of 50% points were within ± 10% of the value given. [b] Kindly provided by Dr. Frank Maley, New York State Department of Health. [c] Kindly provided by Dr. Karen Anderson, Yale Univerisy, New Haven CT. [d] Kindly provided by Dr. J. H. Freisheim, Medical College of Ohio, Toledo, OH. [e] Kindly provided by Dr. R. L. Blakley, St. Jude Children's hospital, Memphis TN. [f] Data derived from ref 2. nd = not determined. [g] Kindly provided by Dr. Chuan Shih, Eli Lilly and Co. [h] Kindly provided by Dr. M. G. Nair, University of South Alabama.

Table 16: DHFR inhibitory activity of **301-306**

	DHFR inhibition IC_{50} μM and selectivity								
	hDHFR	RL	E.coli	*tg*	*pc*	*mav*	*pj*	h/*tg*	h/*pj*
301	>30(31)	40	0.15	1.5	28.59	12.04		>20	
302	>27(21)	9.1	1.4	0.54	13.26	9.06		>50	
303	>30(6)	2.35	0.11	1.5	2.49	0.73		>20	
304	>26(30)	0.43	0.087	0.24	0.164	0.31		>108	
305	>30(8)	4.05	2.2	3	5.28	2.89		>10	
306	>28(25)	2.68	0.21	0.28	2.36	2.02		>100	

Table 17. FRα binding percentages and IC_{50}s (nM) for thienopyrimidine compounds **314**-**317** in cell proliferation inhibition of RFC- , PCFT- and FR-expressing cell lines.

Antifolate	name	FRα binding %	RFC		hFRα		RFC/ FRα		RFC/ FRα		PCFT	
			PC43-10	R2	RT16	RT16 (+FA)	KB	KB (+FA)	IGROV1	IGROV1 (+FA)	R2/PCFT4	R2/VC
314	G64	20.6	N	N	21	nd	149	nd	nd	nd	>1000nM	>1000nM
315	G55	31.2	N	N	N	nd	N	nd	nd	nd	>1000nM	>1000nM
316	G102	nd	>1000nM	>1000	3.1	nd	2.1	nd	nd	nd	>1000nM	nd
317	G103	nd	>1000nM	>1000	13.1	nd	6.1	nd	N	nd	>1000nM	nd
308	ZD2	14.5	>1000	>1000	13(3.4)	>1000	23(5.5)	>1000	4.7(1.9)	>1000	>1000nM	>1000nM
309	ZD1	16.3	>1000	>1000	9(2.9)	>1000	4.9(1.3)	>1000	5.9(1.9)	>1000	>1000nM	>1000nM
Methotrexate		nd	12(1.1)	216(8.7)	114(31)	461(62)	6.0(0.6)	20(2.4)	21(3.4)	22(2.1)	120.5(16.8)	>1000nM
Pemetrexed		nd	138(13)	894(93)	42(9)	388(68)	68(12)	327(103)	102(25)	200(18)	13.2(2.4)	974.0(18.1)
Raltitrexed		nd	6.3(1.3)	>1000	15(5)	>1000	5.9(2.2)	22(5)	12.6(3.3)	20(4.3)	99.5(11.4)	>1000nM
Lometrexol		nd	12(2.3)	>1000	12(8)	188(41)	1.2(0.6)	31(7)	3.1(0.9)	16(6)	248.0(18.2)	>1000nM
Trimetrexate		nd	25(7.3)	6.7(1.3)	13(1)	4.1(1)	58(18)	155(38)	12(4)	8.6(1.9)	nd	nd

FR experiments, cytotoxicity assays were performed in the absence and presence of 200 nM folic acid (FA). The data shown are mean values from three experiments (plus/minus SEM in parentheses). N = not active. nd = not determined. IC_{50} data of classical antifolate compounds, methotrexate, pemetrexed, raltitrexed, lometrexol, trimetrexate, **308** and **309**, were previously published from our laboratory.

Table 18. FRα binding percentages and IC_{50}s (nM) for thienopyrimidine compounds **318-322** and **456** in cell proliferation inhibition of RFC- , PCFT- and FR-expressing cell lines.

Antifolate	name	code	FRα binding %	RFC		hFRα		RFC/ FRα		RFC/ FRα		PCFT	
				PC43-10	R2	RT16	RT16 (+FA)	KB	KB (+FA)	IGROV1	IGROV1 (+FA)	R2/PCFT4	R2/VC
318	G69	XLZ/AG/156-239	35.2	N	N	66	N	N	nd	nd	nd	>1000nM	>1000nM
319	G68	XLZ/AG/156-238	36.1	N	N	60	N	N	nd	nd	nd	>1000nM	>1000nM
320	G67	XLZ/AG/156-237	16.7	N	N	13	N	N	nd	nd	nd	>1000nM	>1000nM
321	G66	XLZ/AG/156-235	19.4	N	N	25	N	N	nd	nd	nd	>1000nM	>1000nM
322	G77	XZ/AG/153-439	20.7	N	N	nd	nd	N	nd	N	nd	>1000nM	>1000nM
456	G76	XZ/AG/153-435	15.6	N	N	nd	nd	N	nd	N	nd	>1000nM	>1000nM
308	ZD2	XLZ/AG/156-148	14.5	>1000	>1000	13(3.4)	>1000	23(5.5)	>1000	4.7(1.9)	>1000	>1000nM	>1000nM
309	ZD1	XLZ/AG/156-146	16.3	>1000	>1000	9(2.9)	>1000	4.9(1.3)	>1000	5.9(1.9)	>1000	>1000nM	>1000nM
Methotrexate			nd	12(1.1)	216(8.7)	114(31)	461(62)	6.0(0.6)	20(2.4)	21(3.4)	22(2.1)	120.5(16.8)	>1000nM
Pemetrexed			nd	138(13)	894(93)	42(9)	388(68)	68(12)	327(103)	102(25)	200(18)	13.2(2.4)	974.0(18.1)
Raltitrexed			nd	6.3(1.3)	>1000	15(5)	>1000	5.9(2.2)	22(5)	12.6(3.3)	20(4.3)	99.5(11.4)	>1000nM
Lometrexol			nd	12(2.3)	>1000	12(8)	188(41)	1.2(0.6)	31(7)	3.1(0.9)	16(6)	248.0(18.2)	>1000nM
Trimetrexate			nd	25(7.3)	6.7(1.3)	13(1)	4.1(1)	58(18)	155(38)	12(4)	8.6(1.9)	nd	nd

FR experiments, cytotoxicity assays were performed in the absence and presence of 200 nM folic acid (FA). The data shown are mean values from three experiments (plus/minus SEM in parentheses). N = not active. nd = not determined. IC_{50} data of classical antifolate compounds, methotrexate, pemetrexed, raltitrexed, lometrexol, trimetrexate, **308** and **309**, were previously published from our laboratory.

Table 19. Tumor cell inhibitory activity GI_{50} (nM) of **373** (NCI).

Panel/ Cel line	**GI_{50} (nM)**	**Panel/ Cell line**	**GI_{50} (nM)**	**Panel/ Cell line**	**GI_{50} (nM)**	**Panel/ Cell line**	**GI_{50} (nM)**
NSCLC		**Renal Cancer**		**Ovarian cancer**		**Prostate Cancer**	
A549/ATCC	<10	786 - 0	<10	IGROV1	<10	PC-3	<10
EKVX	<10	A498	<10	OVCAR-3	<10	DU-145	<10
HOP-62	<10	ACHN	16.5	OVCAR-4	96.8	**Breast Cancer**	
HOP-92	<10	CAKI-1	<10	OVCAR-5	<10	MCF7	<10
NCI-H226	<10	RXF 393		OVCAR-8	<10	MDA-MB-231/ATCC	<10
NCI-H23	<10	SN 12C	<10	NCI/ADR-RES	<10	HS 578T	<10
NCI-H322M		TK-10	41.1	SK-OV-3		BT-549	<10
NCI-H460	<10	UO-31		**Melanoma**		MDA-MB-468	<10
NCI-H522	<10	**Colon Cancer**		LOX IMVI	<10	**Leukemia**	
CNS Cancer		COLO 205	<10	MALME-3M		CCRF-CEM	<10
SF-268	11.1	HCC-2998	<10	M14	<10	HL-60(TB)	<10
SF-295	<10	HCT-116	<10	MDA-MB-435		K-562	<10
SF-539	<10	HCT-15	<10	SK-MEL-2	<10	MOLT-4	11.9
SNB-19	<10	HT29	<10	SK-MEL-28	<10	RPMI-8226	<10
SNB-75	<10	KM12	<10	SK-MEL-5	<10	SR	<10
U251	<10	SW-620	<10	UACC-62	<10		

Table 20. Cytotoxicity to JC murine mammary adenocarcinoma cells

	384	**383**	**388**	**387**
IC_{50}(μM)	26±5	28±2	3±1	13±3

Figure 68. microtubule structures in A10 cells

DMSO control 10nM vinblastine 50μM **388**